University of Alberta

Monitoring and Analysis of a Temporary Grandstand

by

David A. Crick ©

A thesis submitted to the Faculty of Graduate Studies and Research
in partial fulfillment of the requirements for the degree of

Master of Science
in
Structural Engineering

Department of Civil AND ENVIRONMENTAL ENGINEERING.

Edmonton, Alberta
Spring 2008

Library and
Archives Canada

Published Heritage
Branch

395 Wellington Street
Ottawa ON K1A 0N4
Canada

Bibliothèque et
Archives Canada

Direction du
Patrimoine de l'édition

395, rue Wellington
Ottawa ON K1A 0N4
Canada

Your file Votre référence
ISBN: 978-0-494-45800-6
Our file Notre référence
ISBN: 978-0-494-45800-6

NOTICE:
The author has granted a non-exclusive license allowing Library and Archives Canada to reproduce, publish, archive, preserve, conserve, communicate to the public by telecommunication or on the Internet, loan, distribute and sell theses worldwide, for commercial or non-commercial purposes, in microform, paper, electronic and/or any other formats.

The author retains copyright ownership and moral rights in this thesis. Neither the thesis nor substantial extracts from it may be printed or otherwise reproduced without the author's permission.

AVIS:
L'auteur a accordé une licence non exclusive permettant à la Bibliothèque et Archives Canada de reproduire, publier, archiver, sauvegarder, conserver, transmettre au public par télécommunication ou par l'Internet, prêter, distribuer et vendre des thèses partout dans le monde, à des fins commerciales ou autres, sur support microforme, papier, électronique et/ou autres formats.

L'auteur conserve la propriété du droit d'auteur et des droits moraux qui protège cette thèse. Ni la thèse ni des extraits substantiels de celle-ci ne doivent être imprimés ou autrement reproduits sans son autorisation.

In compliance with the Canadian Privacy Act some supporting forms may have been removed from this thesis.

While these forms may be included in the document page count, their removal does not represent any loss of content from the thesis.

Conformément à la loi canadienne sur la protection de la vie privée, quelques formulaires secondaires ont été enlevés de cette thèse.

Bien que ces formulaires aient inclus dans la pagination, il n'y aura aucun contenu manquant.

Canada

ABSTRACT

A temporary grandstand was instrumented to measure the static and dynamic response when occupied. The measurements were made at the Toronto Molson Indy Car race on July 18, 1999. The members strain, sway displacements, and sway accelerations were measured. The results were analyzed and found to be within acceptable limits.

The natural frequency and mode shape were identified using the frequency domain decomposition method. A finite element analysis (FEA) model was created for the temporary grandstand to: a) demonstrate that FEA can accurately model the dynamic properties (natural frequency and mode shape) of the temporary grandstand; and b) to validate the mode shape identified from the frequency domain decomposition. The final FEA model correlated well with the experimental results, demonstrating that FEA is a useful tool for predicting the dynamic properties of a temporary grandstand and validating the identified mode shape from the ambient vibration survey.

ACKNOWLEDGEMENT

The author wishes to acknowledge the following for their contribution and support of this work:

- Dr Gilbert Grondin, for serving as my thesis advisor; for his help and support in setting up and monitoring the equipment in Toronto; and for his patience during the long process of writing this thesis.

- Dr. Shahab Afami, for his help in gathering equipment, calibrating, shipping, setting up, and monitoring. For providing guidance for the analysis of the large quantities of data collected. Without Dr. Afami's help I would have never had all of the equipment in place in time for the event

I would also like to acknowledge: Scaffold Connection Corporation for providing funding for the instrumentation phase of the project and providing access to the temporary grandstand; the Alberta Research Council for providing time and financial support towards the preparation of the thesis and the completion of the Master's of Science program.

Finally, I wish to thank my wife, Aileen Mac Isaac, for her patience and loving support during the long days and weekends spent working on my thesis.

TABLE OF CONTENTS

1 INTRODUCTION 1
1.1 GENERAL BACKGROUND 1
1.2 OBJECTIVES 3
1.3 SCOPE OF RESEARCH 4
2 LITERATURE REVIEW 7
2.1 INTRODUCTION 7
2.2 MATERIALS, DESIGN, AND CODES. 7
2.2.1 Scaffolding 7
2.2.2 Frame Scaffold 8
2.2.3 Tube and Clamp Scaffold 8
2.2.4 System Scaffold 8
2.2.5 Allround Scaffold 10
2.2.6 Scaffold Design 11
2.2.7 Temporary Grandstands 14
2.2.8 Design of Temporary Grandstands 15
2.3 CONCLUSIONS: MATERIALS, DESIGN, AND CODES 22
2.4 DYNAMIC PROPERTY MEASUREMENTS 22
2.4.1 Output-only modal parameter identification 26
2.4.2 Frequency Domain Decomposition 27
2.5 DYNAMIC PROPERTY MEASUREMENTS CONCLUSIONS 30
3 INSTRUMENTATION AND MEASUREMENTS 48
3.1 INTRODUCTION 48
3.2 EQUIPMENT 48
3.2.1 Strain gauges 48
3.2.2 Linear Variable Differential Transformer 49
3.2.3 Cable Transducers 50
3.2.4 Accelerometers 50
3.2.5 Data Acquisition System 50

3.3 Location of Measuring Devices. 51
3.4 Measurements. 56
3.4.1 Static Loads and Displacements 57
3.4.2 Standards 58
3.4.3 Brace Members 59
3.5 Sway Displacements 60
3.6 Vertical Displacements 60
3.7 Accelerations 61
3.8 Instrumentation Accuracy 64
4 NATURAL FREQUENCY AND MODE SHAPE 99
4.1 Introduction 99
4.2 Ambient Vibration Survey 99
4.3 Natural Frequencies 100
4.3.1 Fundamental Natural Frequency 101
4.3.2 Higher Frequencies 102
4.4 Frequency Domain Decomposition 103
4.5 Mode Shape 106
5 FINITE ELEMENT ANALYSIS OF TEMPORARY GRANDSTAND 123
5.1 Introduction 123
5.2 Preliminary Finite Element Analysis. 125
5.3 Macro Updating 126
5.4 Micro-updating. 128
5.4.1 Ledger Connection Stiffness 128
5.4.2 Brace Stiffness 129
5.4.3 Mass of Occupants 130
5.5 Optimization. 131
5.6 Conclusion. 133
6 DISCUSSION AND CONCLUSIONS 141
6.1 Introduction 141

6.2 MONITORING OF THE TEMPORARY GRANDSTAND 141
6.3 OUTPUT-ONLY MODAL IDENTIFICATION 143
6.4 MODELLING THE DYNAMIC RESPONSE WITH FEA. 143
6.5 CONCLUSIONS 145
6.6 RECOMMENDATIONS 145
7 REFERENCES 147

LIST OF TABLES

Table 2.1. Strength reduction factors for metal scaffold [CSA, 1987] 32

Table 2.2. National building code requirements relevant to the design of temporary grandstands [NRC, 2005] 33

Table 2.3. Recommended Loading Function for Rhythmic Events [NRC, 2005] 34

Table 2.4. Notional horizontal loads for design of temporary demountable grandstands (as a percentage of the vertical load specified in BS 6399: *Part 1*:1996) [IStructE, 2001] 35

Table 2.5 Representative types of activities and their applicability to different actual activities and types of structures [Bachmann, 1995] 36

Table 2.6 Suggested vibration limits for activities on floors: 1.5 - 8 Hz [Allen,1984] 37

Table 2.7. Human response to wind-induced vibration [Simiu, 1986] 37

Table 2.8. Techniques for Dynamic Testing of Grandstands and Seating Decks [IStructE, 1999] 38

Table 3.1. Monitoring Equipment List 65

Table 3.2. Observed crowd actions during race 66

Table 3.3. Average distributed load on tributary area (kPa) 67

Table 3.4 Maximum static strain on sway braces 68

Table 3.5. Maximum sway displacements front-back motion 69

Table 3.6. Maximum sway displacement side-side motion 69

Table 3.7. Maximum vertical displacements 69

Table 3.8. Maximum accelerations 70

Table 4.1 List of peak picked frequencies for each data set 108

Table 4.2 List of peak picked frequencies for each data set from day before event 109

Table 5.1. Element properties for FEA 134

Table 5.2. Preliminary analysis modal frequencies. 134

Table 5.3 Natural frequency (mode with highest MAC value) with respect to rotational stiffness of joints 134

Table 5.4 Natural frequency (mode with highest MAC value) with respect to maximum axial brace stiffness 135

Table 5.5 Natural frequency (mode with highest MAC value) with respect to the equivalent uniformly distributed load. 135

LIST OF FIGURES

Figure 1.1 Temporary grandstands at Deer Valley for Salt Lake Winter Olympics ... 6
Figure 2.1 Scaffold bays ... 39
Figure 2.2 Frame scaffolding ... 39
Figure 2.3 Tube and clamp scaffold ... 40
Figure 2.4 Connection for *Cuplock* scaffold ... 40
Figure 2.5 (a) ledger head connected to rosette, (b) rosette ... 41
Figure 2.6 *Kwikform* system scaffold ... 42
Figure 2.7 Typical 2.0 m by 2.13 m *Allround* scaffold frame ... 43
Figure 2.8 Folding bleacher ... 44
Figure 2.9 Accordion bleacher ... 44
Figure 2.10 Modular temporary grandstand on scaffold structure ... 45
Figure 2.11 Annoyance criteria for floor vibrations: residences, offices, and school rooms ... 46
Figure 2.12. Power Spectral Density plot ... 47
Figure 2.13. Spectral Estimate of Power Spectral Density ... 47
Figure 3.1. Schematic of LVDT ... 71
Figure 3.2. Data acquisition system ... 71
Figure 3.3. Temporary grandstand plan view ... 72
Figure 3.4. Rear frame (#13) of temporary grandstand ... 73
Figure 3.5. Typical cross section of temporary grandstand ... 74
Figure 3.6. Location of strain gauges on standards ... 75
Figure 3.7. Strain gauges mounted on standard ... 76
Figure 3.8. Location of strain gauges on sway braces (G16-G24) and U-head support (G25& G26) ... 77
Figure 3.9. Strain gauges mounted on brace ... 78
Figure 3.10. Strain gauges mounted on U-head post ... 78
Figure 3.11. LVDT attachment on the ledger near the base of the structure ... 79
Figure 3.12. Side cross section showing line to LVDT to measure front-back sway motion ... 80
Figure 3.13. Rear cross section showing line to LVDT to measure side-side sway 81

Figure 3.14. Location of LVDTs for front-back sway on plan view of grandstand 82
Figure 3.15. Location of LVDT measuring side-side sway on plan view of grandstand 83
Figure 3.16. Location of cable transducers measuring vertical displacement on plan view of grandstand 84
Figure 3.17. Cable transducer mounted at base of structure 85
Figure 3.18. Location of accelerometers on plan view of grandstand 86
Figure 3.19. Accelerometers 87
Figure 3.20. Track map for Molson Indy, location of grandstand highlighted in southeast corner 87
Figure 3.21. Temperature for July 18, 1999, as measured at Toronto City Centre Airport 88
Figure 3.22. Hourly wind speed for July 18, 1999, as measured at the Toronto City Centre Airport 88
Figure 3.23. Map of track location in Toronto 89
Figure 3.24. Temporary grandstand empty 90
Figure 3.25. Temporary grandstand full 90
Figure 3.26. Recorded strains - standards G0 to G3 91
Figure 3.27. Recorded strains - standards G4 toG7 91
Figure 3.28 Recorded strains- standards G8 to G11 92
Figure 3.29. Recorded strains - standards G12 to G15 92
Figure 3.30. Recorded strains - sway braces G16 to G19 93
Figure 3.31. Recorded strains - sway braces G20 to G22 93
Figure 3.32. Recorded strains - sway braces G23 to G24 94
Figure 3.33. LVDT front-back sway displacement L0 to L4 94
Figure 3.34. LVDT front-back sway displacement L5 to L9 95
Figure 3.35. LVDT front-back sway displacement L10 to L12 95
Figure 3.36. LVDT side-side sway displacement L13 to L16 96
Figure 3.37. LVDT side-side sway displacement L17 to C19 96
Figure 3.38. Cable transducers vertical displacement C20 to C22 97
Figure 3.39. Cable transducers vertical displacement C23 to C25 97
Figure 3.40. Running Root-Mean-Square accelerations for data set 3:32 98

Figure 4.1 Power spectra from various channels at 4:05 July 18, 1999 110
Figure 4.2. Power spectra of LVDT "L0" 112
Figure 4.3. Power spectra of LVDT "L2" 113
Figure 4.4. Power spectra of LVDT "L16". 114
Figure 4.5. Power spectra of cable transducer "C21" 115
Figure 4.6. Power spectrum of voltage channel "V1" from data set 03:20, July 18, 1999 116
Figure 4.7. Singular Value Decomposition of 2 DOF system 117
Figure 4.8. Identified portion of the auto spectrum of 2 DOF system 117
Figure 4.9. Free decay from identified portion of auto spectrum, with peaks and crossings marked 118
Figure 4.10. Singular value decomposition of the 20 DOF system 118
Figure 4.11. Identified portion of the auto spectrum of the 20 DOF model 119
Figure 4.12. Free decay from identified portion of the auto spectrum of 20 DOF model 120
Figure 4.13. 20 DOF model of the grandstand 121
Figure 4.14. Fundamental frequency mode shape 122
Figure 5.1. Preliminary FEA model 136
Figure 5.2. Preliminary FEA model side view 136
Figure 5.3. Preliminary FEA model, first mode shape 137
Figure 5.4. Preliminary FEA model, second mode shape 137
Figure 5.5. Preliminary FEA model, third mode shape 138
Figure 5.6 Mode shape of optimized result 140
Figure A.1. Location of strain gauges on standards 154
Figure A.2. Location of strain gauges on sway braces (G16-G24) and U-head support (G25& G26) 155
Figure A.3. Side cross section showing line to LVDT to measure front-back sway motion 156
Figure A.4. Rear cross section showing line to LVDT to measure side-side sway .. 157
Figure A.5. Location of LVDTs for front-back sway on plan view of grandstand... 158
Figure A.6. Location of LVDT measuring side-side sway on plan view of grandstand 159

Figure A.7. Location of cable transducers measuring vertical displacement on plan view of grandstand.. 160

Figure A.8. Location of accelerometers on plan view of grandstand........................ 160

LIST OF SYMBOLS

A_{red}	Reduced cross sectional area
$a_w(t)$	Instantaneous frequency-weighted acceleration;
$a_w(t)$	Weighted acceleration as a function of time in metres per second squared.
A	Cross sectional area
a_0/g	Acceleration limit
a_m	Peak acceleration
a_0	Limiting acceleration
a_{wx}, a_{wy}, a_{wz}	Weigthed r.m.s. accelerations with respect to orthogonal axis x,y,z
β	Damping ratio
C.F.	Crest Factor
δ	Logarithmic decrement,
Δ_s	Static deflection
E	Elastic modulus.
f	Forcing frequency
f	Natural frequency
f_d	Damped natural frequency
f_0	Fundamental natural frequency
$\hat{G}_{yy}(j\omega)$	Estimate the output PSD matrix
$H(\omega)$	Frequency Response Function (FRF)
K	1.3, except for jumping exercises, where K= 2.0 is recommended.
k	Axial stiffness of the connection
k_x, k_y, k_z	Multiplying factors, which in this case $k_x=k_y=k_z= 1.0$
L	Length of brace
P	Axial load
ρ	Dynamic response factor
ψ	Modal vectors
r_0	Intial value of the decay function,
r_k	k^{th} value of the decay function
ς	Damping ratio
S_i	Diagonal matrix holding the singular values s_{ij}
t	Time (integration variable);
T	Duration of the measurement, in seconds.
t_0	Time of observation (instantaneous time).
τ	Integration time for the running averaging;

U_i	Unitary matrix holding singular vectors u_{ij}
VDV	Fourth power vibration dose value
Wp	Weight of the participants
W_t	Total weight supported
$[w]$	Weighting matrix
$X(\omega)$	Input signal
$Y(\omega)$	Response signal

LIST OF ABBREVIATIONS

ARMA	Autoregressive moving average
AVT	Ambient vibration test
CSA	Canadian Standards Association
DOF	Degree of Freedom
ERA	Eigenvalue Realization Algorithm
FDD	Frequency Domain Decomposition
FEA	Finite Element Analysis
FEM	Finite Element Method
FFT	Fast Fourier Transform
FRF	Frequency Response Function
FVT	Forced Vibration Test
IFFT	Inverse Fast Fourier Transform
LVDT	Linear Variable Differential Transformer
MAC	Modal Assurance Criterion
MTVV	Maximum Transient Vibration Value
NBCC	National Building Code of Canada
PSD	Power Spectral Density
RMS	Root Mean Square
RRMS	Running Root Mean Square
SDOF	Single Degree of Freedom
SVD	Singular Value Decomposition
VDV	Vibration Dose Value

1 INTRODUCTION

1.1 General Background

A grandstand is a structure that provides seating for spectators at entertainment and sporting events. Grandstands typically have seats, or benches, arranged in tiered rows with access to the seats from aisles that run perpendicular to the rows of seating. The term grandstand is commonly used to refer to permanent sports stadiums. The term *bleacher* is sometimes used interchangeably with grandstands, particularly when bench seating is used. A *temporary grandstand* is one that is erected for a particular event and removed once the event is complete.

Temporary grandstands are frequently being used for sporting and entertainment events. These structures are being used as a replacement for permanent venues at events, such as the Olympic Games, and may have occupancies of several thousand people. One recent example was the 2001 Salt Lake Winter Olympics where a large portion of the seating was provided using temporary grandstands. Figure 1.1 shows a temporary grandstand used at the Salt Lake Winter Olympics in 2001. In Canada they have been used for many race car events including the Montreal Grand Prix, Toronto Molson Indy, and Vancouver Indy, and to supplement the seating capacity of sports stadiums for large events. For example, 10 000 seats were added behind the end zone of Calgary's McMahon stadium for the 2001 Grey Cup.

There have been several documented accidents involving the collapse of temporary grandstands. Incidents in Corsica in 1992 [Jacob, 1996], and the UK in 1993 and 1994, involved thousands of people and resulted in several deaths [ISTRUCTE, 1999]. One of the problems cited in these instances was improper engineering of the structures. Until recently, few guidelines were available for the design of temporary grandstands and it has been up to the individual engineers to apply the design codes for permanent structures to these temporary structures. However, temporary grandstands have significant differences in their construction, structural elements, and member connections; and they have been found to have different structural performance compared to permanent grandstands. The UK has recognized these differences and has prepared guidelines for the design and construction of temporary grandstands, but similar guidelines have not been introduced in North America. The UK guidance was first published in 1999 just prior to our research at the Toronto Molson Indy.

The question of safety of temporary grandstands has been raised in Canada. The Ontario Building Code Commission ruled on a case where the Chief Building Official of Toronto had concerns that horizontal bracing members were not installed on a temporary grandstand [OBCC, 1995]. The builder's position was that they provided adequate vertical diagonal braces to resist the occupant sway load and wind loads as required by the National Building Code of Canada. The Chief Building Officials' position was that the dynamic behaviour of the grandstand was not considered in its design and the use of vertical diagonal braces alone would not properly address this short coming. It was the opinion of the Chief Building Official that the structure would have a natural sway frequency mode in the range of 1Hz to 3Hz, which would have the potential of resonance due to occupant movement. Despite the Chief Building Officials' objections the Ontario Building Commission ruled that no additional bracing was required.

The investigation presented in the following chapters was initiated due to complaints from grandstand occupants regarding their perception of sway motion of the grandstand. These complaints were often associated with a sudden synchronized motion of the occupants that may have induced a swaying motion. One such incident was reported to have occurred when spectators rose in unison for the singing of the national anthem. The complainant's perception of the motion was significant and caused them concern about the safety of the structure. Generally, the complaints were from only a few individuals, and it may be suggested that these individuals may be more sensitive to the acceleration due to vibration. Hence, the frequency and magnitude of the sway vibrations of a temporary grandstand will be measured as part of this project to determine if the vibrations are a comfort issue or a safety concern.

A temporary grandstand, built in Canada, must be designed to meet the National Building Code of Canada (NBCC) and any other jurisdictional requirements. These codes specify load and safety requirements for temporary grandstands. However there is little guidance with respect to the use of scaffolding for the main load bearing structure. The standards that govern scaffolding were not created for publicly accessed structures. In the case of temporary grandstands, scaffolding is being used for an application that it was not designed for, and there is a lack of guidance as to how to use scaffolding for this non-standard application.

The main difference between scaffolding and permanent grandstand construction, is how they are assembled. In particular, scaffolding is designed to be repeatedly assembled and disassembled, so the connections are designed to make this operation quick and easy. As a result, scaffold connections are quite different than bolted or welded connections that are found on permanent steel structures. Another difference is that scaffold structures use many light slender members instead of large heavy members. The temporary grandstands tend to have very short spans between supports; where as permanent grandstands may have long spans or balconies and may have issues with vertical vibration [Manheim and Honeck, 1987]. However, for temporary grandstands, vertical vibration is not a significant problem, but both side sway and front sway have been found to be an issue [Ji and Ellis, 1997].

The temporary grandstand system that is the focus of this research is one that has a scaffold structure to which a modular aluminum floor and seating system is fixed at the top. This arrangement allows great flexibility in the layout of the grandstand. The grandstand can be assembled in a variety of shapes and sizes to accommodate any need. With infinite possible configurations of the temporary grandstand it is important that a reliable method of predicting the performance of a temporary grandstand be developed, since each configuration may have different dynamic characteristics.

1.2 Objectives

It is the purpose of this research to monitor the static and dynamic behaviour of a temporary grandstand due to occupant load. The data will be analyzed to determine the sway displacements, member forces, vertical deflections, and lateral accelerations. The dynamic properties (natural frequency and mode shape) of the structure will be determined by output-only signal analysis of the ambient vibration survey data. The results of the testing will be compared to the results of a finite element analysis (FEA) model of the structure. The FEA model serves two purposes: firstly, to demonstrate that the dynamic properties of the temporary grandstand can be accurately modelled by FEA; and secondly to validate the mode shape identified by the ambient vibration analysis. If the field results and the FEA results do not match then the assumptions for the FEA model will be reviewed to determine if they were correct for this analysis. The FEA model will be an important tool to provide insight into the dynamic performance of the temporary grandstand.

By the conclusion of this research it will be determined whether the loads, displacements, and vibrations were at an acceptable level for this structure; the dynamic properties (natural frequency and mode shape) will be identified; and it will be determined whether a Finite Element Analysis model is a useful tool for predicting the dynamic properties of a temporary grandstand.

1.3 Scope of Research

The scope of research involved recording the static and dynamic behaviour of a temporary grandstand due to occupant load during an event. The instrumentation and data collection was conducted by a team that included Dr. Gilbert Grondin, Dr. Shahab Afami, and Mr. David Crick. The data collected was analyzed to determine structural loads, sway displacements, vertical displacements, lateral accelerations, and natural frequency. The results have been used to verify and modify a finite element model of the structure. It is determined whether FEA is a useful tool for accurately modelling the dynamic behaviour of a temporary grandstand.

The steps followed for the research included:

1. Instrumentation of a temporary grandstand to measure displacements, accelerations and member strains, due to occupant load at a sporting event. Strain readings were recorded on structural members, displacement transducers were

placed to measure vertical and horizontal displacements, and accelerometers were placed to measure the lateral acceleration of the grandstand. The instruments were installed by Dr. Afami and Mr. Crick. The data and observations were collected by Dr Grondin and Dr. Afami.

2. The data collected was analyzed to estimate the static loads, sway displacements, and sway accelerations. Ambient vibration survey data was analysed using an output-only signal analysis technique to determine the dynamic characteristics (natural frequency and mode shape) of the structure.

3. A FEA model of the grandstand was created and the natural frequency and mode shape were compared to the experimental results. Several factors (modelling assumptions) were proposed that may be responsible for the differences between the analytical and experimental results. A sensitivity analysis was performed to determine which factors were significant, and the FEA model was refined based upon these results.

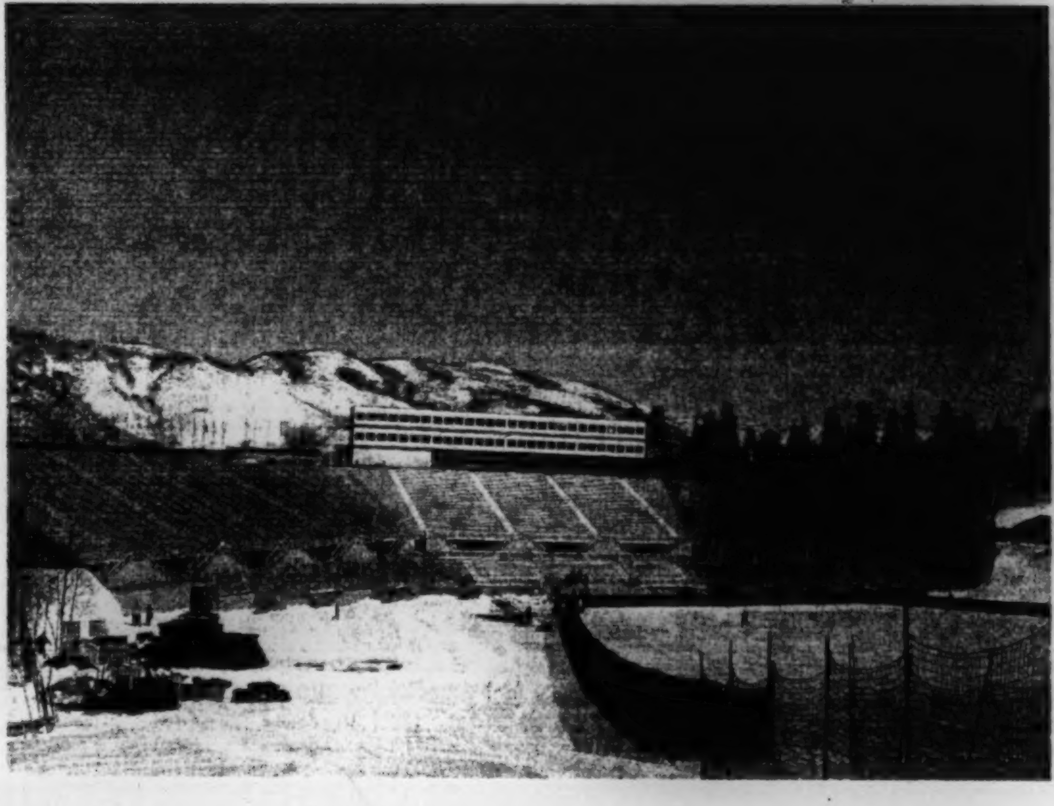

Figure 1.1 Temporary grandstands at Deer Valley for Salt Lake Winter Olympics

2 LITERATURE REVIEW

2.1 Introduction

This literature review will focus on two areas that are of interest to this research. The first area is related to how the temporary grandstands are designed and constructed. It provides details with respect to the scaffolding materials and the design codes that are applicable to scaffolding and temporary grandstands. The second area is related to the analysis of the collected data and describes the different methods of dynamic property measurement based on output-only data. It describes in detail an output-only signal analysis procedure called Frequency Domain Decomposition that will be used in this analysis to identify the dynamic properties of the temporary grandstand.

2.2 Materials, Design, and Codes.

2.2.1 Scaffolding

Scaffolding is designed to be erected and dismantled repeatedly and quickly. Scaffolds are designed for construction and industrial settings to provide access for workers or as false work to temporarily support structures and forming. The public are rarely intended to be in contact with scaffold structures in most applications.

Common terminology for scaffolding is used to describe the members and scaffold configuration. The most basic building block of a scaffold structure, referred to as a *scaffold bay*, which is a box like structure that consists of four vertical members connected together by horizontal members (Figure 2.1). Vertical members are referred to as *standards*. Horizontal members that connect standards are referred to as *ledgers*. Horizontal members that span across ledgers are called *transoms* (Figure 2.1). A brace that is used to prevent horizontal sway is referred to as a *sway brace*, or a *bay brace*.

Scaffold bays may be built on top of one another or adjacent to one another to created large scaffold structures. Adjacent bays share a common set of standards forming a continuous structure.

There are three main types of scaffold that include, frame, tube and clamp, and system scaffold.

2.2.2 *Frame Scaffold*

Frame scaffold is manufactured as a planar moment-resisting frame that attaches to a matching frame using sway braces. A frame can be attached on top of another frame with a frame coupler. Frame scaffolding is used most commonly in building construction where it is used for access to the walls of the building for masonry, fenestrations, siding, etc. Figure 2.2 shows a typical frame scaffold tower.

2.2.3 *Tube and Clamp Scaffold*

Tube and clamp scaffold, as illustrated in Figure 2.3, uses steel or aluminum tubes that are connected by specialized clamps (right-angle and swivel clamps). Tube and clamp is the simplest and most versatile scaffolding system, and is similar to the bamboo scaffolding that is still in use in some countries today. Tubes may be attached perpendicular to each other using a right angle clamp. Swivel clamps are used to attach tubes at an angle to create a sway brace. To connect tubes end-to-end *joint pins* (also called *spigots*) or *sleeve couplers* are used, or both together. The versatility of tube and clamp is due to the fact that there are no fixed joint locations. Joints can be added at any position along the length of the vertical member or horizontal member. This gives flexibility in the lift height, bay length, and scaffold width. This versatility makes it easier to build around pre-existing structures or obstacles. The main disadvantage of the tube and clamp is that it is labour intensive to assemble. Scaffolders require greater skill and care to assemble the structure properly since there are no fixed locations for joints.

2.2.4 *System Scaffold*

System scaffold refers to a type of scaffolding that has separate components for the vertical members and horizontal members, which attach at evenly spaced connection points on the vertical members. "System scaffold" means a scaffold consisting of posts with fixed connection points that accept runners, bearers and diagonal braces that can be fixed at predetermined levels" [BC.OH&S, 2004]. These connection points are spaced typically every 0.5 m along the length of the vertical member. There are many variations of the type of connection used on system scaffolding, but the most popular includes *Allround*™ (Wilhelm Layher GmbH & Co. KG), *Cuplock*™ (SGB Group Ltd), and *Kwikform*™ (RMD Kwikform). These types of system scaffold have spawned many imitators who have duplicated their styles of connection.

The *Cuplock* ledger to standard connection has a cup like element fixed to the standard at set intervals along its length. A second cup that is free to slide along the standard sits above the bottom cup. To make a connection, the ledger end is placed into the bottom cup and the top cup is screwed down on to the top of the ledger end locking it into place. A hammer blow is used on the top cup to tighten the connection. Thus the top and bottom of the ledger head is secured against the standard. This connection method allows four members to be connected at one location (Figure 2.4).

The *Allround* system has a circular plate with slots, called a rosette, attached at fixed intervals along the length of the standard. The ledger has a ledger head at each end that has a horizontal slot that mate with a rosette and a wedge pin that fit through the rosette's slot. To make a connection the ledger head is inserted into the rosette in line with a slot; the wedge pin drops down into the slot on the rosette; a hammer blow is used to force the wedge pin into the slot securing the ledger to the standard. The rosettes has 8 slots that allows up to eight members at one connection (Figure 2.5).

The *Kwikform* system has metal loops attached to the standard at fixed intervals. The ledger has a hooked head that fits into the loop and a wedge pin to tighten the connection. A hammer blow is used to drive the wedge pin between the ledger head and the loop creating a secure connection (Figure 2.6).

In Canada, *Allround* type scaffold is used more frequently than *Cuplock* or *Kwikform*. One of the reasons for the *Allround*'s popularity in Canada is that there are national manufacturers of this style of system scaffold. These manufacturers include Etobicoke Iron Works Ltd, producers of *Total System Scaffold*, and Mills Construction Products, producers of *Versa Scaffold*.

Each type of scaffolding (frame, tube and clamp, system) balances its capabilities in terms of speed of erection and versatility, this helps to determine which system is used for an application. In order of speed of erection, the fastest is frame, followed by system, and tube and clamp. In order of versatility, the most versatile is tube and clamp, followed by system, and frame. Frame scaffold is used in building construction because it can be erected quickly and can be used on a building face where there are few obstructions or obstacles. Tube and clamp scaffold are used in industrial settings around process piping and areas where it is difficult to gain access. System scaffold falls somewhere in between and is used for building construction and industrial access.

For temporary grandstands both frame and system scaffold are used most frequently; tube and clamp is considered too slow and labour intensive. Frame scaffold is most suitable for areas that have relatively flat ground, such as parking lots and playing fields. System scaffold is more versatile when the temporary grandstand is built on an area with elevation changes, such as a side of a hill, or over pre-existing structures. Both types of scaffold have been successfully used for temporary grandstands, but the system scaffold has an advantage for larger structures, since there are many venues where it is difficult to provide a large level surface suitable for frame scaffold.

2.2.5 Allround Scaffold

The structure that is the focus of this research is constructed of *Allround* type system scaffold. The following gives a more detailed description of the *Allround* system scaffold. Figure 2.7 shows a typical 2.0 m by 2.13 m *Allround* scaffold frame consisting of a pair of standards, a pair of ledgers, and a sway brace.

The standards and ledgers are made from tubular steel with an outside diameter of 49 mm and a wall thickness of 3.2 mm. The steel is generally of G40.21 300W steel or equivalent grade depending on the country of origin.

The standards and ledgers are available in set dimensions. The standards are typically available in 0.5, 1.0, 1.5, 2.0, and 3.0 m lengths. These may be attached end to end up to the required elevation. The ledgers are available in many different lengths, which may vary from country to country. In North America the most common ledger lengths are 2.13 m (7 ft) and 3.05 m (10 ft). The particular temporary grandstand system investigated in this study was developed in Europe and requires two sizes of ledgers that are common in the European market, which are 2.25 m and 1.35 m.

The bay braces are often manufactured of lighter weight steel tube by either reducing wall thickness (typically 2.3 mm) or outside diameter (typically 45 mm). The bay braces are all designed for a 2.0 m elevation, but their lengths differ depending on the width of bay that they are designed for. The ends of the bay braces have modified ledger heads that are oriented to fit into the diagonal slots on the rosette and attach to the brace tube by a pin connection.

The base of the scaffold structure is supported on adjustable base jacks. The adjustable base jacks have a screw tube with an adjustable nut on which the standard rests (Figure 2.7). The nut is adjusted up or down to allow for differences in the elevation of the ground. This allows the scaffold to be built on uneven terrain. The manufacturer of the base jack specifies a maximum allowable extension based upon the leg loading. When extensions are required that exceed the maximum allowable, then an additional length of standard is added.

2.2.6 Scaffold Design

Allowable Stress Design has traditionally been used for the design of scaffold structures. It is a requirement of many provincial Occupational Health and Safety authorities that a safety factor of 4 be used when designing a scaffold for access purposes [Alberta Human Resources and Employment, 2003]. The safety factor for scaffold is higher than the safety factor of 2 which would typically be used in the design of buildings. However, for scaffolding the safety factor of 4 is applied to the ultimate capacity of the scaffold member instead of the yield capacity.

The Canadian design standard for scaffolds is "Access Scaffolding for Construction Purposes", CAN/CSA-S269.2-M87, and it provides:

> *...rules and requirements for the design, fabrication, erection, inspection, testing, maintenance, and use of scaffolding equipment,*

> *materials and components where scaffolds are erected to provide working platforms for workers and materials during the construction, alteration, repair, or demolition of buildings and other structures.*

The CAN/CSA-S269.2-M87 states that scaffolding is for workers and materials. The standard does not mention the use of scaffold for the design of structures for public occupation. However, the design standard does specify how to determine the load capacities of scaffold equipment and the acceptable construction tolerances.

When assembling a scaffold, one of the concerns is the vertical alignment of the standards. Therefore, it is important that the scaffolders are trained in proper scaffold erection. The scaffold design standard requires that the vertical plumb of a scaffold be 12 mm in 3 m, 19 mm in 6 m and 38 mm for the total height of the structure [CSA, 1987]. The design standard requires that 2% of the vertical load be applied as a horizontal load at the level of the deck, partially to account for any vertical misalignment. For vertical loads the effective load distribution for each column is to be taken as the area immediately above the column that is bounded by the line halfway across to each of the adjacent bays.

The CSA design standard allows the strength of the members to be determined by testing. The allowable loads are determined by dividing the ultimate strengths by the reduction factors given in Table 2.1.

One issue with scaffolds that is not addressed by the CSA design standard is the stiffness of the connections. Godley and Beale [1997, 2001] have researched the apparent stiffness of different scaffold bay braces and ledger to standard connections for a *Cuplock* scaffold (Godley and Beale, 1997) and for a *Kwikform* scaffold (Godley and Beale, 2001).

In both cases the bay braces were constructed of steel tubes with pin connected swivel fittings at each end, and had the same tube dimensions. In both papers they determined that the cross braces had a reduced effectiveness due to the small stiffness of the connections. For their analysis they calculated a reduced cross sectional area, A_{red}, for the brace based upon the following equations:

$$\Delta = \frac{PL}{AE} + \frac{2P}{k} = P\left(\frac{L}{AE} + \frac{2}{k}\right) = \frac{PL}{A_{red}E}$$ Equation 2.1

$$A_{red} = \frac{L}{A}\frac{1}{\frac{1}{AE} + \frac{1}{2k}}$$ Equation 2.2

where,

k = axial stiffness of the connection
P = axial load
A = cross sectional area
L = length of brace
A_{red} = reduced cross sectional area
E = modulus of elasticity.

The steel braces had an outside diameter of 48 mm and a wall thickness of 3.2 mm, with a cross sectional area of 451 mm^2. However, in the case of the *Cuplock* type brace they determined a reduced cross sectional area of 10.4 mm^2, and for the *Kwikform* scaffold a reduced area of 4.79 mm^2. The difference in the reduced stiffness of the bay braces is presumably due to the different stiffness of the end connections.

Godley and Beale measured the connection stiffness of the ledger to standard connection for the *Kwikform* scaffold. They found that the connections had a non-linear moment-rotation curve due to the looseness in the connection [Godley and Beale, 2001]. They used a bilinear moment-rotation curve in their finite element analysis models of the system scaffold.

2.2.7 Temporary Grandstands

Temporary grandstands come in many different forms including: folding (Figure 2.8), accordion style (Figure 2.9), and modular (Figure 2.10). The folding and accordion styles have fixed dimensions; where as the modular systems can be constructed to various dimensions. It is the modular grandstands that are of particular interest for this thesis. Each modular grandstand must be designed for a particular location and application. The modular grandstands can be built to virtually any size due to their modular nature; and they are not limited to rectangular layouts, but can have varying depth, elevation, or a curved layout.

The modular temporary grandstand's components are designed to be assembled and disassembled several times, and to be erected quickly with simple tools and minimal heavy machinery. Currently, there are many suppliers of modular temporary grandstand systems, and each differs in how they are assembled. Some modular systems include components that provide the structure as well as the seating, while others use modular components for the seating but use scaffold for their support structure. The latter is the most common type since scaffold components tend to be cheaper than proprietary structural components. In many cases the scaffold components can be rented locally, so only the modular seating must be supplied. Also, the cost of erection can be lower since local scaffolders can be used to erect the structure and specially trained crews are only required to install the modular seating.

The temporary grandstand system that is the subject of this research is a modular type, manufactured by SitDown Systems. The seating system is assembled from proprietary aluminum elements that make the seats, floorboards, and guardrails. The main structural elements are aluminum stringer beams that are mounted on the top of the scaffold and run parallel to the side of the grandstand. All the seating, floorboards, and guardrails lock into the aluminum stringers.

2.2.8 Design of Temporary Grandstands

In North America there are currently no specific guidelines that address the structural requirements of temporary grandstands. Instead, the same building design codes used for permanent grandstands are applied to temporary grandstands. In Canada, grandstand design begins with the National Building Code of Canada (NBCC) [NRC, 2005]. This code specifies the loading requirements for structures for assembly occupancy. The code provides specifications for floor loads, occupancy sway forces, concentrated loads on seating, and wind loads. Table 2.2 gives a brief summary of the specified loading requirements that are applicable to a grandstand. The NBCC also provides specifications with regards to aisle widths, number of exits, guard rails, etc, but only the structural requirements will be considered for this thesis.

Vibration in assembly occupancies has been investigated with respect to long span floors [Allen *et al.*, 1985]. Allen *et al.* developed the procedure for determining dynamic load factors that are used in the NBCC. NBCC Commentary "A" offers a guide requiring dynamic analysis for floor structures when the fundamental vibration frequency is less than 6 Hz. Commentary "A" deals primarily with vertical vibrations, as they are a common problem in structures with long span floors. No mention is given with respect to natural frequency due to horizontal or sway vibration. There is no reference to whether the dynamic response factor may be applied to the static horizontal loads.

To determine the potential for overloading Commentary "A" provides an equation to calculate the dynamic response factor, ρ:

$$\rho = \frac{1}{\sqrt{\left[1-\left(\frac{f}{f_0}\right)^2\right]^2 + \left(\frac{2\beta f}{f_0}\right)^2}}$$ Equation 2.3

where:

f = forcing frequency

f_0 = fundamental natural frequency

β = damping ratio

ρ = dynamic response factor

The total effect on the structure is the sum of the static load and the dynamic loading components. The dynamic loading component is given by $\Sigma\ \rho_i\ \alpha_i\ w_p$, where α_i and ρ_i are the dynamic load and response factors for each harmonic multiple, i, of the rhythmic frequency. Values of α_i, ρ_i, w_p, and f are listed in Table 2.3. Overloading occurs if the total load, including static and dynamic components ($\Sigma\ \rho_i\ \alpha_i\ w_p$), exceeds the total specified load that the structure is allowed to carry.

In order to apply the guide from Commentary "A" one must be able to determine the dynamic properties of the structure, i.e. natural frequency and damping ratio. Many temporary bleachers are unique in their configuration and are designed and erected for a specific purpose and venue, and therefore their dynamic properties will be unique as well. Hence, an analytical method for determining the dynamic properties of the structure would be beneficial.

In recent years, several publications in the UK have been introduced that deal with the concerns of permanent and temporary grandstand design. The UK organization, the Institution of Structural Engineers (IStructE), published a guidance that provides information on the structural design of temporary grandstands [IStructE, 1999]. They also published an interim guidance that recommends dynamic performance criteria for different occupancy categories, for use with permanent grandstand structures [IStructE, 2001].

The guidance for temporary grandstands [IStructE, 1999] introduces the concept of using notional horizontal loads to account for, spectator action, and geometrical imperfections of frames (e.g. the lack of alignment of vertical members). The notional horizontal loads are taken as a percentage of the imposed vertical load. The notional horizontal loads should be applied in combination with operational wind loads. Table 2.4 gives the recommended notional horizontal loads for the design of temporary grandstands for different end uses.

The bracing for a temporary bleacher must be sufficient to resist the notional horizontal loads and the wind loads, but the guidance [IStructE, 1999] also recommends that the bracing be designed to avoid disproportionate collapse due to the removal of two adjacent braces. The guidance also recommends that the connection capacities of the bracing members be considered in the design requirements.

The bracing pattern that should be used for a temporary grandstand constructed of scaffolding is the topic of a paper by Ji and Ellis [1997]. They recommend criteria for selecting a bracing system for temporary grandstands based upon two principles: 1) the direct force path, and 2) uniform force distribution. The direct force path principle is, simply stated, that the load will take the shortest path to the supports. The uniform force distribution principle states that for a pinned structure the more uniformly distributed the inner forces, the greater the static stiffness.

The criteria presented for selecting the most effective bracing method, based upon the two principles are:

1. Bracing members in different storeys should be provided from the top to the support (base) of the structure.
2. Bracing members in different storeys should be directly linked where possible.
3. Bracing members should be linked in a straight line where possible.

4. Bracing members at the top of adjacent bays should be directly linked where possible.
5. If extra bracing members are required, they should be used following the above four criteria.

Ji and Ellis [1997] present examples of different bracing patterns as means of demonstrating the application of their criteria. By following these criteria the authors demonstrated in some practical applications that the lateral stiffness could be improved while using fewer braces. They also observed that the better the structure is braced, the less that there is a difference between the stiffness as a pinned structure and one with rigid joints. The effect of rigid joints is therefore assumed to be negligible in most cases.

Ji and Ellis [1997] investigated the effect of joint eccentricity on the stiffness of the bracing system. It was found that the eccentricity at the joints resulted in a greater percentage reduction in stiffness on the bracing systems. However, this was not enough to offset the improvements gained by applying their bracing methods compared to other inefficient bracing systems.

For the design of any structure subject to dynamic loads the avoidance of resonance effects is important. The forcing frequency for different types of rhythmical human body motions are given in Table 2.5 [Bachmann *et al.*, 1995]. When the frequency of a spectator activity is near one of the natural frequencies then resonance may occur. The resonance can build rapidly from cycle to cycle, the resulting cyclic motion could result in spectator discomfort, panic, or in extreme cases structural damage. However, even at resonance, the response will be limited by the mass of the structure, the level of damping and by the inability of the crowd to sustain the motion in a synchronized manner [IStructE, 2001].

In terms of the comfort of spectators in grandstands, most of the research has involved permanent grandstand structures, which differ from temporary grandstands in that they usually have longer floor spans and sometimes cantilevered seating areas. For permanent grandstands, the guidance [IStructE, 2001] recommends for viewing events including sports that the minimum vertical natural frequency should be 3.5Hz for an empty stand. For pop concerts the lowest vertical natural frequency should be 6Hz, which will be outside the range for the effect of a second harmonic. For the control of horizontal motion it is recommended that the minimum horizontal natural frequency of 3Hz for all grandstands as a substitute for a full dynamic evaluation.

Ji and Ellis [1997] recommend a vertical frequency greater than 8.4 Hz and the horizontal frequencies greater than 4.0 Hz for temporary grandstands to avoid resonance effects, as evaluated for an empty structure. Bachmann *et al.* [1995] recommend a vertical frequency of greater than 3.4 Hz for classical or "soft" pop concerts, or greater than 6.5 Hz for "hard" pop concerts, and a horizontal frequency greater than 2.5 Hz.

The degree of comfort for the occupants on the stands is dependent on the frequency of vibration and the acceleration experienced. The sensitivity of occupants to acceleration is dependent on the type of activity that they are engaged in. Someone sitting in an office may become uncomfortable if the acceleration exceeds 0.005 g, but someone dancing may tolerate accelerations up to 0.05 g. It has been suggested that the lower acceleration limit for the onset of panic is 0.35 g [IStructE, 2001]. NBCC Commentary "A" recommends a maximum level of 0.04-0.07 g for rhythmic activities. A spectator sport such as car racing would not be considered a rhythmic activity, so it may be more appropriate to assume a maximum level of 0.015-0.025 g (recommended for dining and weightlifting).

If the harmonic forcing frequency corresponds to a natural frequency then resonance will occur and the accelerations may exceed the recommended value. So, it is important to have a natural frequency that is greater than the harmonic forcing frequency. Commentary "A" recommends the following criterion for vertical vibration of a long span floor:

$$\frac{f_0}{f} \geq \sqrt{1+\frac{K}{a_0/g}\left(\frac{\alpha_i w_p}{w_t}\right)} \qquad \text{Equation 2.4}$$

where:

f_0 = fundamental natural frequency

f= forcing frequency (I times the jumping frequency for jumping exercises),

a_0/g – acceleration limit

K = 1.3, except for jumping exercises, where K= 2.0 is recommended.

w_t= total weight supported

w_p=weight of the participants

The purpose of controlling vibration is not only to prevent structural damage or failure, but also for limiting the effect on human perception. When people are exposed to excessive structural vibration it can lead to discomfort and, in extreme cases, panic. People are most sensitive to the amplitude of vibration and the accelerations [IStructE, 2001]. By limiting the displacements and accelerations at the natural frequencies we can reduce the effect on the occupants. Other factors such as the type of loading, structural mass and damping must be considered [IStructE, 2001].

Allen *et al.* [1985] suggest an acceleration limit of 0.05 g for lively concerts or sporting events for spectators who are not directly participating in the activity. Other vibration limits are suggested as vibration limits for activities on floors (Table 2.6). Allen and Rainer [1975] present a graph of annoyance criteria for floor vibrations with respect to frequency and damping ratio (Figure 2.11)

For acceptable sway acceleration limits it may be appropriate to look at the recommendations for buildings subjected to wind induced vibration. Simiu and Scanlan [1986] present levels of discomfort with respect to the acceleration experienced and their results are presented in Table 2.7.

Rainer describes most vibration problems in terms of the source, the transmission path, and the receiver [Rainer, 1984]. The source in this case is the synchronized motion of the grandstand occupants. The transmission path is through the temporary grandstand structure. The receiver is a person who is sensitive to the vibration. Rainer mentions that human's sensitivity varies depending on whether they are sitting or standing and on the direction of vibration (vertical, horizontal, rotational).

When considering remedial measures it is useful to consider the source, and the transmission path. It may be possible to reduce the vibrations being created by the source (e.g. some form of crowd control). For the transmission path the structure can be stiffened of supplied active devices (controlled mass dampers), passive devices (viscoelastic damping layers, tuned-mass dampers) [Rainer, 1984].

2.3 Conclusions: Materials, Design, and Codes

In Canada there is a design standard for scaffolding, primarily for access applications for construction workers, and the National Building Code which specifies the structural requirements for grandstands and bleachers. However, there is no guide as to how scaffolding equipment, which is designed for materials and workers, may be used for temporary grandstand applications. In the UK they have recognized that the temporary grandstands behave differently than permanent grandstands, and they have created design guides for these structures.

The issue of vibration for assembly occupancies has been studied, but primarily for vertical vibrations related to long-span floors. The effects of these vibrations on humans have also been studied and it has been shown that human perception can occur at levels that are significantly lower than what would be considered a safety issue.

The bracing patterns have a significant effect on the natural frequency of scaffold structures used for temporary grandstands. Joint stiffness and eccentricities may also have an influence on the overall stiffness of a scaffold structure.

The monitoring of the temporary grandstand will provide important insight into how these structures behave in real life conditions. This information may be used to improve the design and analysis of these structures.

2.4 Dynamic Property Measurements

One of the goals of the monitoring of the temporary grandstand is to determine the dynamic properties of the structure. The dynamic properties are the natural frequencies, vibration mode shapes, and modal damping factors. For the measurement of the dynamic properties of grandstands, two distinct approaches have been utilized: 1) forced vibration measurement, and 2) ambient vibration measurement. Of these two approaches, forced vibration is the easiest to implement from the analysis perspective.

The properties of the forcing vibration can be measured accurately using forced vibration measurement. By using the Fourier transform of the input signal, $X(\omega)$, and the Fourier transform of the response signal, $Y(\omega)$, it is possible to determine the Frequency Response Function (FRF), $H(\omega)$, where the following relationship exists:

$$Y(\omega) = H(\omega)X(\omega) \qquad \text{Equation 2.5}$$

The FRF is the basis for determining the modal parameters (frequency, mode shape, and damping coefficient) for forced vibration analysis [Gatti and Ferrari, 1999]

Electro-dynamic, hydraulic or mechanical shakers are used to create the forced vibration. These typically vibrate at one frequency but some can be operated to produce a broadband signal. The forced vibration source is moved to different locations on the structure and the vibrations are measured from fixed locations. The limitations of forced vibration analysis include: heavy and bulky equipment is required to achieve moderate levels of vibration, and tests need to be performed while the structure is unoccupied [Schiff, 1972]. These limitations make forced vibration testing disruptive to normal facility operation [Schiff, 1972].

Ambient vibration survey relies on measuring the response of the structure that is excited by ambient vibrations only. The advantage of ambient vibration measurements is that the test can be performed while the structure is occupied, and it does not require forced vibration equipment. Hence, ambient vibration tests are significantly less expensive than forced vibration tests [Krämer, 1999]. However, with ambient vibration testing the forcing vibration is unknown, so the modal parameters must be recovered based upon the response measurement.

The Institute of Structural Engineers [2002] published an advisory note on the "Dynamic testing of grandstands and seating decks". They recommend dynamic testing to verify the calculated values for natural frequencies of a structure since calculations may have inaccuracies due to short-cut methods and rules of thumb to estimate the natural frequencies. They divide the types of dynamic testing into two categories: a "Type 1" test provides basic information concerning the natural frequencies; a "Type 2" test provides more detailed information including natural frequencies, mode shapes and modal damping.

The common dynamic testing techniques that are considered in the advisory note are:

- Ambient vibration survey
- Heel-drop testing
- Measured impact testing
- Shaker testing of different types and complexities.

Table 2.8 shows a comparison of the different dynamic measurement techniques.

Reynolds and Pavic [2002] describe the use of forced vibration testing on a permanent grandstand. The grandstand contained two tiers of seating, with one cantilevered over the back of the other. The structure was constructed of steel frames spaced 7.025m on center with precast concrete elements spanning between adjacent frames. A pre-test finite element analysis was performed to determine the possible vibration modes. Testing was done using an electro-dynamic shaker to provide the excitation force and measurements were made using nine piezoelectric accelerometers, with a nominal sensitivity of 1000 mV/g. The primary digital data acquisition system was a portable spectrum analyzer that was capable of providing immediate calculation of the frequency response function (FRF).

A case study by Manheim and Honeck [1987] investigated the spectator-induced vibrations of an auditorium balcony. Dynamic testing was performed on the structure using an electromagnetic shaker as the input force and an accelerometer moved to different locations to measure the response vibration. The modal parameters were determined for the structure and a computer model created to reproduce the physical behaviour of the structure. The computer model was then used to perform an analysis of the structure to assess the effects of spectator loading and resonance.

There are many examples where ambient vibration testing has been used on civil engineering structures to determine the dynamic properties.

Meyyappa *et al.* [1986] performed tests on a 24 story steel frame office tower. The measurements were made using five low-level force-balance type accelerometers. Eight sets of measurements were made, with each lasting up to 6 hours.

Tamura *et al.* [2002] conducted measurements of the dynamic characteristics of a high-rise building during construction. The ambient response of the structure was measured at four different construction stages. The measurements were made using servo-type accelerometers with high sensitivity and resolution (10^{-6} V/g) with a sampling rate of 20 Hz, the duration of each record was 1800 seconds.

Ventura *et al.* [2002] performed a series of tests on a 48-storey building in Vancouver, British Columbia. The building is the tallest building in Vancouver. The measurements were taken using force balanced accelerometers. Data was recorded for periods of 12 minutes per set-up.

Reynolds *et al.* [2003] used ambient vibration measurements to continuously monitor the dynamic response of a stadium remotely. First, they conducted forced vibration tests to determine the stadiums dynamics. An electrodynamic shaker was moved to 15 test points and the response read by six reference accelerometers. Based upon the results of the forced vibration tests, 12 accelerometers were placed within the stadium. For the ambient vibration readings the 12 accelerometers were continuously sampled at a rate of 80 Hz for every event at the stadium. A video camera was set up to capture video that could be synchronized with the recorded data. They used the frequency domain decomposition technique on portions of the acquired data to determine the natural frequencies and mode shapes. This work demonstrates the usefulness of ambient vibration testing since the authors are able to determine the dynamic response of the structure while it is occupied and can correlate the results with the occupants' activities. The forced vibration tests had to be performed with the stands empty and required that the vibration equipment be moved to several positions.

2.4.1 Output-only modal parameter identification

For ambient vibration testing the forcing vibration is unknown, so the modal properties can only be determined from the response of the structure. The natural frequencies can sometimes be identified by looking at the Power Spectral Density plot for the response and picking prominent peaks, which indicate a large response at a particular frequency. This process is sometimes referred to as "peak picking". However, with peak picking, extraneous noise or forcing frequencies may be misinterpreted as natural frequencies. Therefore, more sophisticated methods are required to identify the modal properties from the output-only signal.

To determine the modal parameters from the response requires an output-only system identification procedure. Some of these procedures include: Frequency Domain Decomposition (FDD) [Brincker *et al*, 2000], Eigensystem Realization Algorithm (ERA) [Juang, 1985], parametric curve-fitting [Meyyappa, 1986], Auto-Regressive Moving Average models (ARMA) [Brincker and Andersen, 1999], and Stochastic Subspace Identification (SSI) [Andersen and Brincker, 2003; Peeters and de Roeck, 1999]. The Frequency Domain Decomposition method was selected for this research, because it was relatively easy to implement. The procedure for implementing this procedure was outlined in papers by Brinker *et al.* [1999, 2000, and 2001] and is discussed in detail in the next section.

The first step of any output-only identification system is to simplify the representation of the structure. Most identification systems ignore nonlinearities and time dependent characteristics. Most identification schemes are limited to determining the lower natural frequencies and modal damping. Typically, the schemes ignore modal coupling, which can be done since lightly damped multi-degree of freedom systems can be closely approximated by a single degree of freedom system [Schiff, 1972].

Identification procedures usually rely on estimates of the power spectral density (PSD) instead of the true PSD. The estimates are used to eliminate the statistical variability and to smooth the PSD. Figure 2.12 shows a PSD plot and Figure 2.13 shows the spectral estimate of the PSD from the same input signal. The spectral estimate is smoother and has much less variability, which makes it better suited for further analysis. However, there are four main considerations associated with using spectral estimates for system identification [Schiff, 1972]:

1. Aliasing: Aliasing results when a continuous signal is discretely sampled and may appear at a lower frequency in the Fourier transform. For example, if an event occurs at a frequency of 6 Hz, but the sampling rate is 2 Hz then when looking at the sampled data it would appear that the event was occurring at 2 Hz. To avoid aliasing the signal is filtered using a low pass filter that is set to at least one-half the sampling rate. Therefore, the rate at which the analog data is digitized must be at least twice the highest frequency presented. So, for the previous example the sampling rate would have to be set to at least 12 Hz to capture the 6 Hz event.

2. Statistical variability. In order to smooth the spectra and reduce the variability a spectral estimate is used. However the characteristics of the variability (standard deviation, etc) of the estimate might not be the same as with the true spectra.

3. Bias. The spectral estimate of the power spectral density allows the degree of smoothing to be adjusted. However, as the degree of spectral smoothing increases, the peaks in the spectra will, on average, tend to be underestimated. Therefore, if there is a very high sharp peak it will become lower and less sharp in the spectral estimate.

4. Resolution. The resolution, the separation required to distinguish two distinct spectral peaks, has a lower bound that increases as the spectral smoothing increases. The spectral estimate has a lower resolution than the true Power Spectral Density. Therefore, if there are two peaks that are very close to each other they may be merged into one peak after the smoothing is performed.

2.4.2 Frequency Domain Decomposition

The frequency domain decomposition (FDD) method will be used in this research to identify the natural frequency, damping coefficient, and mode shape for the temporary grandstand. Frequency domain decomposition is a system identification method that is similar to the common peak picking technique. Brincker *et al* [1999, 2000, 2001] and Tamura *et al* [2002] describe the procedure in several papers. Tamura *et al* [2002], and Ventura *et al* [2002] describe practical applications of this procedure in papers.

This procedure is relatively simple compared to some of the other procedures and it gives the user a better feel for the data [Brincker and Zhang, 2000]. Frequency domain decomposition decomposes an estimate of the PSD matrix into a set of single degree of freedom systems using singular values decomposition (SVD). The SDOF system is then identified using the Modal Assurance Criterion (MAC). The result is exact in the case where the loading is white noise, the structure is lightly damped, and the modes are geometrically orthogonal [Brincker *et al*, 2000]. For cases where these assumptions are not true then the results are approximate.

The Modal Assurance Criterion measures the degree of proportion between two vectors. As a correlation coefficient its value varies from 0 to 1. The Modal Assurance Criterion is defined as:

$$MAC(\psi_a, \psi_e) = \frac{\left(\{\psi_a\}^t [w] \{\psi_e\}\right)^2}{\left(\{\psi_a\}^t [w] \{\psi_e\}\right)\left(\{\psi_e\}^t [w] \{\psi_a\}\right)} \qquad \text{Equation 2.6}$$

where : ψ : modal vectors,
$[w]$: weighting matrix,
index a: analytical entity, and
index e: experimental entity [Heylen and Janter, 1988]

The frequency domain decomposition method uses the output-only signal and can be used to identify the natural frequency, damping coefficient and the mode shape. The frequency domain decomposition technique is relatively simple to implement, which makes it attractive for this application. The procedure is described as follows [Brincker *et al.*, 2001]:

- Estimate the output PSD matrix, $\hat{G}_{yy}(j\omega)$. The values of the PSD will be known at discrete frequencies, $j\omega$.

- Decompose the PSD matrix using SVD,

$$\hat{G}_{yy}(j\omega) = U_i S_i U_i^H$$ Equation 2.7

where $U_i = [u_{i1}, u_{i2}, ..., u_{im}]$ is a unitary matrix holding singular vectors u_{ij}, and S_i is a diagonal matrix holding the singular values s_{ij}

- The first singular vector is an estimate of the mode shape, $\hat{\varphi} = u_{i1}$, and with the corresponding singular value represents the auto PSD function of the SDOF system.

- Pick a peak on the SVD plot for the mode of interest.

- Identify the PSD function of the SVD around the peak by comparing the modes shape estimate, $\hat{\varphi}$, with the singular vectors by using the MAC for each frequency line.

- If a singular vector exists that has a larger MAC value than a certain limit value then the search for parts of the SDOF PSD will continue.

- When no singular vectors with a large enough MAC value exist then the remaining parts of the PSD are set to zero.

- The identified SDOF PSD is then taken back to the time domain by Inverse Fast Fourier Transform (IFFT).

- The natural frequency and damping are determined by the logarithmic decrement method.

For the logarithmic decrement method the free decay time function is used [Brincker *et al*, 2001]. The extreme values from the decay function, r_k, are found. The logarithmic decrement, δ, is found by the equation:

$$\delta = \frac{2}{k}\ln\left(\frac{r_0}{|r_k|}\right) \qquad \text{Equation 2.8}$$

where:

r_0 is the initial value of the decay function,

r_k is the kth value of the decay function

The damping ratio, ς, can then be found by the following equation:

$$\varsigma = \frac{\delta}{\sqrt{\delta^2 + 4\pi^2}} \qquad \text{Equation 2.9}$$

The natural frequency is determined by performing a linear regression on the crossing times and the extreme value times to determine the damped natural frequency, f_d. The damped natural frequency is then related to the natural frequency, f, by the following equation:

$$f = \frac{f_d}{\sqrt{1-\varsigma^2}} \qquad \text{Equation 2.10}$$

2.5 Dynamic Property Measurements Conclusions

Both forced vibration and ambient vibration methods have been used to identify the modal properties of structures. The ambient vibration survey methods are typically less expensive to implement because it can be performed while the structure is in use and it does not require large and heavy equipment to excite the structure. With ambient vibration survey only the response of the structure is measured and therefore, output-only signal analysis methods are required to identify the modal properties. Several output-only signal analysis methods are available, but for this research the Frequency Domain

Decomposition Method was chosen. This method was relatively easy to implement and has been used for the analysis of structural vibrations.

Table 2.1. Strength reduction factors for metal scaffold [CSA, 1987]

	Reduction Factor (Metal)
Vertical Frames	2.5
Vertical Members	3.0
Horizontal Members	2.2
Tube and Clamp	2.5

Table 2.2. National building code requirements relevant to the design of temporary grandstands [NRC, 2005]

Design Requirement	Code Section	Requirement
Specified Uniformly Distributed Live Loads	Table 4.1.5.3	Minimum specified load = 4.8 kPa Grandstands, reviewing stands and bleachers
Bleachers	4.1.5.13	1) Bleacher seats shall be designed for uniformly distributed love load of 1.75 kN for each linear metre or for a concentrated load of 2.2 kN distributed over a length of 0.75 m, whichever produces the most critical effect on the supporting members. 2) Bleachers shall be checked by the erector after erections to ensure that all the structural members including bracing specified in the design have been installed"
Resonance	4.1.3.6 (2)	"Where the fundamental vibration of a structural system supporting an assembly occupancy used for rhythmic activities, such as dancing, concerts, jumping exercises or gymnastics, is less than 6 Hz, the effects of resonance shall be investigated by means of dynamic analysis. (See Appendix A)"
Sway	4.1.5.11	"The floor assembly and other structural elements that support fixed seats in and *building* used for *assembly occupancies* accommodating large numbers of people at one time, such as grandstands, stadia and *theatre* balconies, shall be designed to resist a horizontal force of 0.3 kN for each metre of length of seats acting parallel to each row of seats, and not less than 0.15 kN for each metre length of seats acting at right angles to each row of seats, assuming such forces to be acting independently of each other."

Table 2.3. Recommended Loading Function for Rhythmic Events [NRC, 2005]

Activity Property	Activity		
	Dancing	Lively Concert (1) or Sports Event	Aerobics
Weight of Participants(2) w_p, kPa	0.6 (2.5 m2/person)	1.5 (0.5 m2/person)	0.2 (3.5 m2/person)
First harmonic, (3) α_1 (forcing frequency, f)	0.5 (1.5 to 2.7 Hz)	0.25 (1.5 to 2.7 Hz)	1.5 (2 to 2.75 Hz)
Second harmonic, (3) α_2 (forcing frequency, $2f$)	0.3 (3 to 5 Hz)	0.05 (3 to 5 Hz)	0.6 (4 to 5.5 Hz)
Third harmonic, (3) α_3 (forcing frequency, $3f$)			0.1 (6 to 8.25 Hz)

(1) Values given are for concerts where there is fixed seating. For rock concerts at which seating is not provided, α_1=0.40 and α_2=0.15.

(2) Weight of participants is uniformly distributed over activity area. For long-span floors where dancing occurs only on part of the span, the effective uniformly distributed weight over the whole span may be reduced accordingly.

(3) Values of the dynamic coefficient for the i'th harmonic, α_i, are based on commonly encountered events involving a minimum of 20 persons.

Table 2.4. Notional horizontal loads for design of temporary demountable grandstands (as a percentage of the vertical load specified in BS 6399: *Part 1*:1996) [IStructE, 2001]

Category of spectator activity	Notional horizontal load
Category 1 Nominal potential for spectator movement, which excludes synchronized and periodic crowd movement, e.g. at: • Lectures/exhibitions • Displays/shows • Athletic events • Golf tournaments • Agricultural shows • Military tournaments	5%
Category 2 Potential for spectator movement more vigorous than Category 1 but excluding synchronized and periodic crowd movement, e.g. at: Major musical concerts Rugby or football matches	7.5%
Category 3 Stands with potential for synchronized and periodic crowd movement and having vertical and horizontal fundamental frequencies which avoid resonance effects, e.g. at most pop concerts where strong musical beats are expected.	10%

Table 2.5 Representative types of activities and their applicability to different actual activities and types of structures [Bachmann, 1995]

Representative types of activity			Range of applicability		
Designation	Definition	Design Activity rate [Hz]	Actual activities	Activity rate [Hz]	Structure type
"walking"	Walking with continuous ground contact	1.6 to 2.4	▪ slow walking (ambling) ▪ normal walking ▪ fast, brisk walking	~ 1.7 ~ 2.0 ~ 2.3	▪ pedestrian structures (pedestrian bridges, stairs, piers, etc.) ▪ office buildings, etc.
"running"	Running with discontinuous ground contact	2.0 to 3.5	▪ slow running (jog) ▪ normal running ▪ fast running (sprinting)	~ 2.1 ~ 2.5 > 3.0	▪ pedestrian bridges on jogging tracks, etc.
"jumping"	Normal to high rhythmical jumping on the spot with simultaneous ground contact of both feet	1.8 to 3.4	▪ fitness training with jumping, skipping and running to rhythmical music ▪ jazz dance training	~1.5 to 3.4 ~1.8 to 3.5	▪ gymnasia, sport halls ▪ gymnastic training rooms
"dancing"	Approximately equivalent to "brisk walking"	1.5 to 3.0	▪ social events with classical and modern dancing (e.g. English Waltz, Rumba, etc.)	~1.5 to 3.0	▪ dance halls ▪ concert halls and other community halls without fixed seating
"hand clapping with body bouncing while standing"	Rhythmical hand clapping in front of one's cheat or above the head while bouncing vertically by forward and backward knee movement of about 50 mm	1.5 to 3.0	▪ pop concerts with enthusiastic audience	~1.5 to 3.0	▪ concert halls and spectator galleries with and without fixed seating and "hard" pop concerts
"hand clapping"	Rhythmical hand clapping in front of one's chest	1.5 to 3.0	▪ classical concerts, "soft" pop concerts	~1.5 to 3.0	▪ concert halls with fixed seating (no "hard" pop concerts)
"lateral body swaying"	Rhythmical lateral body swaying while being seated or standing	0.4 to 0.7	▪ concerts, social events		▪ spectator galleries

Table 2.6 Suggested vibration limits for activities on floors: 1.5 - 8 Hz [Allen,1984]

Activity or occupancy	**Limiting peak acceleration a_o/g**	**Reiher and Meister rating at 3 Hz**	**ISO duration for reduced comfort h**
Threshold of perception	0.001-0.002	Just perceptible	24
Offices and residences (daytime)	0.005	Perceptible	24
Dancing and dining	0.02	Annoying	4
Physical exercise, sports, and lively concerts (gymnasia, arenas, stadia)	0.05	Unpleasant	1

Table 2.7. Human response to wind-induced vibration [Simiu, 1986]

Degree of Discomfort	**Acceleration**
Imperceptible	$< 0.005g$
Perceptible	$0.005g$-$0.015g$
Annoying	$0.015g$-$0.05g$
Very Annoying	$0.05g$-$0.15g$
Intolerable	$> 0.15g$

Table 2.8. Techniques for Dynamic Testing of Grandstands and Seating Decks [IStructE, 1999]

Test Characteristics			**Test Outcomes and their Relation to Interim Guidance Requirements**				
			Essential outcome	**Desirable outcome**	**Outcomes not needed to meet requirements of the Interim Guidance but may be specified by the Engineer for detailed design checks requiring data from type 2 testing**		
Test Type	**Excitation**	**Force Measurement**	**Natural frequencies**	**Mode shapes**	**Damping ratio**	**Frequency response function**	**Modal mass**
Type 1	Ambient	Not possible	Yes, but care needed with interpretation. Can combine with other Type 1 techniques to assist interpretation	Yes, if excitation energy is sufficient	Not reliable	No	No
Type 1	Heel-drop	Not normally done	Suitable for simple structures. Difficulties with complex structures or closely separated vibration modes	Provides coarse indication sufficient for simple structural arrangements	Not reliable	No	No
Type 1	Drop-weight or sledge hammer	Measured	Yes	Yes	Better than heel-drop	Possible with further development if excitation energy is adequate	
Type 1 or type 2 according to techniques and instrumentation employed	Shaker with variety of possible types and techniques	Measured or inferred depending on technique	Yes and provides more repeatable results than heel-drop, impact or AVS	Yes	Yes	Quality of results dependent on technique and instrumentation. Most reliable results obtained with instrumented shaker giving direct measurement of force time history	

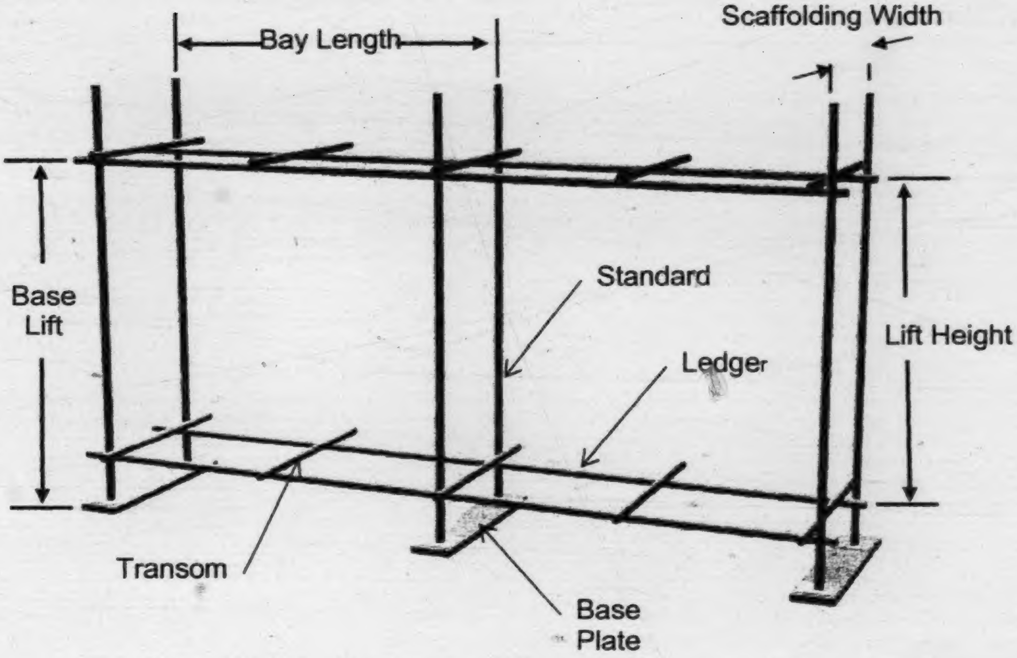
Bay Length
Scaffolding Width
Base Lift
Standard
Ledger
Lift Height
Transom
Base Plate

Figure 2.1 Scaffold bays

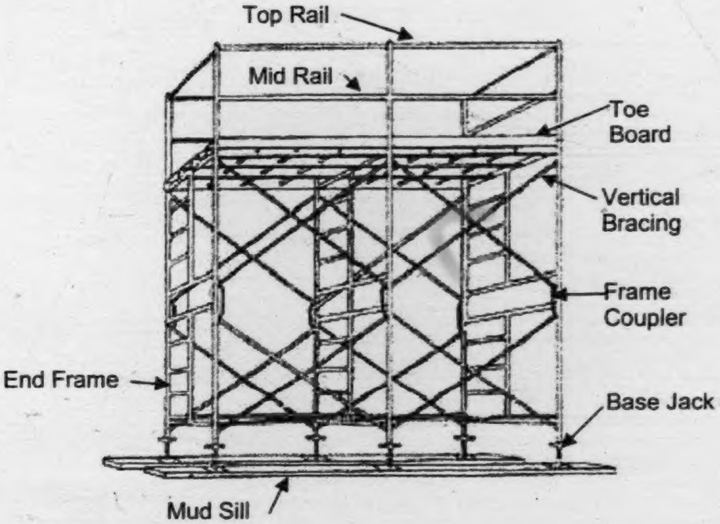
Top Rail
Mid Rail
Toe Board
Vertical Bracing
Frame Coupler
End Frame
Base Jack
Mud Sill

Figure 2.2 Frame scaffolding

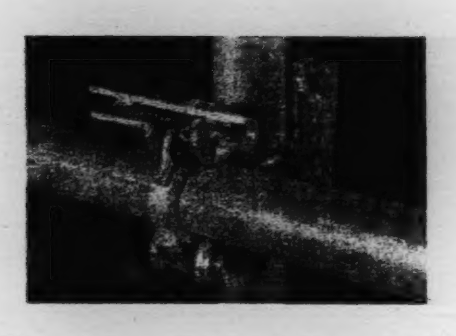

Figure 2.3 Tube and clamp scaffold

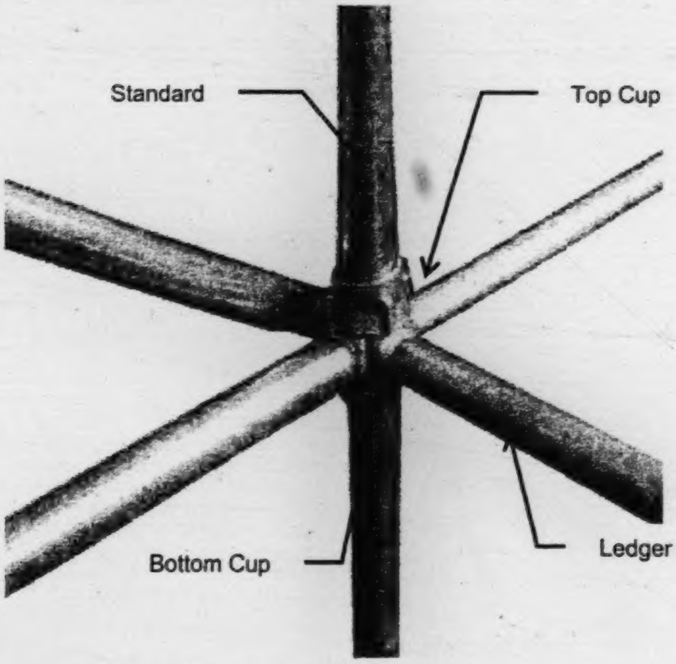
Standard
Top Cup
Bottom Cup
Ledger

Figure 2.4 Connection for *Cuplock* scaffold

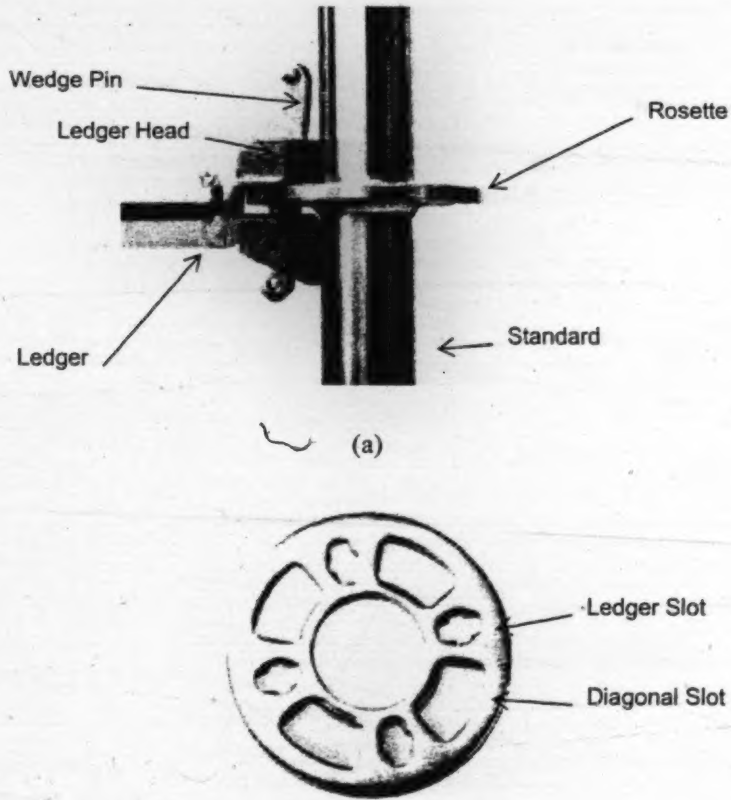
Wedge Pin
Ledger Head
Rosette
Ledger
Standard
Ledger Slot
Diagonal Slot

(a)

(b)

Figure 2.5 (a) ledger head connected to rosette, (b) rosette.

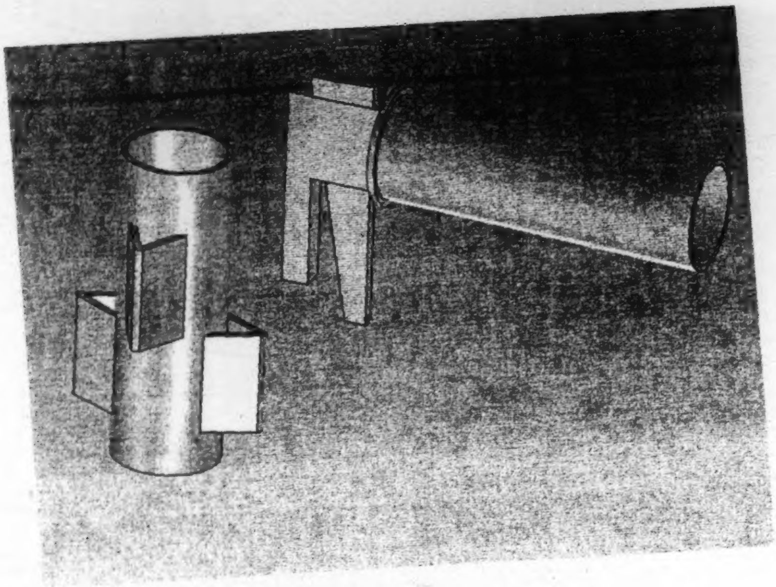

Figure 2.6 *Kwikform* system scaffold

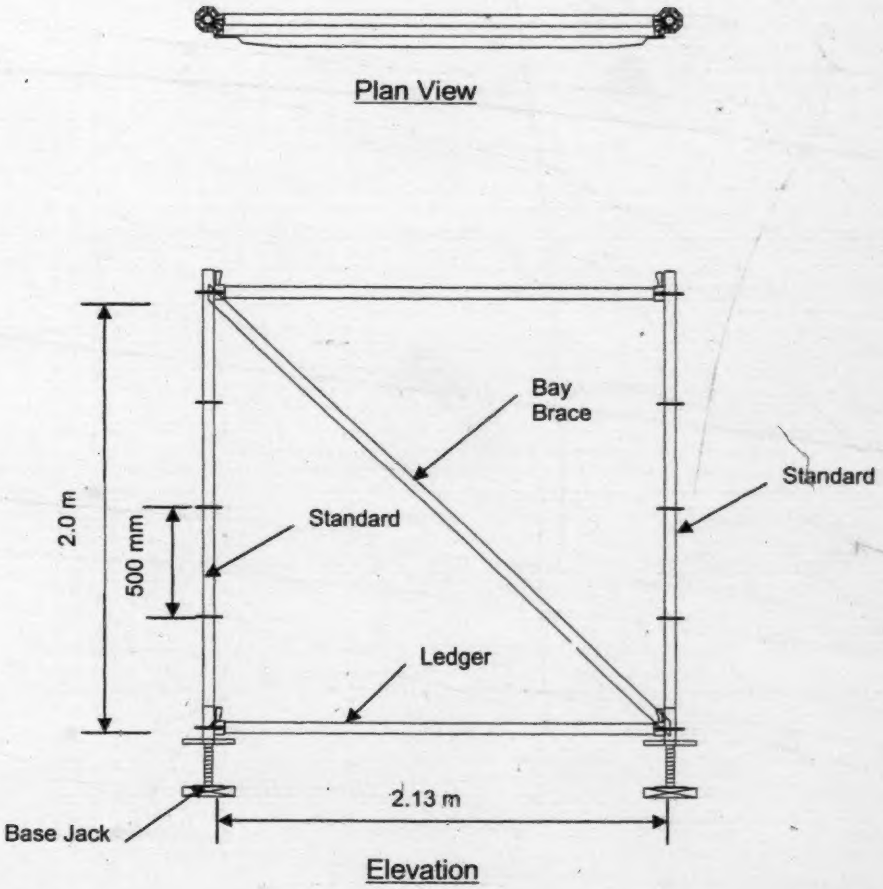
Plan View
Bay
Brace
Standard
Standard
2.0 m
500 mm
Ledger
2.13 m
Base Jack
Elevation

Figure 2.7 Typical 2.0 m by 2.13 m *Allround* scaffold frame

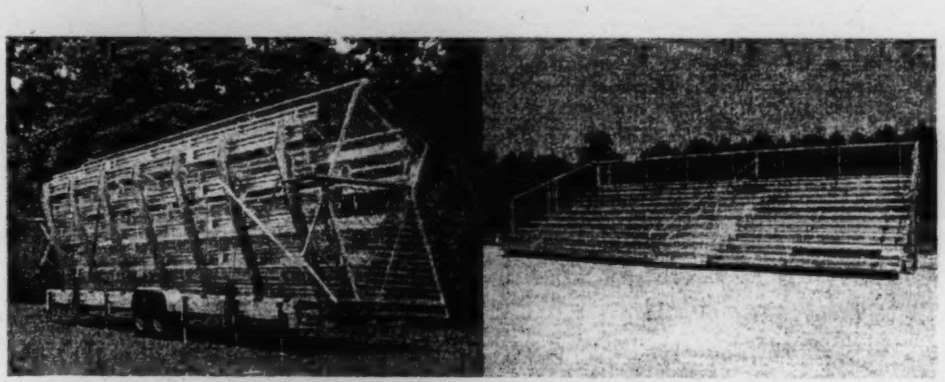

Figure 2.8 Folding bleacher

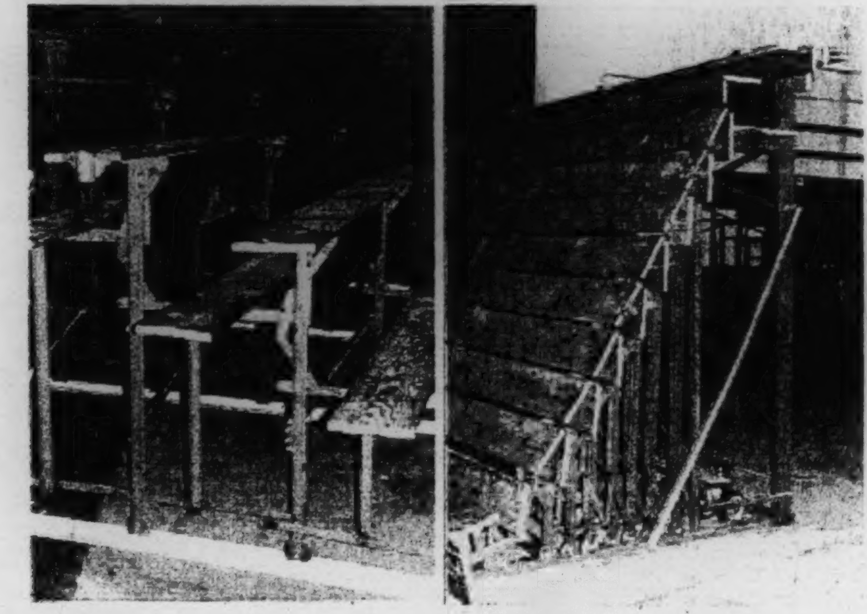

Figure 2.9 Accordion bleacher

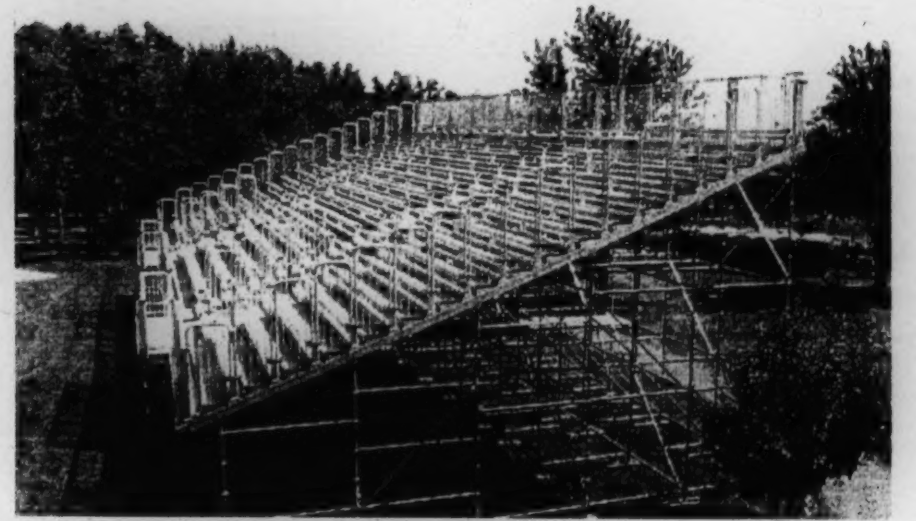

Figure 2.10 Modular temporary grandstand on scaffold structure

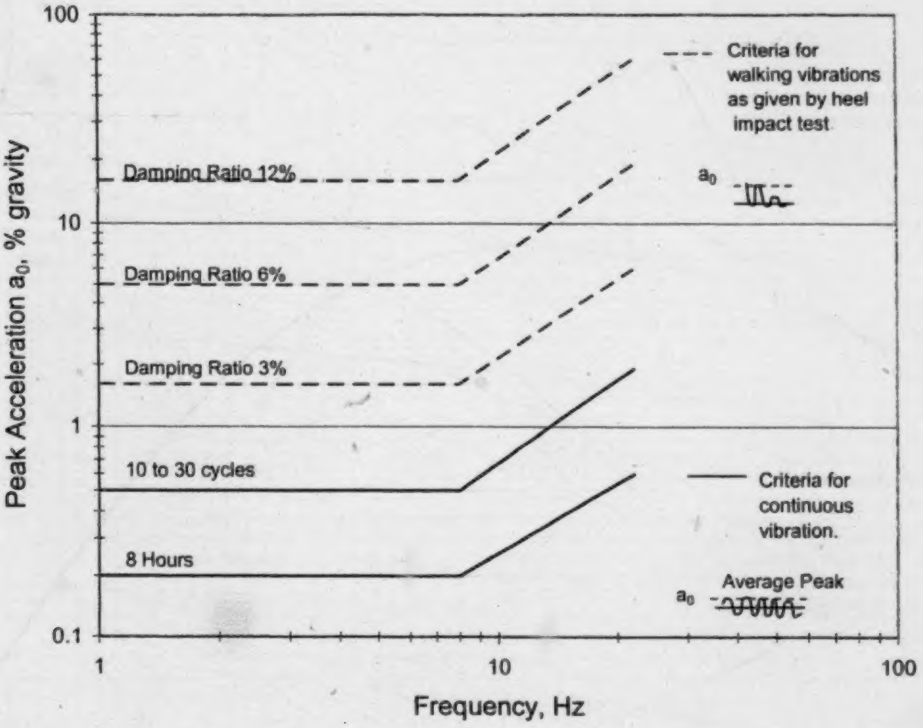

Figure 2.11 Annoyance criteria for floor vibrations: residences, offices, and school rooms.

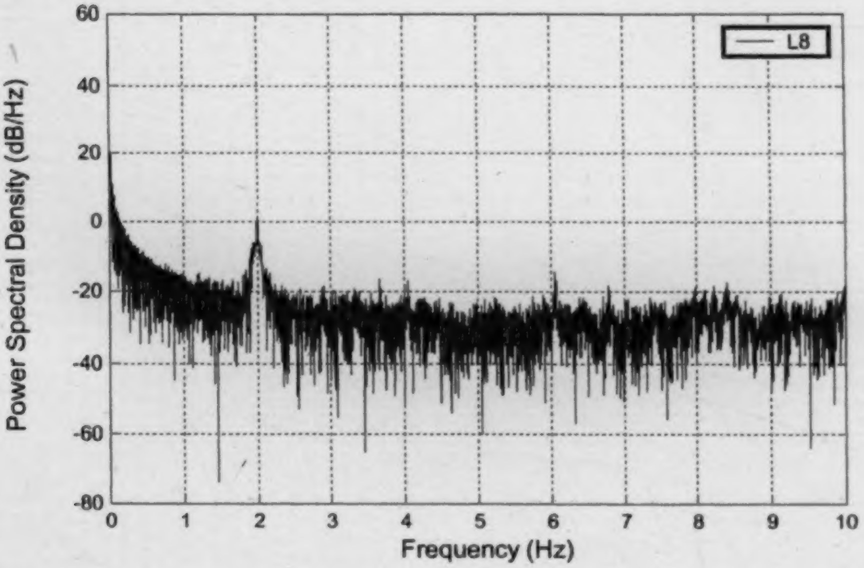

Figure 2.12. Power Spectral Density plot

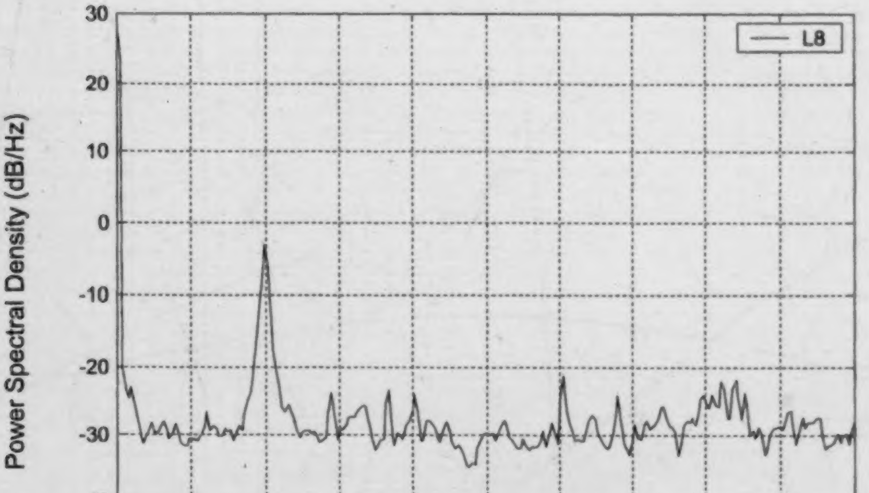

Figure 2.13. Spectral Estimate of Power Spectral Density

3 INSTRUMENTATION AND MEASUREMENTS

3.1 Introduction

A temporary grandstand was selected at the Toronto Molson Indy to be instrumented during a sporting event to measure any motion of the grandstand due to occupant movement. The particular grandstand was selected for its uniform shape and relative small size. Also, since it was an independent structure it would be free to respond to vibration without additional damping. The particular grandstand had seating capacity for 2811 spectators within 40 rows; it was 37 m wide, 26 m deep, and more than 2 m high at the front and 12m high at the rear.

The temporary grandstand was instrumented to measure lateral displacements, vertical displacements, member strains, and lateral accelerations. Table 3-1 lists the equipment that was used for the instrumentation of the temporary grandstand. The data generated by these instruments was recorded by a high speed data acquisition system located under the grandstand. The data acquisition system was capable of monitoring up to 60 channels of data at a rate of 80 Hz. The channels were setup to monitor the following:

- 28 strain gauge channels,
- 19 LVDT's,
- 7 cable transducers,
- 4 accelerometers, and
- 2 excitation voltages (for strain gauges and LVDT).

3.2 Equipment

3.2.1 Strain gauges

Strain gauges are lightweight resistive elements that change their resistance as they are elongated or contracted. The strain gauges have an insulating back carrier on which a foil grid is etched. The back carrier is bonded to the test specimen and has an important function in transferring the strain from the test area to the foil grid. The small changes in strain can be measured with great sensitivity by the arrangement of the strain gauge into a Wheatstone bridge. The strain gauges light weight makes them suitable for dynamic measurement, since they add negligible mass to the system.

The strain gauges applied to the standards and the sway braces were arranged in a half-bridge configuration, which uses two strain gauges. The first gauge is aligned with the axis of the member. The second gauge is mounted perpendicular to the axis of the member. The purpose of the half-bridge configuration is to improve the sensitivity of the strain reading. The gauge normal to the axial gauge compensates for the Poisson effect and temperature on the axial gauge resulting in improved sensitivity.

3.2.2 Linear Variable Differential Transformer

The Linear Variable Differential Transformer, or LVDT, is a transducer that utilizes the magnetic induction principle to measure displacement. The device has a primary coil and two secondary coils with a moveable ferromagnetic core. The core is arranged so that it can move between the primary and secondary coils without touching them. A schematic of the LVDT is shown in Figure 3.1. As the coil moves it causes a variation in the magnetic field between the primary and secondary coils. An excitation voltage is applied to the primary coil, V_{in}. An induced voltage is generated at the secondary coils, V_{out}, which is related to the position of the core. When the core is in the middle the voltage V_{out} will be zero. As the core moves one way or the other the voltage will change becoming higher positive or negative depending on the direction.

LVDTs typically have very good resolution, which are typically better than 0.01% of their range [Gatti, 1999]. The action of the LVDT is generally friction free since there is no contact between the core and the coils. For dynamic measurements the useful bandwidth for most LVDT is generally limited to several kilohertz, well within the range for this application.

Before placing the LVDTs in the field they were each individually calibrated in the laboratory. The individual calibrations were recorded for use in the field.

3.2.3 Cable Transducers

Cable transducers measure the change in distance by a cable that turns a high precision rotary potentiometer as it is pulled. The potentiometer is attached to a spring to maintain tension in the cable. The cable transducers were used to measure the vertical displacement of the grandstand.

The cable transducers are suitable for measuring displacement, but may not be responsive enough to measure vibration accurately. No information was available with respect to their ability to measure vibration, so they will only be used for displacement data.

As with the LVDTs the cable transducers were also calibrated in the laboratory.

3.2.4 Accelerometers

The accelerometers contain a crystal sensing element that emits a charge when subjected to a force. A mass is attached to the crystal such that when the accelerometer is subjected to acceleration ('g' force) it emits a signal which is related to the intensity of the acceleration.

The accelerometers were installed to measure vibration of the structure for the purposes of determining occupant's comfort and the dynamic parameters of the structure. The locations for the accelerometers were determined by a pre-test finite element analysis, to estimate the possible mode shapes.

Four accelerometers were used: 2 with a range of 20 μg to 2000 g, and 2 with a range of 2 μg to 1 g. The accelerometers were set to 1 volt/g. The accelerometers used an independent power source that consisted of a 9 volt battery.

3.2.5 Data Acquisition System

The data acquisition system included a National Instruments Analog to Digital converter with 60 channels. Two Hewlett Packard power supplies were used to supply excitation for the displacement transducers. A laptop computer running LabView software controlled the data acquisition system. The data acquisition system held special terminal boxes for the strain gauges (SCXI1520) and for voltage measurements (SCXI1120). The strain gauge terminal boxes could each hold up to eight strain gauges in the quarter or half-bridge configuration. The voltage boxes contained circuitry for the measurement of voltage for up to 32 channels.

To run the data acquisition system at maximum record rate the integration time for the voltage measurements was minimized. This results in less accuracy but a higher frequency of measurements. For the 60 channels the data acquisition system was capable of a scan rate of 0.0125 sec or 80 Hz. The data acquisition software was set to take readings for 300 seconds before pausing to save the data to the hard drive. However, the user could force the software to record the data before the 300 second interval. While the system saved data to the hard drive, no data was recorded this resulted in a gap of approximately 30 seconds between data sets. The data was saved in tab delimited text files, to be analyzed later. The data acquisition software automatically converted the strain signals into microstrain and the LVDT and cable transducers into mm. The accelerometer and voltage data was recorded in millivolts. The data file also included a time stamp for each set of readings.

Power was supplied to the data acquisition system and instruments by a small gas powered generator that was located at the rear of the grandstand. A long steel rod was hammered into the soil under the grandstand to provide ground for the system. The soil around the grounding rod was kept wet to improve the conductance. Figure 3.2 shows the data acquisition system under the grandstand.

3.3 Location of Measuring Devices.

The location of the measurement devices was carefully considered prior to their placement. A preliminary FEA was conducted, based upon the pre-construction drawings, to determine the possible vibration modes of the structure (the details of this FEA are discussed in Chapter 5).

For the purpose of the placement of the instruments the temporary grandstand structure was considered as being arranged in a grid, with cross sections running front to back and frames running lengthwise. The cross sections of the structure, as viewed from the side, are repeated at every bay length and are identified in Figure 3.3 by letters A to S. The bay lengths between adjacent cross sections are either 2.25 m or 1.35 m. Perpendicular to the cross sections are a series of frames identified from front to back in Figure 3.3 by numbers 1 to 13. These frames are spaced at a distance of 2.13 m and vary in elevation, due to the slope of the temporary grandstands seating (Frame #1 and # 13 have nominal elevations of 2.0 m and 12.0 m, respectively). The measurement devices were arranged on the structure to measure the movement of the temporary grandstand with respect to the cross sections and frames. However, there were not enough channels in the data acquisition system to monitor every cross section and frame, so typically every alternate one was used.

The location of the measurement devices was also influenced by the bracing pattern used on the structure. The style of bracing pattern that was used on the cross sections differs from that used on the frames. The frames used a continuous bracing pattern, where a run of braces is continuous from the top of the frame to the ground. The direction of the runs was alternated, typically, every fourth bay. Figure 3.4 shows a typical braced frame. The cross sections have individual bay bracing, where a single bay is braced, in a zig-zag fashion; typically, alternate bays were braced creating a "shear wall" to resist horizontal forces. Figure 3.5 shows a typical cross section.

The reason for the different bracing patterns is to relieve congestion at the rosette connection. If the continuous bracing pattern was used on the cross sections as well as the frames, there is the potential for eight braces to intersect at one rosette connection. However by using different bracing patterns, the maximum number of braces at one rosette connection is six. Since the rosette can accommodate only four braces, the remaining two braces are attached on the standard, near the rosette, using wedge clamps.

The location of the strain gauges placed on the standards was determined considering layout of the cross section and its bracing pattern. It was desirable to have the strain gauges on an interior standard, so that the maximum tributary area would be supported by the standard. Due to the "shear wall" type bracing pattern, horizontal forces at the top of the "shear wall" (in the plane of the cross section) would result in a difference in leg loads for the front and rear standards of the braced bay. Pairs of standards were therefore strain gauged: one on the front side of the "shear wall" and one on the back side. The strain gauges were located on the rear most "shear wall", since it was the tallest and any horizontal forces at the top would result in the greatest difference in leg loading. It was not known if the difference in leg load would be detectable, given the variability in the supported live load.

Figure 3.6 shows the locations of the strain gauges on the plan view of the grandstand. Strain gauges were mounted on standards located at G0 to G15. Figure 3.7 shows a typical strain gauge mounted on a standard. The strain gauges were mounted twelve inches above the lowest level of ledgers.

Strain gauges were also mounted on brace members. The locations of the strained gauged brace members were determined by the bracing pattern. In all cases the strain gauges were located on the braces at the lowest elevation of the structure. For the brace members in the plane of the cross sections, two locations in the front most braced bay were selected. These locations are identified in the plan view of the temporary grandstand as G23 and G24 on Figure 3.8. The strain gauges on the sway braces in the frame direction are identified in Figure 3.8 as locations G16 to G22. These locations were selected since the braces were part of a continuous run from the top to the bottom of the structure. Figure 3.9 shows typical strain gauges mounted on a sway brace.

Strain gauges were also mounted on a "U-head" support for the modular seating at locations G25 to G26. Figure 3.10 shows the strain gauges mounted on a "U-head" support. The "U-head" support is a solid post with a channel on the top that supports the stringers from the seating system. The solid post of the "U-head" is inserted in the top standard and is the interface between the aluminum seating system and the scaffold substructure. The strain gauges on the U-head were placed in the bending configuration to measure bending (front to back or side to side). In the bending configuration two strain gauges are used on opposite sides of each other in the same circuit. This configuration increases the sensitivity of the strain readings for flexural bending. However, this configuration for this application was not appropriate since the "U-head" is not in pure bending, but in a combination of compression and bending. Therefore, the results from these strain gauges are not included in the analysis.

One dummy strain gauge was created that was not attached to the structure, but was used to monitor any drift in the strain gauge readings that might occur over time.

LVDTs were arranged to measure the swaying motion of the grandstand. Figure 3.11 shows the attachment of a LVDT to a ledger near the base of the structure. The bodies of the LVDT were held in wooden blocks that were fixed to ledgers at the base of the structure with nylon wire ties. Spectra fibre fishing line (Spider Wire) was attached to the end of the LVDT and run at an angle of approximately 45° to the top of the scaffold structure. Figures 3.12 and 3.13 show how the lines were connected from the LVDT to the top of the structure. The LVDT and the line were placed inside the structure so that the spectators at the venue would not interfere with them.

The distance between the LVDT and the top of the structure changes with the swaying motion in the direction of the LVDT, causing the line to pull on the LVDT. The spectra line was kept in tension by rubber bands that attached from the wooden blocks to the end of the LVDT. The spectra line was selected due to its high strength and low elongation. The LVDT's used a 7-volt excitation and all of the LVDT's had a 6 inch range from +3 to –3 inches. The LVDT core was positioned near the middle of their range when they were installed on the structure.

Figures 3.14 and 3.15 show the location of the LVDT's on a plan view of the grandstand. The LVDT's were arranged on a grid with one LVDT attached along each bay at the rear of the structure to measure front-back sway, L0-L9. Another row of LVDT's were arranged parallel to the rear of the structure to measure side-side sway, L13-C19. Three additional LVDT's were added to the front of the structure to measure front-back sway, L10-L12. Due to the shortage in the number of LVDT's, one cable transducer was substituted in one location (C19) measuring side-side sway at the front.

The LVDT's were attached to a lower level of ledgers that were at a consistent elevation throughout the structure. Ideally the LVDT would not have been attached to the structure but would have been attached to independent points on the ground. The initial plan was to drive wooden stakes into the ground to which the LVDT's would be attached. Unfortunately the wooden stakes did not provide a solid foundation for the LVDT's so they could not be used. Attaching the LVDT's to the structure provides some advantages and disadvantages. One advantage is that the elevation of the LVDT's is consistent throughout the structure; all movements are therefore referenced to the same elevation. The ground at the site was uneven so a reference to the ground would have been necessary to take into account changes in elevation. Another advantage is that the movement at the foundation is not measured so the structure-foundation interaction does not need to be modeled in the finite element analysis, thus simplifying the model. This may also be a disadvantage since the foundation is ignored although it may contribute to the overall dynamic response of the structure.

There were six cable transducers available, five were arranged at the rear of the structure, where it was anticipated that the largest vertical deflections would occur. One cable transducer was placed in the midway between the front and back to measure vertical displacement. The cable transducers were attached at the base of the structure and spectra fishing line was used to attach the cable transducer to the top of the scaffold structure. It was anticipated that the vertical displacements would be small in comparison to the sway motion, due to the nature of the structure. Figure 3.16 shows the location of the cable transducers measuring the vertical displacement on the grandstand. Figure 3.17 shows a cable transducer at the base of the structure.

The accelerometers were mounted in pairs perpendicular to each other. The main axis of the accelerometers was at 45° to the front-back direction of the grandstand. The accelerometers were mounted on hoarding clamps that were attached to the rear of the grandstand at 12 m elevation at the mid and quarter point locations. A hoarding clamp has a ledger head to attach it to a rosette and has a "U" shaped metal plate for attaching tarps to scaffolding. The accelerometers were bolted to the "U" shaped plate.

Based upon the pre-test finite element analysis the large pair of accelerometers was located at the mid point of the rear of the grandstand and the smaller pair was located at the quarter point along the rear of the grandstand. Figure 3.18 shows the location of the accelerometers, measuring lateral accelerations, on a plan view of the grandstand. Figure 3.19 shows the attachment of the accelerometers at the top rear of the structure.

3.4 Measurements.

The grandstand that was instrumented had a width of 36.9 m, a depth of 26.4 m, a rear height of 12 m, and a front height of 2 m. The stand was designed to accommodate 2811 spectators and had three aisles and entrances. The event was held in Toronto, Ontario at the National Exhibition Park on July 18, 1999. The grandstand was located at the southeast corner of the track south of Lake Shore Boulevard, shown in Figure 3.20. The weather conditions at the time of the event were sunny and hot (25 °C to 28 °C) with wind conditions from 11 to 17 km/h. Figure 3.21 shows the hourly temperatures for July 18, 1999, and Figure 3.22 shows the hourly wind speeds. The weather conditions were obtained from Environment Canada, at the Toronto Island Airport, which is close to the event location as shown in Figure 3.23.

Readings were taken the day before the main event with the grandstands empty (Figure 3.24). These readings were stored in a separate file to be used as base line data. There were smaller races occurring the day before the main race, but the grandstand was not open for general admission. The readings from that day are therefore only the result of ambient vibration, primarily due to wind. Four data sets were collected between 4:27 PM and 4:59 PM.

During the day of the feature race the grandstand was open to the public in the morning. The feature race was not set to start until 2:00 PM, but there were other races held throughout the day. As a result, the grandstand filled slowly throughout the day. A set of readings was taken in the morning, but we were unable to measure the filling of the grandstand because it would occur over several hours. The main set of readings was collected just prior to the commencement of the event. This included the introduction of the drivers and the singing of the national anthem. At the start of the feature race the grandstand was nearly full but there were still spectators arriving at the venue; the maximum capacity was not reached until sometime after the start of the race (Figure 3.25).

It was intended that a video camera would be set up to record the movement on the grandstand during the event, but equipment failure prevented this from happening. Instead, notes were kept of any notable movement such as the rising for the singing of the national anthem; these are listed in Table 3.2. During the event there was little coordinated motion from the spectators other than the rising for the national anthem and at the end of the race the crowd rose to applaud the victor and then proceeded to exit the venue. Within a half hour of the end of the race the grandstand was mostly empty. At this point the recording of data was stopped. One more data set was gathered at approximately 1.5 hours after the end of the race to be used for comparison with the baseline data.

3.4.1 Static Loads and Displacements

The data gathered during the event were stored in data files for post processing. The data files were tab-delimited files that stored the data from each channel. The data from the strain gauges were recorded in microstrain, the data from the LVDT's and cable transducers were recorded in millimetres, and the accelerometers and voltmeters were recorded in millivolts.

For each data file, 60 channels were recorded at a rate of 80 Hz for up to a maximum of 300 seconds of data recording, so a maximum of 1,440,000 data points were generated for each data set. To determine the static results the data was filtered using a low pass filter set at 1.0 Hz and averaged over one minute. Filtering and data reduction were used to reduce the variability in the recorded data.

The static results apply only to the strain gauges and displacements; the accelerometers record only dynamic motion so these are presented as instantaneous maximum accelerations. The filtering and data reduction applied only to the analysis of the static results. For the dynamic analysis, discussed later, the data was left unfiltered and had no data reduction applied.

3.4.2 Standards

The strain gauge readings on the standards were used to determine the average maximum static load on the structure during the event. The maximum strain reading during the event from the filtered data set was recorded for each of the channels G0 to G15. The minimum strain reading was determined as the average of the strain values taken at 5:32 PM, when the grandstand was empty. The change in strain was therefore the difference between the average of the final readings, taken at 5:32 PM, and the maximum strain during the event. The load is then calculated by multiplying the change in strain by the nominal cross sectional area (451 mm^2) and Young's modulus (200 GPa) of the standard. The distributed static load was determined by dividing the load on the standard by the tributary area supported by it. Table 3.3 shows the maximum static load for each strain location. Based upon the tributary area supported by each of the standards an average distributed load was calculated at each location for each time period. An overall average for the grandstand was calculated for each time period and the maximum average distributed load was 1.4 kPa at 2:45 PM. The overall maximum distributed load was 2.2 kPa at location G10 at 2:45 PM.

To determine if the average distributed load is reasonable, a rough calculation was made to estimate the distributed load based upon the occupancy, an estimate of the average spectator weight, and the area of the grandstand. The occupancy for this particular grandstand was 2811 people; the average weight of the spectators was taken as 68 kg [Pernica, 1982]; and the grandstand plan area was 962 m^2. Therefore, the estimated distributed load was 1.95 kPa (2811 x 68 kg x 9.81 N/kg / 962 m^2 = 1950 Pa). The estimated distributed load is very close to the distributed load based on the strain measurements.

At the start of the data recording most of the spectators were already in the stands, however, there was a steady increase in load at the beginning as many spectators were still entering the grandstand. Figures 3.26 to 3.29 show the strain readings on the vertical members. The peak load for most areas occurs approximately one hour after the start of the race. At the end of the event, when people are exiting the grandstand, the load drops off sharply and stabilizes when the grandstand is empty. The load next to the aisles increases substantially at the end of the event, as seen at locations G6-G9 (Figures 3.27 and 3.28), as the spectators moved from their seats to the aisles. The data recording was stopped after 4:35 PM and a final data set was gathered at 5:30 PM with the grandstand completely empty.

3.4.3 Brace Members

Most of the braces that were instrumented were oriented to resist sway in the side-to-side direction (locations G16-G22 in Figure 3.8); and two braces at the front of the structure measured front-back sway (locations G23 and G24 in Figure 3.8). For the calculation of the brace load the nominal cross sectional area (337 mm^2) was used. Averages of the strain reading for the last data set, when the grandstand was empty, were used as the baseline to calculate the change in strain for the occupied stand. The last data set was used instead of the first data set for the day because the grandstand was already partially occupied when the first data set was collected. The load was estimated using the change in strain, the cross sectional area, and Young's modulus. The maximum brace member loads are given in Table 3.2. Figures 3.30 to 3.32 show the strains in the brace members during the event.

A wide variation in the load on the brace members was observed, which suggests that they may not be sharing load equally. This could be due to the looseness of some of their connections, causing the load to not be evenly distributed.

The sway braces towards the rear of the structure tended to have less load variations during the event. One possible explanation is that there is better load sharing due to the height of the structure at the rear; the load has more opportunities to be shared as it travels from the top to the base of the structure. The braces towards the front of the structure show greater load variation. The largest load was measured on brace G24 (3.86kN), a brace at the front of the grandstand resisting front-back motion. This result is significantly higher than the other brace forces; however, this load does not exceed the factored resistance of the brace (16 kN).

The sway braces near the front of the grandstand, G20 to G22 and G24, show a sharp change in load at the end of the event.

3.5 Sway Displacements

The sway displacements shown in this section are the static sway displacements. The vibrations that oscillated about these static displacements will be used in the next section for the determination of the dynamic properties of the grandstand. Table 3.5 and 3.6 give the maximum static sway deflections in the front-back and side-side directions respectively. The maximum sway displacements were determined as the difference between the maximum and minimum values measured during the monitoring period. Figures 3.33 to 3.35 show the front-back sway; Figures 3.36 and 3.37 show the side-side sway of the temporary grandstand.

The raw data for the sway displacements show a lot of variability. The low pass filter and averaging over a minute reduces the variability and reveals the static sway displacement. The results show that the changes in the sway displacements correspond to the loading and unloading of the grandstand. In particular, the graphs of the sway displacements show an abrupt shift corresponding to the time that the grandstand emptied.

3.6 Vertical Displacements

The vertical displacements were measured using cable transducers. The vertical measurements were taken along the rear of the structure (C20-C24) and one location (C25), halfway from the front to the back of the structure. The vertical displacement readings were offset to zero at the start of the event, so the results would be on a comparable scale. The changes in vertical displacements during the event are shown in Figures 3.38 and 3.39. As with the sway displacements, the vertical displacement varied with the loading and unloading of the temporary grandstand. Table 3.7 gives the maximum vertical displacements during the event.

?

3.7 Accelerations

Acceleration has a great effect on how spectators respond to movement of a structure. Humans tend to have a greater sensitivity to acceleration than to the frequency of vibration. To evaluate the vibration it is necessary to use standard methods for measuring the acceleration. ISO 2631-1 [1997] uses the weighted root-mean-square (RMS) acceleration as the basic measurement. The weighted root-mean-square acceleration is defined as:

$$a_w = \left[\frac{1}{T}\int_0^T a_w^2(t)\,dt\right]^{\frac{1}{2}} \qquad \text{Equation 3.1}$$

where:

$a_w(t)$ is the weighted acceleration as a function of time in m/s^2.

T is the duration of the measurement, in seconds.

The weightings are given in the frequency domain and are based on the effects on human perception. To apply the weightings the accelerations are transformed into the frequency domain by Fast Fourier Transform (FFT). The weightings are applied and the accelerations are transformed back into the time domain by Inverse Fast Fourier Transform (IFFT). The accelerations from the two accelerometers were combined using the following equation from ISO 2631-1[ISO, 1997]:

$$a_v = (k_x^2 a_{wx}^2 + k_y^2 a_{wy}^2 + k_z^2 a_{wz}^2)^{\frac{1}{2}} \qquad \text{Equation 3.2}$$

where:

a_{wx}, a_{wy}, a_{wz} are the weighted RMS accelerations with respect to orthogonal axis x, y , z

k_x, k_y, k_z are multiplying factors, which in this case k_x=k_y=k_z= 1.0

The use of the weighted RMS is useful for determining the "average" vibration level over a specified time period. In this case the weighted RMS values were calculated for each 300 seconds block of data. However, there may be cases where there are large transient vibrations, such as those caused by shock. In these cases the weighted RMS may greatly underestimate the effect on the spectators. A crest factor is used to determine the difference between the extreme vibration and the average vibration. The crest factor is the ratio of the largest instantaneous peak value of the frequency-weighted acceleration to its RMS value. When the crest factor is greater than 9.0 it may be more suitable to use an alternative method for evaluating the vibration. Two alternative methods are available. They include: the Running RMS (RRMS), and the fourth power Vibration Dose Value (VDV).

The RRMS evaluation method uses a short integration time to take into account transient vibrations. It is defined by:

$$a_w(t_0) = \left\{ \frac{1}{\tau} \int_{t_0-\tau}^{t_0} \left[a_w(t) \right]^2 dt \right\}^{\frac{1}{2}}$$

Equation 3.3

where:

$a_w(t)$ is the instantaneous frequency-weighted acceleration;

τ is the integration time for the running averaging;

t is the time (integration variable);

t_0 is the time of observation (instantaneous time).

The Running RMS can be used to evaluate the Maximum Transient Vibration Value (MTVV). An integration time of $\tau = 1$ sec is used and the MTVV is defined by:

$$MTVV = \max\left[a_w(t_0) \right]$$

Equation 3.4

The crest factor is calculated as:

$$C.F. = \frac{MTVV}{a_w}$$

Equation 3.5

where a_w is the weighted RMS value.

The fourth power vibration dose method uses the fourth power rather than the second power that is used for the RMS method. As a result it is more sensitive to the peaks and transient vibrations. The VDV is defined by:

$$VDV = \left\{ \int_{0}^{T} \left[a_w(t) \right]^4 dt \right\}^{\frac{1}{4}} \qquad \text{Equation 3.6}$$

where:

$a_w(t)$ is the instantaneous frequency-weighted acceleration;

t is the duration of the measurement

The units for VDV are in m/sec$^{1.75}$. When more than one period of time is evaluated the total vibration dose value can be calculated by:

$$VDV_{total} = \left(\sum_{i} VDV_i^4 \right)^{\frac{1}{4}} \qquad \text{Equation 3.7}$$

For each data set the weighted RMS, VDV, MTVV, and crest factor were calculated and are given in Table 3.8. The average RMS value for the event was less than 0.02 g, which would be considered annoying based on Table 2.6. However, accelerations of up to 0.07 g are considered acceptable for rhythmic activities based upon the NBCC guidelines. The highest RMS reading occurred in data set 4:05 (0.03 g), which corresponded to the end of the race and the exiting of the spectators. This indicates that there was an average high level of vibration for this data set. The VDV was highest in data set 3:32 (5.1 m/s$^{1.75}$), which also corresponded with the highest MTVV (0.34 g) and Crest Factor (12.51). This was due to a short duration event (< 5 seconds) as shown in the RRMS in Figure 3.40. The MTVV value of 0.34 g was approaching the lower limit to incite panic (0.35 g [IStructE, 2001]), but due to its short duration it may have been tolerated by the occupants. Had the vibration acceleration been sustained for a much longer time then it definitely would have caused concern for the occupants.

3.8 Instrumentation Accuracy

There are a number of factors that can affect the accuracy of the data that is collected. The data acquisition system recorded the values to 3 decimal places, but the actual precision is based on the accumulated error from the instruments, wire losses, analog to digital conversion, etc. It would be difficult to exactly identify the error in the readings based on the number of factors that would have to be taken into account.

For the strain gauges no effort was made to identify the error in the measurement system. Typically, strain gauge measurements have less than 5% error and this was assumed to be satisfactory for this research. However, efforts were made to improve the accuracy by arranging the strain gauges in a half- bridge configuration, with the primary gauge aligned axially and a secondary gauge perpendicular. This configuration provides temperature compensation and compensates for the effect of Poisson's ratio on the axial measurement. This configuration also improves the sensitivity as compared to a quarter-bridge arrangement. To monitor the fluctuations or drift in the strain gauge readings an extra strain gauge was mounted (in the same configuration) on a small piece of metal that was not attached to the structure. This strain gauge was kept close to the data acquisition system throughout the project and was not subject to any loading. During the duration of the event the strain gauge readings fluctuated a maximum of 9 microstrain.

The LVDT's and cable transducers were calibrated in the laboratory prior to being placed in the field, and validated upon return to the laboratory.

Table 3.1. Monitoring Equipment List

Equipment	**Details**
Data Acquisition System	▪ National Instruments Analog-Digital Converter DAQ Card-AI-16E-4 ▪ Mainframe SCXI 1001 ▪ Strain gauge signal conditioner SCXI 1121 ▪ Signal conditioner SCXI 1100 ▪ Two HP power supplies
Accelerometers	▪ Signal conditioner, charge amplifier type 2635 ▪ 2 accelerometers, Type 4370, charge sensitivity 100pC/g, range 20 μg to 2000 g ▪ 2 accelerometers, Type 8306, charge sensitivity 10000 pC/g, range 2 μg to 1g
Strain Gauges	▪ SHOWA Measuring Instruments Co., type N11-FA-5-120-11 ▪ 120 ohm, 5mm gauge length
LVDT, Cable Transducer	▪ LVDT: +/- 3 inch travel ▪ Cable transducers: 2 and 3 inch travel

Table 3.2. Observed crowd actions during race

Time	**Crowd Action**
1:47	National Anthem, people standing
1:49	People clapping and moving
1:50	People sitting after national anthem
1:56	Cheers for the Canadian driver
1:58	Cheering for the call to start engines
2:06	Cheering as race starts
4:02:30	End of race, people standing and cheering
4:03 to 4:20	People leaving the grandstand

Table 3.3. Average distributed load on tributary area (kPa)

	Location																
Time	G0	G1	G2	G3	G4	G5	G6	G7	G8	G9	G10	G11	G12	G13	G14	G15	Average
1:49:45 PM	0.79	0.42	1.13	1.38	0.70	0.61	0.76	0.50	0.47	0.28	1.26	0.52	0.92	0.99	0.97	1.00	0.79
1:55:19 PM	0.95	0.45	1.29	1.42	1.17	0.86	0.96	0.82	0.57	0.31	1.21	0.49	1.04	1.24	1.51	1.46	0.98
2:00:53 PM	1.19	0.54	1.50	1.52	1.30	0.86	0.98	0.82	0.72	0.29	1.45	0.59	1.12	1.29	1.74	1.69	1.10
2:06:28 PM	1.24	0.68	1.70	1.63	1.32	0.88	1.03	0.84	0.80	0.29	1.46	0.59	1.36	1.68	1.79	1.72	1.19
2:12:02 PM	1.31	0.84	1.78	1.81	1.35	0.98	1.00	0.80	0.78	0.31	1.52	0.69	1.43	1.69	1.92	1.80	1.25
2:17:41 PM	1.38	0.90	1.71	1.90	1.37	1.04	1.05	0.81	0.76	0.34	1.55	0.68	1.43	1.67	2.01	1.89	1.28
2:23:15 PM	1.34	0.86	1.68	1.90	1.36	1.04	1.06	0.91	0.75	0.34	1.67	0.72	1.44	1.67	2.12	2.02	1.31
2:28:50 PM	1.22	0.72	1.63	1.84	1.41	1.06	1.10	0.96	1.04	0.56	2.02	0.91	1.42	1.64	2.13	2.02	1.36
2:39:58 PM	1.30	0.79	1.62	1.71	1.50	1.19	0.95	0.90	0.96	0.56	2.15	1.14	1.40	1.64	2.15	2.00	1.37
2:45:52 PM	1.40	0.94	1.58	1.72	1.44	1.20	0.95	0.93	1.15	0.69	**2.19**	1.18	1.35	1.64	2.09	1.88	**1.40**
2:51:28 PM	1.34	0.95	1.50	1.70	1.33	1.21	0.86	0.91	1.15	0.74	2.16	1.16	1.25	1.58	2.00	1.77	1.35
2:57:04 PM	1.48	0.96	1.58	1.57	1.39	1.23	0.72	0.83	0.99	0.58	2.00	1.00	1.16	1.43	1.94	1.62	1.28
3:02:38 PM	1.53	0.95	1.62	1.54	1.40	1.26	0.81	0.90	0.99	0.66	2.01	1.02	1.15	1.44	2.00	1.69	1.31
3:08:18 PM	1.50	0.92	1.61	1.57	1.39	1.26	0.83	0.88	1.01	0.66	2.03	1.01	1.14	1.37	2.01	1.68	1.30
3:15:04 PM	1.48	0.98	1.61	1.69	1.38	1.24	0.82	0.85	1.02	0.60	2.04	0.95	1.14	1.21	1.95	1.62	1.29
3:20:41 PM	1.23	0.97	1.62	1.68	1.42	1.23	0.79	0.76	0.95	0.62	2.07	0.98	1.12	1.15	1.66	1.35	1.22
3:26:42 PM	1.05	0.82	1.60	1.78	1.19	1.03	0.89	1.13	1.05	0.54	2.01	0.83	1.08	1.00	1.63	1.18	1.17
3:32:16 PM	1.29	0.90	1.57	1.77	1.20	1.10	0.94	1.21	1.20	0.67	2.03	0.83	1.13	1.11	1.62	1.29	1.24
3:37:50 PM	1.28	0.94	1.52	1.72	1.20	1.06	0.99	1.20	1.16	0.67	2.11	0.96	1.14	1.18	1.56	1.33	1.25
3:43:32 PM	1.36	0.91	1.52	1.64	1.27	1.09	1.09	1.22	1.18	0.64	1.98	1.01	1.12	1.14	1.37	1.16	1.23
3:49:05 PM	1.44	0.88	1.52	1.69	1.25	1.09	1.05	1.14	1.15	0.59	1.97	0.94	1.14	1.18	1.55	1.28	1.24
3:54:40 PM	1.42	0.86	1.48	1.66	1.27	1.13	1.00	0.92	1.07	0.54	1.98	0.90	1.13	1.18	1.65	1.35	1.22
4:00:14 PM	1.53	0.96	1.49	1.69	1.28	1.15	1.00	0.96	1.15	0.63	2.01	0.98	1.13	1.16	1.68	1.39	1.26
4:05:48 PM	1.54	0.94	0.98	1.00	0.65	0.55	0.86	1.17	1.13	0.67	1.51	0.73	0.80	0.73	1.46	0.92	0.98
4:11:28 PM	0.57	0.40	0.33	0.53	0.45	0.27	0.15	0.35	0.18	0.16	0.44	0.09	0.34	0.23	0.59	0.36	0.34
4:17:13 PM	0.22	0.09	0.22	0.40	0.31	0.20	0.12	0.27	0.19	0.14	0.17	0.02	0.19	0.19	0.42	0.24	0.21
4:22:41 PM	0.20	0.08	0.08	0.27	0.19	0.14	0.25	0.20	0.02	0.07	0.02	0.02	0.17	0.14	0.25	0.14	0.14
4:28:17 PM	0.07	0.03	0.00	0.01	0.09	0.06	0.05	0.07	0.04	0.07	0.05	0.04	0.01	-0.04	-0.01	0.00	0.03
4:33:51 PM	0.00	0.00	0.00	0.00	0.00	0.00	0.00	0.00	0.00	0.00	0.00	0.00	0.00	0.00	0.00	0.00	0.00

Table 3.4 Maximum static strain on sway braces

Location	Average Strain (empty stand) (με)	Max Compressive Strain (με)	Δ Strain (με)	Compressive Force (kN)
G16	18	6	-12	-0.8
G17	12	-8	-20	-1.3
G18	20	18	-2	-0.1
G19	6	1	-5	-0.3
G20	16	-25	-41	-2.8
G21	45	10	-35	-2.4
G22	20	3	-17	-1.1
G23	28	-15	-43	-2.9
G24	-4	-61	-57	-3.8

Table 3.5. Maximum sway displacements front-back motion

Location	Max. Displacement (mm)	Height (m)	H/Δ
L0	1.3	12.0	8960
L1	1.4	12.0	8467
L2	1.3	12.0	9129
L3	2.7	12.0	4481
L4	1.8	12.0	6636
L5	1.2	12.0	9658
L6	1.6	12.0	7405
L7	3.4	12.0	3493
L8	2.9	12.0	4131
L9	1.6	12.0	7366
L10	0.8	2.0	2536
L11	1.4	2.0	1407
L12	1.5	2.0	1330

Table 3.6. Maximum sway displacement side-side motion

Location	Max. Displacement (mm)	Height (m)	H/Δ
L13	3.6	12.0	3348
L14	2.3	10.0	4388
L15	1.9	8.5	4566
L16	2.2	7.0	3172
L17	2.3	4.5	1959
L18	1.5	3.5	2400
C19	1.0	2.0	2070

Table 3.7. Maximum vertical displacements

Location	Vertical Displacement (mm)
C20	1.2
C21	2.4
C22	1.5
C23	1.8
C24	1.8
C25	1.5

Table 3.8. Maximum accelerations

Data Set	**RMS**		**VDV**	**MTVV**		**Crest**
	(g)	**m/s^2**	**m/s$^{1.75}$**	**(g)**	**m/s^2**	**Factor**
1:49	0.0209	0.205	1.34	0.074	0.729	3.55
1:55	0.0172	0.169	1.63	0.078	0.765	4.54
2:01	0.0153	0.150	1.03	0.059	0.574	3.84
2:06	0.0161	0.158	1.39	0.066	0.645	4.08
2:12	0.0146	0.143	0.82	0.032	0.311	2.17
2:17	0.0153	0.150	0.98	0.055	0.540	3.60
2:23	0.0182	0.178	2.19	0.119	1.169	6.55
2:28	0.0159	0.156	1.21	0.065	0.641	4.12
2:40	0.0208	0.204	2.63	0.176	1.728	8.48
2:46	0.0204	0.200	1.95	0.101	0.988	4.95
2:51	0.0227	0.223	1.69	0.103	1.015	4.56
2:57	0.0220	0.216	1.52	0.094	0.919	4.26
3:02	0.0180	0.176	1.06	0.051	0.499	2.83
3:08	0.0214	0.210	1.74	0.118	1.157	5.50
3:15	0.0161	0.158	0.90	0.042	0.411	2.61
3:20	0.0187	0.183	1.35	0.067	0.659	3.60
3:26	0.0255	0.250	1.88	0.108	1.064	4.26
3:32	0.0270	0.265	**5.13**	**0.338**	**3.311**	**12.51**
3:37	0.0206	0.202	3.01	0.187	1.836	9.08
3:43	0.0146	0.143	0.90	0.047	0.463	3.24
3:49	0.0150	0.147	1.18	0.082	0.805	5.46
3:54	0.0163	0.160	1.91	0.097	0.954	5.97
4:00	0.0144	0.142	0.94	0.038	0.371	2.62
4:05	**0.0290**	**0.284**	1.69	0.067	0.659	2.32
4:11	0.0218	0.214	1.85	0.098	0.959	4.48
4:17	0.0207	0.203	1.81	0.100	0.983	4.83
4:22	0.0185	0.182	1.28	0.074	0.726	4.00
4:28	0.0146	0.143	1.20	0.062	0.609	4.25
4:33	0.0170	0.167	1.67	0.089	0.869	5.20
5:39	0.0178	0.174	1.18	0.064	0.626	3.59

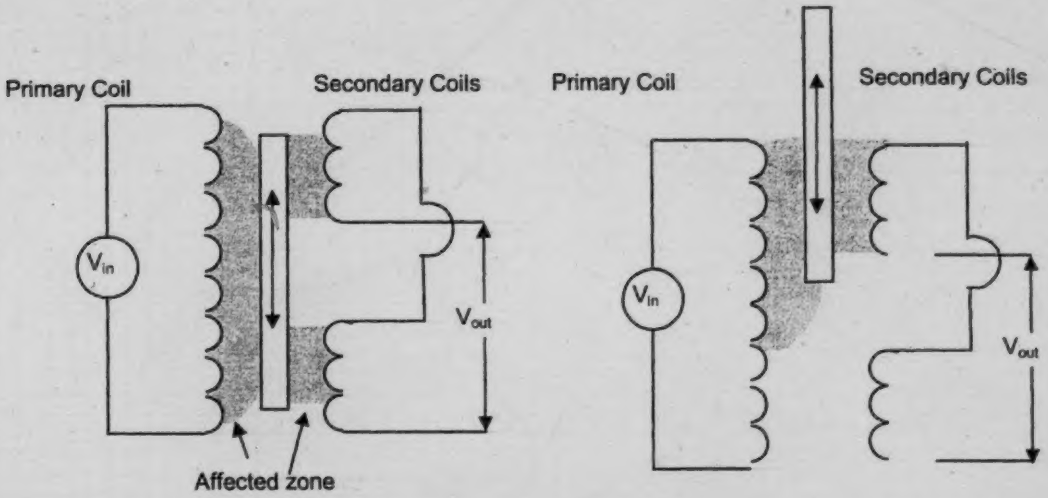
Primary Coil
Secondary Coils
V_{in}
V_{out}
Affected zone
Primary Coil
Secondary Coils
V_{in}
V_{out}

Figure 3.1. Schematic of LVDT

Figure 3.2. Data acquisition system

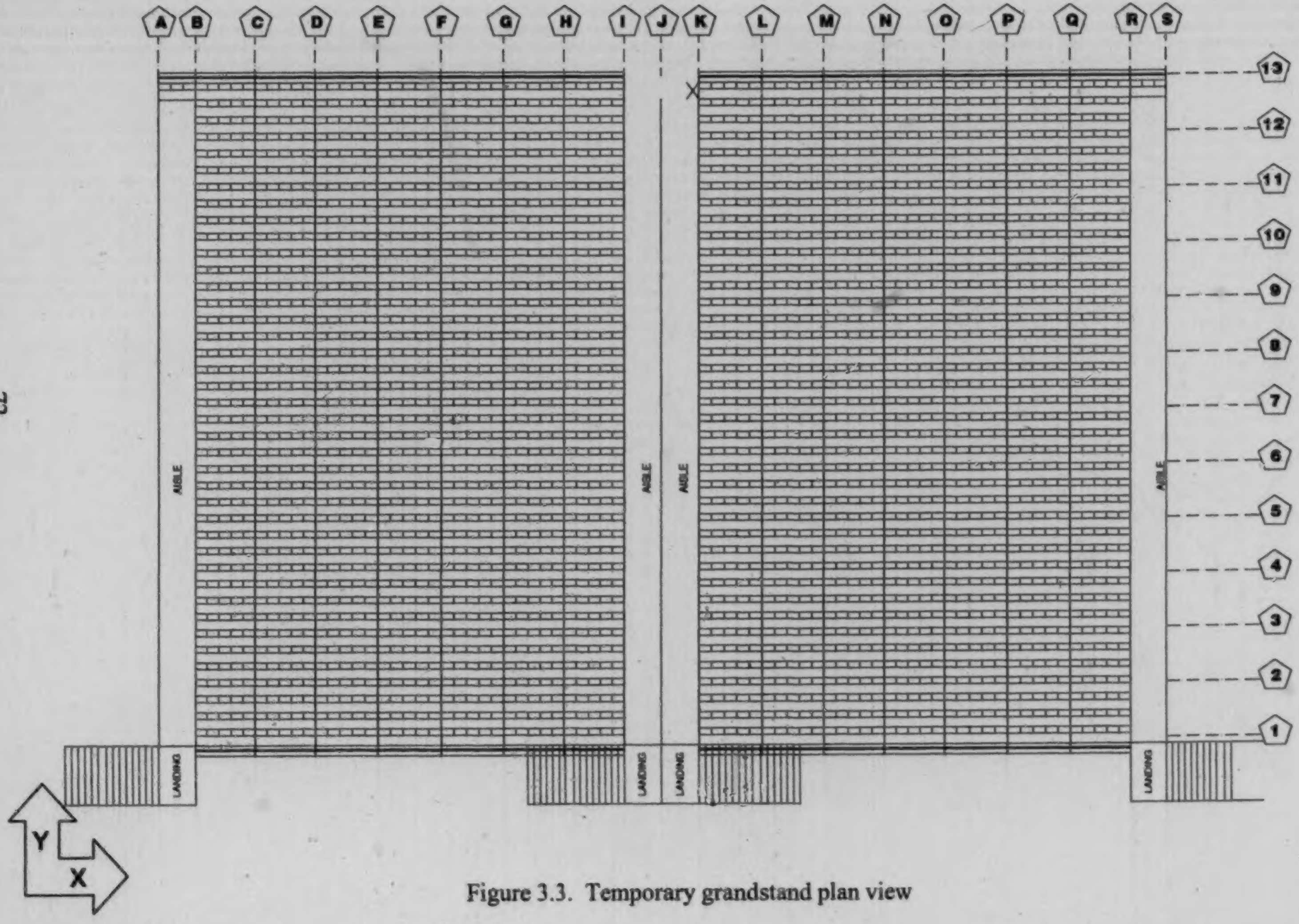
A
B
C
D
E
F
G
H
I
J
K
L
M
N
O
P
Q
R
S
13
12
11
10
9
8
7
6
5
4
3
2
1
AISLE
AISLE
AISLE
AISLE
LANDING
LANDING
LANDING
LANDING
Y
X

Figure 3.3. Temporary grandstand plan view

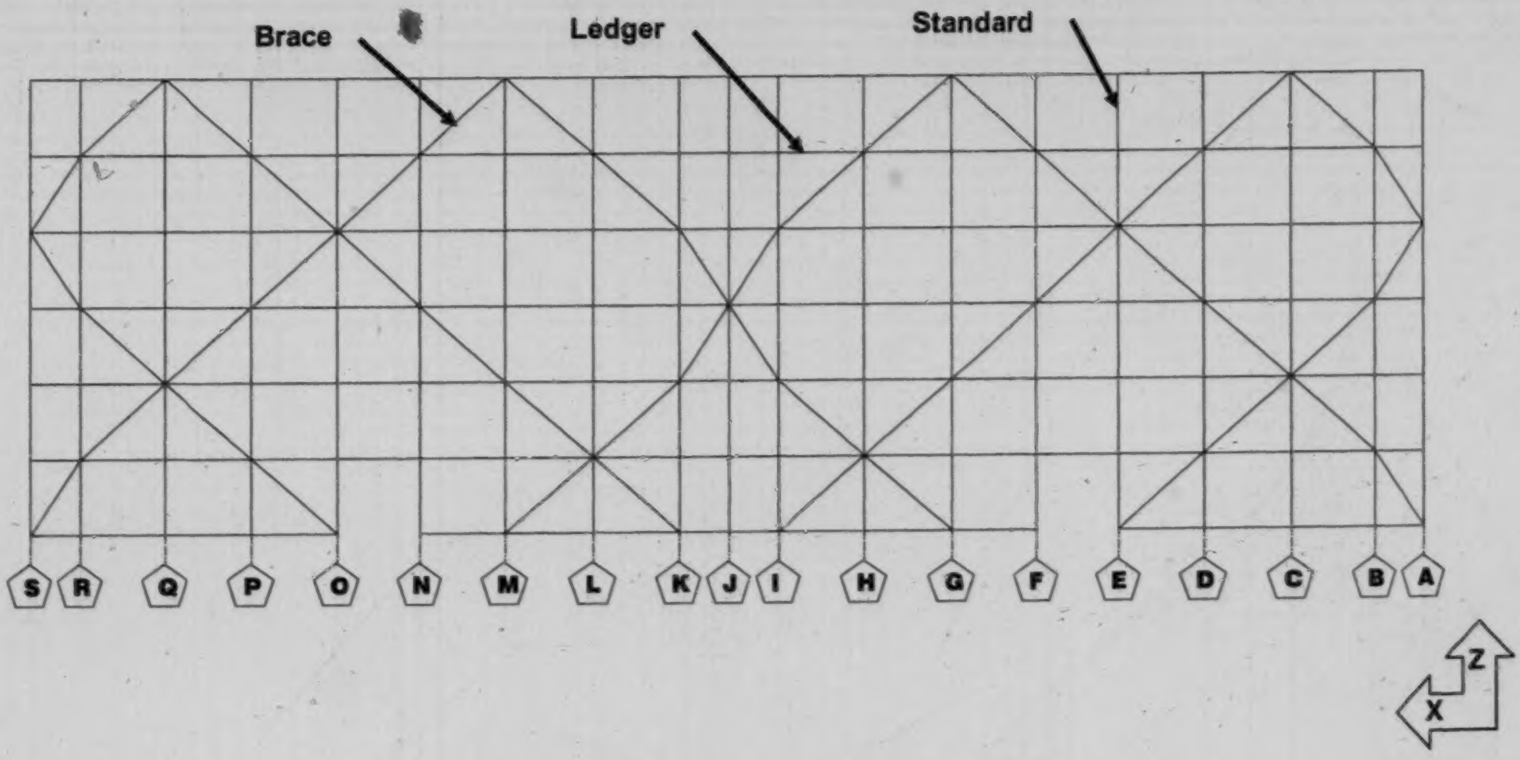
Brace
Ledger
Standard
S
R
Q
P
O
N
M
L
K
J
I
H
G
F
E
D
C
B
A
Z
X

Figure 3.4. Rear frame (#13) of temporary grandstand

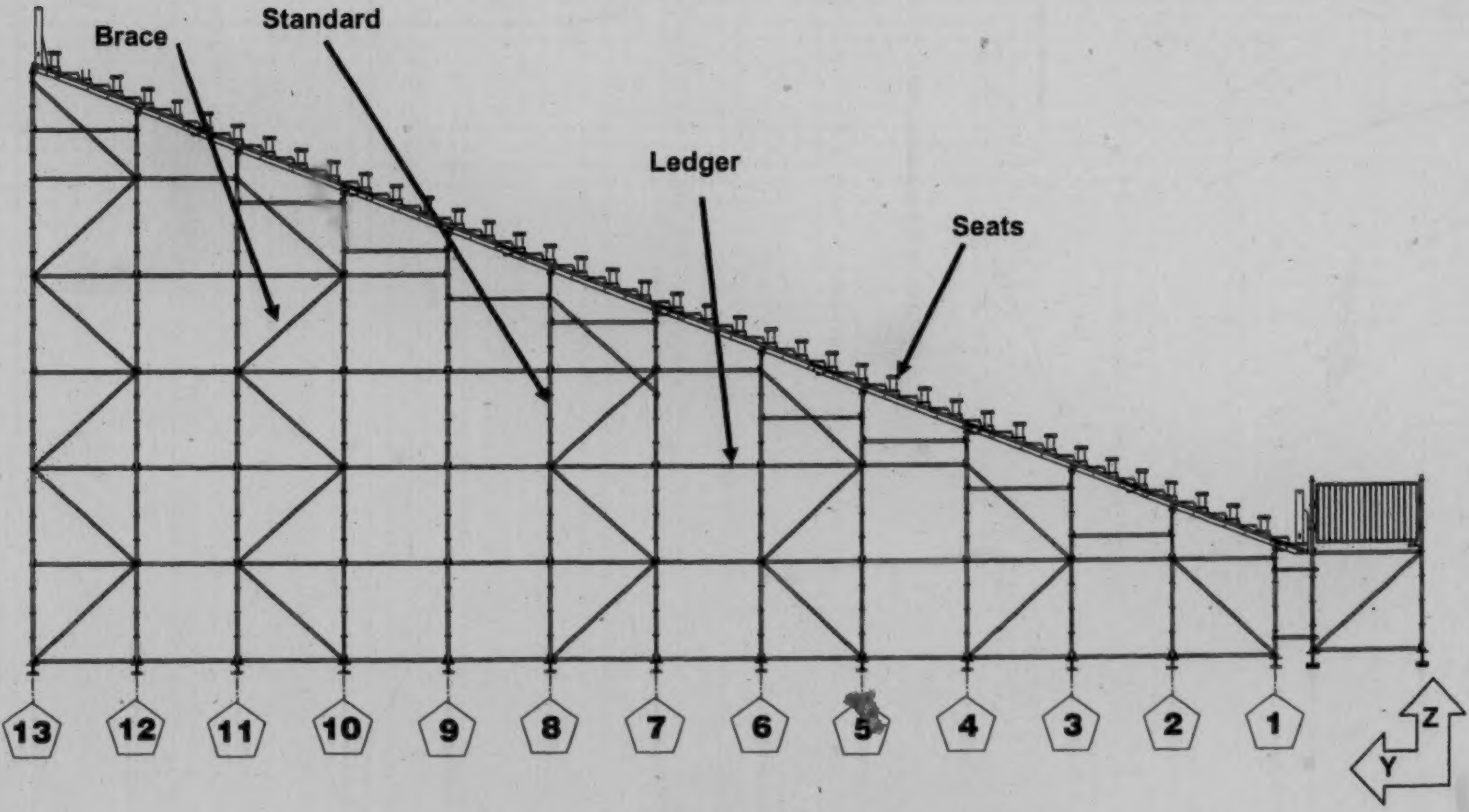
Brace
Standard
Ledger
Seats
13
12
11
10
9
8
7
6
5
4
3
2
1
Z
Y

Figure 3.5. Typical cross section of temporary grandstand

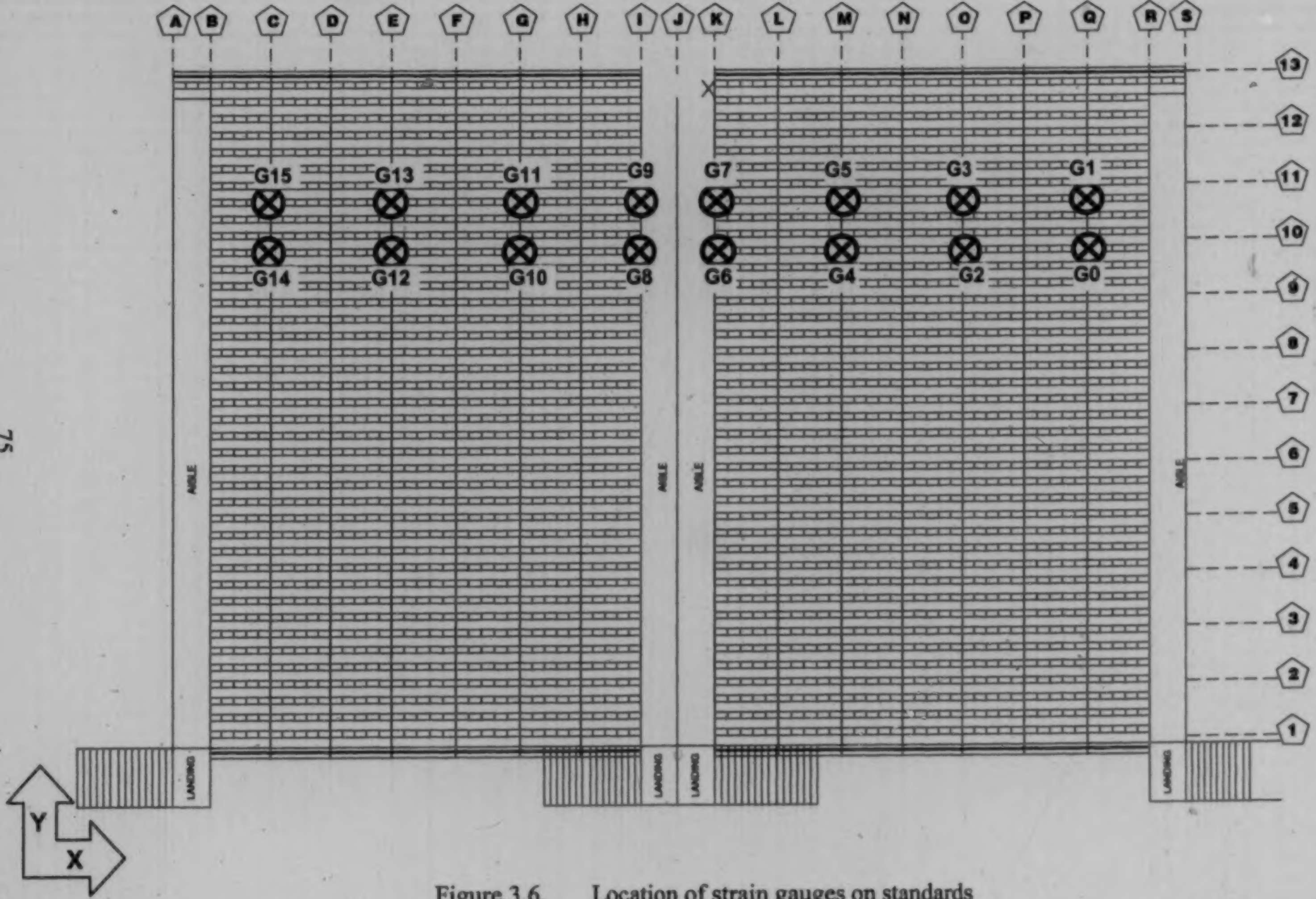
A
B
C
D
E
F
G
H
I
J
K
L
M
N
O
P
Q
R
S
13
12
11
10
9
8
7
6
5
4
3
2
1
G15
G13
G11
G9
G7
G5
G3
G1
G14
G12
G10
G8
G6
G4
G2
G0
AISLE
AISLE
AISLE
AISLE
LANDING
LANDING
LANDING
LANDING
Y
X

Figure 3.6. Location of strain gauges on standards

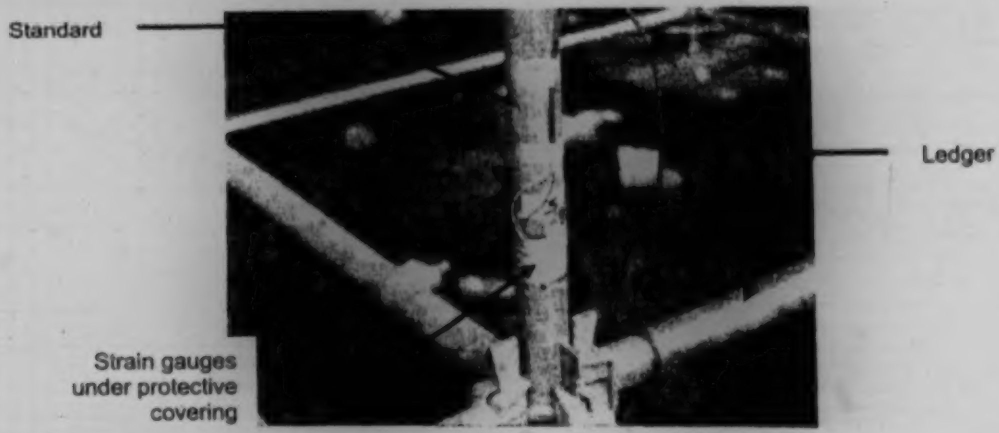
Standard
Ledger
Strain gauges under protective covering

Figure 3.7. Strain gauges mounted on standard

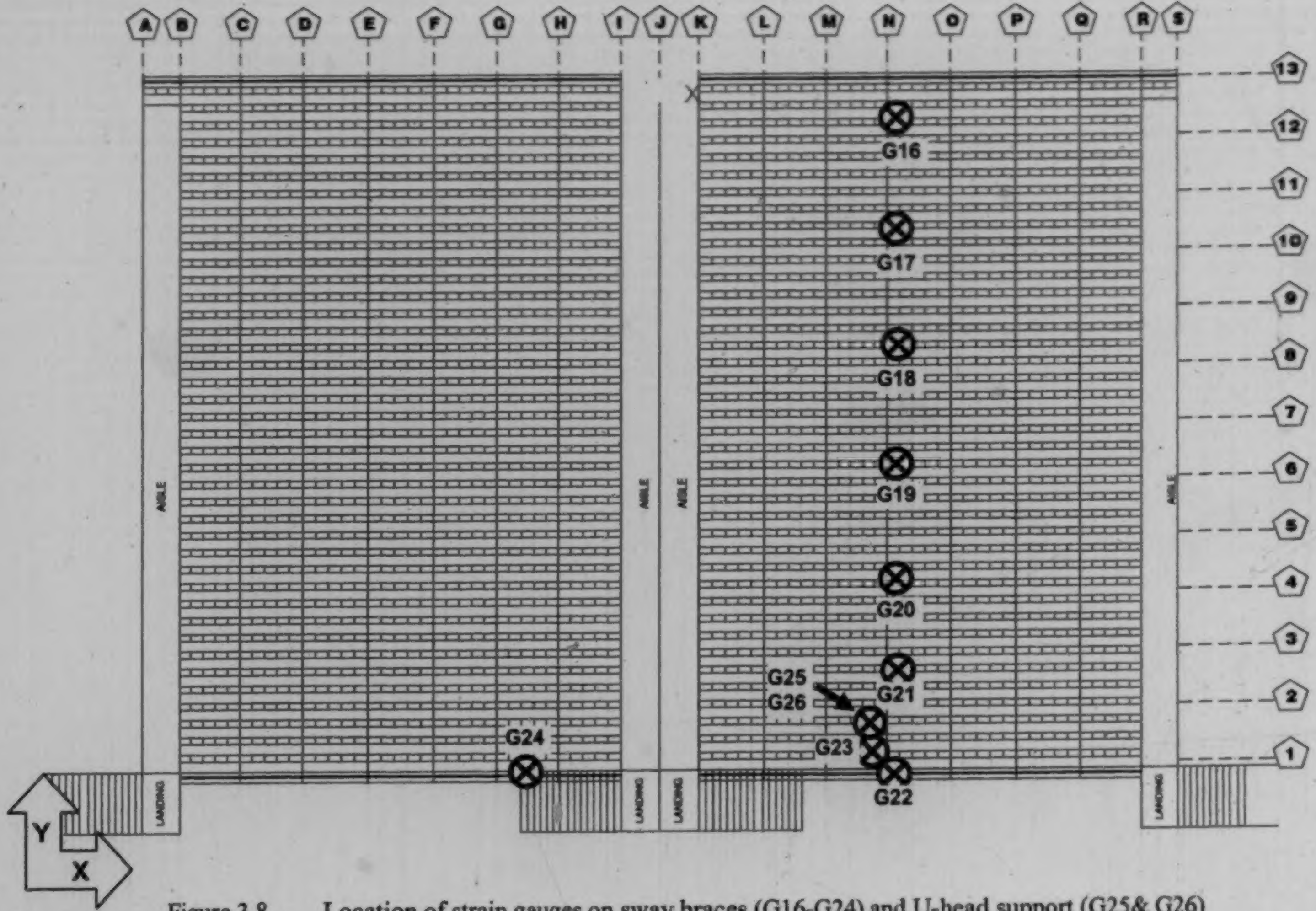
A
B
C
D
E
F
G
H
I
J
K
L
M
N
O
P
Q
R
S
13
12
11
10
9
8
7
6
5
4
3
2
1
AISLE
AISLE
AISLE
AISLE
LANDING
LANDING
LANDING
LANDING
G16
G17
G18
G19
G20
G21
G22
G23
G24
G25
G26
Y
X

Figure 3.8. Location of strain gauges on sway braces (G16-G24) and U-head support (G25& G26)

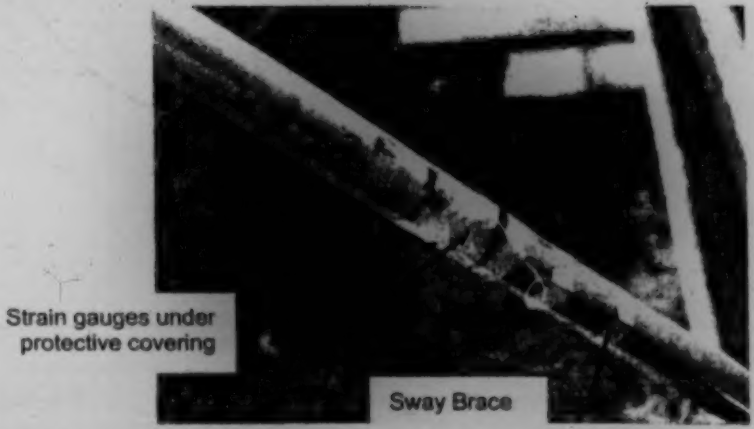
Strain gauges under protective covering
Sway Brace

Figure 3.9. Strain gauges mounted on brace

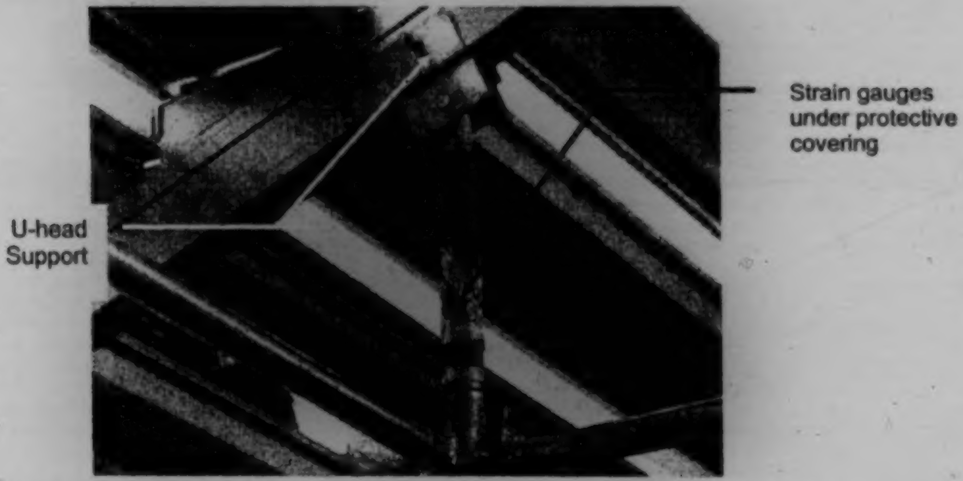
Strain gauges under protective covering
U-head Support

Figure 3.10. Strain gauges mounted on U-head post

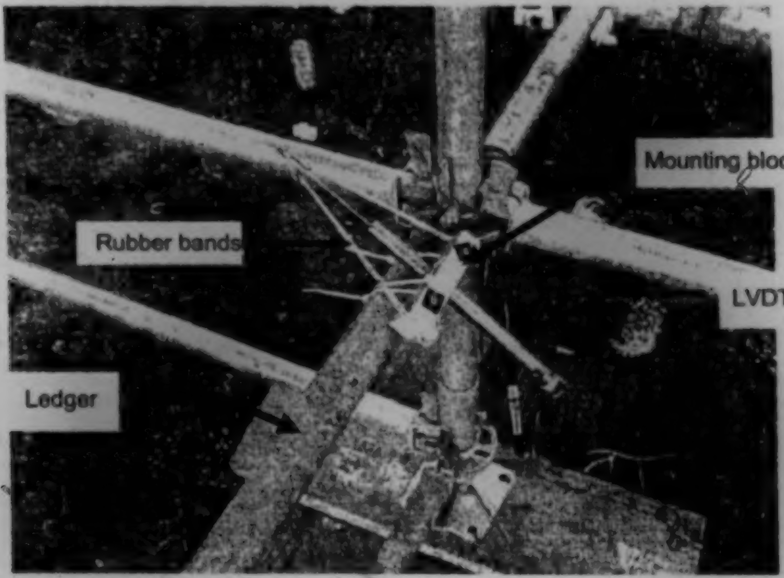
Mounting block
Rubber bands
LVDT
Ledger

Figure 3.11. LVDT attachment on the ledger near the base of the structure

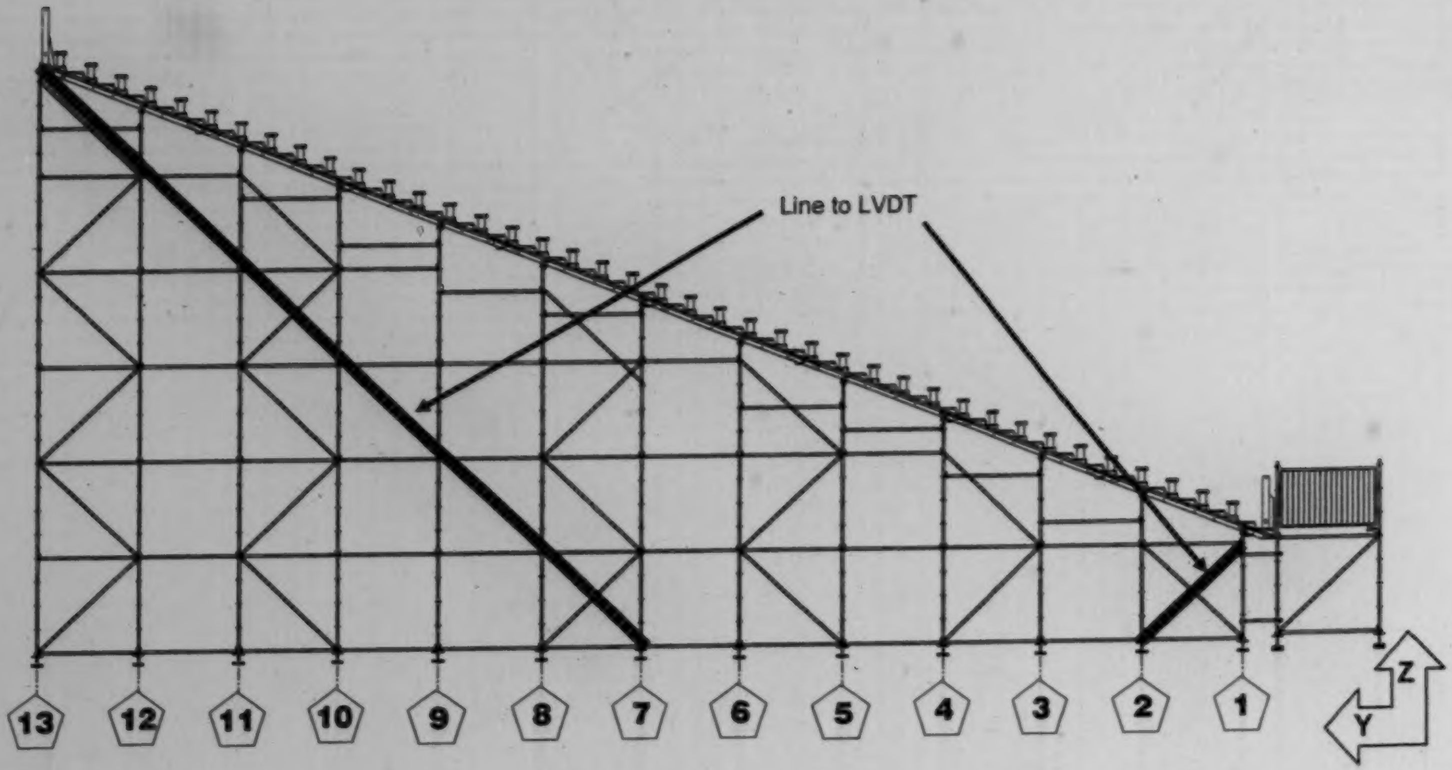
Line to LVDT
13
12
11
10
9
8
7
6
5
4
3
2
1
Z
Y

Figure 3.12. Side cross section showing line to LVDT to measure front-back sway motion

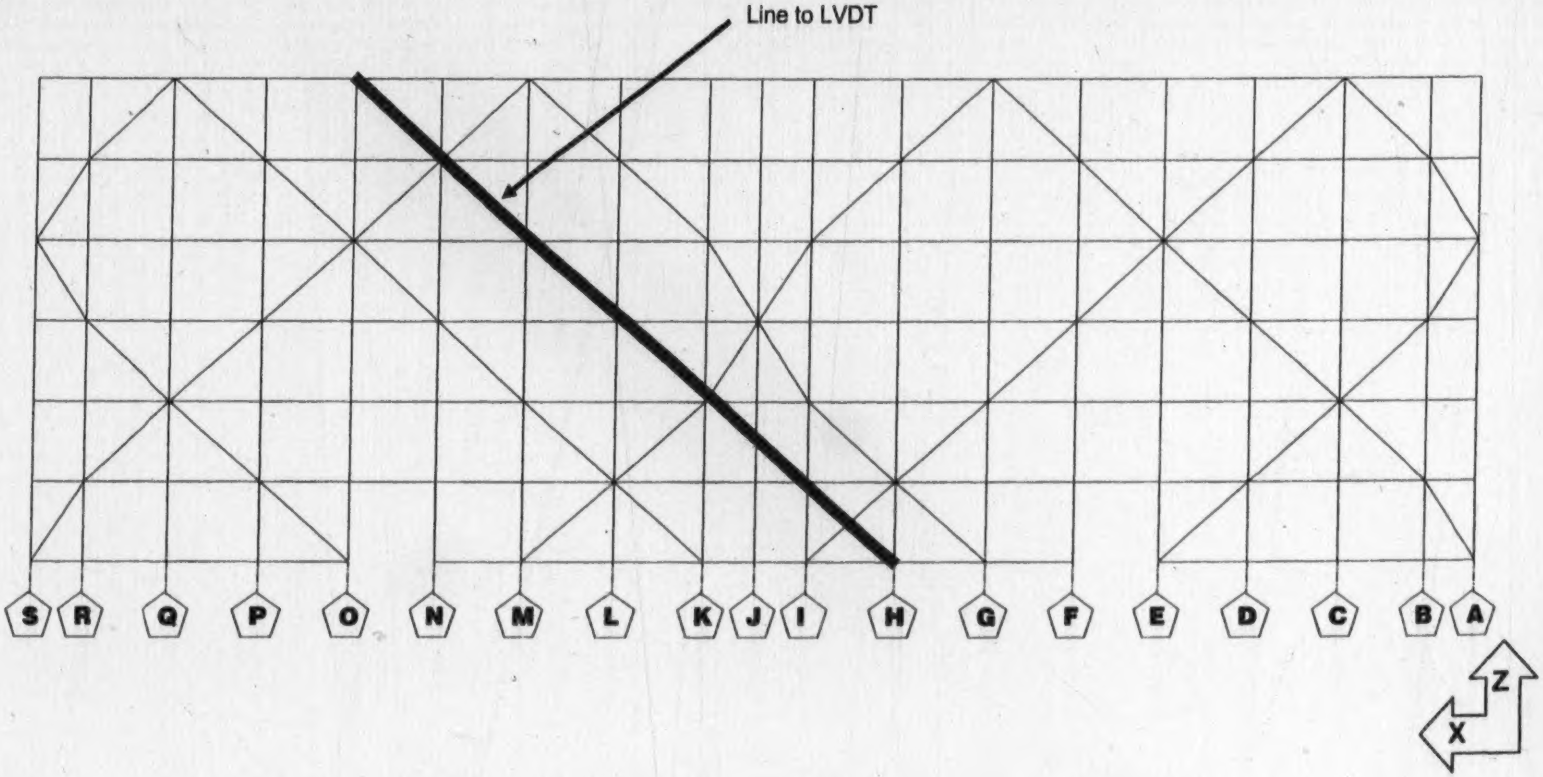
Line to LVDT
S
R
Q
P
O
N
M
L
K
J
I
H
G
F
E
D
C
B
A
Z
X

Figure 3.13. Rear cross section showing line to LVDT to measure side-side sway

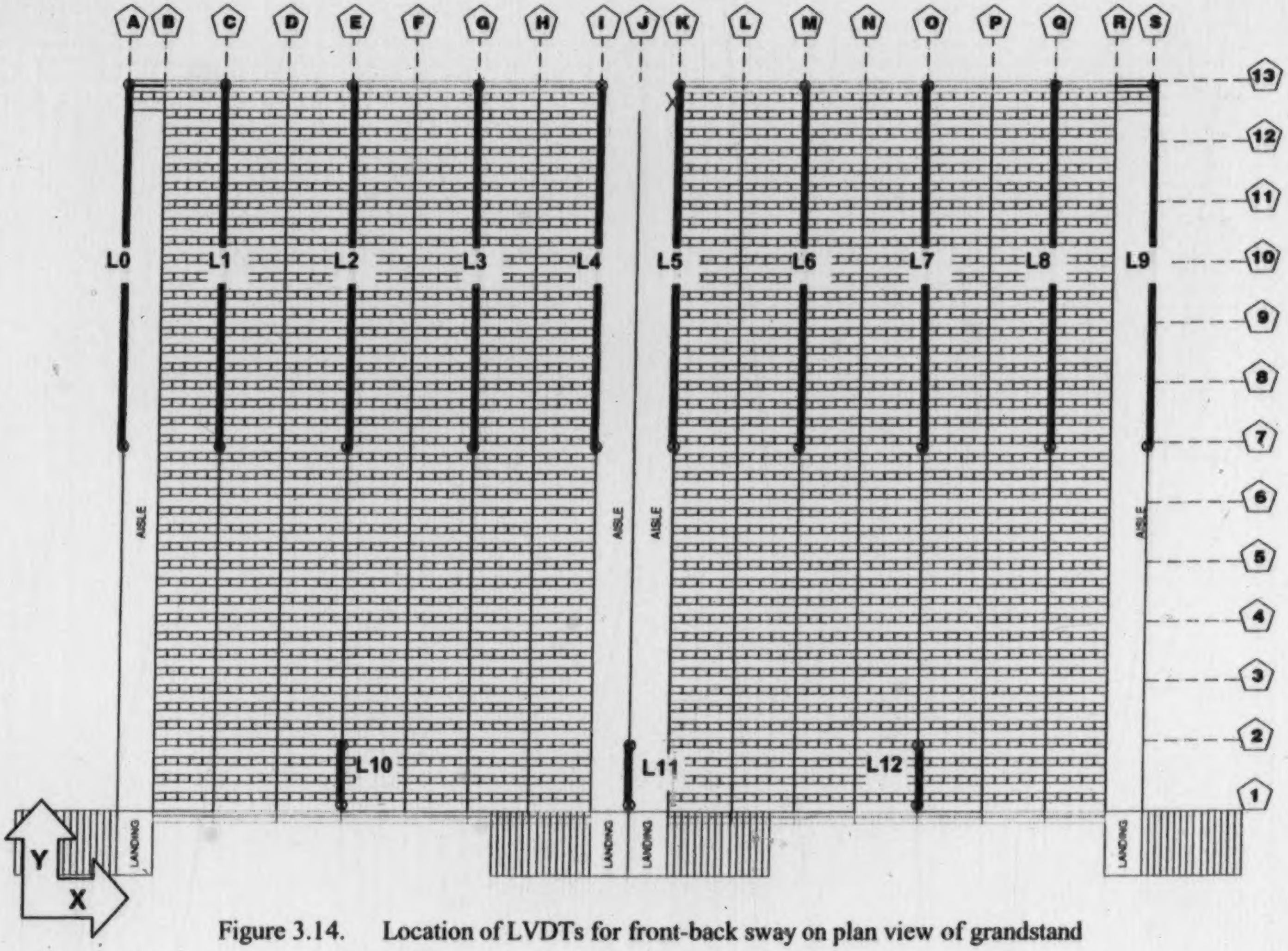
A
B
C
D
E
F
G
H
I
J
K
L
M
N
O
P
Q
R
S
13
12
11
10
9
8
7
6
5
4
3
2
1
L0
L1
L2
L3
L4
L5
L6
L7
L8
L9
L10
L11
L12
AISLE
AISLE
AISLE
AISLE
LANDING
LANDING
LANDING
LANDING
Y
X

Figure 3.14. Location of LVDTs for front-back sway on plan view of grandstand

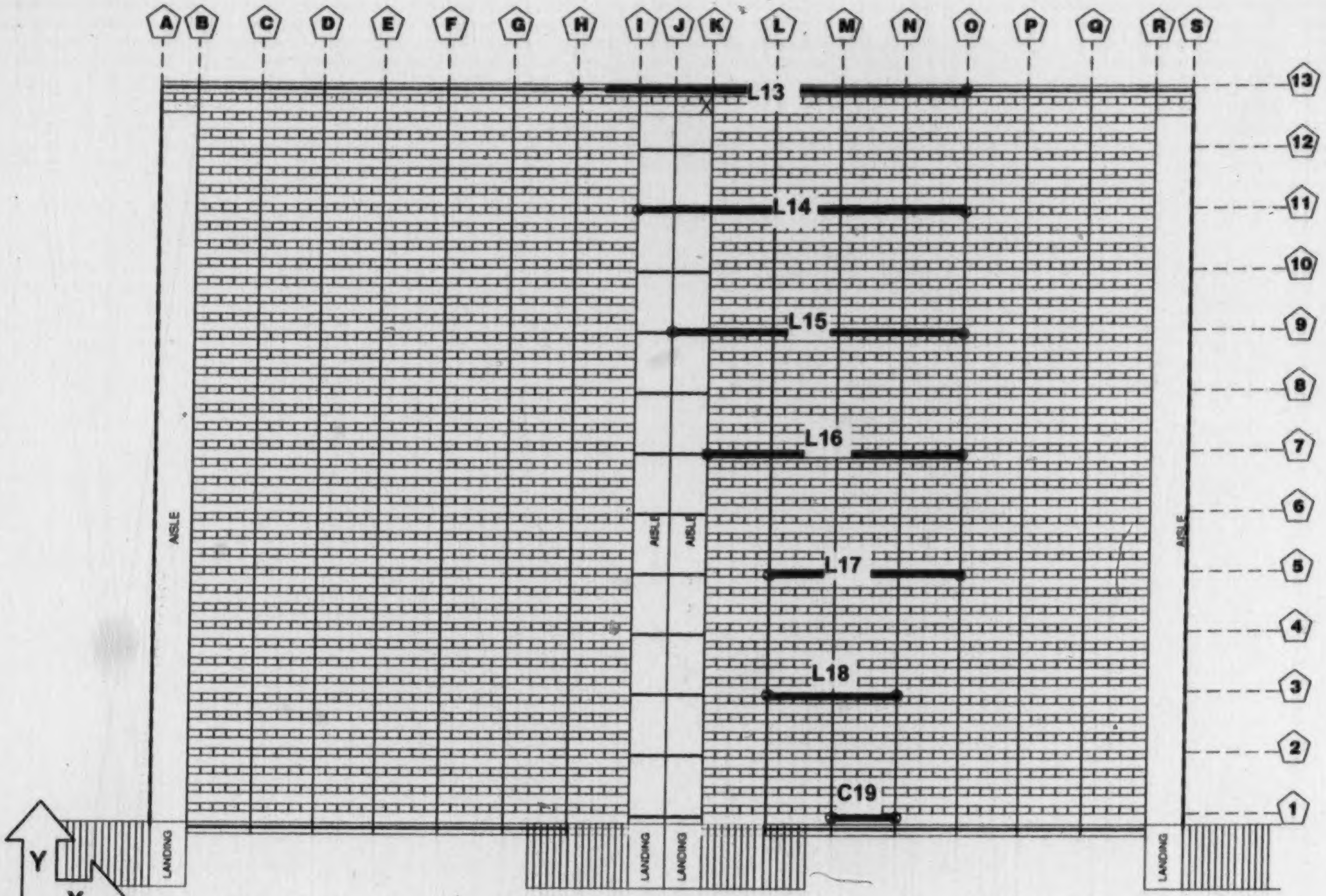
A
B
C
D
E
F
G
H
I
J
K
L
M
N
O
P
Q
R
S
13
12
11
10
9
8
7
6
5
4
3
2
1
L13
L14
L15
L16
L17
L18
C19
AISLE
AISLE
AISLE
AISLE
LANDING
LANDING
LANDING
LANDING
Y
X

Figure 3.15. **Location of LVDT measuring side-side sway on plan view of grandstand**

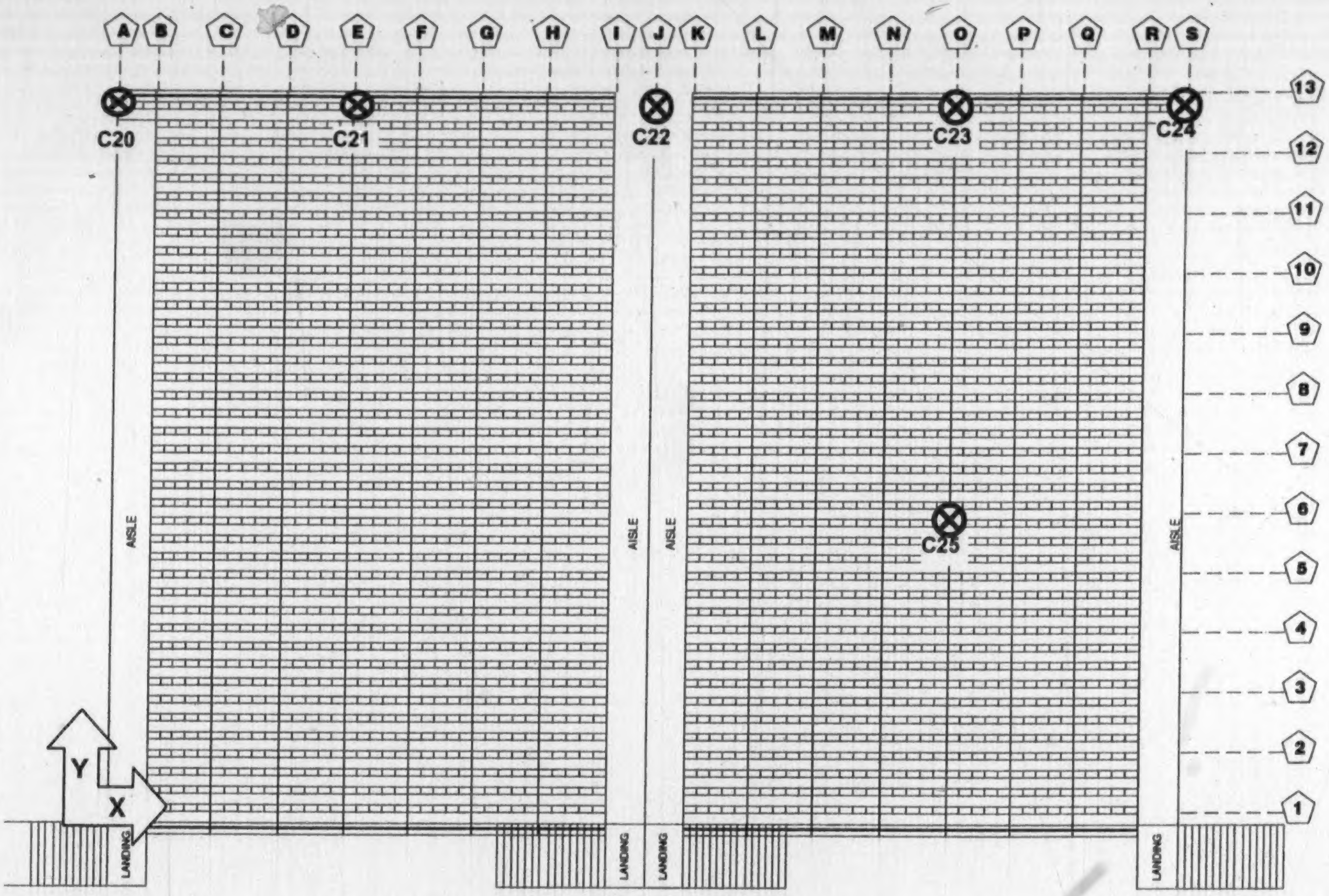
A
B
C
D
E
F
G
H
I
J
K
L
M
N
O
P
Q
R
S
13
12
11
10
9
8
7
6
5
4
3
2
1
C20
C21
C22
C23
C24
C25
AISLE
AISLE
AISLE
AISLE
LANDING
LANDING
LANDING
LANDING
Y
X

Figure 3.16. Location of cable transducers measuring vertical displacement on plan view of grandstand

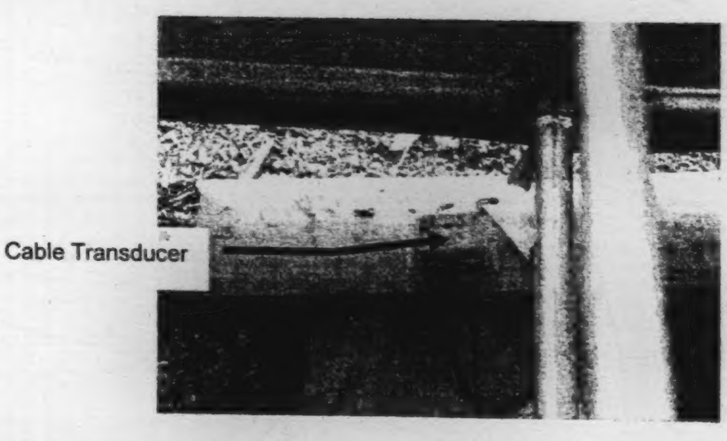
Cable Transducer

Figure 3.17. Cable transducer mounted at base of structure

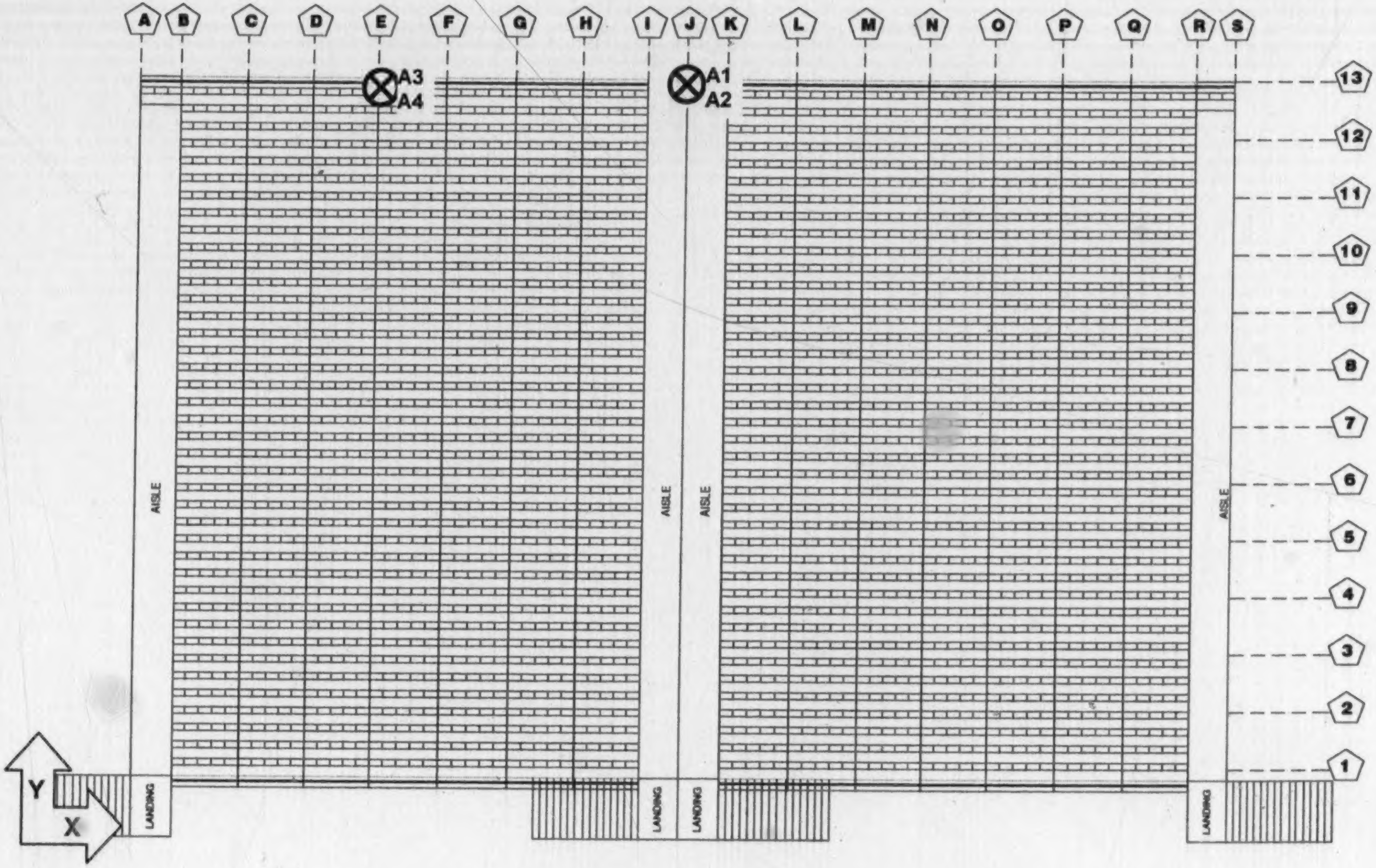
A
B
C
D
E
F
G
H
I
J
K
L
M
N
O
P
Q
R
S
13
12
11
10
9
8
7
6
5
4
3
2
1
A3
A4
A1
A2
AISLE
AISLE
AISLE
AISLE
LANDING
LANDING
LANDING
LANDING
Y
X

Figure 3.18. Location of accelerometers on plan view of grandstand

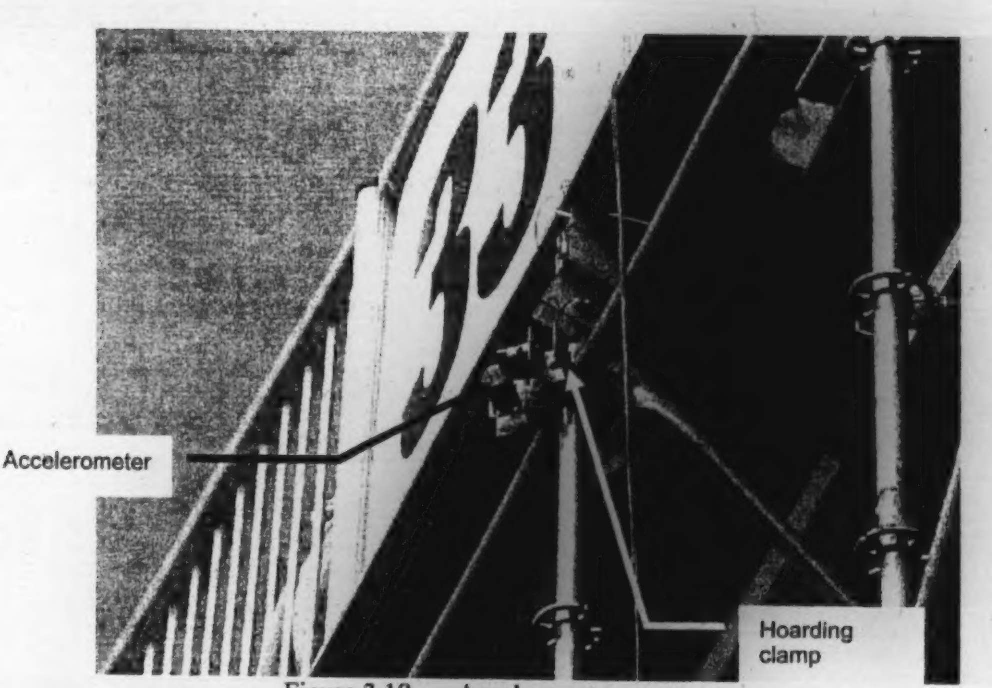
Accelerometer
Hoarding clamp

Figure 3.19. Accelerometers

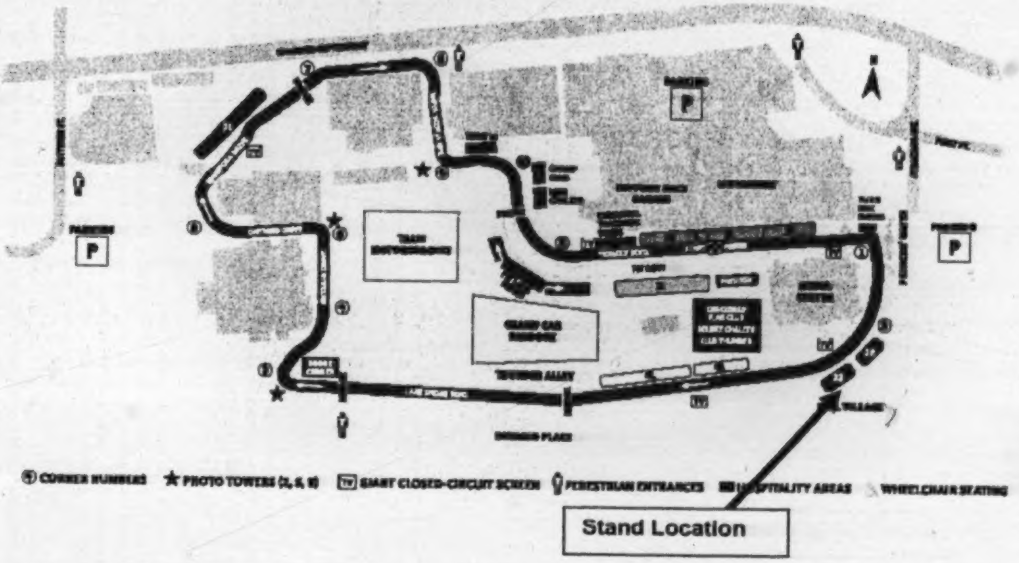
P
P
P
CORNER NUMBERS
PHOTO TOWERS (2, 6, 8)
GIANT CLOSED-CIRCUIT SCREEN
PEDESTRIAN ENTRANCES
HOSPITALITY AREAS
WHEELCHAIR SEATING
Stand Location

Figure 3.20. Track map for Molson Indy, location of grandstand highlighted in southeast corner.

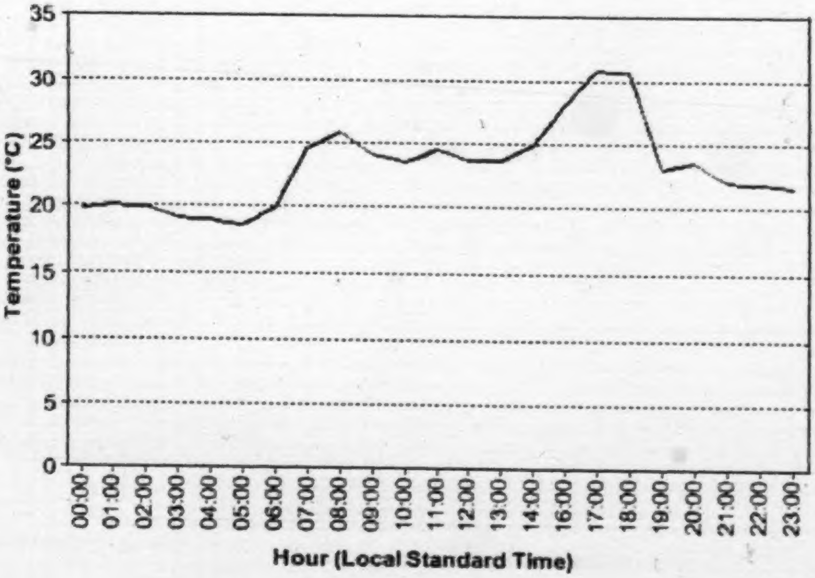

Figure 3.21. Temperature for July 18, 1999, as measured at Toronto City Centre Airport

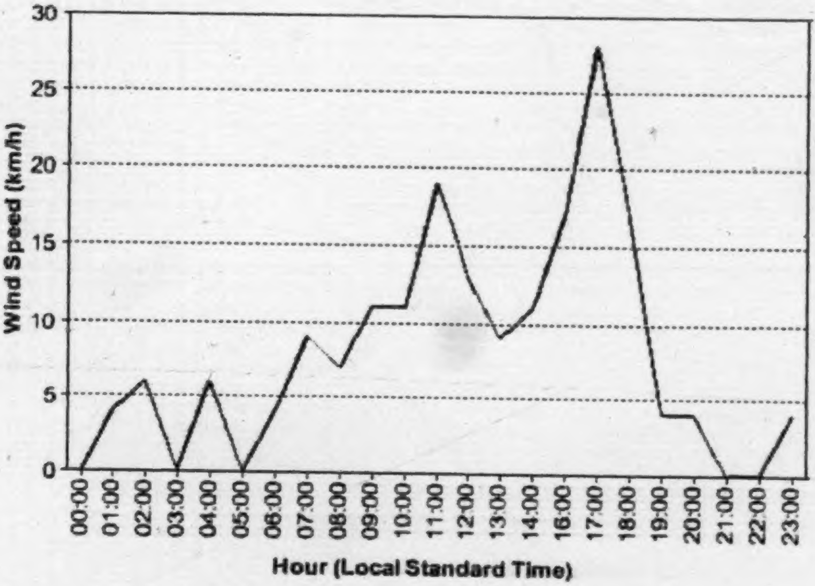

Figure 3.22. Hourly wind speed for July 18, 1999, as measured at the Toronto City Centre Airport

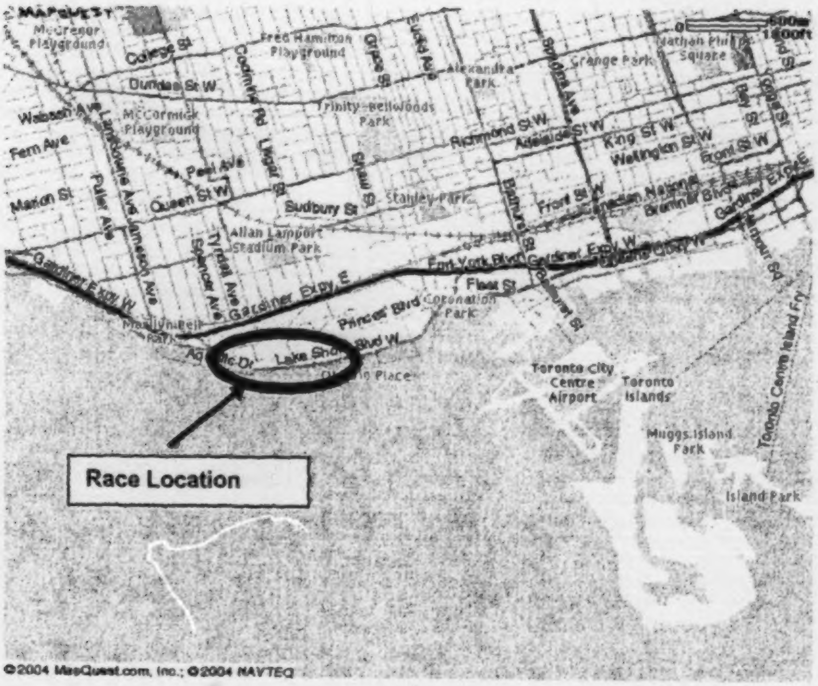
Race Location
Gardiner Expy W
Gardiner Expy E
Lake Shore Blvd W
Princes' Blvd
Queen St W
Dundas St W
College St
Toronto City Centre Airport
Toronto Islands
Coronation Park
©2004 MapQuest.com, Inc.; ©2004 NAVTEQ

Figure 3.23. Map of track location in Toronto

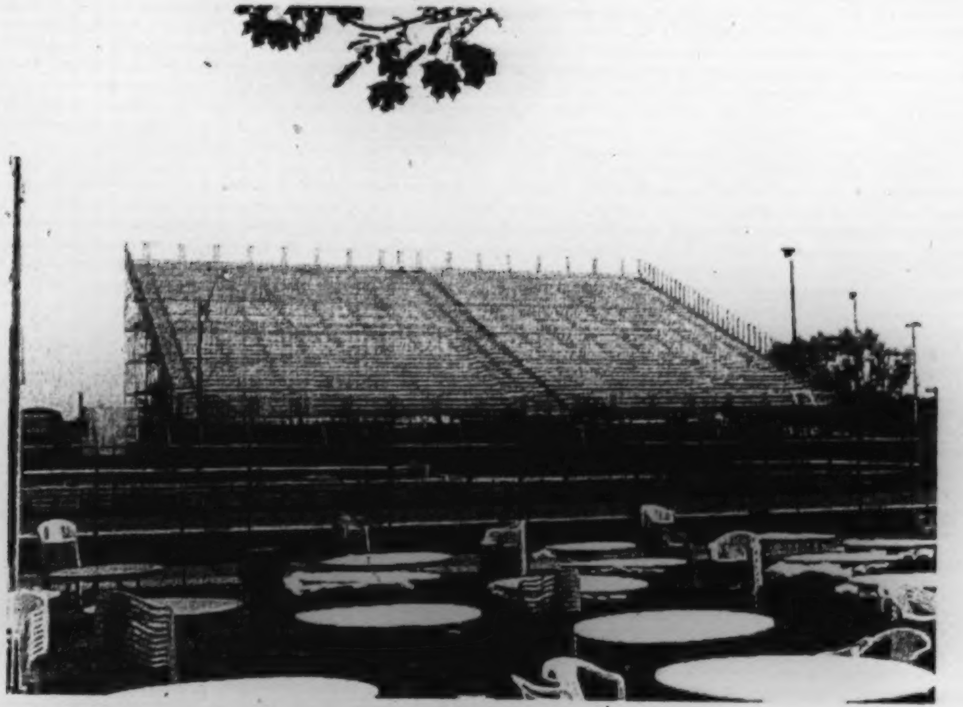

Figure 3.24. Temporary grandstand empty

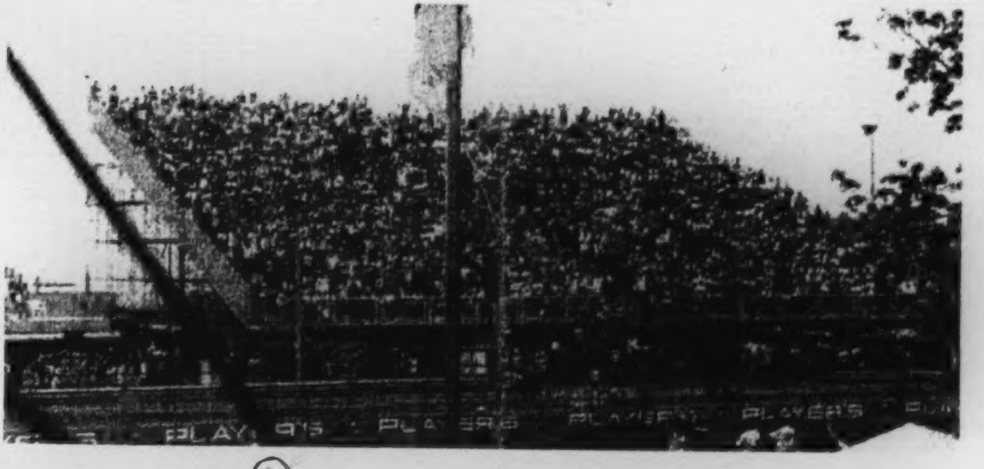
PLAYER'S
PLAYER'S
PLAYER'S
PLAYER'S

Figure 3.25. Temporary grandstand full

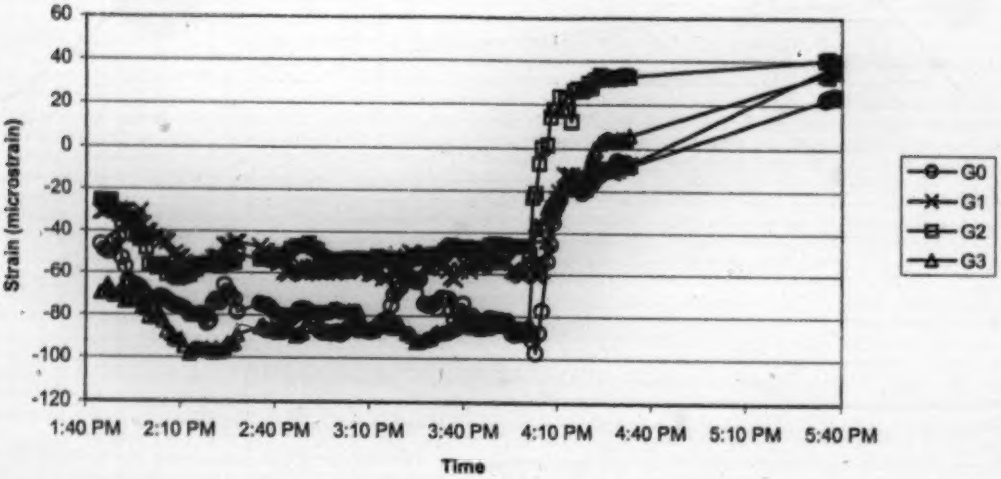

Figure 3.26. Recorded strains - standards G0 to G3

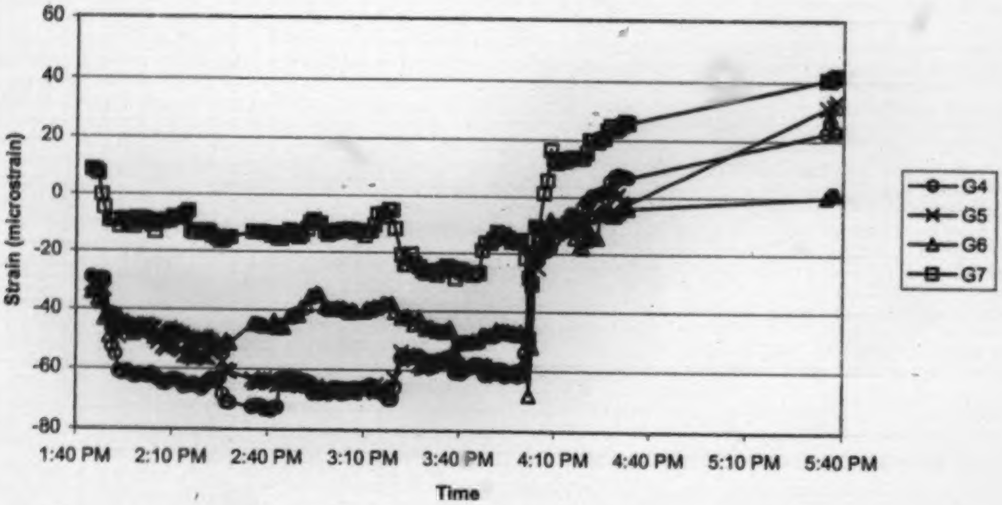

Figure 3.27. Recorded strains - standards G4 toG7

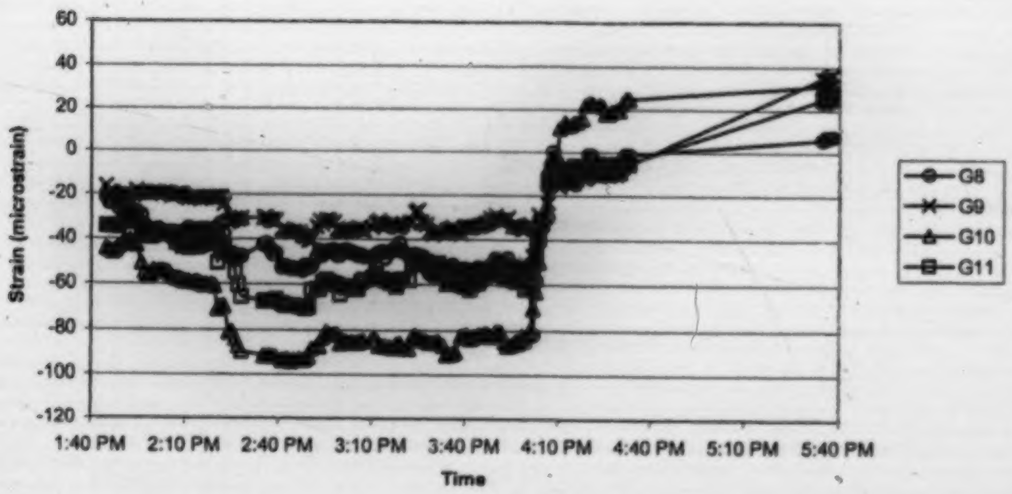

Figure 3.28 Recorded strains- standards G8 to G11

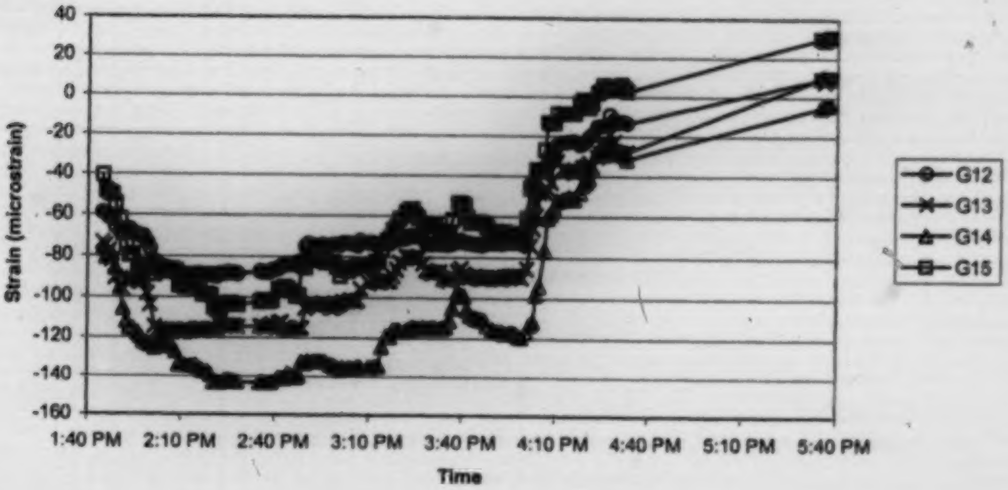

Figure 3.29. Recorded strains - standards G12 to G15

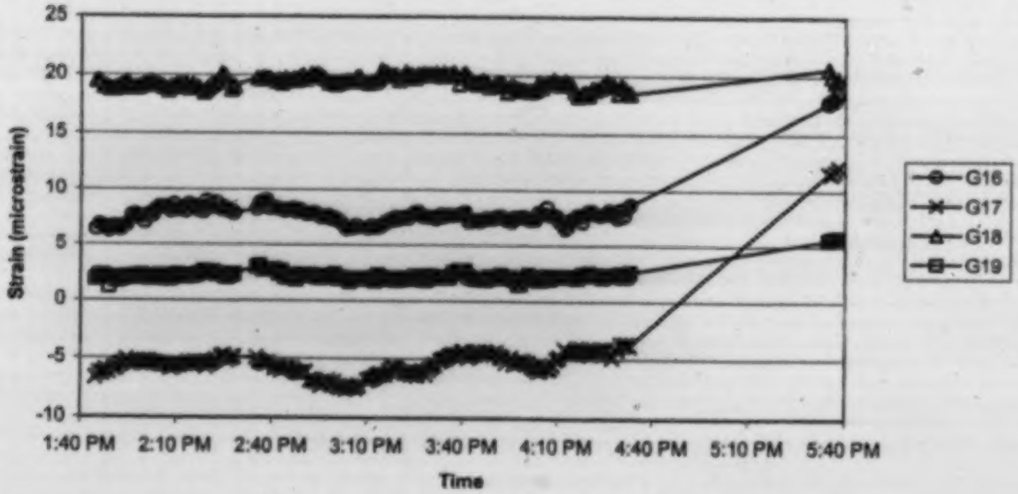

Figure 3.30. Recorded strains - sway braces G16 to G19

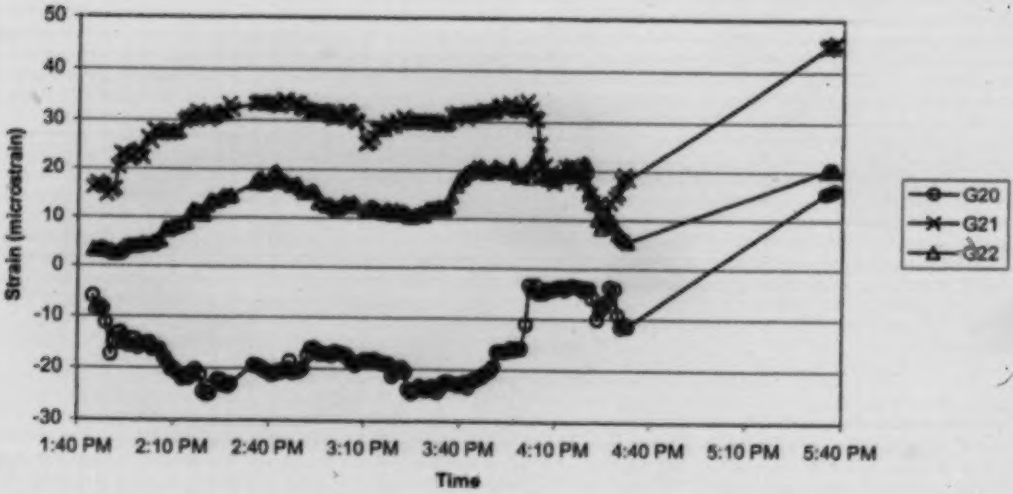

Figure 3.31. Recorded strains - sway braces G20 to G22

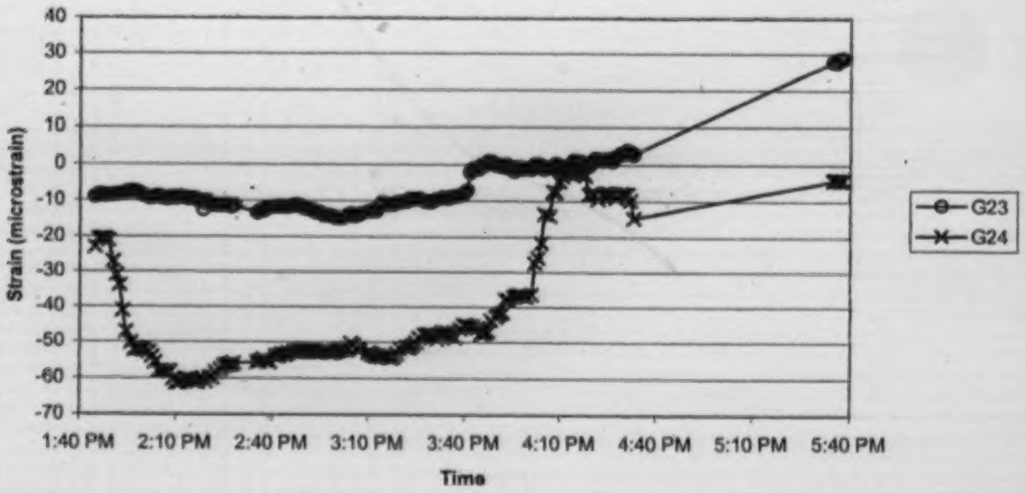

Figure 3.32. Recorded strains - sway braces G23 to G24

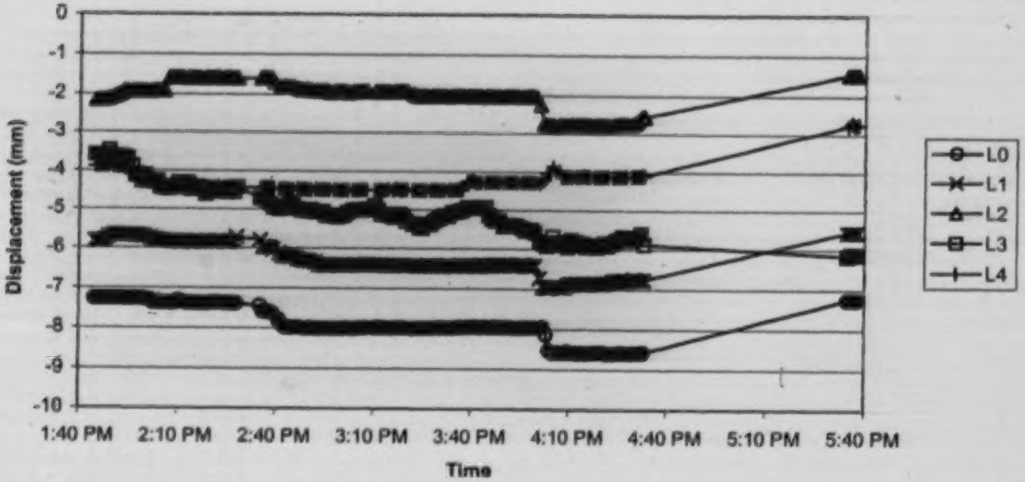

Figure 3.33. LVDT front-back sway displacement L0 to L4

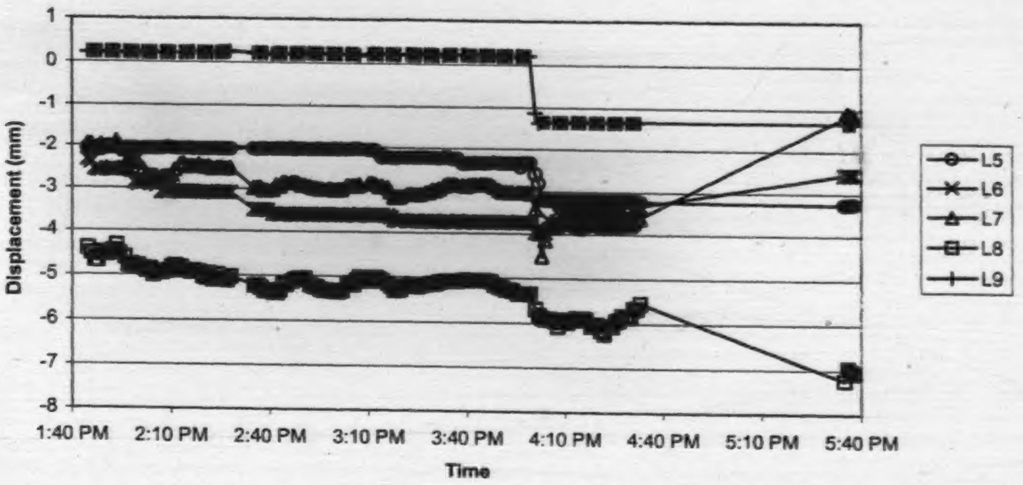

Figure 3.34. LVDT front-back sway displacement L5 to L9

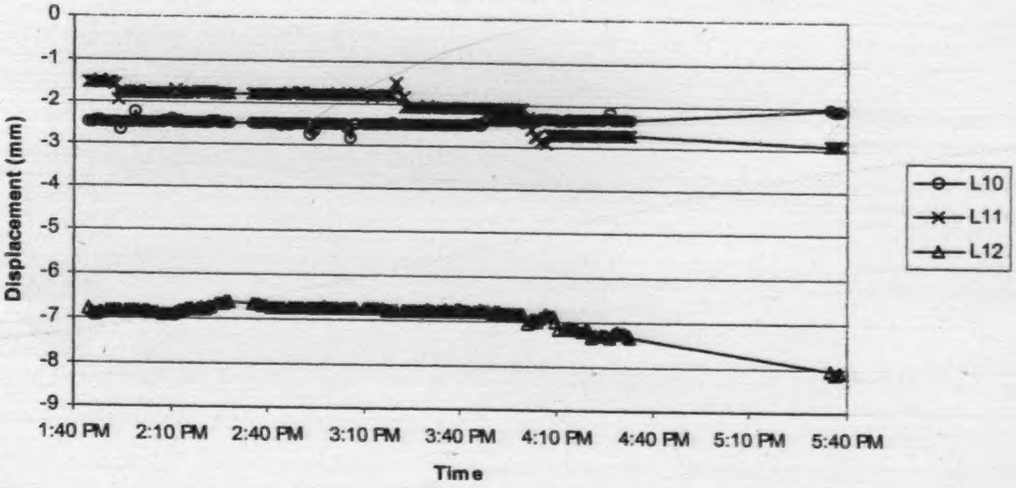

Figure 3.35. LVDT front-back sway displacement L10 to L12

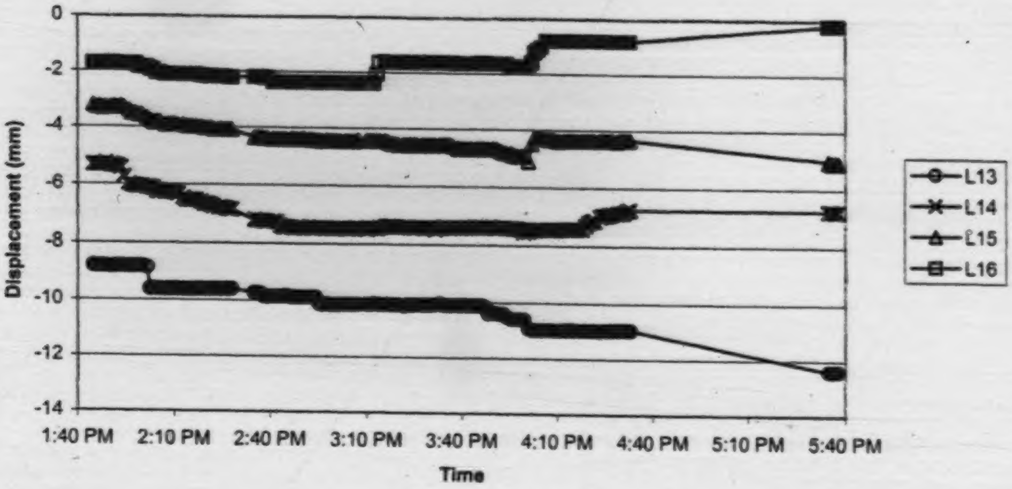

Figure 3.36. LVDT side-side sway displacement L13 to L16

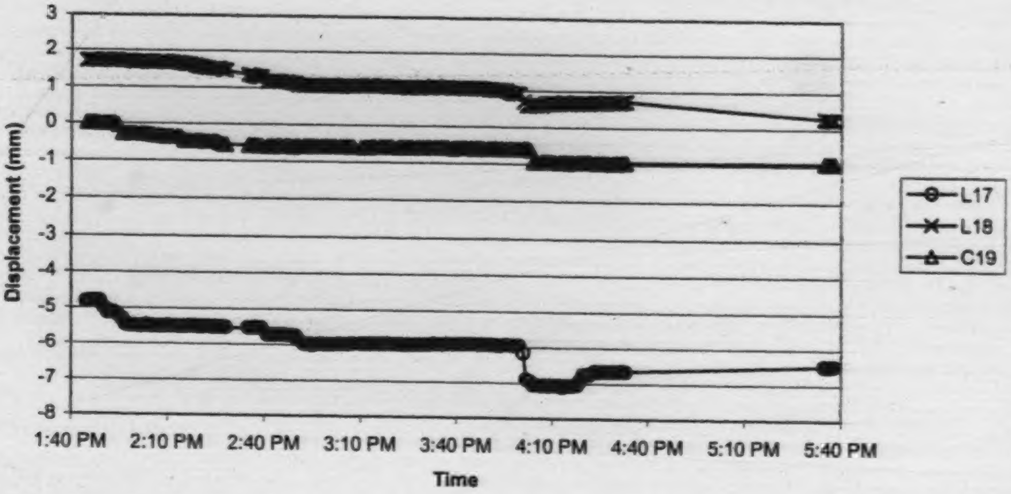

Figure 3.37. LVDT side-side sway displacement L17 to C19

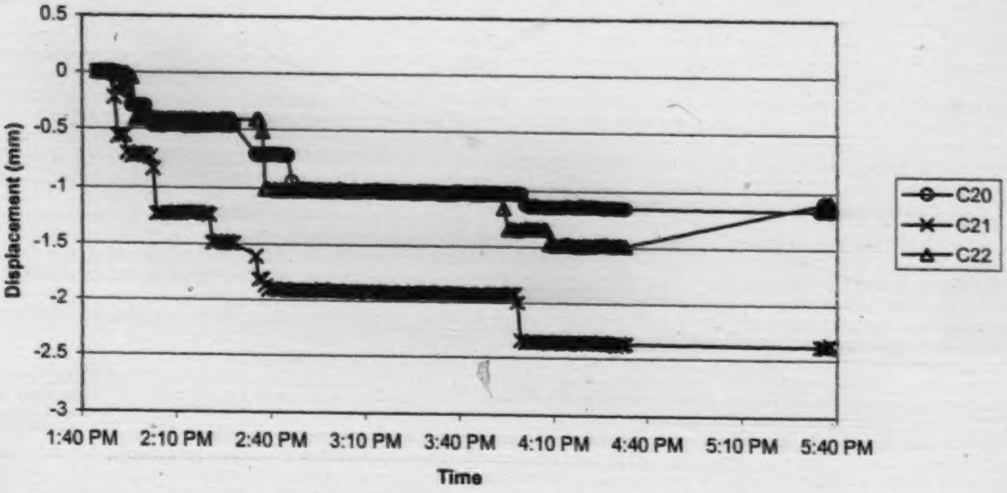

Figure 3.38. Cable transducers vertical displacement C20 to C22

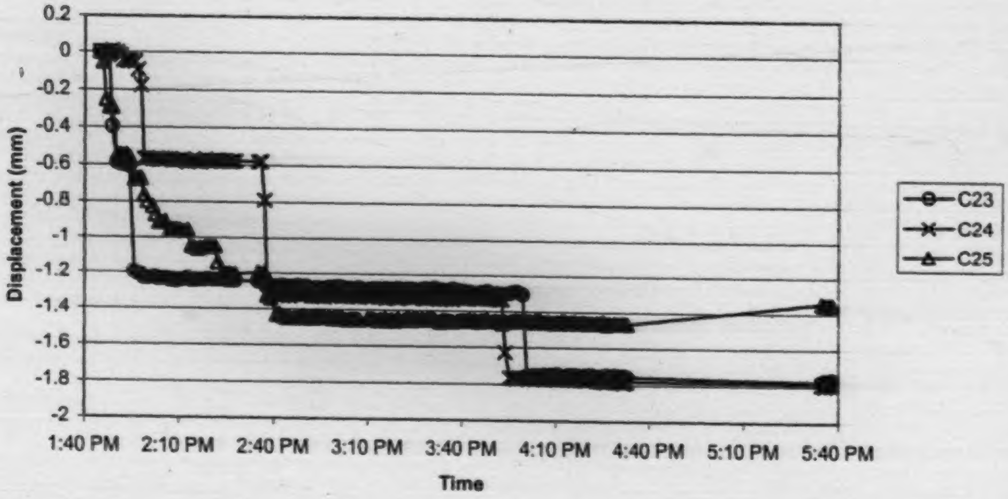

Figure 3.39. Cable transducers vertical displacement C23 to C25

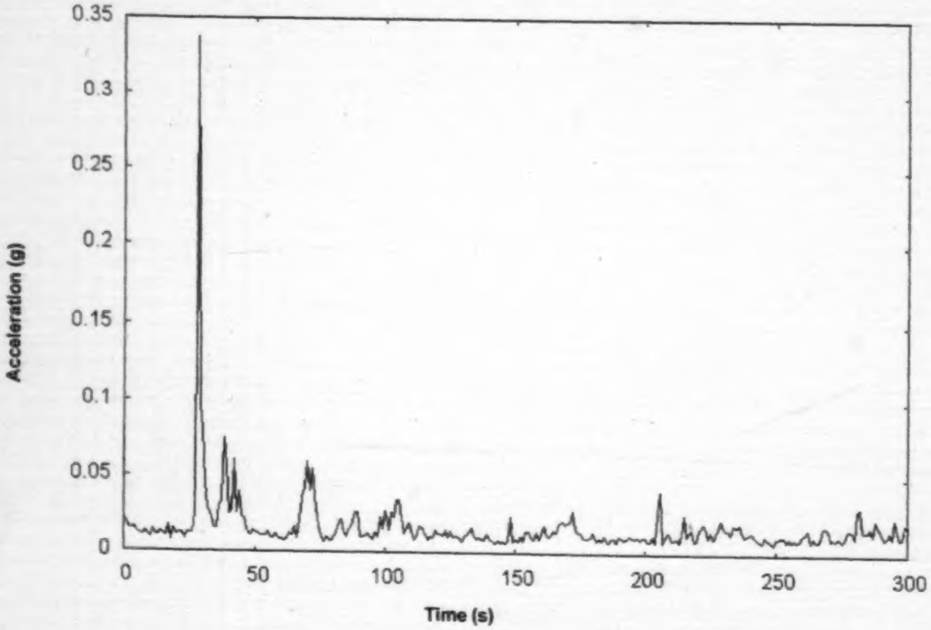

Figure 3.40. Running Root-Mean-Square accelerations for data set 3:32

4 NATURAL FREQUENCY AND MODE SHAPE

4.1 Introduction

The affect of occupant induced vibration is of greatest concern when it occurs at a frequency that is close to the natural frequency due to the potential for resonance. Resonance can amplify the vibration causing large displacements that could cause structural damage, or potentially worse, panic. It is the purpose of the dynamic property measurement to identify the natural frequency and mode shape of the temporary structure from the output-only signal data.

A simple method of identifying the natural frequency is visually observe the power spectral density plots of the output signal and picking the clearly identifiable peaks, referred to as "peak-picking". However, there are potential problems with this method since the peaks may be due to other sources such as noise, interference, or forcing vibrations. So it is not sufficient to identify only the frequency, it is also necessary to identify a mode shape. Identifying the mode shape requires more sophisticated analysis than peak picking and several different methods are available that are discussed later in this chapter.

4.2 Ambient Vibration Survey

An Ambient Vibration Survey relies on the ambient vibration from various sources to excite the structure and only the response of the structure is measured. Therefore, it requires output-only signal analysis to identify the dynamic properties for the structure from the response data.

For this research the ambient vibration survey method was chosen over forced vibration methods since it is relatively inexpensive and it was anticipated that the occupants' movement would provide sufficient ambient vibrations to excite the structure. The movements of the occupants may be synchronized, as when participants rise for the national anthem, dancing or swaying to music; or they may be random due to individuals shifting in their seats or moving about the grandstand. When the grandstand is unoccupied, the excitation of the structure will rely on ambient sources of vibration such as noise, traffic, and wind. Since we are relying only on the response of the structure there is no direct information on the excitation level or how it is distributed on the structure. However, one of the assumptions for the output-only analysis is that the excitation spectrum will be relatively smooth across all frequencies. With output-only analysis care must be taken to not misinterpret the dominant frequencies in the ambient excitation spectrum (such as due to vortex shedding, adjacent machinery, or by the occupants) for the fundamental frequency [IStructE, 2002]

A concern with using ambient vibration survey for this research was that the structural damping caused by the looseness of the scaffold joint connections may over-damp low level vibration. Since the magnitude of the ambient vibration due to spectator movement is not known, the effect of damping can not be anticipated. It has been suggested that the looseness in the connections is reduced when the structure is loaded [Godley and Beale, 2001. So, the over-damping may only be a concern for the measurements of the empty grandstand.

4.3 Natural Frequencies

All of the data sets were used to generate power spectra plots for each of the instruments (Appendix A). The power spectra plots are based on spectral estimates of the power spectra. The spectral estimates are used to reduce the statistical variability and to smooth the power spectra at the risk of reduced amplitude and resolution. The spectral estimates were made using Welch's Spectral Estimation technique [Welch, 1967]. The power spectra are shown using the decibel scale for magnitude, which is a logarithmic scale of the relative power, and frequency (Hz).

Potential natural frequencies were identified by "peak picking" of the power spectra of each of the instruments. Natural frequencies in the power spectra appear as peaks when the power is plotted versus frequency. By observation it is possible to identify specific frequencies that appear repeatedly on several power spectra. Many of these peaks appear repeatedly in the power spectra of instruments and across several data sets.

The peak picking was limited to frequencies below 6 Hz. For the grandstand the frequencies below 6 Hz are of the greatest interest due to the potential for resonance effects. Frequencies above 6 Hz are less of concern because they are not sustainable by crowd action and would therefore not be subject to resonance effects [IStructE, 2001].

For most of the data sets, the strain gauges and accelerometers have few significant peaks below 6 Hz, this may be due to the low amplitude of vibration (small displacement). When sway displacement is the dominant mode, it would be expected that the strain gauges on the standards (vertical members) would not be sensitive to the vibration, since the movement is perpendicular to the direction of the members. The strain gauges mounted on the sway braces may not record significant strain for small sway displacements, due to the looseness of the brace connections. Also, small displacements at low frequencies produce very low levels of acceleration. Therefore the accelerometers would not be sensitive to the low amplitude vibration. The LVDTs however, were arranged to measure the sway displacement, and had greater sensitivity to this mode of vibration. Hence, most of the peaks are observed in the power spectra of the LVDTs.

4.3.1 Fundamental Natural Frequency

A fundamental natural frequency of 2.0 Hz was observed in the 4:05 data set. This coincided with the end of the race when people were exiting the grandstand, as observed by the static readings. The simultaneous movement of the spectators towards the exit may have resulted in an increased excitation level. This frequency was not observed in any other data set. However the frequency was recorded by a wide range of instruments including strain gauges, LVDTs, and accelerometers.

The fundamental natural frequency was most prominent on strain gauges G2 to G5, with lower magnitude signals on strain gauges: G0, G1, G7, G8, G9, G22, and G23.

LVDT L6 to L8 and L12, and accelerometers A1 to A3 show significant peaks at the frequency. Figure 4.1 shows the power spectra for these instruments.

Based on the location of the instruments that recorded the fundamental frequency, the mode of vibration affected only half of the grandstand. This half of the grandstand differed from the other half of the structure since the entire base was lowered 0.5 m (and the lower 0.5 m was unbraced). The other half of the structure had part of the base at the proper elevation which may have made the base stiffer.

4.3.2 Higher Frequencies

Other peaks were observed in the power spectra at higher frequencies. These peaks were observed over a wide range of data sets, unlike the fundamental frequency. These frequencies varied slightly with each data set but had approximate values of 2.9, 3.7, and 4.1 Hz. Table 4.2 lists the peaks observed by data set for race day (July 18). These same frequencies were observed the day before the event (July 17) when the grandstand was empty, as listed in Table 4.2. The average values for the frequencies for the empty grand stand were 3.1, 3.9, and 4.1, indicating a slight shift in the lower frequencies. Figure 4.2 to 4.5 shows the typical power spectra plots with these peaks for the full stand and the empty stand. With the stands full or empty the peaks show a very sharp with very high damping. The amplitude of the peaks for the full stand was typically higher than for the empty stand.

The higher frequencies also appear in the power spectra of the voltage channels. This may indicate that these frequencies were due to noise from the power supplies. However, the peaks were observed at different channels at and at different times. Some channels show only one peak and others have all three, and some channels show peaks in one data set but not another. Also amplitude of the peaks is smaller for the empty grandstand than for the occupied grandstand, which suggests that the peaks related to the excitation level. Therefore, it is unlikely that these peaks are the result of noise created by the power supplies.

4.4 Frequency Domain Decomposition

To determine the dynamic parameters of the grandstand the Frequency Domain Decomposition (FDD) technique will be applied to the fundamental frequency (2.0 Hz). This frequency showed a strong response in terms of amplitude and damping, so it should yield the best estimate of the dynamic parameters. The Frequency Domain Decomposition analysis was performed using Matlab for the numeric processing.

First the Frequency Domain Decomposition technique will be applied to the data from the accelerometers and then the data from the LVDTs. The two results will be compared and should be similar if they are measuring the same mode of vibration.

The signals from two accelerometers, A1 and A2, will be used for spectral identification. The two accelerometers were located at the same point (Figure 3.18) and were oriented orthogonal to each other, which eliminates any coupling due to twisting of the structure. The accelerometers are on the same plane measuring acceleration in X and Y directions. Since only two accelerometers were used the vibration model will have 2 degrees of freedom

The first step of the Frequency Domain Decomposition process is to create spectral estimates of the signals. The spectral estimates are performed using the Welch's Spectral Estimation technique; this technique uses averaged periodograms of overlapped windowed signals. The Matlab function, *pwelch,* is the implementation of this technique for the estimation of power spectrums. The degree of smoothing is controlled by the functions variable, *window*. Increasing the value of *window* reduces the smoothing but increases the resolution. For the spectral estimates of the accelerometers, *window* was set to 1024. Their power spectral estimates are shown in Figures 4.6(9) and (10).

The next step of the Frequency Domain Decomposition technique is to perform a singular value decomposition of the spectral matrix. The singular value decomposition separates noisy data from disturbances caused by un-modeled dynamics and measurement noise [Tamura, 2002]. The singular value decomposition breaks the signal down into component parts based on the number of DOF. For the 2 DOF system, two singular vectors are created. The first singular vector is the best estimate of the power spectrum of the SDOF system. A plot of the two singular vectors is shown in Figure 4.7. A peak is manually picked from the first singular vector and a portion of the estimate is identified using the Modal Assurance Criterion function (Equation 4.2) to compare points around the peak with the other singular vectors. A MAC threshold value of 0.85 was used for this analysis. Those points that have a MAC value above the threshold are retained and the remaining points are assigned zero. This isolates the *bell* associated with the particular peak. The identified portion of the estimate is shown in Figure 4.8

The identified portion of the SDOF is then returned to the time domain by using an IFFT function. A plot of the time domain free decay is shown in Figure 4.9. The damped natural frequency is determined by the crossing times, and the damping coefficient is determined by the logarithmic decrement method of the peaks. Using the Equations 4.4 to 4.6 the undamped natural frequency was determined to be 2.03 Hz and the damping coefficient was 0.10.

$$\begin{aligned}
&k = 6 \\
&r_0 = 1.03\times10^{-4} \\
&r_k = 1.41\times10^{-5} \\
&\delta = \frac{2}{6}\ln\left(\frac{1.03\times10^{-4}}{1.41\times10^{-5}}\right) = 0.663 \\
&\zeta = \frac{\delta}{\sqrt{\delta^2+4\pi^2}} = 0.10 \\
&f_d = 2.016Hz \\
&f = \frac{f_d}{\sqrt{1-\zeta^2}} = 2.03
\end{aligned}$$

where:

r_0 is the initial value of the decay function,

r_k is the kth value of the decay function,

δ is the logarithmic decrement,

ς is the damping ratio,

f_d is the damped natural frequency, and

f is the natural frequency.

A similar procedure was performed for the LVDT measurements. In this case the measured data are sway displacements and each point represents a displacement in the X or Y direction. In this case there were 20 discrete locations along the edge of the grandstand, so the vibration model will have 20 degrees of freedom. However three of the degrees of freedom are redundant since they represent the LVDTs on the front of the grandstand and are measuring the same sway along the same bay as the LVDTs at the rear.

The spectral estimates of the LVDT data were produced using the Welch's technique for spectral estimates. The LVDTs signal required less smoothing than the accelerometers so a *window* value of 3000 was used to improve the resolution. The spectral matrix was decomposed using the singular value decomposition method. For this case the 20 DOF system resulted in 20 singular vectors as shown in Figure 4.10. The peak, corresponding to the fundamental frequency, was picked in the first singular vector. A MAC threshold value of 0.93 was used to identify the portion of the first spectral estimate, shown in Figure 4.11. The spectral estimate was returned to the time domain by use of the IFFT. From the peak and crossing times of the free decay, the frequency and the damping were calculated; the free decay is shown in Figure 4.12. The undamped natural frequency was 2.11 Hz and the damping coefficient was 0.204.

$$k = 8$$

$$r_0 = 8.17 \times 10^{-8}$$

$$r_k = 4.34 \times 10^{-10}$$

$$\delta = \frac{2}{6} \ln\left(\frac{8.17 \times 10^{-8}}{4.34 \times 10^{-10}}\right) = 1.309$$

$$\zeta = \frac{\delta}{\sqrt{\delta^2 + 4\pi^2}} = 0.2$$

$$f_d = 2.00 Hz$$

$$f = \frac{f_d}{\sqrt{1 - \zeta^2}} = 2.11$$

The results from the 2 DOF case and the 20 DOF case were close with an undamped natural frequency of 2.03 Hz and 2.11 Hz, respectively. The damping coefficient estimates for the two cases were 0.10 and 0.20 respectively. The results for the 20 DOF model should be more accurate because it involves more degrees of freedom. . These results indicate that the accelerometers and the LVDTs are measuring the same mode of vibration.

4.5 Mode Shape

The LVDTs were located on the structure on alternate bays. So, only the displacements of those bays were recorded and the displacements of the intermediate bays are unknown. Therefore, higher mode shapes might not be plotted correctly due to insufficient degrees of freedom. For lower frequencies, fewer degrees of freedom are required to model the mode shape. Therefore, sufficient resolution should be available to plot the mode shape for the fundamental frequency. So, for this analysis only the mode shape for the fundamental frequency will be identified.

To model the mode shape of the grandstand, it will be represented as a grid of elements at the locations of the LVDTs. Each element has 1 DOF moving in the X or Y direction. The grid that defines the model of the structure is shown in Figure 4.13. For this model there are 20 degrees of freedom, but three DOF are redundant and will be ignored in plotting the mode shapes.

The mode shape will be determined by peak picking the fundamental frequency in the power spectra. The corresponding power spectral densities for each LVDT at the selected frequency represent the magnitude of the response at that frequency. These magnitudes were normalized and assigned as displacements to the elements of the grid. The element displacements were scaled and plotted and the mode shape shown in Figure 4.14.

The mode shape shows that the displacement occurs on one side of the grandstand and is in the front-back direction. This mode shape is consistent with the observed location of the vibration response.

Table 4.1 List of peak picked frequencies for each data set

	Natural Frequency (Hz)		
Time	1	2	3
1:49	3.1	3.8	4.3
1:55	3.1	3.8	4.3
2:01	3.1	3.8	4.2
2:06	3.0	3.8	4.2
2:12	3.0	3.8	4.2
2:17	3.0	3.8	4.2
2:23	3.0	3.8	4.2
2:28	3.0	3.8	4.2
2:34	3.1	3.8	4.3
2:40	3.1	3.8	4.3
2:46	3.0	3.8	4.2
2:57	3.0	3.7	4.2
3:02	3.0	3.8	4.2
3:08	3.0	3.8	4.2
3:15	3.0	3.7	4.1
3:20	2.9	3.7	4.1
3:32	2.9	3.7	4.1
3:37	2.9	3.7	4.1
3:43	2.9	3.7	4.0
3:49	2.9	3.6	4.0
3:54	2.9	3.6	4.0
4:00	2.9	3.6	4.0
4:05	2.1	2.9	3.7
4:11	2.9	3.7	4.0
4:17	2.8	3.6	4.0
4:28	2.8	3.6	3.9
4:33	2.8	3.6	3.9
5:39	2.9	3.7	4.1
Mean	2.9	3.7	4.1
Std. Dev.	0.2	0.2	0.1

Table 4.2 List of peak picked frequencies for each data set from day before event

	Natural Frequency (Hz)		
Time	**1**	**2**	**3.0**
4:32	3.0	3.9	4.2
4:37	3.1	3.9	4.2
4:47	3.0	3.8	4.0
4:59	3.1	3.9	4.2
Mean	3.1	3.9	4.1
Std dev	0.1	0.0	0.1

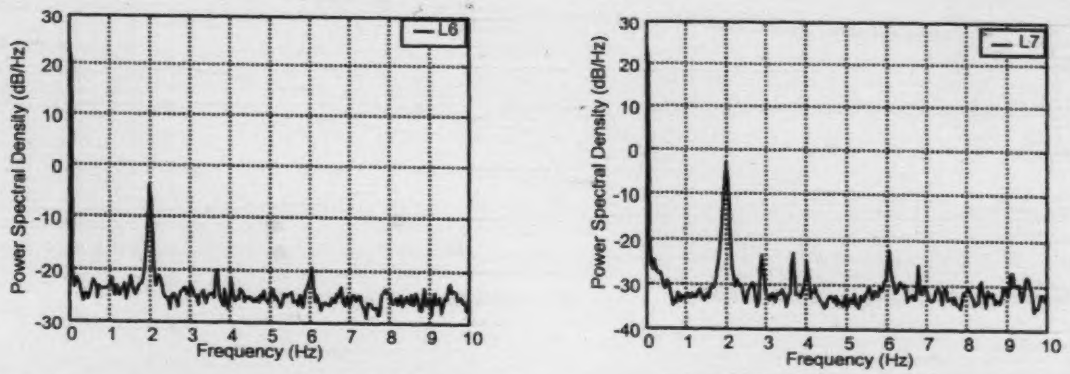

(a) Power spectrum from LVDT "L6" **(b) Power spectrum from LVDT "L7"**

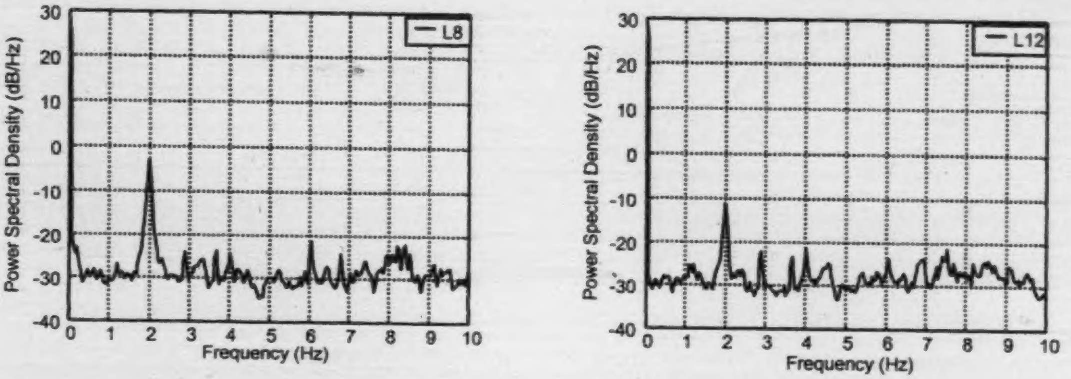

(c) Power spectrum from LVDT "L8" **(d) Power spectrum from LVDT "L12"**

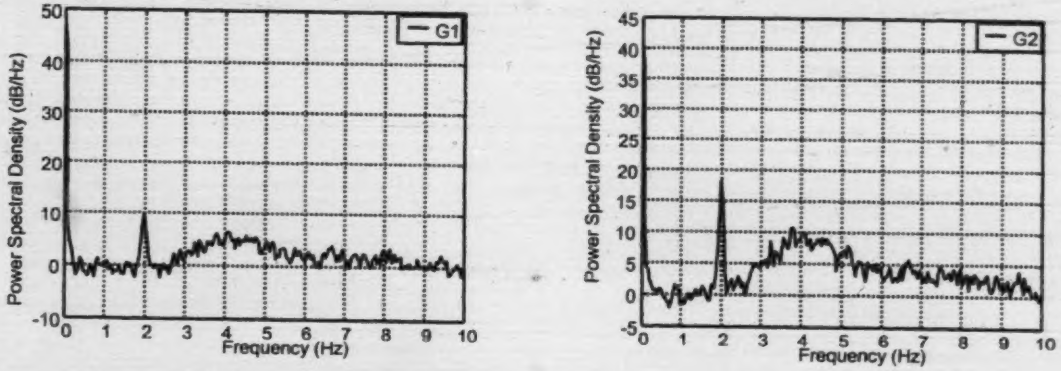

(e) Power spectrum from strain gauge "G1" **(f) Power spectrum from strain gauge "G2"**

Figure 4.1 Power spectra from various channels at 4:05 July 18, 1999

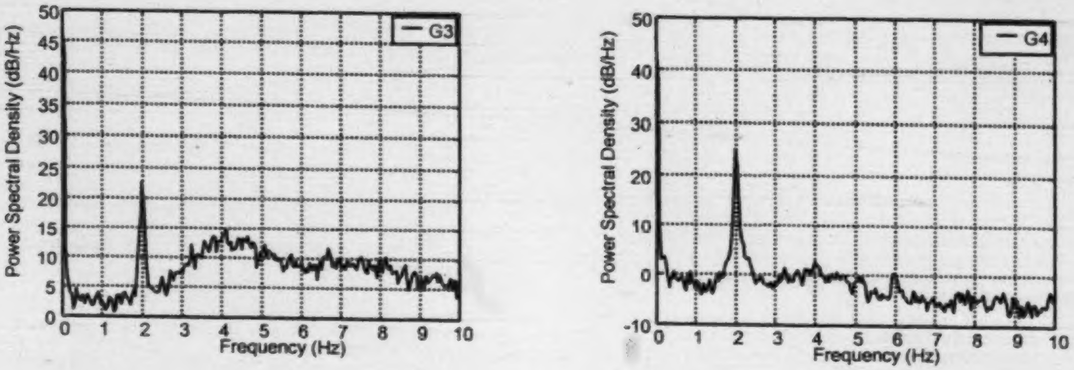

(g) Power spectrum from strain gauge "G3" **(h) Power spectrum from strain gauge "G4"**

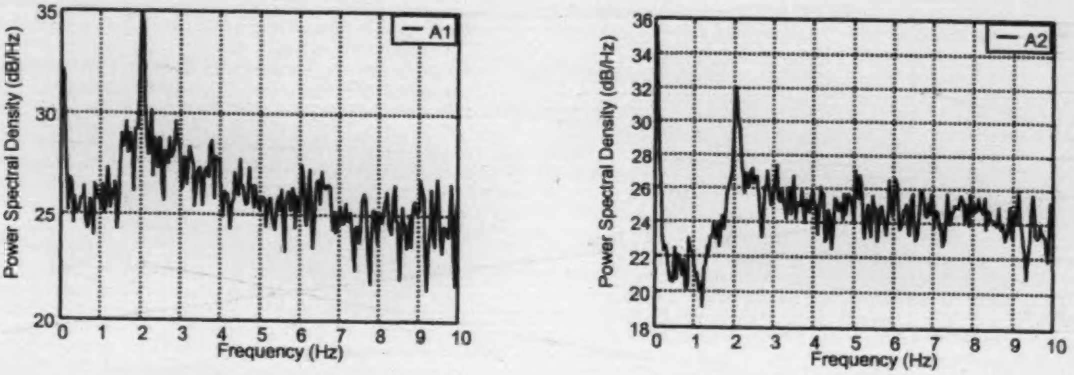

(i) Power spectrum from accelerometer "A1" **(j) Power spectrum from accelerometer "A2"**

Figure 4.1 (cont'd).

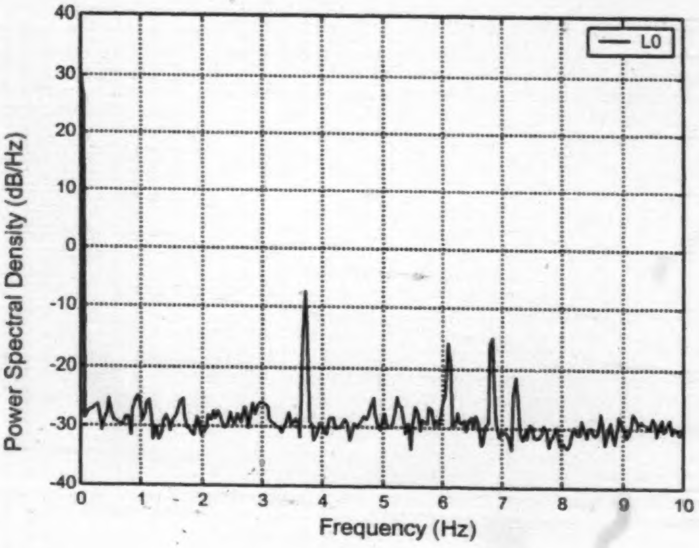

(a) Full grandstand, July 18, 3:20

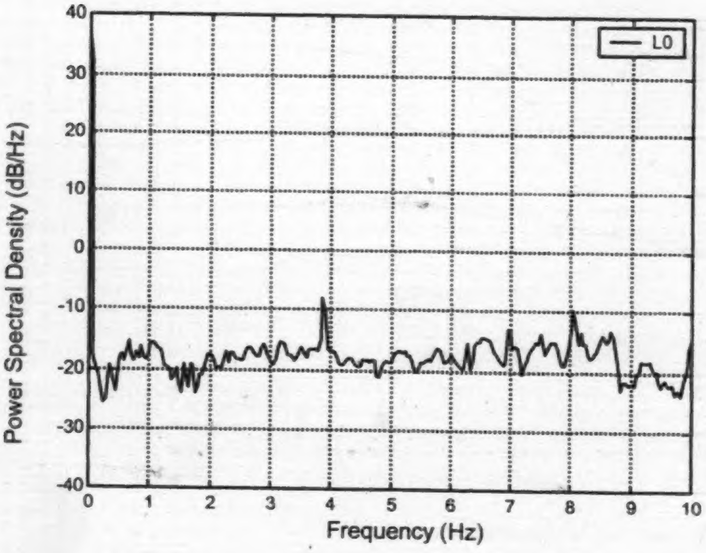

(b) Empty grandstand, July 17, 4:59

Figure 4.2. Power spectra of LVDT "L0"

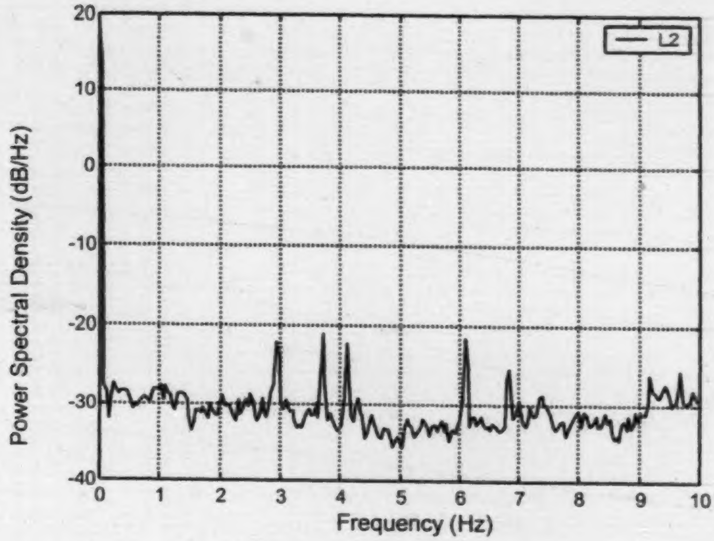

(a) Full grandstand, July 18, 3:20

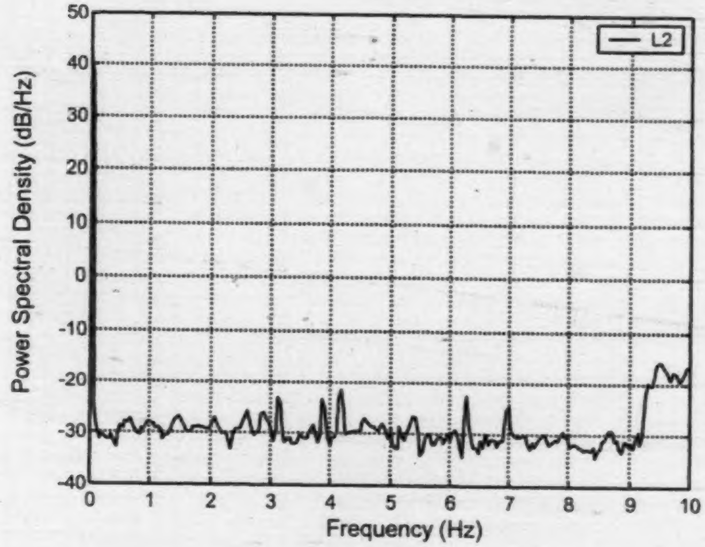

(b) Empty grandstand, July 17, 4:59

Figure 4.3. Power spectra of LVDT "L2"

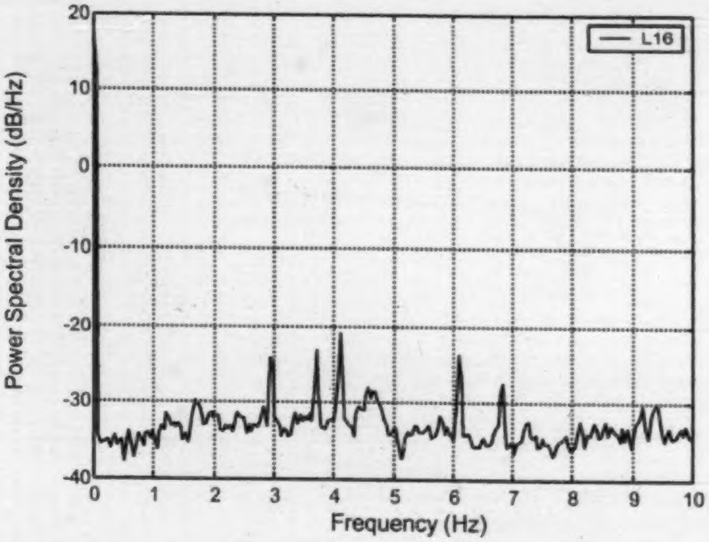

(a) Full grandstand, July 18, 3:20

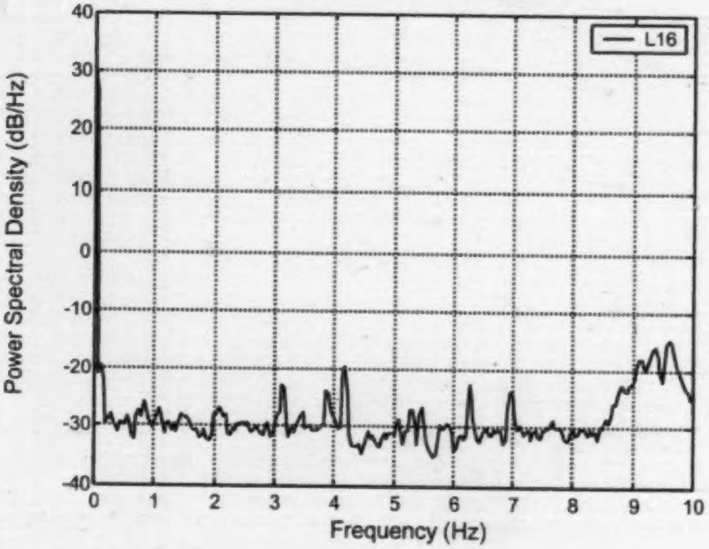

(b) Empty grandstand, July 17, 4:59

Figure 4.4. Power spectra of LVDT "L16".

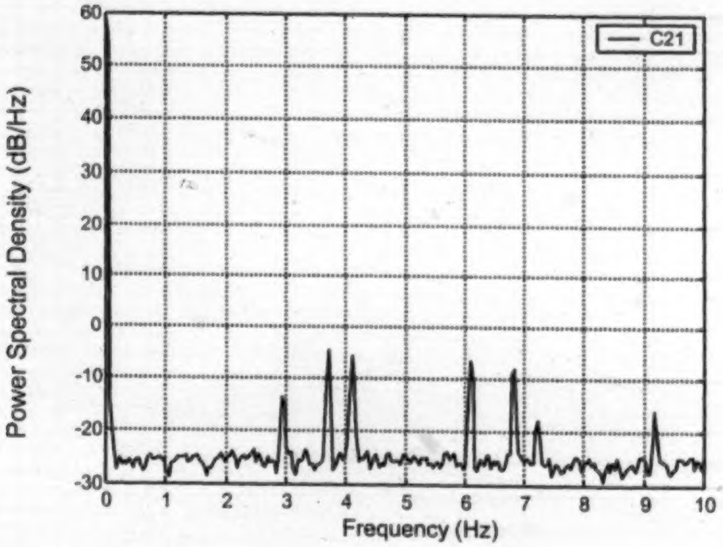

(a) Full grandstand, July 18, 3:20

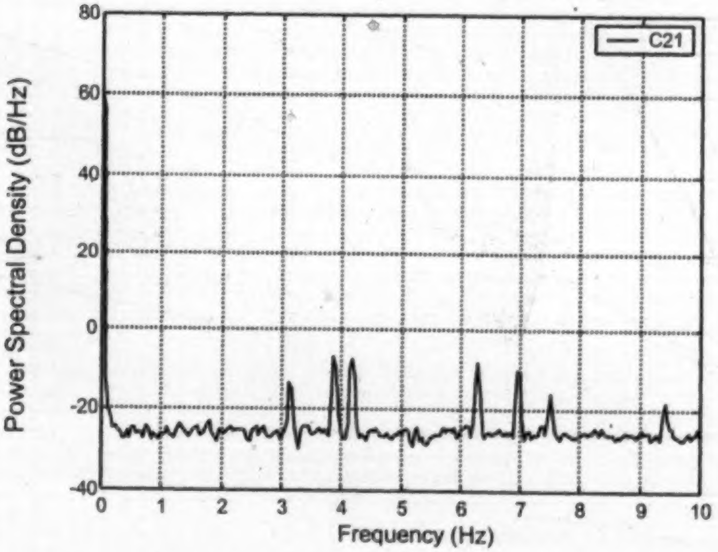

(b) Empty grandstand, July 17, 4:59

Figure 4.5. Power spectra of cable transducer "C21"

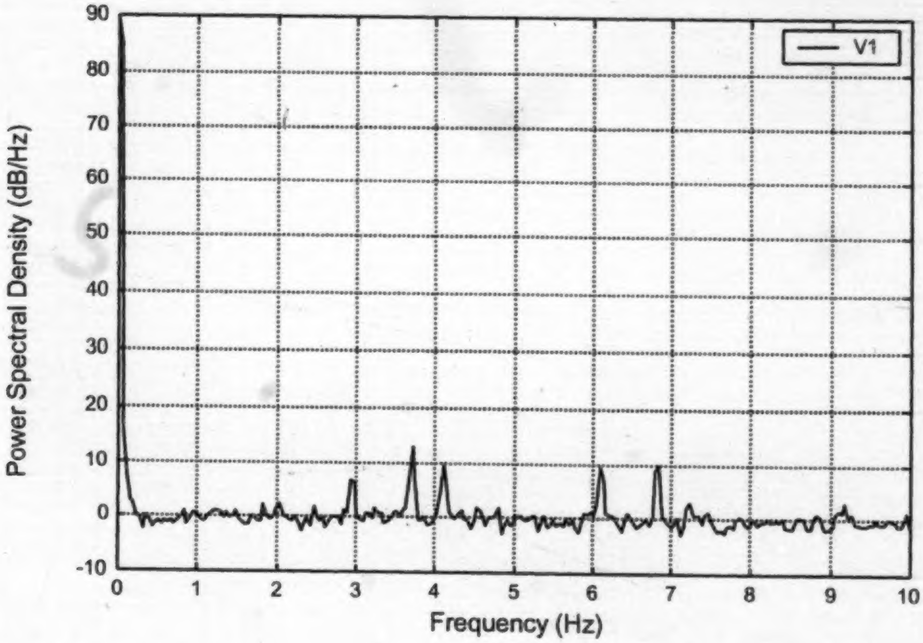

Figure 4.6. Power spectrum of voltage channel "V1" from data set 03:20, July 18, 1999

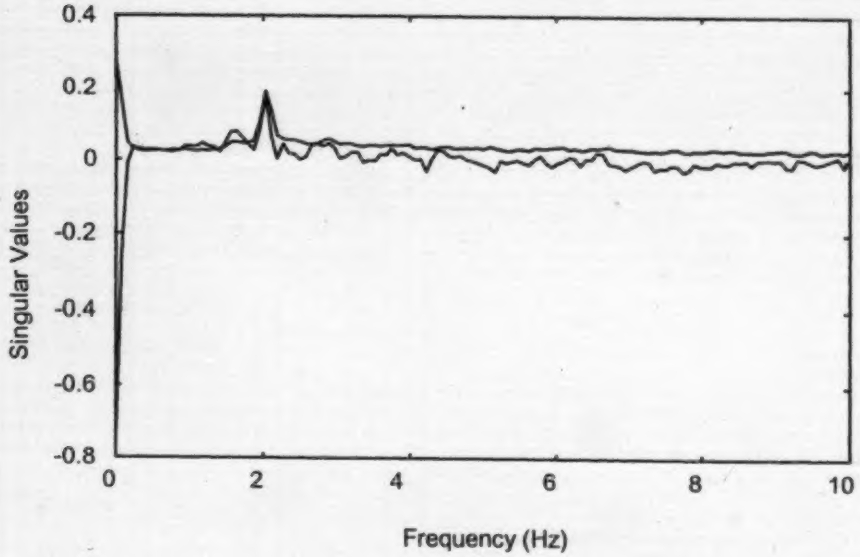

Figure 4.7. Singular Value Decomposition of 2 DOF system

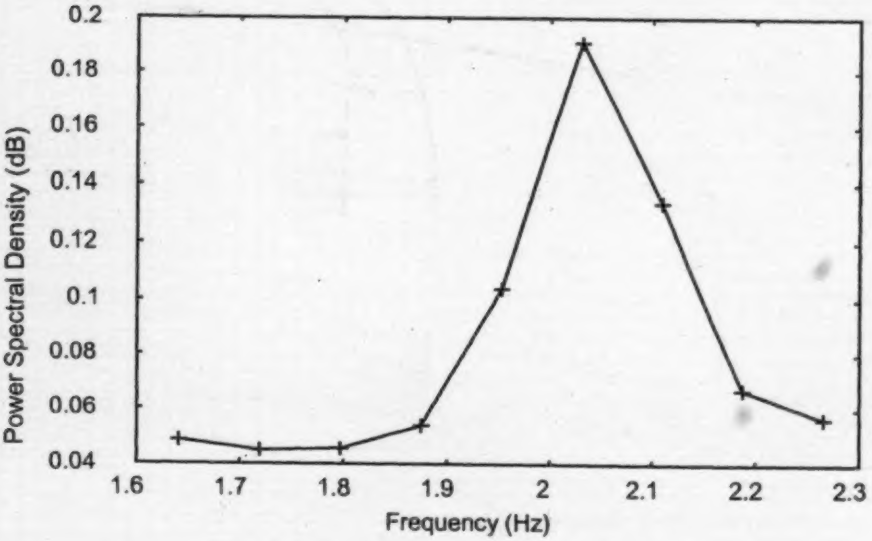

Figure 4.8. Identified portion of the auto spectrum of 2 DOF system

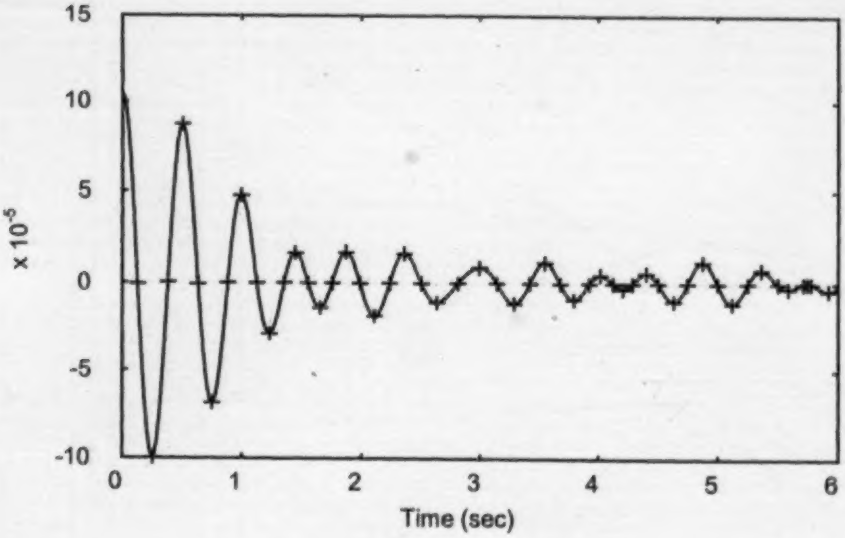

Figure 4.9. Free decay from identified portion of auto spectrum, with peaks and crossings marked

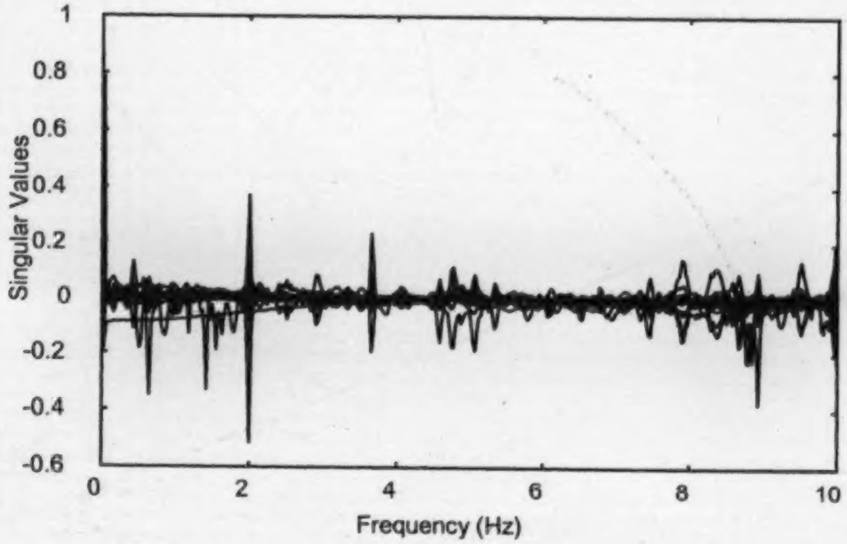

Figure 4.10. Singular value decomposition of the 20 DOF system

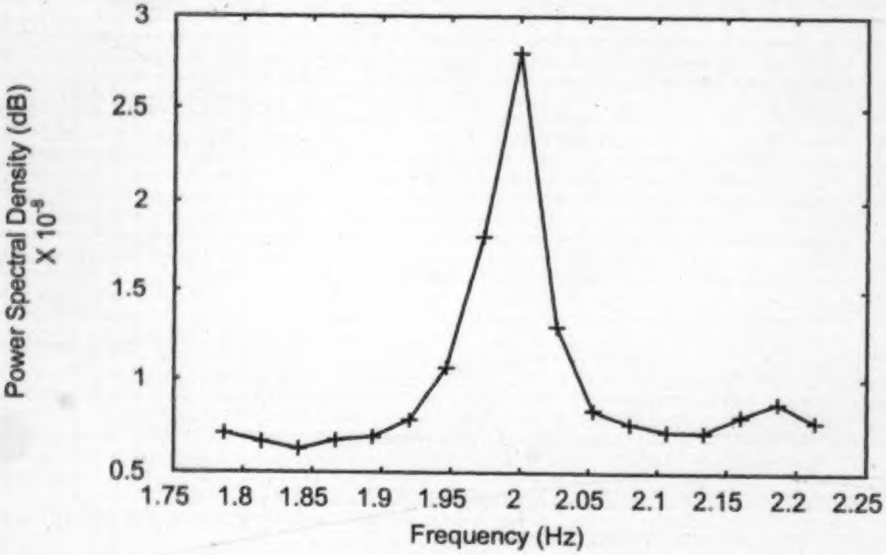

Figure 4.11. Identified portion of the auto spectrum of the 20 DOF model

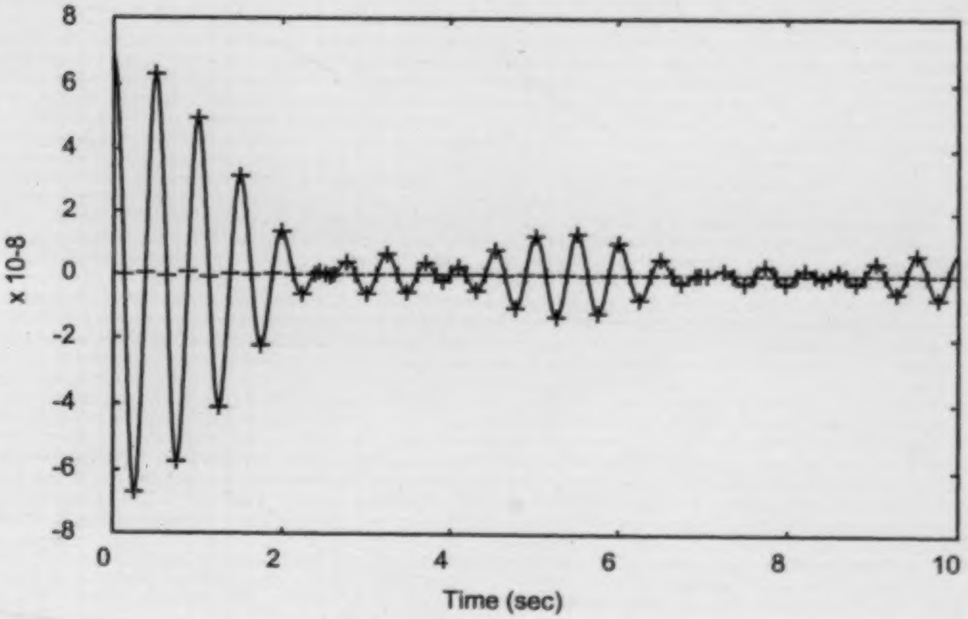

Figure 4.12. Free decay from identified portion of the auto spectrum of 20 DOF model

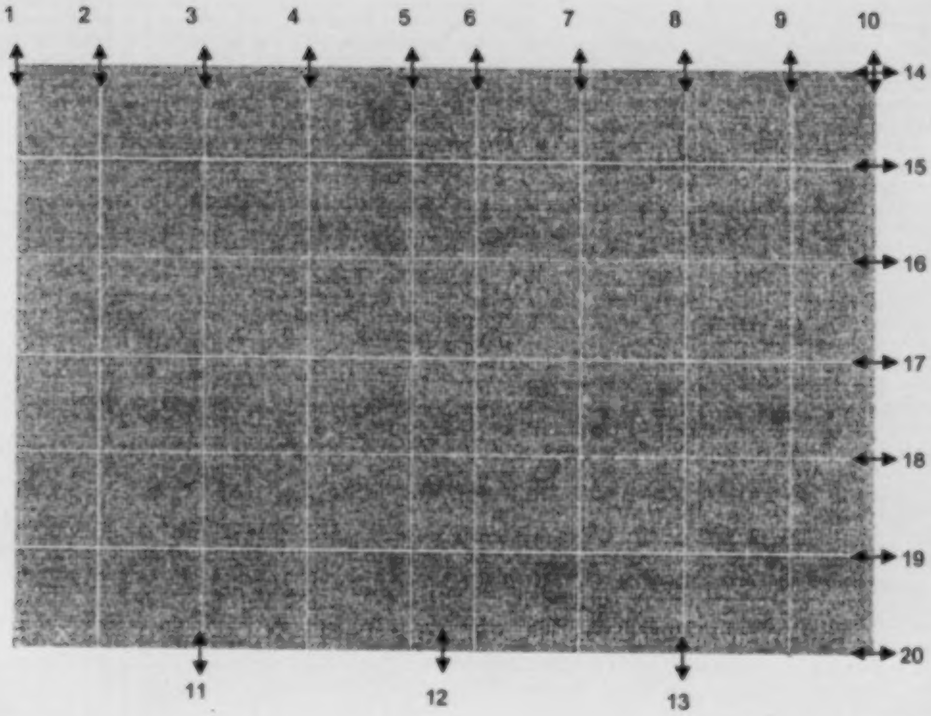
1
2
3
4
5
6
7
8
9
10
14
15
16
17
18
19
20
11
12
13

Figure 4.13. 20 DOF model of the grandstand

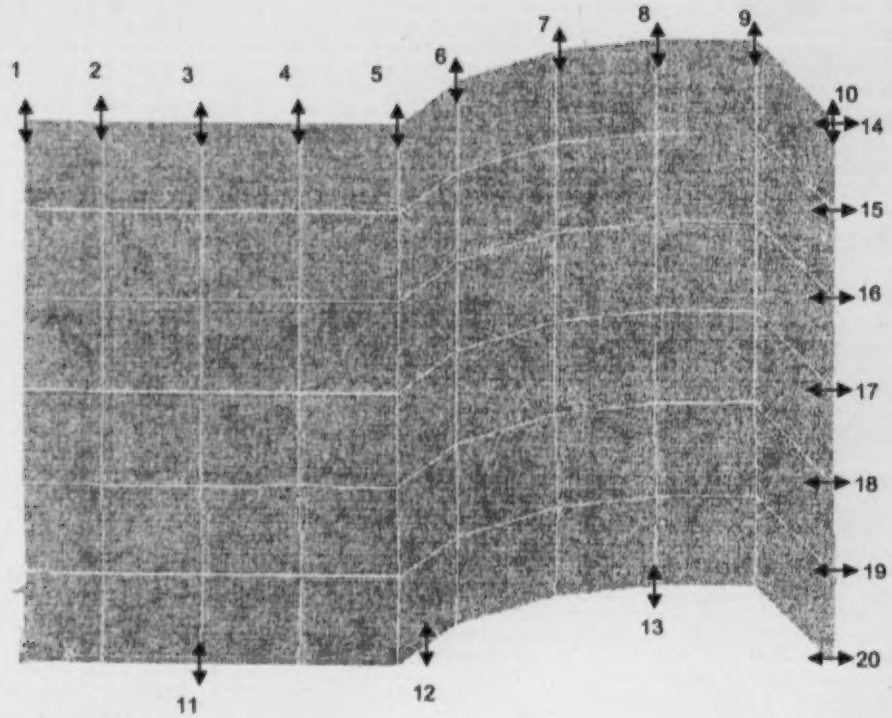
1
2
3
4
5
6
7
8
9
10
14
15
16
17
18
19
20
13
12
11

Figure 4.14. Fundamental frequency mode shape.

5 FINITE ELEMENT ANALYSIS OF TEMPORARY GRANDSTAND

5.1 Introduction

Finite Element Analysis has been used extensively as a tool to predict the dynamic behaviour of structures. The Finite Element Analysis conducted for this research had two goals:

1. To show that FEA can accurately predict the dynamic properties of a temporary grandstand, thus eliminating the need for expensive testing; and

2. To validate the mode shape identified by the output-only modal analysis. A potential problem with output-only modal analysis is that the results could potentially be incorrect. Therefore, to verify the results it should be shown that the mode shape is consistent with the structure. For this purpose FEA models have been used to show that the mode shape is consistent.

At the outset of the research project a preliminary FEA model was created to predict the natural frequency and mode shape of the temporary grandstand. However, the results of the modal analysis were significantly different than the results of the FEA model. Therefore, it became important to identify which, if any, assumptions of the preliminary FEA model had resulted in these significant differences.

Based on the Literature Review and observations of the mode shape, several factors were identified that may have resulted in the differences between the FEA and the observed results. These factors included:

1. Ledger Connection Stiffness: The ledger connections of scaffold structures are designed to be connected and disconnected quickly and therefore may perform

differently than traditional bolted or welded connections. The connection stiffness is unknown and it has been suggested that the semi-rigid connection stiffness may have a significant effect on the analysis predictions [Godley and Beale, 1997].

2. Brace Stiffness: It has been suggested that the brace stiffness should be reduced to due to the connection stiffness [Godley, 1997]. Since the stiffness of the connection is difficult to assess the overall brace stiffness is unknown.

3. Mass of Occupants: The mass of occupants may need to be accounted for in the prediction of the dynamic properties. The recommendation for permanent grandstands is that the occupant mass not be considered in a dynamic analysis [IStructE, 2002]. However, other research has suggested that the mass of the occupants may be significant [Ellis and Ji, 1997]

4. Construction Modifications: The preliminary FEA model was based on the assumption that the ground elevation was consistent for the entire structure. However, due to variations in the ground elevation, a portion of the temporary grandstand was modified to extend downward 0.5 m to accommodate the low areas and to preserve the site lines for the spectators. The additional 0.5 m was unbraced, which may have significantly affected base stiffness of the structure in those areas. These changes may have contributed to the mode shape that was identified from the recorded data. Normally, it is expected that the first mode shape acts like a single degree-of- freedom system and therefore the temporary grandstand should move as a single unit, but the observed mode shape shows only half the structure moving. It is possible that the changes to the structure may have caused parts of it to act independently.

A sensitivity analysis will be performed using macro and micro-updating techniques to determine which of these factors may be responsible for the observed differences.

5.2 Preliminary Finite Element Analysis.

Prior to the instrumentation of the temporary grandstand, a preliminary finite element model was created. The purpose of the model was to provide information on the possible mode shapes of the structure to facilitate the positioning of the instrumentation. The FE model did not take into account any of the factors described in Section 5.1, but used typical assumptions for modeling the structure. The model was three-dimensional based on pre-construction drawings of the temporary grandstand and was used to determine the natural frequencies and the mode shapes of the structure.

The FEA model was created using ALGOR FEA software. The ledgers, standards, stringers and floorboards were modeled using beam elements. The beam elements have 6 DOF at each node: translation in X, Y, and Z direction, and rotation about X, Y and Z axes. For the beam elements the required inputs are: cross sectional area, moments of inertia, and section modulus. The scaffold braces were modeled using truss elements which have three degrees of freedom at each node: translation in X, Y, and Z directions. For the truss elements the required input is the cross sectional area. The truss elements can only accept axial forces, whereas beam elements have axial forces and end moments. The properties of the elements are given in Table 5.1 and the completed model is shown in Figures 5.1 and 5.2

For the seating level of the structure the floorboards were modeled using beam elements that spanned between the stringer beams. The base of the model was considered fixed in translation and rotation. Lumped masses were applied at the top of each standard with a mass equivalent to a live load of 156 kg/m^2 (32 psf) distributed over the seating area.

A finite element modal analysis was performed to determine the first three modal frequencies modes, listed in Table 5.2 and Figures 5.3 to 5.5 present the mode shapes. The mode shapes are plotted from a plan view with the front of the grandstand on the right side. The first mode shape has a double curve towards the front of the grandstand. An inflection point is located at the middle of the grandstand, which would not normally be expected for the first mode shape. However, this inflection point was due to the mass being distributed on the seating areas only (see Figure 3.3 for seating areas). The inflection point occurs at the central aisle which was not considered to have live load when all the spectators are in their seats. This distribution of mass created the doubly curved first mode. The second mode shape is an "S" shaped curve with half the grandstand curved forward and half curved backward, the inflection point is at the middle of the grandstand. The third mode shape is a curve along the edge, which is most pronounced towards the rear of the grandstand. This mode shape differs from the first two since it is a side to side displacement instead of a front to back displacement.

The dynamic characteristics identified by the preliminary finite element analysis differed from the measured values. The first modal frequency of the preliminary FEA was 4.49 Hz, whereas the measured value was 2.1 Hz. Also, the first mode shape from the FEA (Figure 5.3) differs from the observed mode shape (Figure 4.14). Therefore, the FEA model requires further refinement dynamic properties of the temporary grandstand.

Although ALGOR was used for the preliminary FEA, ANSYS finite element software was used for the model refinement. This was due to ANSYS' superior capabilities for defining parameters and model optimization over ALGOR. ANSYS has optimization and sensitivity analysis routines that will simplify the process. As a basis for the ANSYS models the preliminary finite element model was converted from ALGOR to ANSYS using ALGOR's conversion utility.

5.3 Macro Updating

Brownjohn *et al.* [2000] describe *macro-updating* as changing the model by choosing to omit or include structural elements that may have an effect on the structural and dynamic performance, based upon an understanding of how the real structure behaves. The authors determine that through these modifications to the FEA model that they achieve better results and gain a better understanding of how the structure behaves.

The preliminary FEA had assumed that the structure was built on level ground. However, the actual site had uneven ground elevation. Changes in elevation that are greater than can be accommodated by the adjustable base jacks require the base of the structure to be extended down into the low areas. For this structure there was an elevation drop of 0.5 m over a large area, which required an additional 0.5 m to the bottom of the grandstand at the low points. The result was that the bracing terminated at 0.5 m above the ground level for some areas of the grandstand (i.e. the bottom 0.5 m was not braced). Figure 5.6 shows the portion of the grandstand that was affected by this modification. This construction modification resulted in a more flexible base than if the entire structure were built on level ground. Macro-updating will be used to modify the FEA model so that is matches the geometry of the structure that was built on site.

To determine the significance of the construction modifications on the dynamic characteristics of the structure, two FEA models were created. The first model (Model #1) was created assuming level ground and the second model (Model #2) was created to include the uneven elevation and additional base structure that was used for the tested structure. The dynamic properties of each model were compared to the measured dynamic properties. To compare the mode shapes the Modal Assurance Criterion, which is discussed in Section 4.2.1, was used.

The Modal Assurance Criterion value was determined using a displacement vector from the finite element analysis, and the normalized displacement vector from the mode shape estimation from the previous chapter. In both cases the displacement vectors were identified as the front-back displacement corresponding to LVDT locations L0 to L9 (Figure 3.14. A Modal Assurance Criterion value was calculated based on Equation 4.2. with these two vectors.

For the macro-updating, the other parameters were kept constant. The brace stiffness was assumed to be 100% of the maximum axial stiffness, k (where k= AE/L), and the spectator mass was ignored. The modal analysis identified the first five modes for each of the models and compared the mode shapes to the measured mode shape. From the five mode shapes, the one with the highest Modal Assurance Criterion (MAC) value was selected and the frequency recorded.

For Model #1 it was found that the third mode had the highest MAC value (0.88) at a frequency of 6.05 Hz. For Model #2 the first mode had the highest MAC value (0.88) at a frequency of 3.31 Hz. Therefore, Model #2 provided the closest estimate to the measured dynamic properties. This indicates that the unbraced length at the base of the standards has a significant effect on the dynamic response of the temporary grandstand.

Based on the macro-updating results the Model #2 was used for further refinement through micro-updating.

5.4 Micro-updating.

Micro-updating describes the traditional approach of adjusting parameters of the model, such as elastic modulus, cross sectional areas, etc. For micro-updating, it is assumed that the finite element model is fixed with respect to the mesh, boundary conditions, and the element types that are used. Several factors were identified that are suitable for micro-updating, they included: the ledger connection stiffness, the brace stiffness, and the occupant loads. Each of these factors could be assigned as a variable and modified within the FEA model without major modifications to the model. Since there are three factors that may be adjusted it was determined that a sensitivity analysis should be performed to determine the significance of each of these factors with respect to the natural frequency and mode shape. One factor would be modified at a time while the other factors were held constant. If the factor did not significantly effect the natural frequency or mode shape then it could either be eliminated or set as a constant value.

5.4.1 Ledger Connection Stiffness

The ledger connection rotational stiffness is most rigid in the vertical plane of the ledger and standard and is pin connected in the horizontal plane rotation. It is not known whether the rotational connection stiffness in the vertical plane will have a significant effect on the dynamic properties so the stiffness was varied from a pin connection to a rigid connection.

A model was created for which the joint stiffness between the ledgers and standards could be modified. Essentially, rotational springs were inserted into the model between the ledger and standard connections. Coincident nodes were created at the joint between the ledgers and standards, so that the ledgers and standards each have nodes occupying the same space. At each pair of coincident nodes a stiffness-matrix element was inserted connecting the coincident nodes. With the stiffness-matrix elements it is possible to directly modify the individual stiffness values affecting the interaction of the degrees of freedom between the two nodes. With the stiffness-matrix elements it was possible to change the values affecting the rotational stiffness, in particular the rotation in the vertical plane of the ledgers. By varying the rotational stiffness from a very small value to a large value, it was possible to determine the effect of the change in rotational stiffness on the results of the analysis. The stiffness in the model was varied from 1000 N·m/rad to 100 000 N·m/rad. The rotational end stiffness of the ledger or standard, assuming a length of 2.0 m, would be 35 000 N·m/rad.

As with the macro-updating the mode shapes from of the analysis were compared to the measured mode shape. The modal analysis determined the first five modes as a function of the rotational stiffness and the mode shapes were compared to the measured mode shape. The modal frequency of the mode with the highest MAC value was recorded. Table 5.3 shows the frequency, mode number, and MAC value.

It was found that the model is not significantly affected by changes in the rotational stiffness. There was only a small effect on the natural frequency and no effect on the mode shape. So, the effect of the unknown rotational stiffness can be eliminated as a design variable and the connection stiffness can be considered rigid.

5.4.2 Brace Stiffness

It has been suggested that the brace stiffness may be significantly less than the axial stiffness of the brace tube due to the connection stiffness. For the finite element analysis the reduced stiffness of the brace will be modeled assuming a reduced material stiffness instead of reducing the cross sectional area since that would affect the calculated mass of the elements. For this analysis the range for the brace stiffness design variable was from 1% to 100% of the maximum axial stiffness, k (where k = AE/L).

Similar to the previous analysis, the modal analysis determined the first five modes as a function of the brace stiffness. The modal frequency of the mode with the highest MAC value was recorded. Table 5.4 shows the mode, frequency, and MAC values as a function of brace stiffness. For brace stiffness of less than 15%, of the full stiffness, the mode shape of the third mode has the highest MAC value (indicating a greater similarity between the mode shapes) but the first mode does not correlate well with the observed results. For brace stiffness higher than 15%, of the full stiffness, the mode shape of the first mode had the highest values MAC value, indicating greatest similarity with the observed results. Little change was observed in the natural frequency with changes in brace stiffness from 15% to 100%. Hence, assuming a brace stiffness of 100% of the full stiffness will achieve a high correlation for the mode shapes without significantly affecting the correlation with the natural frequency.

5.4.3 *Mass of Occupants*

It is typical for the modal analysis of a structure to ignore the mass of the occupants. The British standard for permanent grandstands [IStructE, 2002] recommends that any dynamic analysis be performed for an empty grandstand. In the case of the temporary grandstands the mass of the occupants may be significant, in part due the lightweight construction. However, the contribution of the occupant mass to the structural response may depend on the occupant's activity. If the occupants are contributing to the dynamic response through some coordinated activity then their mass may be significant. However, if the individual occupants are moving independently then their mass may not contribute at all. A study performed by Ellis and Ji [1997] found that when they measured the dynamic properties of a temporary grandstand, there was a significant difference in the natural frequency between the empty stands and the occupied stands. This would suggest that the occupant mass does have an effect on the dynamic properties of the temporary grandstand.

A sensitivity analysis was performed to determine the effect of mass on the dynamic properties (natural frequency and mode shape) of the model. Mass elements were attached for the seating areas of the structure at the top of each column of standards. The mass was assigned a value based on the tributary area and a distributed load (dead + live load) that varied from 0.48 to 2.4 kPa. The average dead load is 0.48 kPa based on the weights of the aluminum floor boards and seating surfaces, so the live load contribution varied from 0 to 1.92 kPa.

Modal analyses were performed to determine the first five modes as a function of occupant mass. The mode and frequency for the mode with the highest MAC value were recorded. Table 5.5 shows the variation in frequency, mode, and MAC value for the change in distributed load. It was observed that the natural frequency decreases as the distributed load increased. Since the dead load is constant the natural frequency decreases as the live load is increased. Therefore the occupant load can be considered a significant factor in determining the modal frequencies.

For permanent grandstands the affect of occupant mass may not be as significant. For the temporary grandstand the live load was 2.9 times the dead load and the difference between the natural frequency based on dead load only and the combined dead and live load condition was only 1.2 Hz. For a permanent grandstand where the ratio of live load to dead load would normally be much smaller, the difference in natural frequency would be negligible. In this case however, the 1.2 Hz difference is significant because it brings the natural frequency from 3.3 Hz to 2.1 Hz, which is close to the forcing frequency associated with walking (Table 2.5). From a design perspective, one would probably want to achieve a natural frequency greater than 4 Hz, in which case the 1.2 Hz difference may not be an issue.

5.5 Optimization.

To perform an ANSYS optimization one must define the design variables, state variables, and an objective function. The design variables are the quantities that will be varied to achieve the optimized solution. Design variables can be assigned upper and lower limits that act as constraints. State variables are typically a function of the design variables and are evaluated for each iteration. State variables may be assigned maximum and minimum limits, but may also be one-sided having only a single maximum or minimum limit. The limits on the state variables serve to further constrain the solution. The objective function is the dependent variable that we are attempting to minimize. For this analysis the design variable is the occupant mass, the objective function is to minimize the difference between the natural frequency from the experimental and analytical results.

In ANSYS there are two optimization methods available: 1) Subproblem Approximation Method, and 2) First Order Method. The Subproblem Approximation Method uses curve-fitting techniques on the dependent variables, which include the state variables and objective function. For every change in the design variable the resulting change in the state variable and objective function are curve fit. From the equations of the fitted curves the optimization routines are able to close in on a solution. This method is a general-purpose method, which is suitable for a wide range of engineering problems. The Subproblem Approximation method works best when the dependent variables vary smoothly with respect to the design variable. The First Order Method uses the derivative of the dependent variables with respect to the design variables. This method is very accurate but has a higher cost in terms of solution time. Since the frequency varied smoothly with respect to the occupant load the Subproblem Approximation Method was suitable for solving this problem

With the occupant mass set as the design variable and the objective function set as the difference between the natural frequency from the experimental and analytical solutions, the optimization routine converged on a solution after thirteen iterations. The optimum value for the occupant mass (dead load excluded) was equivalent to a distributed live load of 1.39 kPa. For the optimized solution the MAC value was 0.88, indicating a high correlation with the observed mode shape and the natural frequency was 2.1Hz. The mode shape for the optimized result is shown in Figure 5.6 and is very similar to the experimental mode shape in Figure 4.14.

How well did the distributed live load of the optimized solution compare to the observed distributed live load from the static load measurements? At 4:05 PM, when the natural frequency was detected, the estimated distributed load was 0.98 kPa (see Table 3.3), which is 70% of the FEA result. Part of the discrepancy may be due to the assumption that the mass is equally distributed on the structure, when in fact people were moving to the exit so the mass would have been more heavily concentrated towards the aisles. Despite this difference the FEA provided a reasonable estimate of the dynamic properties.

5.6 Conclusion.

A better understanding of how the structure behaves was achieved by performing the FEA. It was determined that the connection stiffness can be considered rigid and the brace stiffness need not be reduced from the full axial stiffness. The other important factors were: the FEA model should closely match the geometry of the completed structure, particularly for variations at the base of the structure; and the occupant mass should be included in the FEA model to accurately predict the natural frequency of the temporary grandstand.

The mode shape that was identified by the FEA closely matched the mode shape that was identified by the output-only modal analysis. This supports the validity of the output-only results, indicating that the measured mode shape identified is due to the response of the structure to ambient vibration and not due to extraneous noise or forcing frequencies in the output signal.

Table 5.1. Element properties for FEA

	Element type	**Area (mm^2)**	**Ix (mm^4)**	**Iy (mm^4)**	**Sx (mm^3)**	**Sy (mm^3)**
Ledger and Standard	Beam	451	115300	115300	4768	4768
Brace	Truss	381				
Stringer	Beam	1944	5.294x106	1.548x106	68710	43010
Floorboards	Beam	2380	0.754x106	34.79x106	16550	189100

Table 5.2. Preliminary analysis modal frequencies.

Mode #	**Frequency (Hz)**
1	4.49
2	5.36
3	5.70

Table 5.3 Natural frequency (mode with highest MAC value) with respect to rotational stiffness of joints

Rotational Stiffness (N·m/rad)	**Natural Frequency (Hz)**	**MAC Value**	**Mode #**
1886	5.62	0.773	3
1891	5.62	0.773	3
1893	5.62	0.773	3
1935	5.62	0.773	3
1942	5.62	0.773	3
2327	5.62	0.773	3
2511	5.63	0.773	3
4219	5.65	0.772	3
82624	5.91	0.746	3
99091	5.93	0.745	3

Table 5.4 Natural frequency (mode with highest MAC value) with respect to maximum axial brace stiffness

Axial Brace Stiffness (% of k=AE/L.)	Natural Frequency	MAC Value	Mode #
1%	1.74	0.89	3
5%	2.35	0.90	3
6%	2.43	0.90	3
15%	2.87	0.89	1
100%	3.31	0.88	1

Table 5.5 Natural frequency (mode with highest MAC value) with respect to the equivalent uniformly distributed load.

Equivalent uniformly distributed load (kPa)	Natural Frequency (Hz)	MAC Value	Mode #
0.48	3.31	0.883	1
0.80	2.86	0.883	1
1.13	2.55	0.883	1
1.47	2.31	0.883	1
1.76	2.15	0.882	1
1.93	2.07	0.882	1
1.97	2.05	0.882	1
1.98	2.05	0.882	1
2.01	2.04	0.882	1

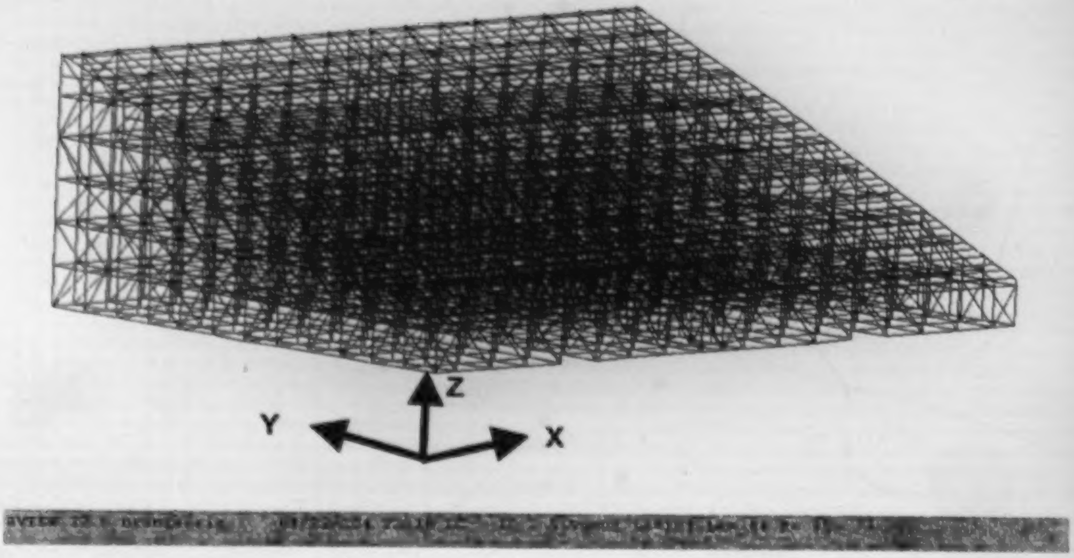

Figure 5.1. Preliminary FEA model

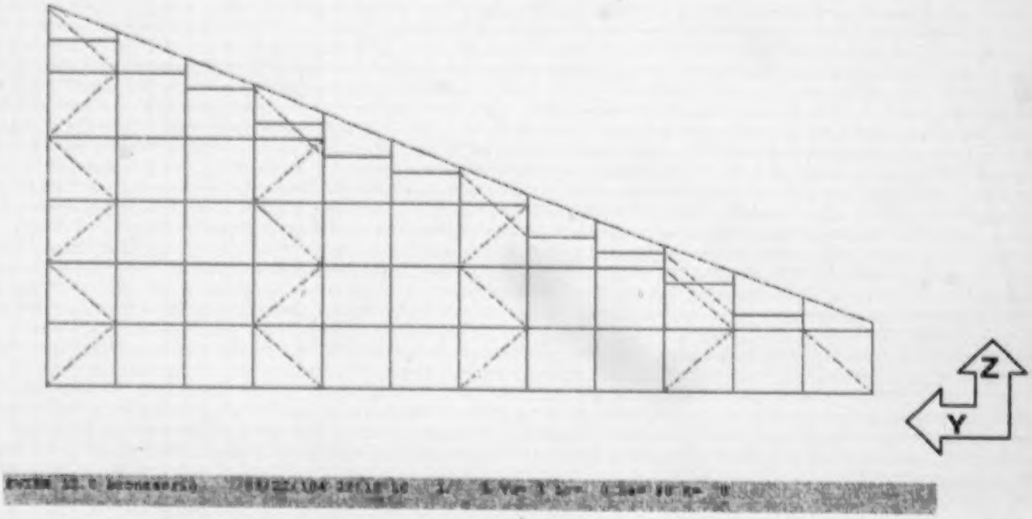

Figure 5.2. Preliminary FEA model side view

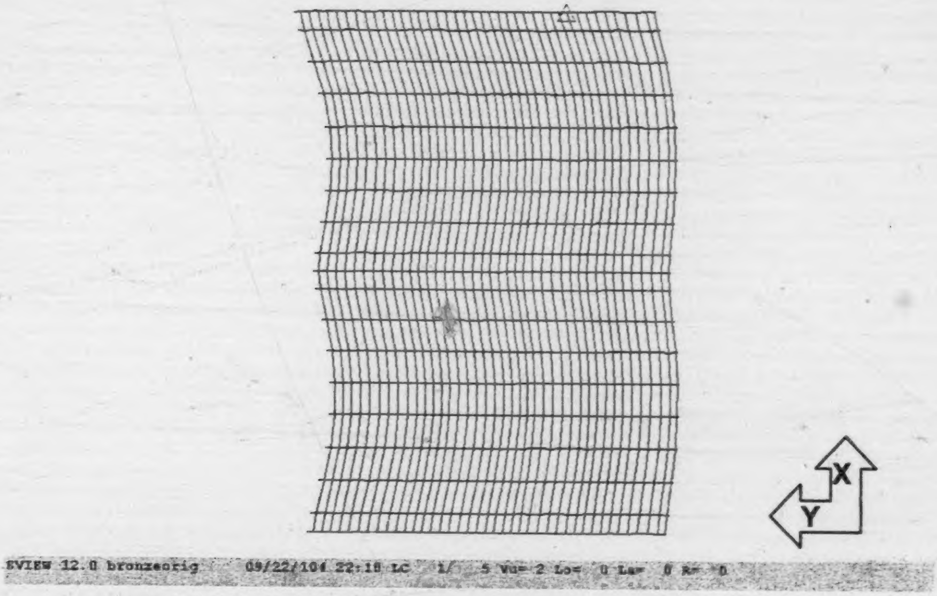
X
Y
SVIEW 12.0 bronzeorig 09/22/104 22:18 LC 1/ 5 Vu= 2 Lo= 0 La= 0 R= 0

Figure 5.3. Preliminary FEA model, first mode shape

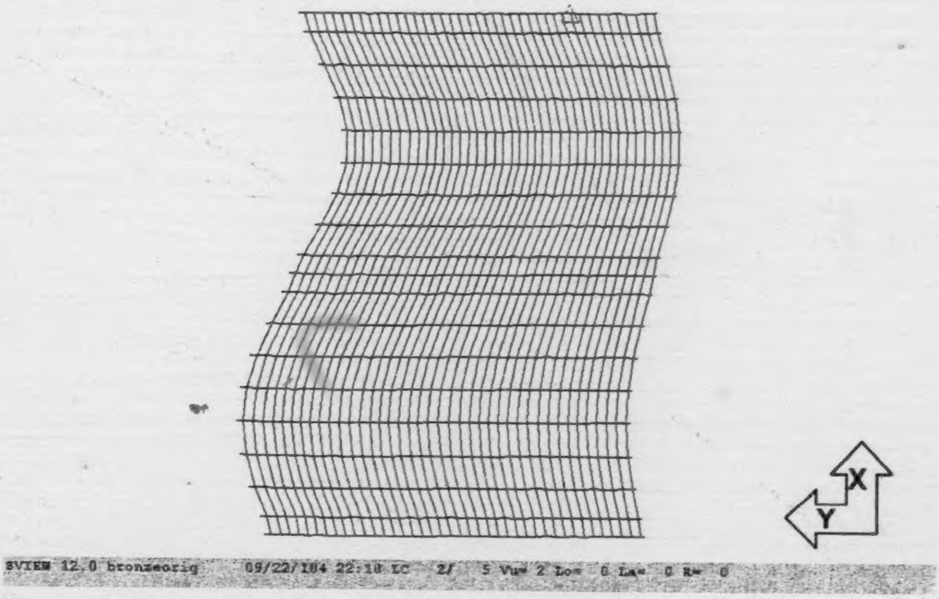
X
Y
SVIEW 12.0 bronzeorig 09/22/104 22:10 LC 2/ 5 Vu= 2 Lo= 0 La= 0 R= 0

Figure 5.4. Preliminary FEA model, second mode shape

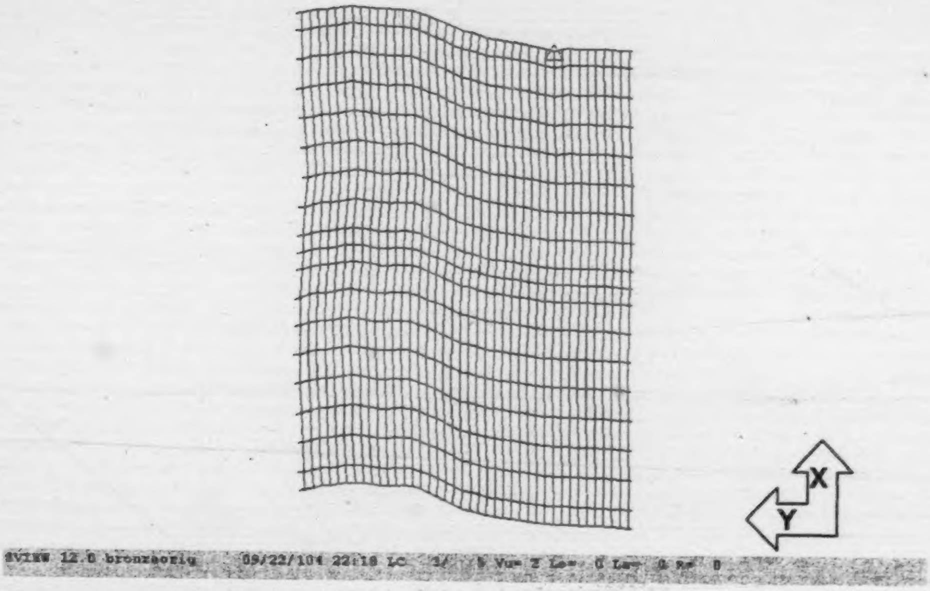
X
Y
SVIEW 12.0 bronzeorig 09/22/104 22:18 LC 3/ 5 Vu= 2 Le= 0 La= 0 R= 0

Figure 5.5. Preliminary FEA model, third mode shape

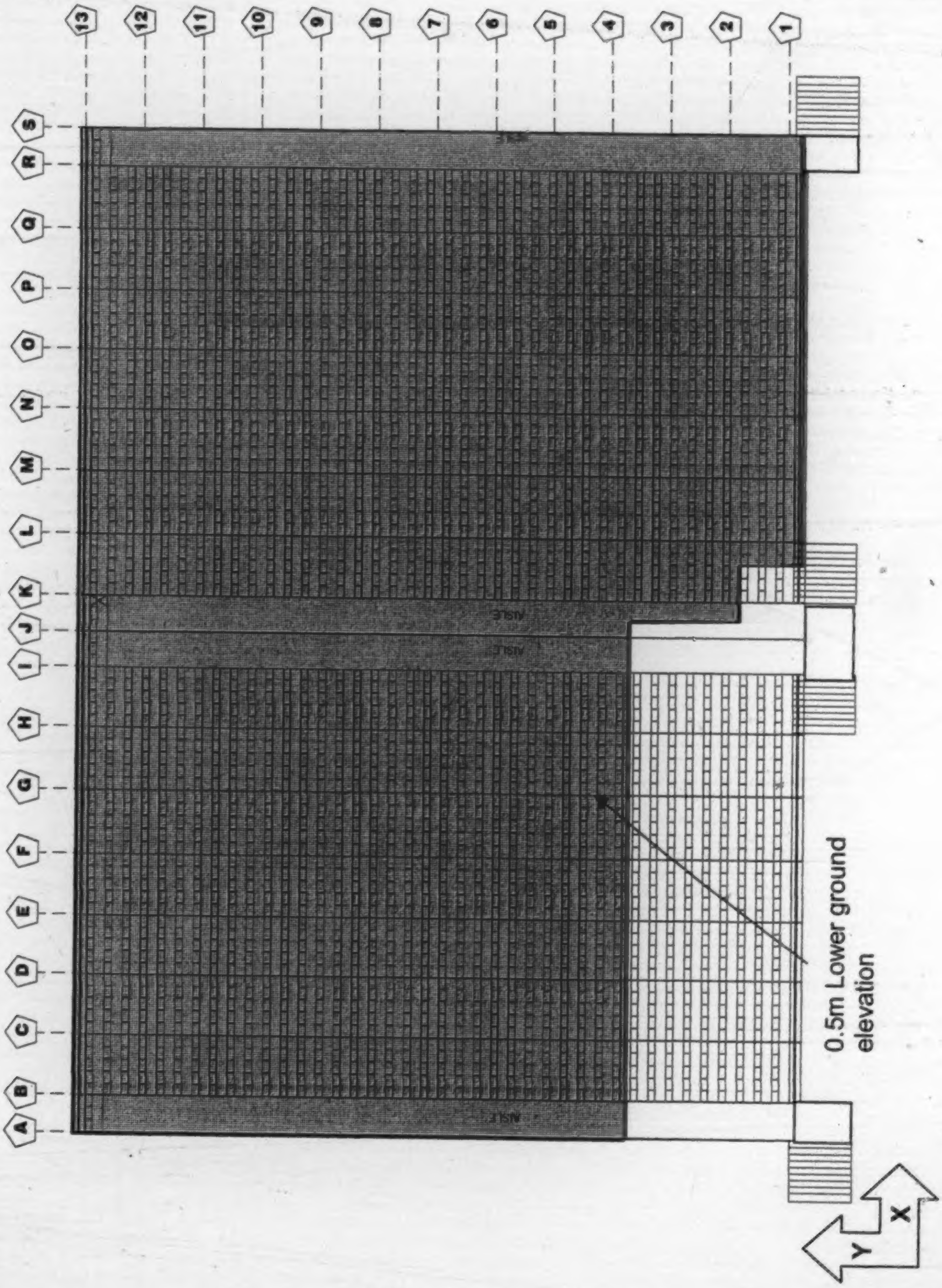
A
B
C
D
E
F
G
H
I
J
K
L
M
N
O
P
Q
R
S
1
2
3
4
5
6
7
8
9
10
11
12
13
AISLE
AISLE
AISLE
AISLE
0.5m Lower ground elevation
X
Y

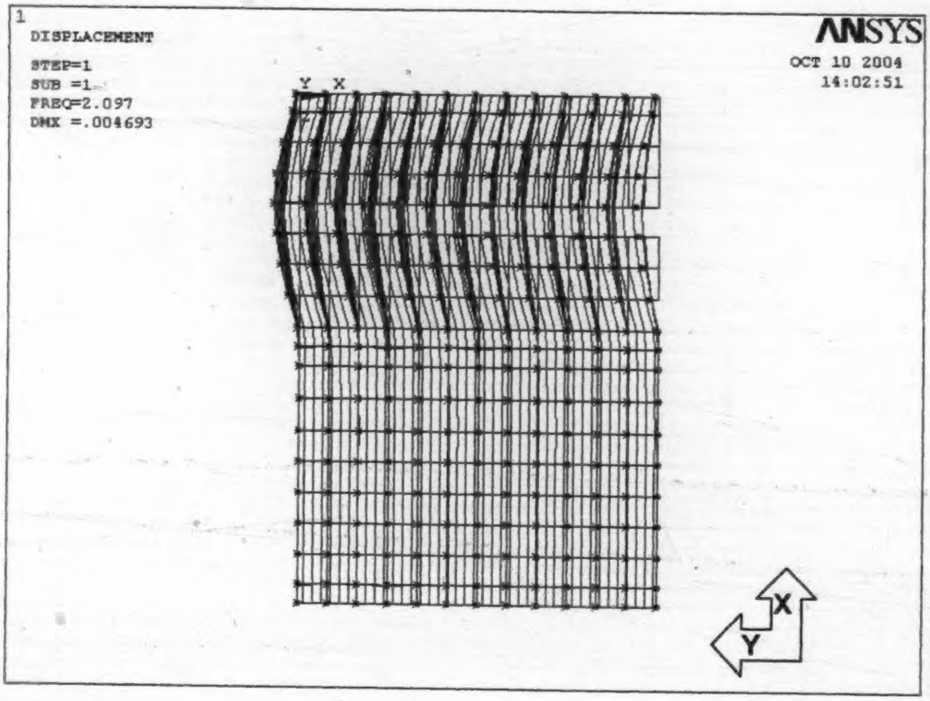
1
DISPLACEMENT
STEP=1
SUB =1
FREQ=2.097
DMX =.004693
ANSYS
OCT 10 2004
14:02:51
Y X
X
Y

Figure 5.6 Mode shape of optimized result

6 DISCUSSION AND CONCLUSIONS

6.1 Introduction

This research project was initiated in response to several complaints regarding unsettling motions of temporary grandstands. The complaints were not specific enough to determine the magnitude of the movement and there were no signs of structural overload or other problems. Hence, it was decided that a temporary grandstand should be instrumented to determine the extent of the problem. The purpose of this investigation was to monitor and analyze the response of a temporary grandstand during an event. Specifically, there were several questions that had to be addressed with this research, they included:

- How severe is the sway movement of temporary grandstands? Is the sway large enough to have concerns for second order (P-Δ) effects? Are members overloaded? Are the sway vibrations severe enough to cause panic or annoyance?
- Can we determine the dynamic response from ambient vibrations and output-only modal identification?
- Can we model accurately the dynamic response using FEA? Can it be used for prediction of the dynamic response for other temporary grandstands?

6.2 Monitoring of the Temporary Grandstand

The temporary grandstand was instrumented with strain gauges, LVDTs, cable transducers and accelerometers to measure the loads, displacement, and vibration accelerations while occupied. The event selected was the 1999 Molson Indy Car Race, held in Toronto, Ontario. The temporary grandstand that was instrumented was 37 m wide, 26 m deep and 12 m high at the rear, and had occupancy of 2811 people.

In Chapter 3, the results of the monitoring of these instruments were discussed. The average distributed load on the structure during the event was calculated based on the strain measurements for specific vertical members. The maximum average distributed load over the course of the event was determined to be 1.4 kPa and the peak load measured at any location was 2.19 kPa. Both these loads are significantly less than 4.8 kPa, which is the NBCC specified load for assembly occupancies. The sway drift as measured at the edge of the structures were relatively small, so second-order load effects could be neglected. Structurally, it could be concluded that the temporary grandstand was safe. The motion of the temporary grandstand would not be considered to be severe.

The occupant comfort, however, is determined by their perception of vibration, and is a function of the vibration acceleration. Accelerometers were used to measure the acceleration of the vibrations on the temporary grandstands. As discussed in Chapter 3 the occupants' sensitivity to vibration is related to their activity. In an office environment the occupant's sensitivity would be higher than at a sporting event, dance, or concert. Several different measures were used to quantify the acceleration that included Root Mean Square (RMS), Vibration Dose Value (VDV), and Maximum Transient Vibration Value (MTVV). RMS provides an average measure of the acceleration and was found to be within an acceptable level, of less than 0.05g, for most of the event. The VDV and MTVV are alternative measures of acceleration which are better at identifying transient vibration accelerations. Very high VDV and MTVV values were identified for one time period during the event. The level of the vibration acceleration would be sufficient to cause concern for some of the occupants, but due to short duration of the event it may have been ignored. Had the vibration been sustained for several cycles it may have resulted in complaints, however no complaints were made at this event.

It should be noted that there was very little occupant motion in the temporary grandstand other than during entry and exit. There were no synchronized activities, such as dancing or "the wave". Therefore, the occupant induced motion may have been at a minimum compared to other events, such as a rock concert.

It can be concluded from the field that the swaying motion for this temporary grandstand was not a structural safety issue. The level of vibration at this particular event was within the acceptable range for the occupants' activity, with an average RMS <0.02g, where the acceptable level is < 0.05g. There was a single short duration vibration acceleration (MTVV = 0.34g), where the lower acceleration limit for the onset of panic is

0.35 g [IStructE, 2001]; but due to the brief nature of the event (< 5 seconds.) it did not appear to cause any significant concern amongst the occupants (at least none was reported)

6.3 Output-Only Modal Identification

Natural frequencies and mode shapes were determined based on ambient vibration and output-only modal identification. The power spectral plots of the instruments showed several prominent frequencies. To identify the natural frequency a corresponding mode shape must be identified as well. A mode shape was successfully identified by Frequency Domain Decomposition at a frequency of 2.1 Hz. This frequency is close to the forcing frequencies associated with walking (1.6 to 2.4 Hz). Since this natural frequency was only observed when the occupants were exiting the temporary grandstand, it may be assumed that their walking may have induced a resonant effect that was observed. Despite this resonant effect the occupants may not have been aware of the vibration since they were moving and not sitting. Also, the relatively short distance that the occupants have to travel to the exit may have mitigated their perception of the motion.

6.4 Modelling the Dynamic Response with FEA.

At the start of the research project it was not known if the dynamic response of temporary grandstand could be modelled with FEA without tailoring the model to the measured response. A preliminary FEA model was created from which natural frequencies and mode shapes were determined. This information was used to establish the location of field instrumentation used to monitor the behaviour of the grandstand. The natural frequencies and mode shapes obtained from the finite element analysis were found to differ significantly from the observed modal properties. Initially, it was thought that the model may require several factors that would be adjusted to fit the measured response. If this were the case then it would seriously limit the usefulness of performing a FEA since each model would have to be adjusted using a measured response.

It was not known why the preliminary FEA and the measured response were so different. However, the literature review identified several factors that could affect the dynamic response of the temporary grandstand and explain the differences. These factors included: the ledger-standard connection stiffness, brace stiffness, and occupant mass. Also it was found that the temporary grandstand was modified when it was constructed and these changes were not included in the preliminary FEA. These factors, and the geometry changes, could account for the differences between the measured response and the predicted response.

A series of sensitivity analysis were conducted to identify which of these factors may have affected the FEA results. From the sensitivity analysis, it was found that the ledger-standard connection stiffness and the brace stiffness did not require reduction factors and their connections could be considered rigid. Modifying the FEA model to reflect the changes to the structure resulted in a significant improvement in the correlation of the mode shapes. The occupant mass was the only variable that was unknown. It was not known if the occupant mass should be ignored or if a partial or full mass should be included in the modal analysis. It was found that the occupant mass, correlating with the measured response, had an equivalent distributed load of 1.39 kPa. This result was close to the estimated average distributed load of 0.98 kPa for the same time period, which further validates the FEA model.

The FEA model closely modeled the dynamic response of the temporary grandstand once the model had been updated to reflect the changes to the geometry and with an accurate estimate of occupant load was applied. No special factors were required to manipulate the FEA model to match the measured response. This suggests that FEA is a useful tool to predict the dynamic response of temporary grandstands. However, this has been shown only for this particular case and additional cases are required to validate this result for other temporary grandstands.

6.5 Conclusions

It was found that the loads, displacements, and vibrations were within acceptable limits for the temporary grandstand. For this particular event there were no extreme movements that would have caused concern for the occupants. A natural frequency was identified at 2.1 Hz, which is close to the average frequency for walking (1.6 to 2.4 Hz) and therefore a potential for resonance existed. However, this natural frequency was observed when the occupants were exiting the grandstand, and their sensitivity to the vibration motion would be much lower than when they were sitting. No complaints of discomfort were reported at this event.

The FEA model of the temporary grandstand was found to correlate very well with the measured natural frequency and mode shape. To achieve these results the model was modified to closely match the geometry of the completed structure and the occupant mass was added. No other modifications were required to the FEA model. While these results are promising, they are only applicable to this particular case, and it cannot be assumed to apply to other temporary grandstands without further verification.

6.6 Recommendations

Although a good correlation between field data and finite element analysis results was observed, other temporary grandstands should be monitored to provide further validation to the procedure used in this research. A wider range of grandstand configurations and different activities, such as rock concerts, should be investigated since the dynamic response of grandstands is affected by the nature of the load and the configuration of the structure.

Strain measurements on sway braces were not reliable due to looseness at the brace connections, which would permit some sway movement before loading the brace. As a result, the strain measurements could not be directly related to the sway displacements. Since the degree of looseness varied from brace to brace, a correction could not be applied to the data. It is recommended for future projects that the instrumented sway braces be modified to include an adjustment that would eliminate slack in the brace. This would allow the strains in the sway braces to be related directly to the sway displacements.

It is recommended that additional accelerometers be located along the side of the grandstand. This would allow modes that are primarily in the side-side direction to be measured accurately. The present configuration had accelerometers mounted only at the rear of the structure, which was only suitable for measuring forward-back sway motions or side-side motion involving the rear of the stand. The additional accelerometers would also provide redundancy, in the case of a failure of one of the accelerometers or in terms of identifying a vibration event.

7 REFERENCES

Alberta Human Resources and Employment (2003), "Occupational Health and Safety Code Explanation Guide, Part 23: Scaffold and Temporary Work Platforms", Alberta Queens Printer, Edmonton, Alberta, November.

Allen, D.E and Rainer, J.H (1975), "Floor Vibration", National Research Council of Canada, Division of Building Research, Canadian Building Digest 173, September.

Allen, D.E, Rainer, J.H., Pernica, G (1985), "Vibration Criteria for Assembly Occupancies", Canadian Journal of Civil Engineering, Vol 12, pp 617-623.

American National Standards Institute (1988), "American National Standard for Construction and Demolition Operations – Scaffolding – Safety Requirements", ANSI A10.8-1988.

Anderson, P. and Brincker, R. (2003), "The Stochastic Subspace Identification Techniques", http://www.svibs.com/literature/Notes/Modal_Analysis/Note_on_SSI.htm.

Bachmann, Hugo, *et al.* (1995), "Vibration Problems in Structures: Practical Guidelines", Birkhäuser Verlag, Berlin

Brincker, R. and Andersen, P. (1999), "ARMA Models in Modal Space", Proceedings of the 17th International Modal Analysis Conference (IMAC), Kissimmee, Florida, pp 330-334.

Brincker, R. and Zhang, L. (2000), "Output-Only Modal Analysis by Frequency Domain Decomposition", Proceedings of The ISMA25 Noise And Vibration Engineering Volume 11, Leuven, Belgium, pp.717-723, September 13-15.

Brincker, R., Zhang, L., Andersen, P. (2000), "Modal Identification from Ambient Responses using Frequency Domain Decomposition", Proceedings of the 18th IMAC, San Antonio, Texas, pp 625-630.

Brincker, R., Ventura, C.E., Andersen (2001), "Damping Estimation by Frequency Domain Decomposition", Proceedings of The 19th International Modal Analysis Conference (IMAC), Kissimmee, Florida, pp.698-703.

British Columbia OH&S (1997), "British Columbia Safety Regulation, Part 13: Ladder, Scaffolds and Temporary Work Platforms".

Brownjohn J M W, Pan T C, Deng X Y (2000), "Macro-Updating of Finite Element Modelling for Core Systems of Tall Buildings", Proceedings of the 14th Engineering Mechanics Conference-ASCE, Austin, Texas, 21-24 May.

Canadian Standards Association (1987), "Access Scaffolding for Construction Purposes", CAN/CSA-S269.2-M87, Rexdale, Ontario.

Ellis, B.R. and Ji, T. (1997), "Human-Structure Interaction in Vertical Vibrations", Proceedings of the Institution of Civil Engineering Structures and Buildings, Feb 1-9.

Gatti, P.L. and Ferrari, V. (1999), "Applied Structural and Mechanical Vibration: theory, methods and measuring instruments", E&FN Spon, London.

Godley, M. H. R. and Beale, R.G. (1997), "Sway Stiffness of Scaffold Structures", The structural engineer, Vol. 75, No. 1, 7 January, pp 4-12.

Godley, M.H.R.and Beale, R.G. (2001), "Analysis of Large Proprietary Access Scaffold Structures", Structures and Buildings: ICE Proceedings, Vol 146, No. 1, UK, Feb, pp 31-39.

Heylen, W and Janter, T. (1988), "Applications of the Modal Assurance Criterion in Dynamic Model Updating", 13th International conference of Noise and Vibration engineering (ISMA13), Leuven, Belgium.

IStructE (1999), "Temporary Demountable Structures: Guidance on Design, Procurement and Use", Second Edition, Clarke, J.N. (ed), The Institution of Structural Engineers, London, England, March.

IStructE (2001), "Dynamic Performance Requirements for Permanent Grandstands Subjected to Crowd Action: Interim Guidance on Assessment and Design", The Institution of Structural Engineers, London, November.

IStructE (2002), "Dynamic Testing of Grandstands and Seating Decks, Advisory Note", Dougill, J.W. (Chair), The Institution of Structural Engineers, London, UK, June.

International Organization of Standards (1997), "Mechanical Vibration and Shock - Evaluation of Human Exposure to Whole-Body Vibration - Part 1: General Requirements", Edition: 2nd, ISO 2631-1, Geneva, May.

Jacobs, N (1996), "Temporary Demountable Structures: the need for guidance. Excursus", The Structural Engineer, v.74, n.5, p 84.

Ji, T. and Ellis, B. R. (1997), "Effective Bracing Systems for Temporary Grandstands", The Structural Engineer", Vol. 75, No. 6, March, p 95-100.

Juang, J-N and Pappa, R.S. (1985), "An Eigenvalue Realization Algorithm for Modal Parameter Identification and Model Reduction", Journal of Guidance, Vol. 8, No. 5, Sept- Oct.

Krämer, C., de Smet, C.A.M., Peeters, B (1999), "Comparison of Ambient and Forced Vibration Testing of Civil Engineering Structures", 17th International Modal Analysis Conference, Kissimee, Florida, February.

Kharrazi, M.H.K, Ventura, C.E, Brincker, R., Dascotte E. (2002), "A Study on Damage Detection Using Output-Only Modal Data", 20th International Modal Analysis Conference (IMAC XX), Los Angeles, USA, February.

Lord, J-F and Ventura, C. (2003), "FEM Updating using Ambient Vibration Data from a 48 Storey Building in Vancouver, British Columbia, Canada", 32nd International Congress and Exposition on Noise Control Engineering, Seogwipo, Korea, August 25-28.

Manheim, D and Honeck, W. (1987), "A Case Study of Spectator Induced Vibrations", Use of Vibration Measurements in Structural Evaluation, Proceedings of the Structural Division of the American Society of Civil Engineers, Atlantic City, April 29.

Meyyappa, M, Palsson, H, Craig, J.I. (1986), "Modal Parameter Estimation For a Highrise Building using Ambient Response Data taken During Construction", Dynamic Response of Structures: Proceedings of the 3rd Conference by the Engineering Mechanics Division, ASCE, Los Angeles, California, March 31-April 2.

National Research Council (2005), "National Building Code of Canada 2005", National Research Council of Canada, Ottawa.

National Research Council (2005), "User's Guide – NBC 2005. Structural Commentaries (Part 4 of Division B), National Research Council of Canada, Ottawa.

Ontario Building Code Commission (1995), "Building Code Commission Decision on B.C.C#95-08-428", Ontario Ministry of Municipal Affairs and Housing, Toronto, February 28.

Peeters, B and de Roeck, G (1999), "Reference-Based Stochastic Subspace Identification for Output-Only Modal Analysis", Mechanical Systems and Signal Processing, 13, 6, pp 855-878.

Pernica, G. (1983), "Dynamic Live Loads at a Rock Concert", Canadian Journal of Civil Engineering, June, pp 185-191.

Rainer, J.H. (1984), "CBD-232. Vibrations in Buildings", National Research Council of Canada, May.

Reynolds, P. and Pavic, A. (2002), "Modal Testing of a Sports Stadium", 20th International Modal Analysis Conference (IMAC XX), Los Angeles, California.

Reynolds, P., Pavic, A., Ibrahim, Z. (2003), "A Remote Monitoring System for Stadia Dynamics", 21st International Modal Analysis Conference, Kissimmee, Florida, Feb 3-6.

Schiff, A.J (1972), "Identification of Large Structures using Data from Ambient and Low Level Excitations", System Identification of Vibrating Structures: Mathematical Models from Test Data, Applied Mechanics Division ASME, New York, pp 87-120.

Simiu, E and Scanlan, R.H. (1986), "Wind Effects on Structures: An Introduction to Wind Engineering", 2nd Edition, John Wiley & Sons, New York.

Tamura, Y., Zhang, L., *et al* (2002), "Ambient Vibration Tests and Modal Identification of Strucutures by FDD and 2DOF-RD Technique", Structural Engineers World Congress (SEWC2002), Yokohama, Japan, Oct 9-12.

Teughels, A., Maeck, J., De Roeck,G. (2001), "A Finite Element Model Updating Method using Experimental Modal Parameters Applied on a Railway Bridge", Proceedings of 7th International Conference on Computer Aided Optimum Design of Structures, Bologna, Italy, May, pp.97-106.✓

Ventura, C. E., Brincker ,R., Dascotte , E., Andersen, P. (2001), "Fem Updating Of The Heritage Court Building Structure", Proceedings of The 19th International Modal Analysis Conference (IMAC), Kissimmee, Florida, pp.324-330.

Ventura, C.E., Lord, J-F, Simpson, R.D. (2002), "Effective use of Ambient Vibration Measurements for Modal Updating of a 48 Storey Building in Vancouver Canada", International Conference on Structural Dynamics Modeling- Test, Analysis, Correlation and Validation, Instituto de Engenharia Macânica, Madeira Island, Portugal.

Welch, P.D (1967), "The Use of Fast Fourier Transform for the Estimation of Power Spectra: A Method Based on Time Averaging Over Short, Modified Periodograms," IEEE Trans. Audio Electroacoustics, Vol. AU-15, pp.70-73.

APPENDIX A

Power Spectra

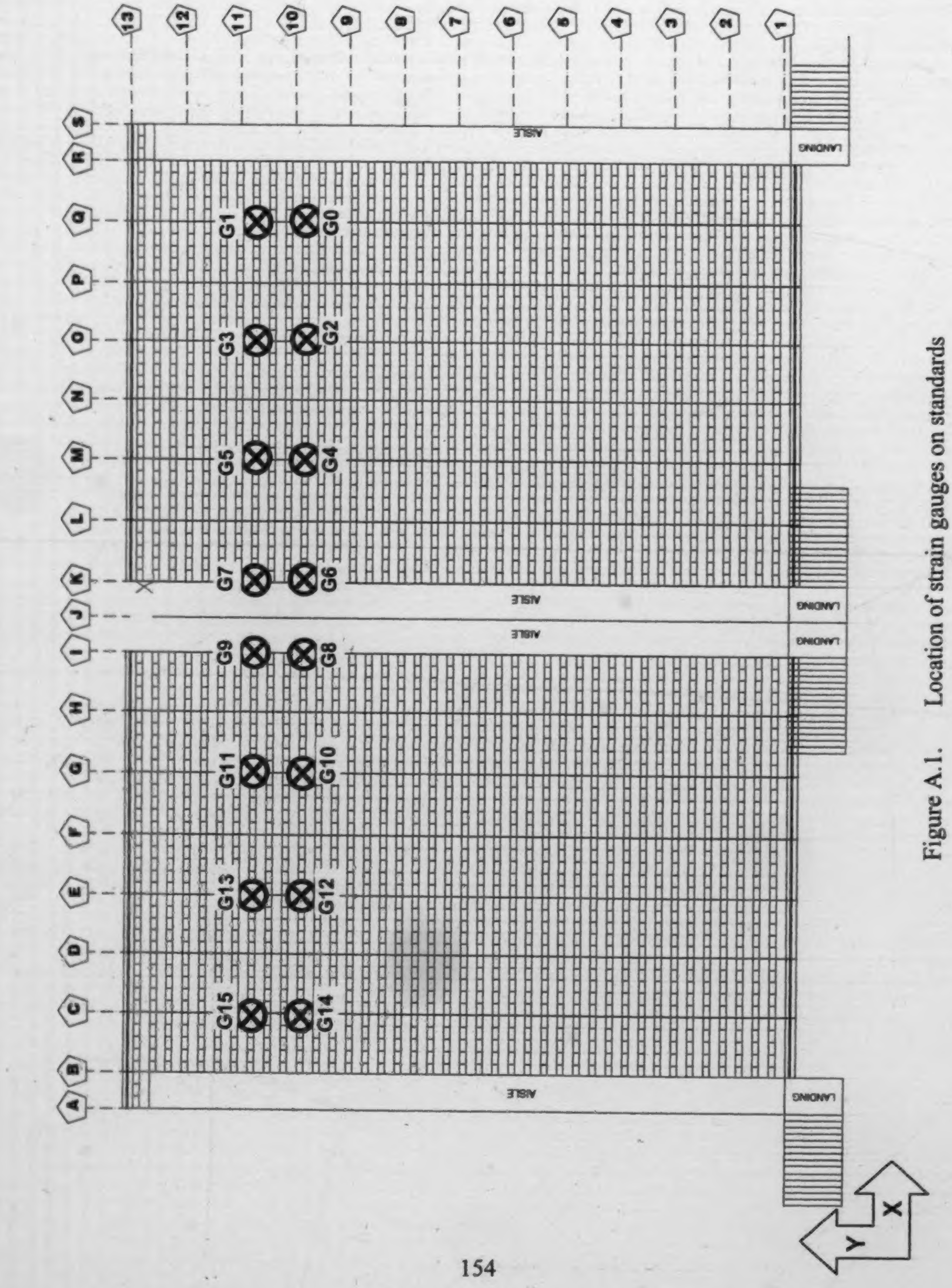
A
B
C
D
E
F
G
H
I
J
K
L
M
N
O
P
Q
R
S
1
2
3
4
5
6
7
8
9
10
11
12
13
G0
G1
G2
G3
G4
G5
G6
G7
G8
G9
G10
G11
G12
G13
G14
G15
AISLE
AISLE
AISLE
AISLE
LANDING
LANDING
LANDING
LANDING
X
Y

Figure A.1. Location of strain gauges on standards

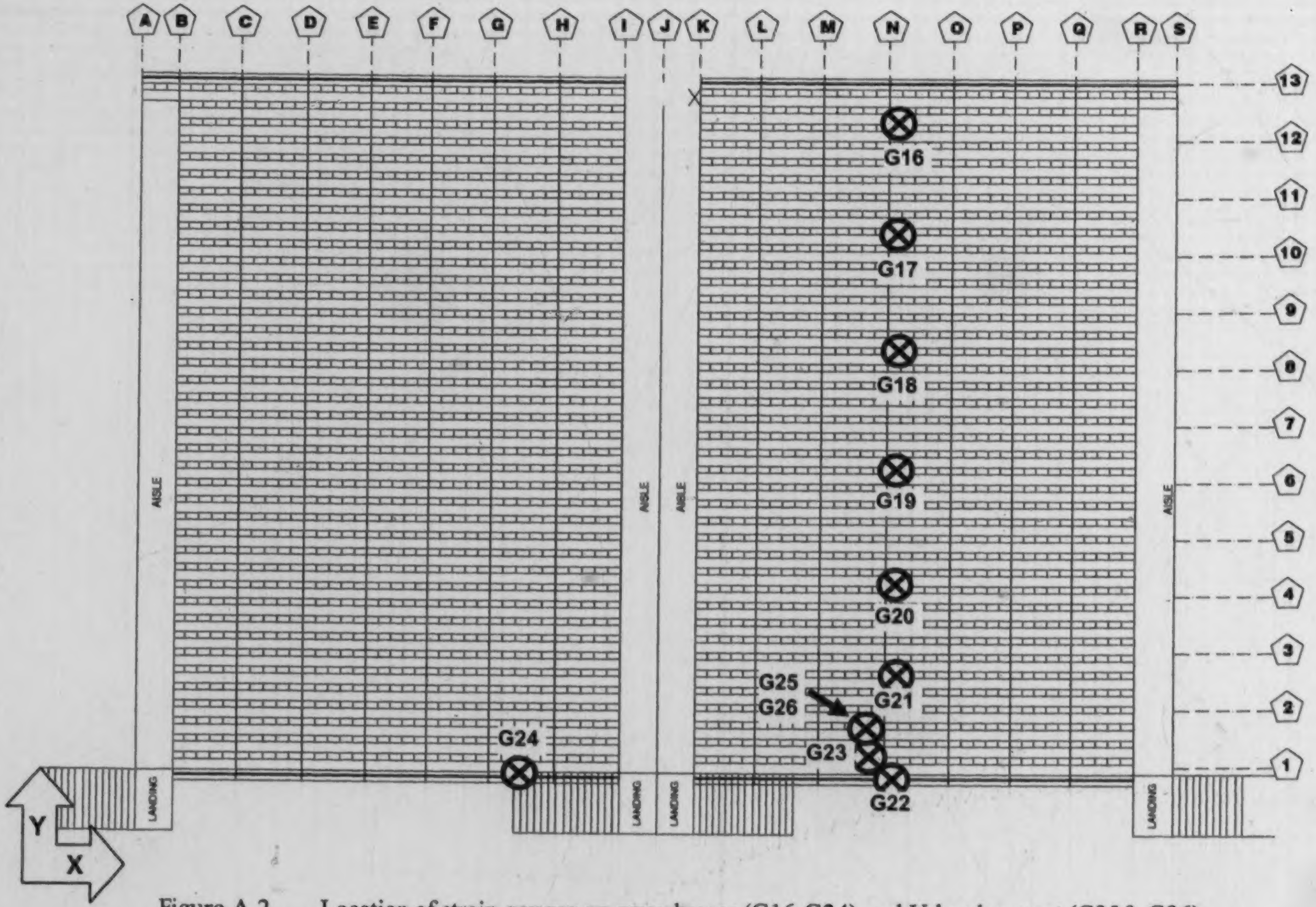
A
B
C
D
E
F
G
H
I
J
K
L
M
N
O
P
Q
R
S
13
12
11
10
9
8
7
6
5
4
3
2
1
G16
G17
G18
G19
G20
G21
G22
G23
G24
G25
G26
AISLE
AISLE
AISLE
AISLE
LANDING
LANDING
LANDING
LANDING
Y
X

Figure A.2. Location of strain gauges on sway braces (G16-G24) and U-head support (G25& G26)

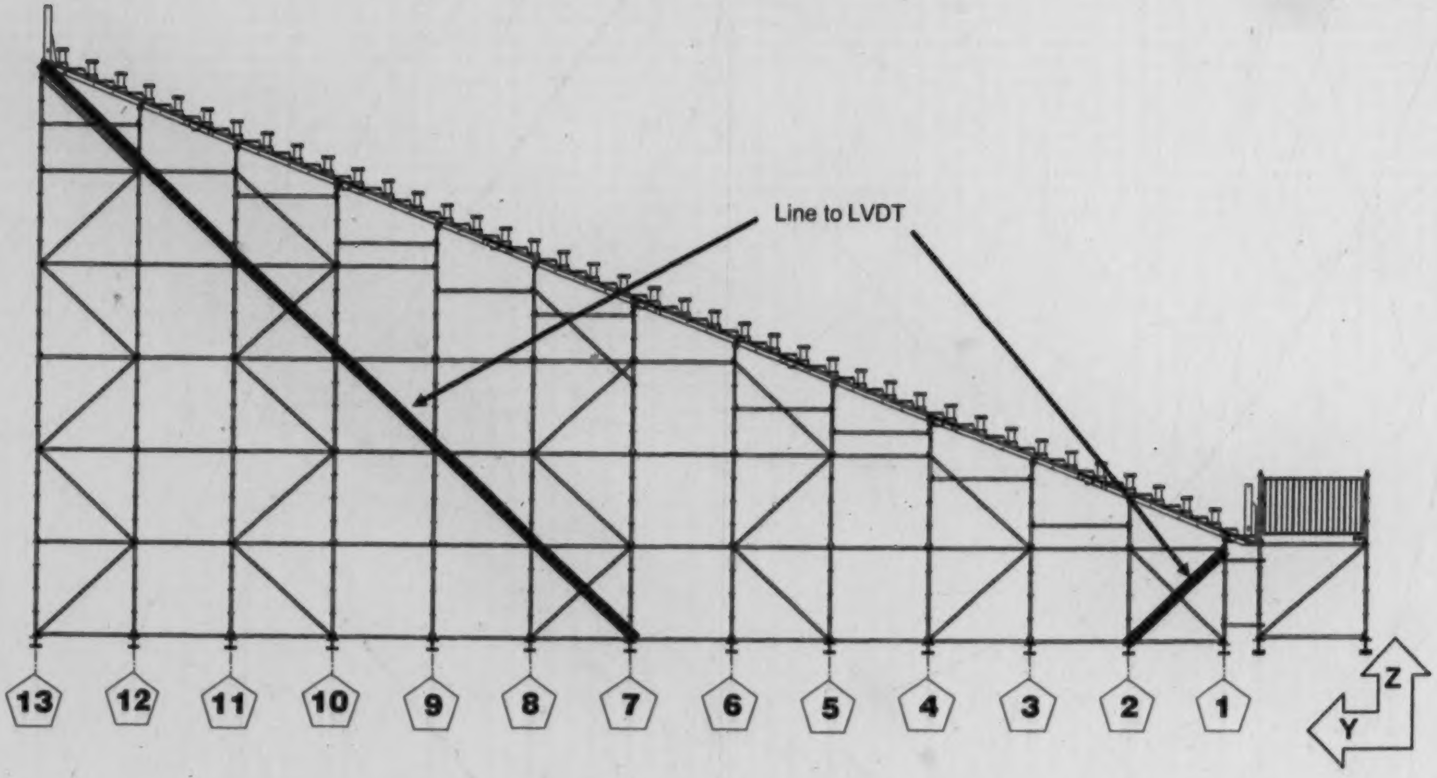
Line to LVDT
13
12
11
10
9
8
7
6
5
4
3
2
1
Z
Y

Figure A.3. Side cross section showing line to LVDT to measure front-back sway motion

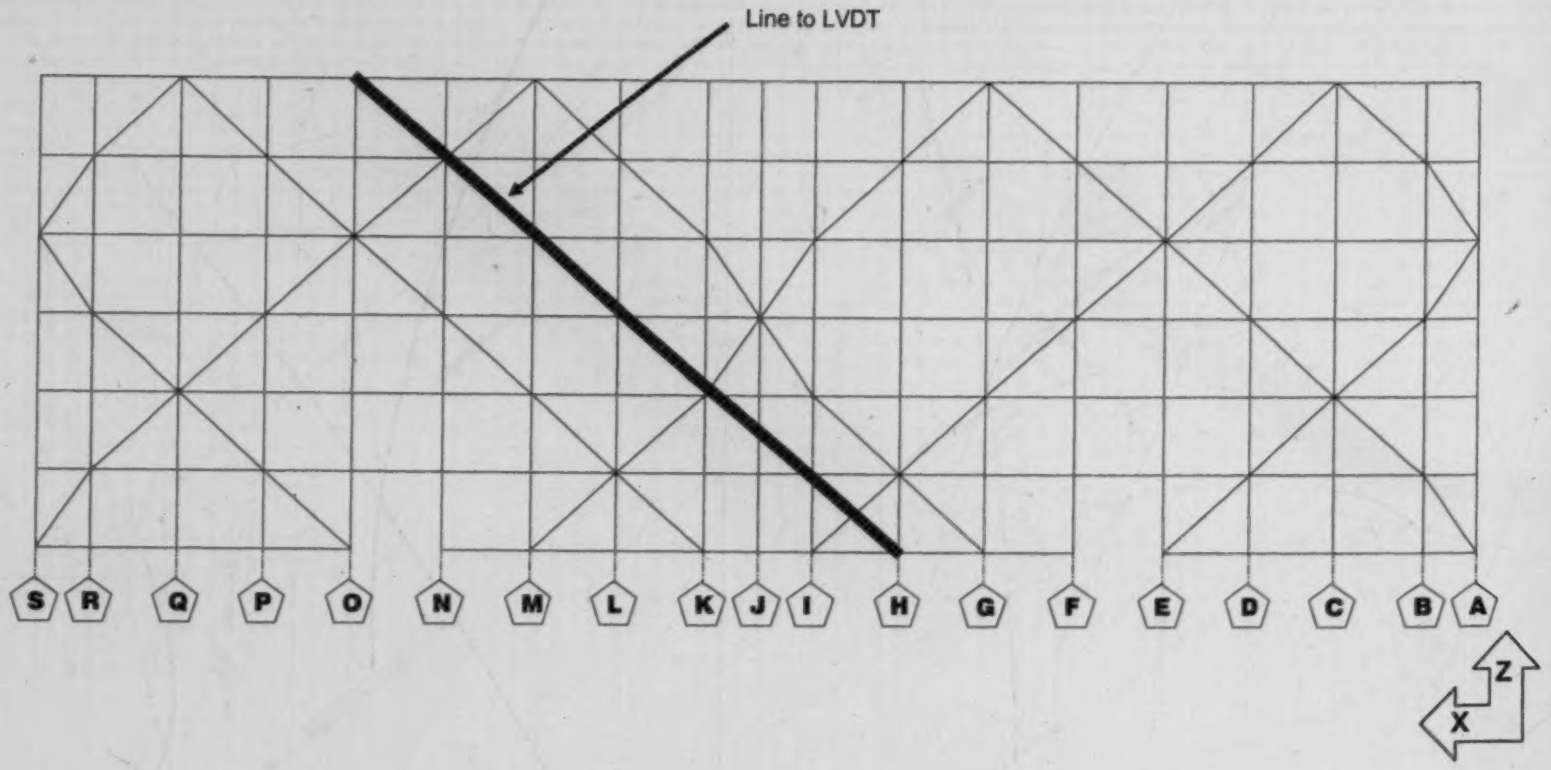
Line to LVDT
S
R
Q
P
O
N
M
L
K
J
I
H
G
F
E
D
C
B
A
Z
X

Figure A.4. Rear cross section showing line to LVDT to measure side-side sway

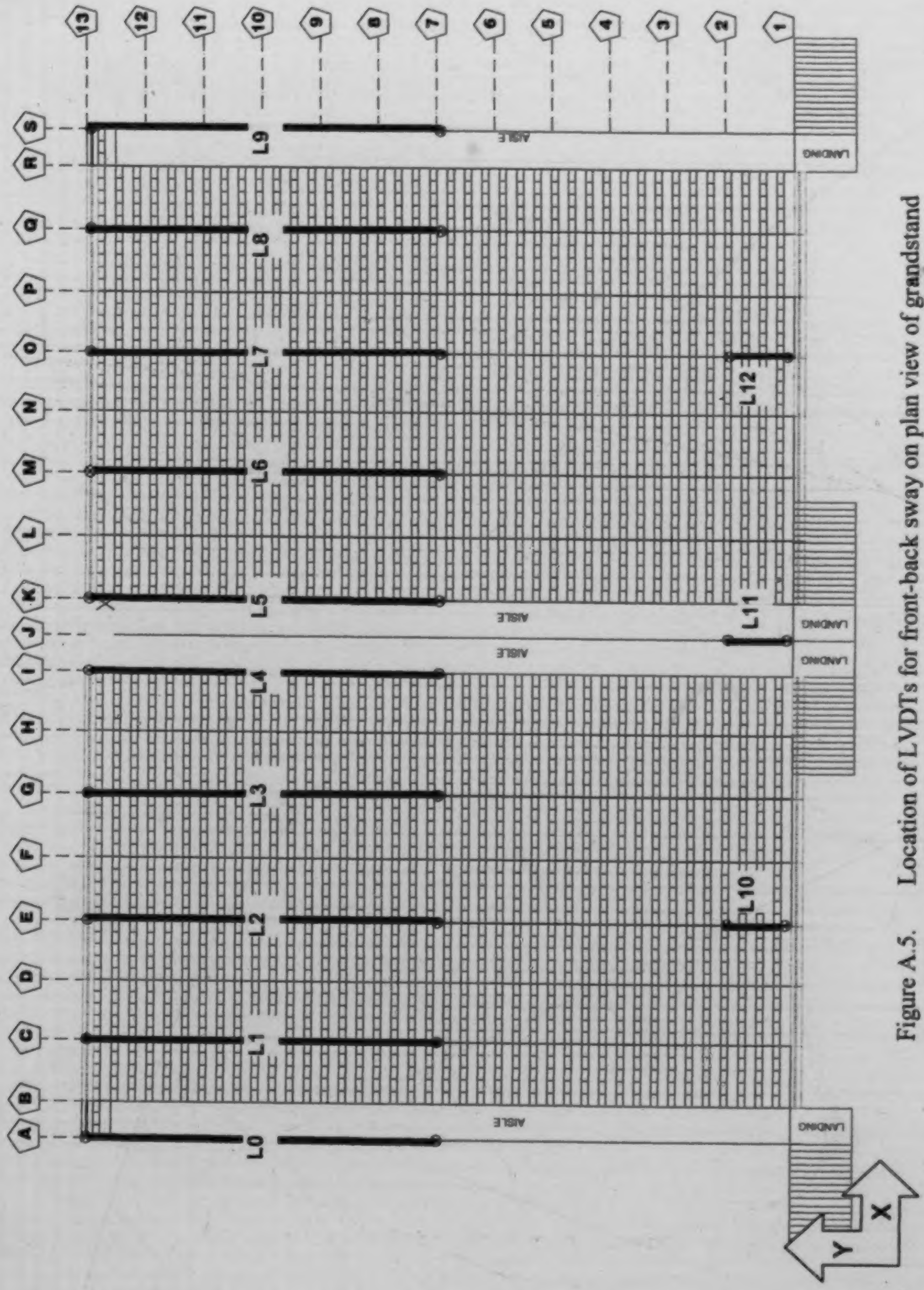

A
B
C
D
E
F
G
H
I
J
K
L
M
N
O
P
Q
R
S
1
2
3
4
5
6
7
8
9
10
11
12
13
L0
L1
L2
L3
L4
L5
L6
L7
L8
L9
L10
L11
L12
AISLE
AISLE
AISLE
AISLE
LANDING
LANDING
LANDING
LANDING
X
Y

Figure A.5. Location of LVDTs for front-back sway on plan view of grandstand

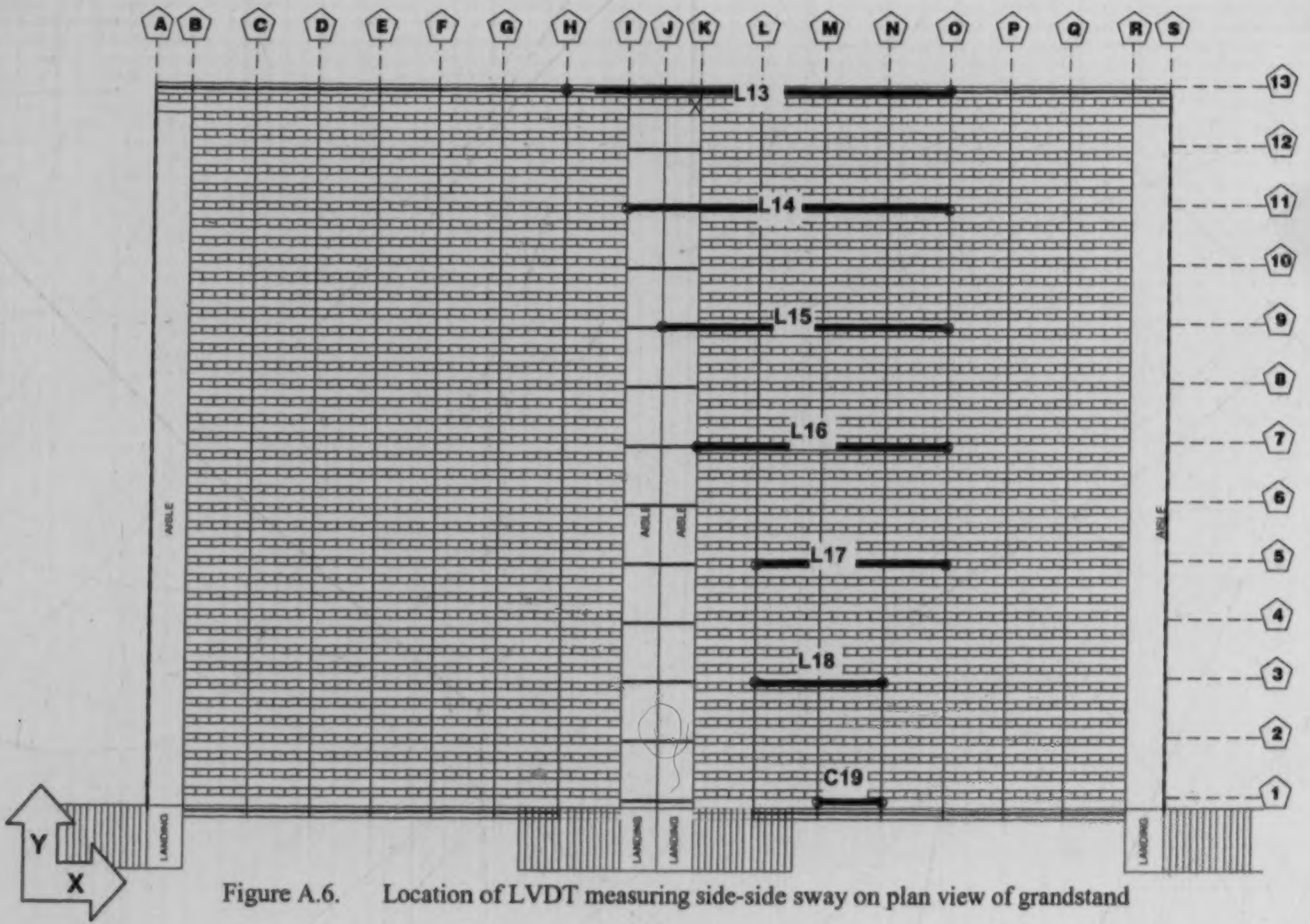
A
B
C
D
E
F
G
H
I
J
K
L
M
N
O
P
Q
R
S
13
12
11
10
9
8
7
6
5
4
3
2
1
L13
L14
L15
L16
L17
L18
C19
AISLE
AISLE
AISLE
AISLE
LANDING
LANDING
LANDING
LANDING
Y
X

Figure A.6. Location of LVDT measuring side-side sway on plan view of grandstand

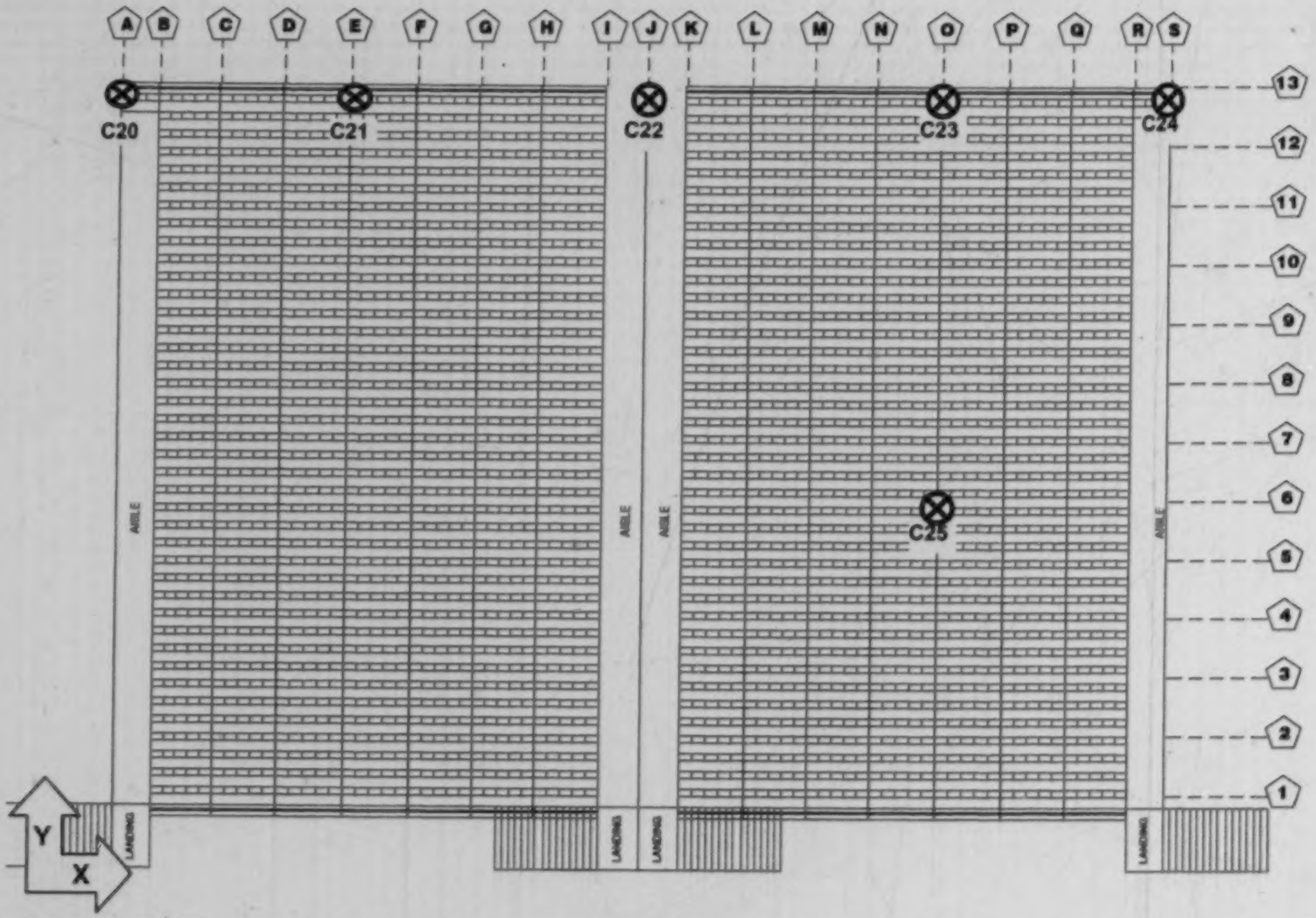
A
B
C
D
E
F
G
H
I
J
K
L
M
N
O
P
Q
R
S
13
12
11
10
9
8
7
6
5
4
3
2
1
C20
C21
C22
C23
C24
C25
AISLE
AISLE
AISLE
AISLE
LANDING
LANDING
LANDING
LANDING
Y
X

Figure A.7. Location of cable transducers measuring vertical displacement on plan view of grandstand

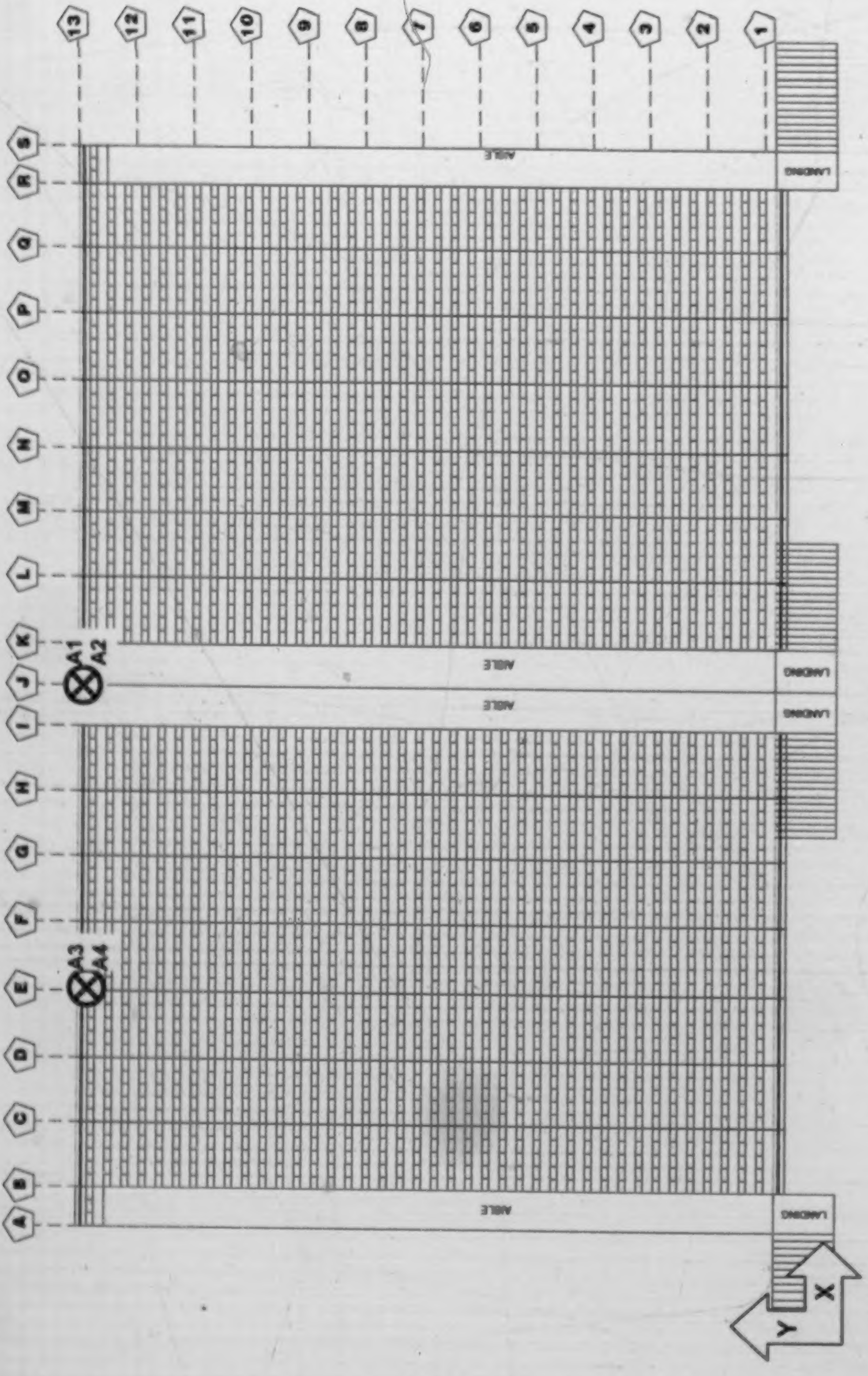
A
B
C
D
E
F
G
H
I
J
K
L
M
N
O
P
Q
R
S
1
2
3
4
5
6
7
8
9
10
11
12
13
A1
A2
A3
A4
AISLE
LANDING
X
Y

Figure A.8. Location of accelerometers on plan view of grandstand

July 17, 1999
4:32 PM

July 17, 1999
4:32 PM

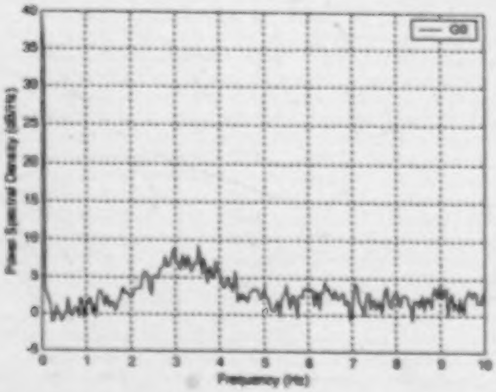

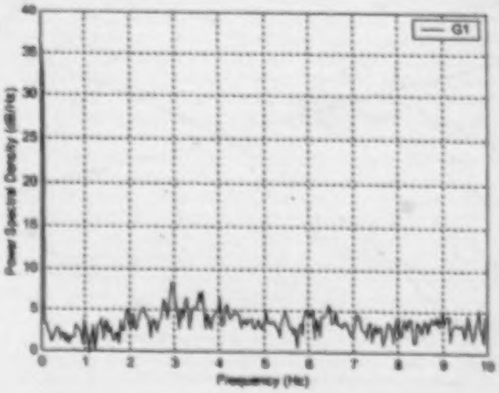

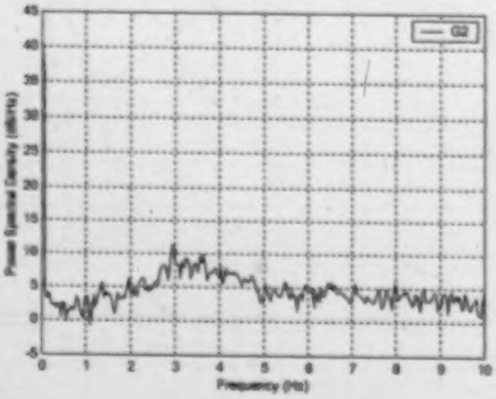

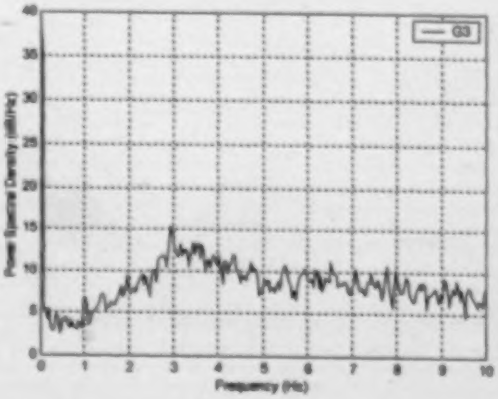

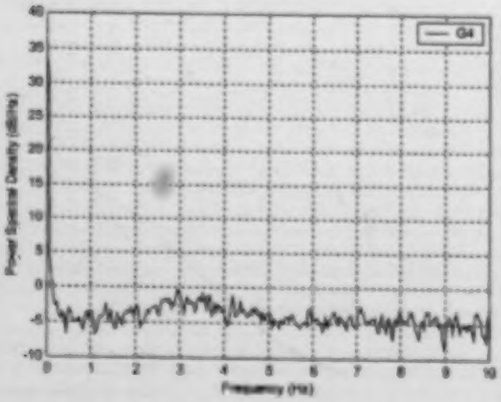

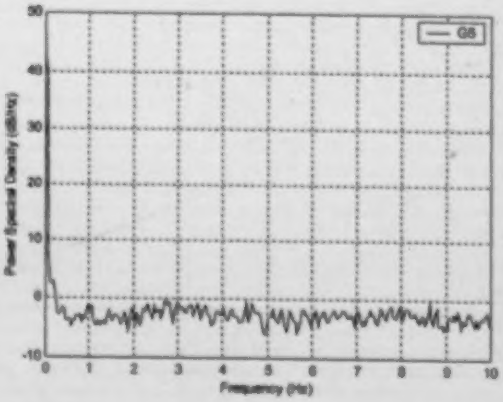

July 17, 1999
4:32 PM

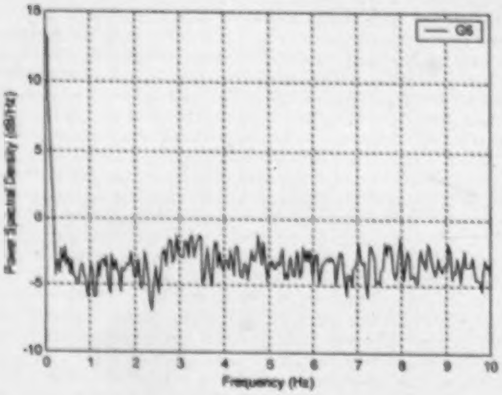

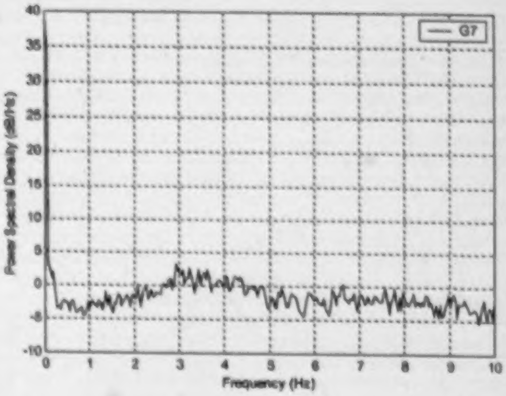

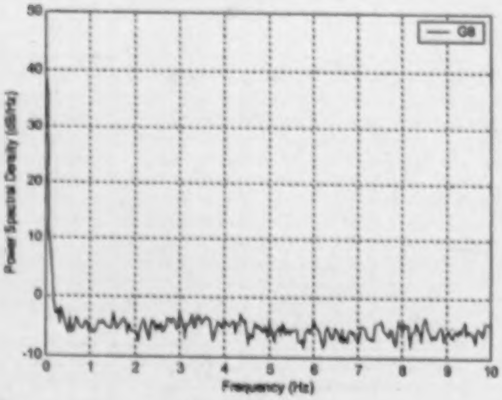

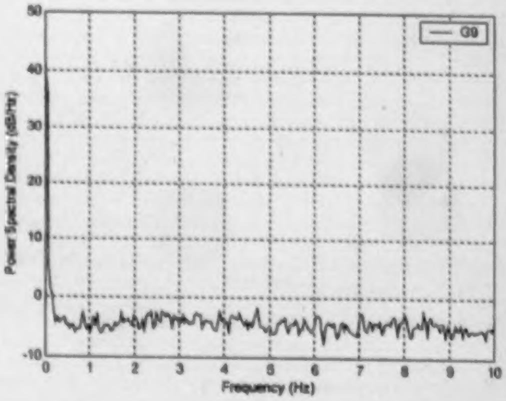

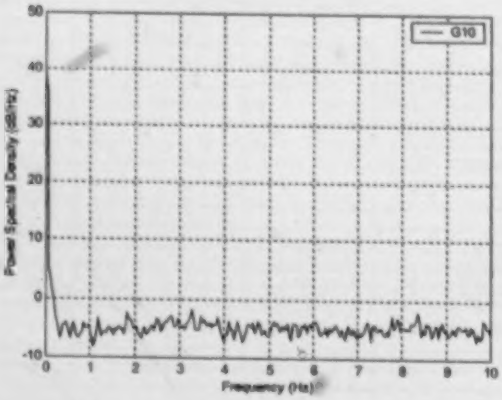

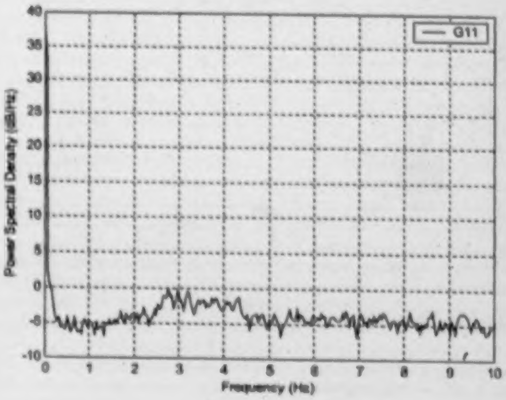

July 17, 1999
4:32 PM

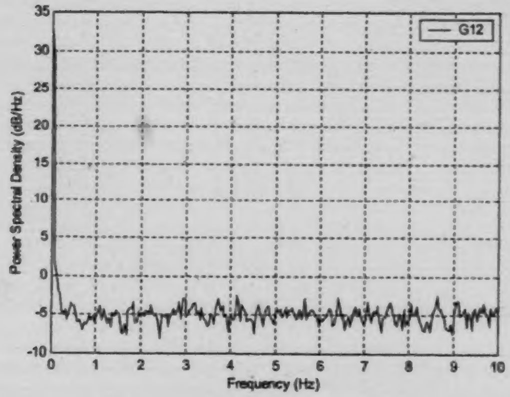

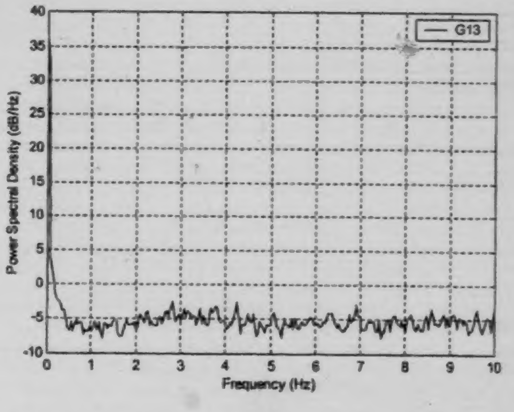

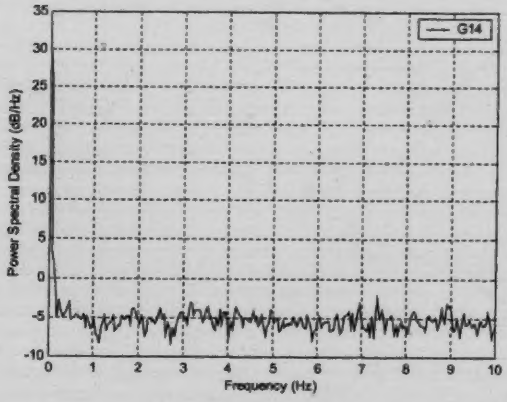

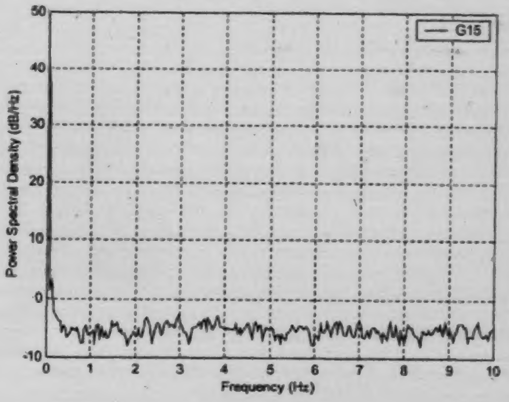

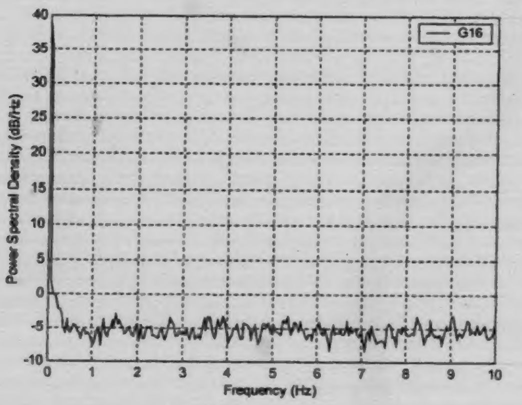

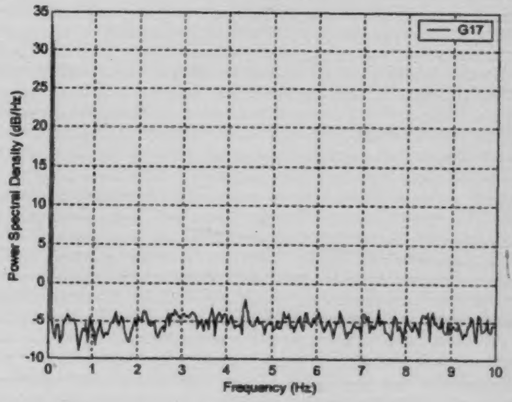

July 17, 1999
4:32 PM

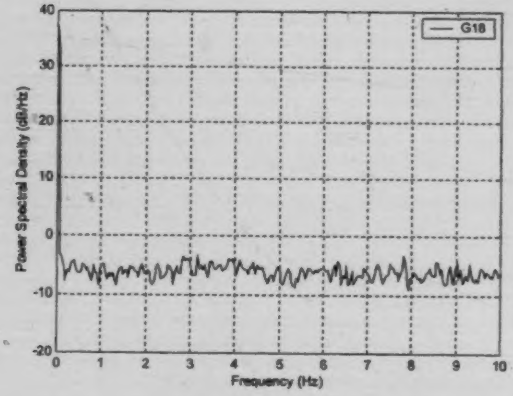

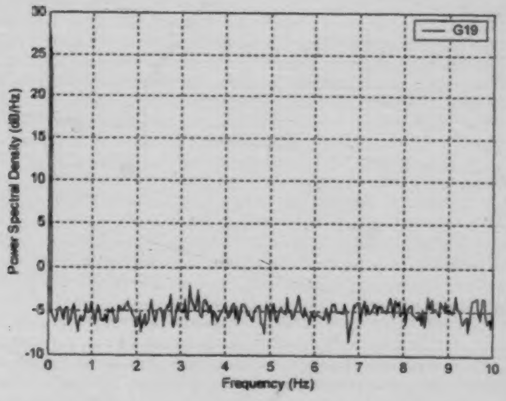

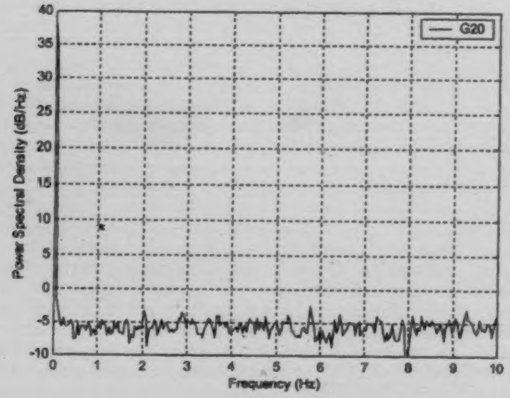

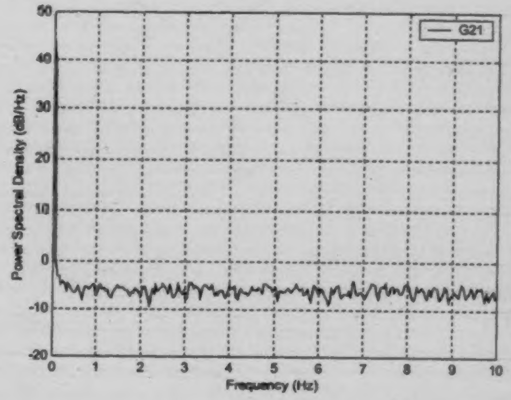

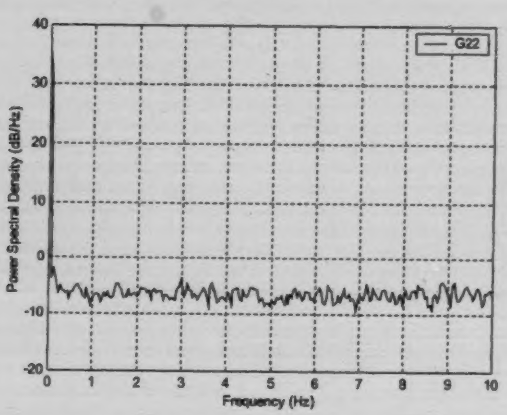

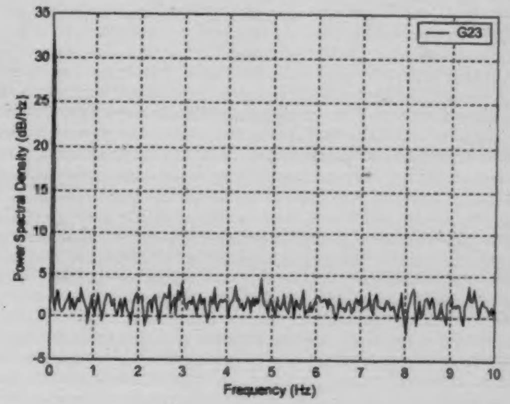

July 17, 1999
4:32 PM

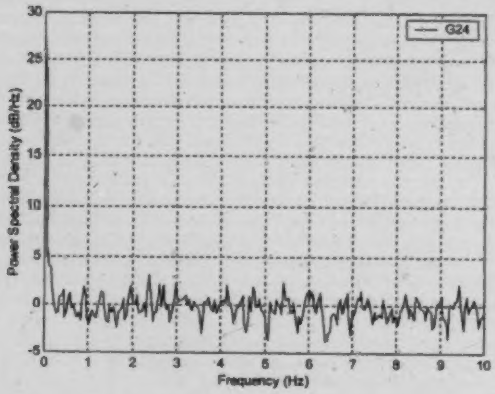

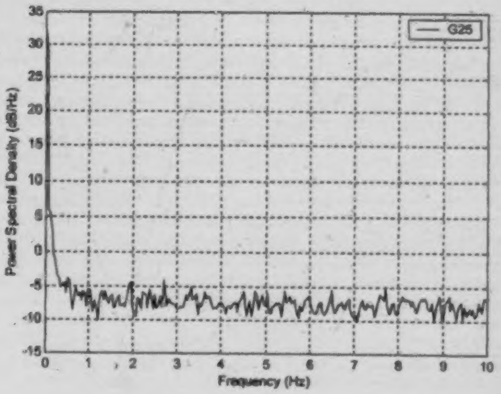

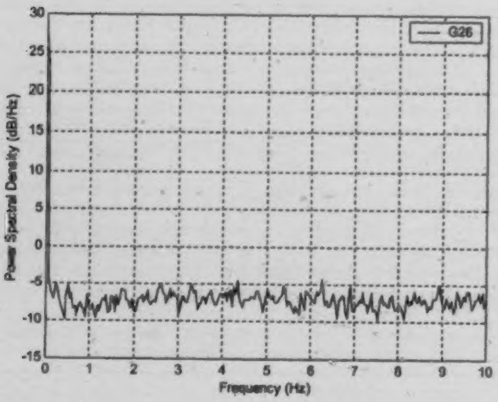

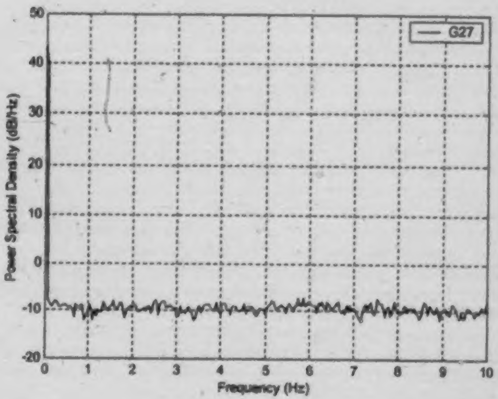

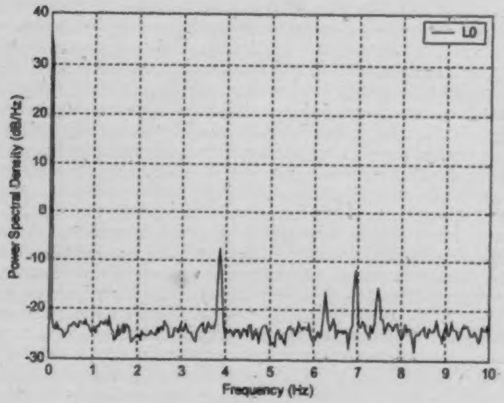

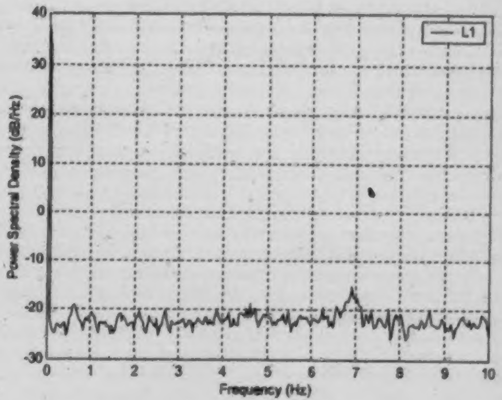

July 17, 1999
4:32 PM

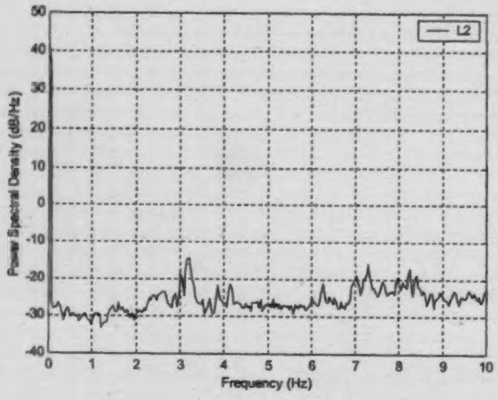

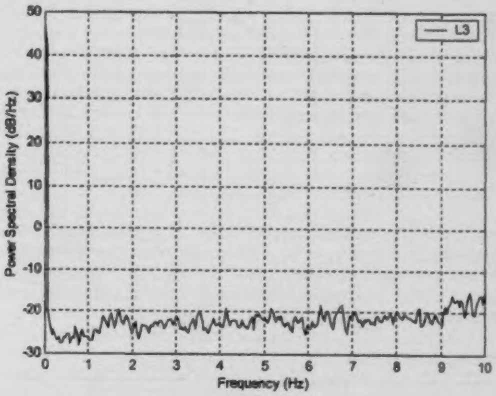

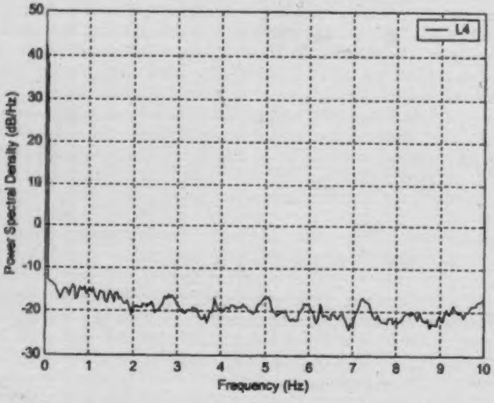

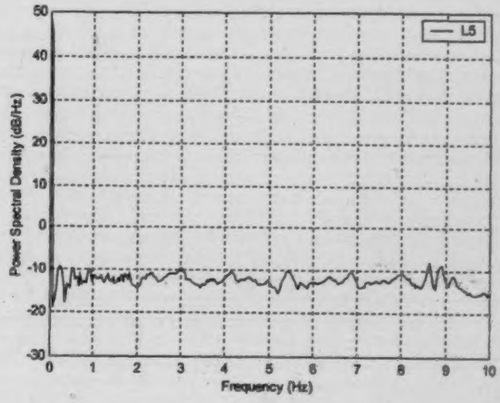

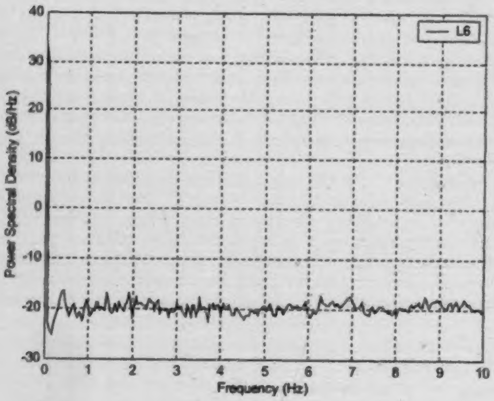

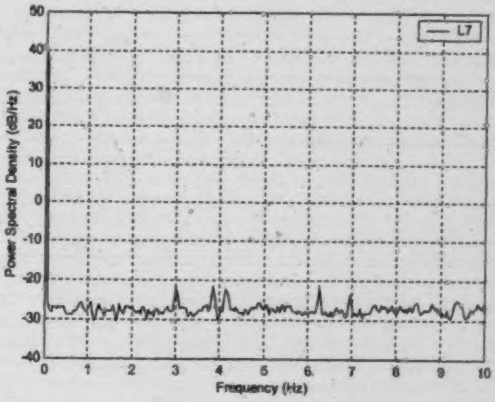

July 17, 1999
4:32 PM

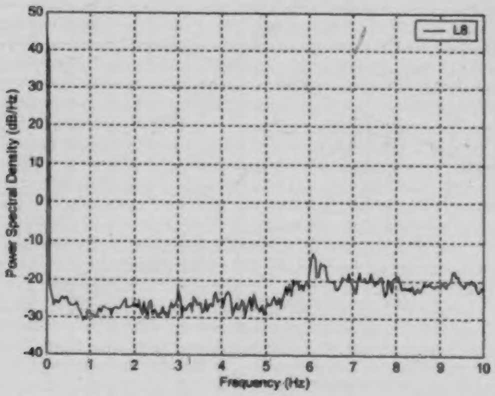

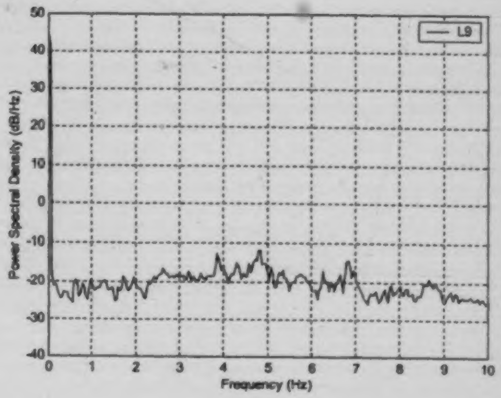

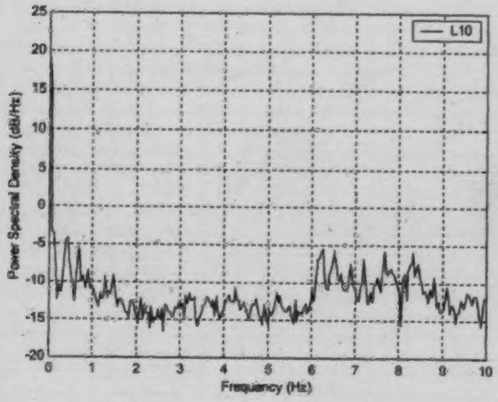

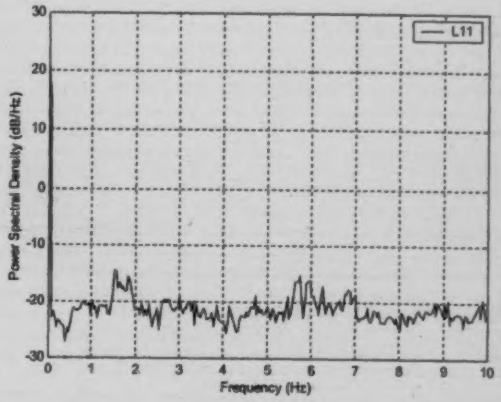

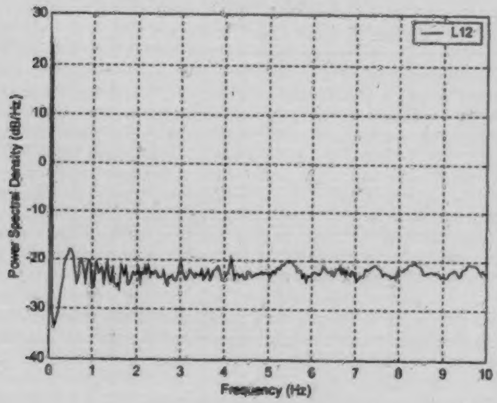

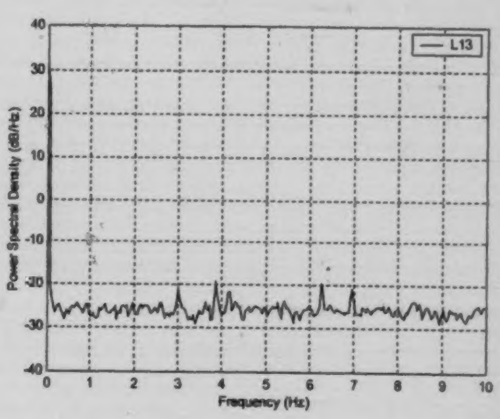

July 17, 1999
4:32 PM

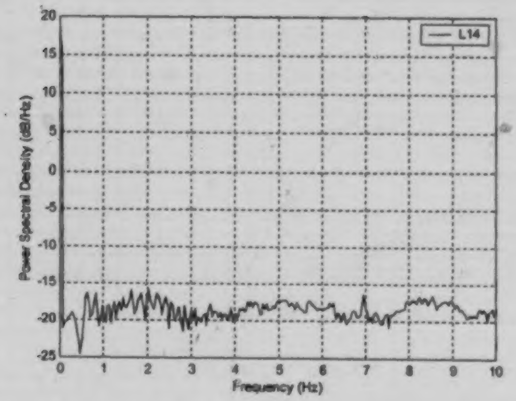

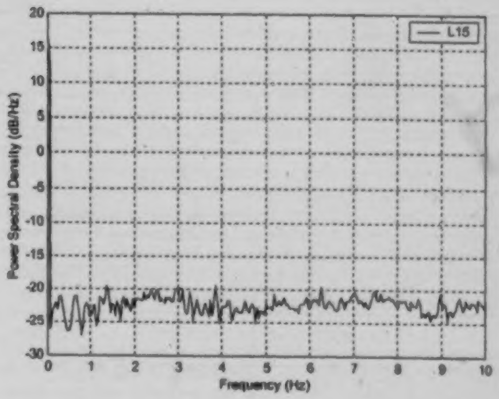

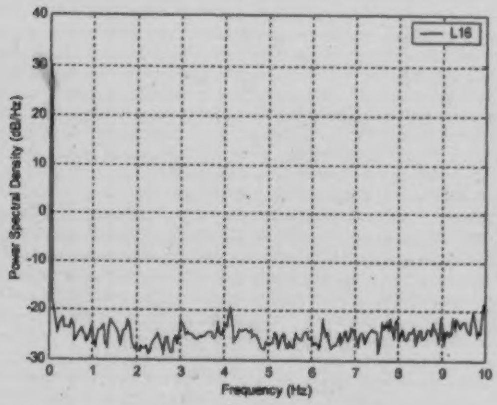

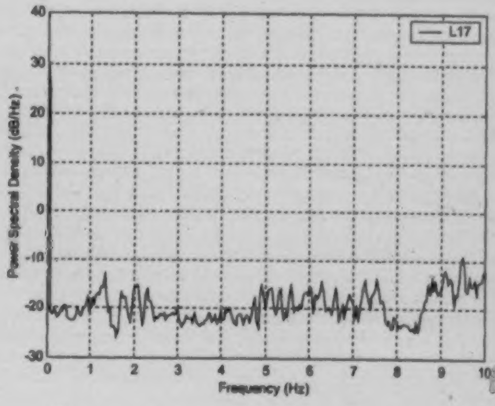

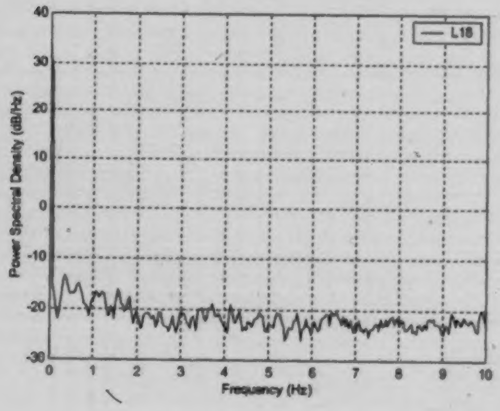

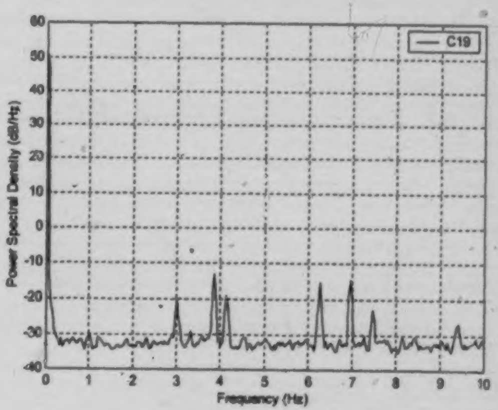

July 17, 1999
4:32 PM

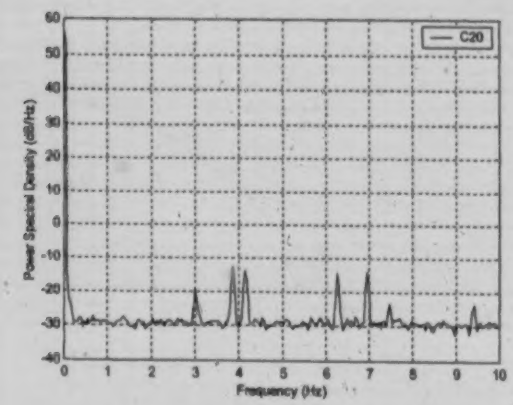

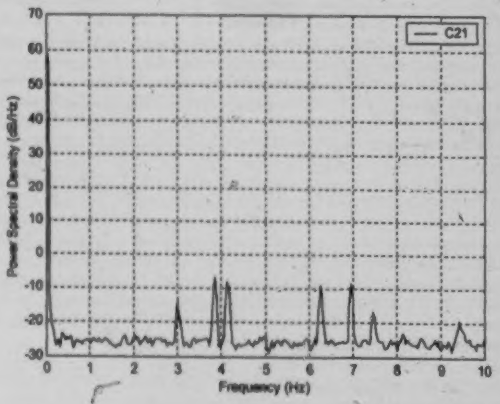

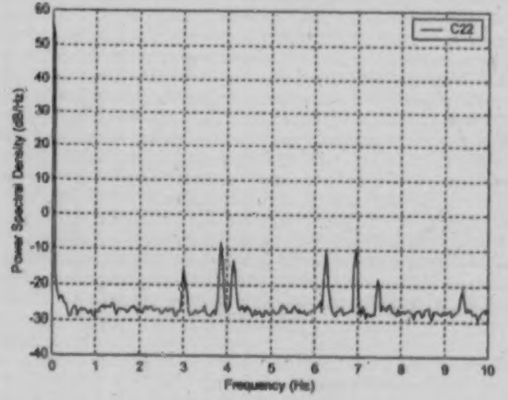

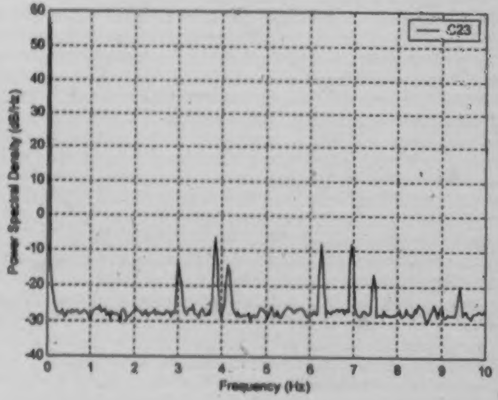

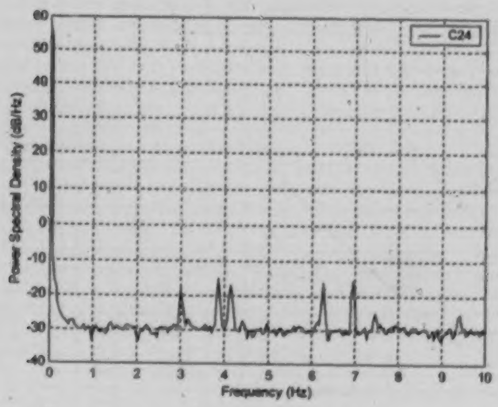

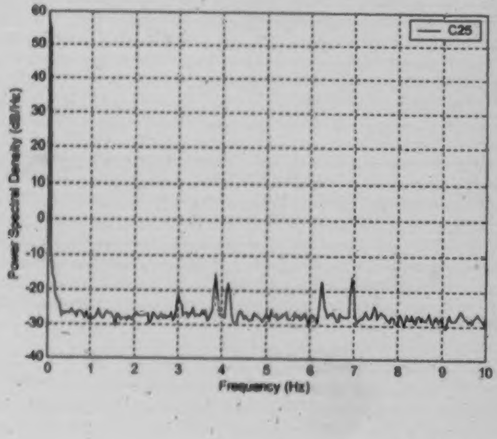

July 17, 1999
4:32 PM

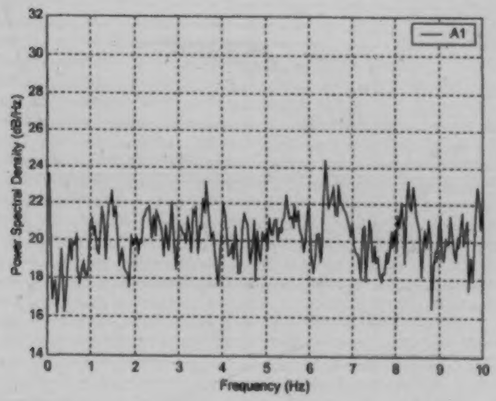

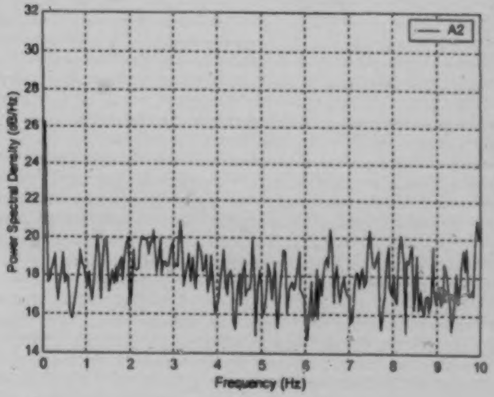

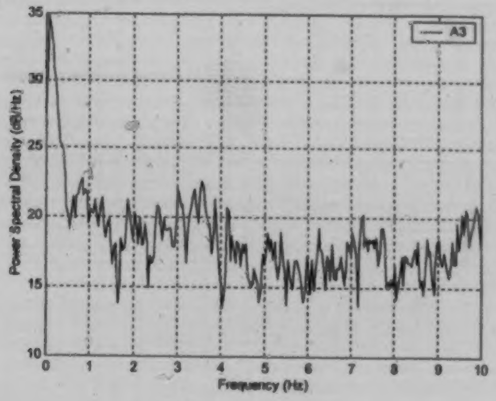

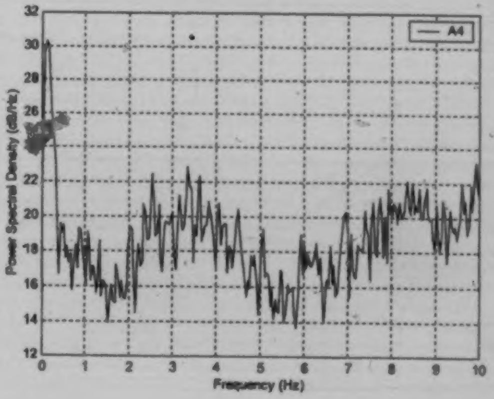

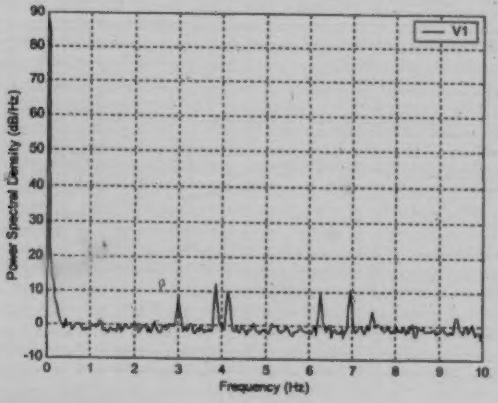

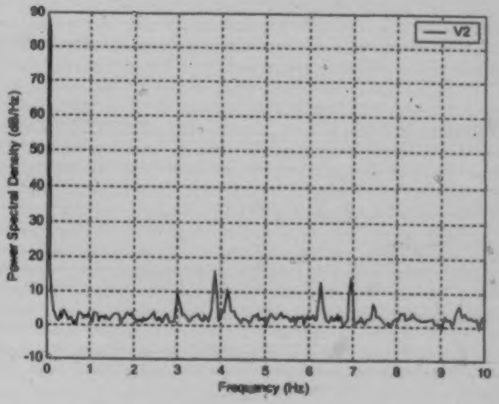

July 17, 1999
4:37 PM

July 17, 1999
4:37 PM

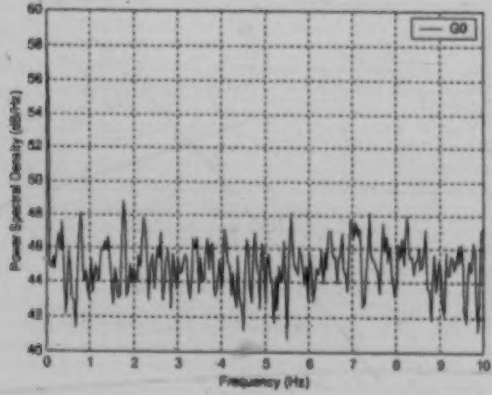

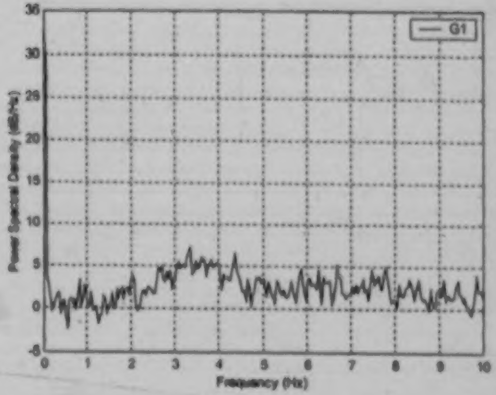

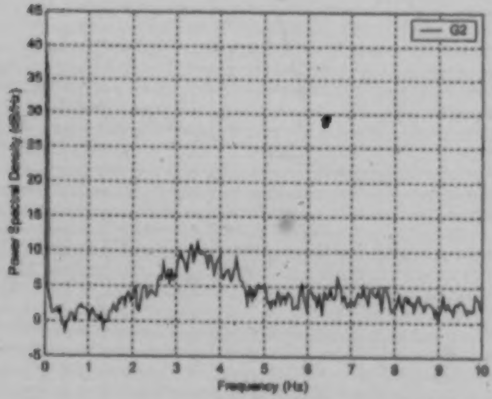

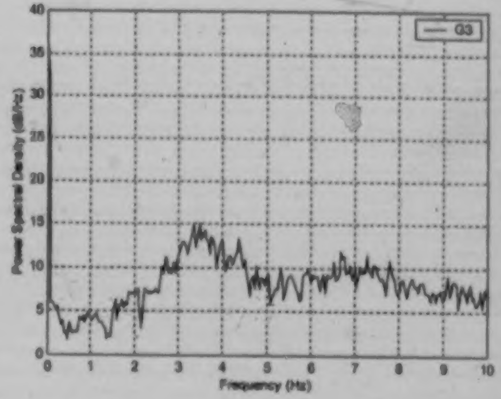

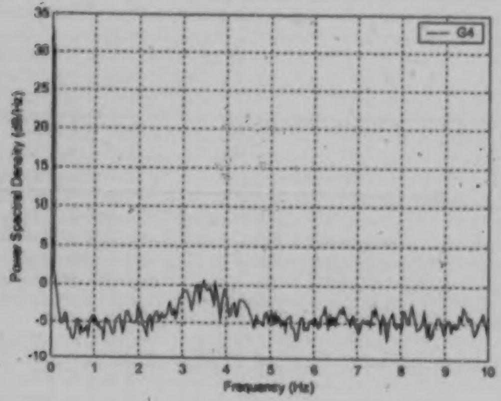

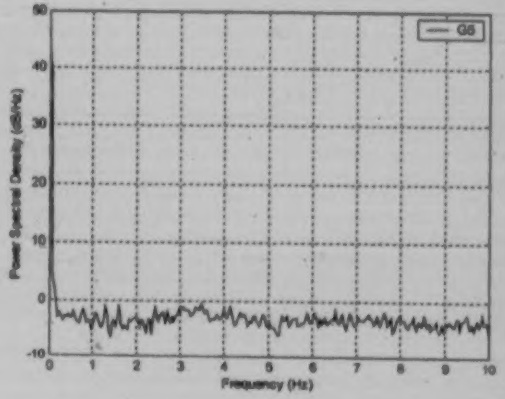

July 17, 1999
4:37 PM

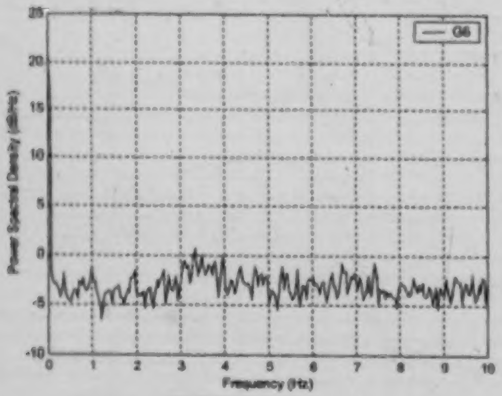

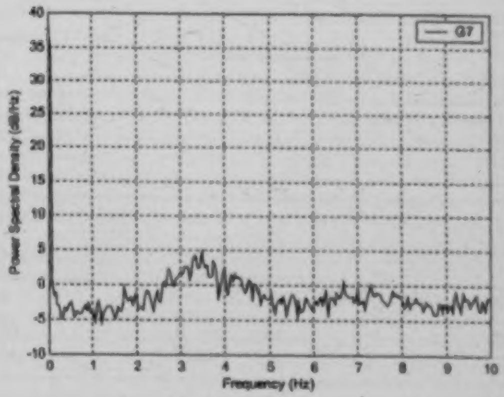

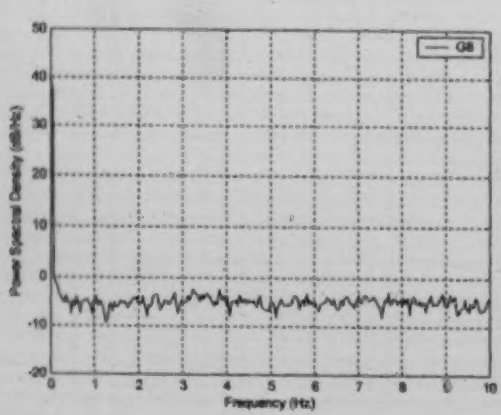

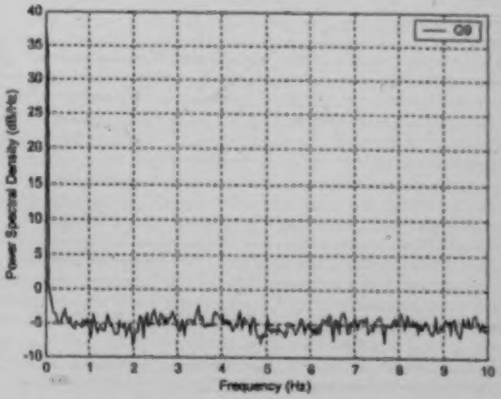

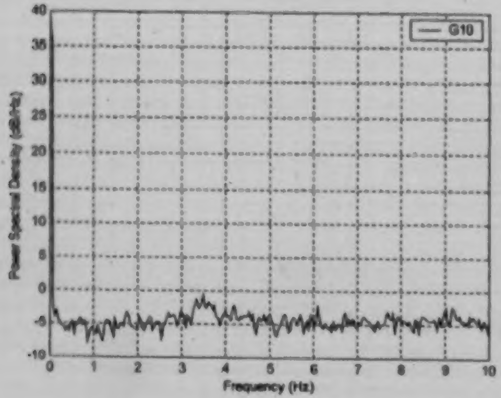

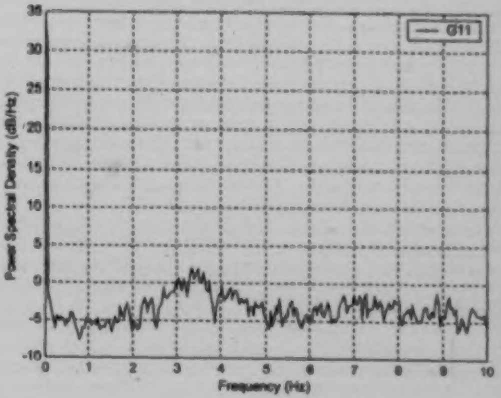

July 17, 1999
4:37 PM

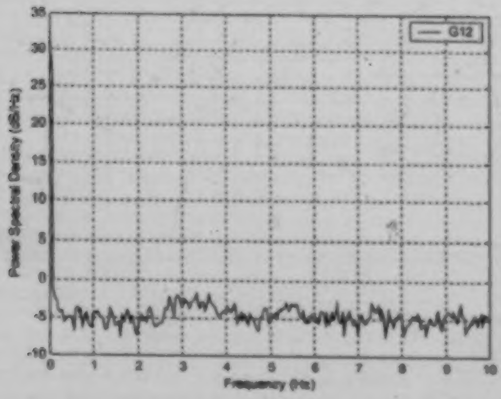

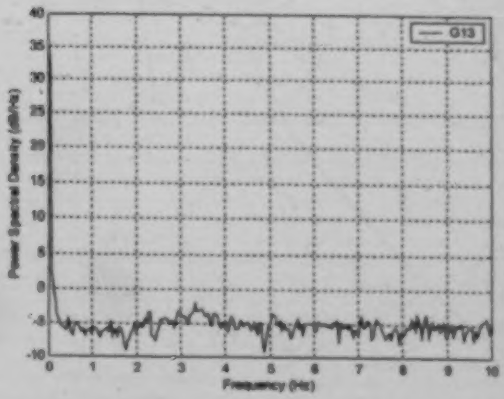

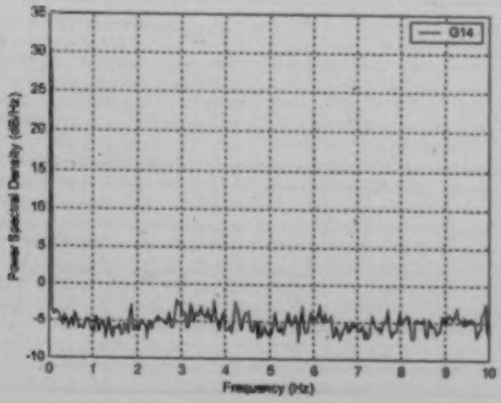

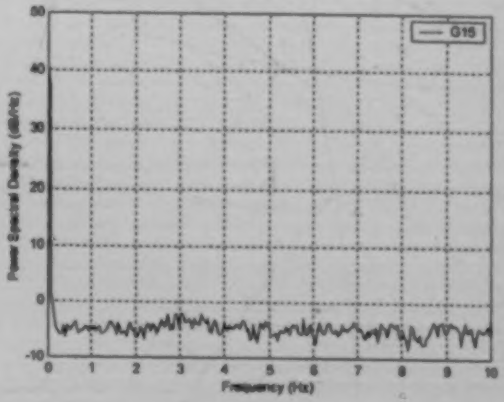

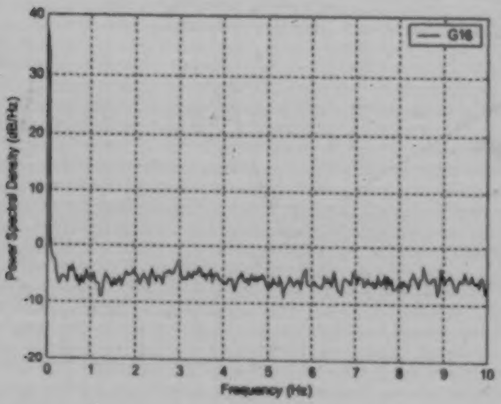

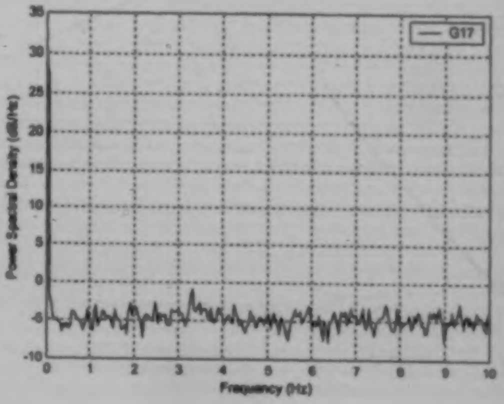

July 17, 1999
4:37 PM

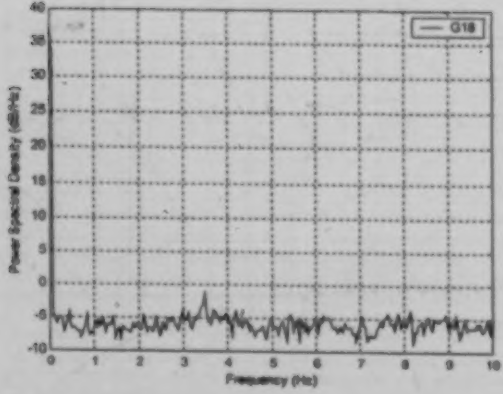

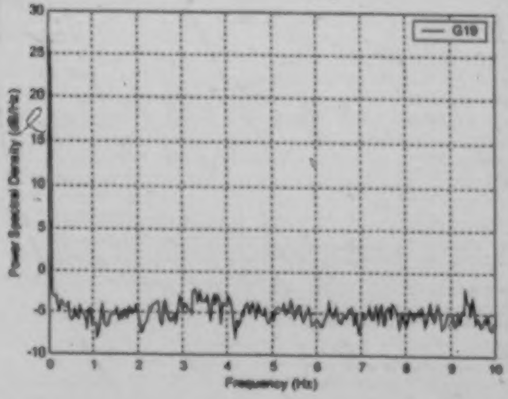

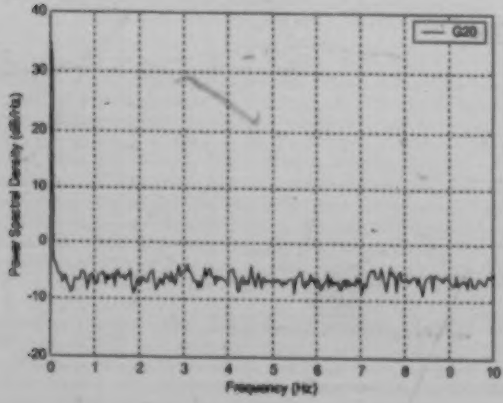

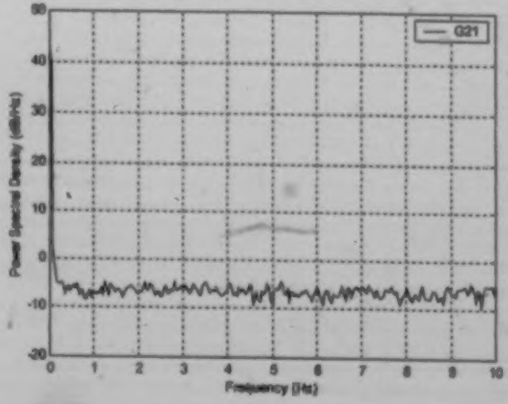

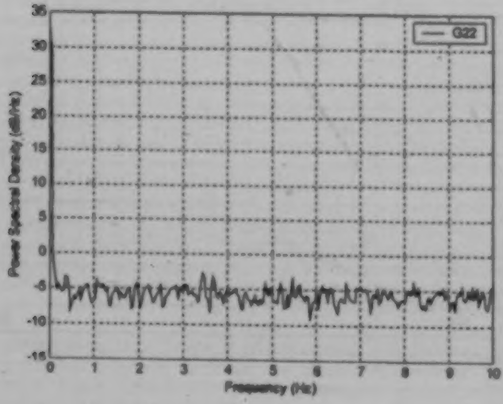

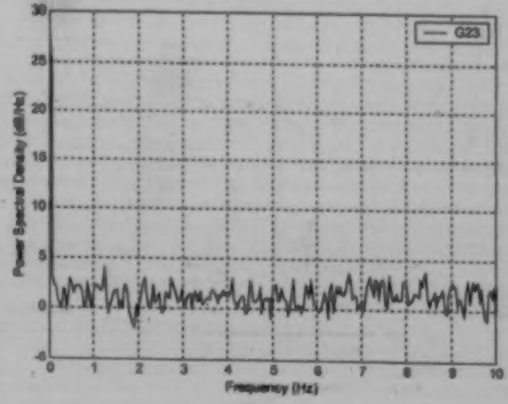

July 17, 1999
4:37 PM

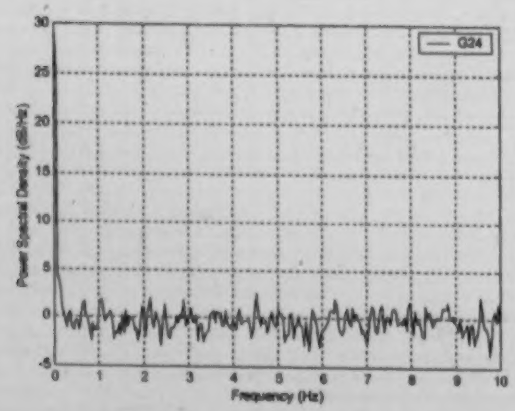

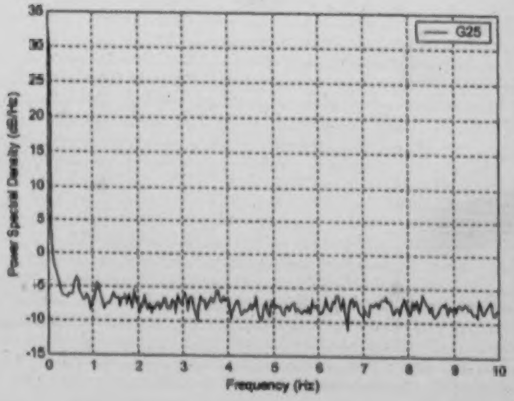

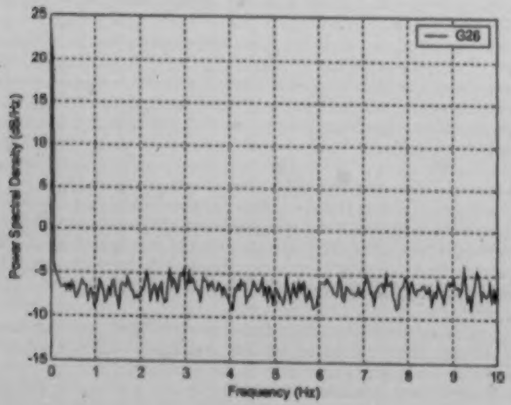

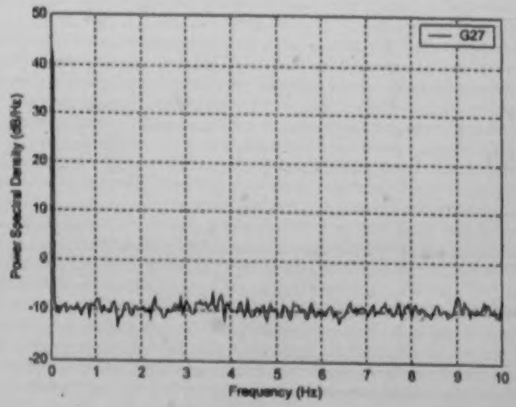

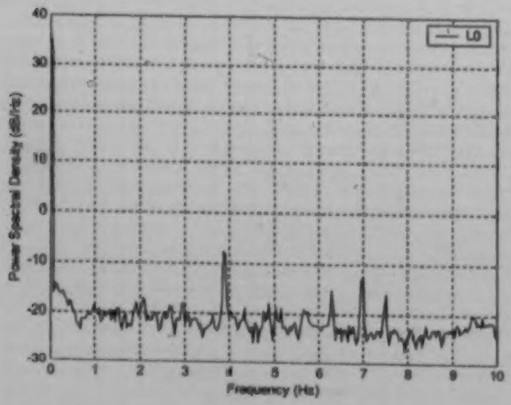

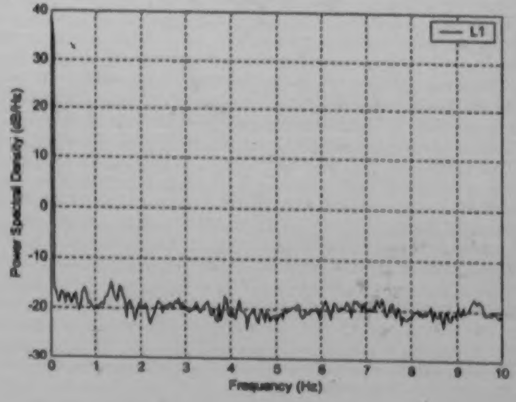

July 17, 1999
4:37 PM

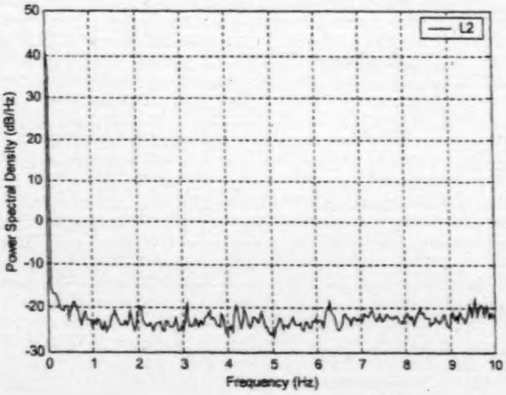

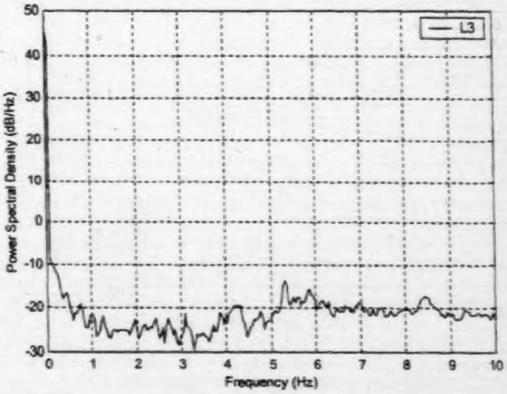

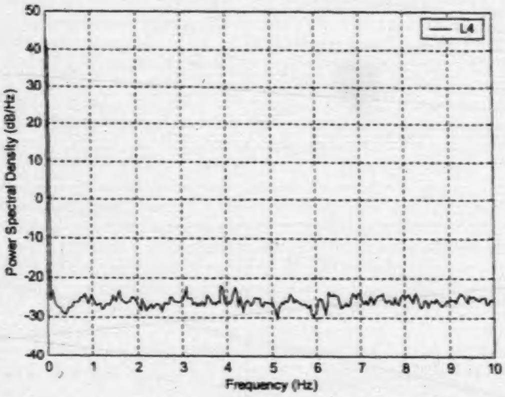

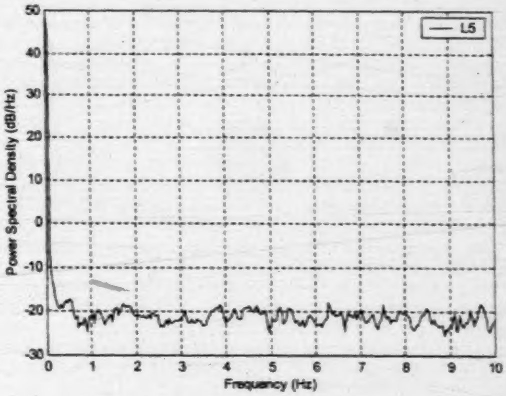

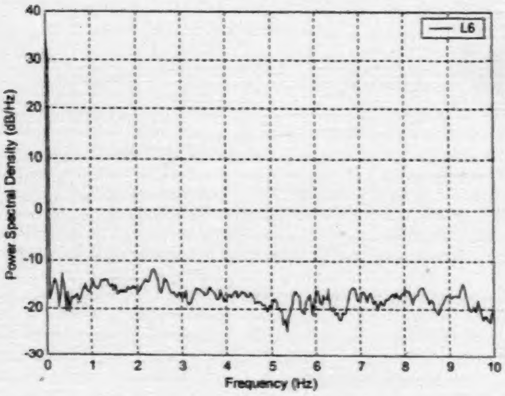

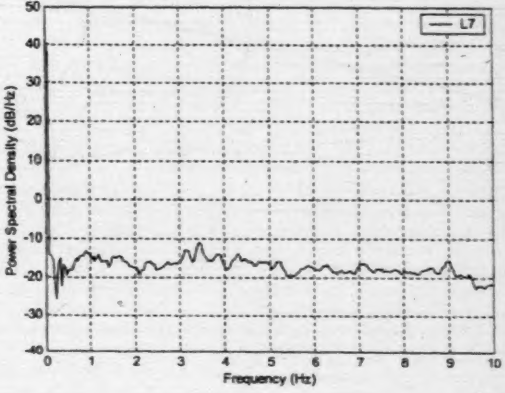

July 17, 1999
4:37 PM

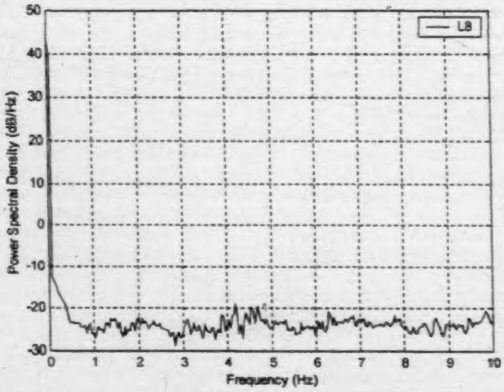

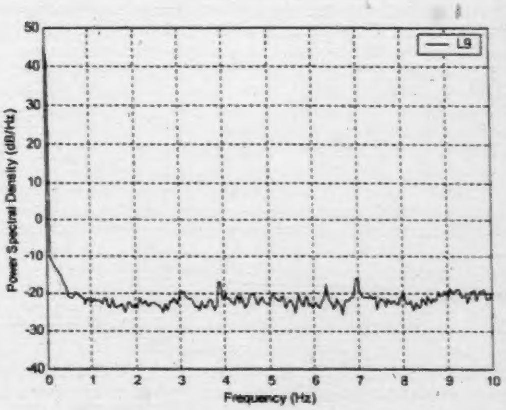

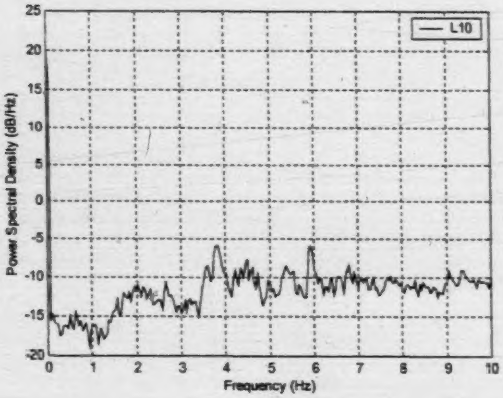

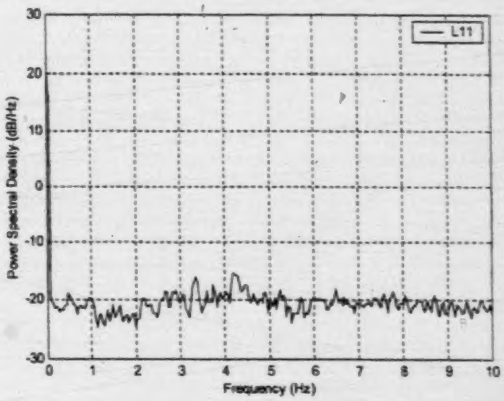

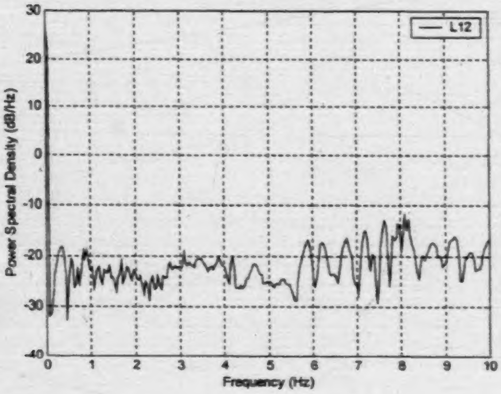

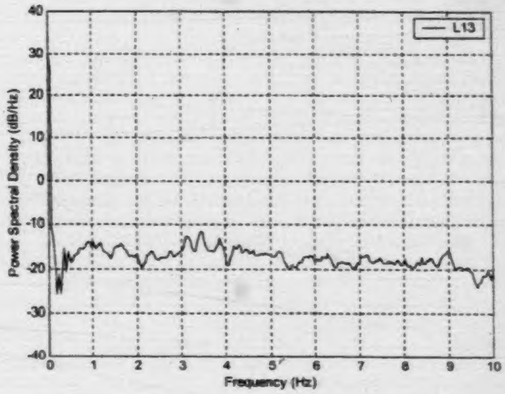

July 17, 1999
4:37 PM

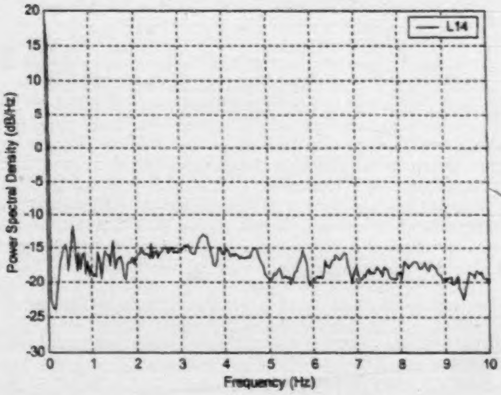

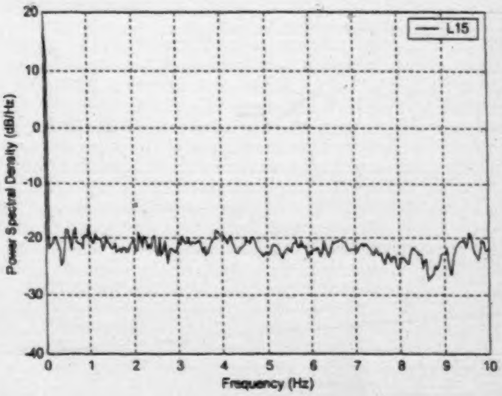

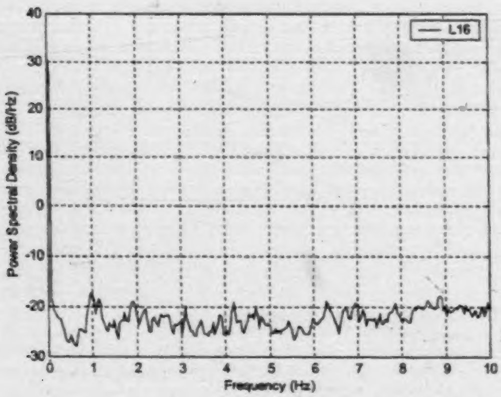

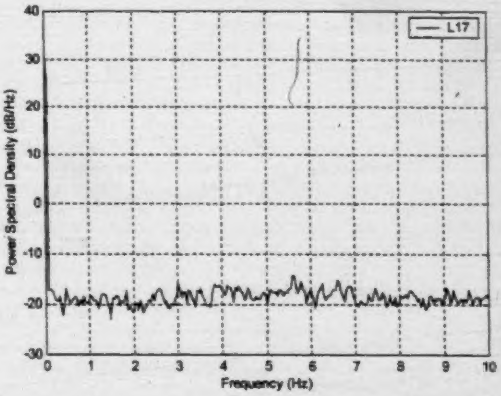

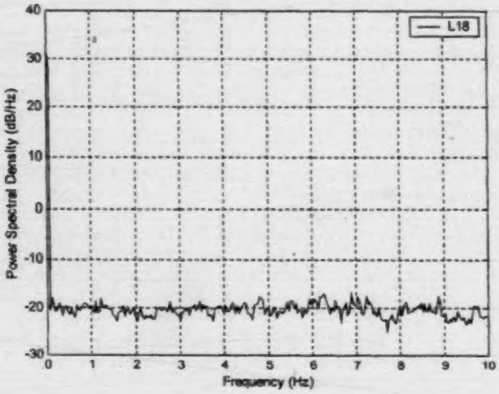

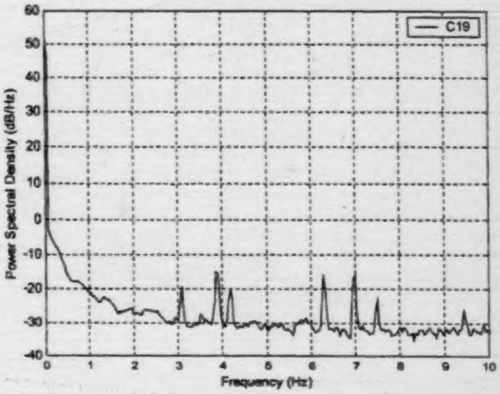

July 17, 1999
4:37 PM

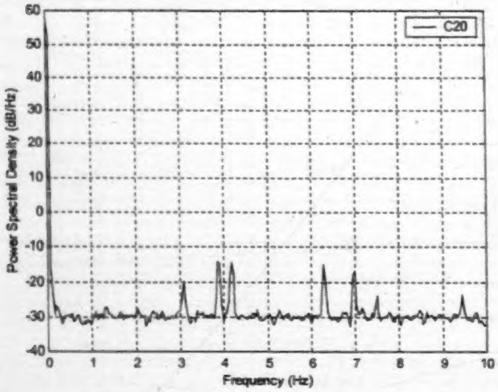

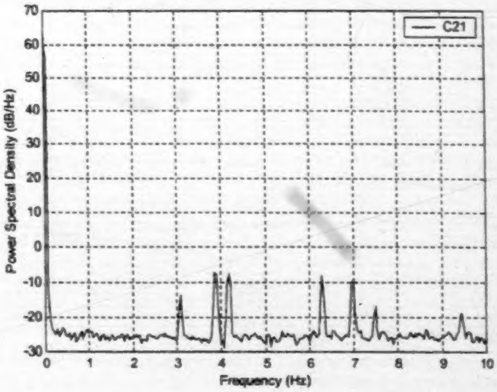

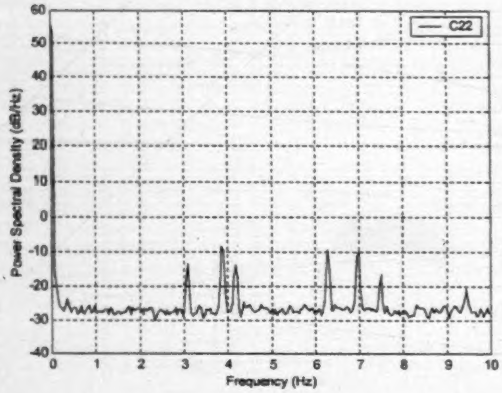

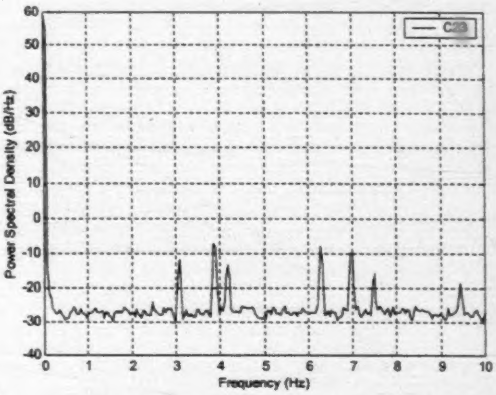

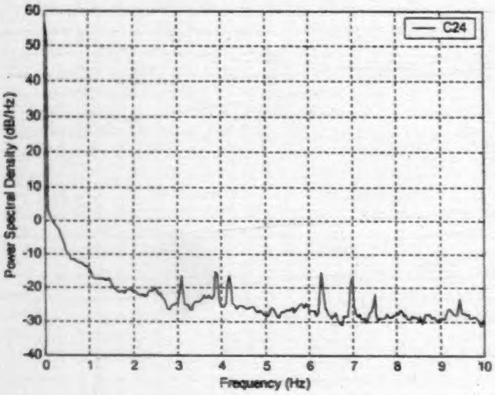

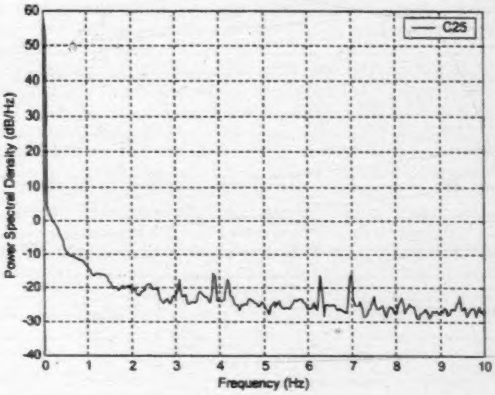

July 17, 1999
4:37 PM

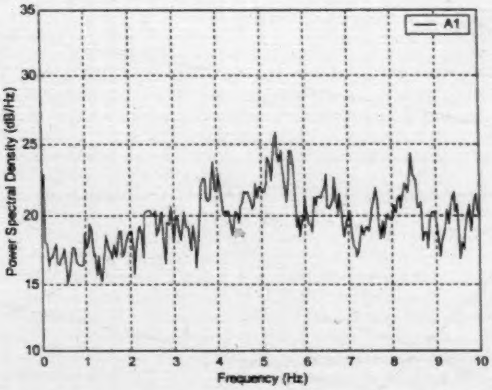

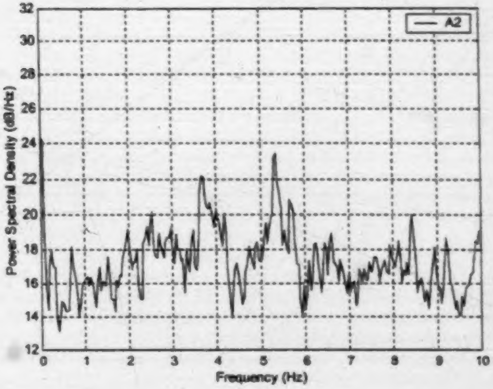

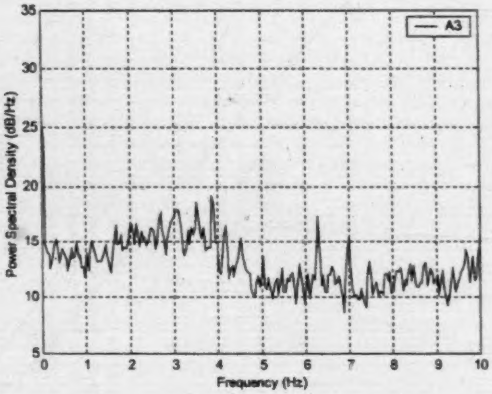

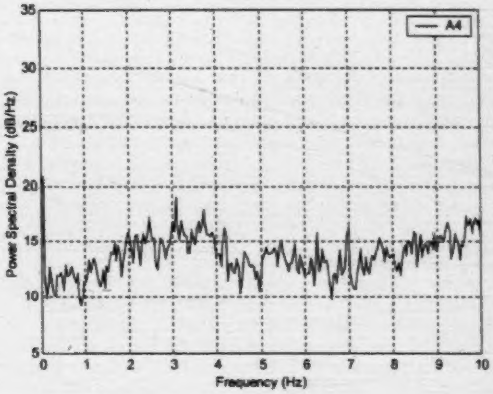

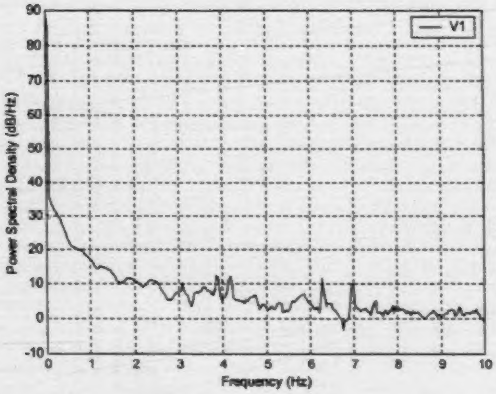

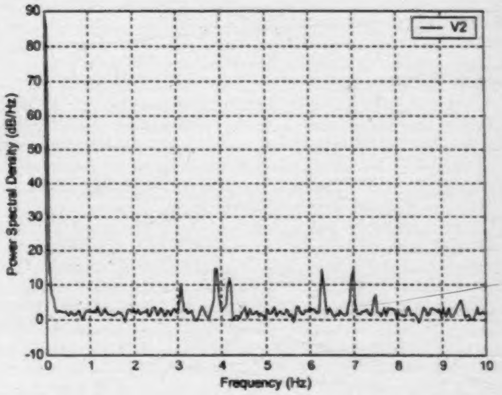

July 17, 1999
4:49 PM

July 17, 1999
4:49 PM

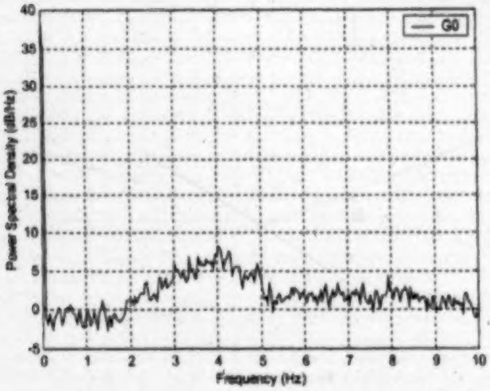

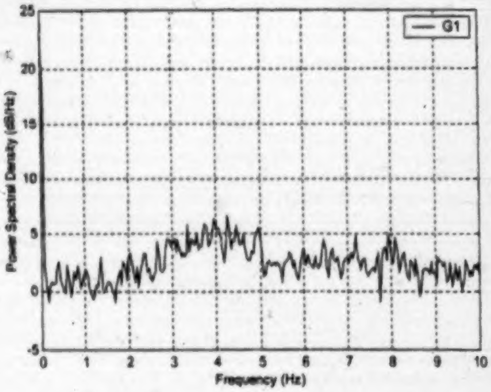

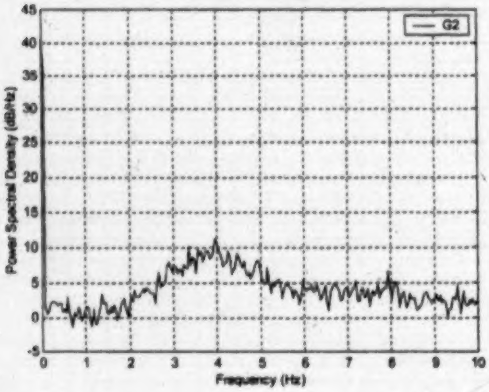

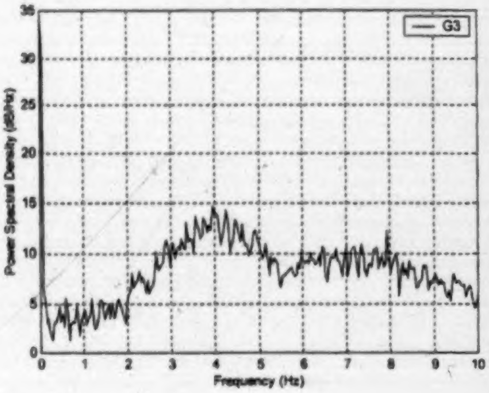

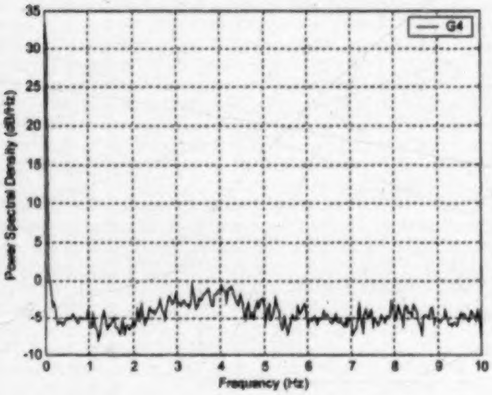

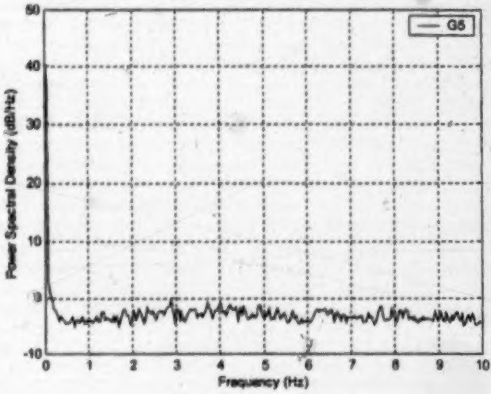

July 17, 1999
4:49 PM

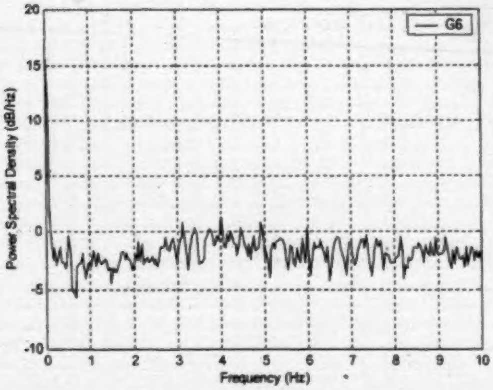

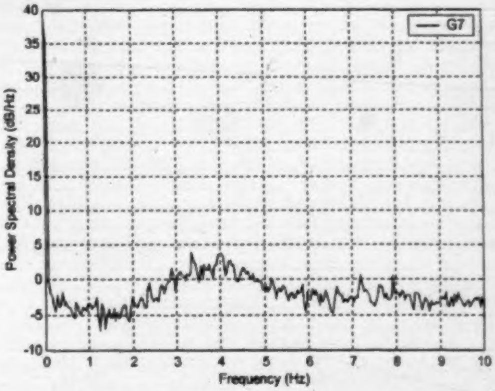

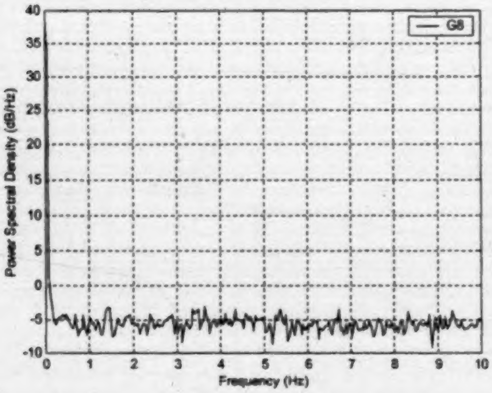

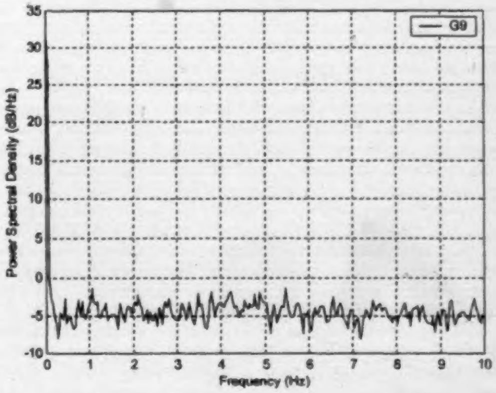

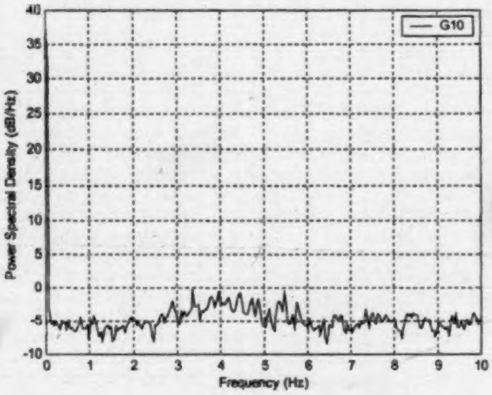

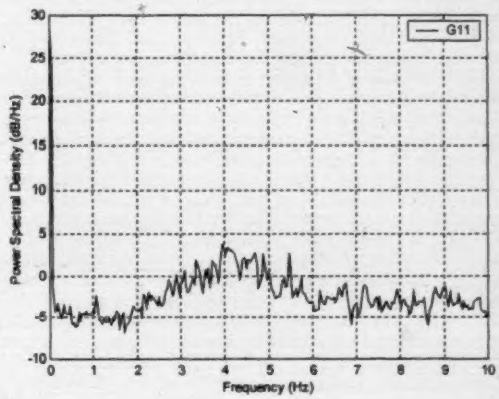

July 17, 1999
4:49 PM

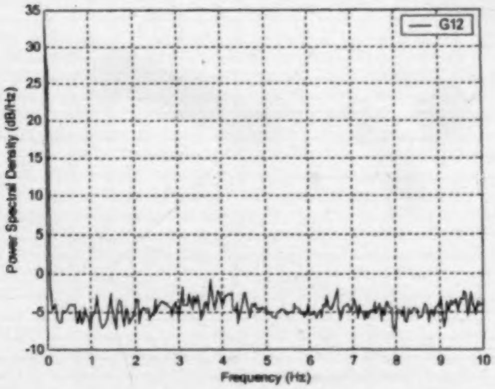

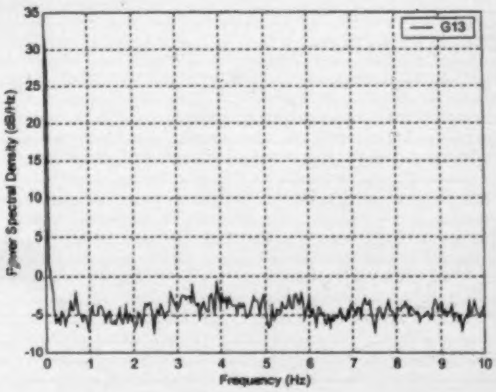

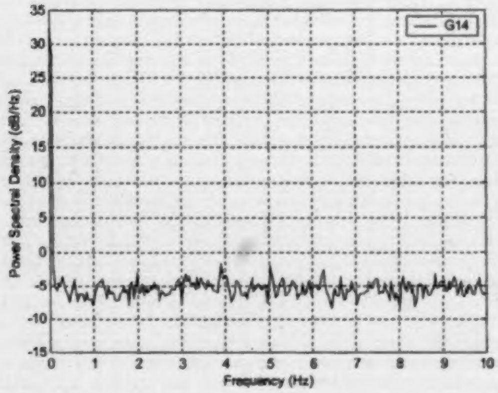

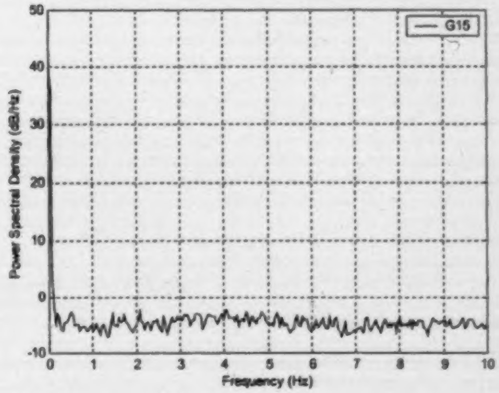

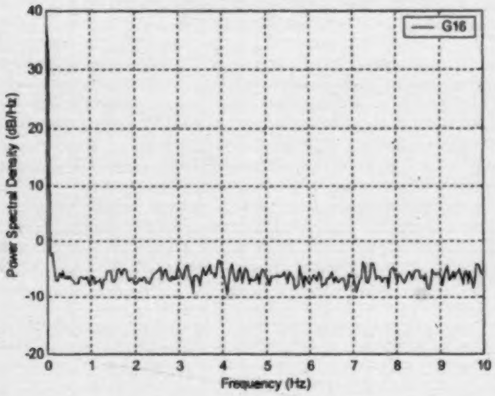

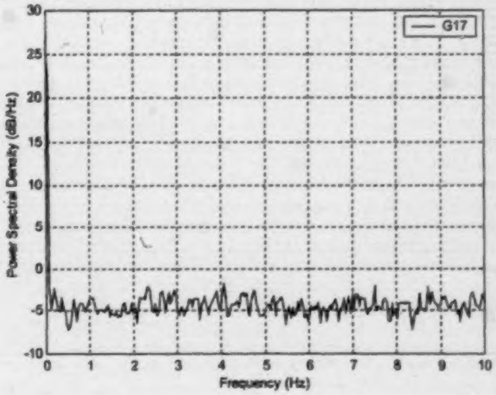

July 17, 1999
4:49 PM

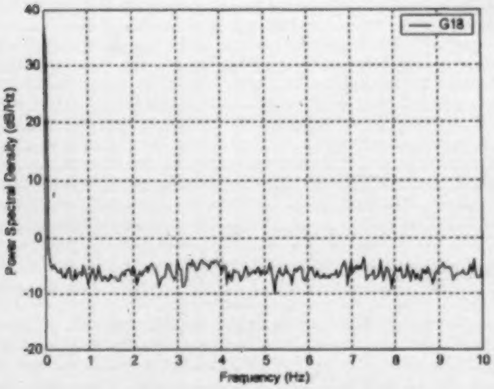

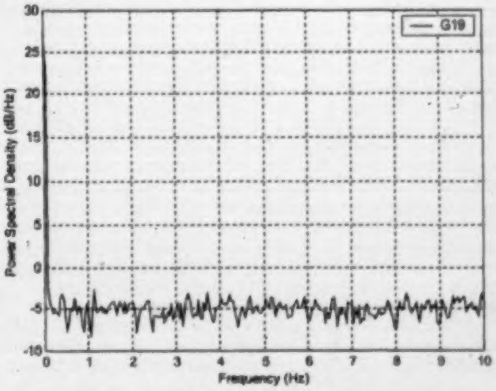

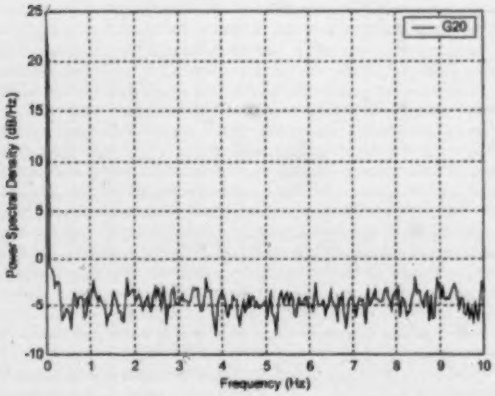

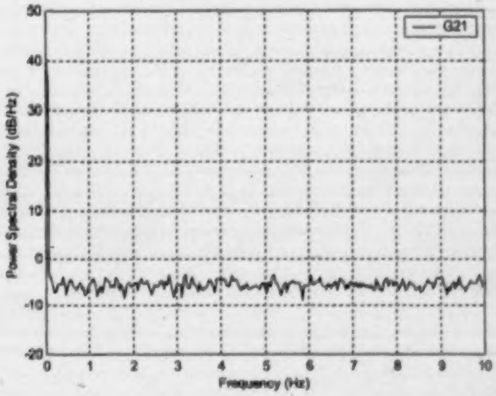

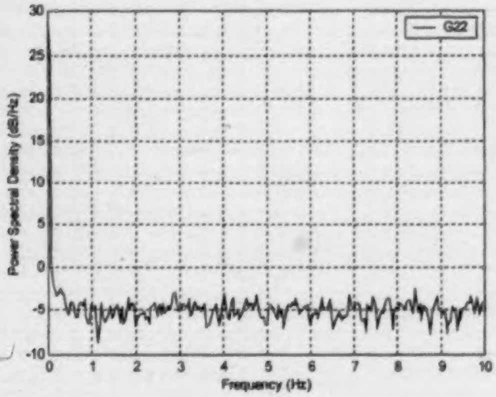

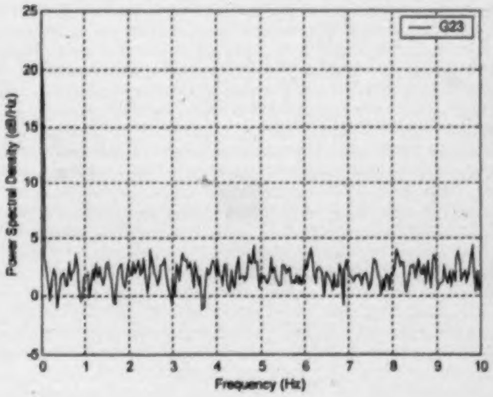

July 17, 1999
4:49 PM

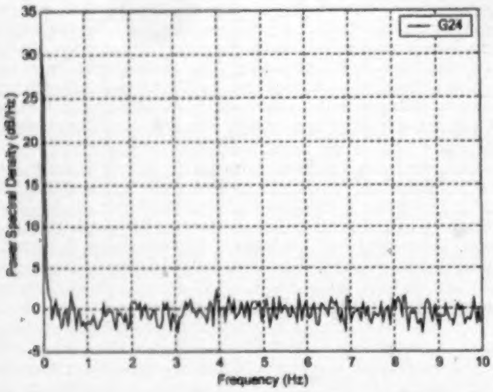

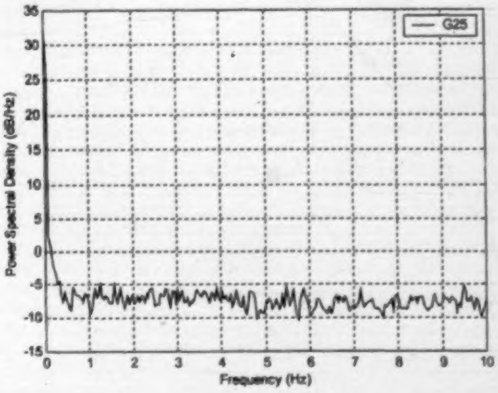

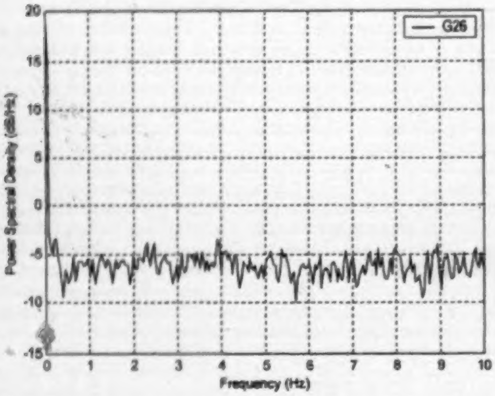

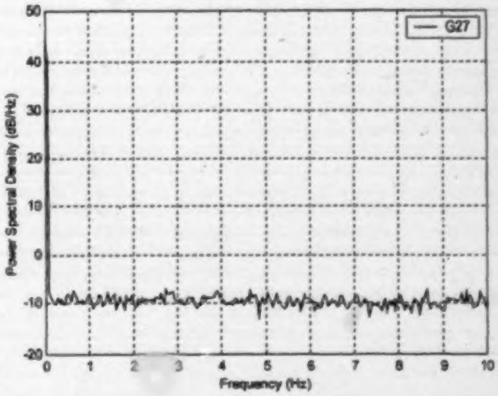

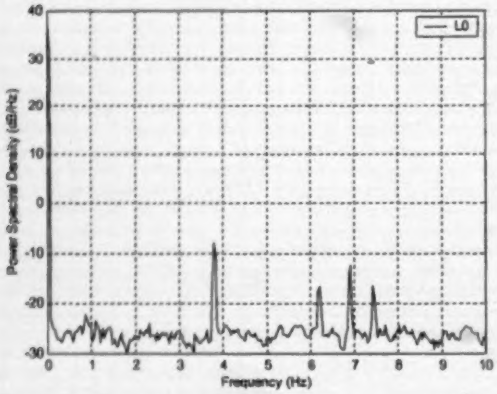

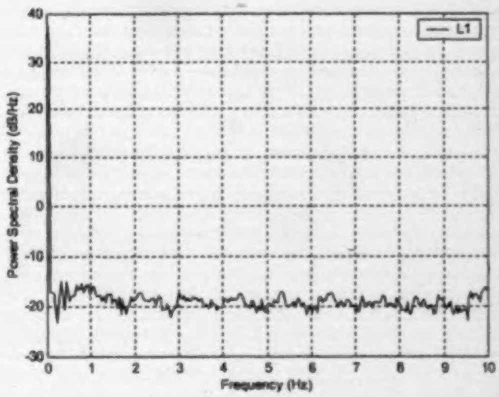

July 17, 1999
4:49 PM

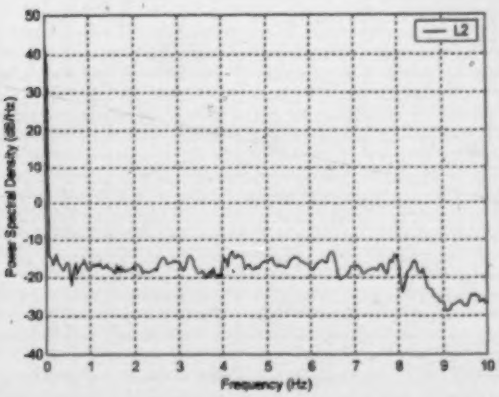

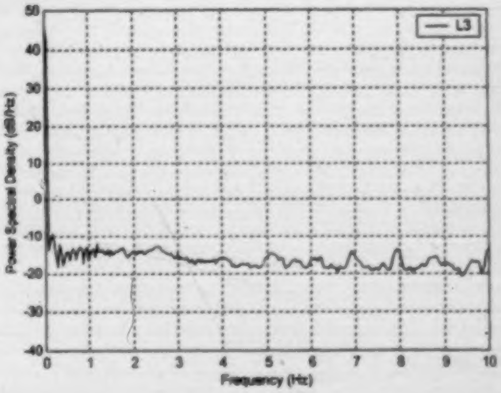

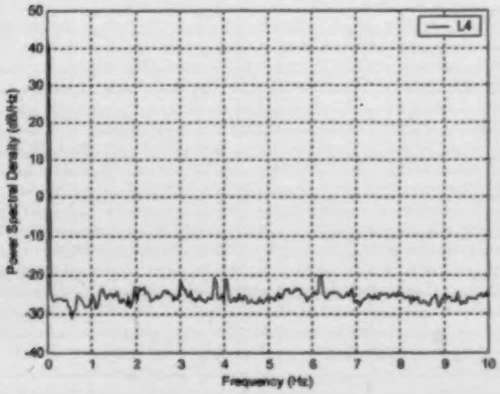

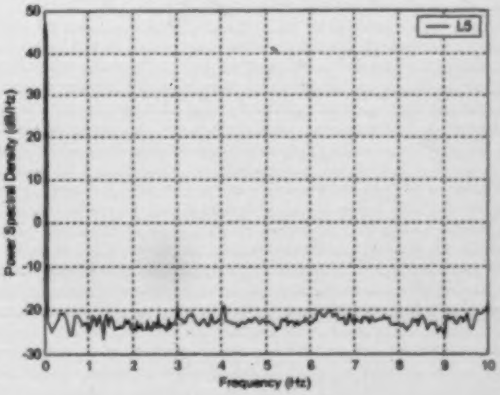

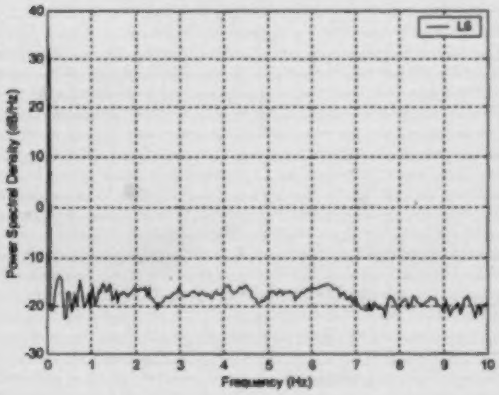

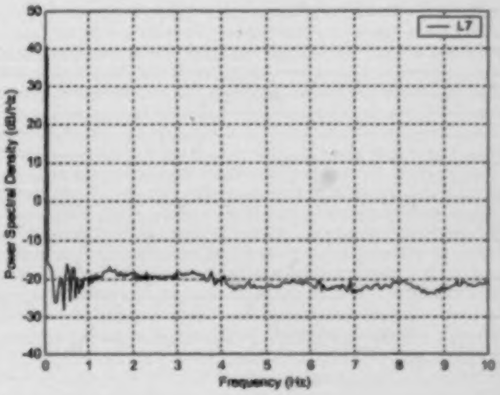

July 17, 1999
4:49 PM

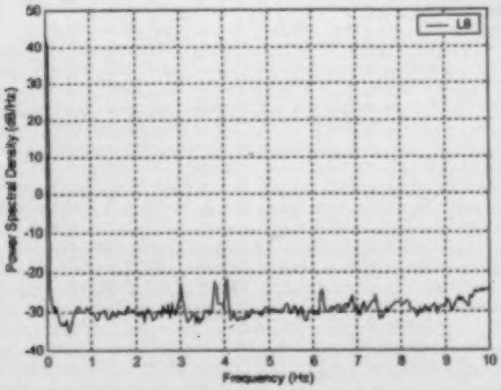

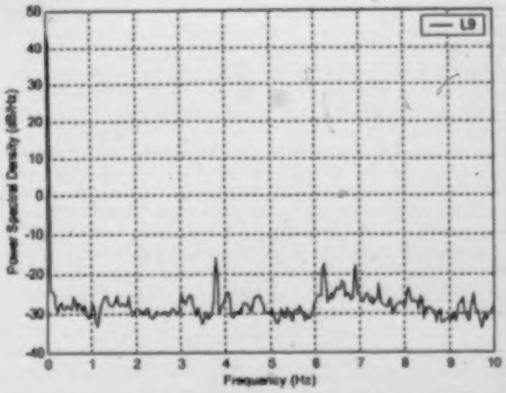

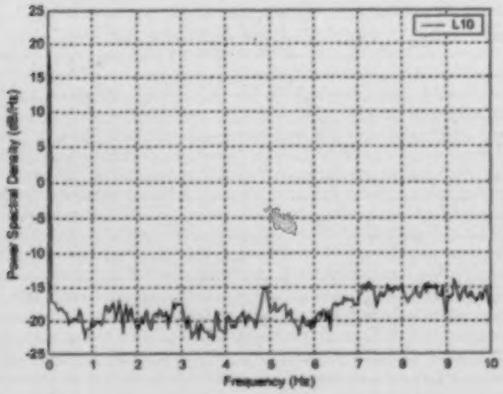

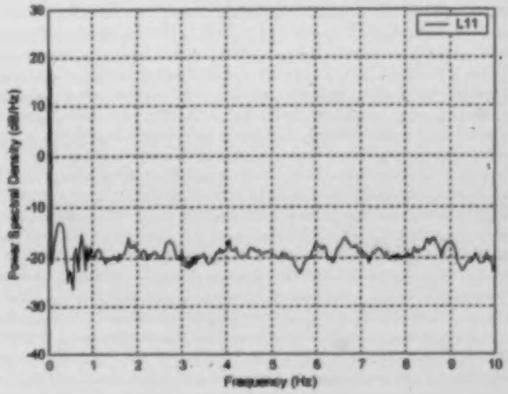

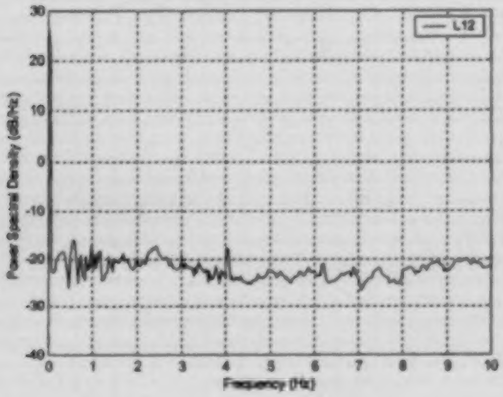

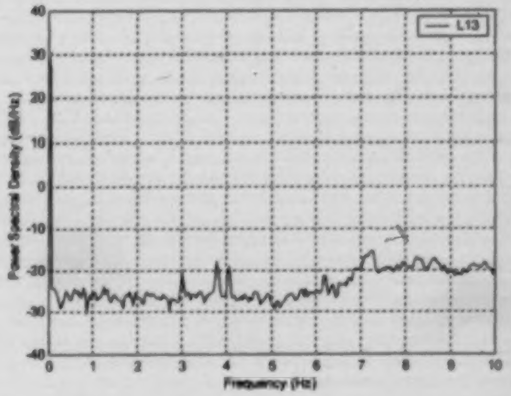

July 17, 1999
4:49 PM

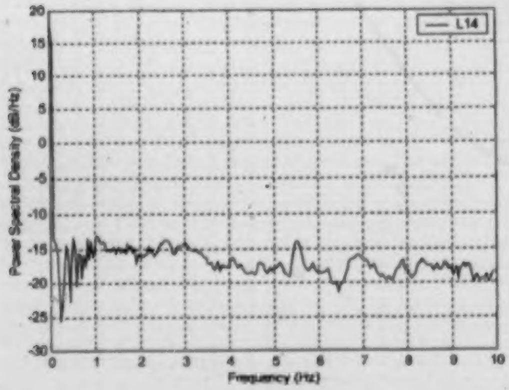

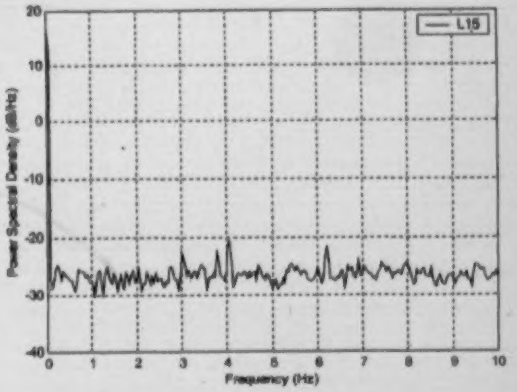

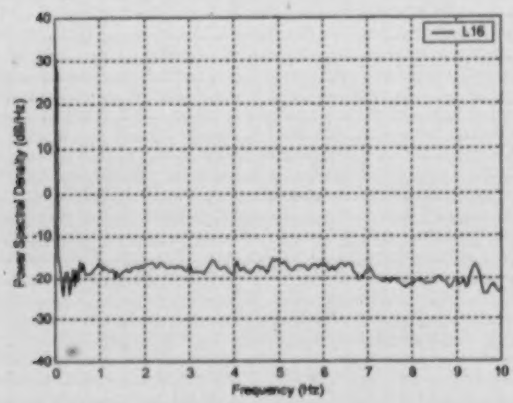

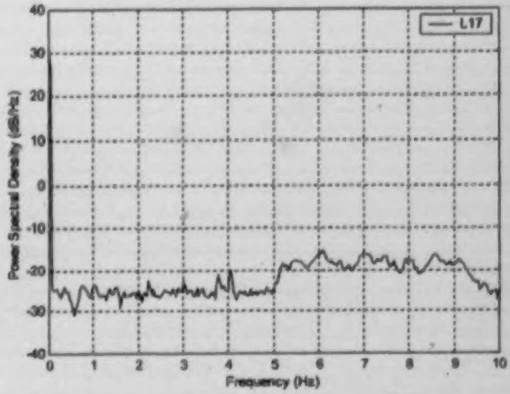

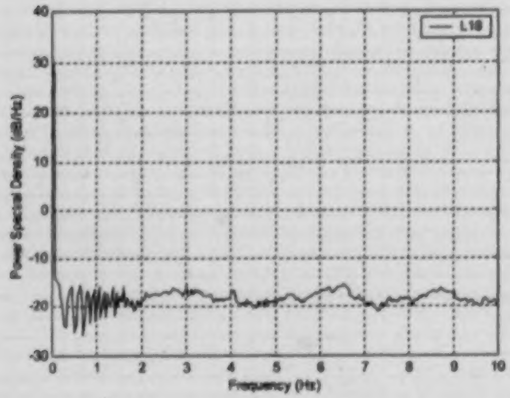

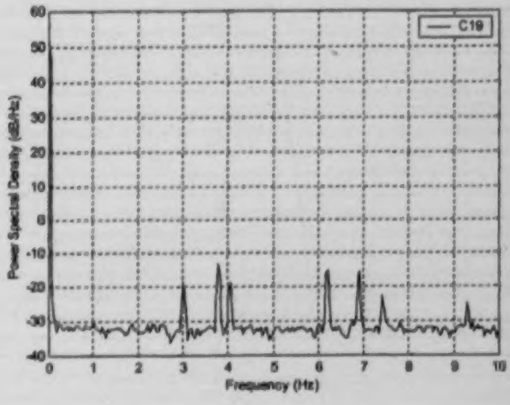

July 17, 1999
4:49 PM

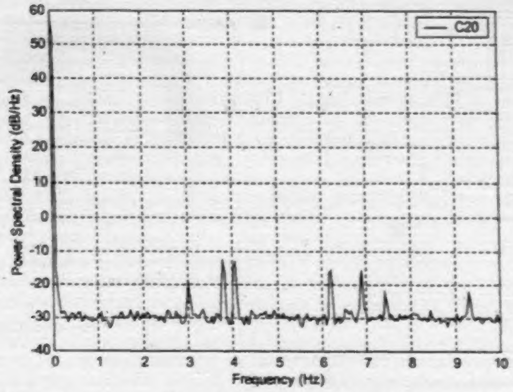

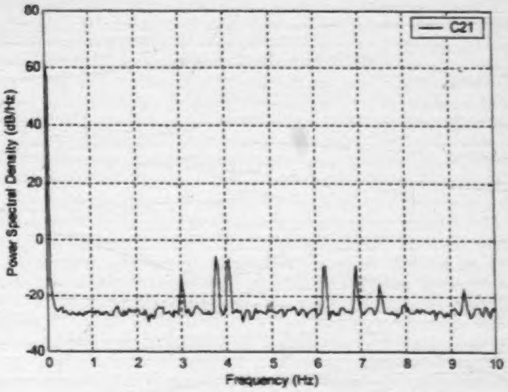

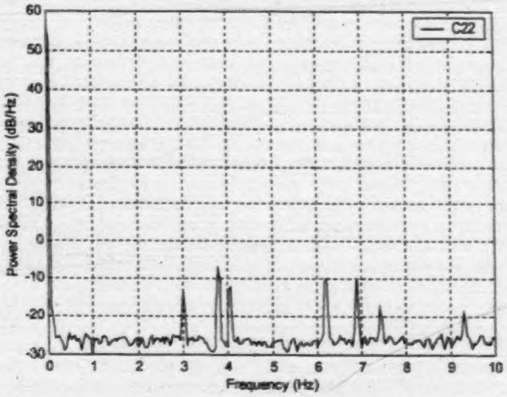

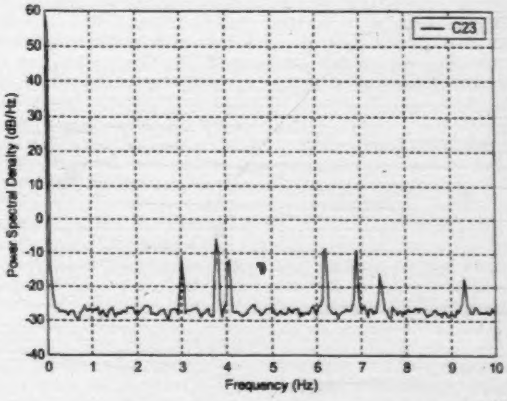

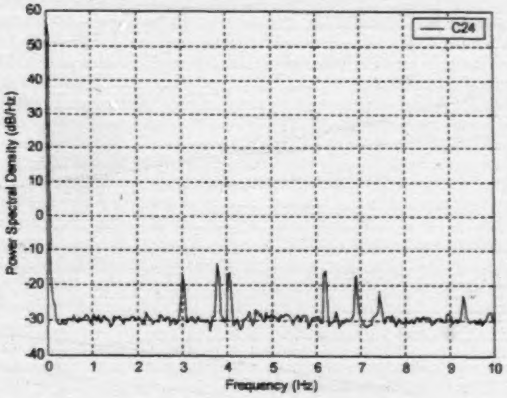

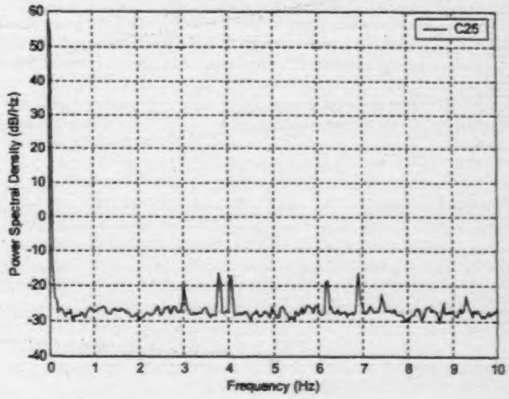

July 17, 1999
4:49 PM

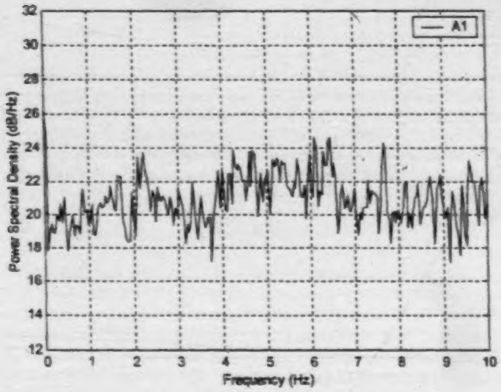

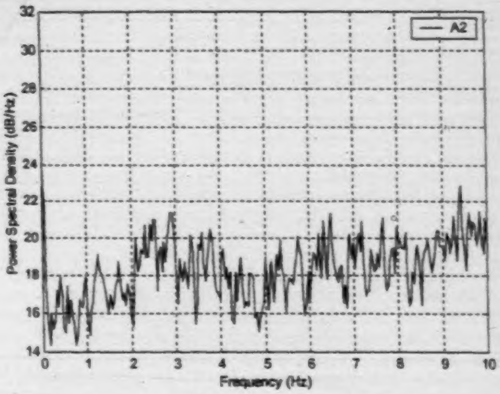

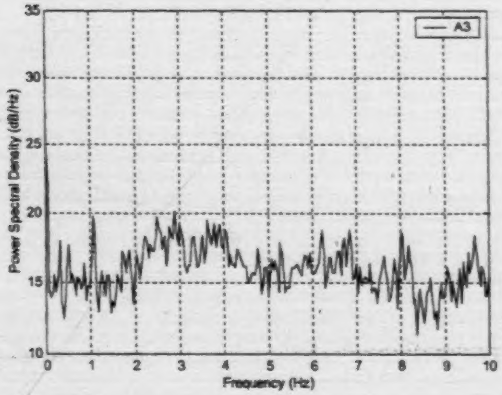

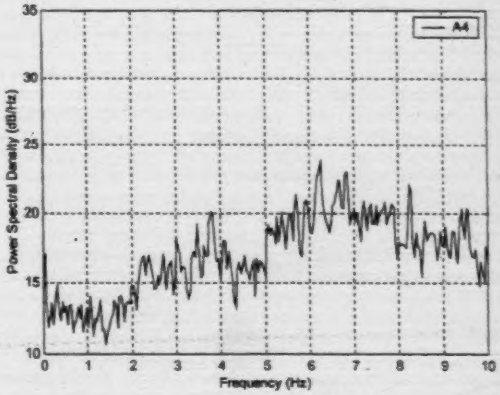

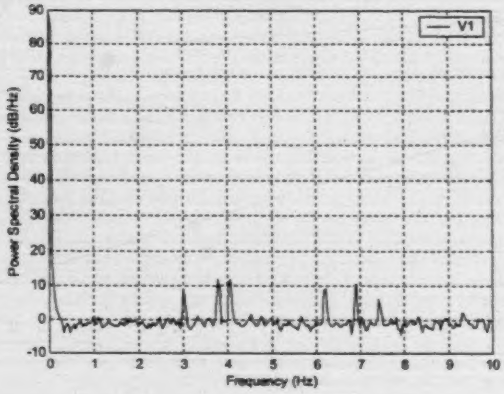

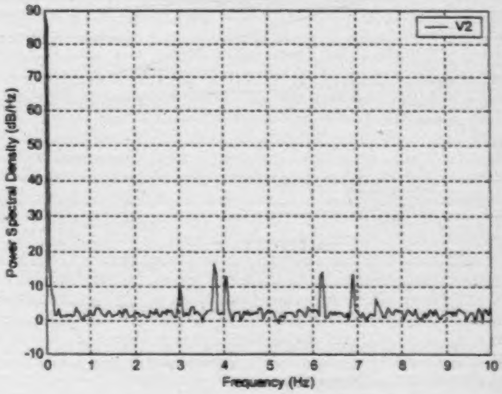

July 17, 1999
4:59 PM

July 17, 1999
4:59 PM

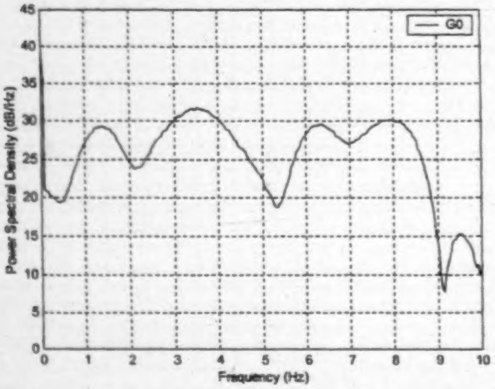

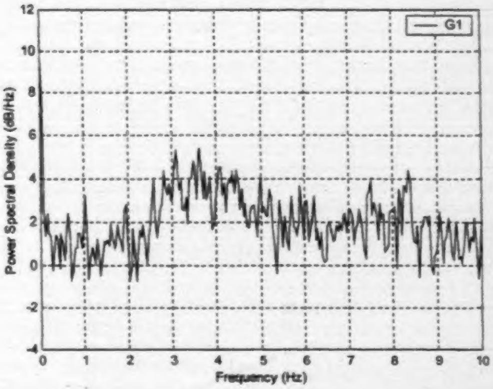

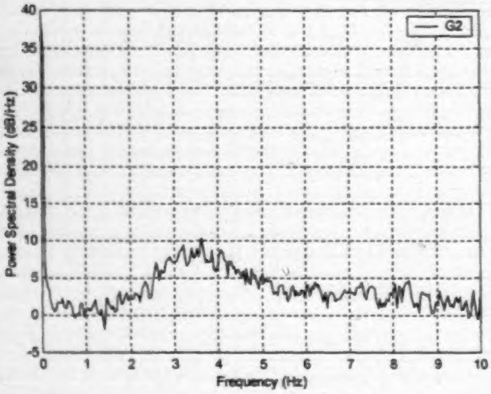

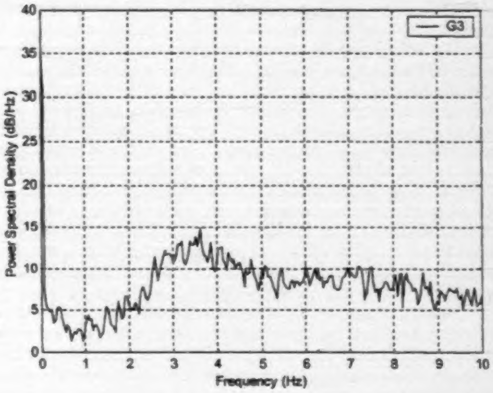

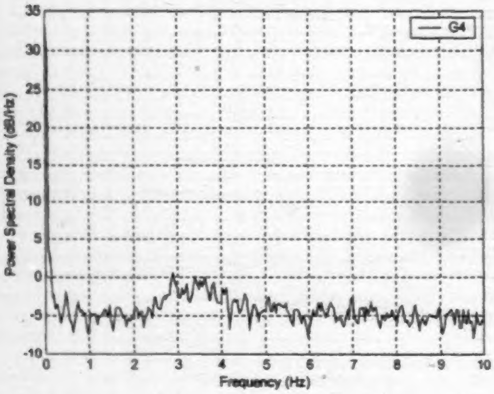

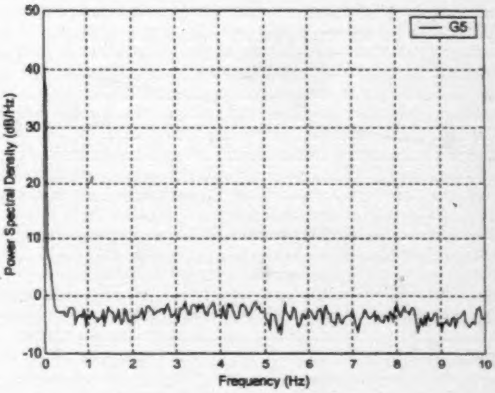

July 17, 1999
4:59 PM

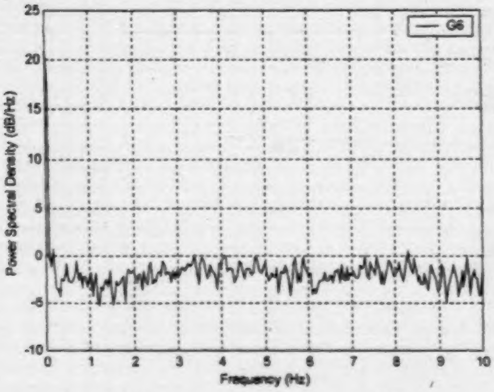

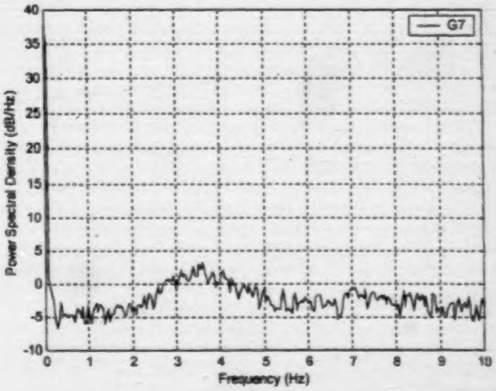

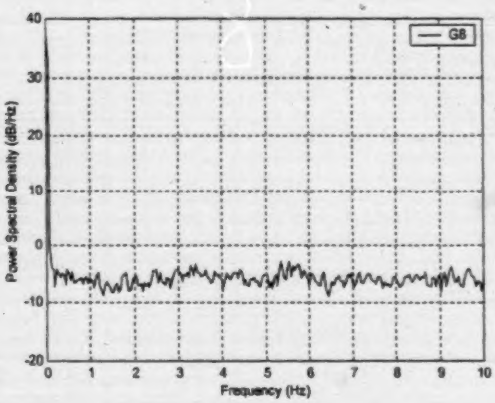

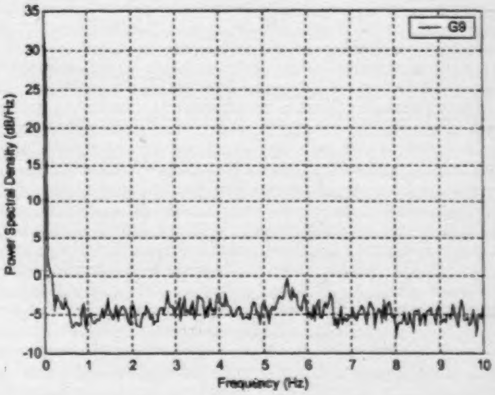

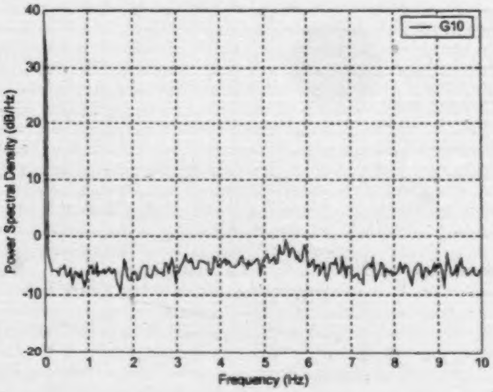

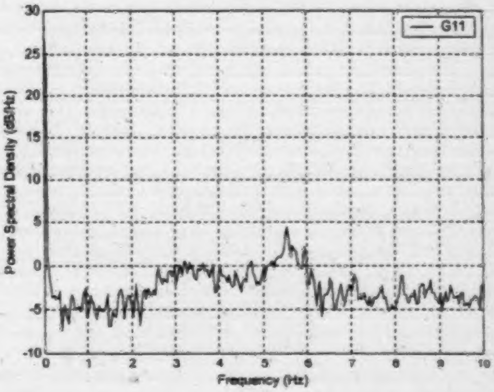

July 17, 1999
4:59 PM

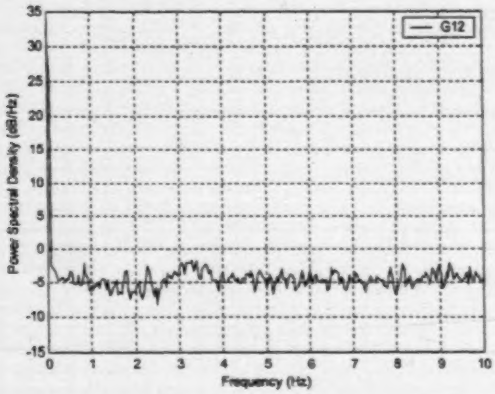

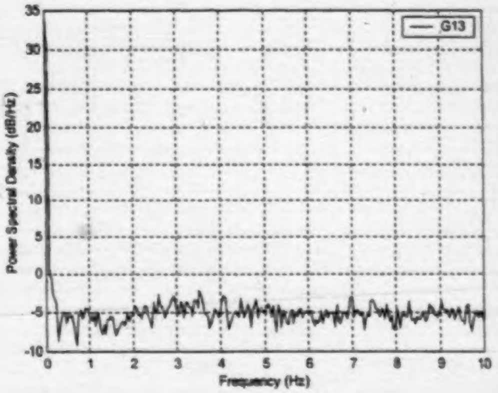

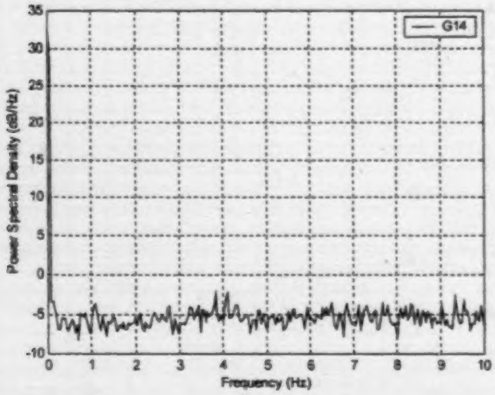

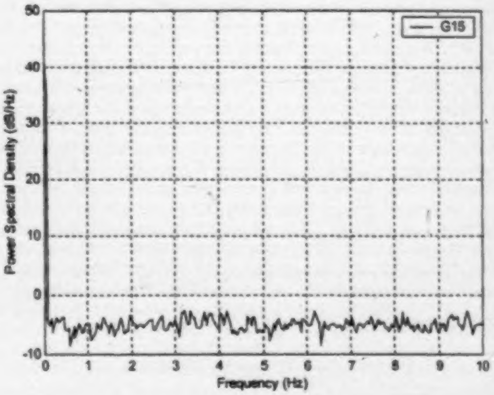

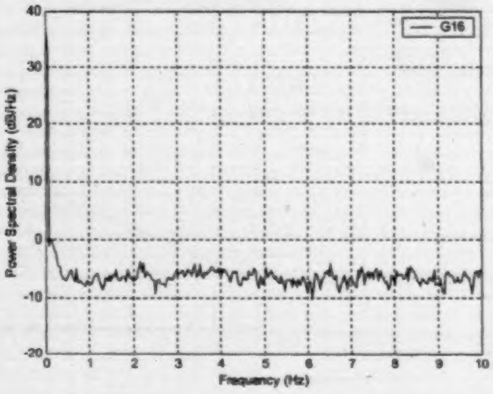

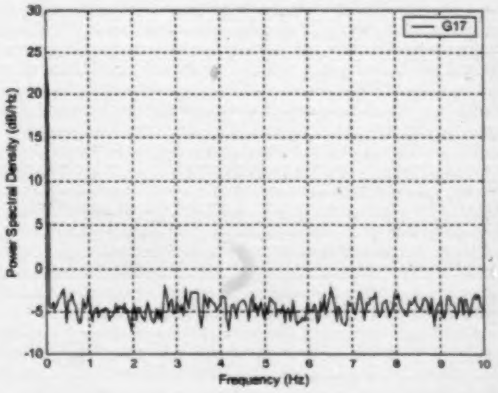

July 17, 1999
4:59 PM

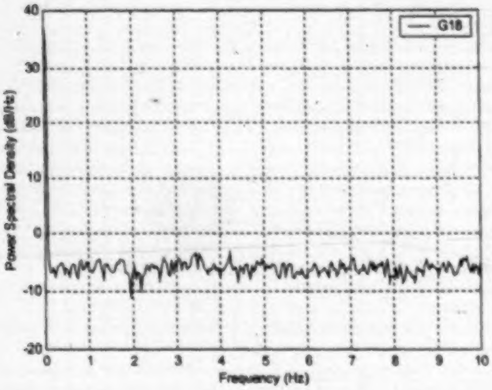

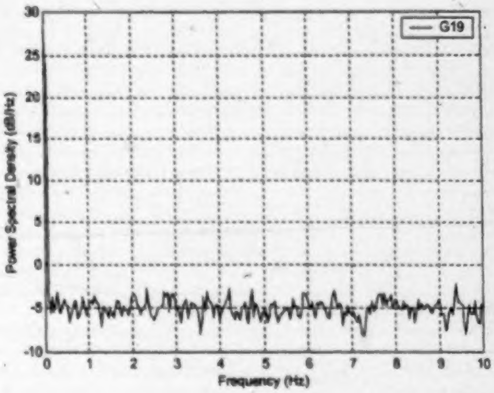

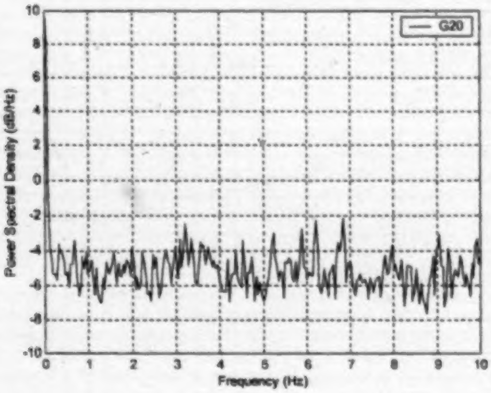

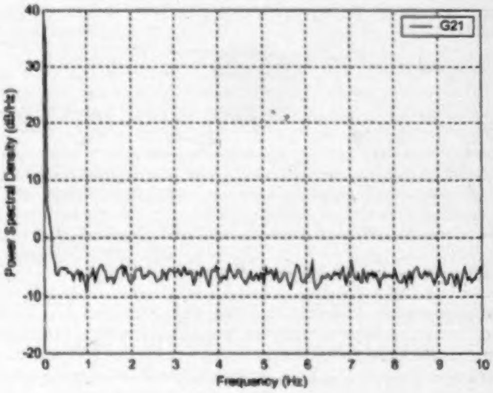

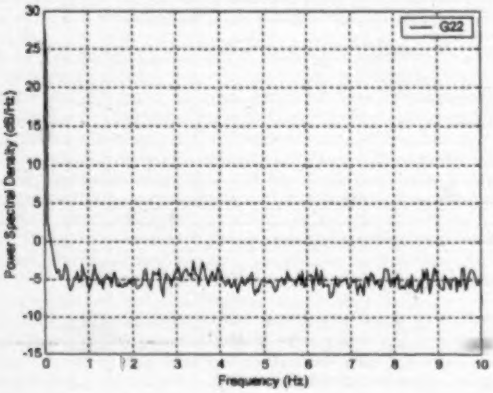

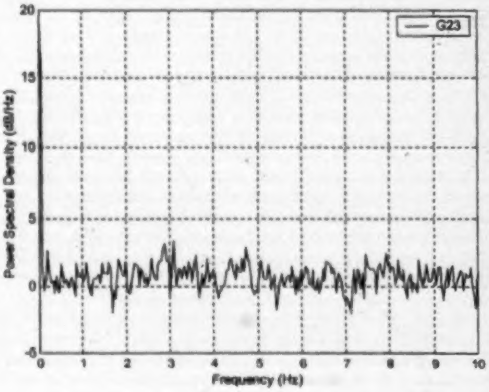

July 17, 1999
4:59 PM

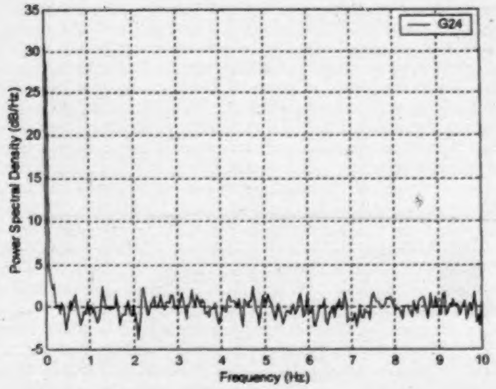

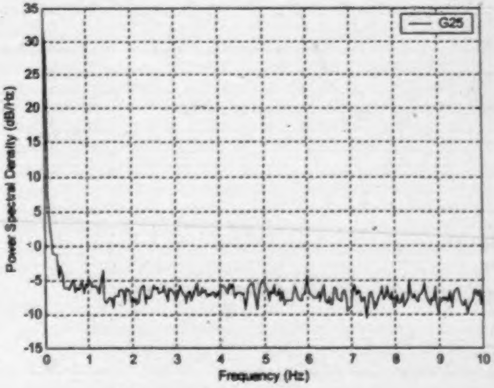

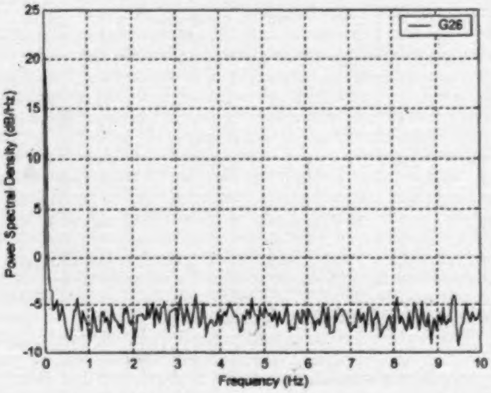

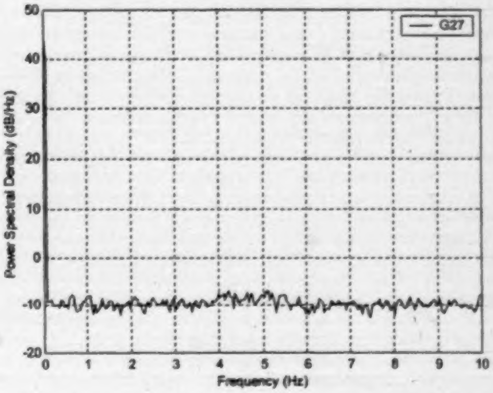

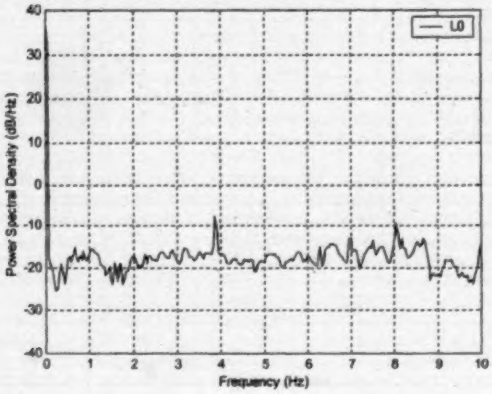

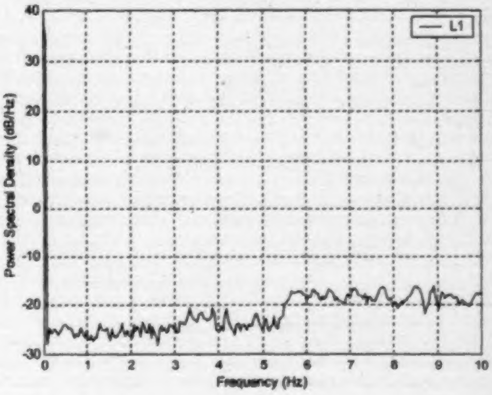

July 17, 1999
4:59 PM

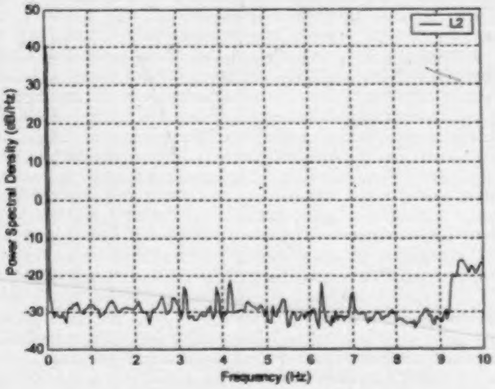

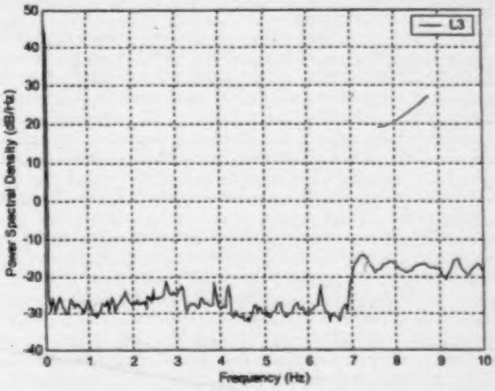

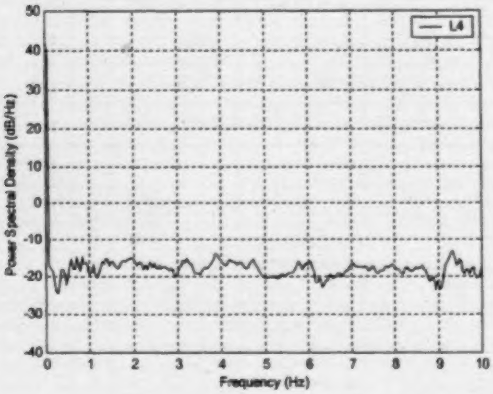

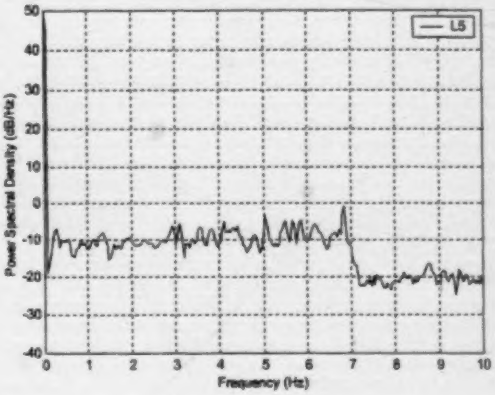

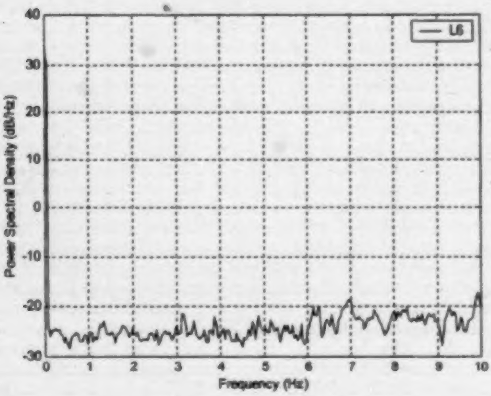

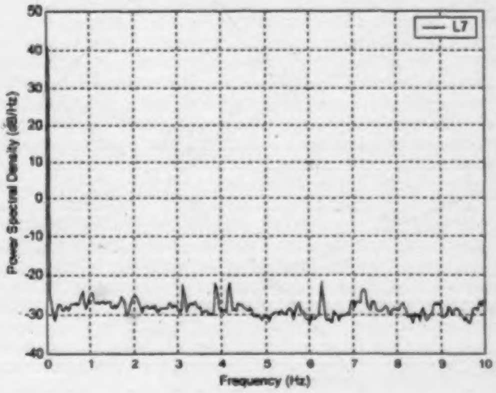

July 17, 1999
4:59 PM

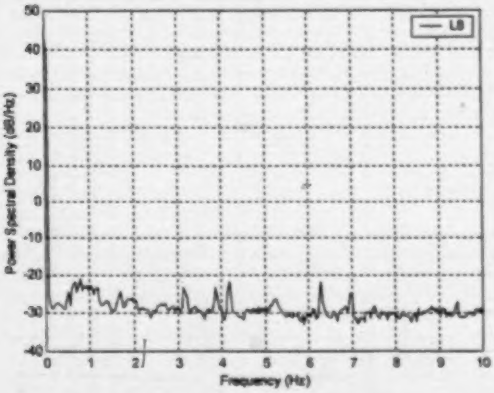

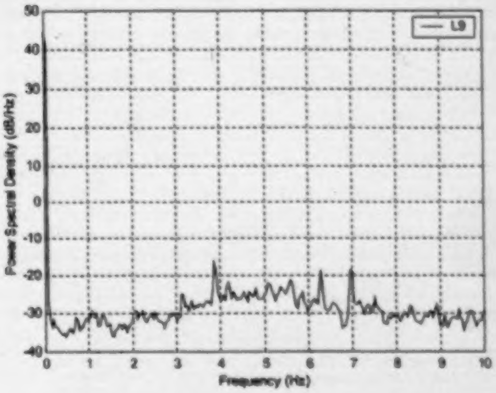

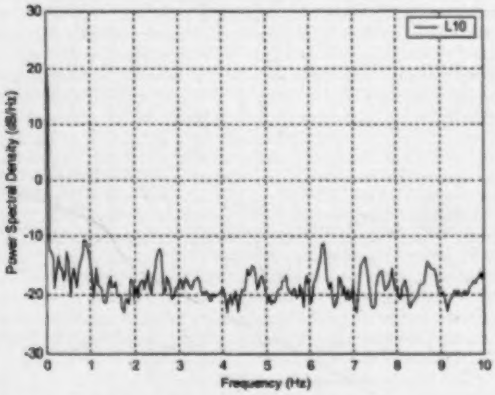

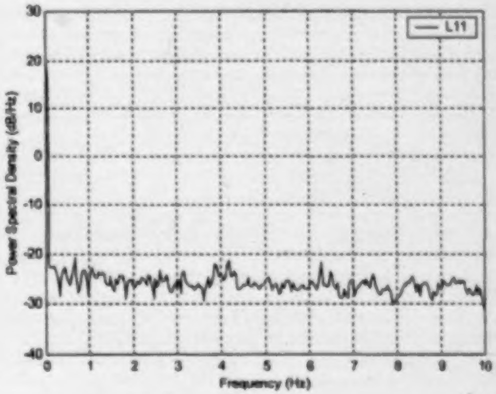

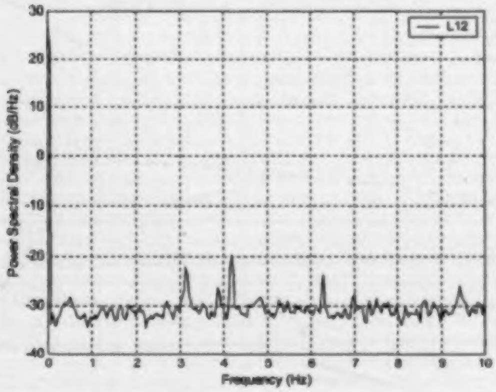

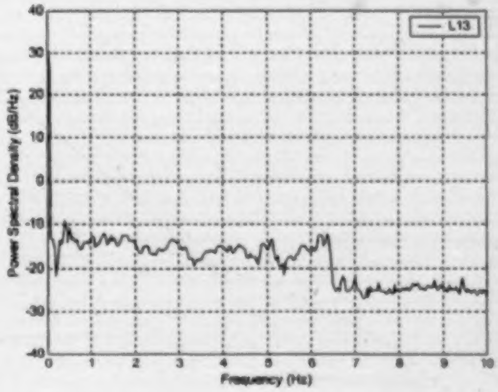

July 17, 1999
4:59 PM

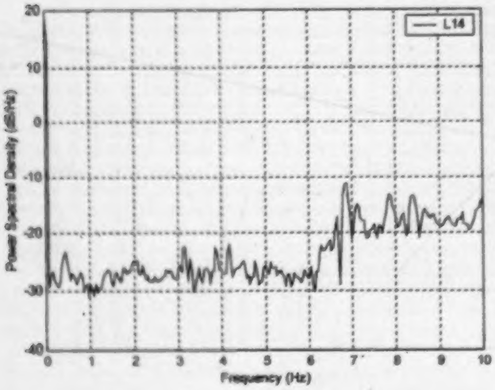

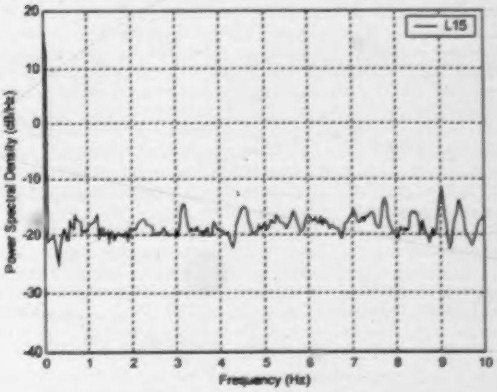

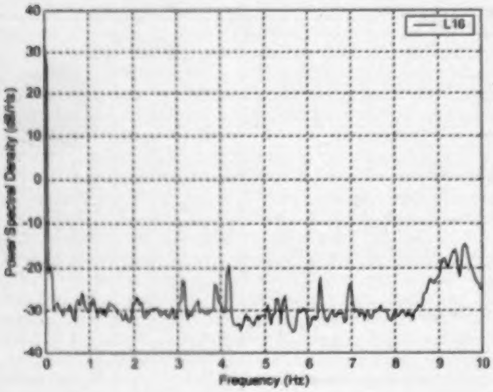

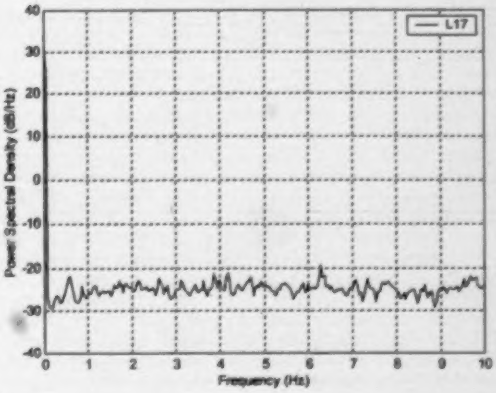

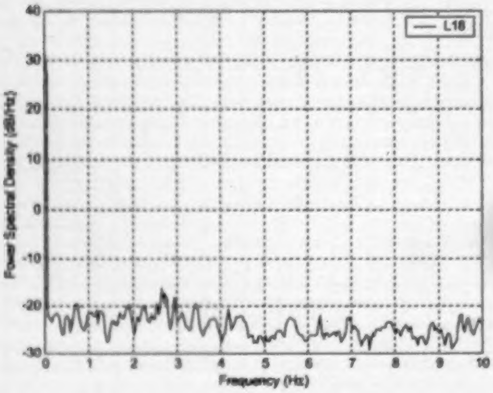

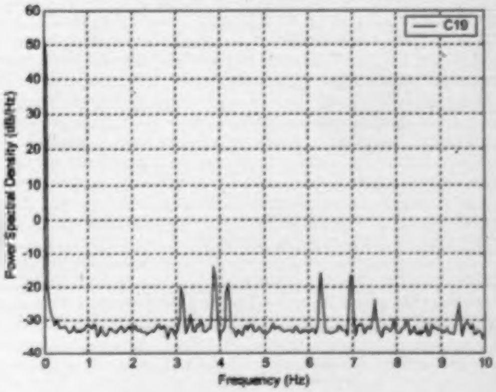

July 17, 1999
4:59 PM

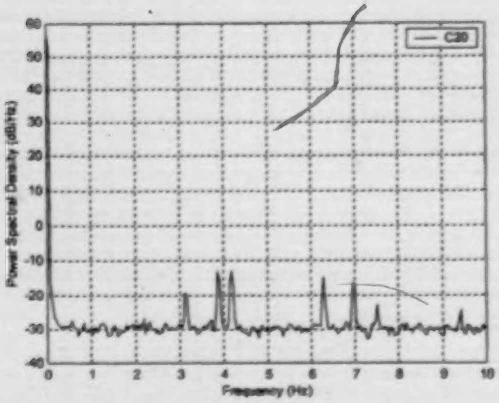

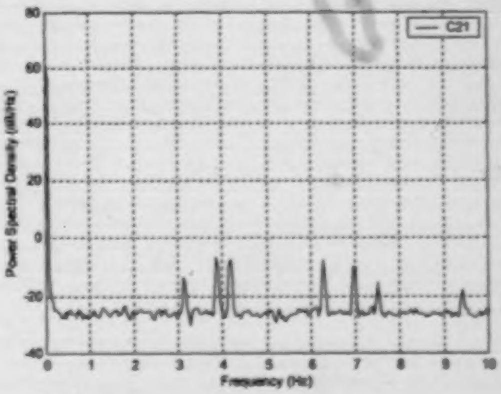

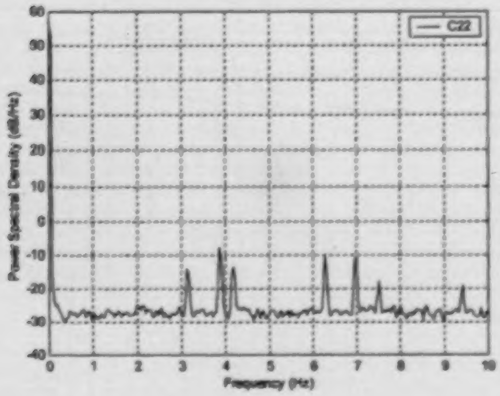

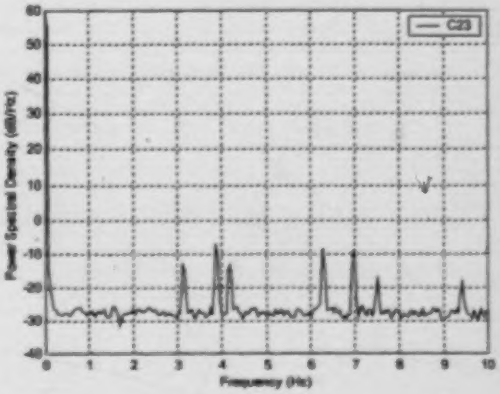

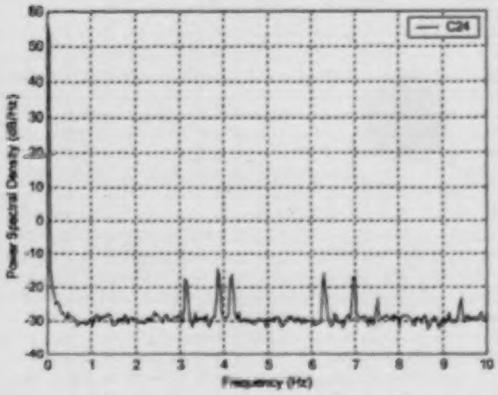

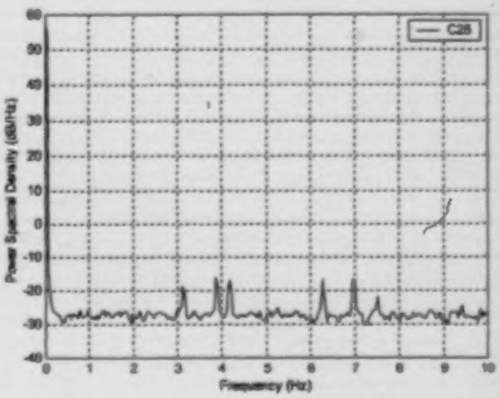

July 17, 1999
4:59 PM

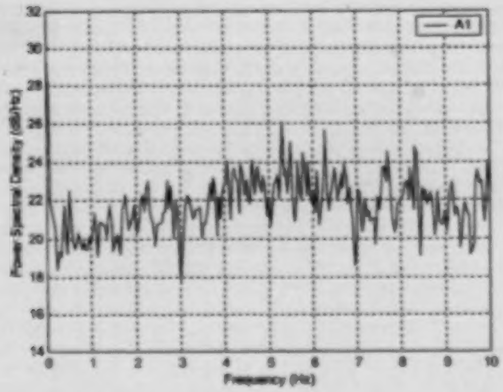

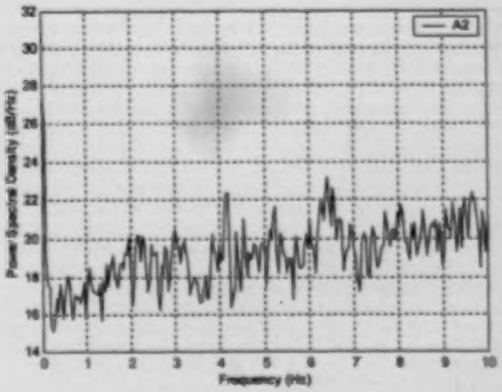

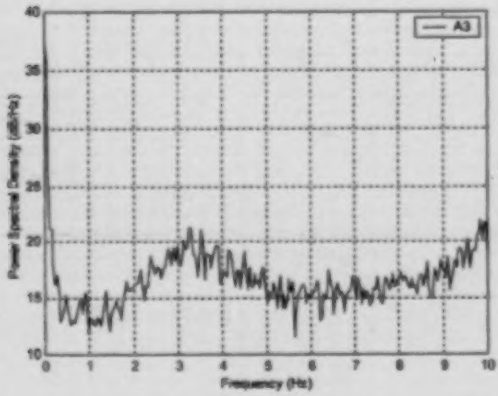

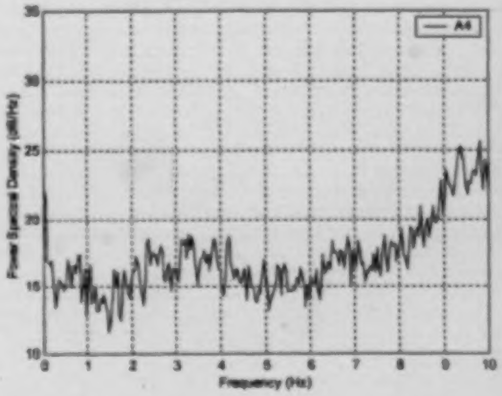

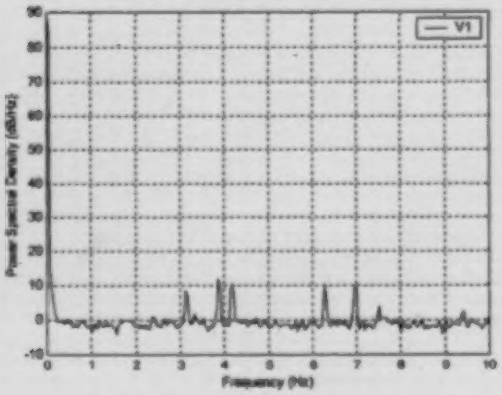

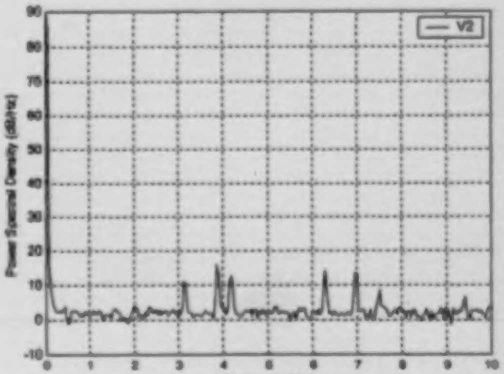

July 18, 1999
1:49 PM

July 18, 1999
1:49 PM

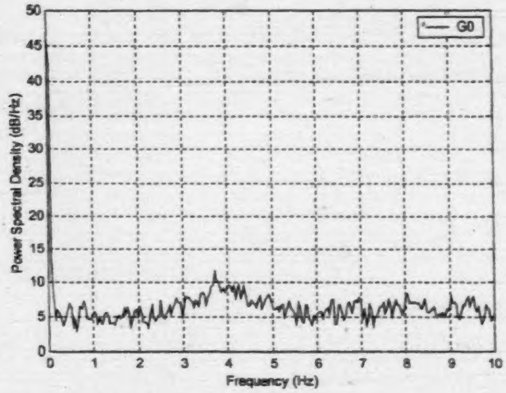

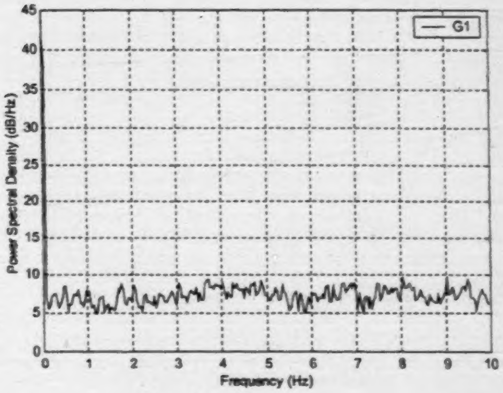

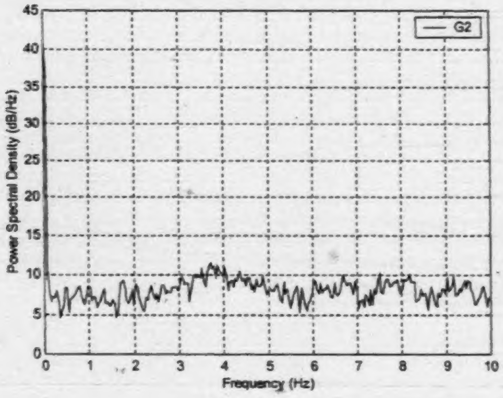

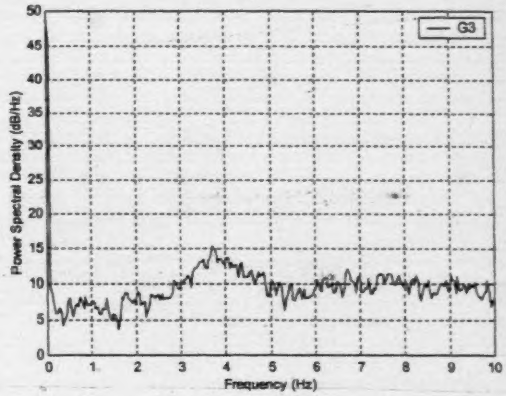

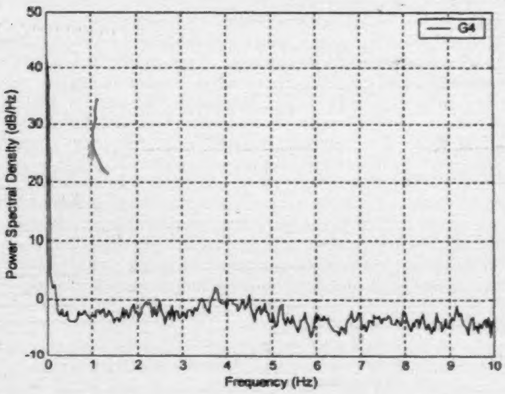

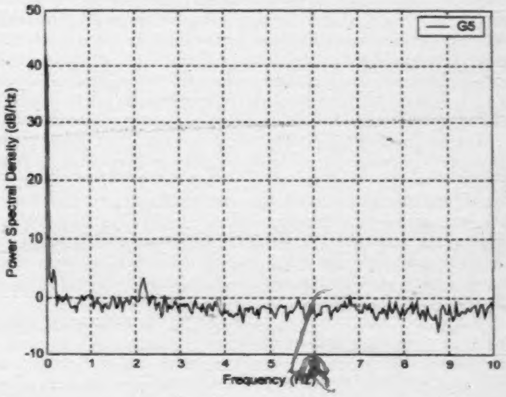

July 18, 1999
1:49 PM

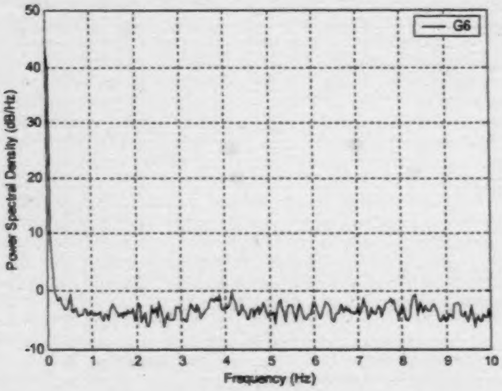

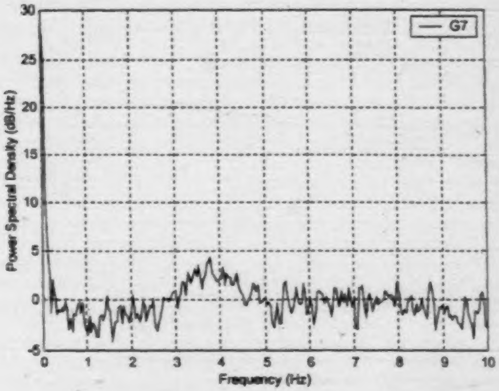

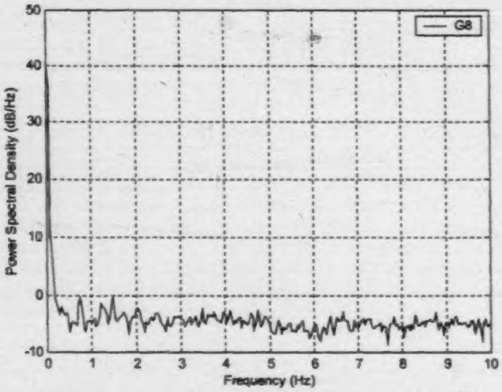

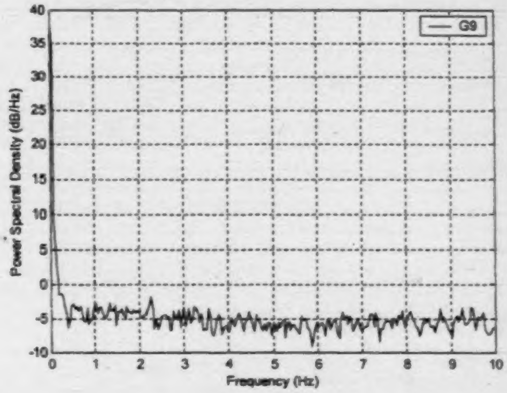

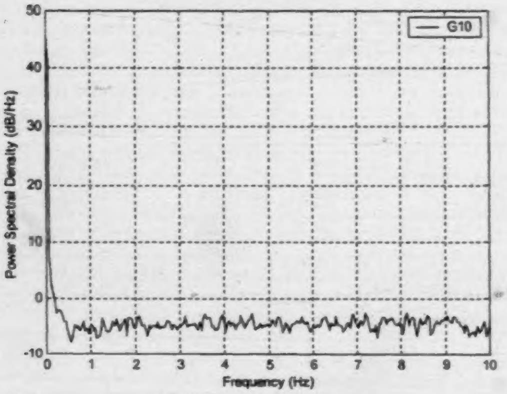

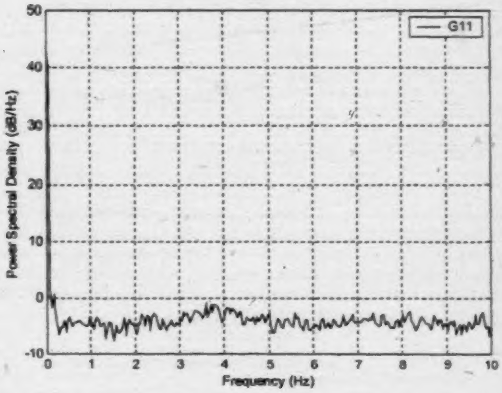

July 18, 1999
1:49 PM

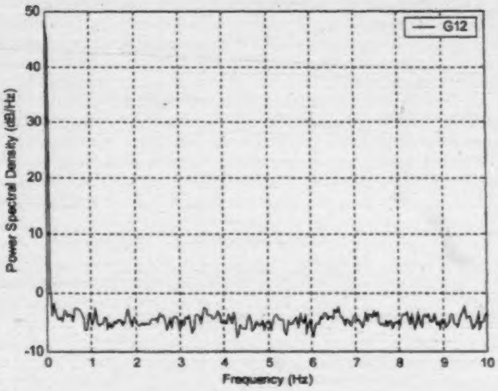

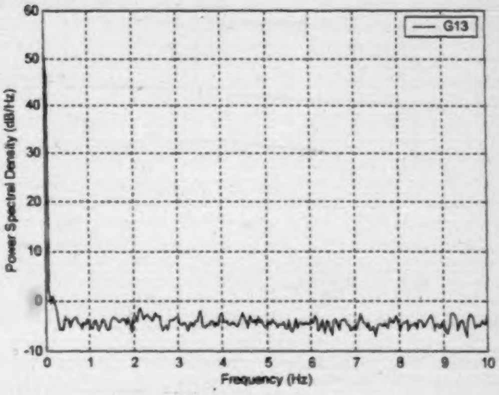

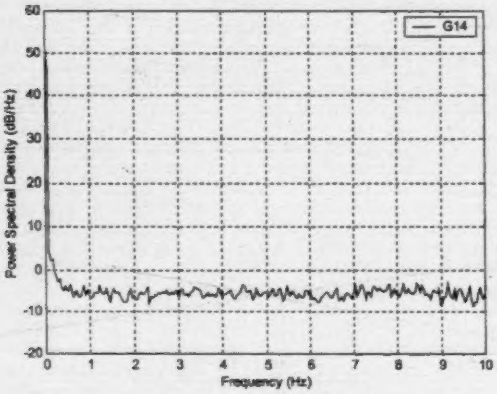

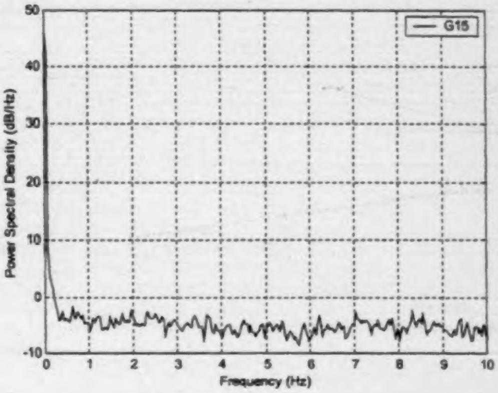

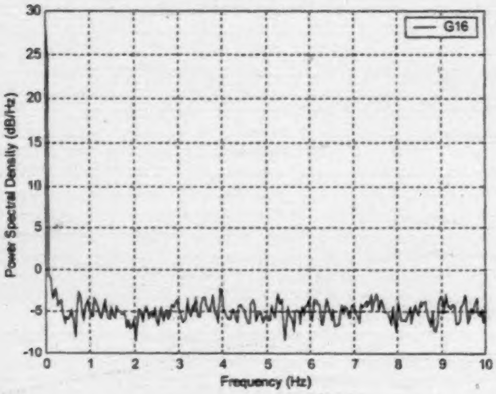

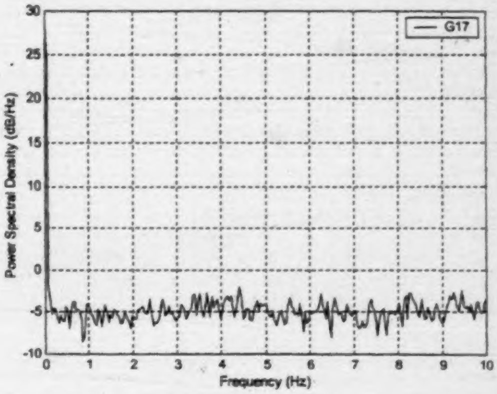

July 18, 1999
1:49 PM

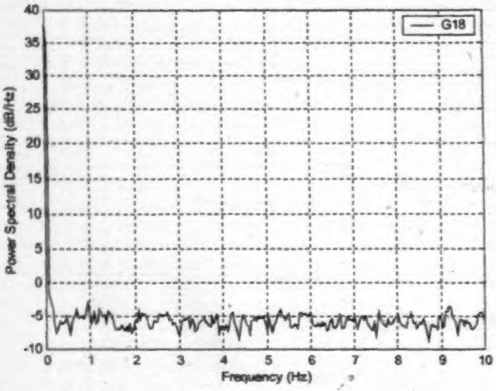

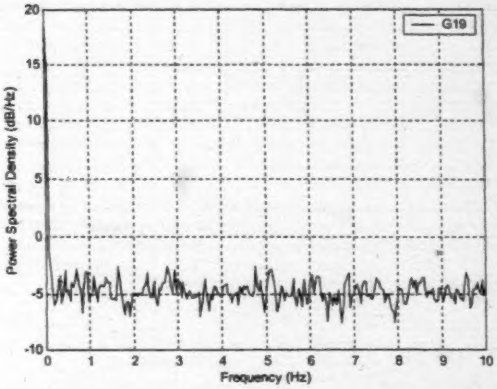

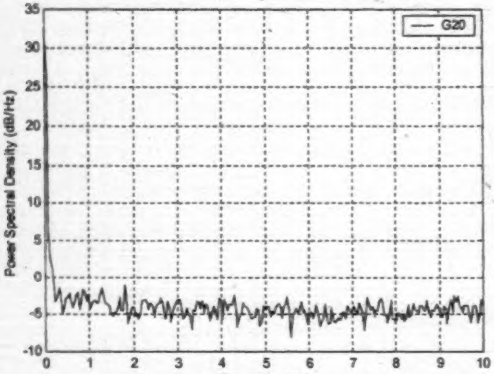

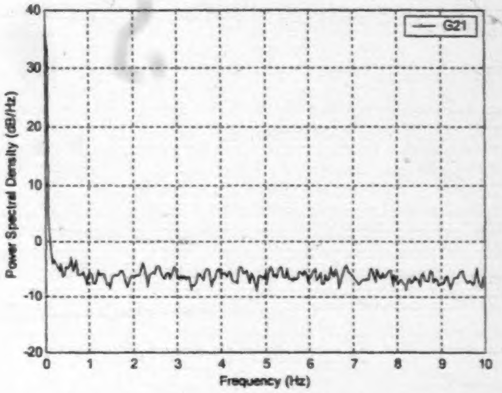

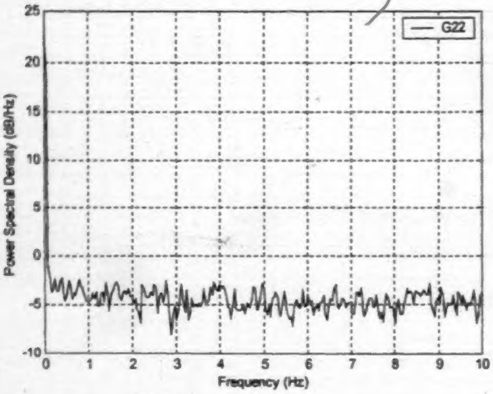

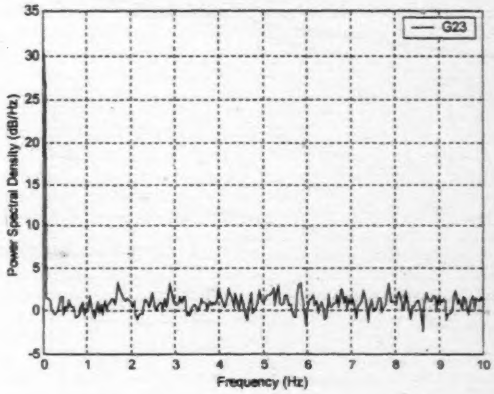

July 18, 1999
1:49 PM

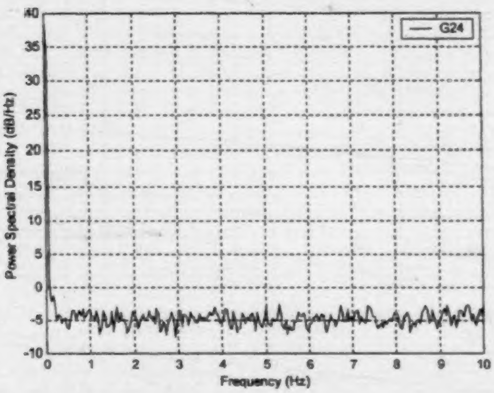

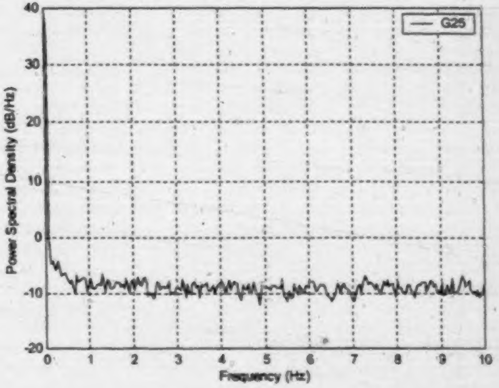

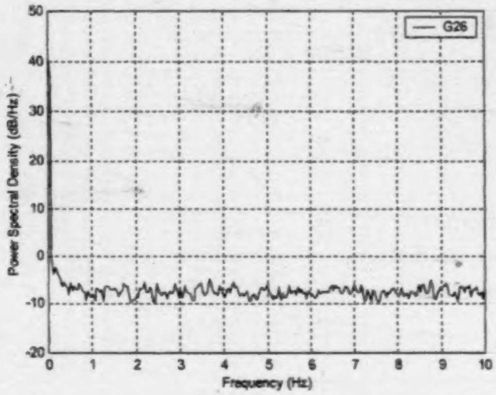

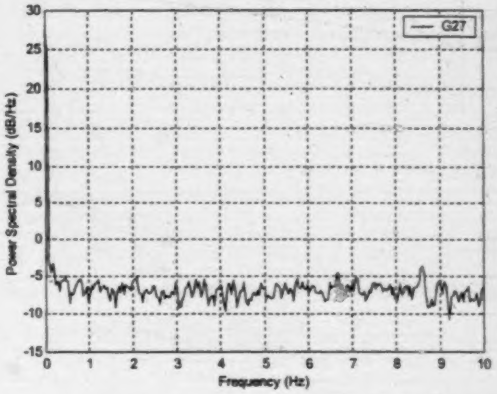

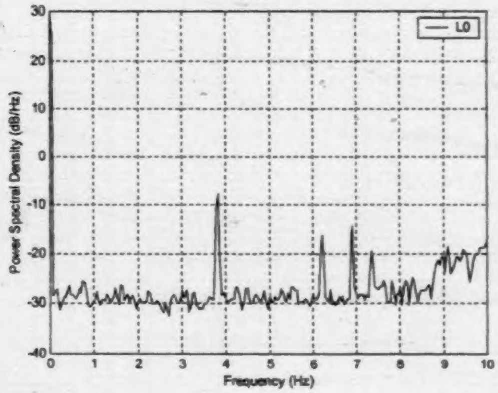

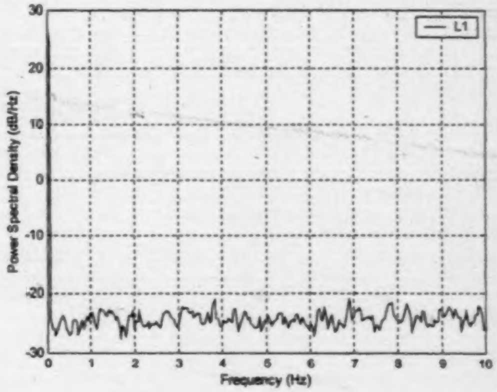

July 18, 1999
1:49 PM

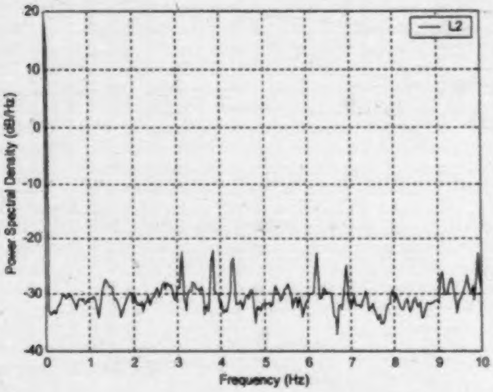

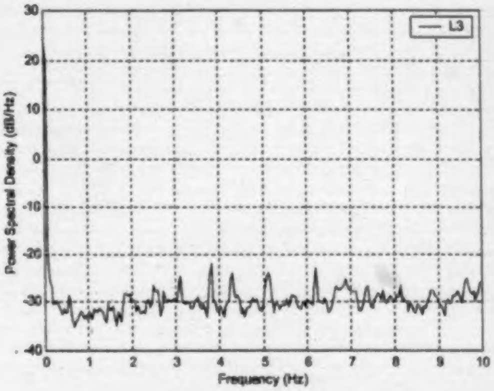

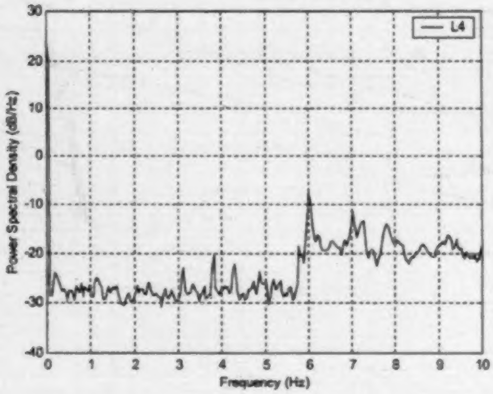

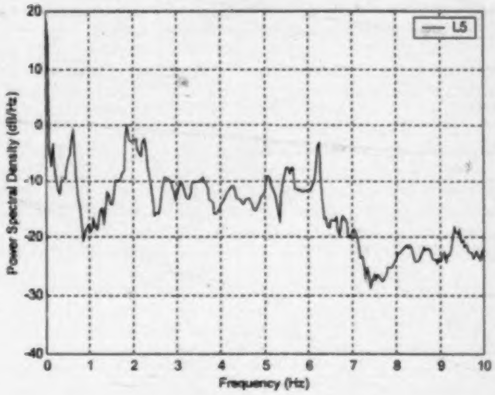

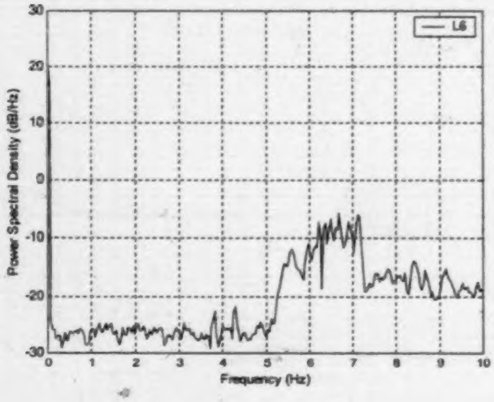

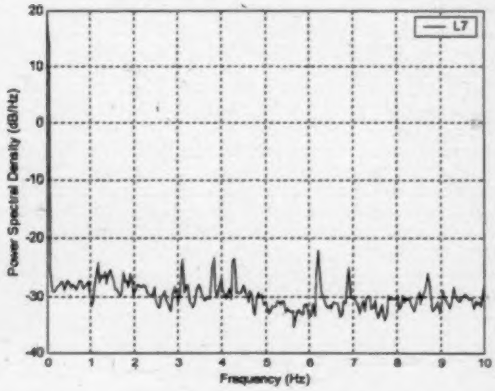

July 18, 1999
1:49 PM

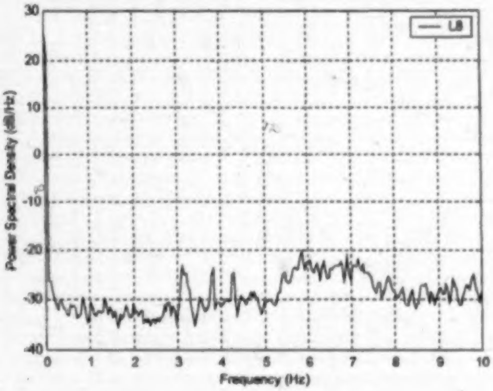

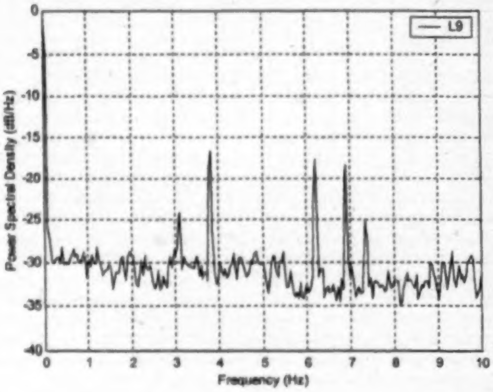

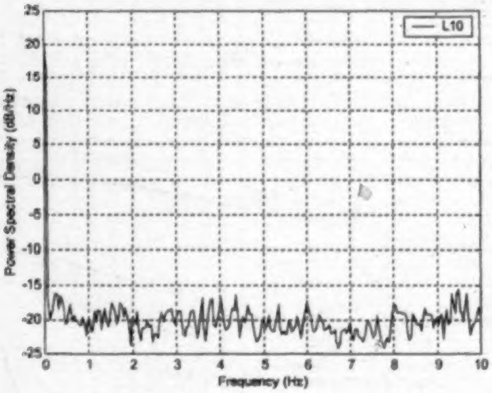

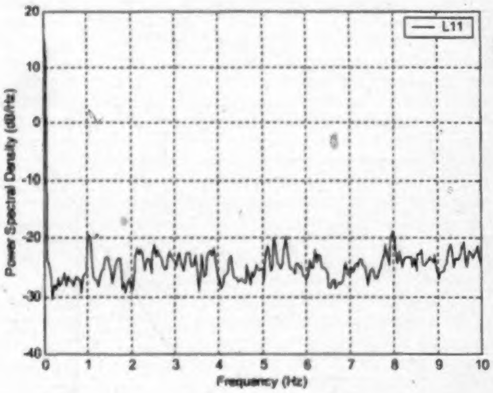

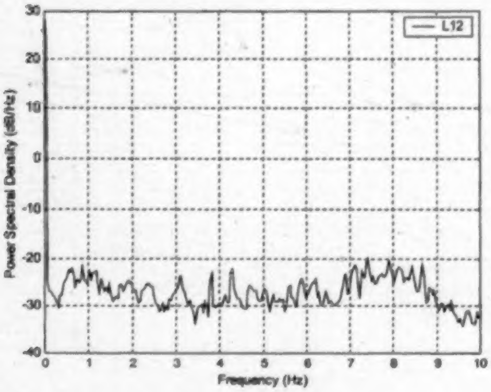

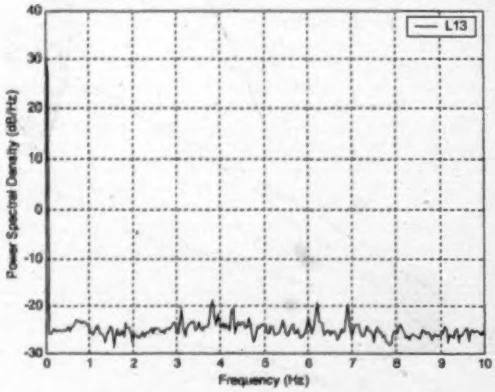

July 18, 1999
1:49 PM

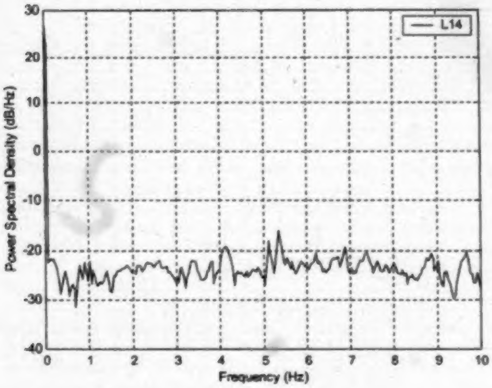

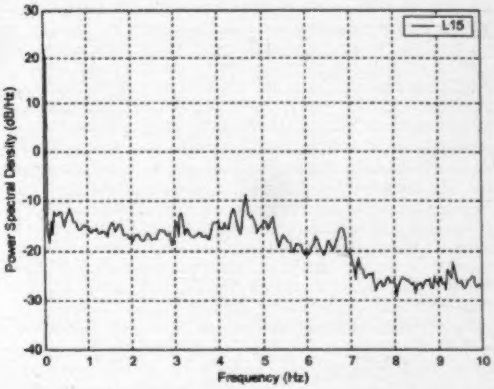

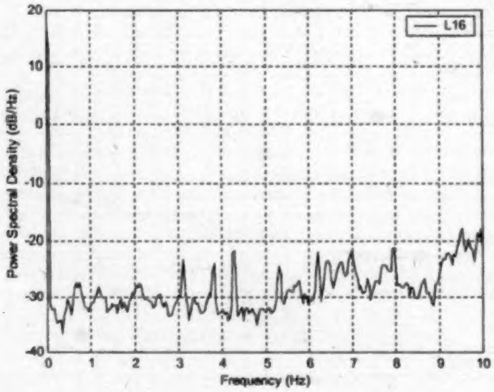

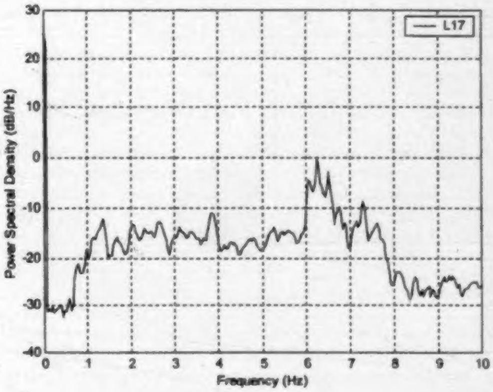

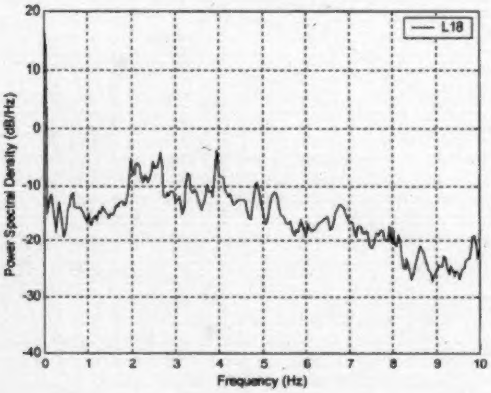

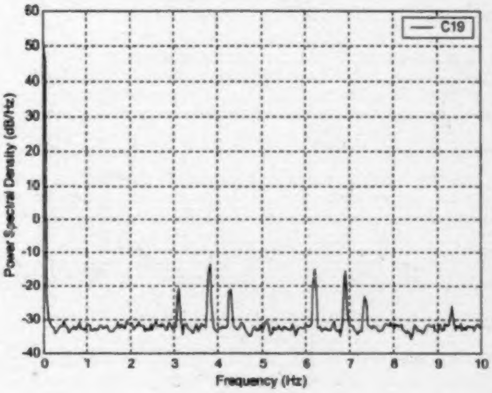

July 18, 1999
1:49 PM

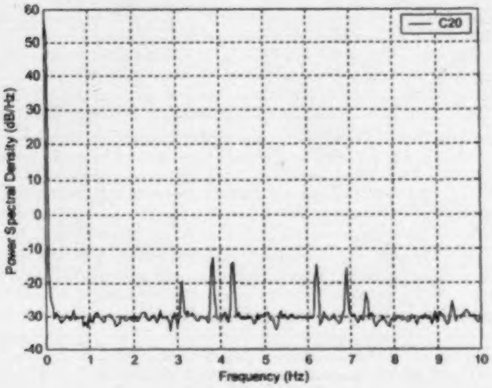

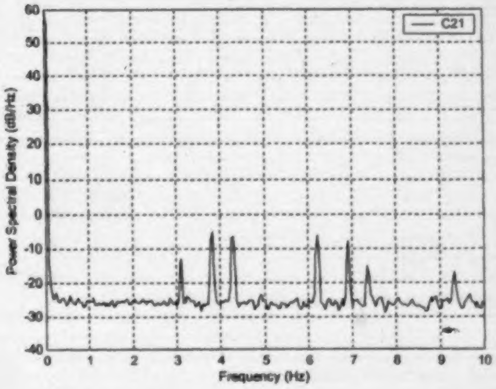

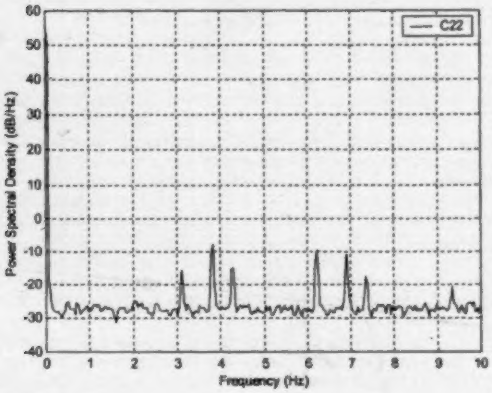

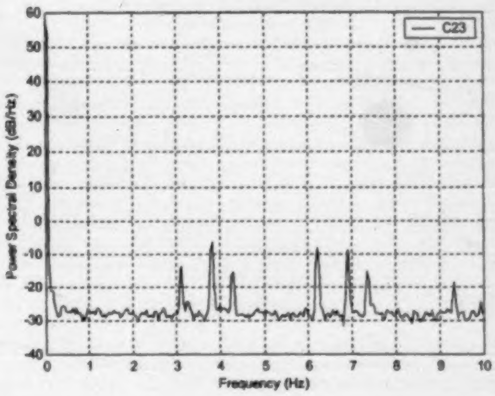

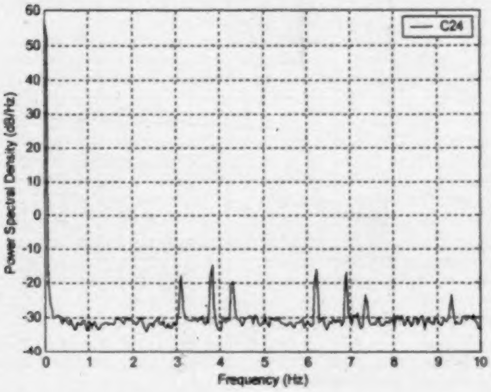

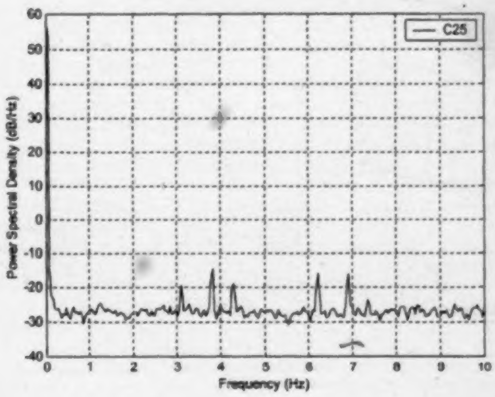

July 18, 1999
1:49 PM

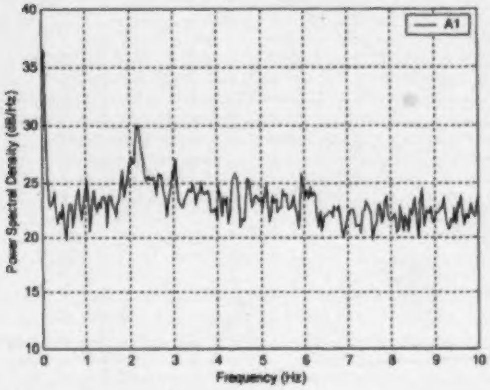

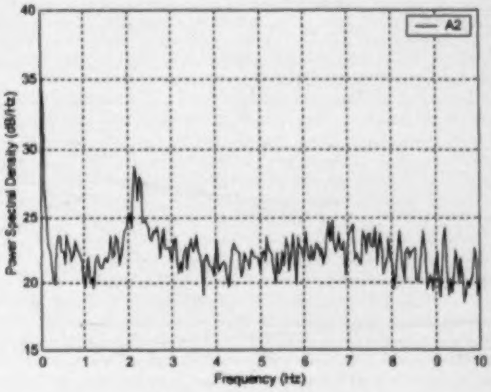

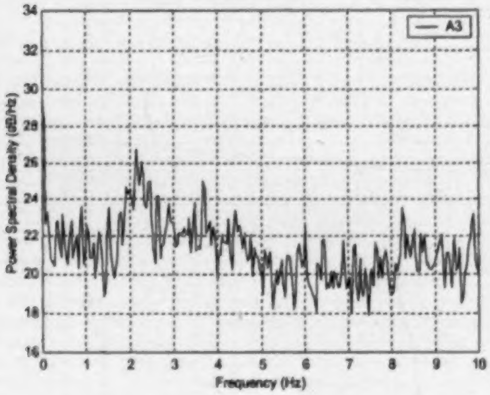

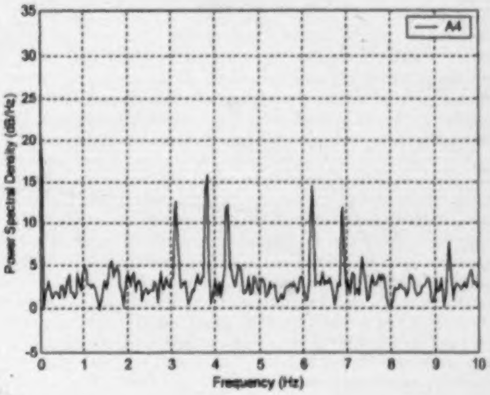

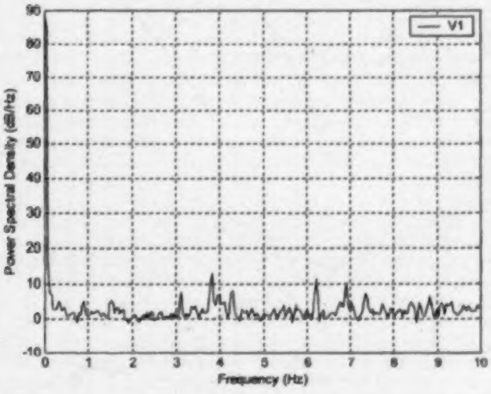

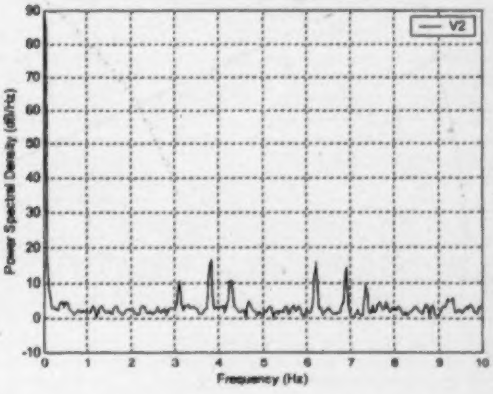

July 18, 1999
1:55 PM

July 18, 1999
1:55 PM

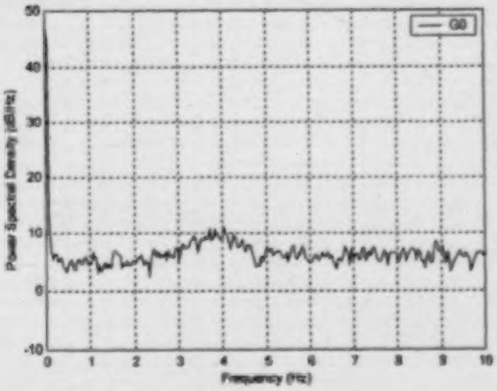

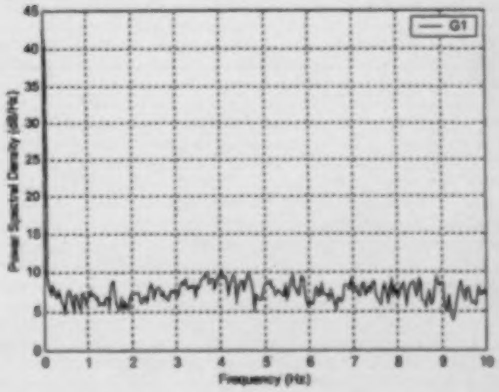

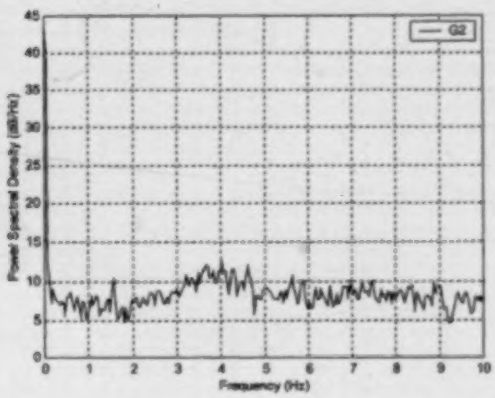

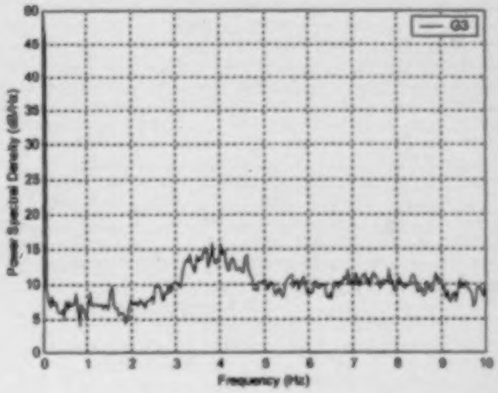

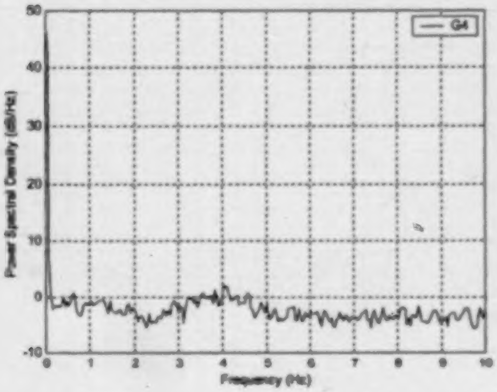

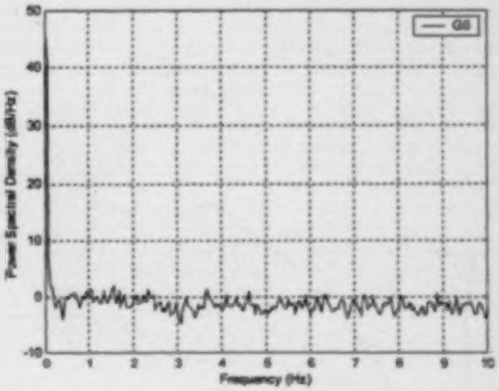

July 18, 1999
1:55 PM

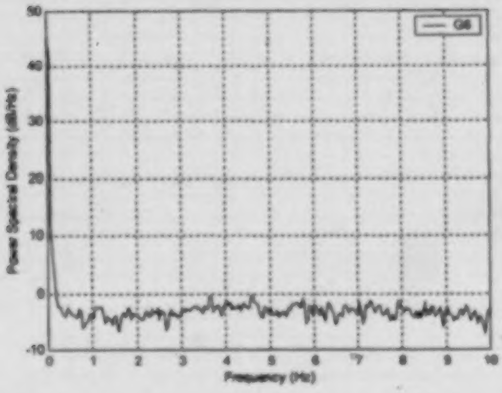

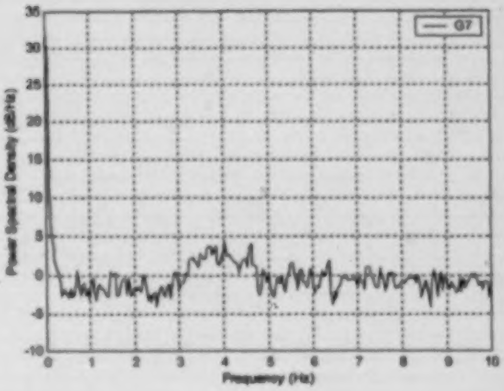

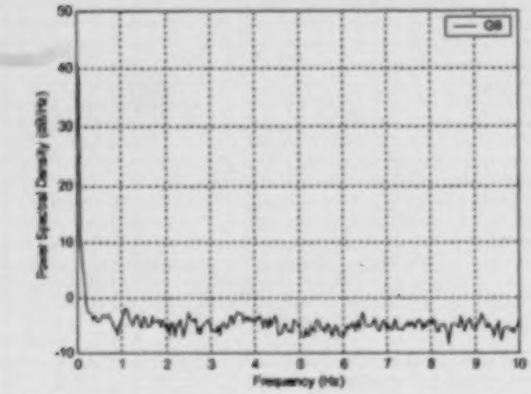

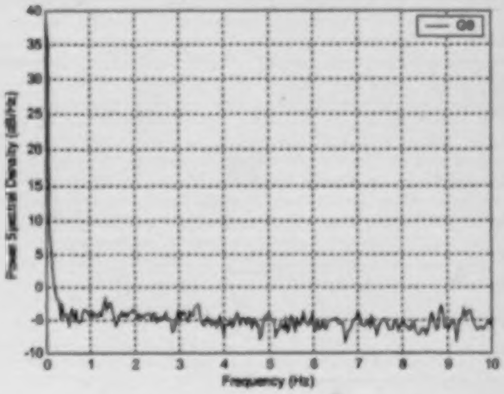

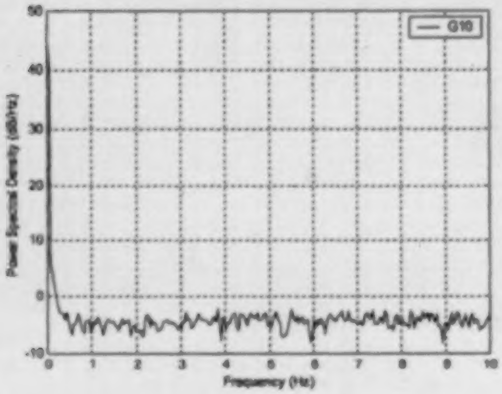

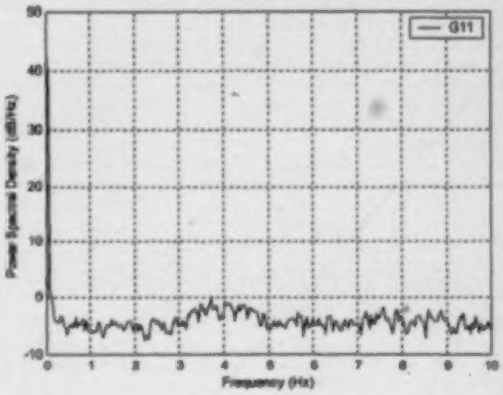

July 18, 1999
1:55 PM

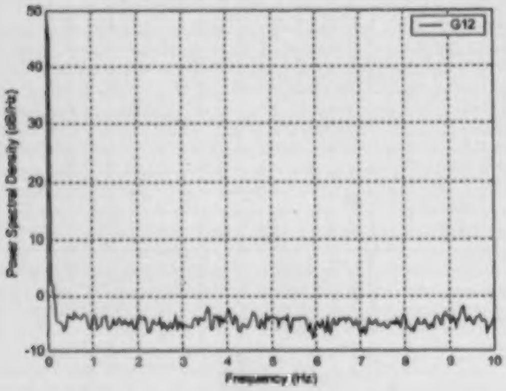

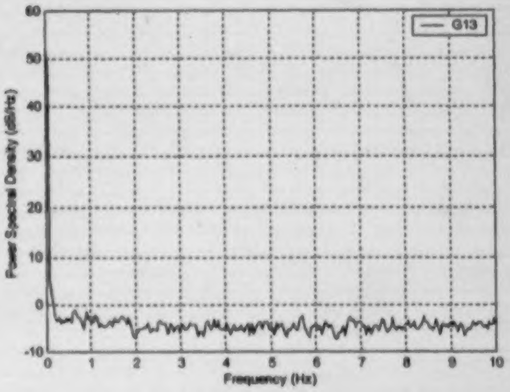

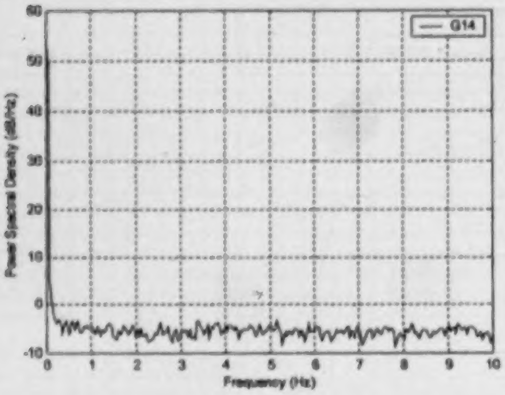

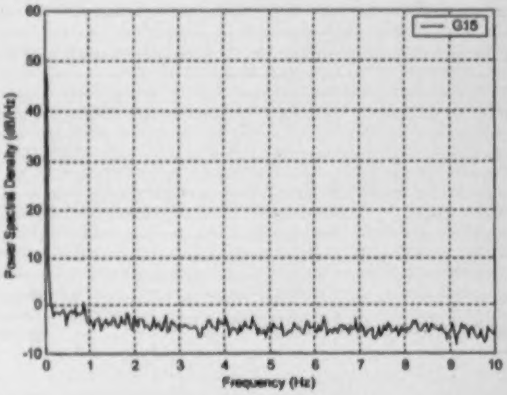

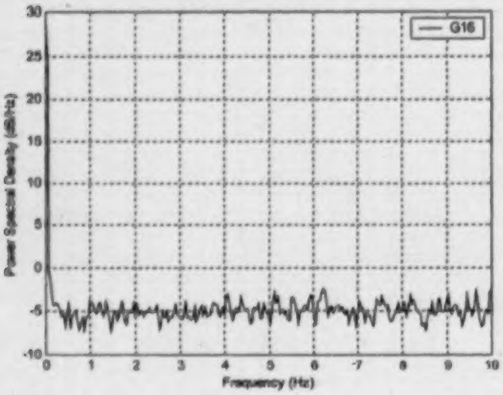

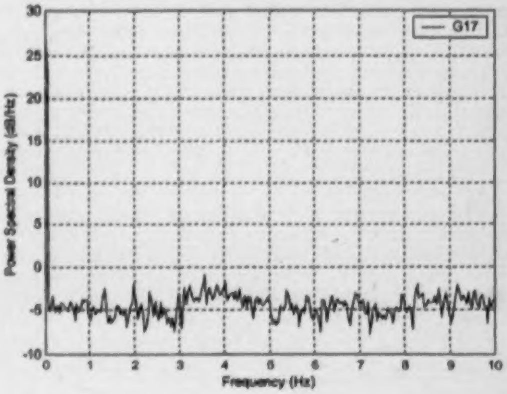

July 18, 1999
1:55 PM

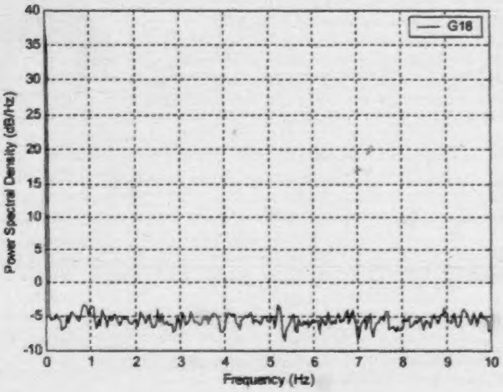

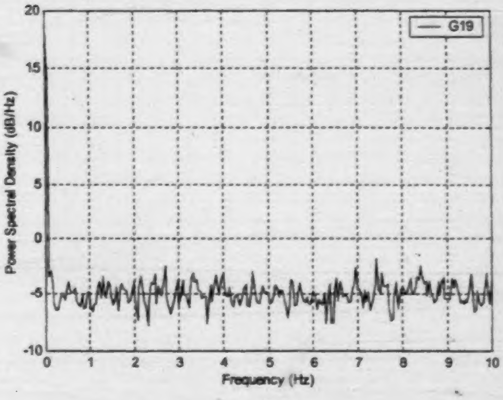

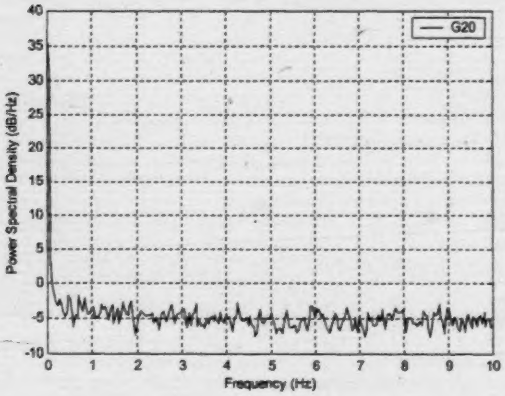

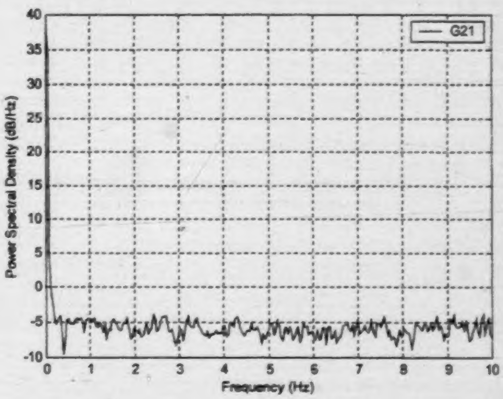

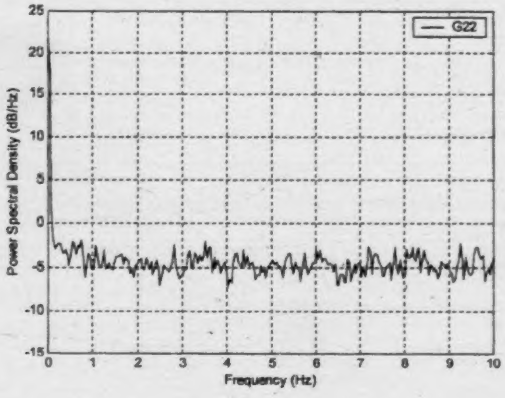

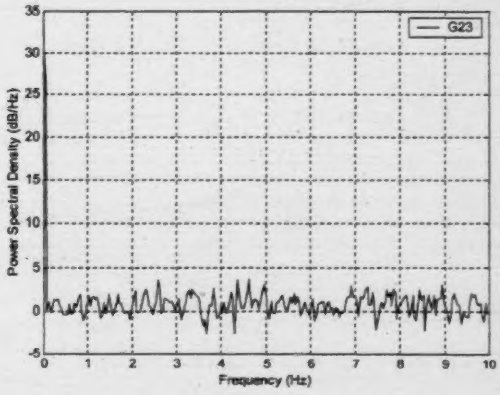

July 18, 1999
1:55 PM

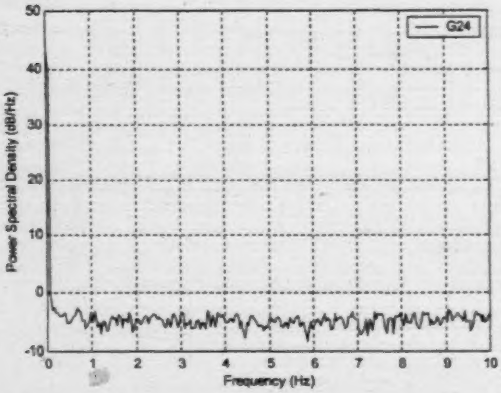

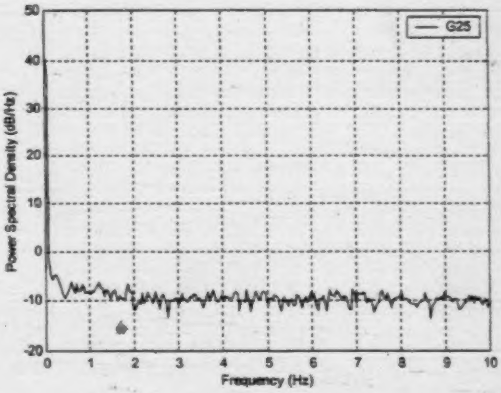

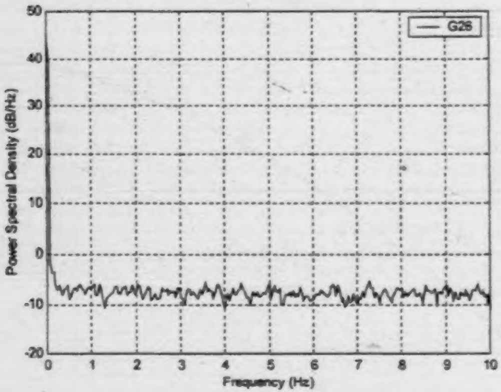

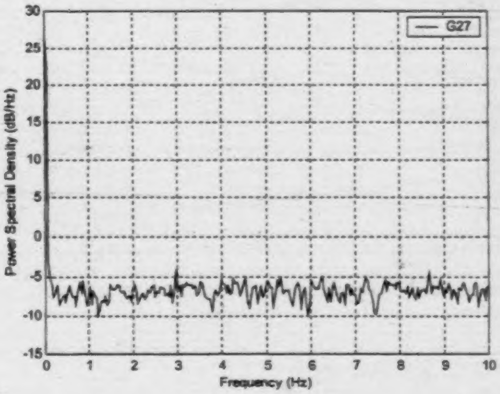

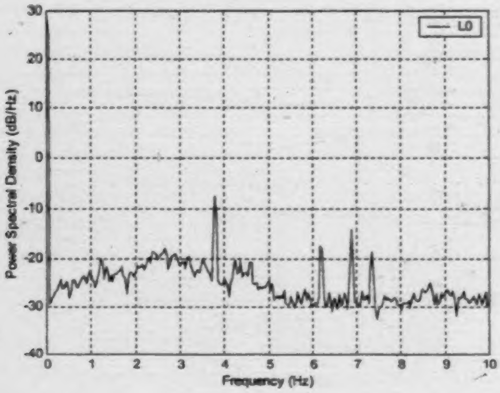

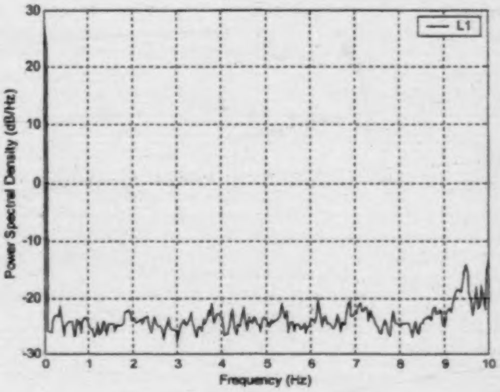

July 18, 1999
1:55 PM

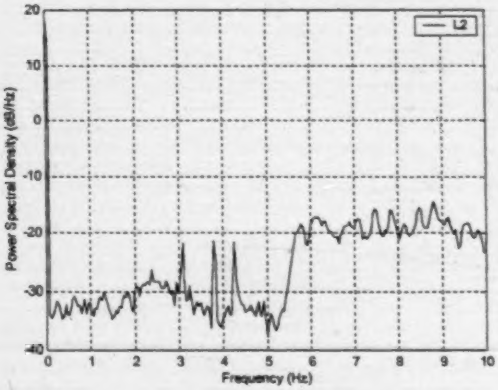

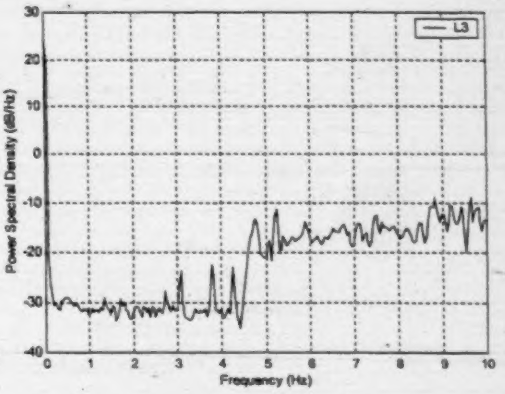

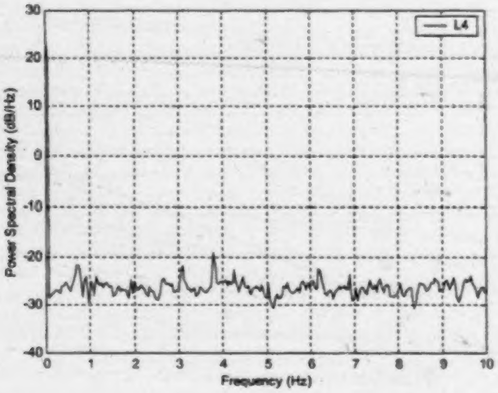

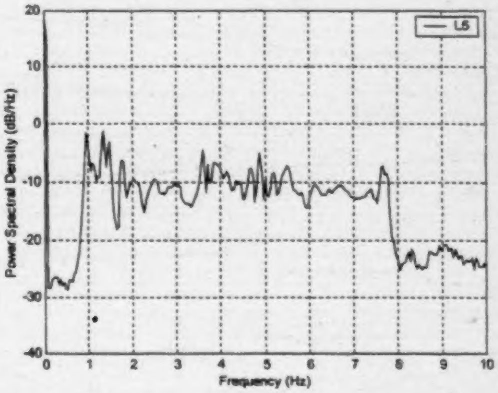

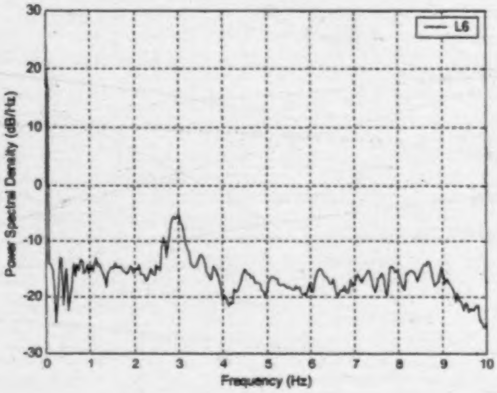

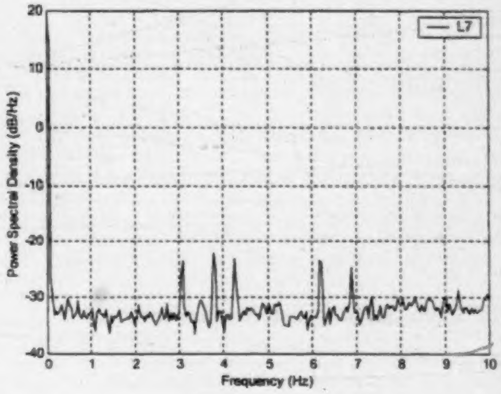

July 18, 1999
1:55 PM

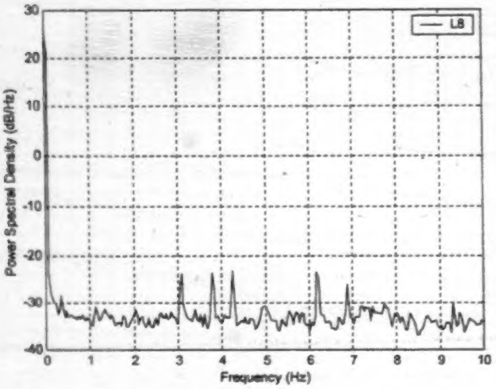

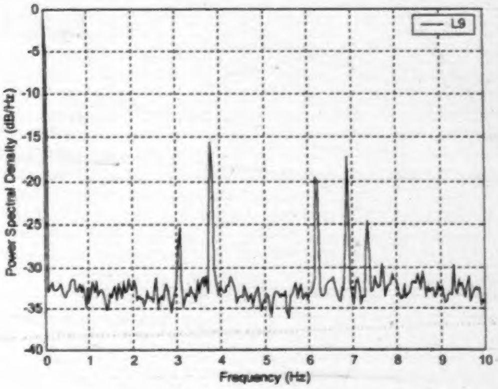

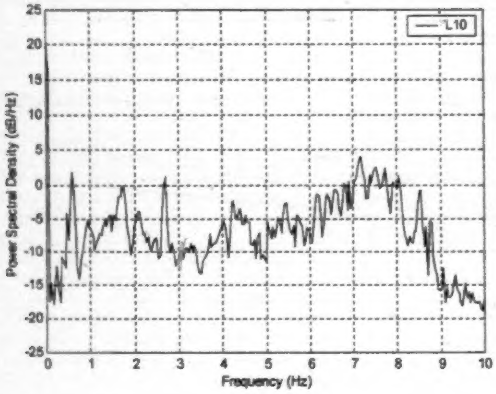

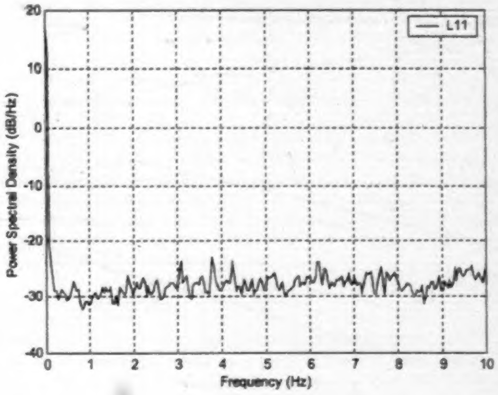

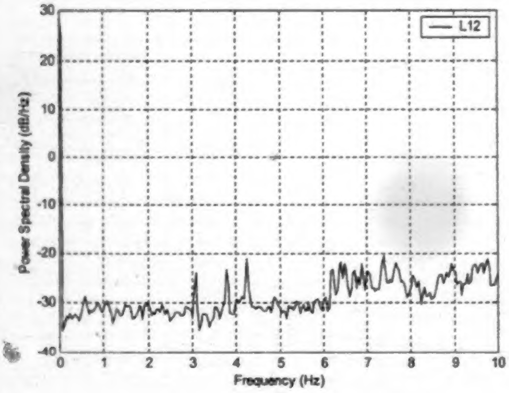

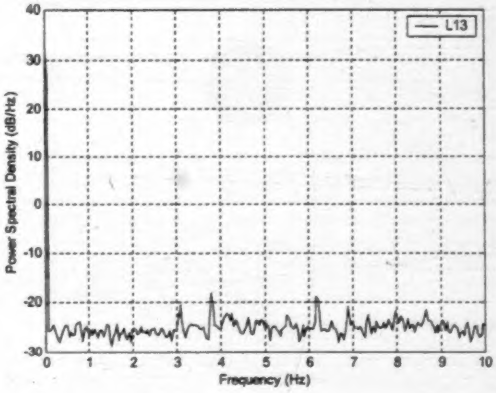

July 18, 1999
1:55 PM

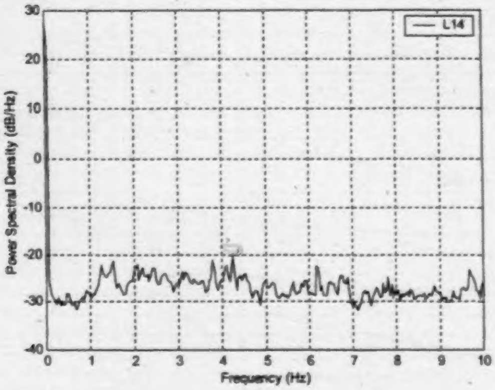

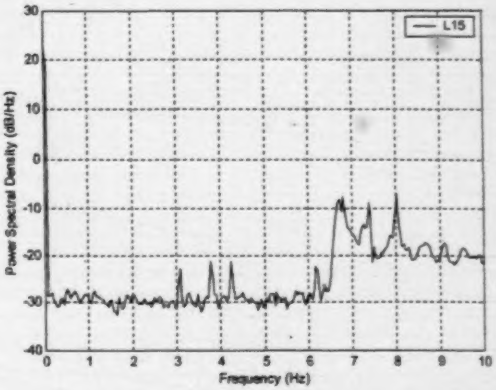

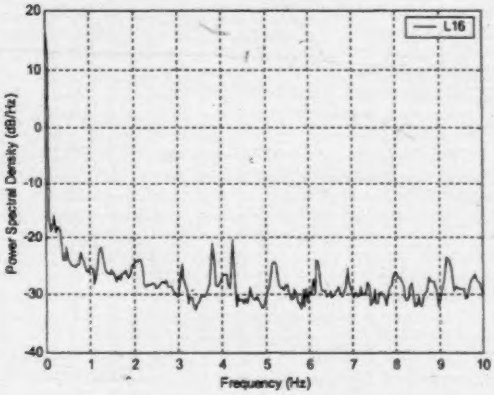

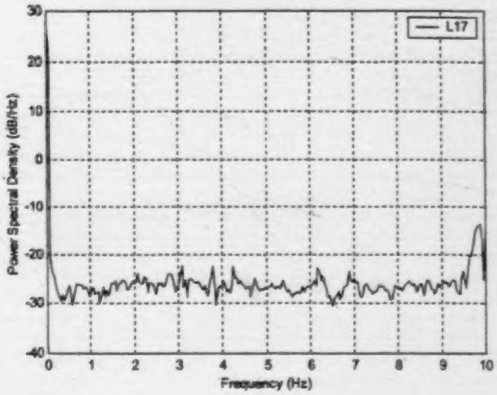

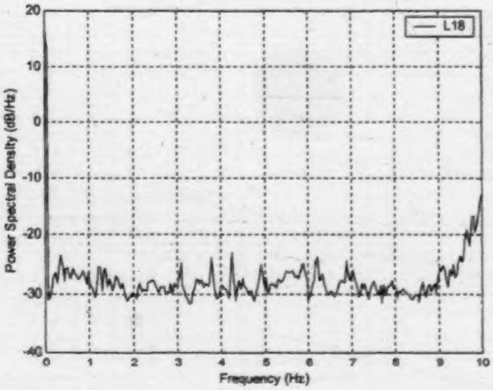

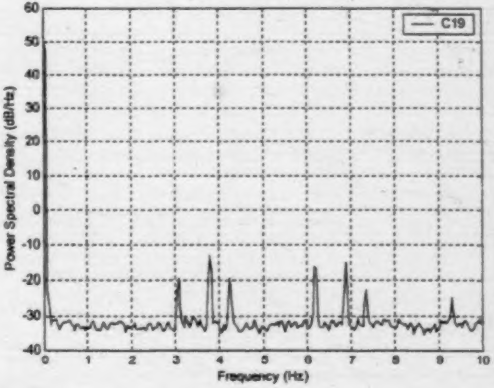

July 18, 1999
1:55 PM

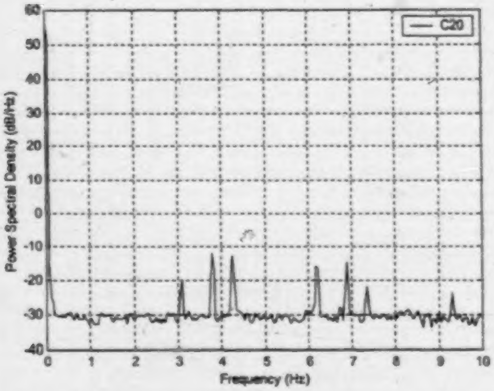

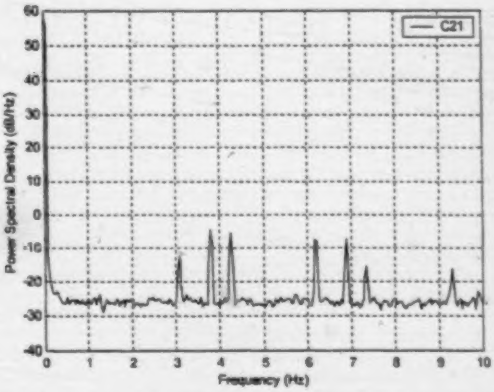

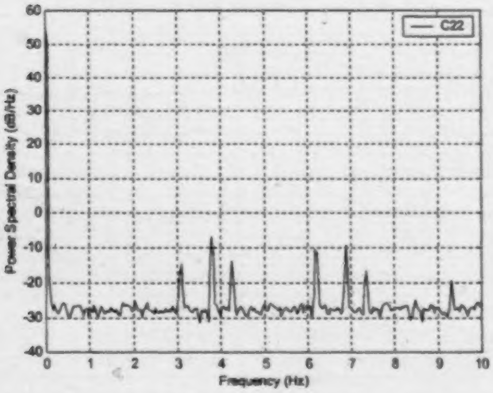

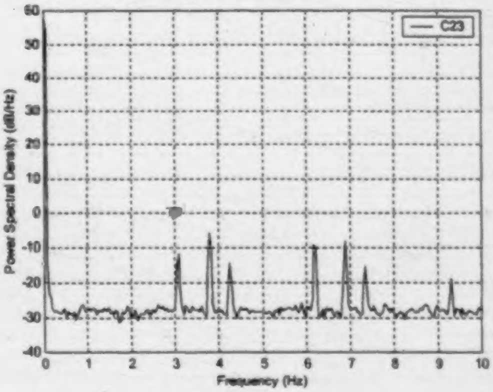

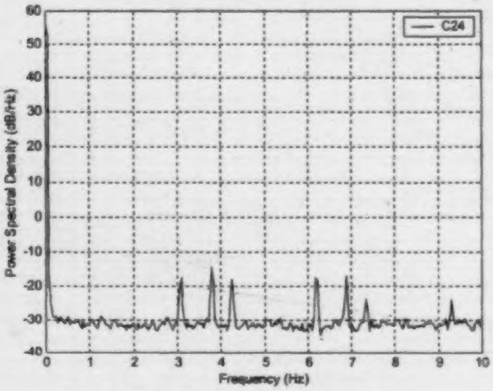

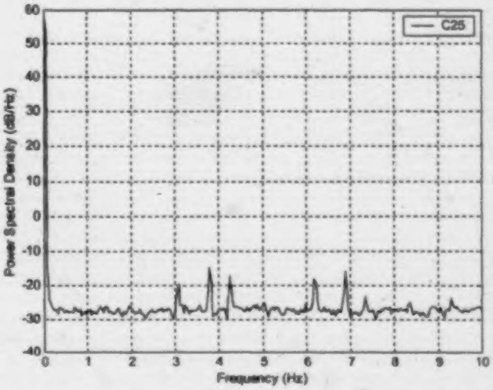

July 18, 1999
1:55 PM

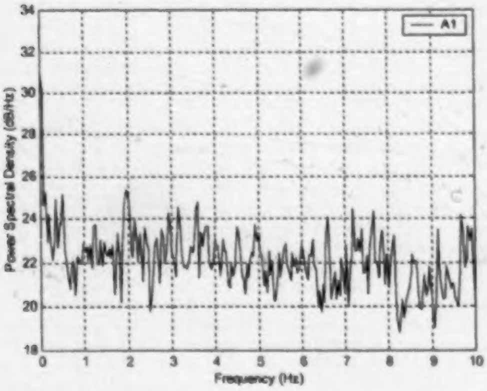

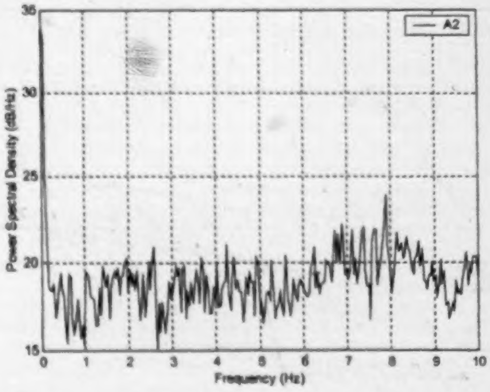

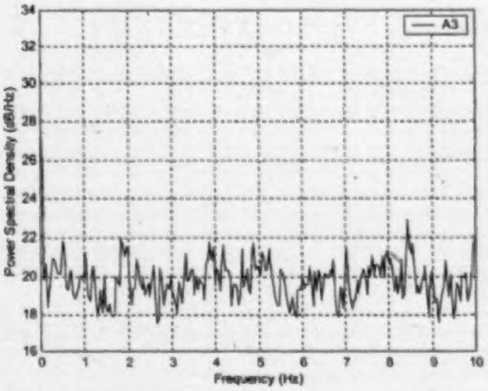

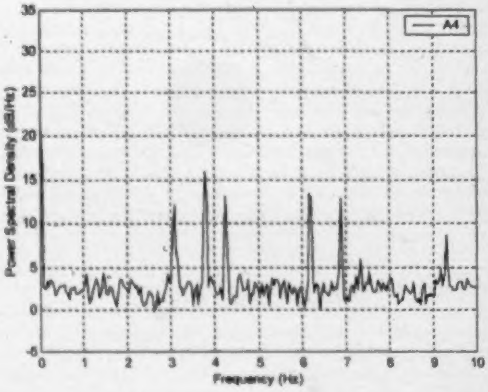

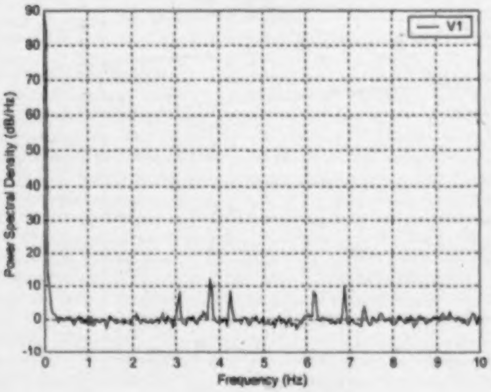

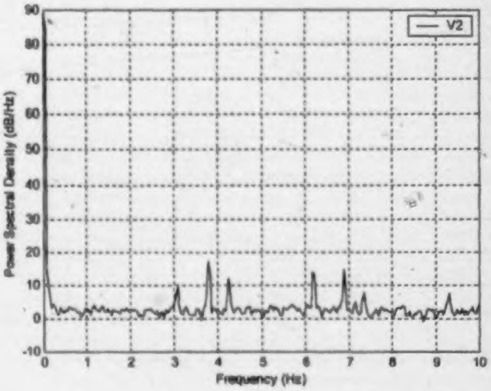

July 18, 1999
2:01 PM

July 18, 1999
2:01 PM

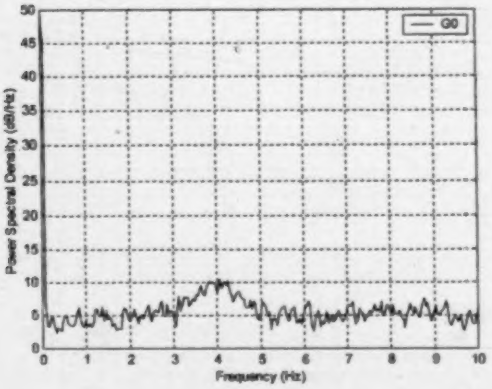

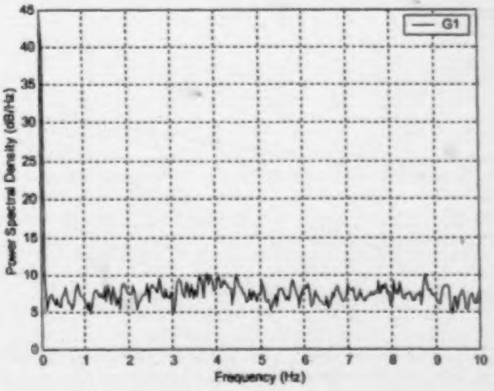

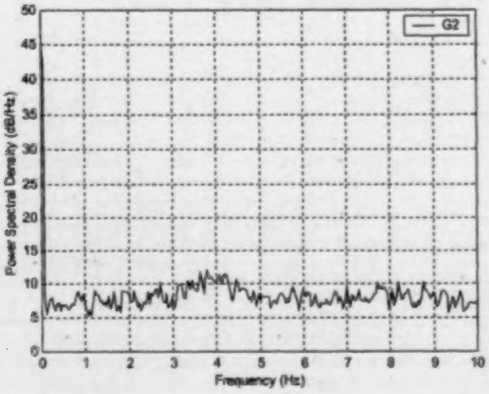

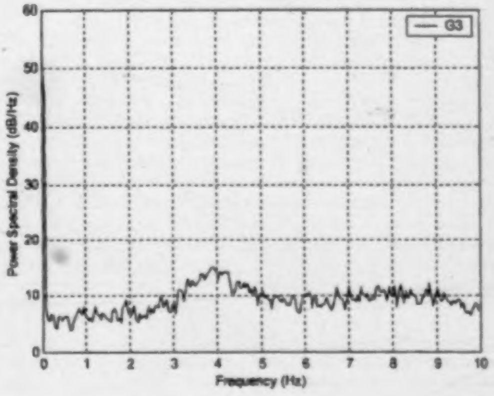

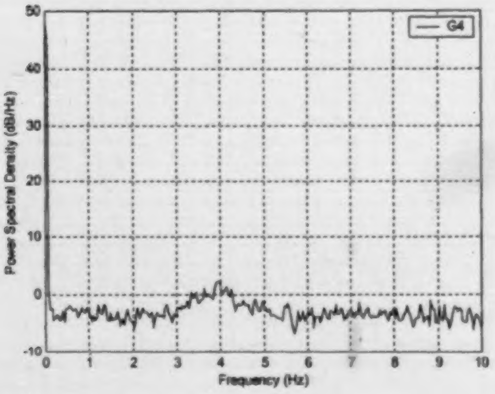

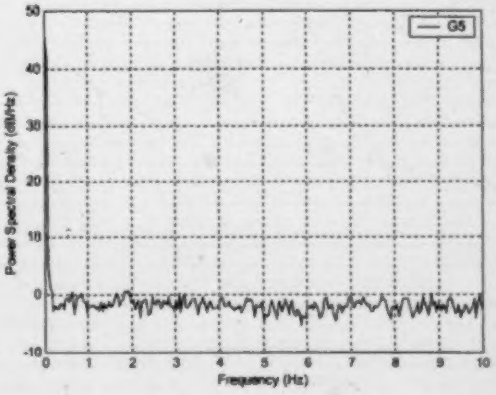

July 18, 1999
2:01 PM

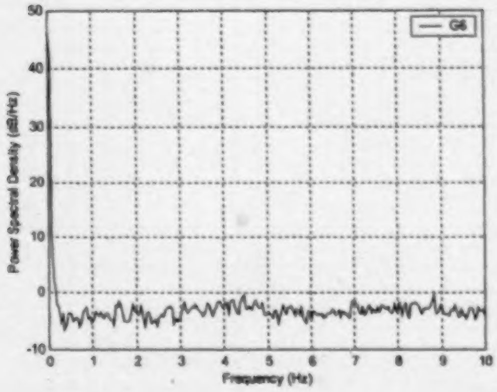

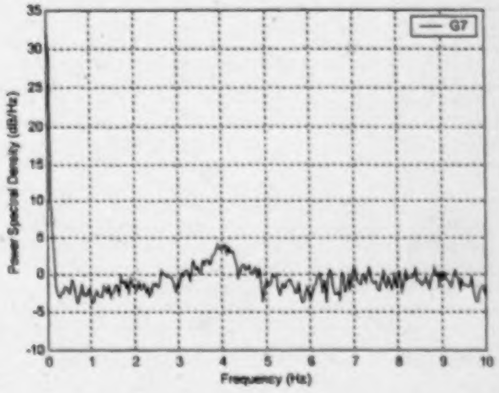

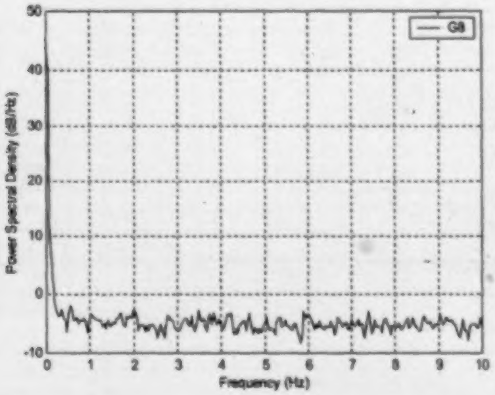

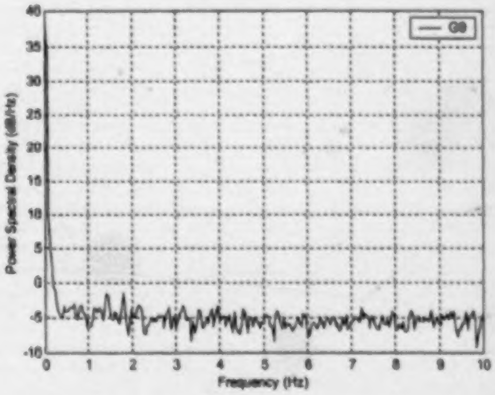

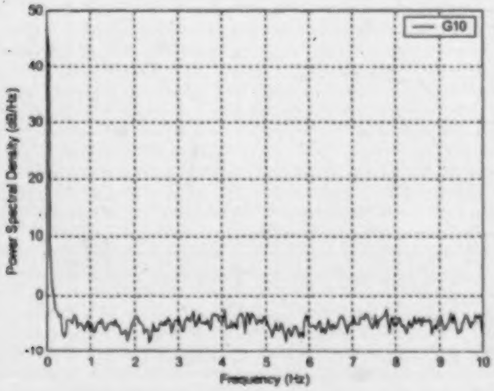

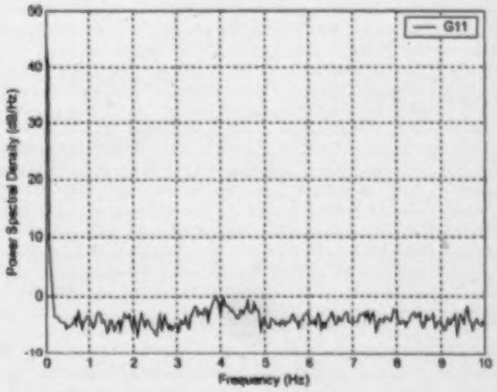

July 18, 1999
2:01 PM

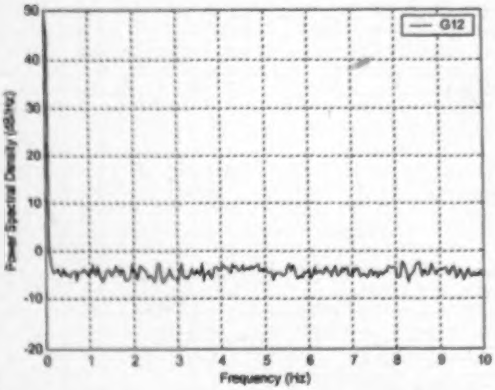

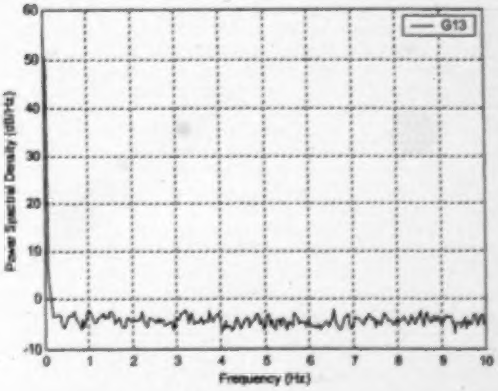

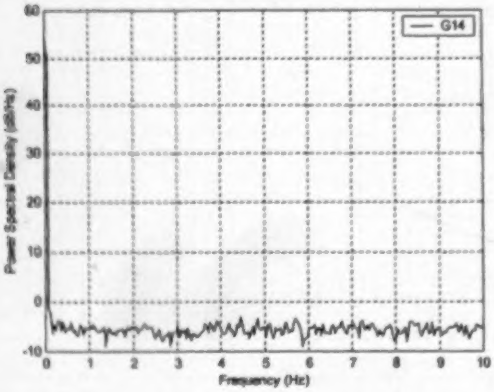

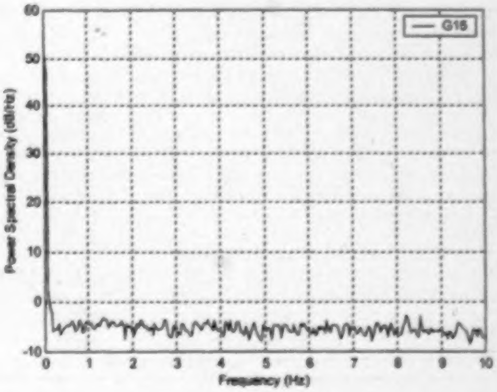

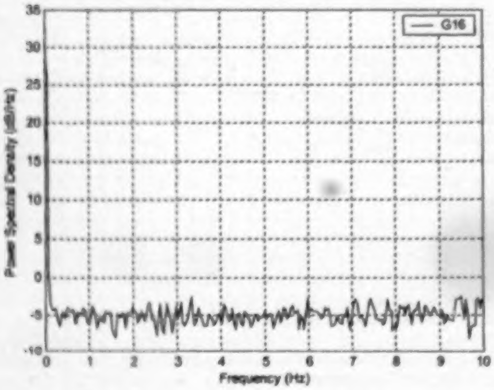

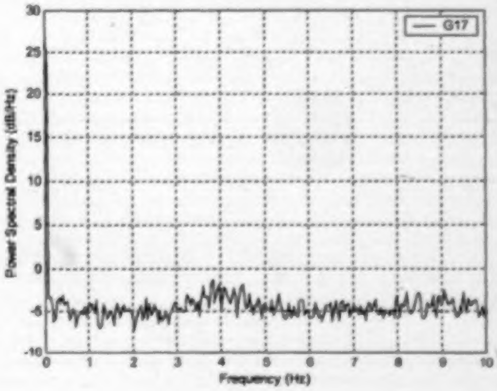

July 18, 1999
2:01 PM

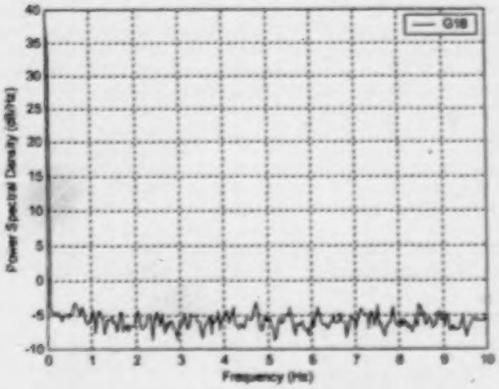

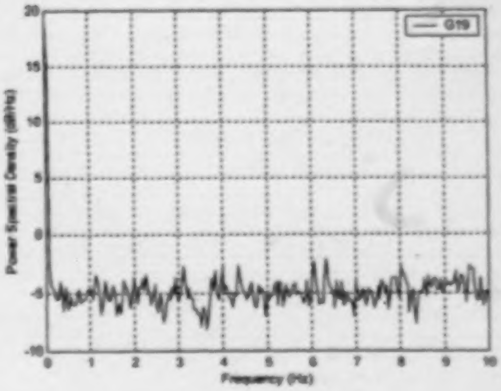

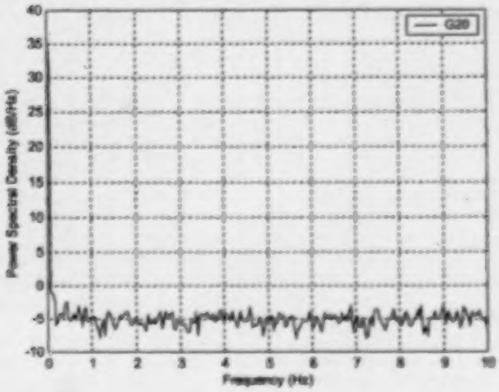

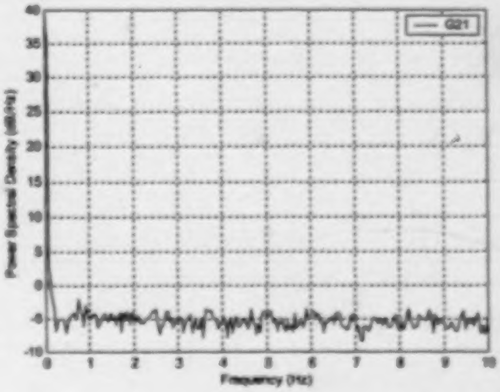

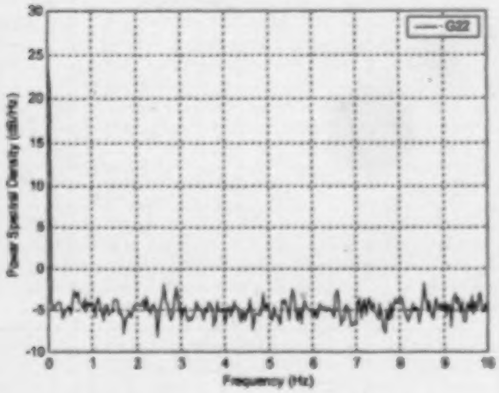

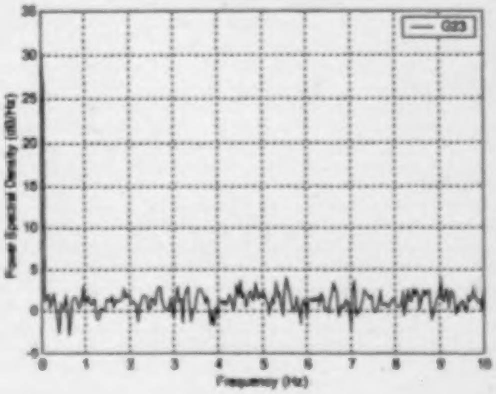

July 18, 1999
2:01 PM

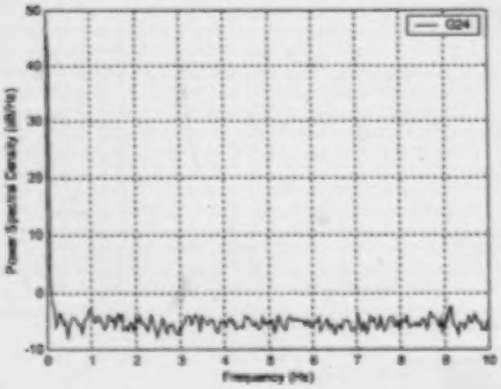

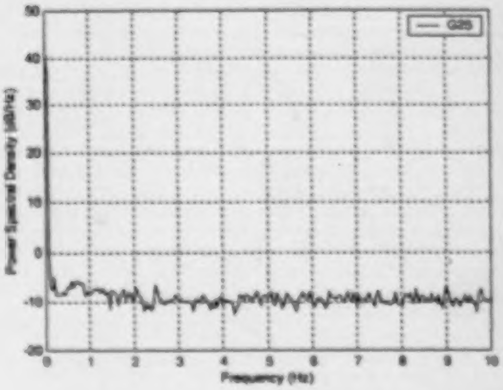

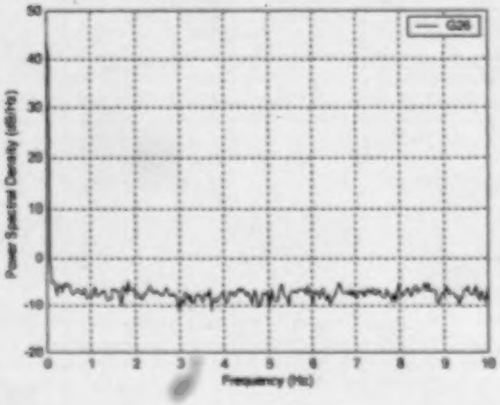

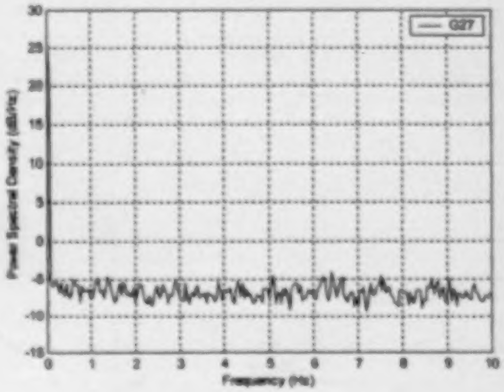

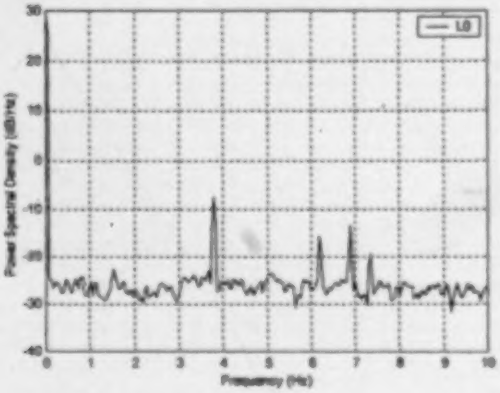

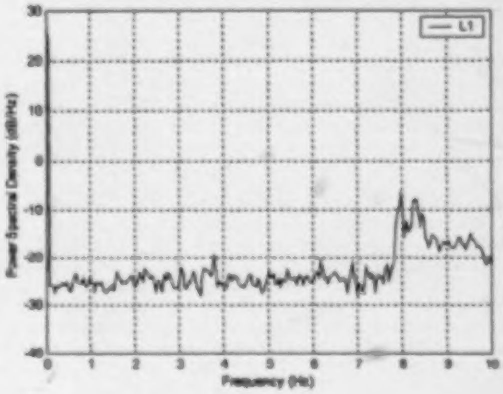

July 18, 1999
2:01 PM

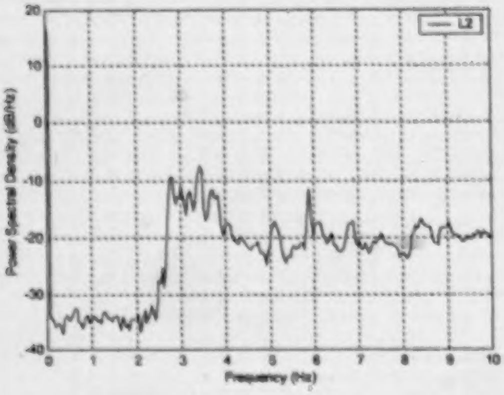

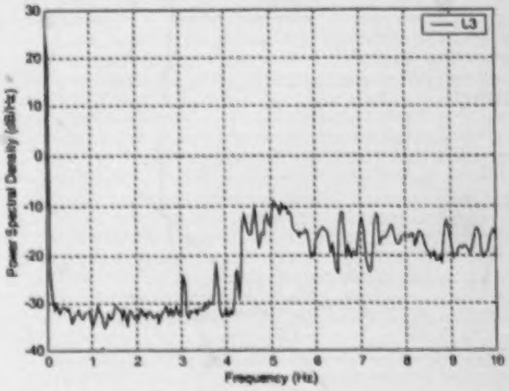

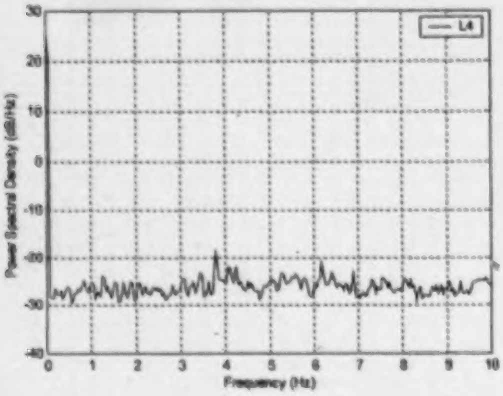

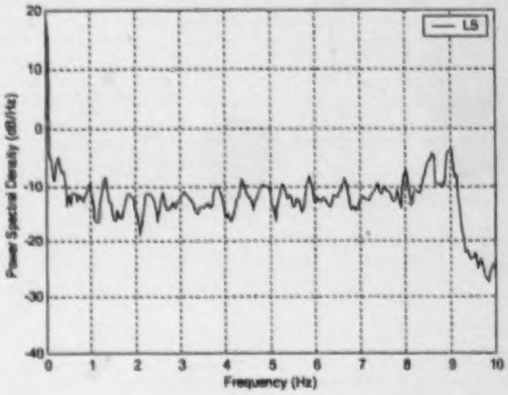

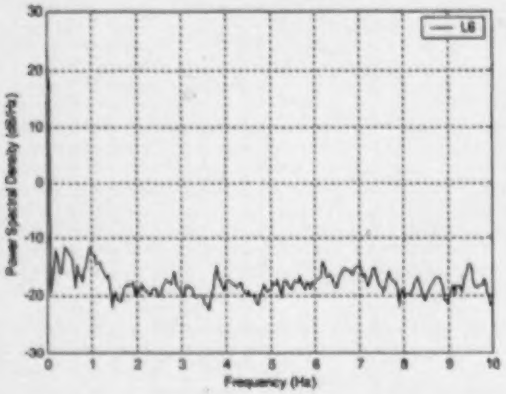

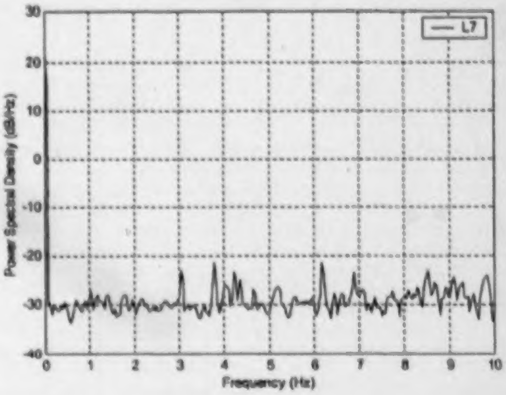

July 18, 1999
2:01 PM

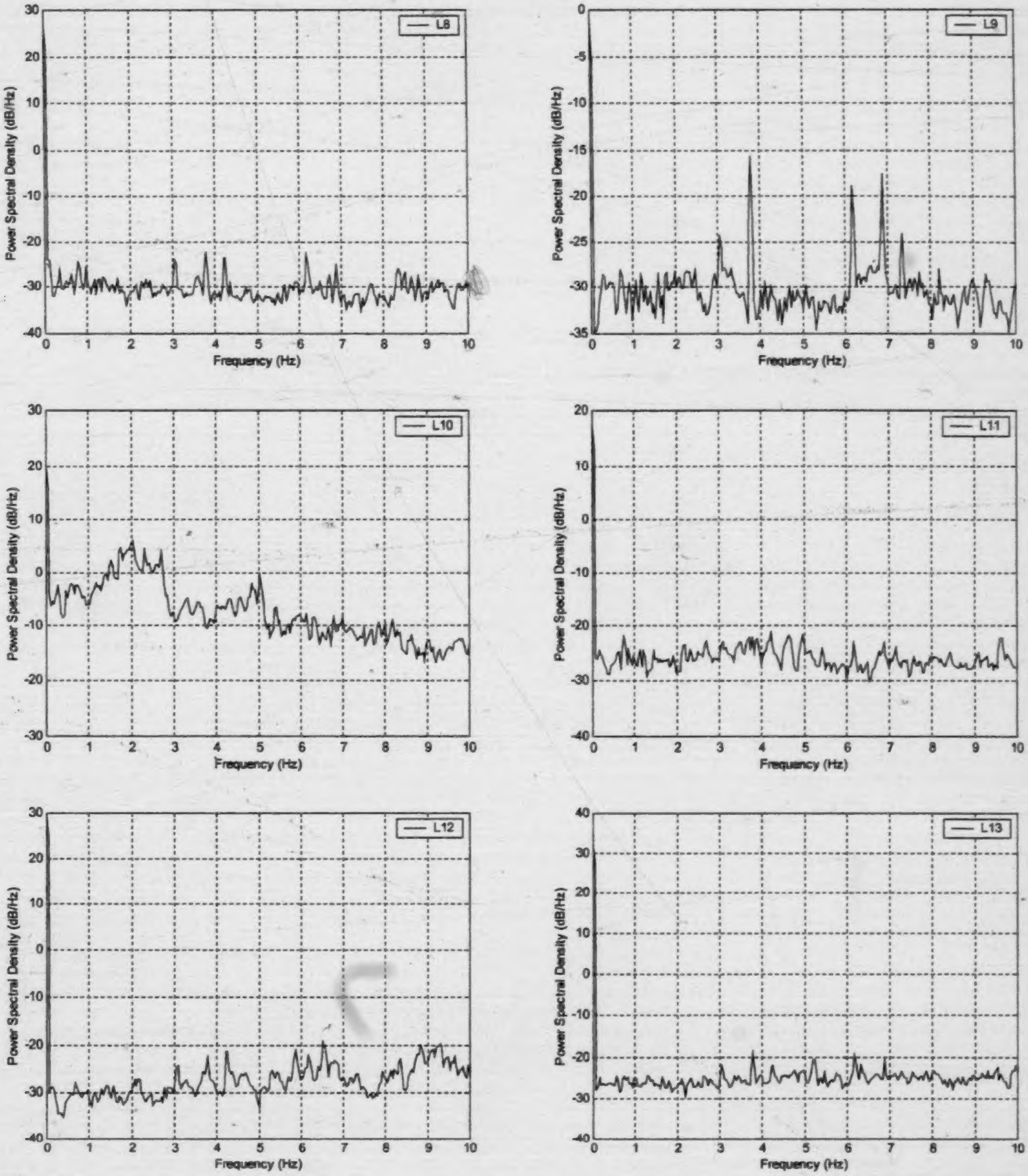

July 18, 1999
2:01 PM

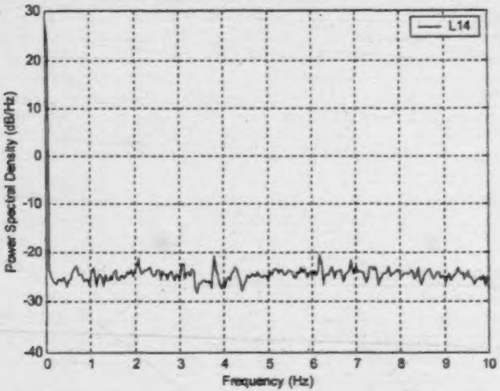

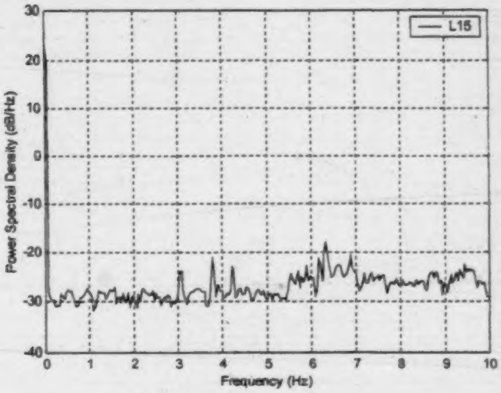

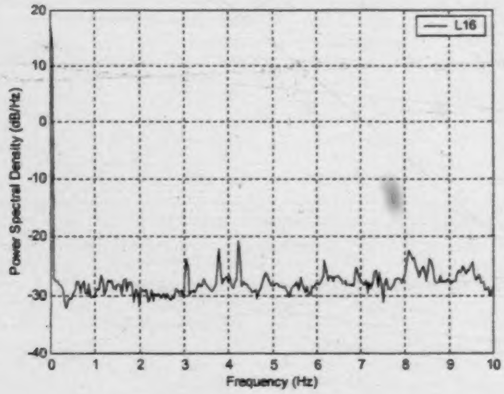

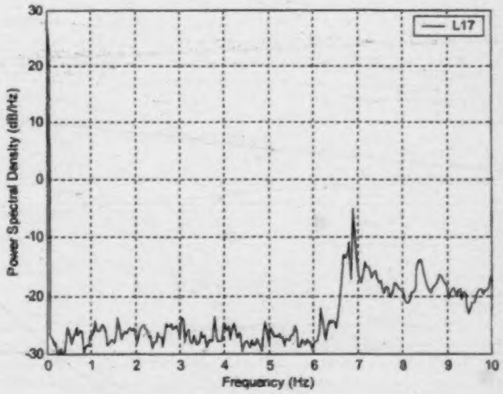

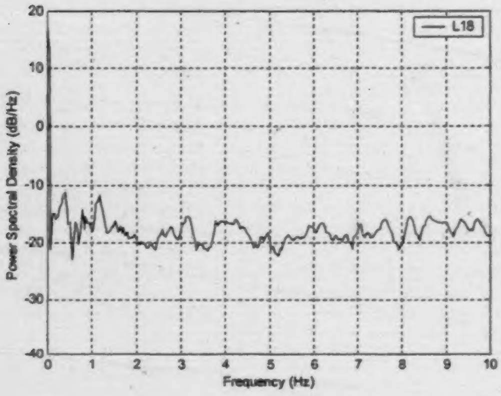

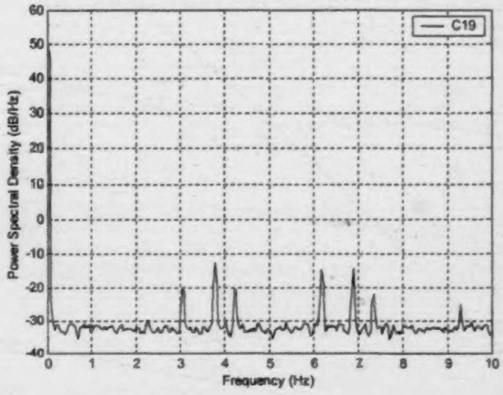

July 18, 1999
2:01 PM

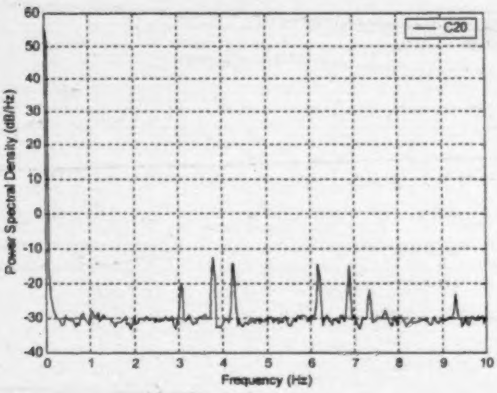

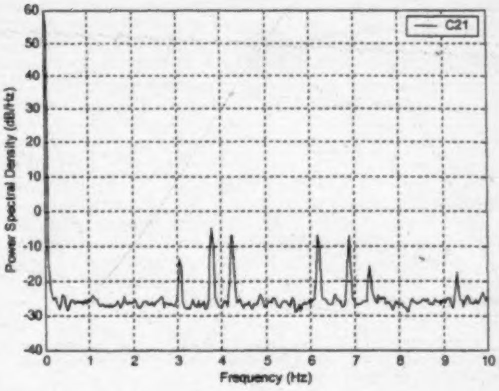

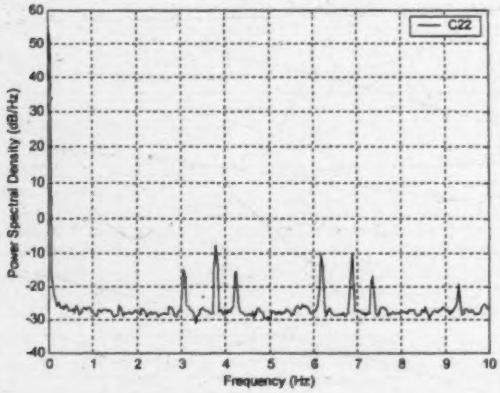

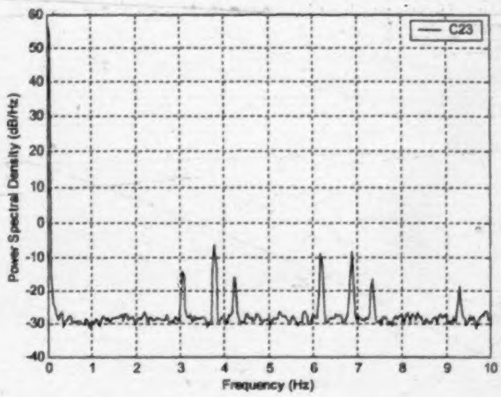

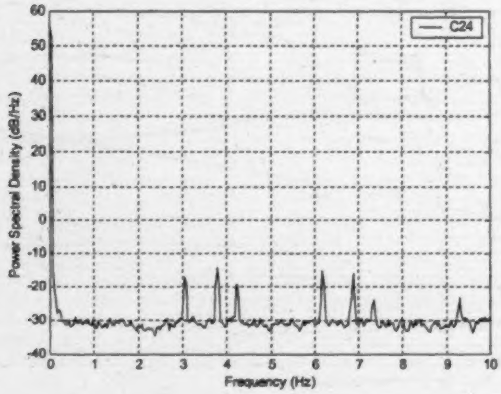

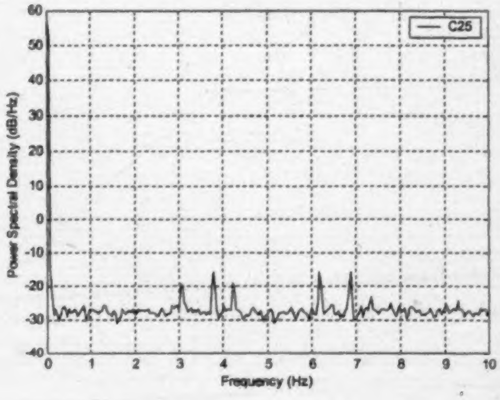

July 18, 1999
2:01 PM

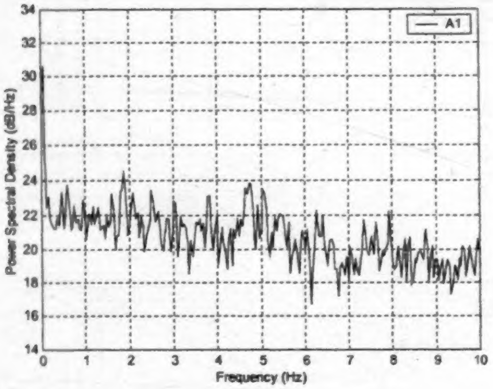

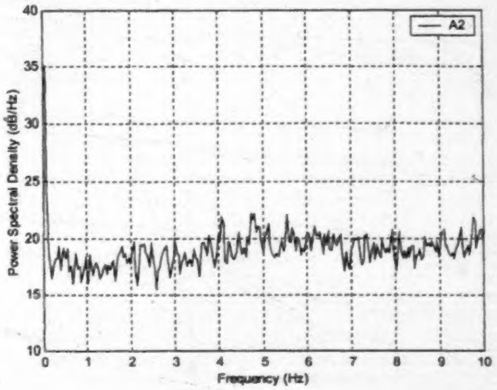

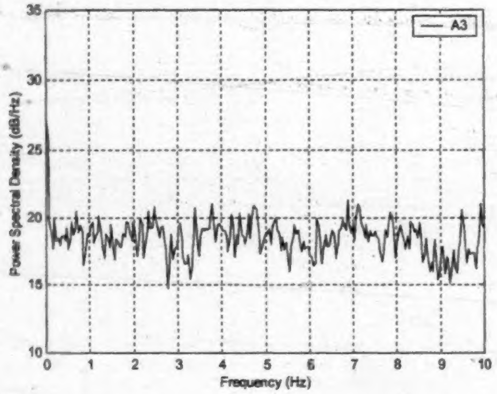

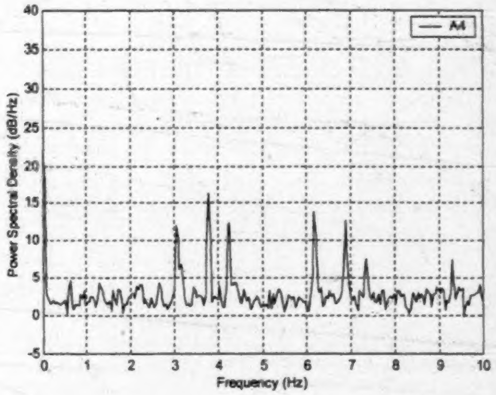

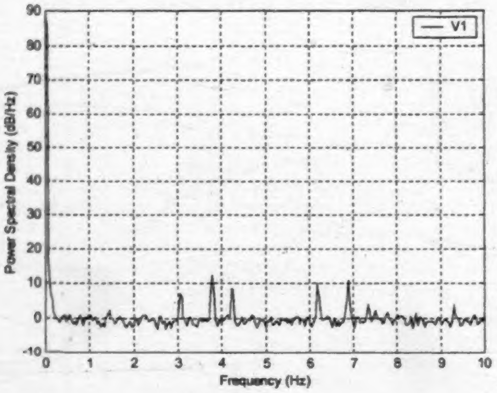

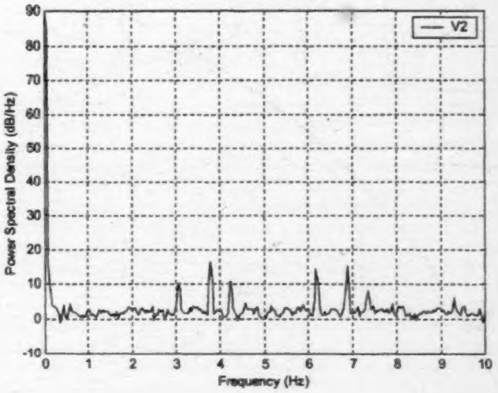

July 18, 1999
2:06 PM

July 18, 1999
2:06 PM

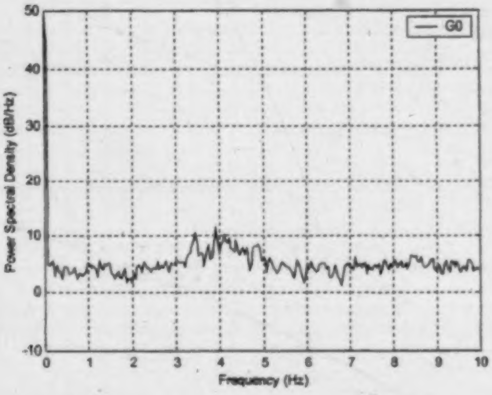

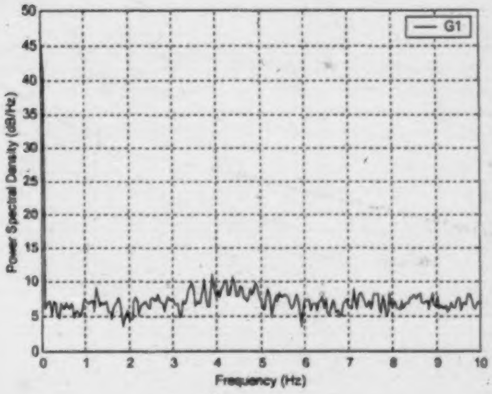

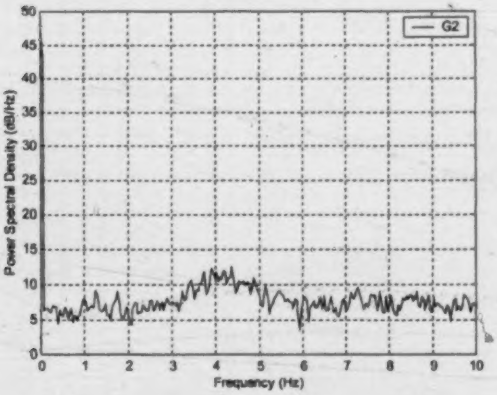

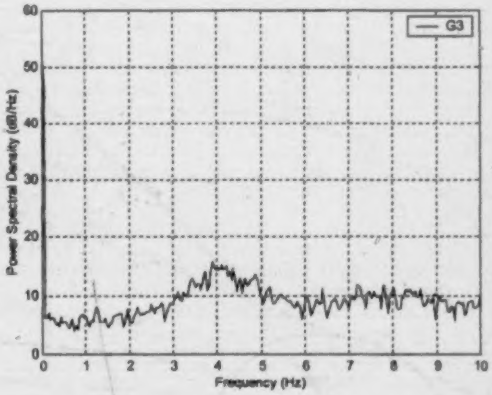

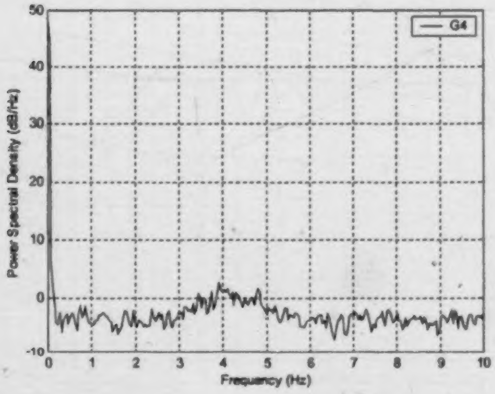

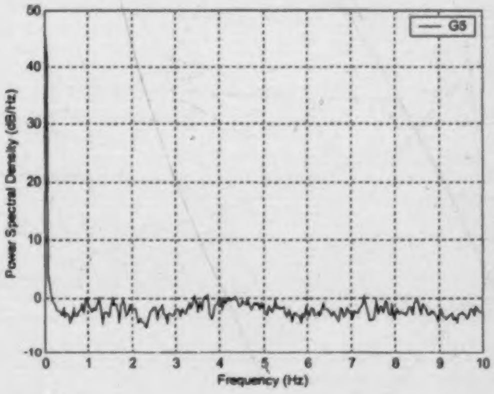

July 18, 1999
2:06 PM

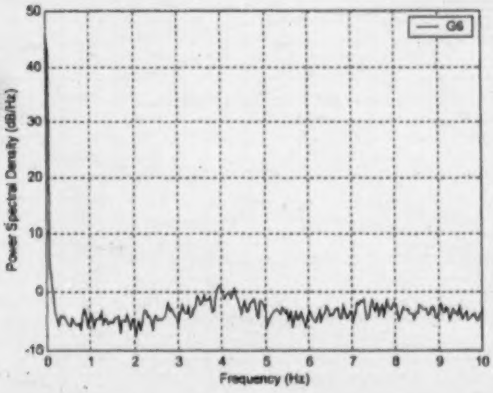

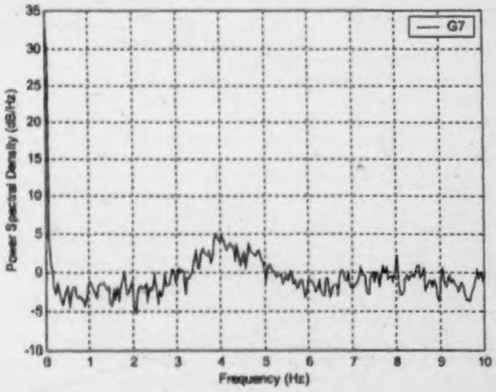

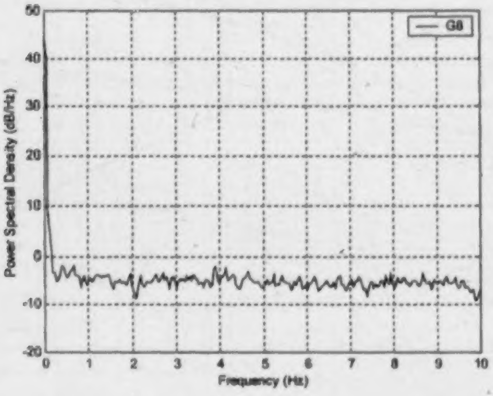

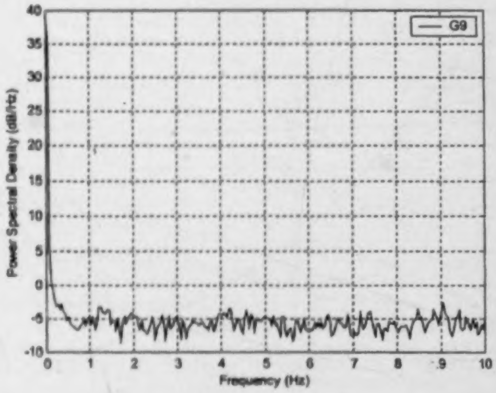

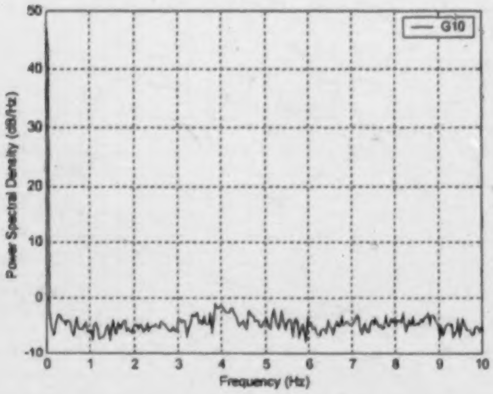

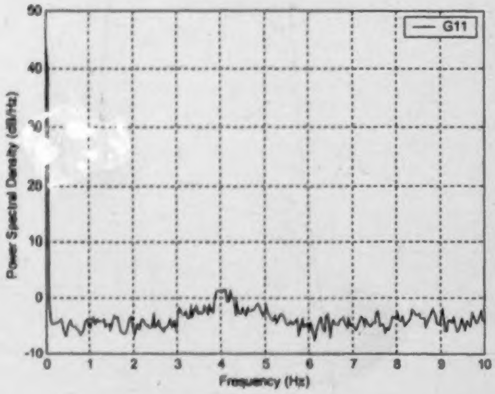

July 18, 1999
2:06 PM

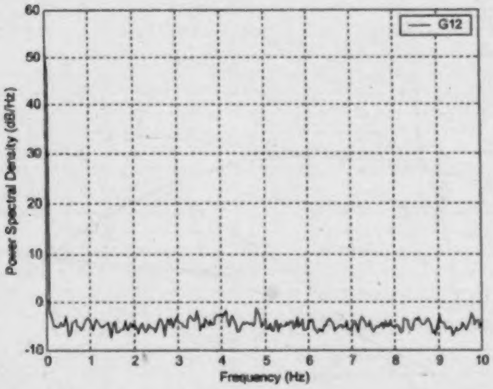

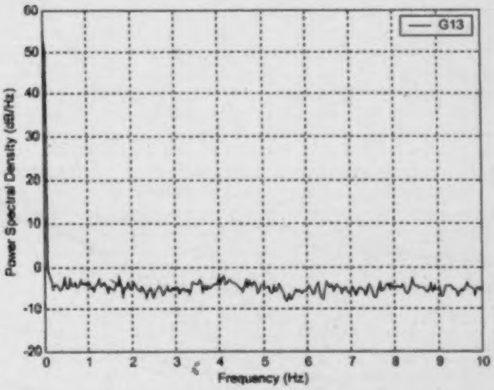

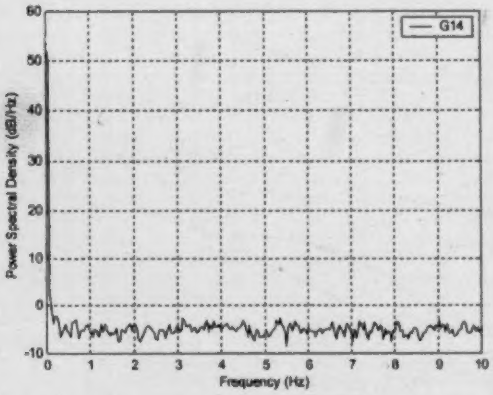

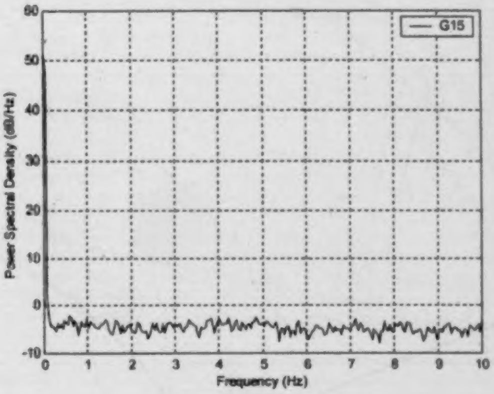

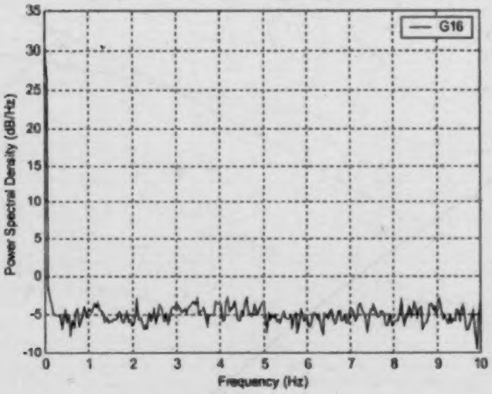

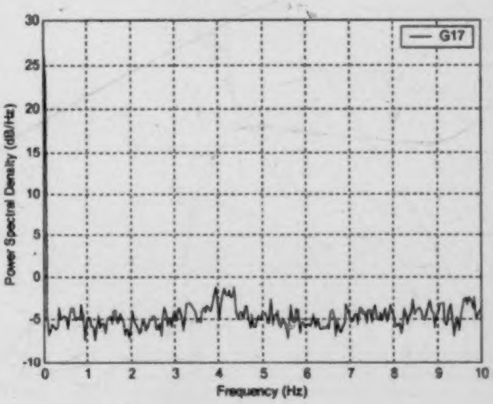

July 18, 1999
2:06 PM

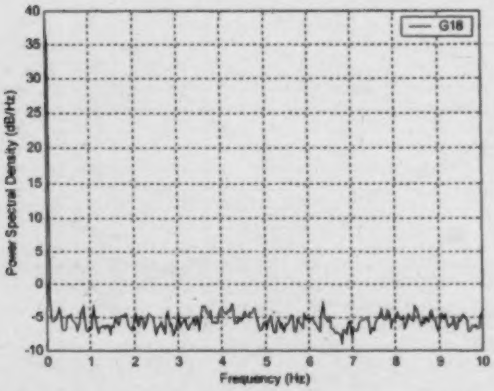

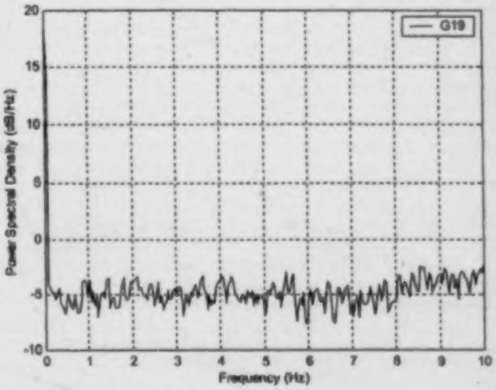

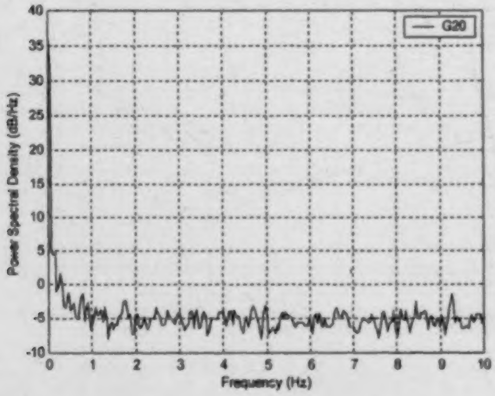

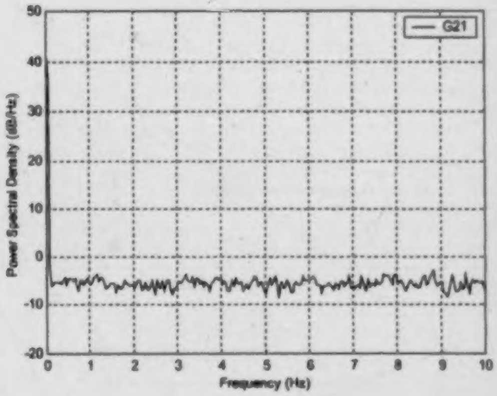

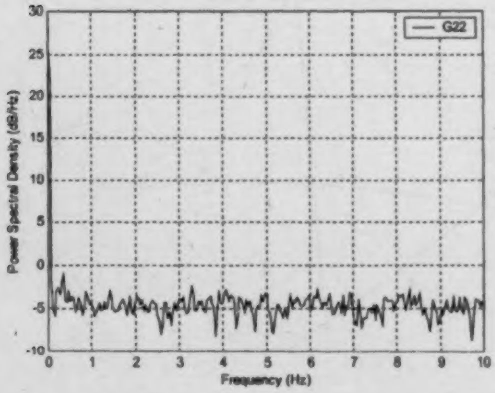

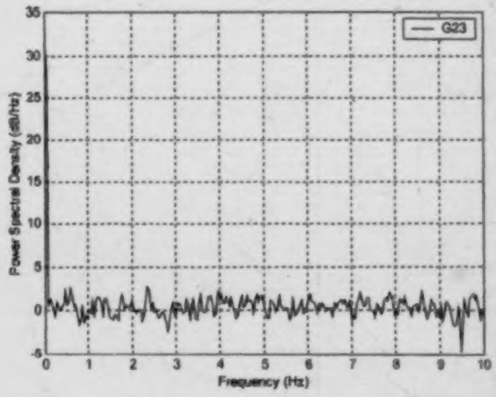

July 18, 1999
2:06 PM

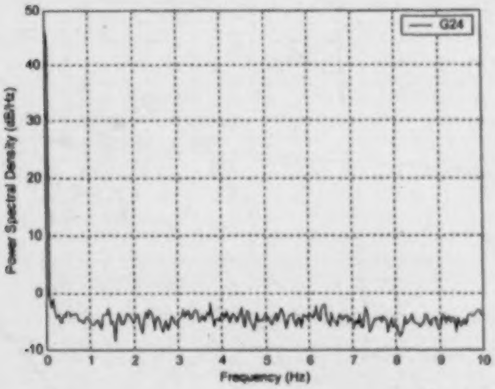

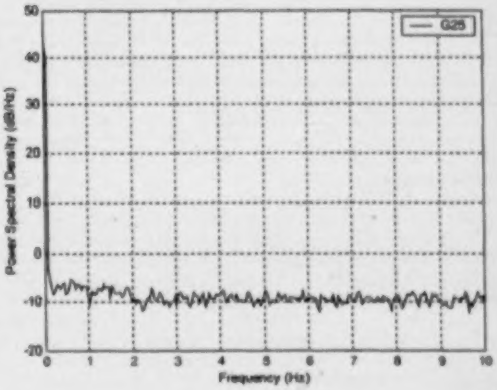

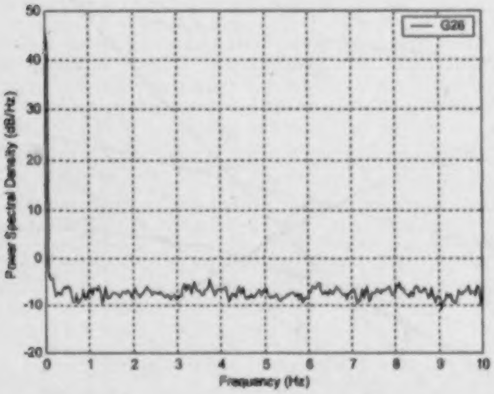

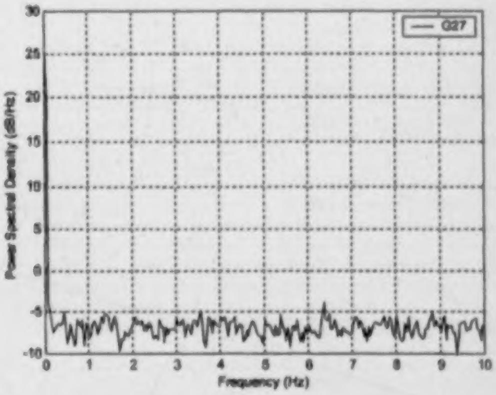

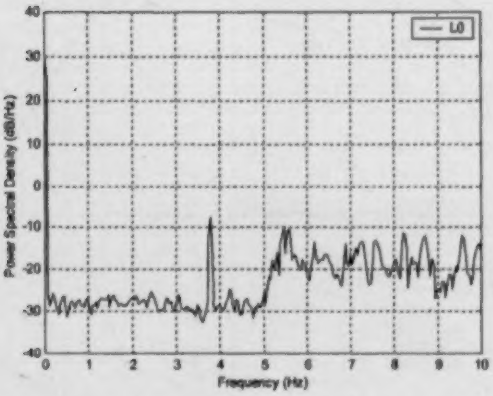

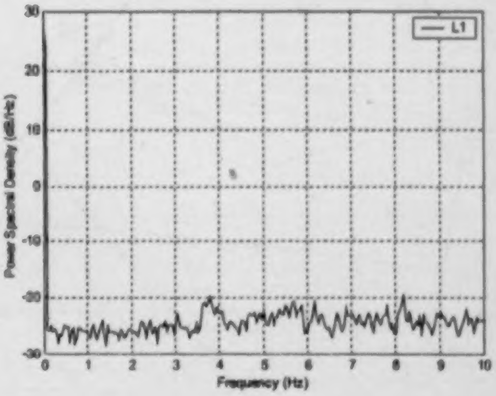

July 18, 1999
2:06 PM

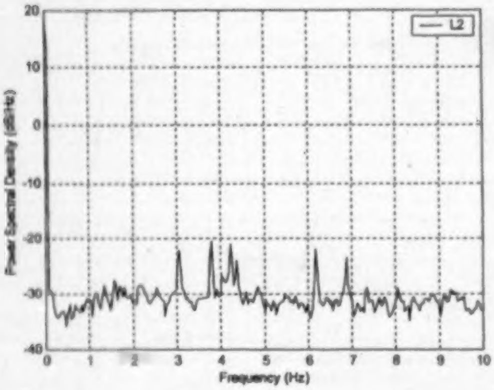

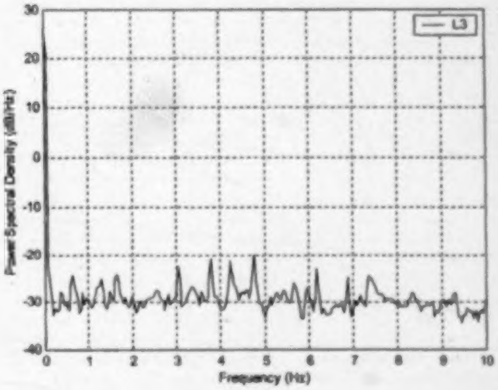

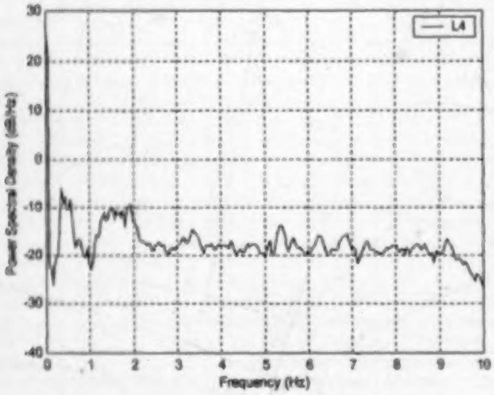

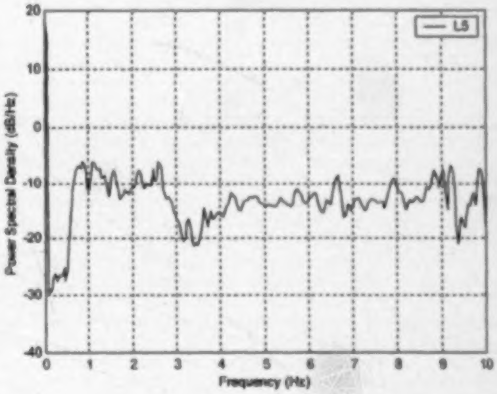

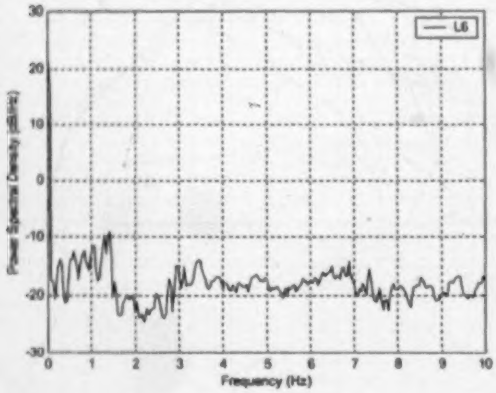

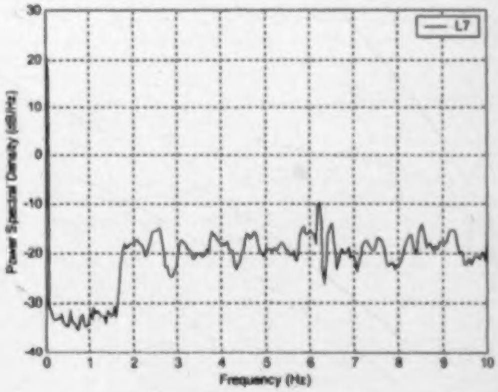

July 18, 1999
2:06 PM

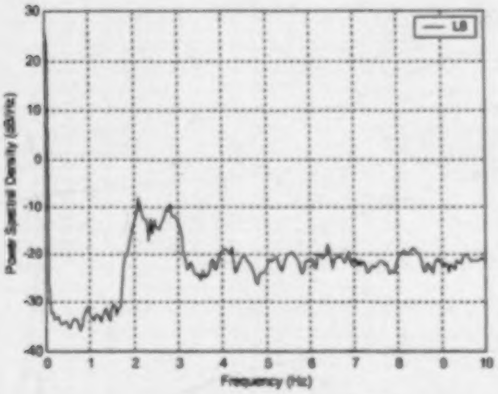

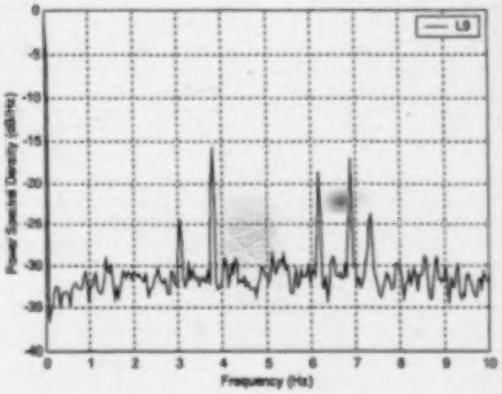

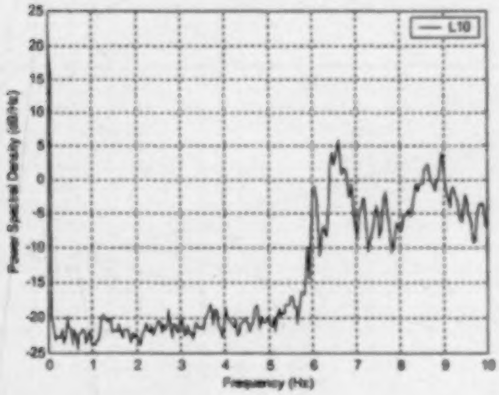

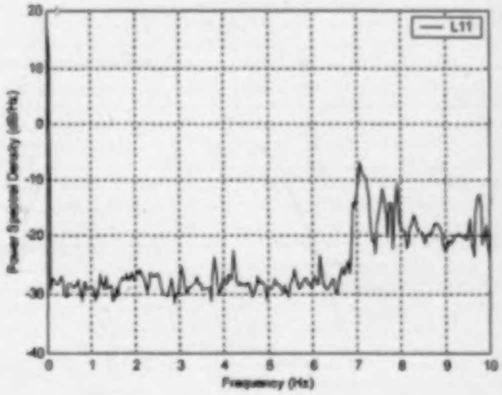

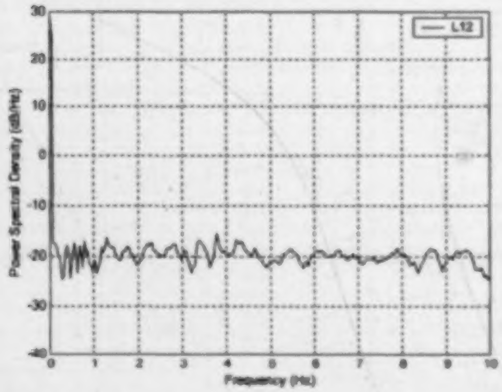

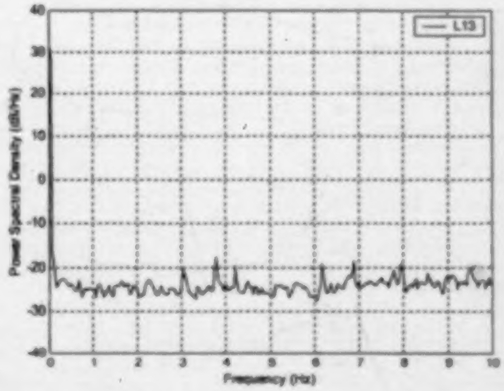

July 18, 1999
2:06 PM

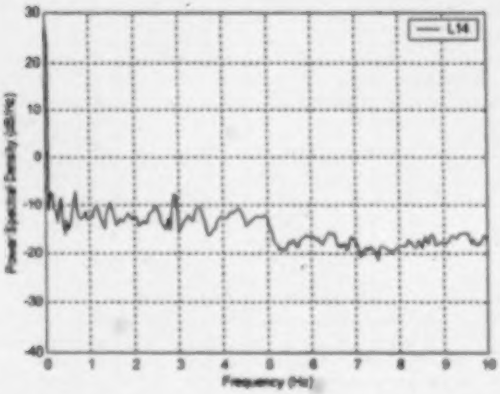

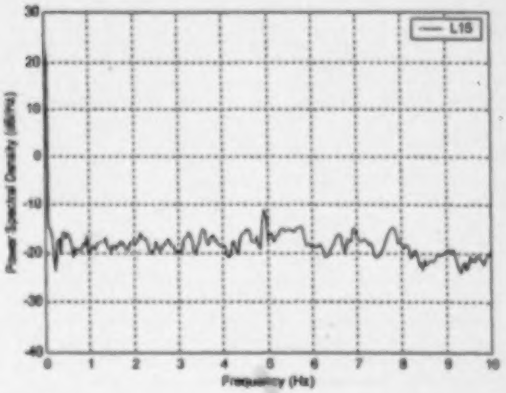

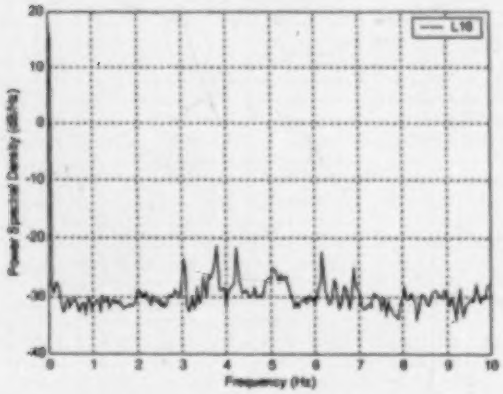

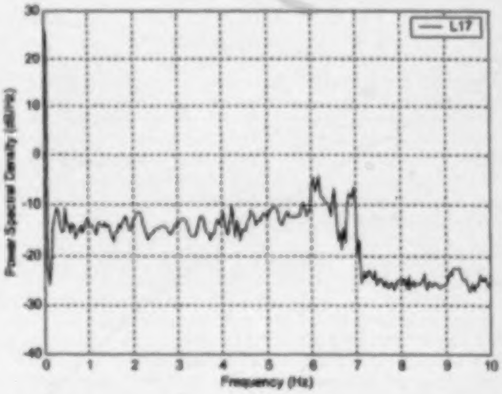

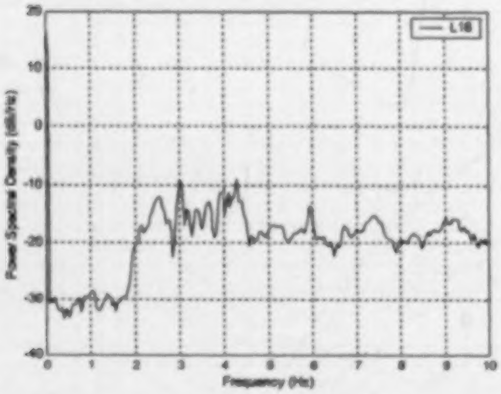

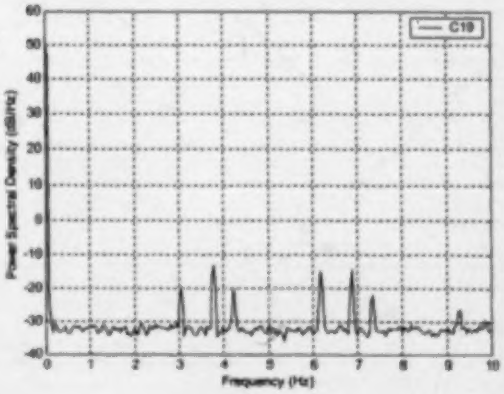

July 18, 1999
2:06 PM

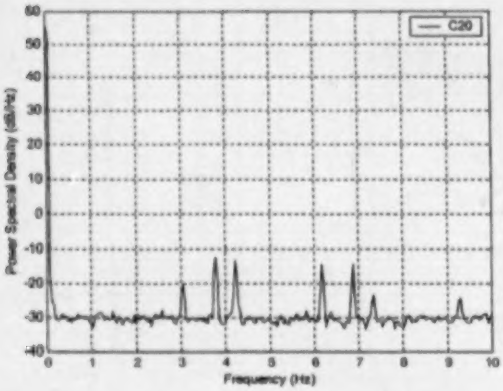

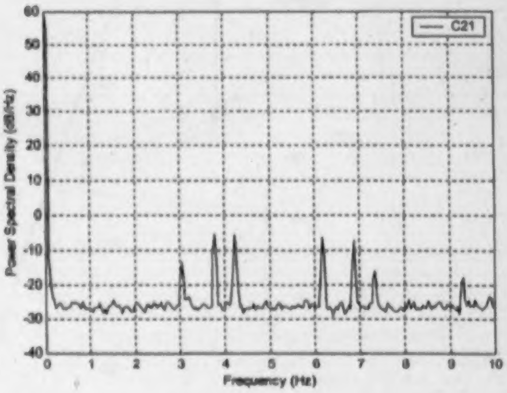

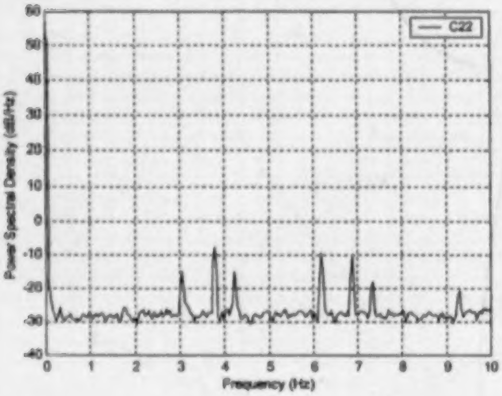

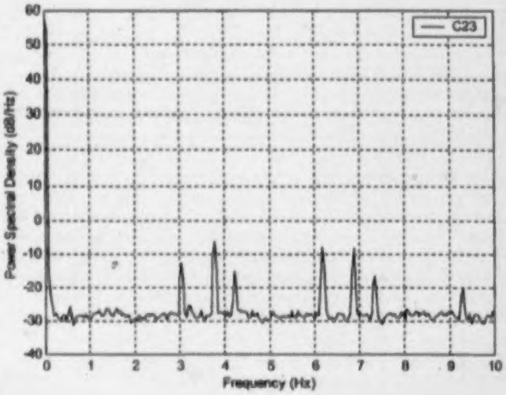

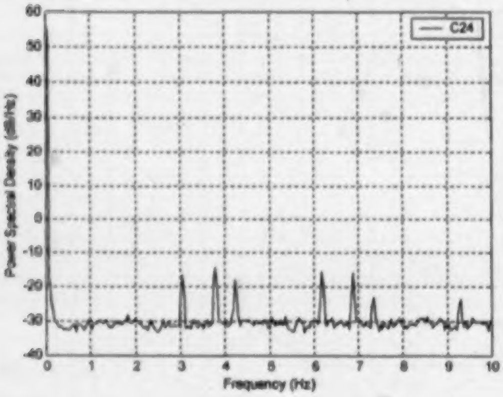

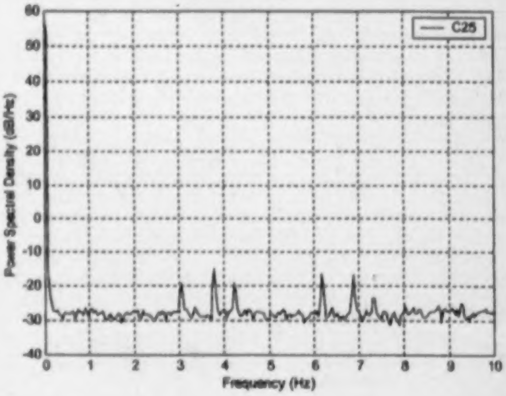

July 18, 1999
2:06 PM

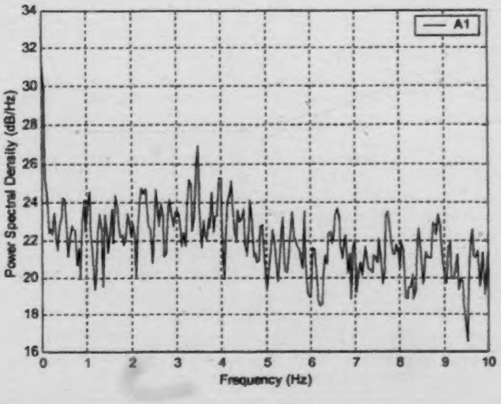

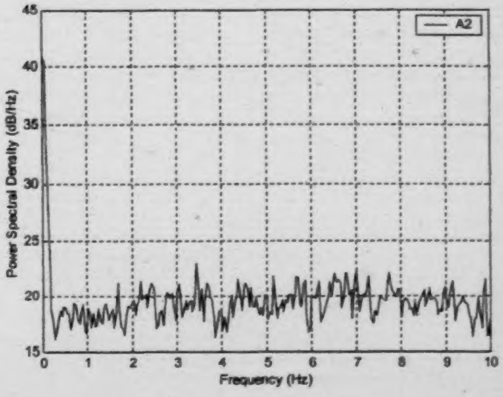

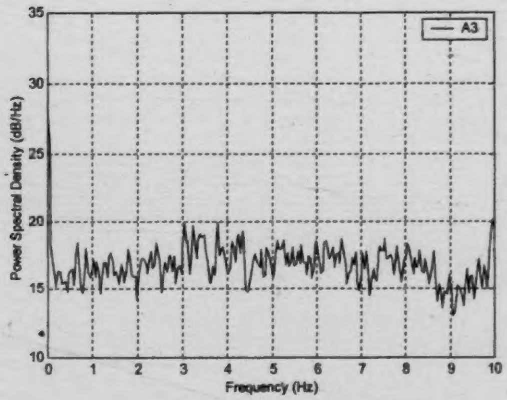

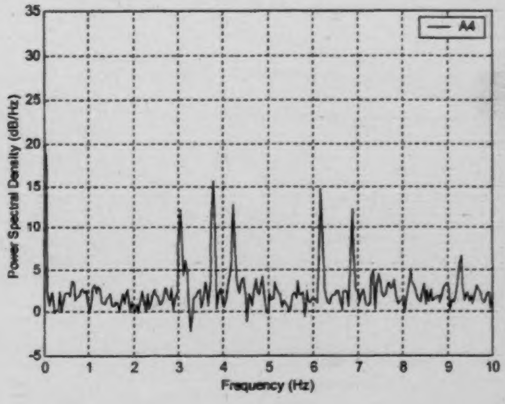

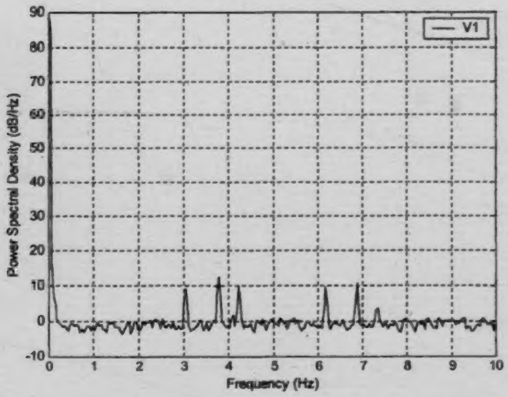

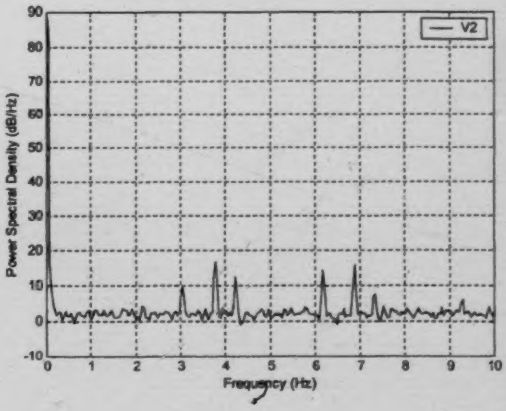

July 18, 1999
2:12 PM

July 18, 1999
2:12 PM

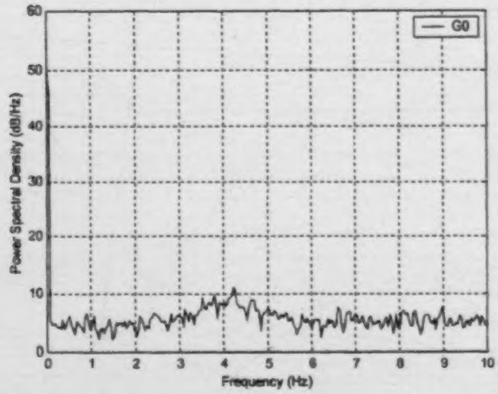

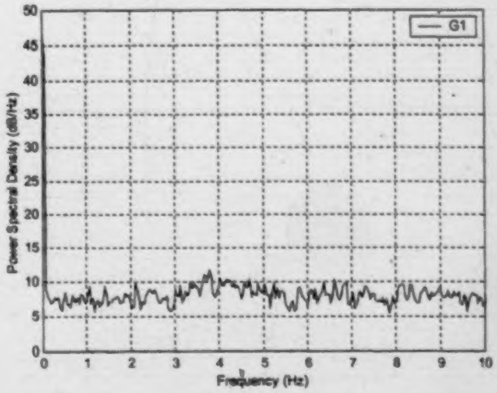

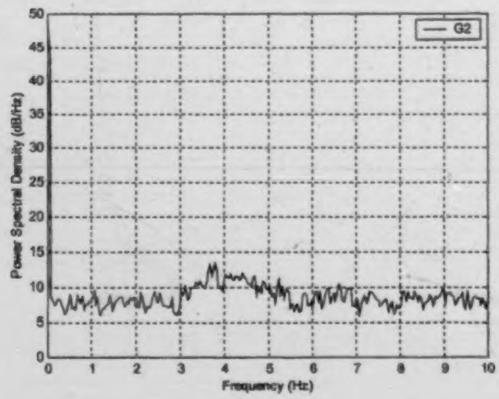

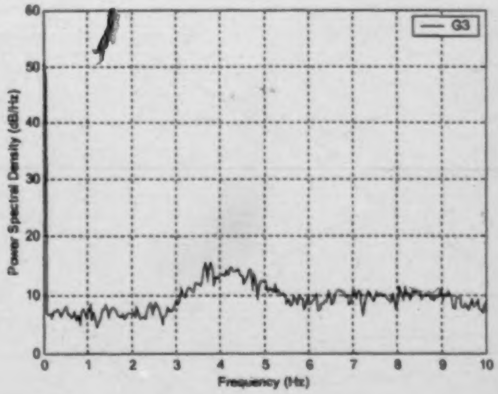

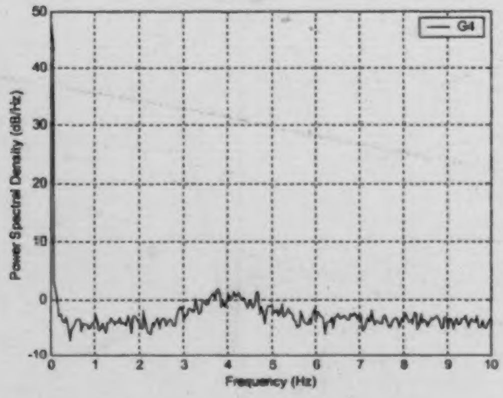

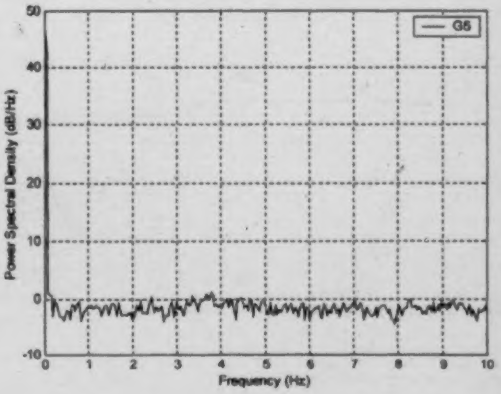

July 18, 1999
2:12 PM

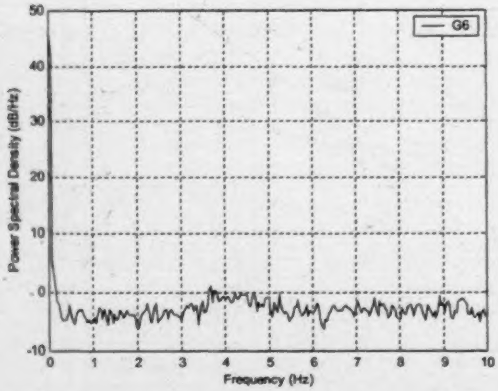

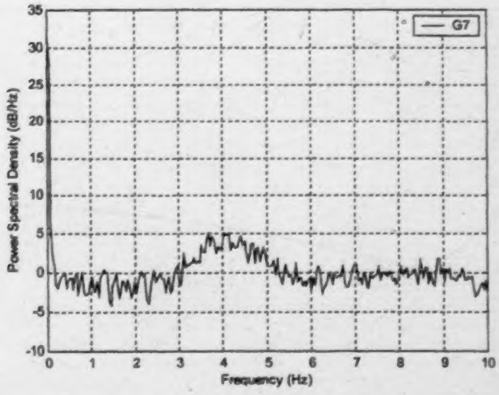

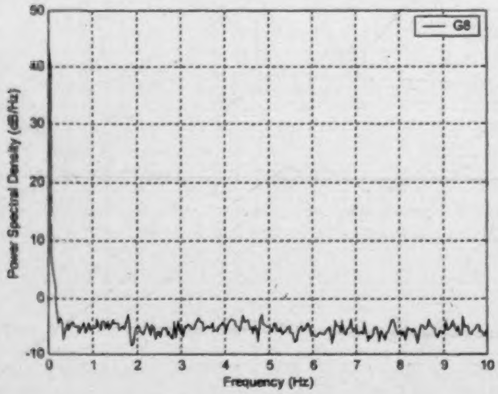

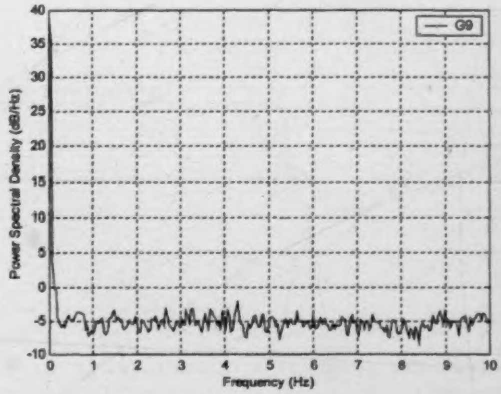

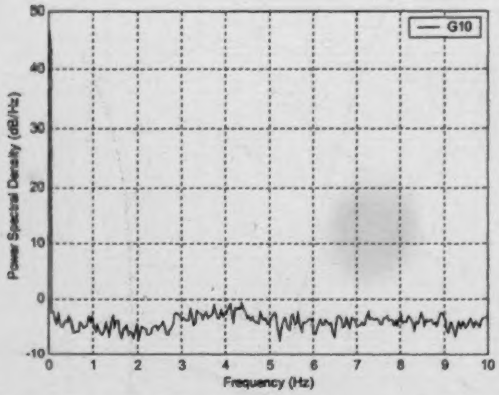

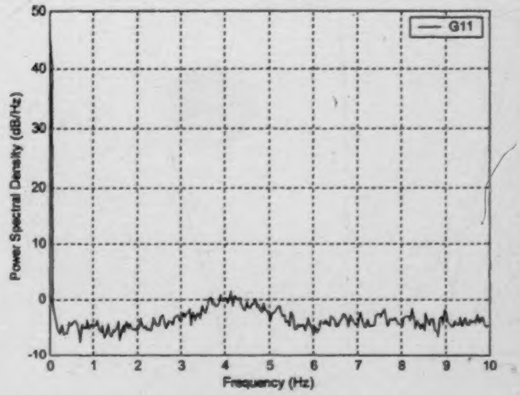

July 18, 1999
2:12 PM

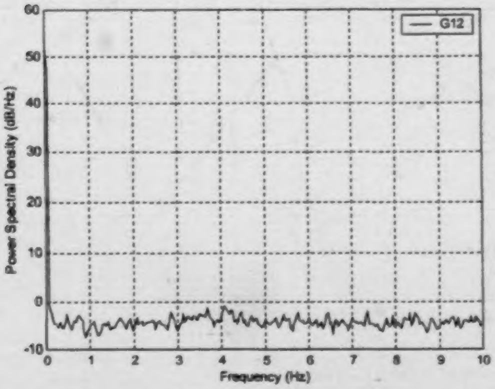

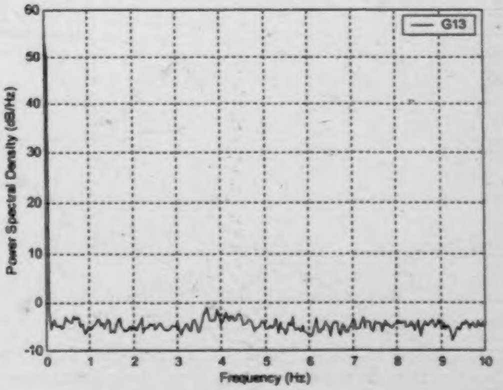

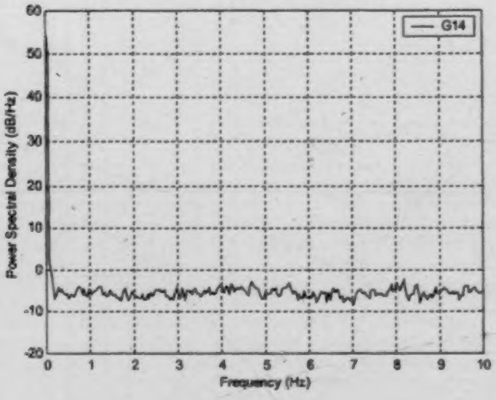

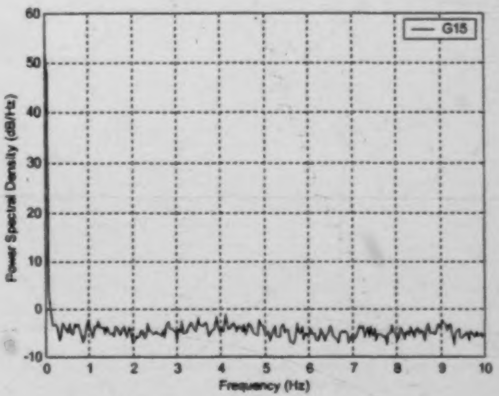

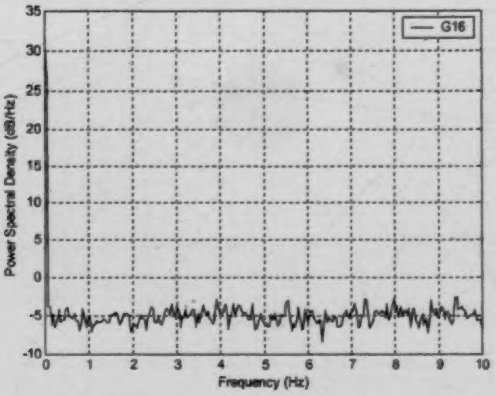

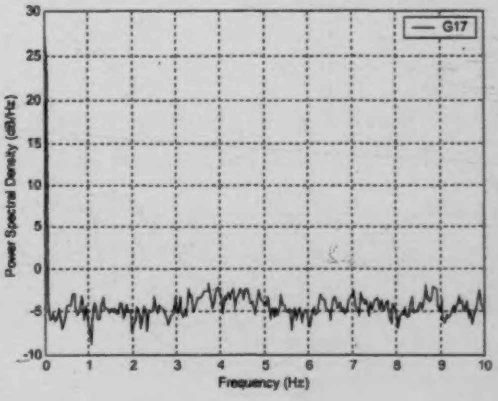

July 18, 1999
2:12 PM

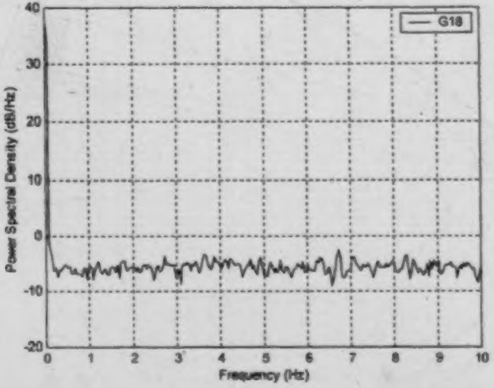

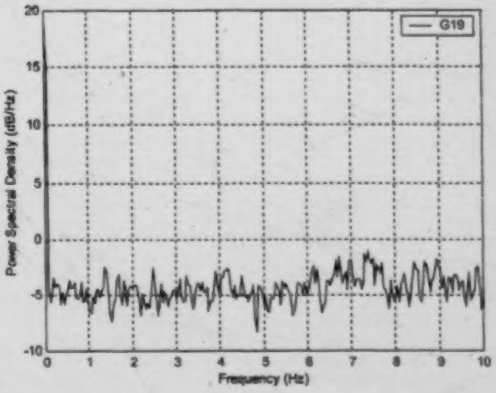

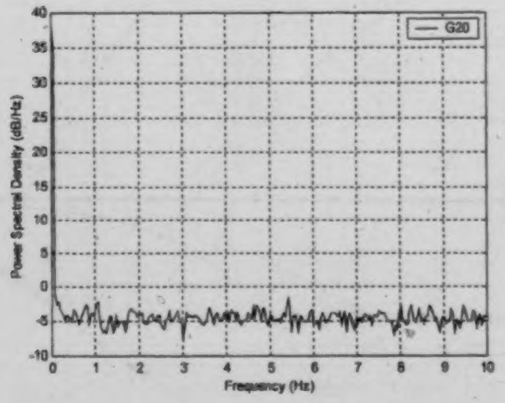

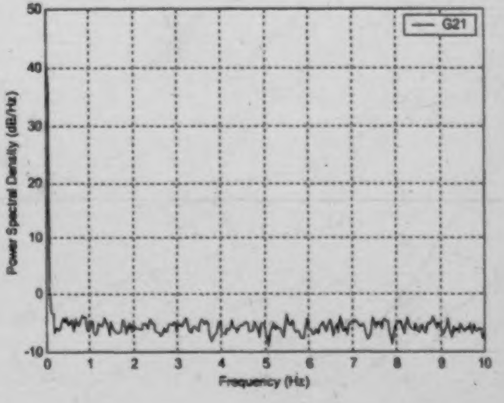

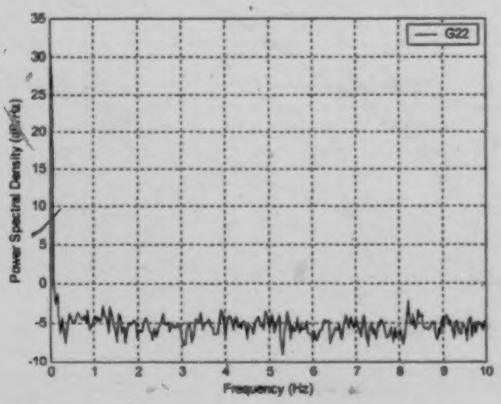

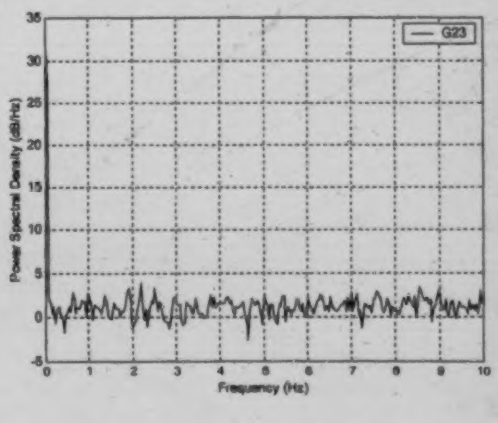

July 18, 1999
2:12 PM

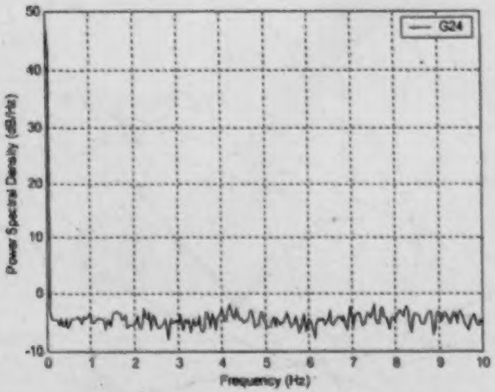

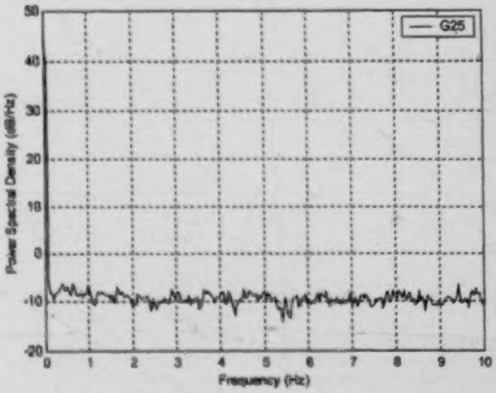

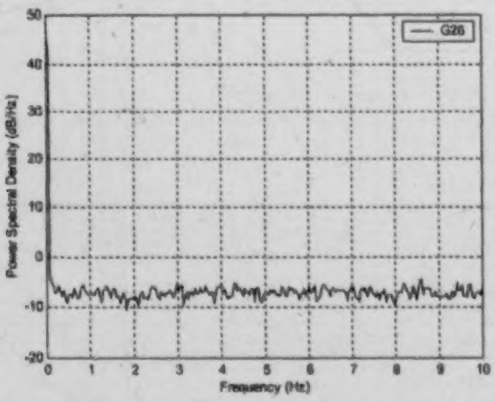

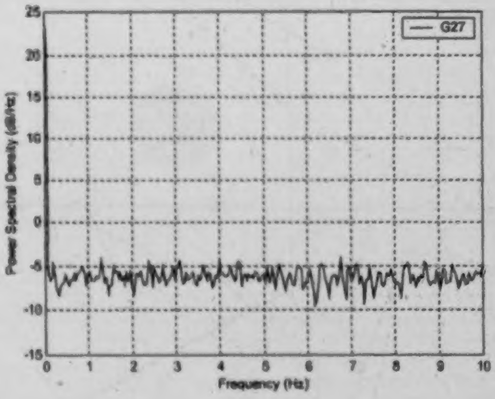

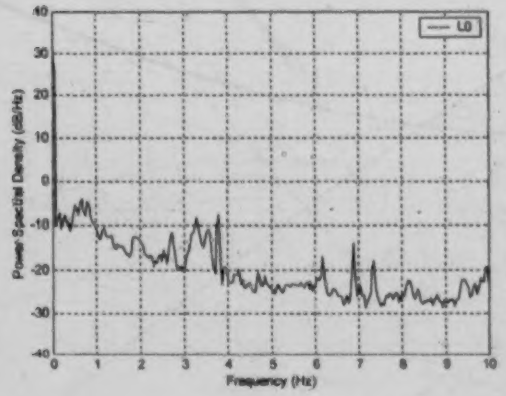

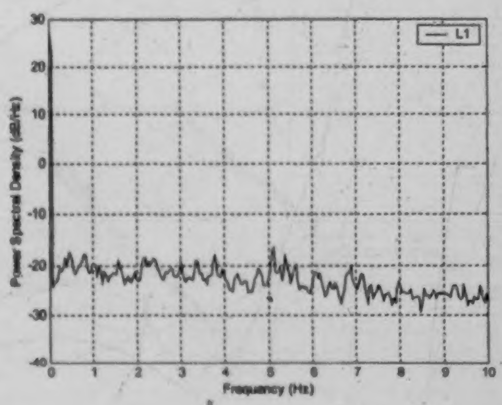

July 18, 1999
2:12 PM

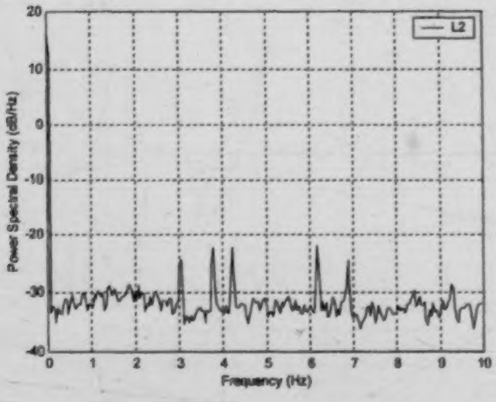

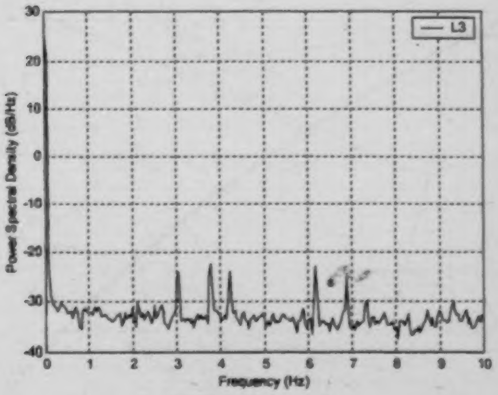

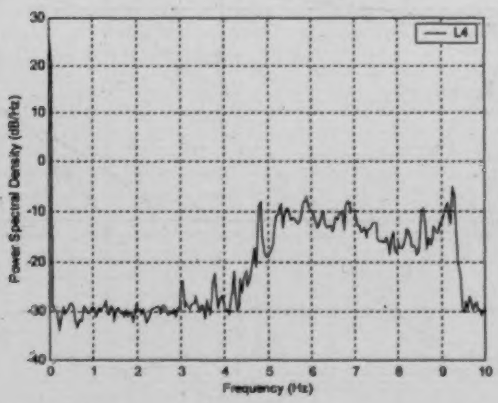

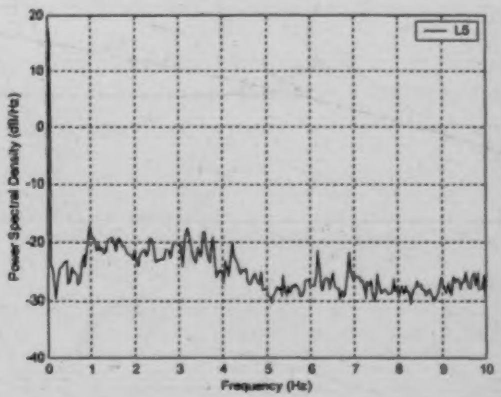

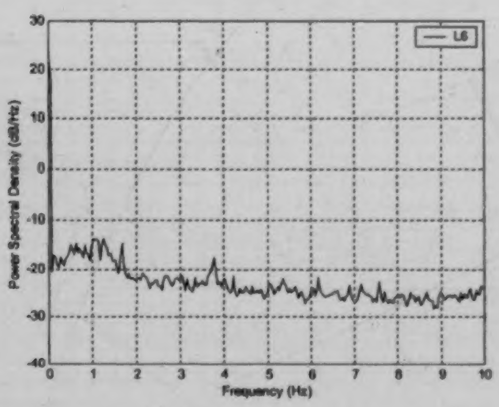

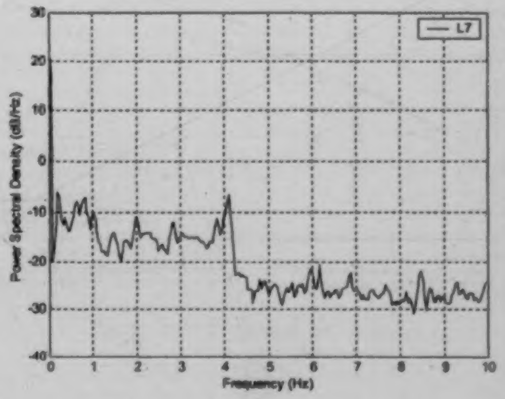

July 18, 1999
2:12 PM

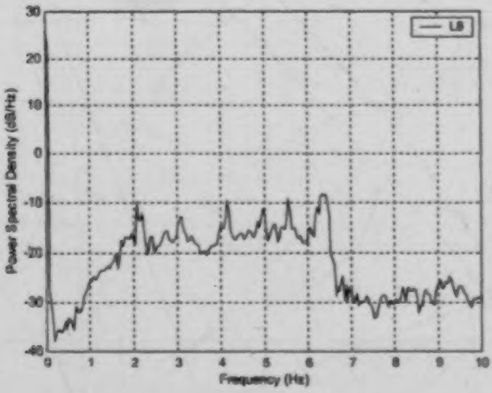

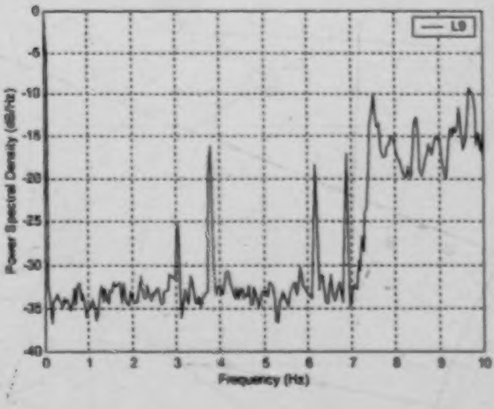

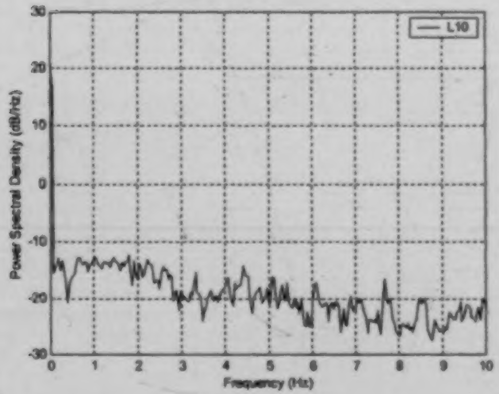

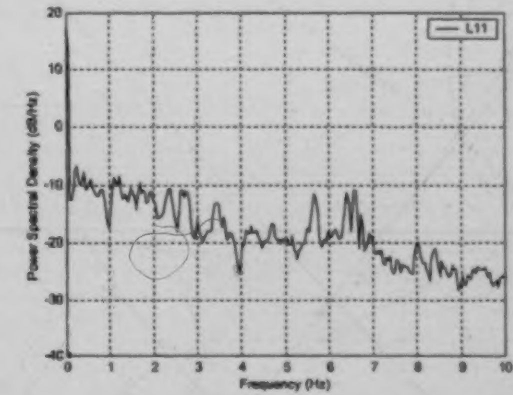

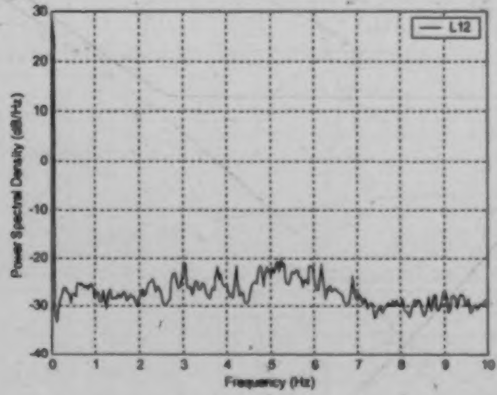

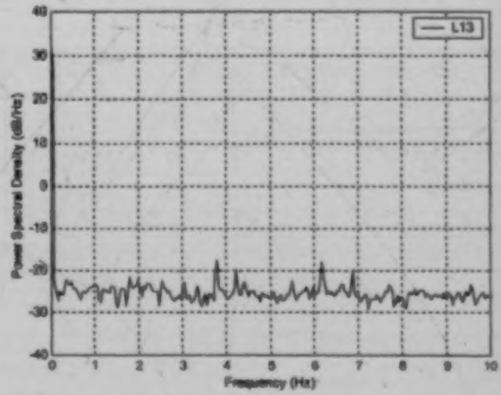

July 18, 1999
2:12 PM

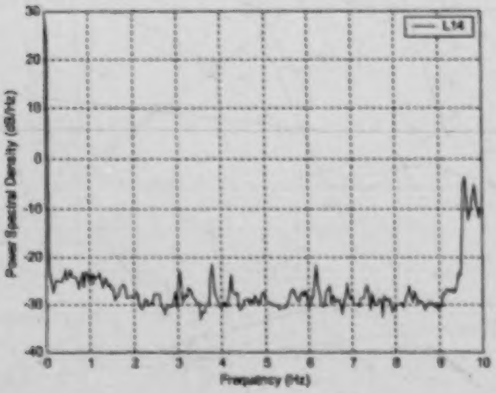

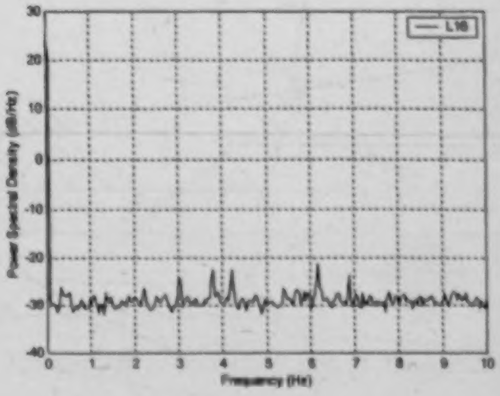

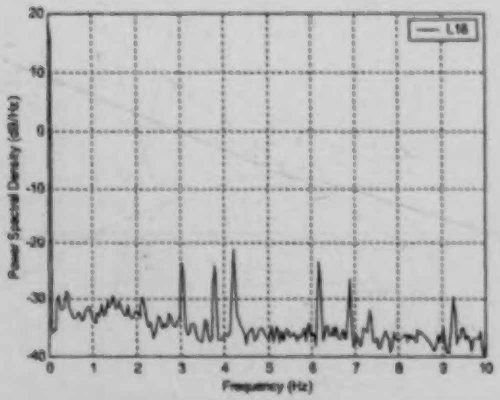

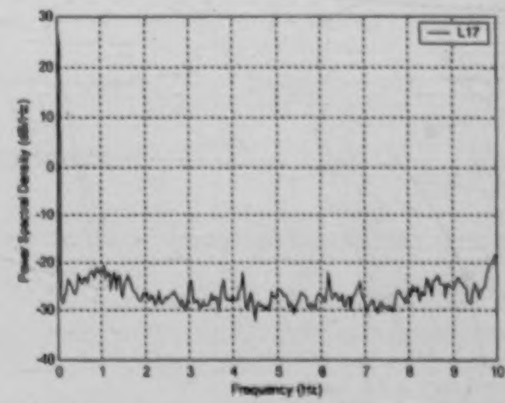

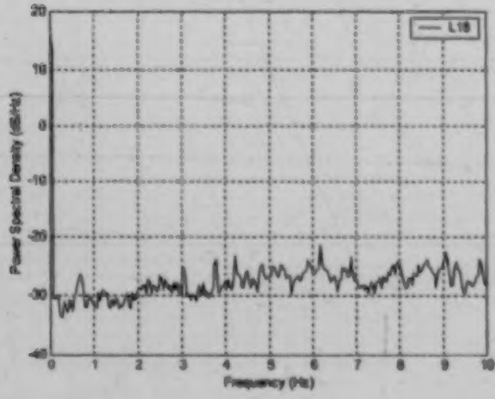

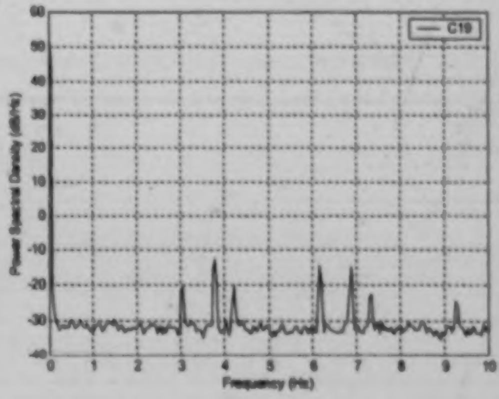

July 18, 1999
2:12 PM

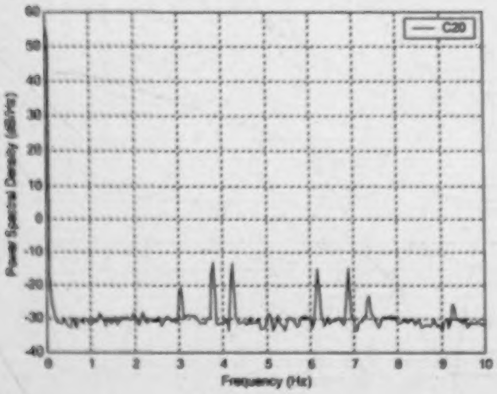

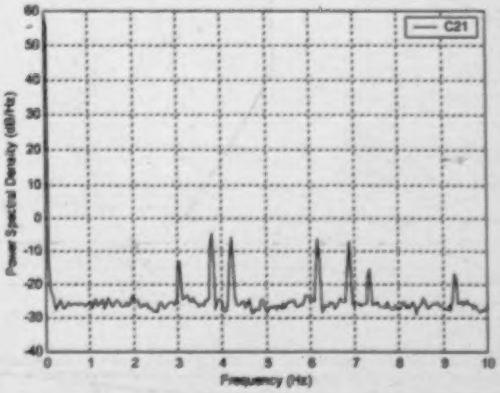

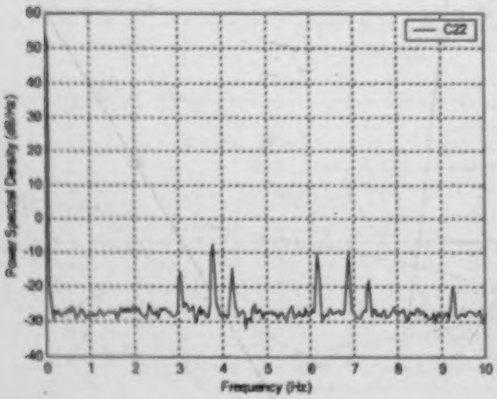

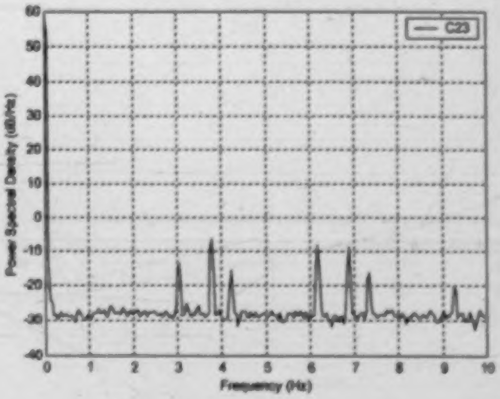

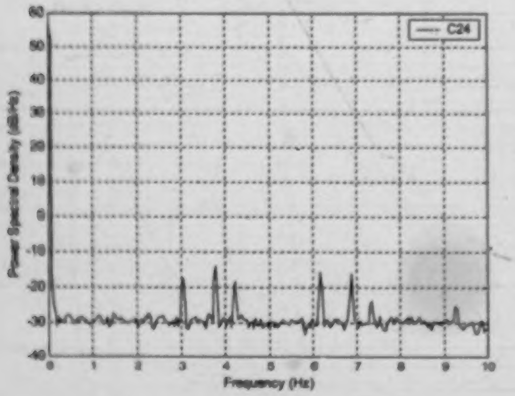

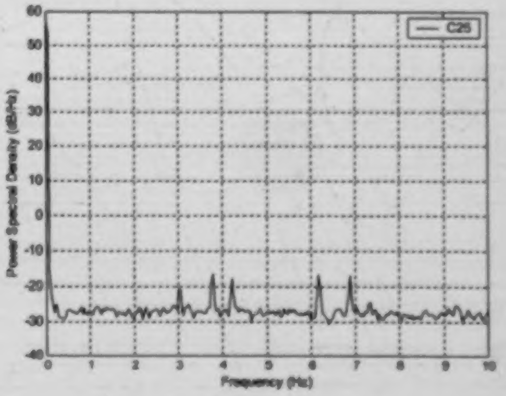

July 18, 1999
2:12 PM

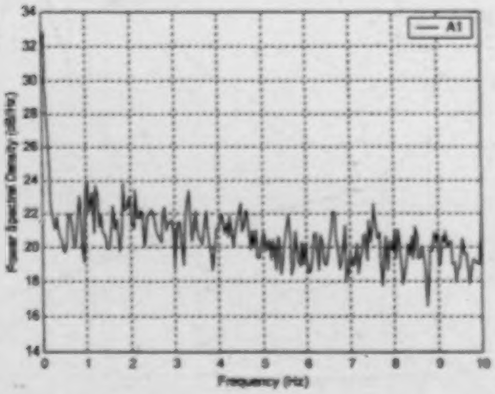

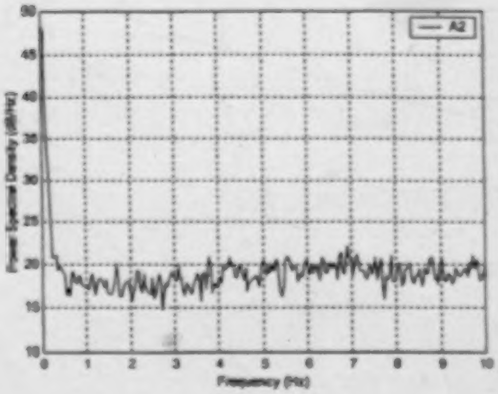

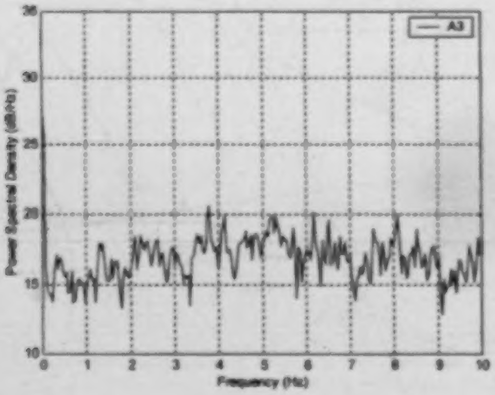

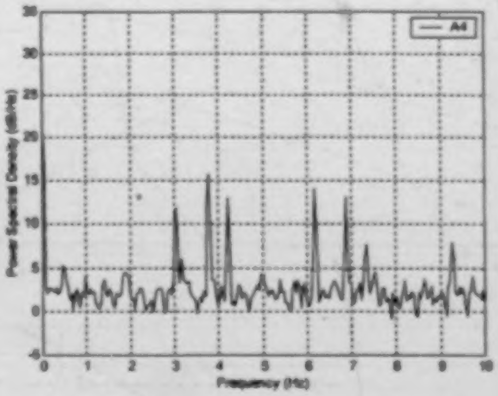

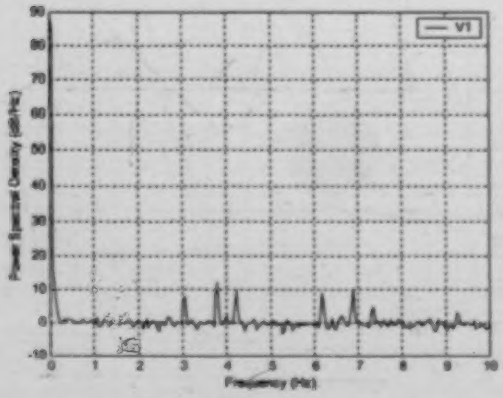

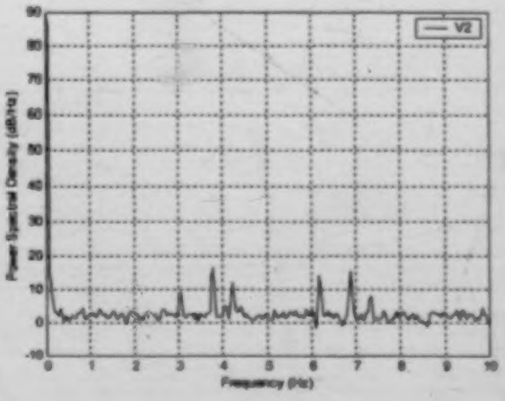

July 18, 1999
2:17 PM

July 18, 1999
2:17 PM

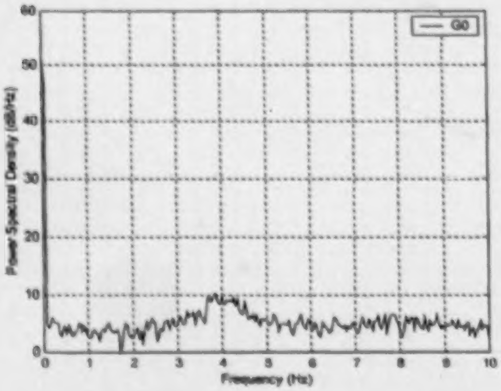

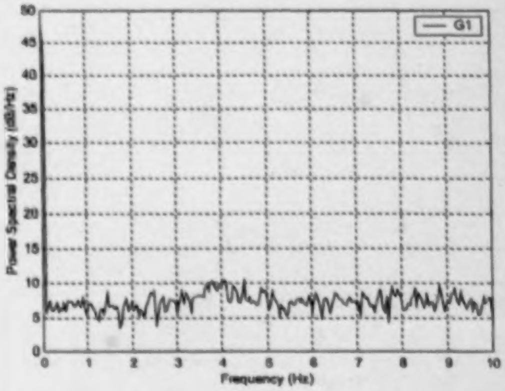

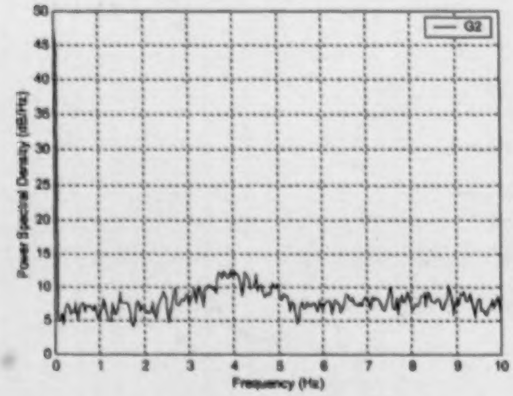

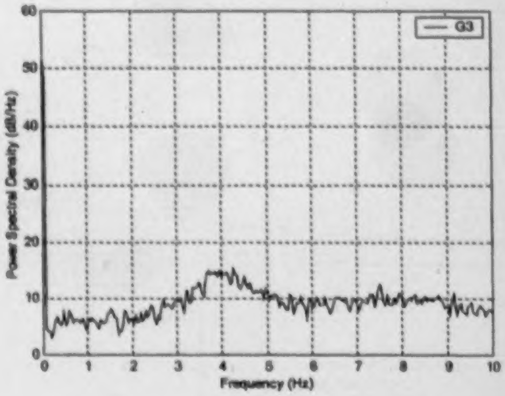

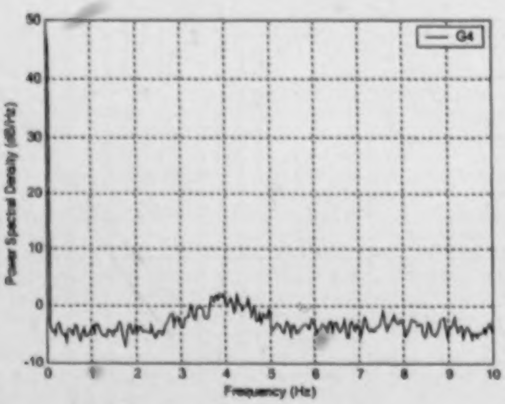

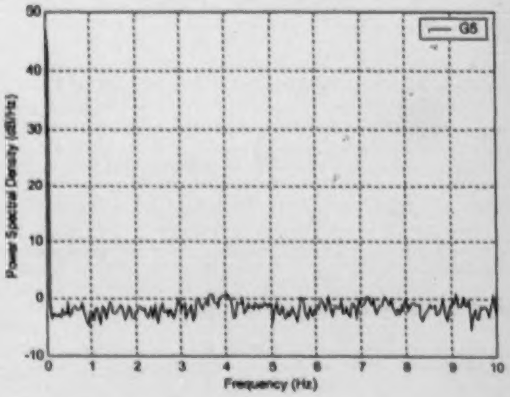

July 18, 1999
2:17 PM

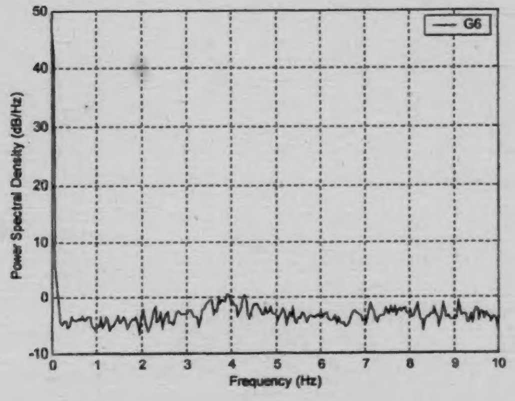

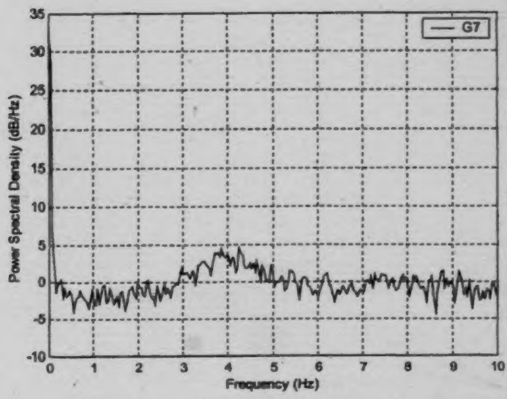

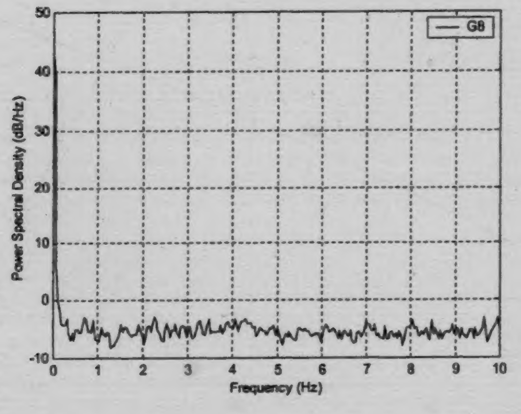

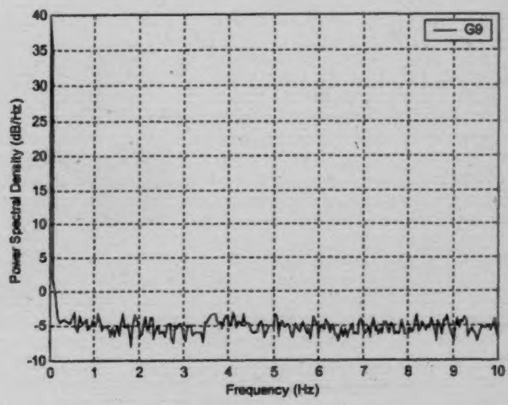

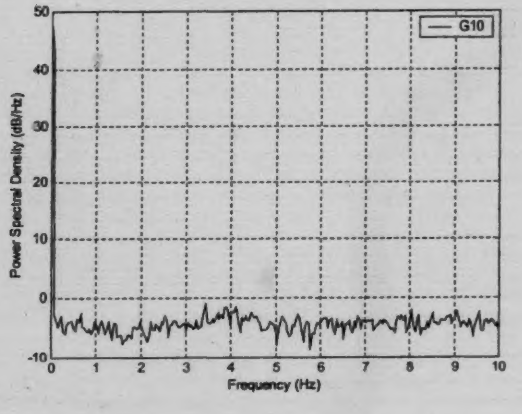

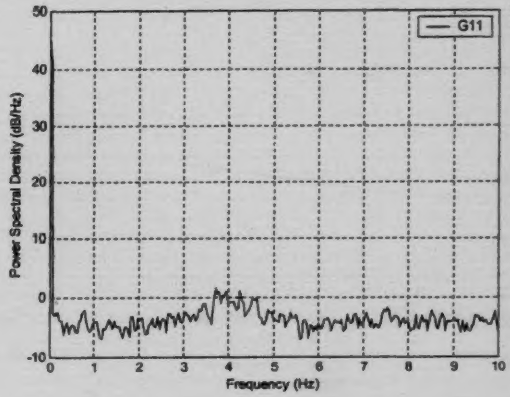

July 18, 1999
2:17 PM

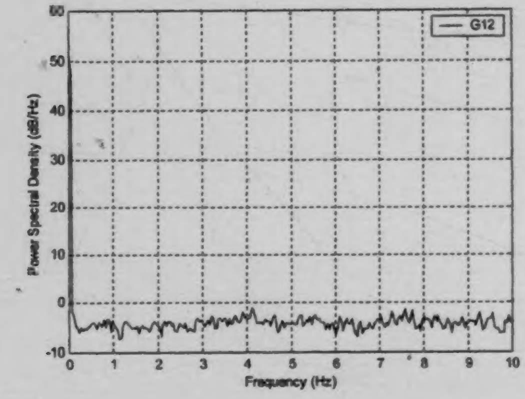

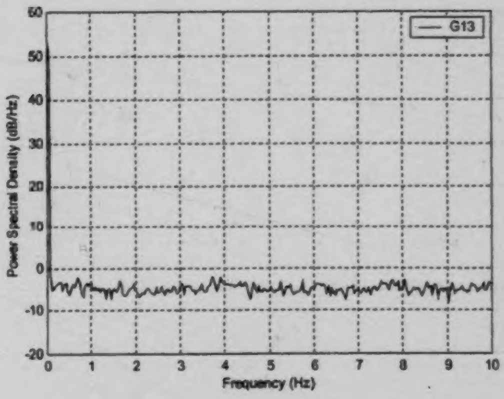

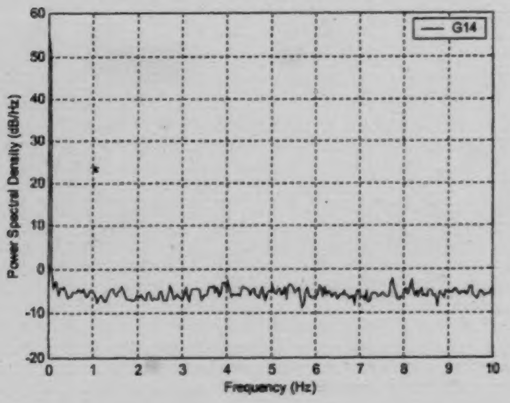

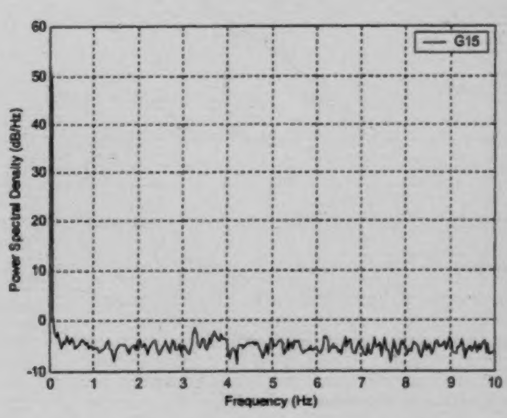

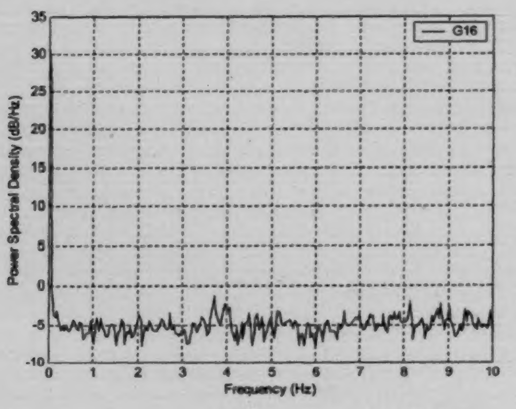

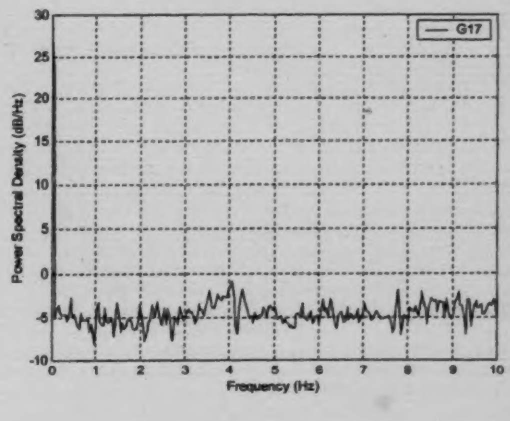

July 18, 1999
2:17 PM

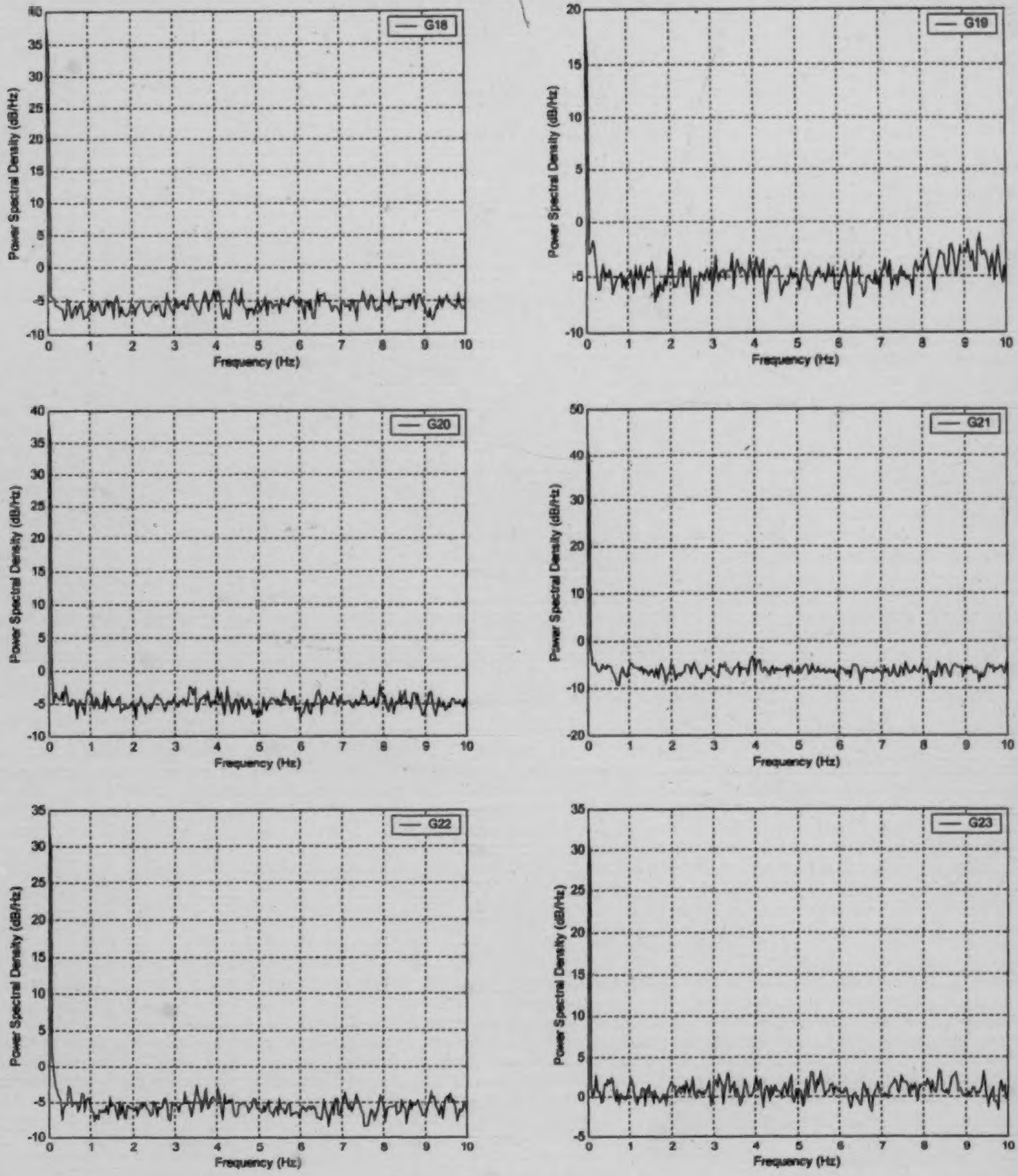

July 18, 1999
2:17 PM

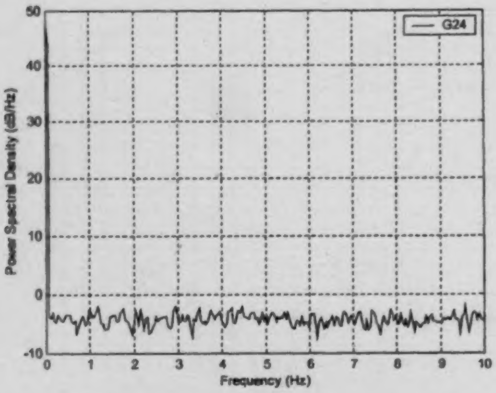

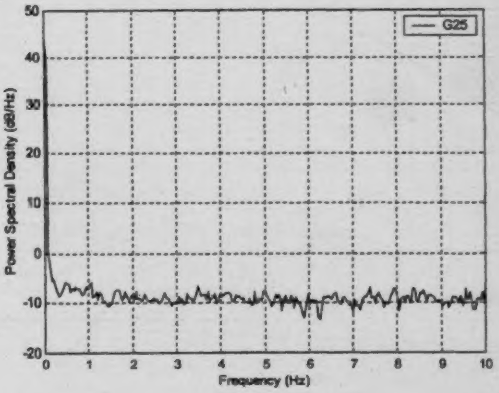

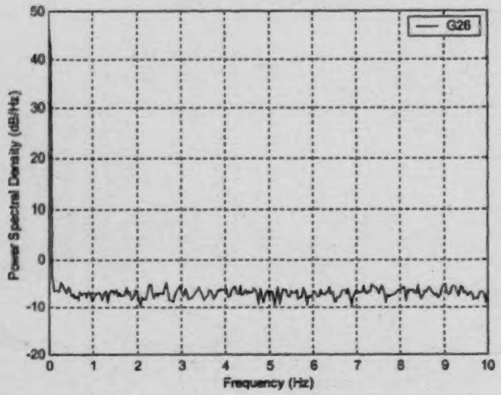

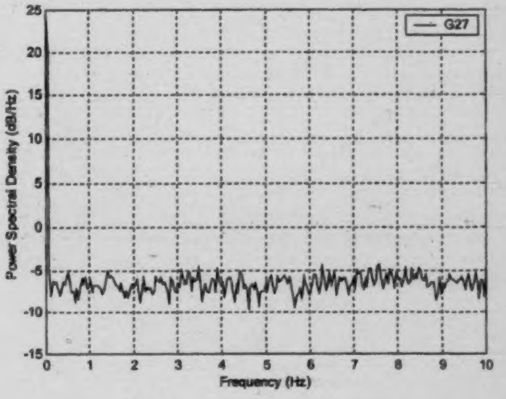

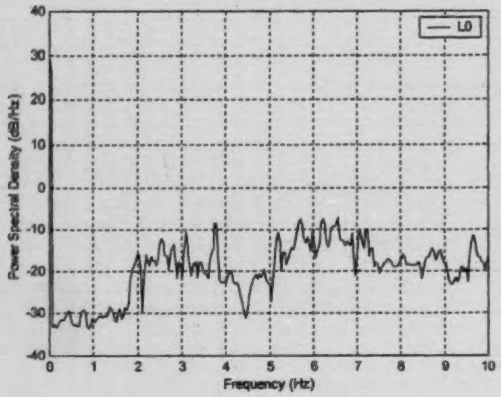

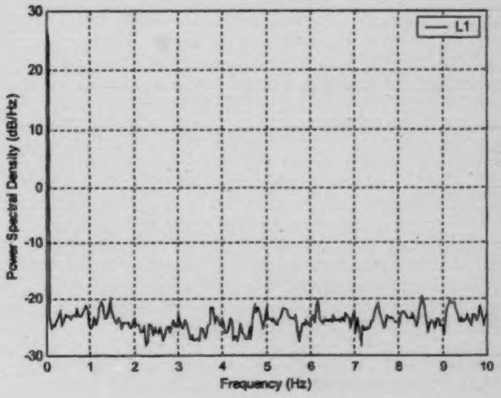

July 18, 1999
2:17 PM

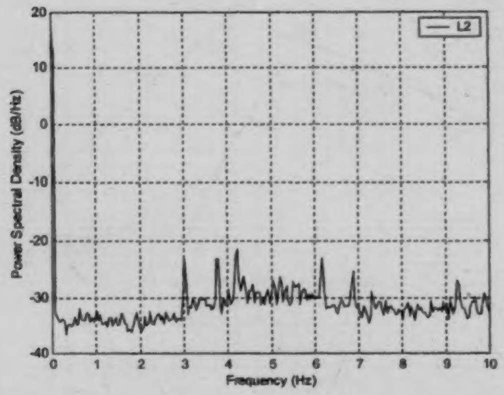

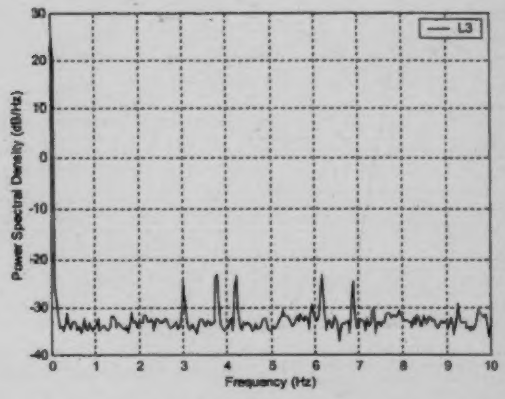

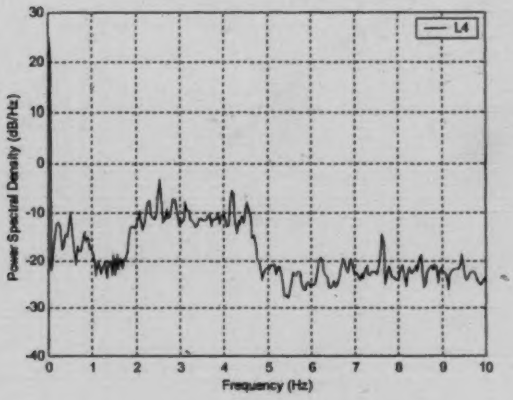

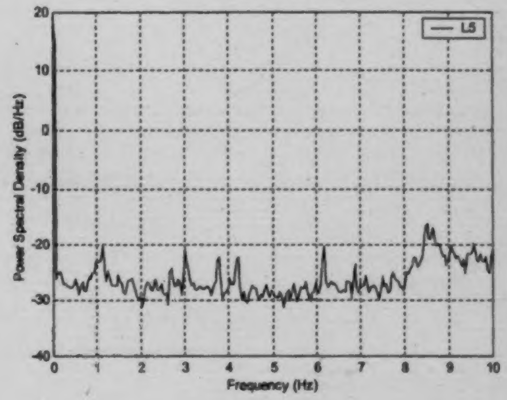

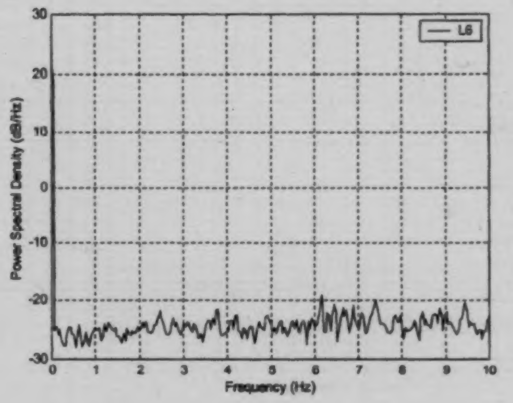

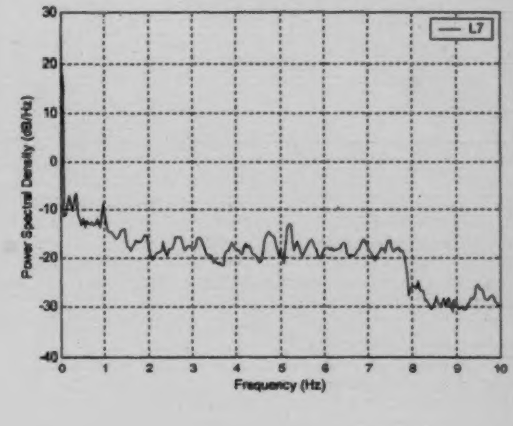

July 18, 1999
2:17 PM

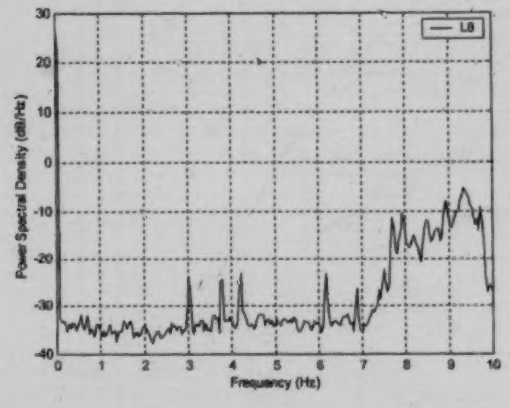

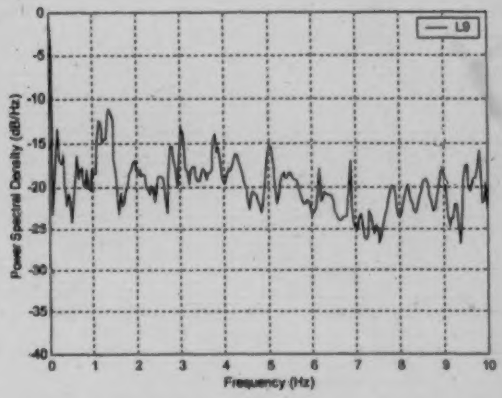

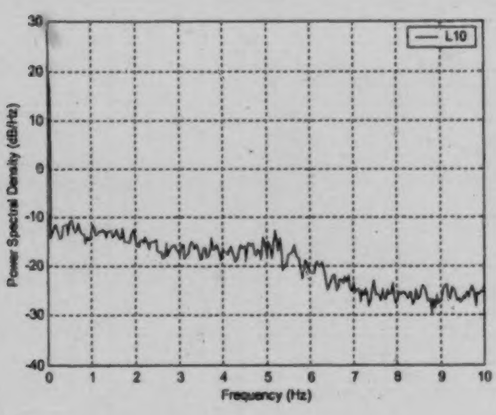

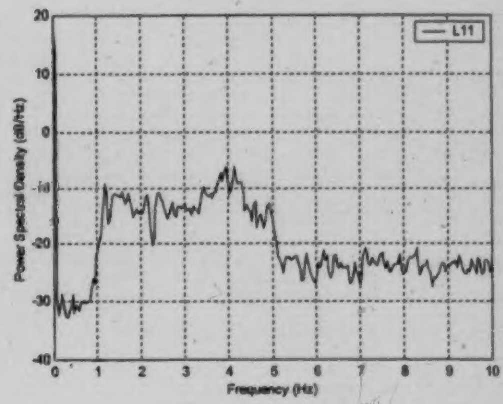

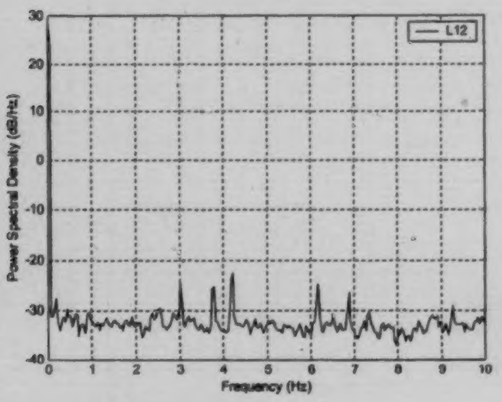

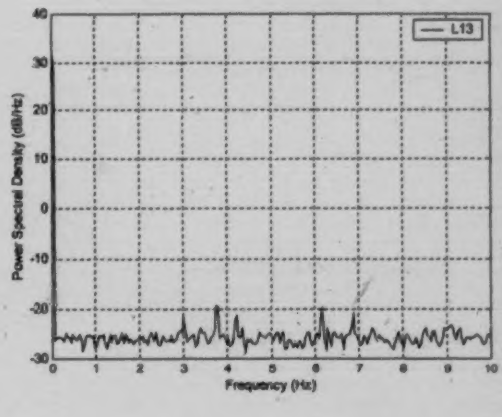

July 18, 1999
2:17 PM

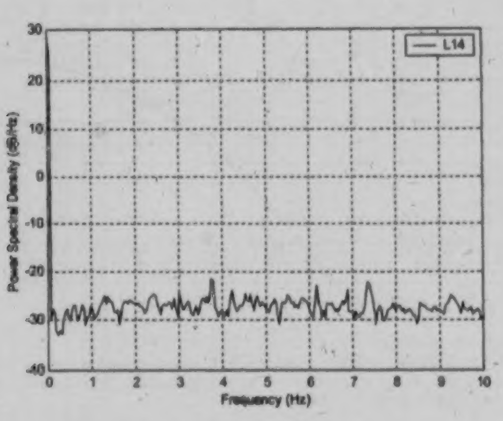

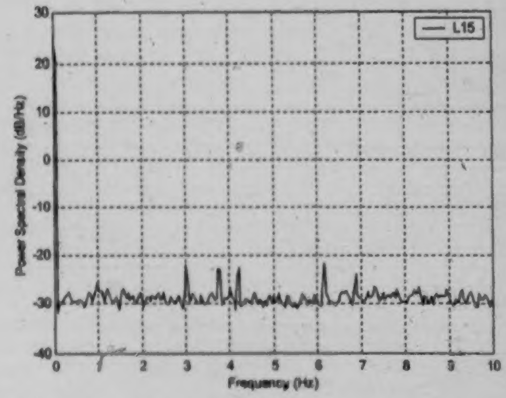

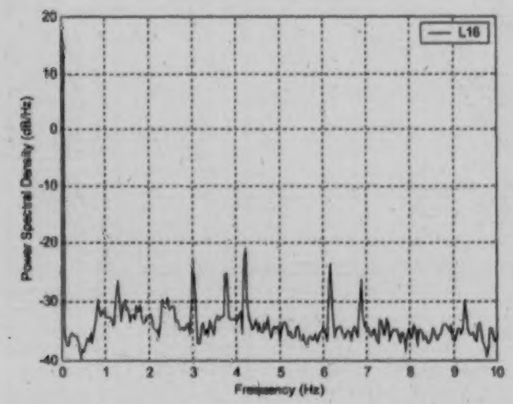

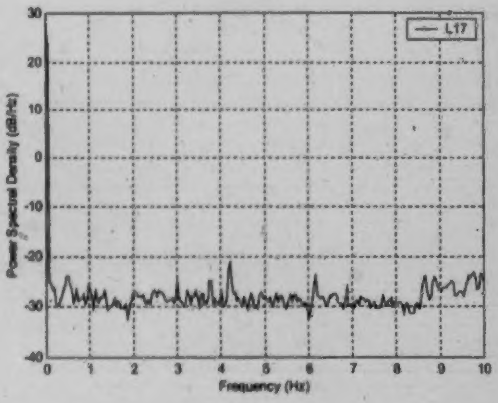

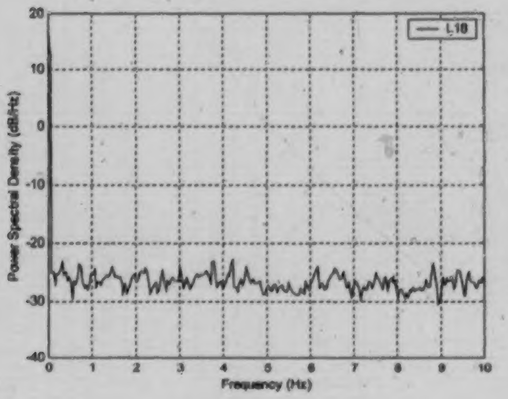

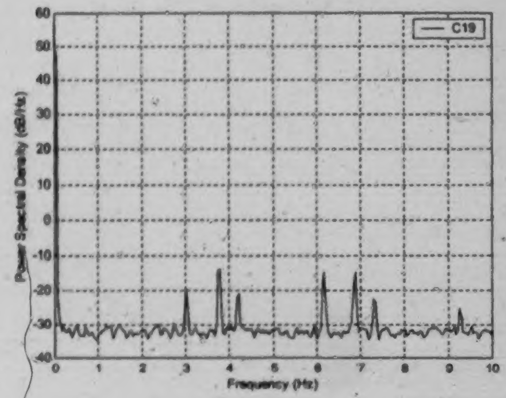

July 18, 1999
2:17 PM

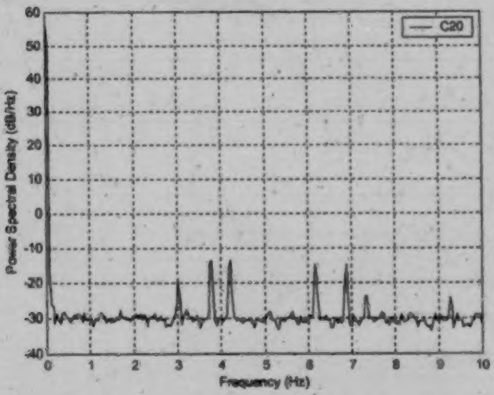

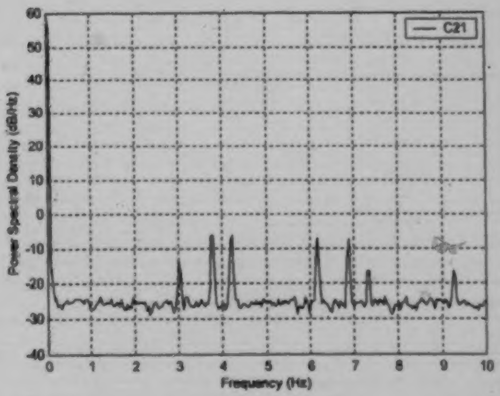

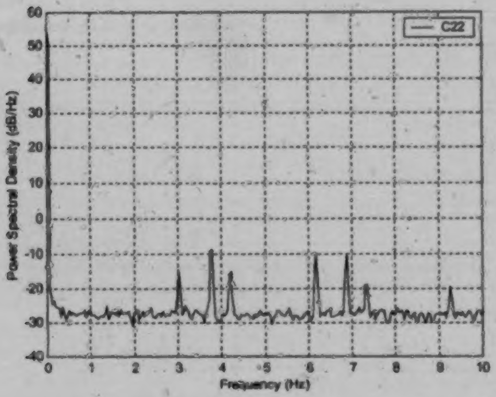

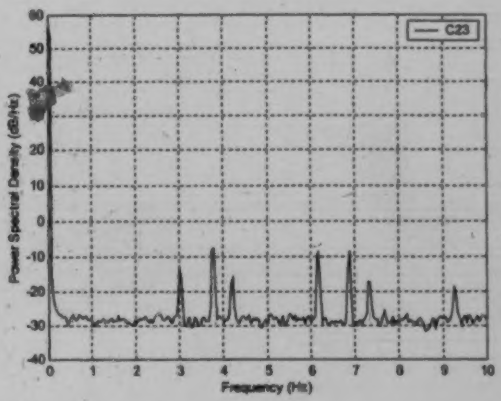

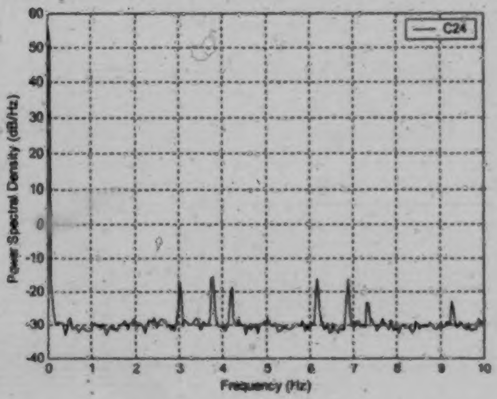

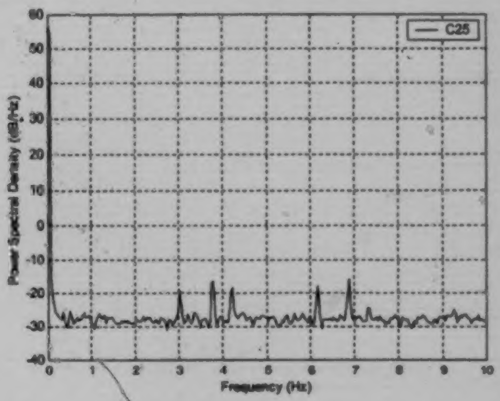

July 18, 1999
2:17 PM

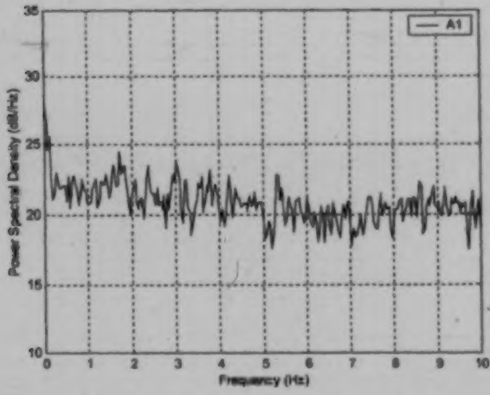

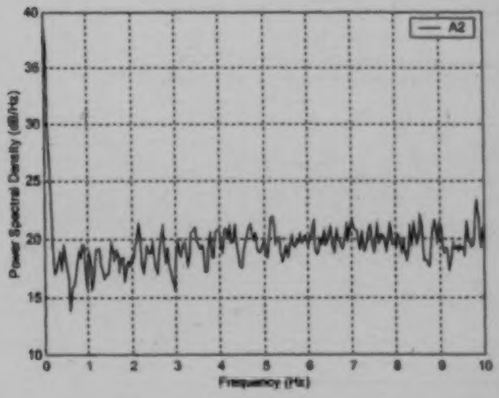

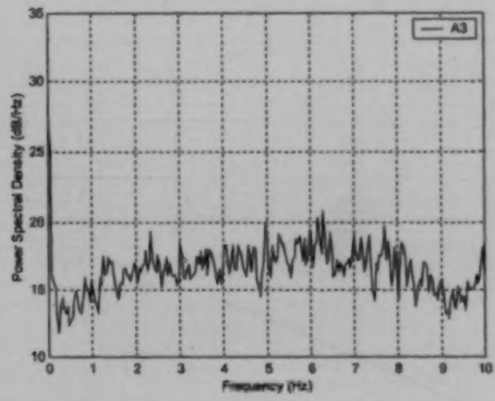

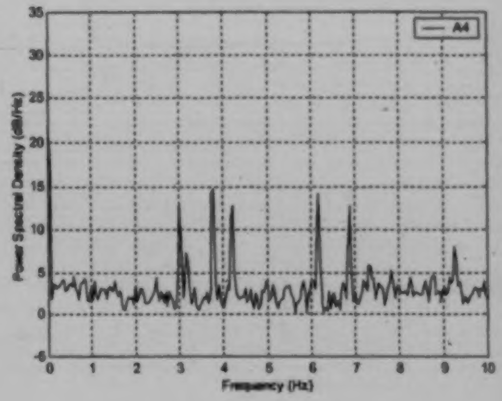

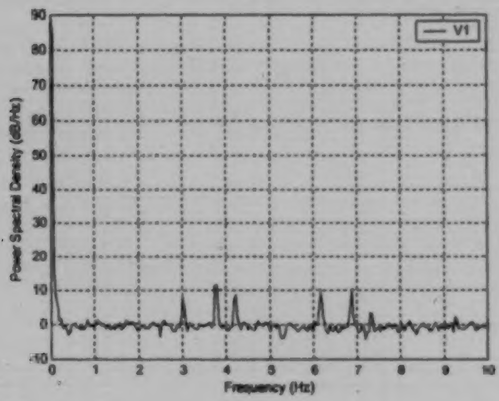

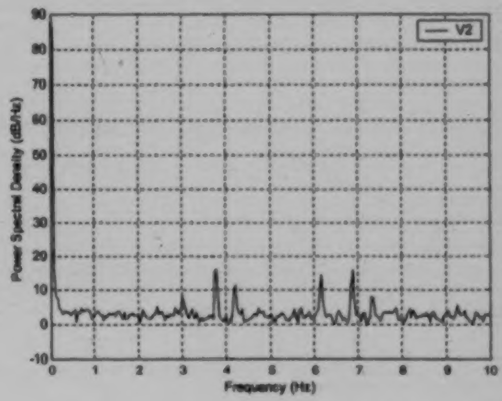

July 18, 1999
2:23 PM

July 18, 1999
2:23 PM

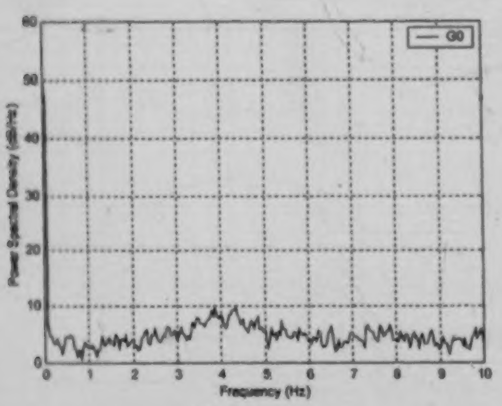

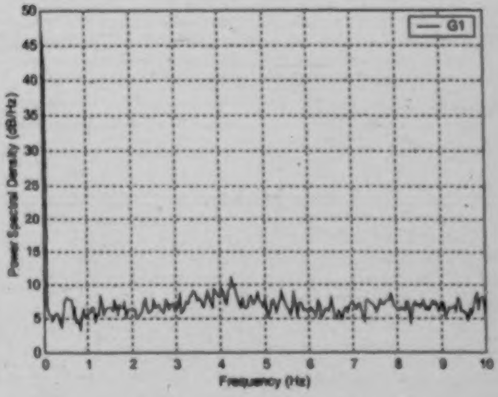

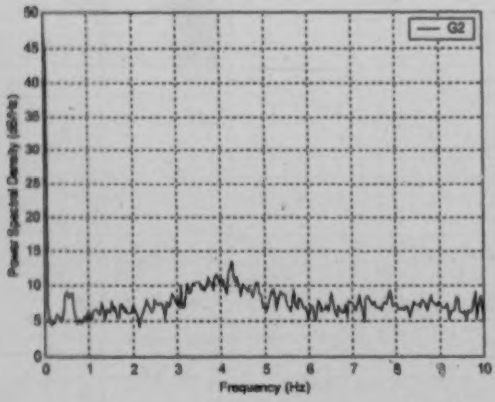

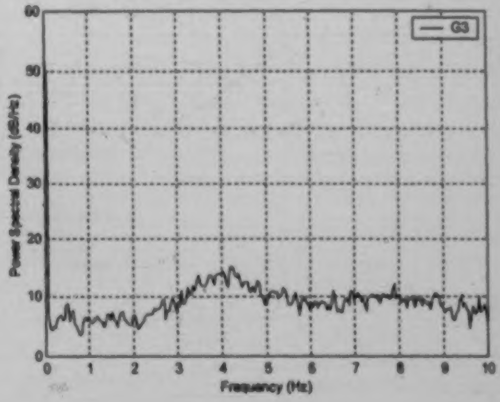

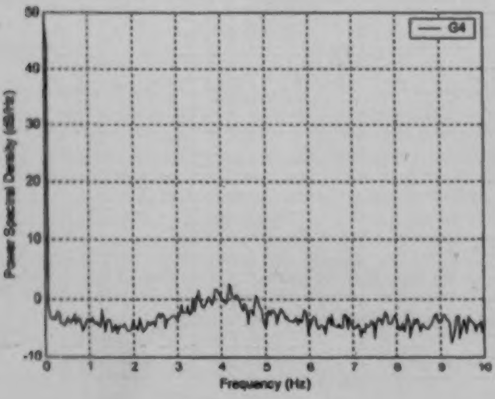

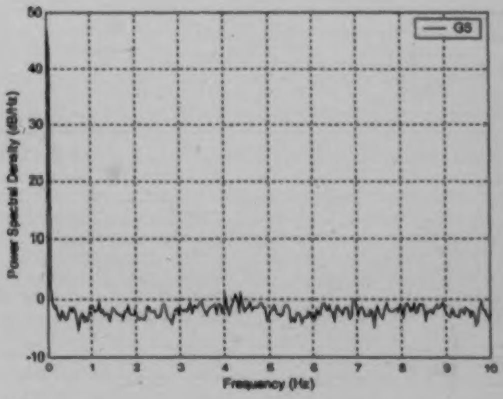

July 18, 1999
2:23 PM

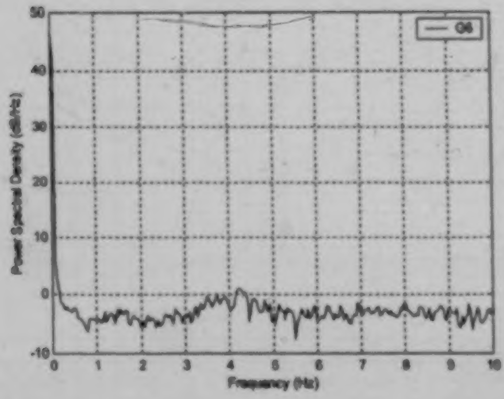

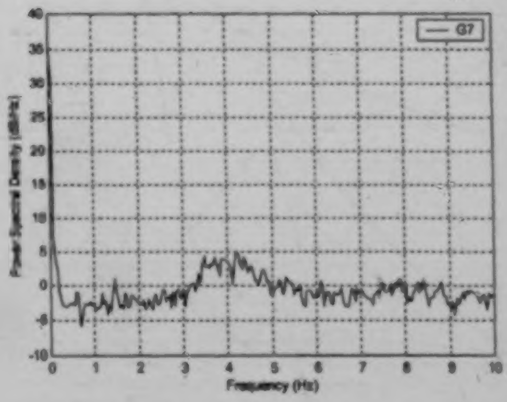

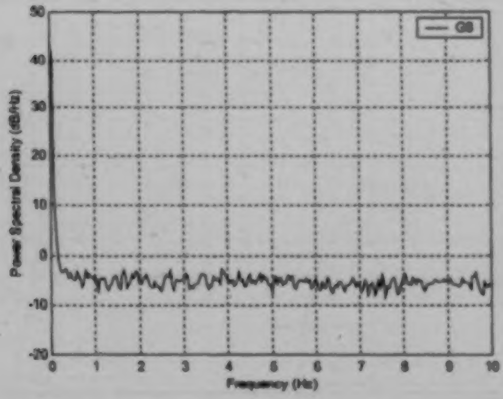

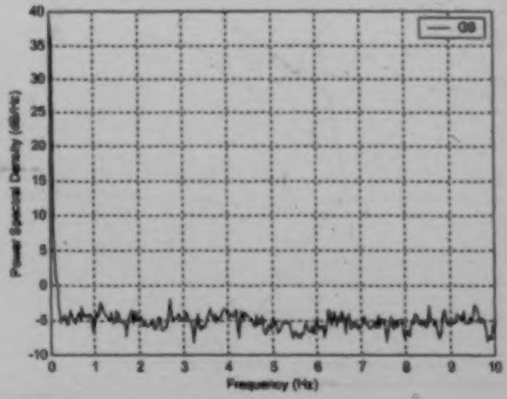

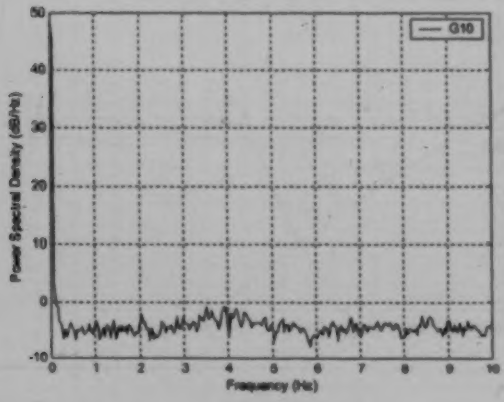

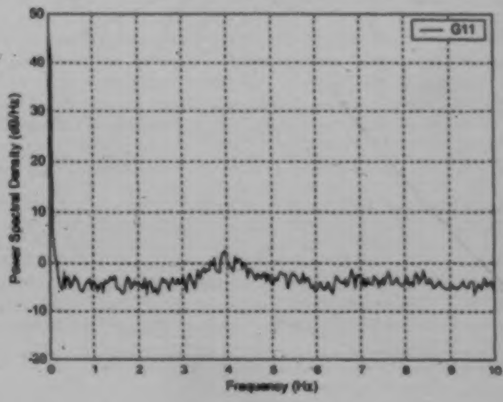

July 18, 1999
2:23 PM

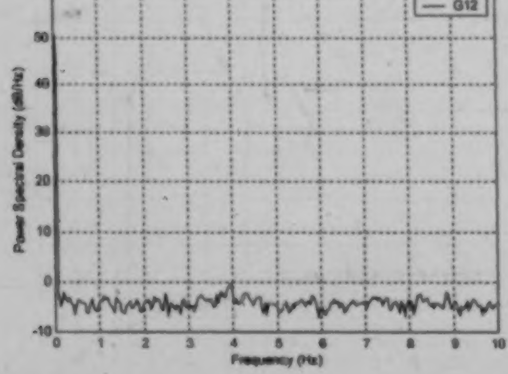

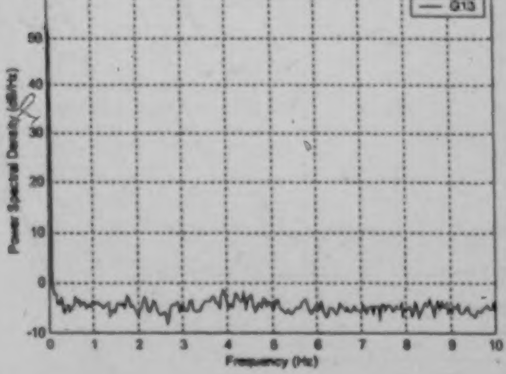

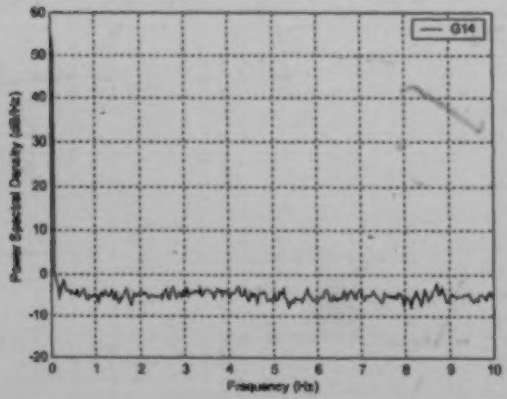

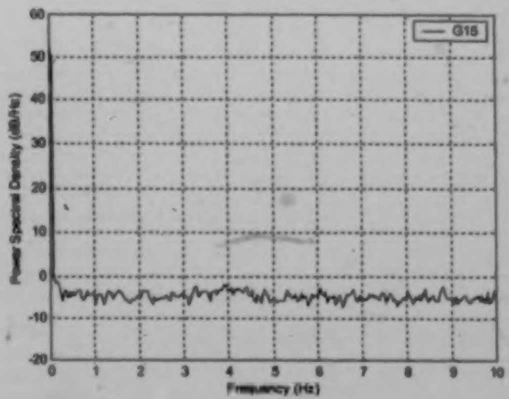

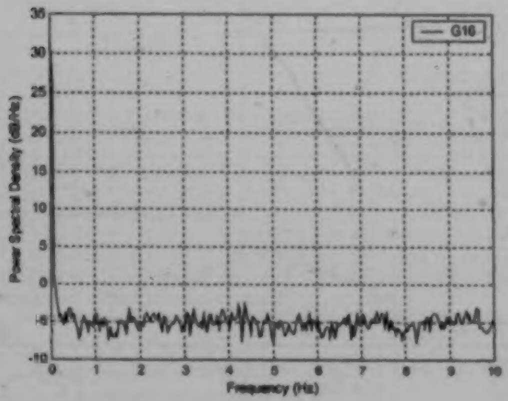

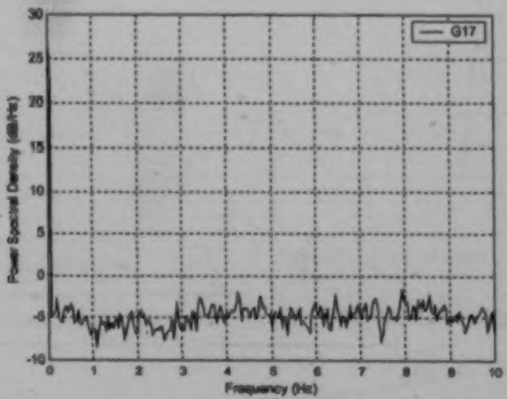

July 18, 1999
2:23 PM

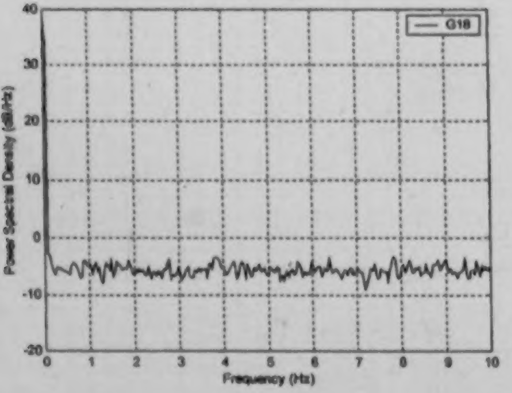

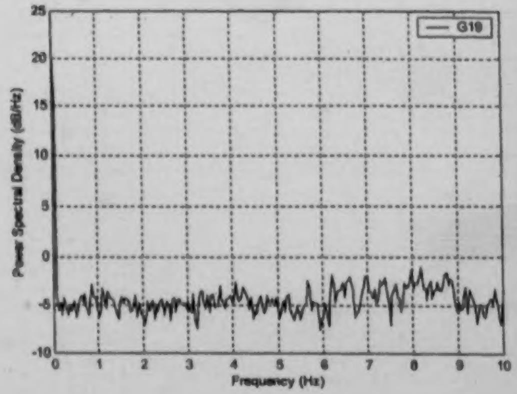

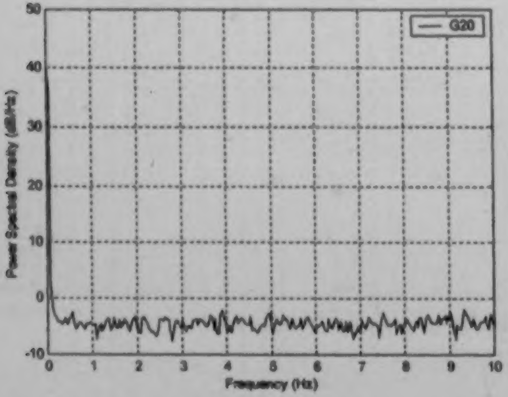

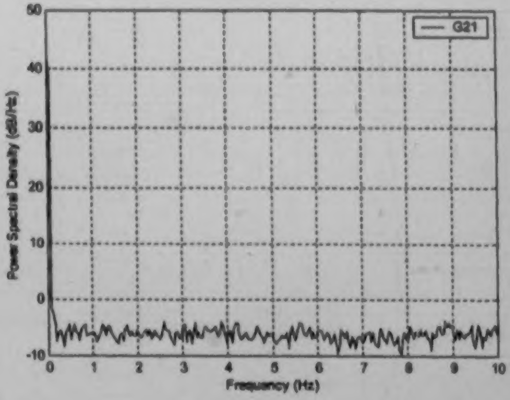

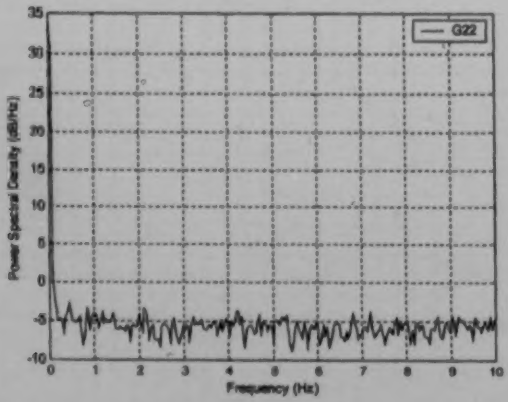

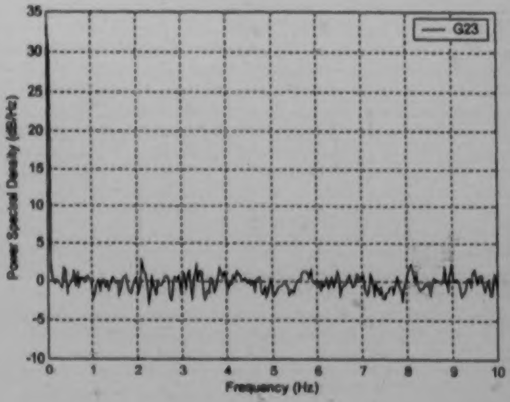

July 18, 1999
2:23 PM

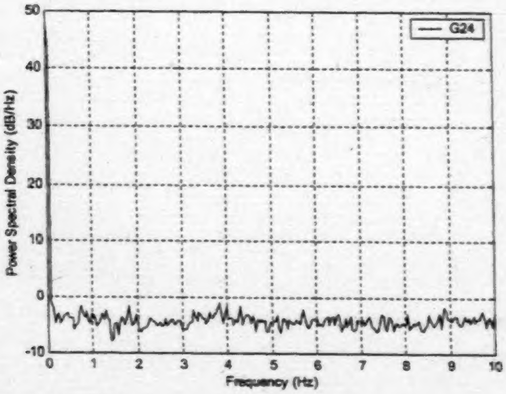

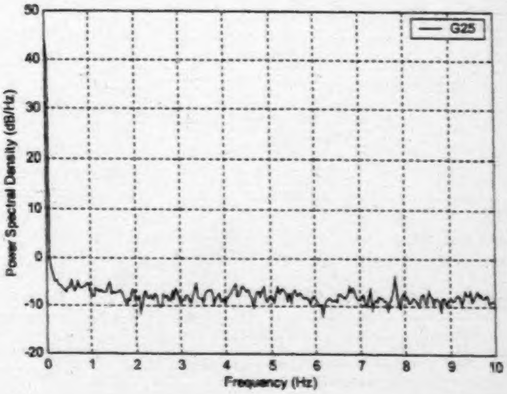

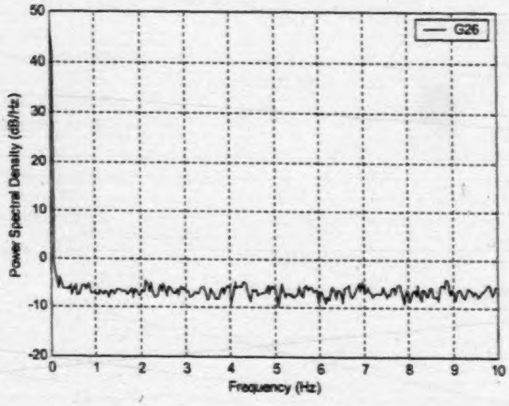

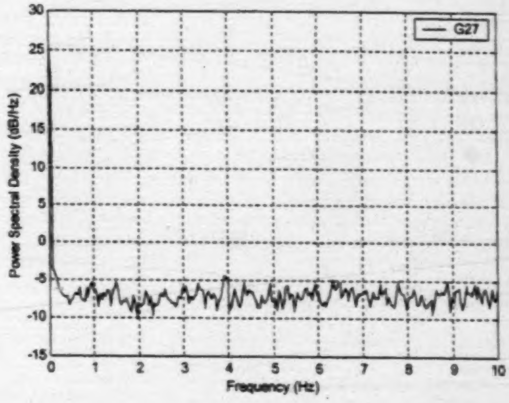

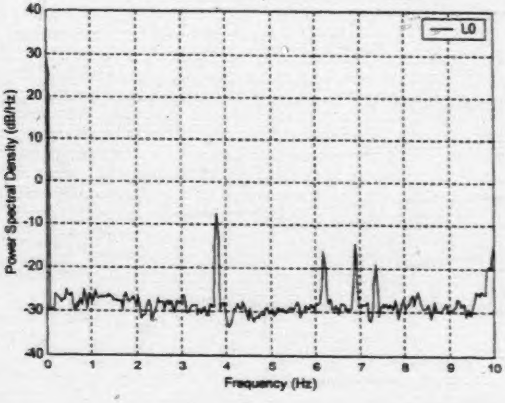

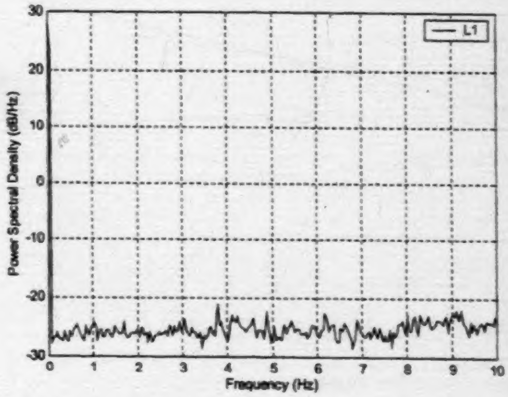

July 18, 1999
2:23 PM

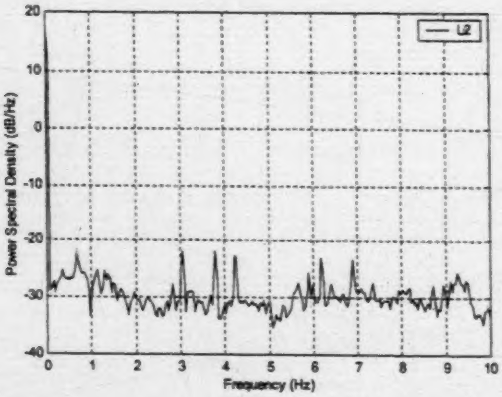

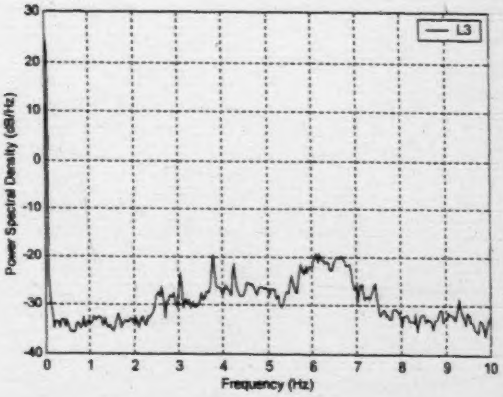

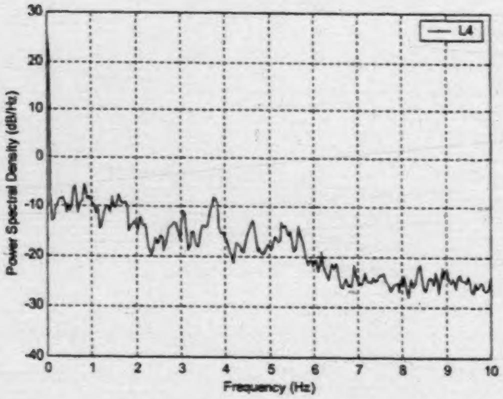

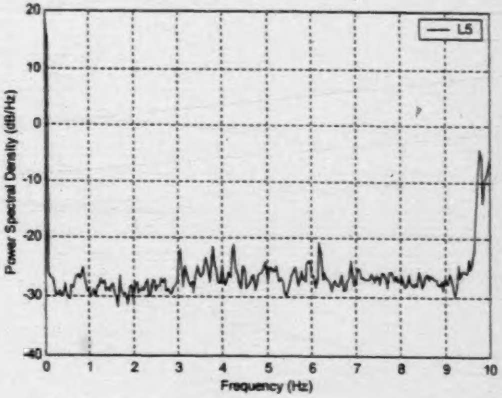

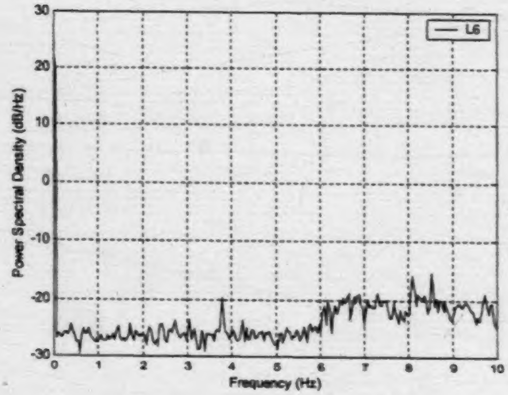

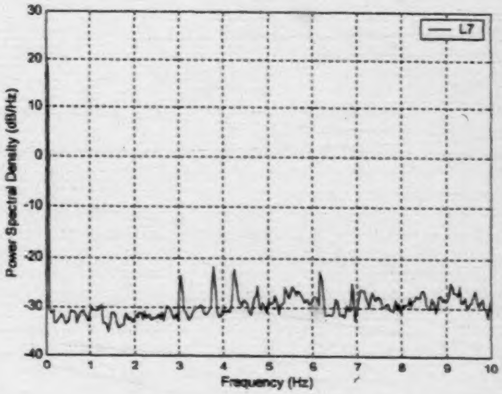

July 18, 1999
2:23 PM

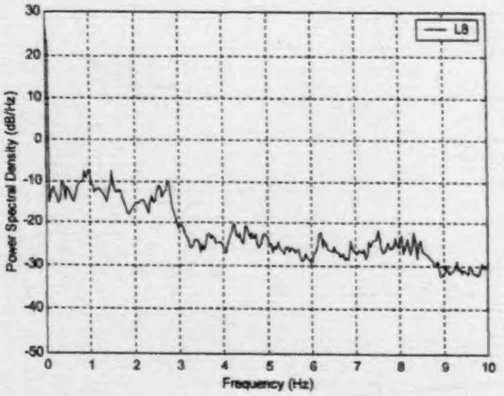

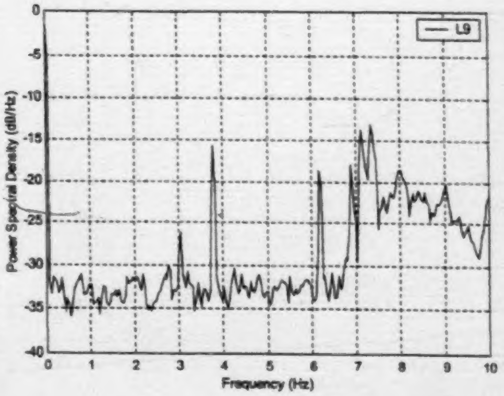

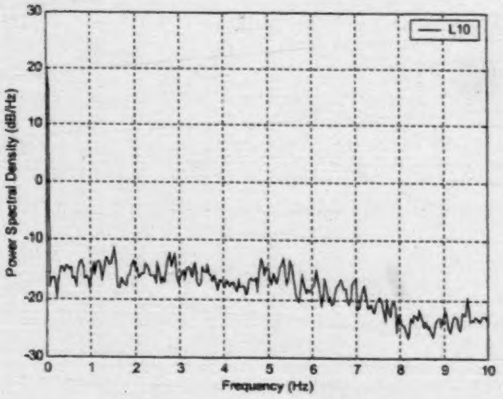

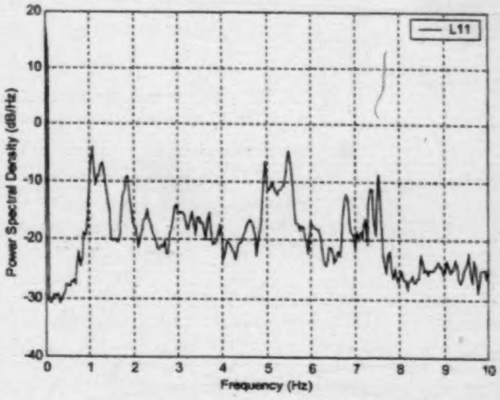

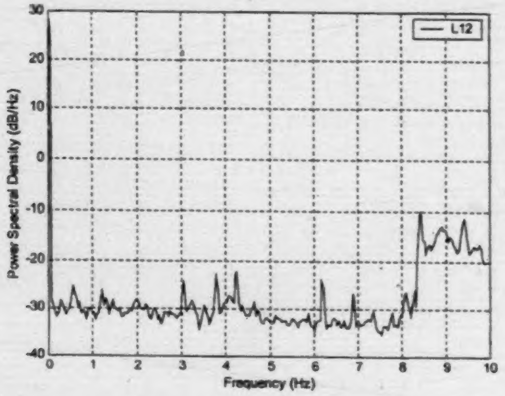

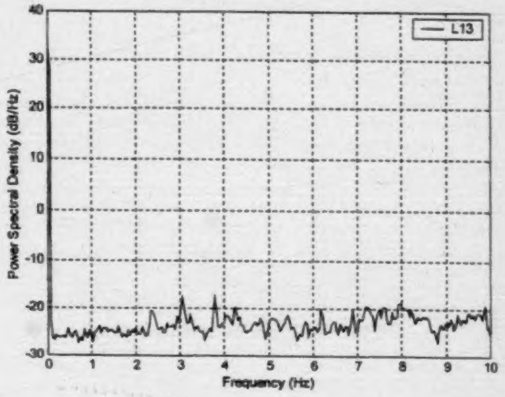

July 18, 1999
2:23 PM

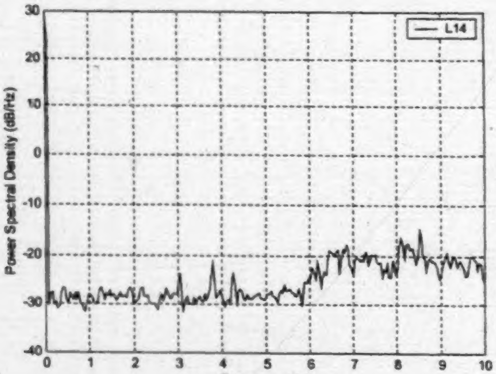

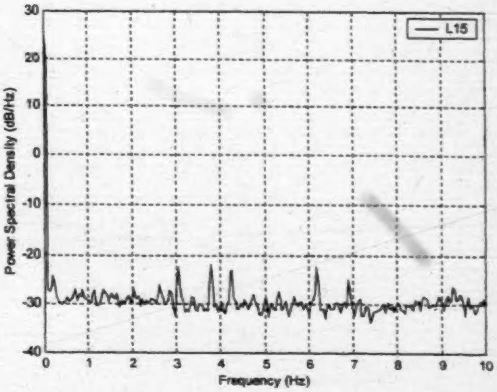

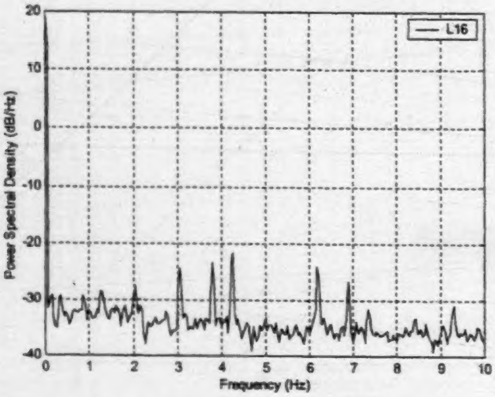

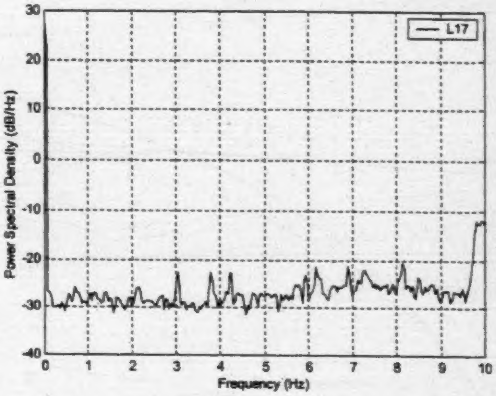

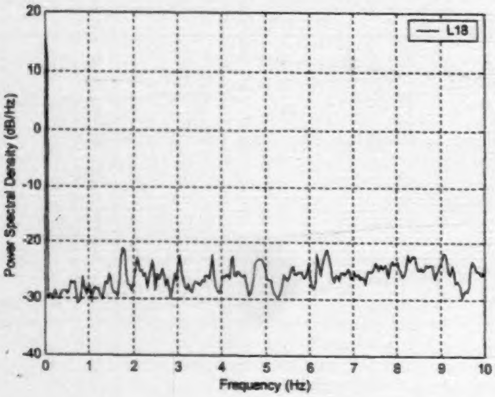

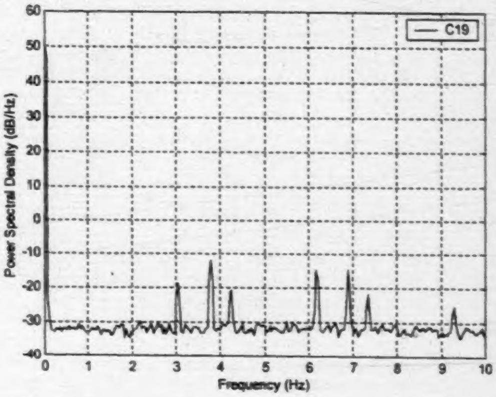

July 18, 1999
2:23 PM

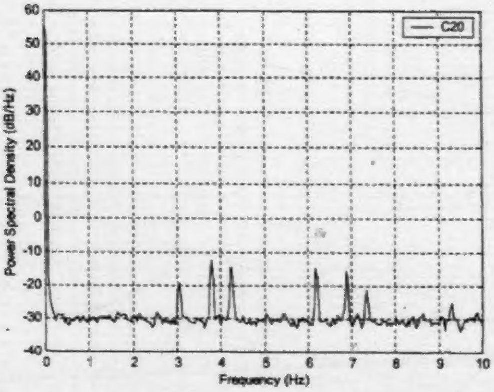

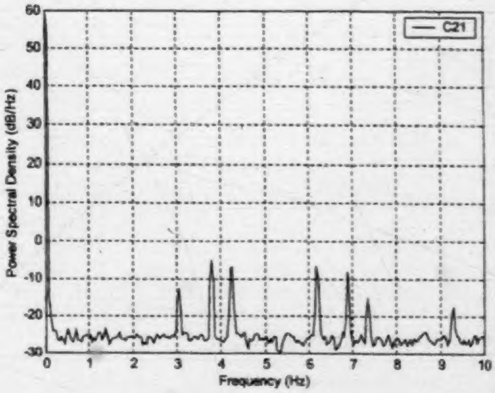

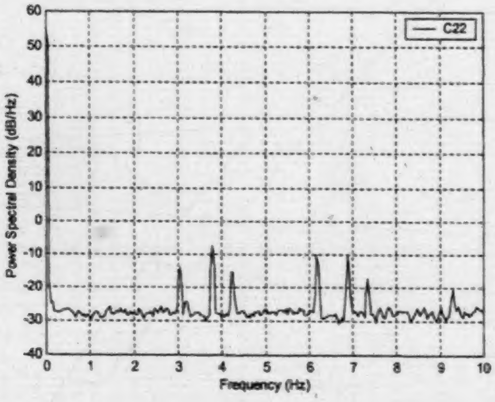

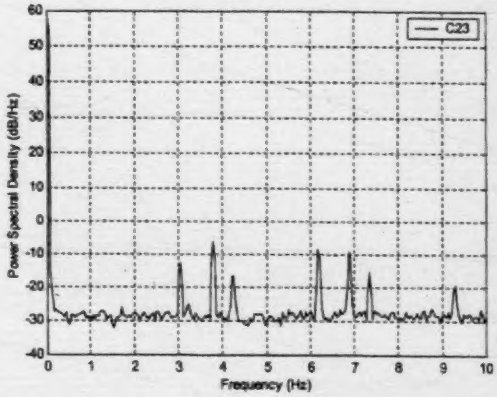

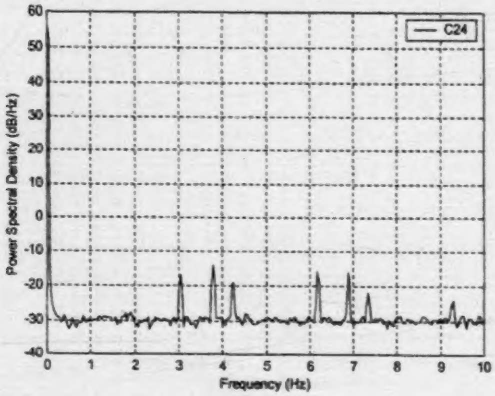

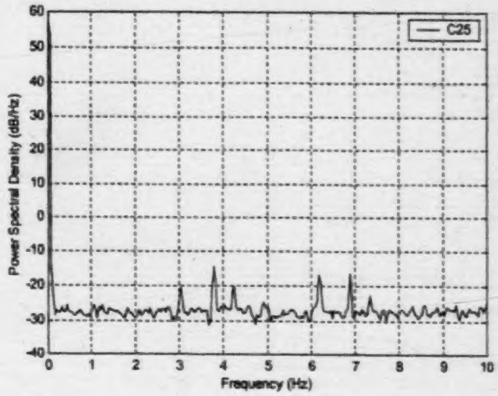

July 18, 1999
2:23 PM

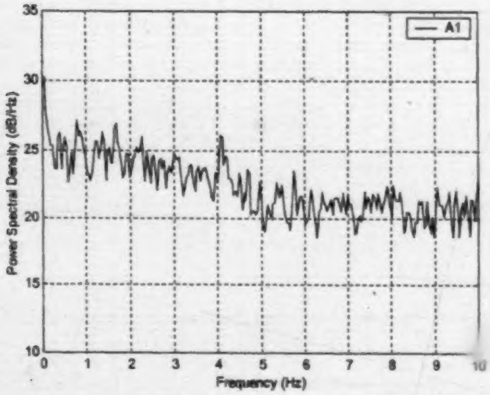

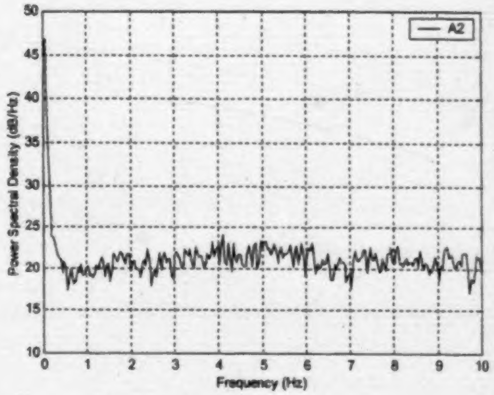

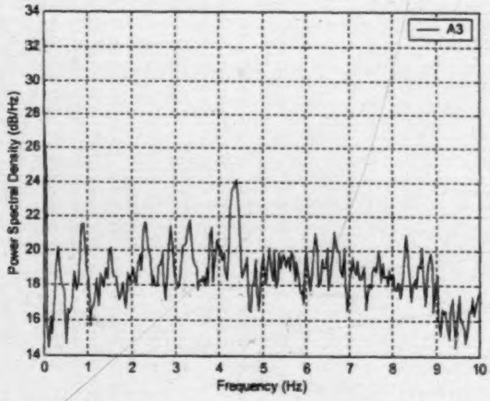

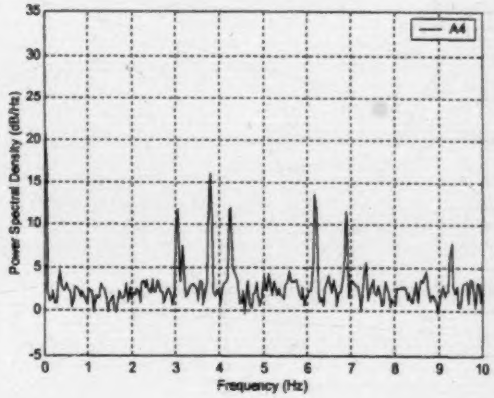

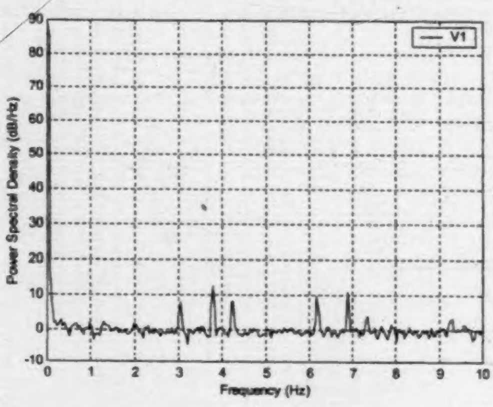

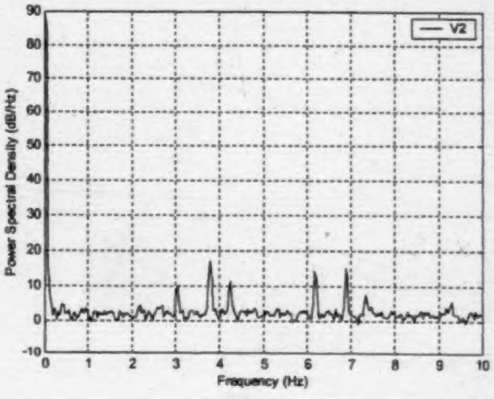

July 18, 1999
2:28 PM

July 18, 1999
2:28 PM

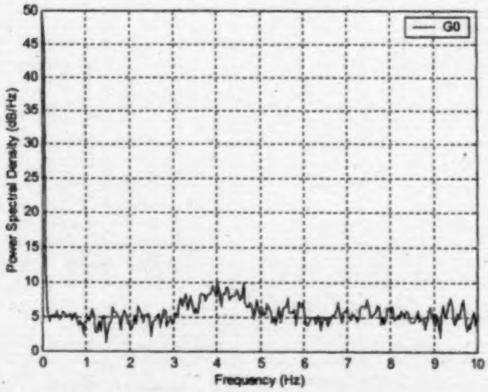

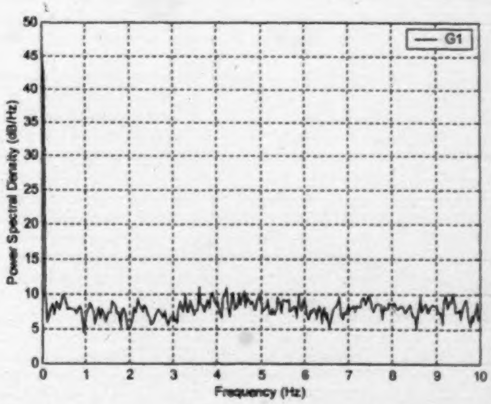

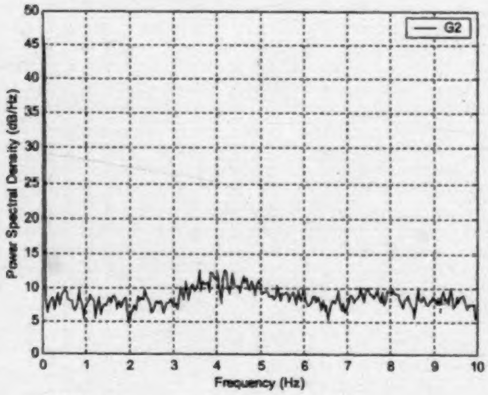

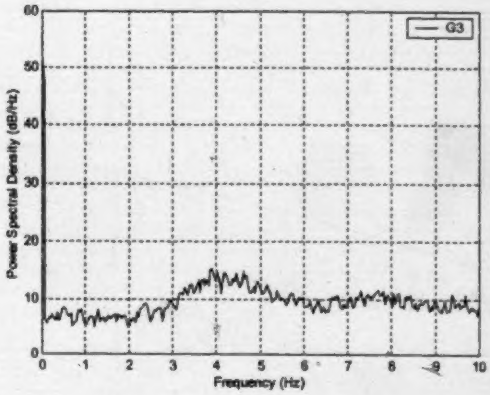

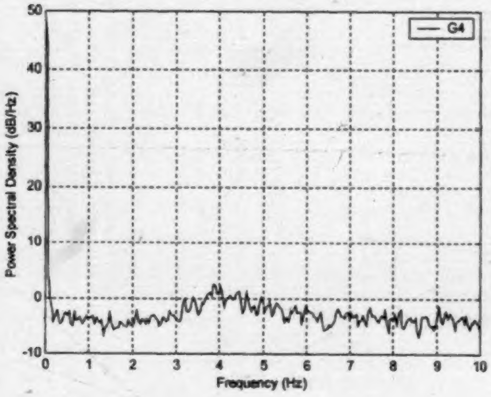

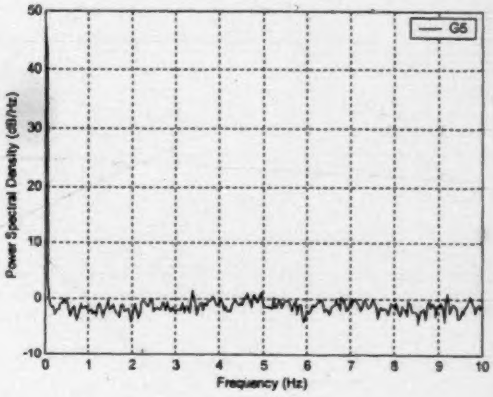

July 18, 1999
2:28 PM

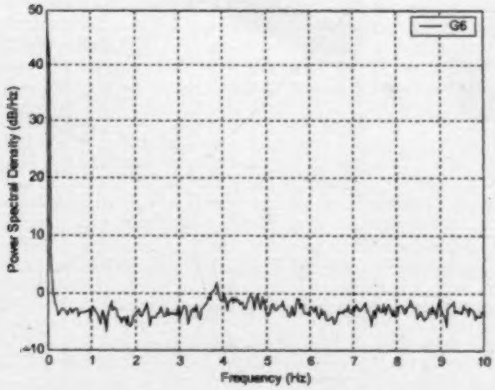

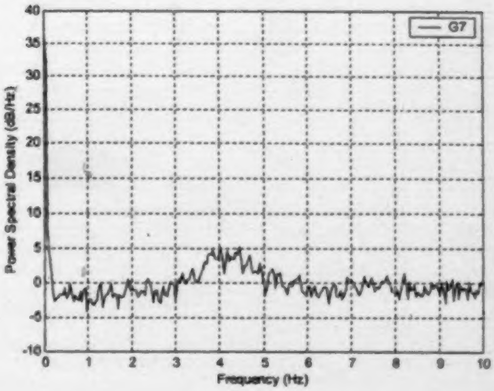

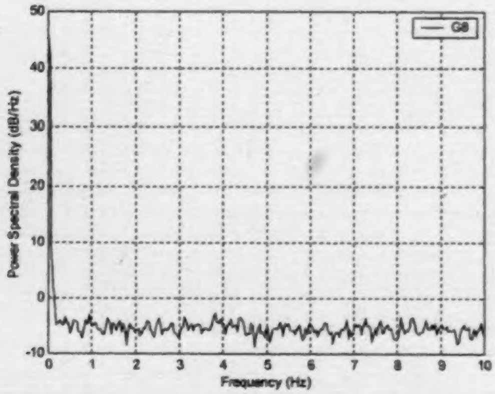

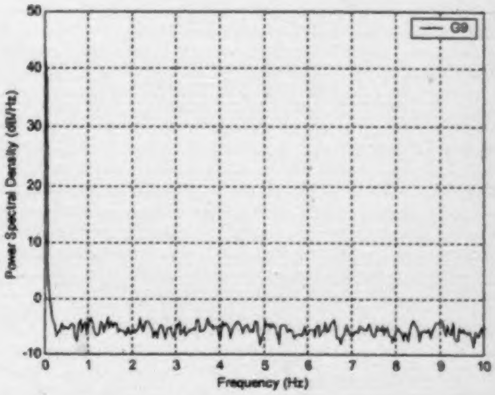

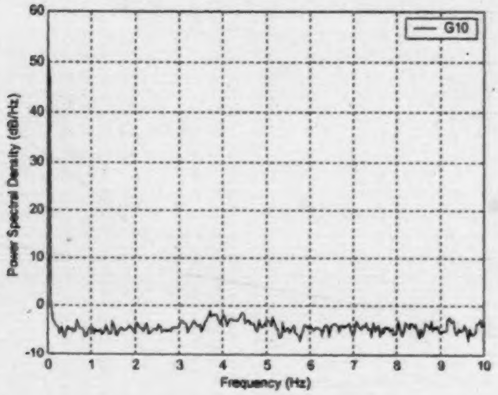

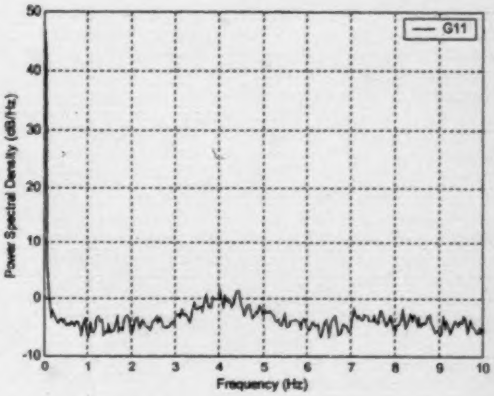

July 18, 1999
2:28 PM

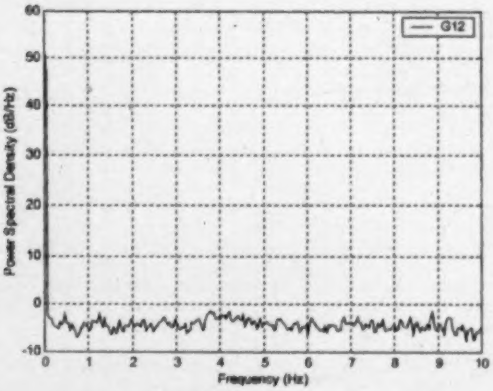

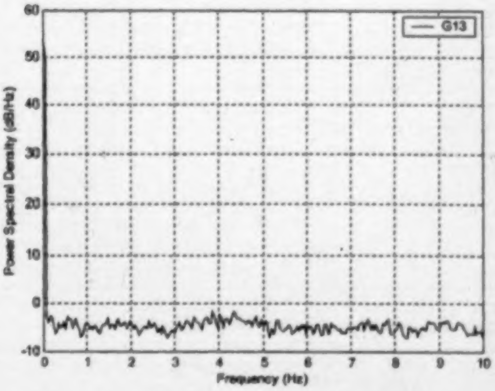

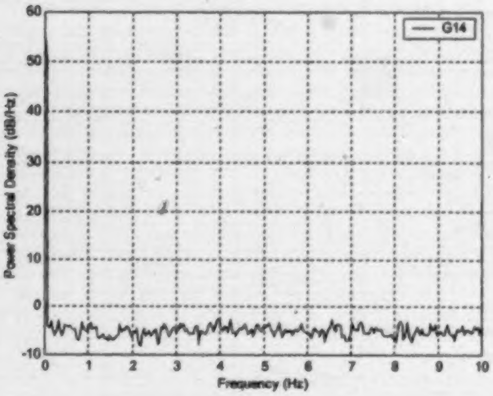

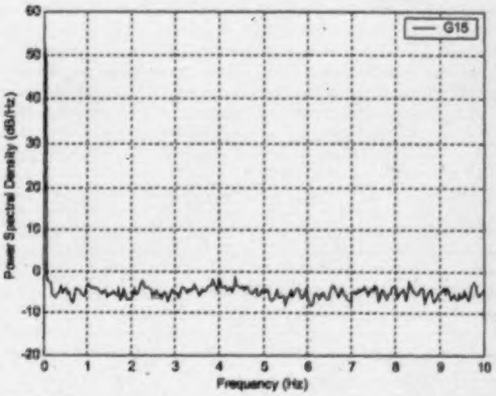

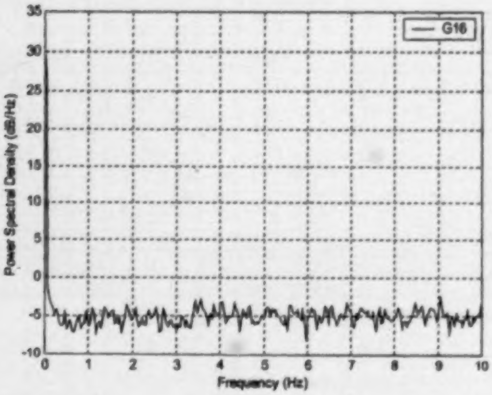

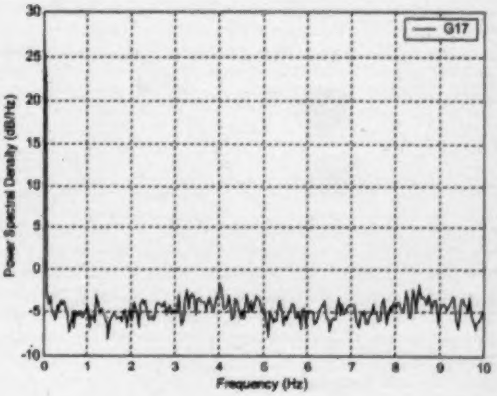

July 18, 1999
2:28 PM

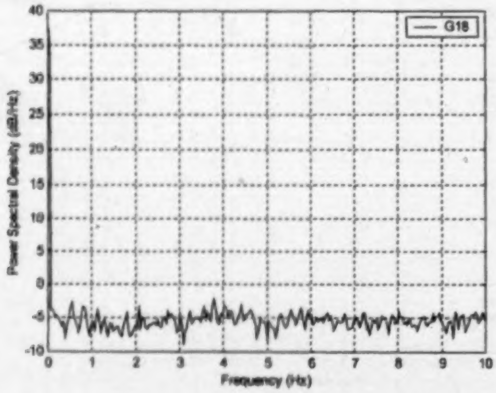

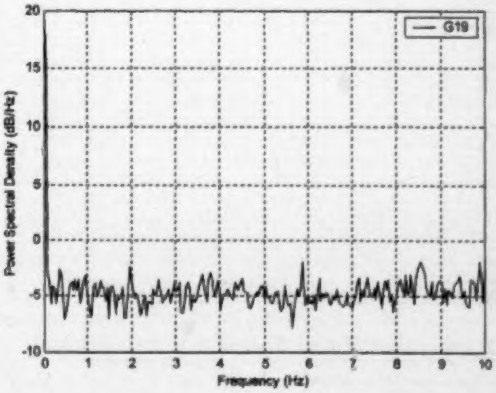

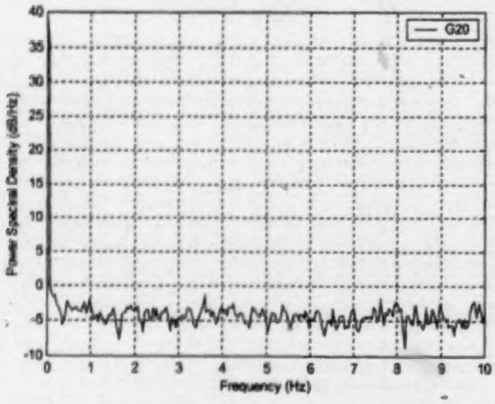

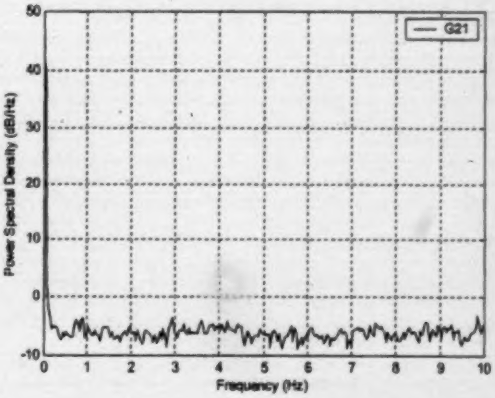

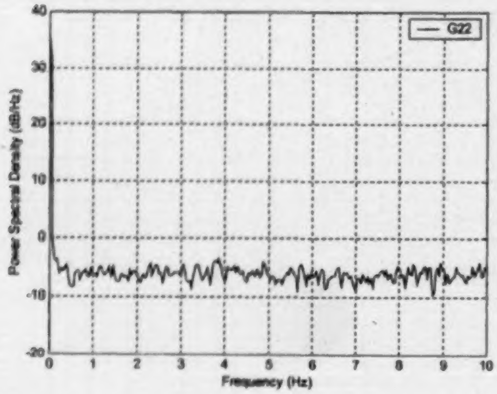

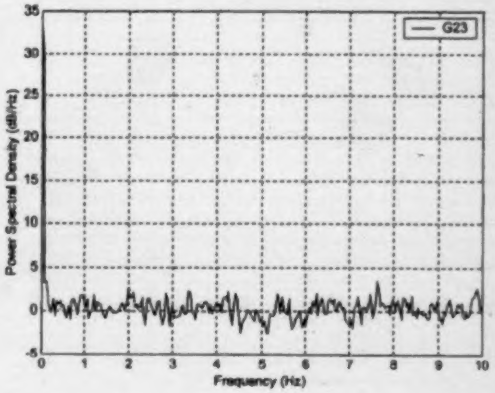

July 18, 1999
2:28 PM

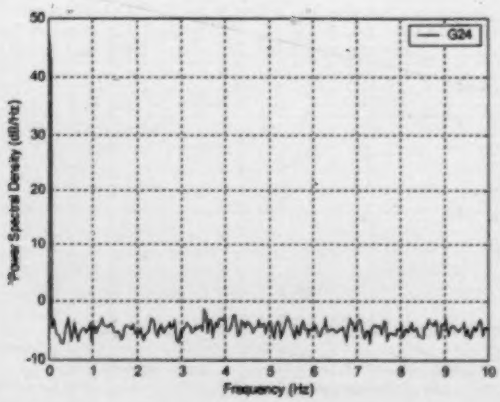

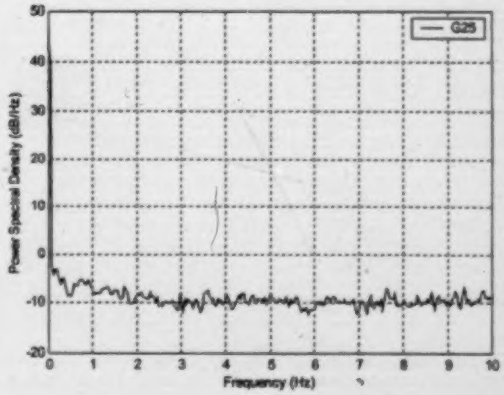

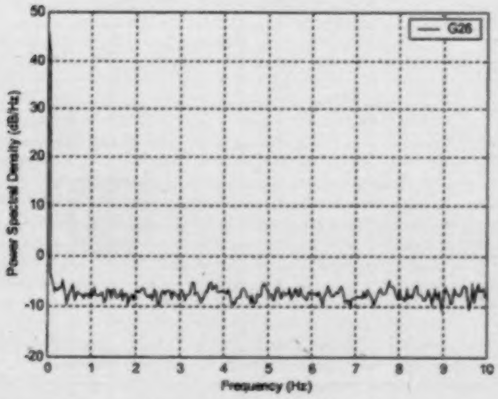

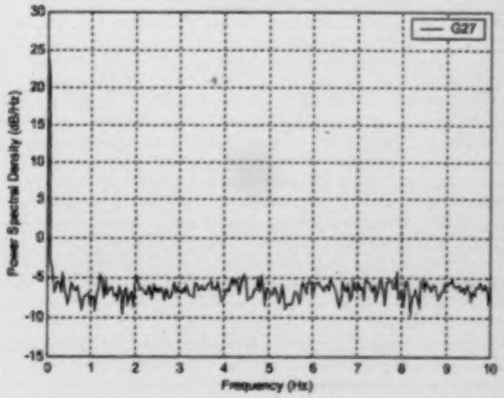

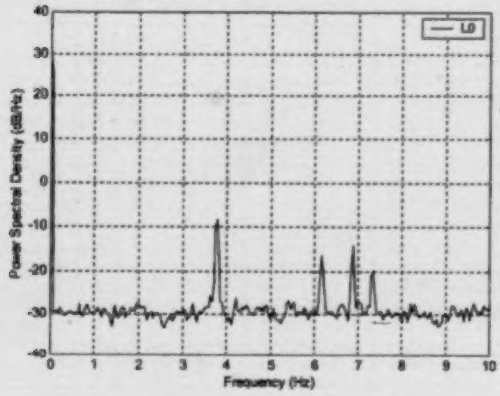

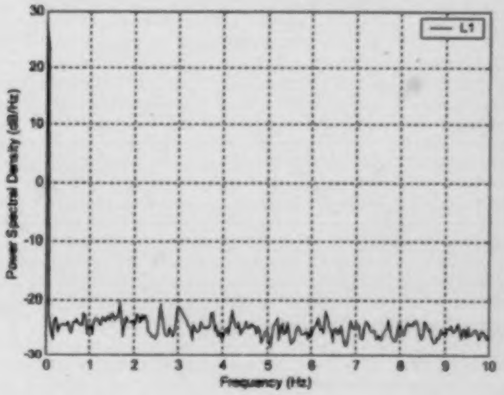

July 18, 1999
2:28 PM

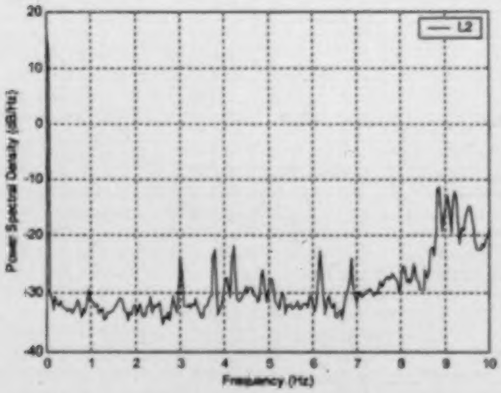

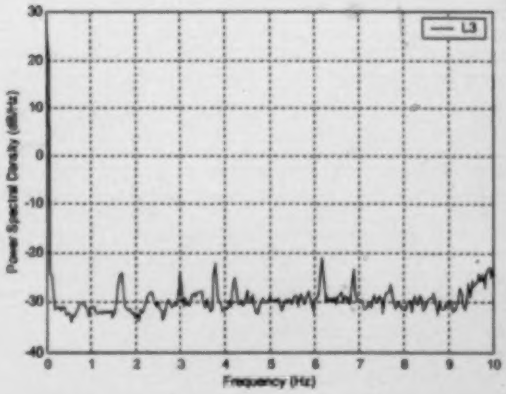

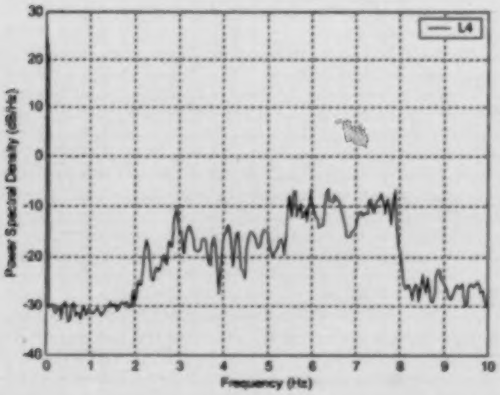

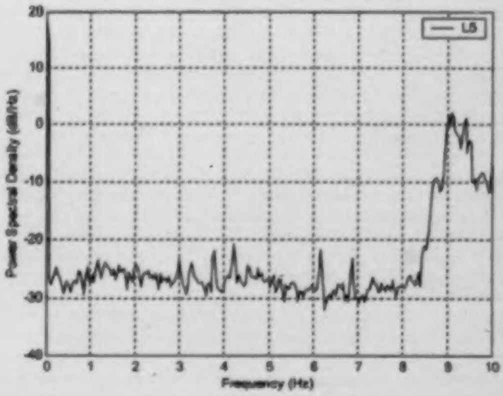

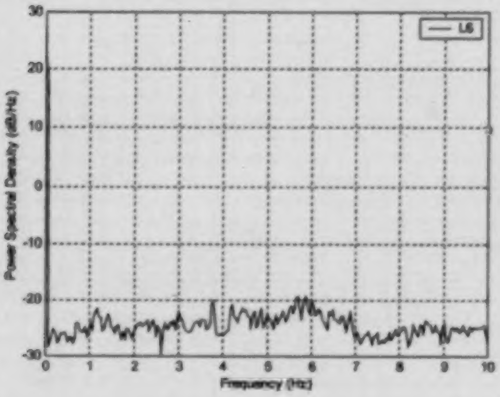

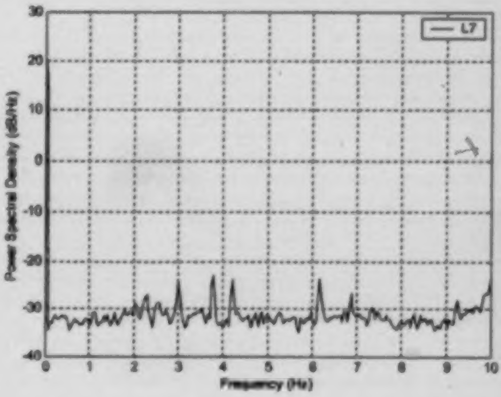

July 18, 1999
2:28 PM

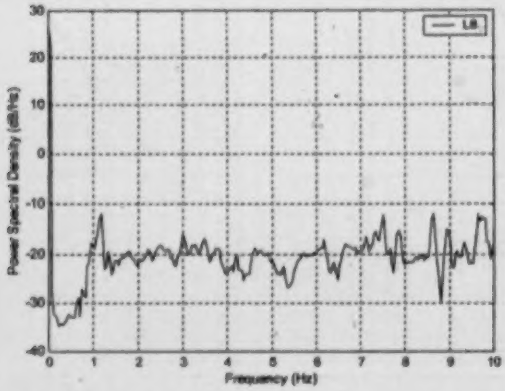

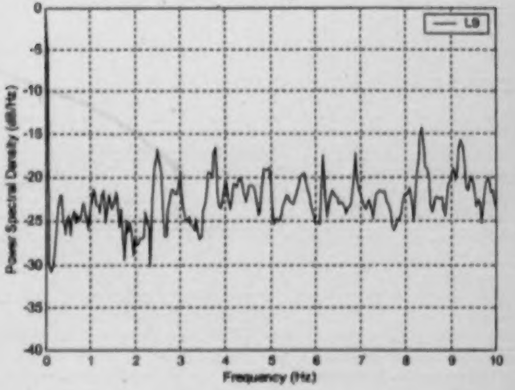

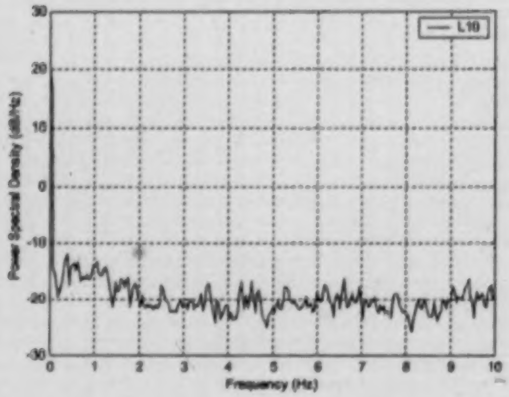

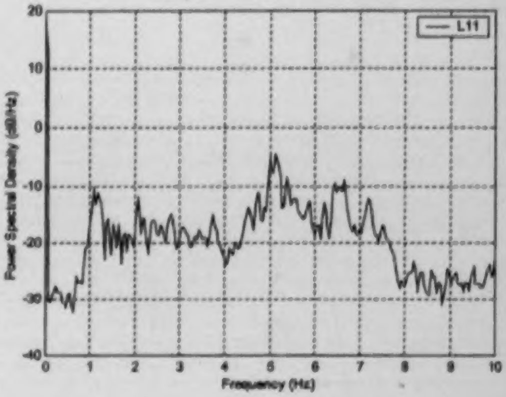

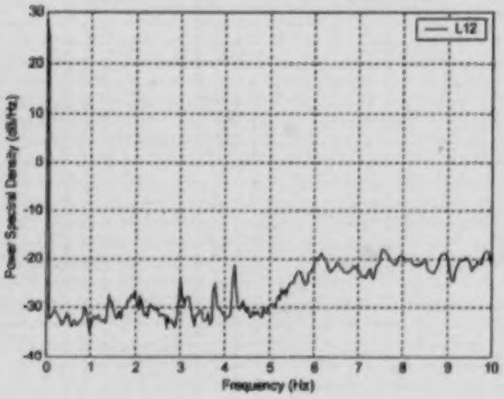

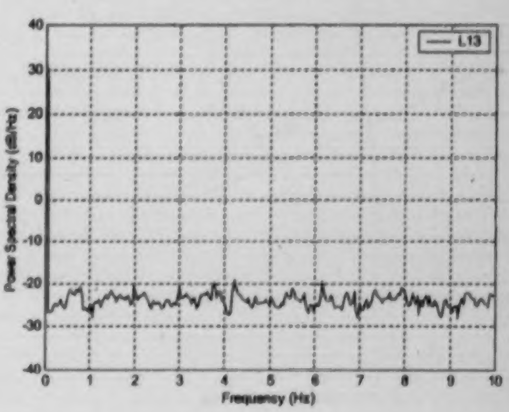

July 18, 1999
2:28 PM

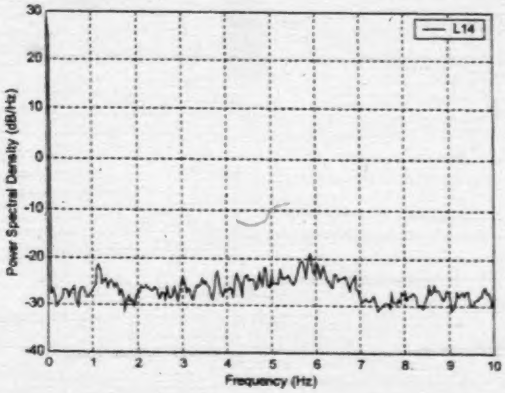

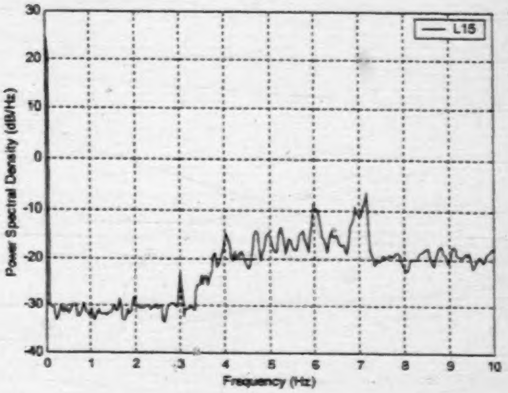

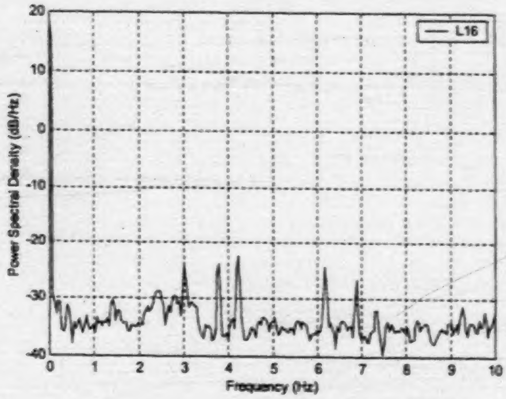

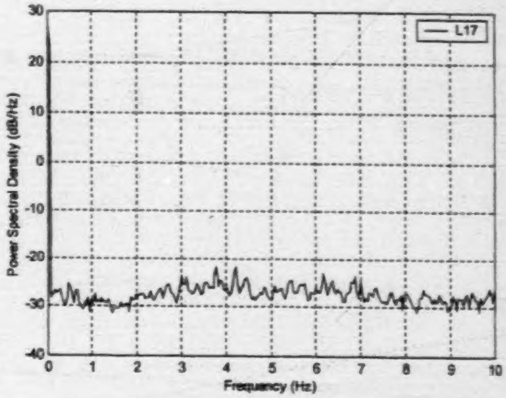

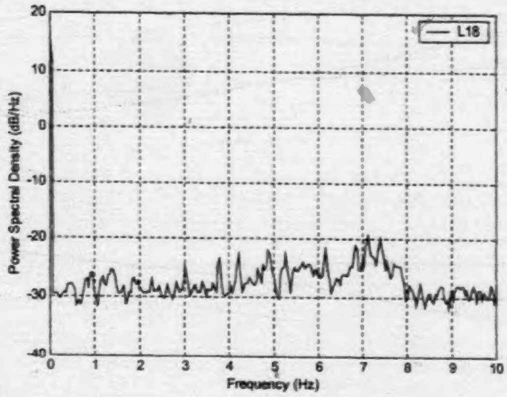

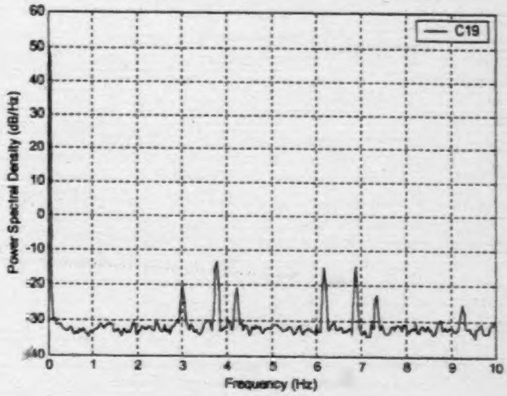

July 18, 1999
2:28 PM

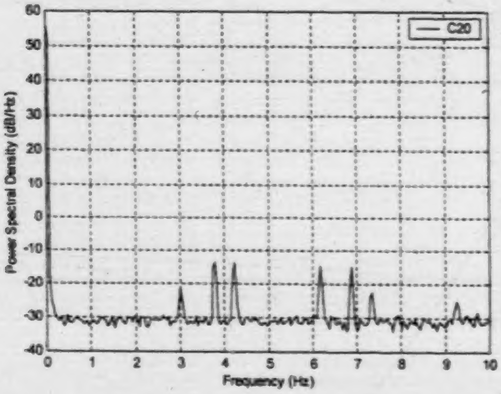

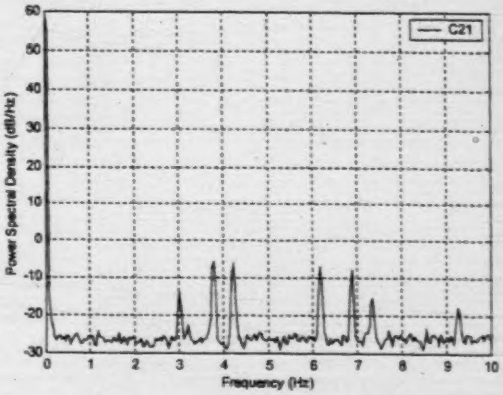

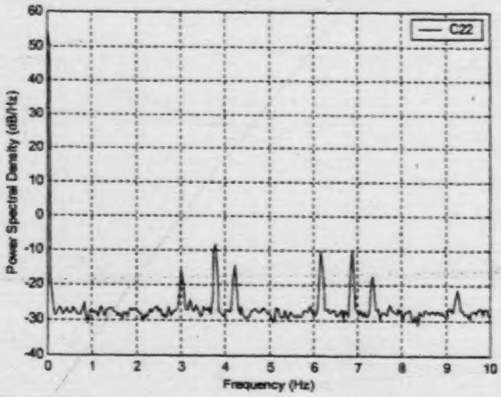

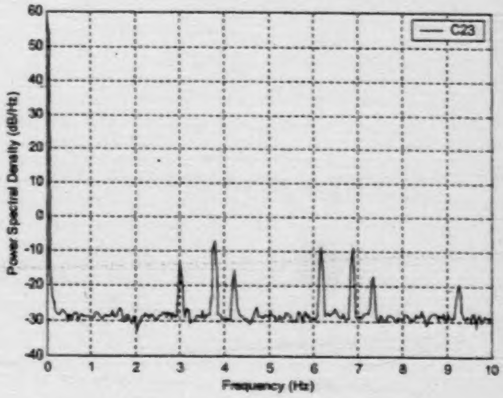

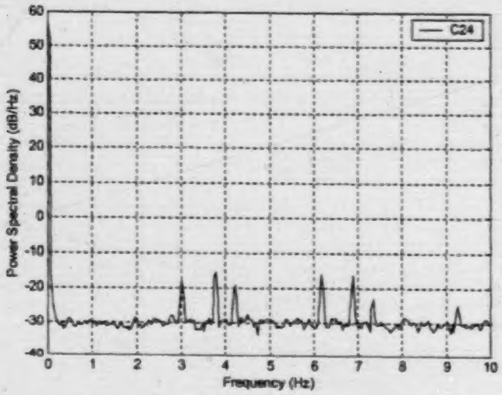

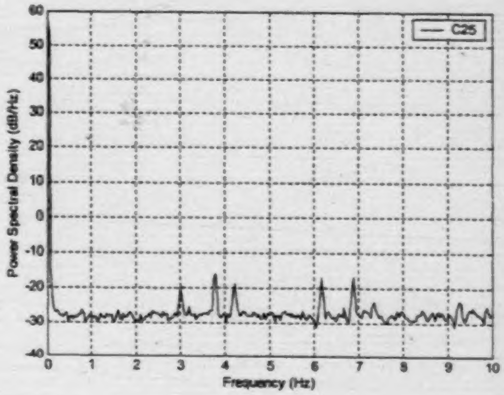

July 18, 1999
2:28 PM

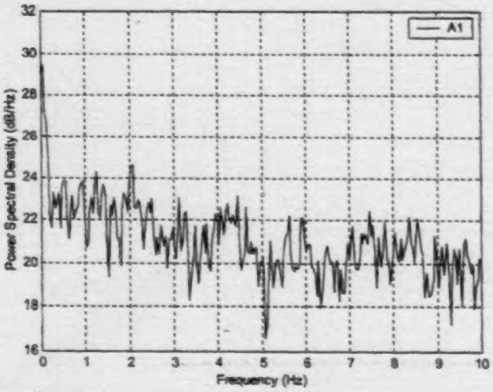

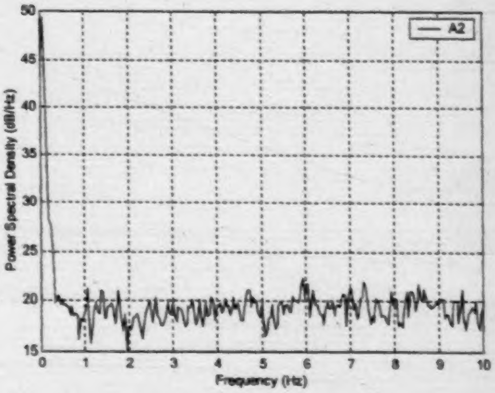

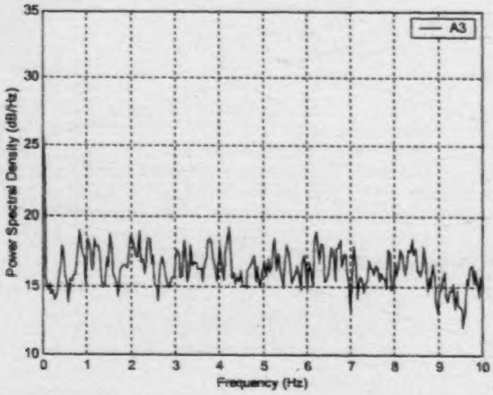

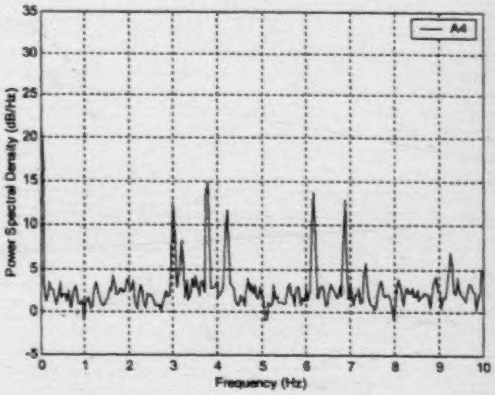

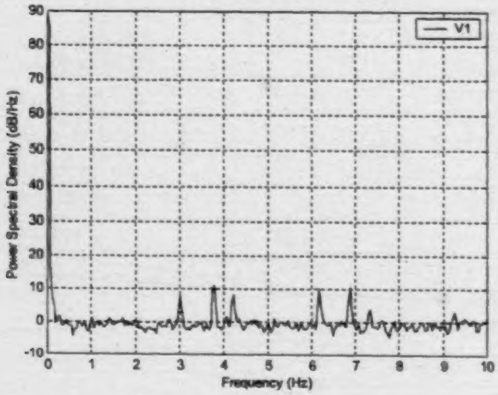

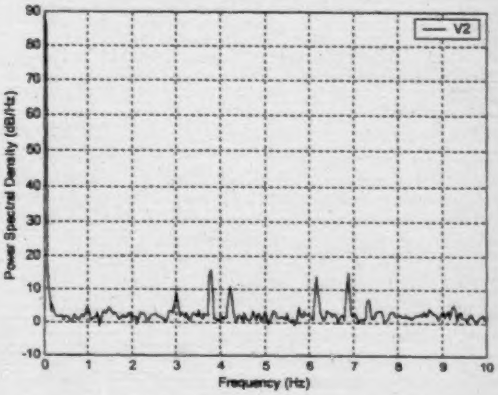

July 18, 1999
2:40 PM

July 18, 1999
2:40 PM

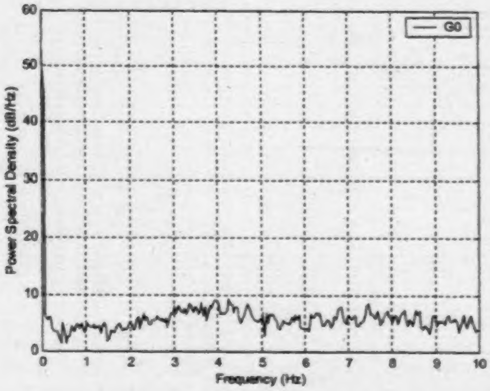

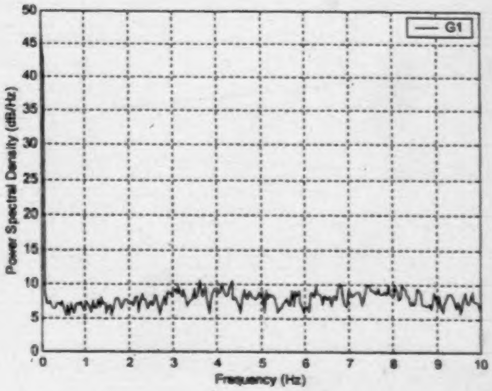

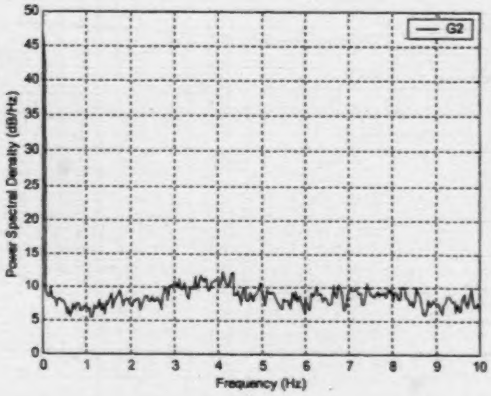

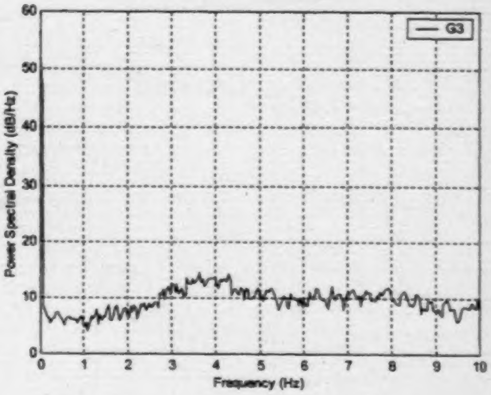

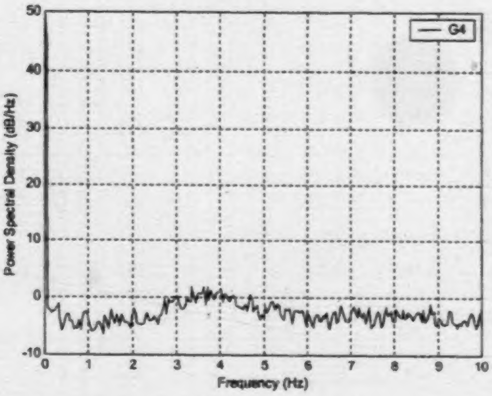

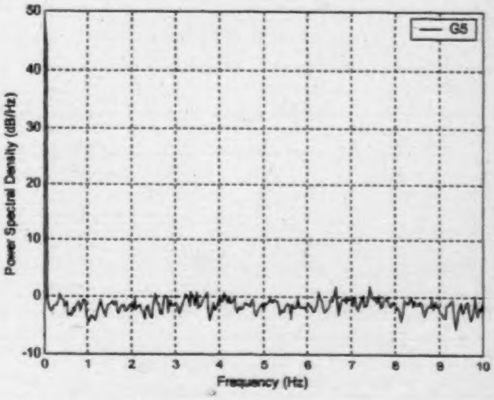

July 18, 1999
2:40 PM

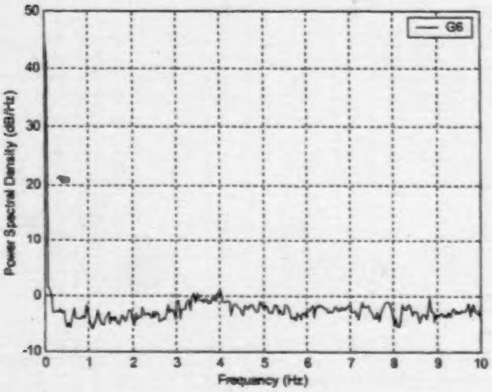

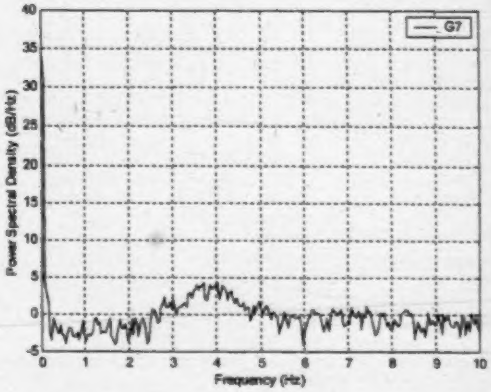

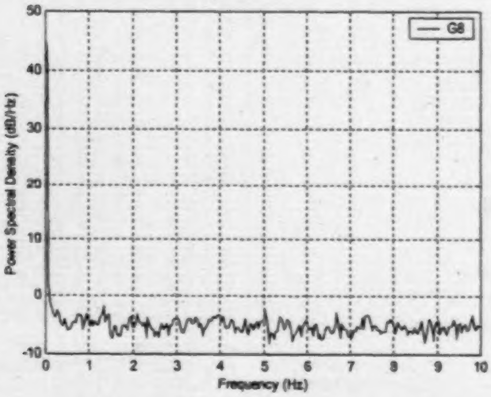

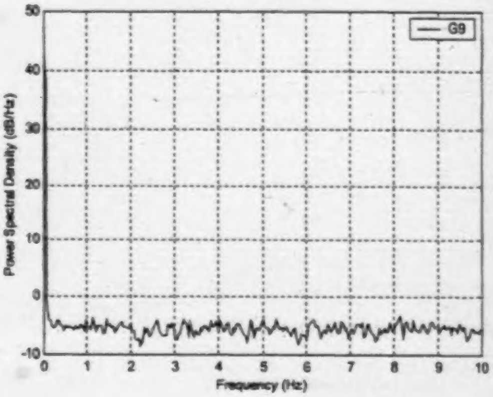

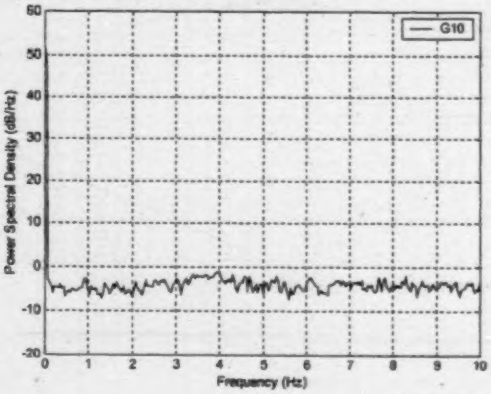

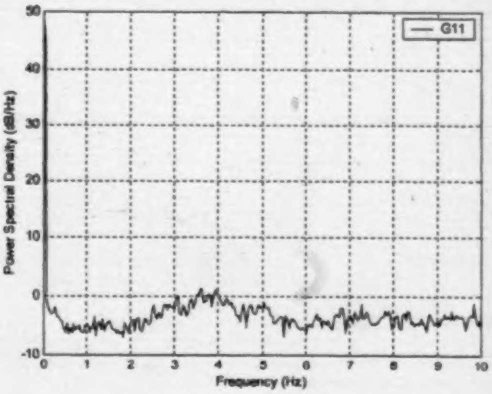

July 18, 1999
2:40 PM

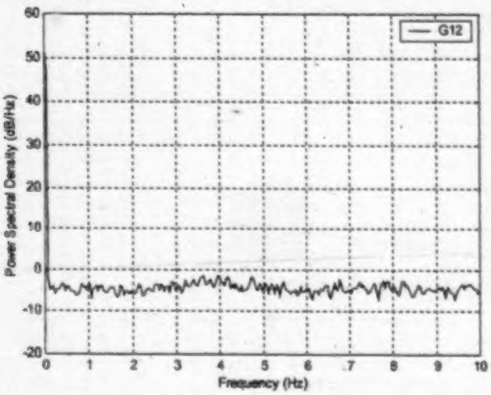

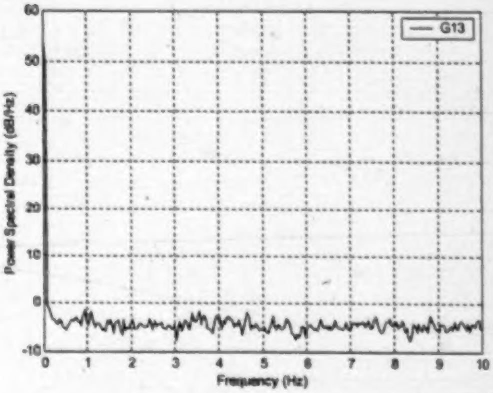

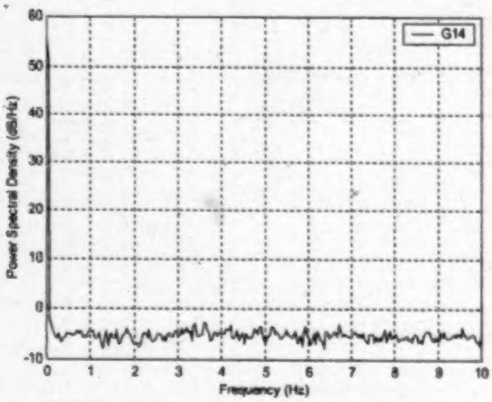

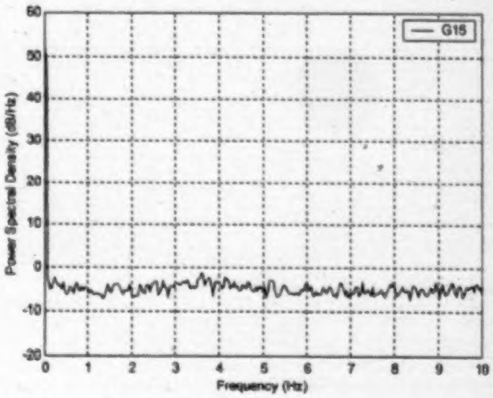

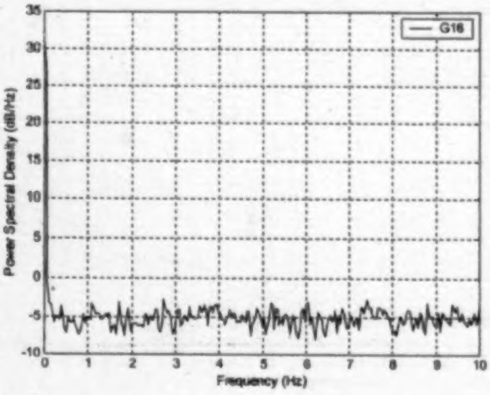

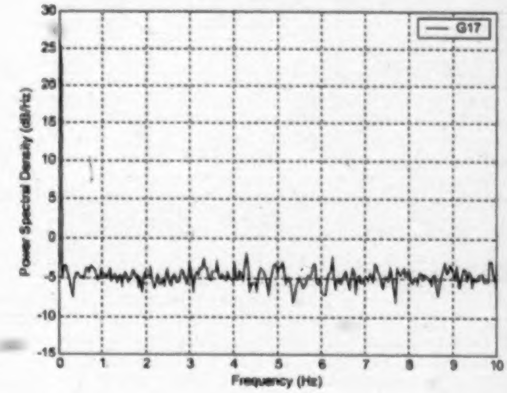

July 18, 1999
2:40 PM

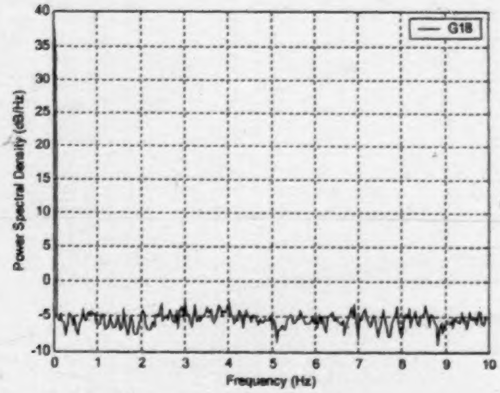

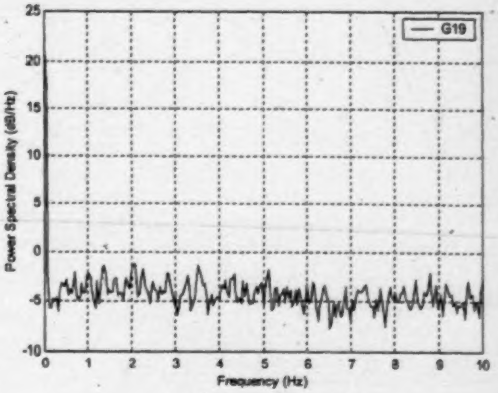

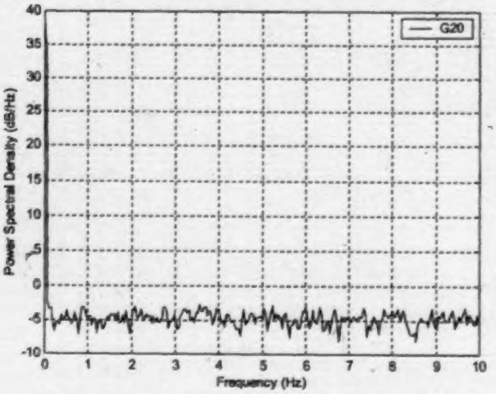

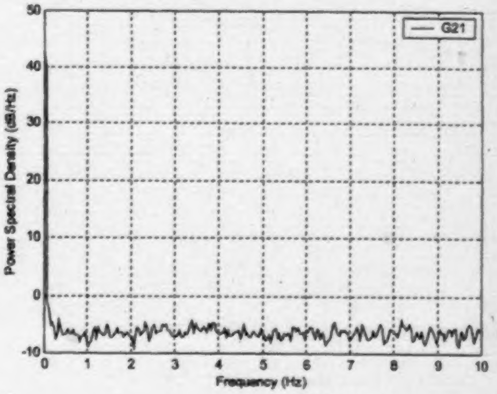

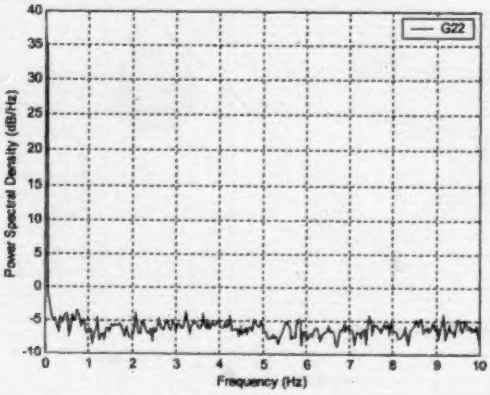

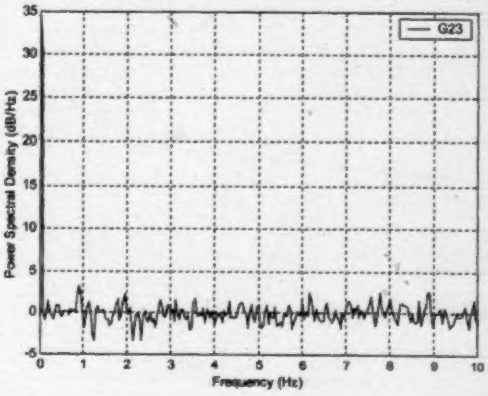

July 18, 1999
2:40 PM

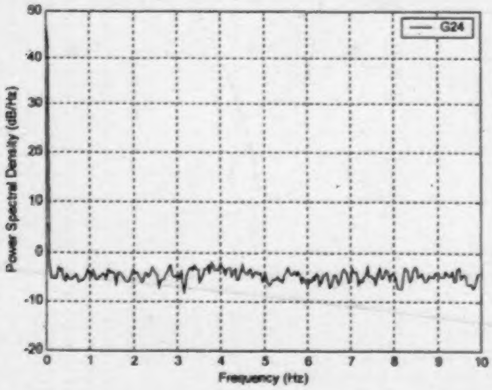

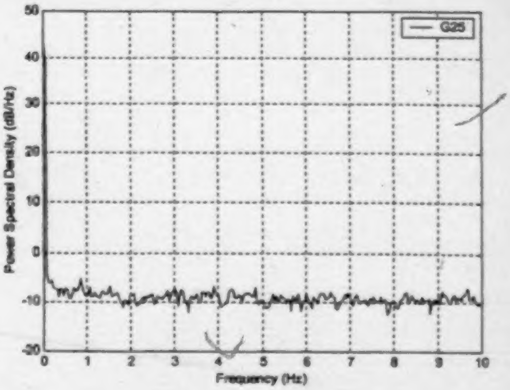

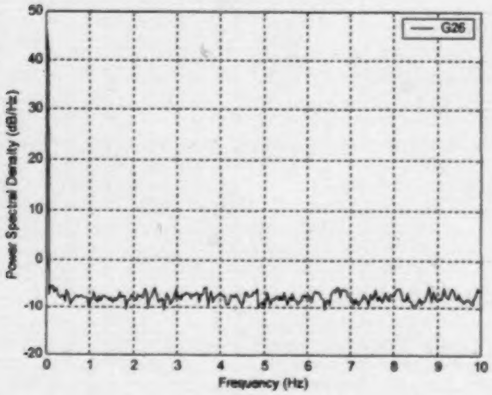

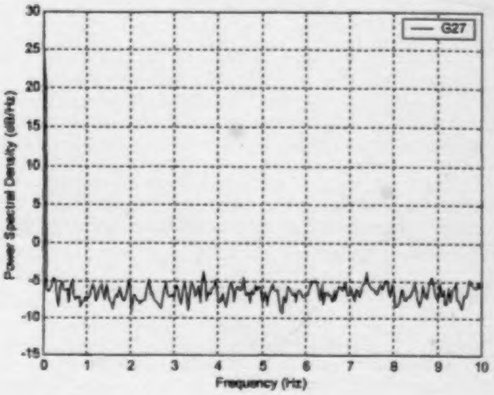

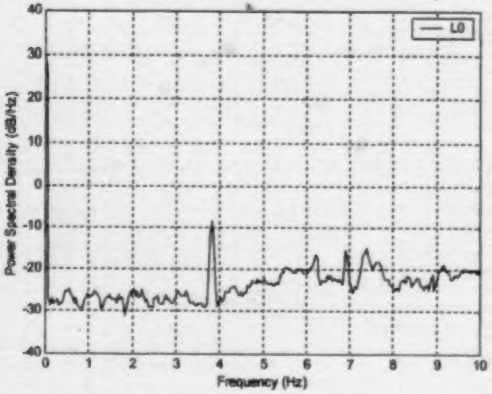

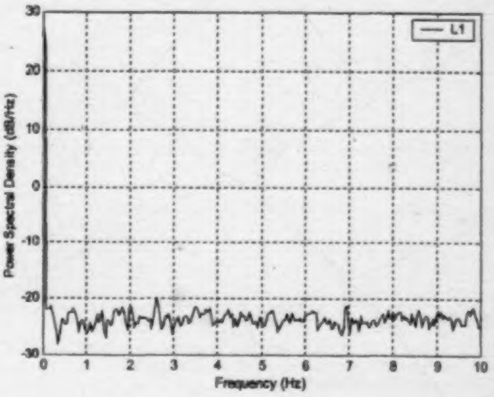

July 18, 1999
2:40 PM

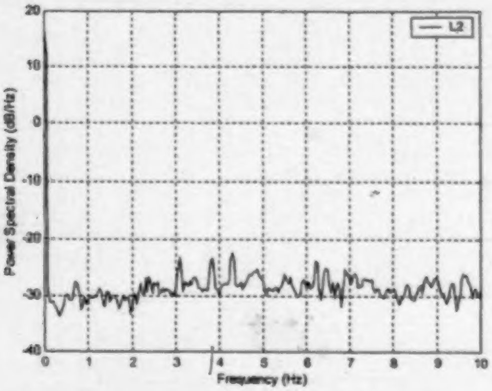

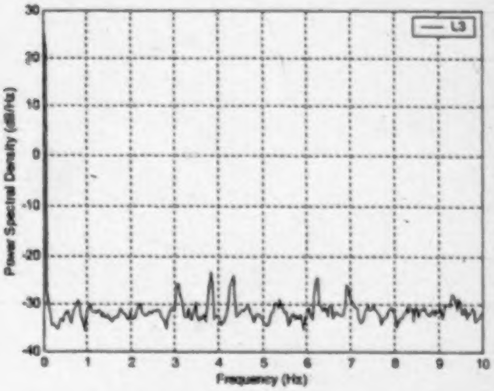

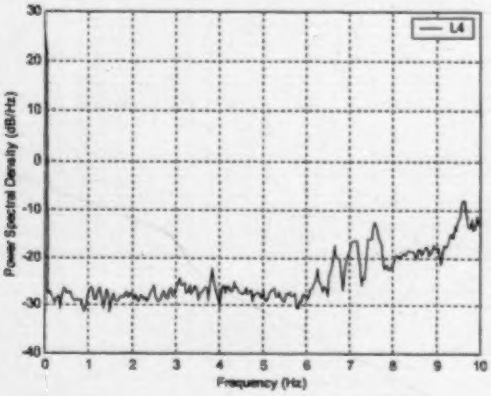

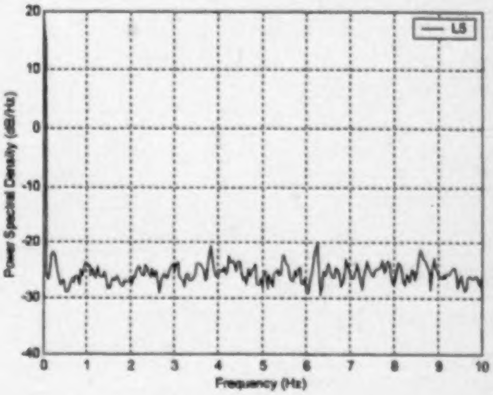

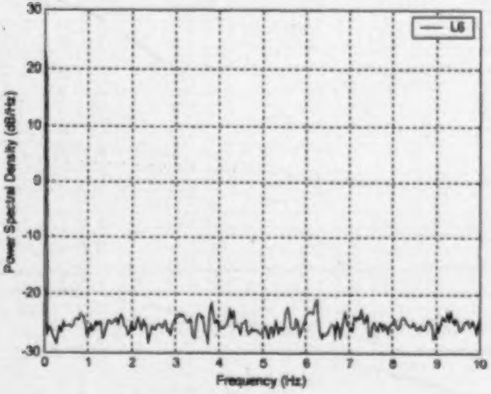

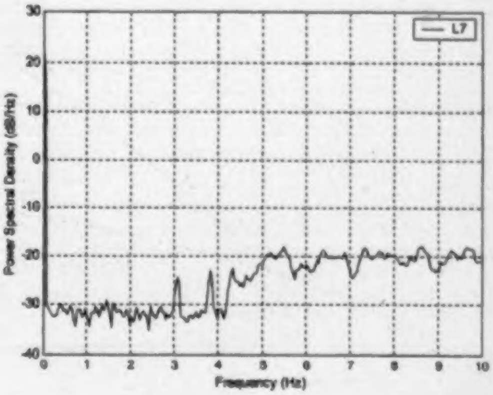

July 18, 1999
2:40 PM

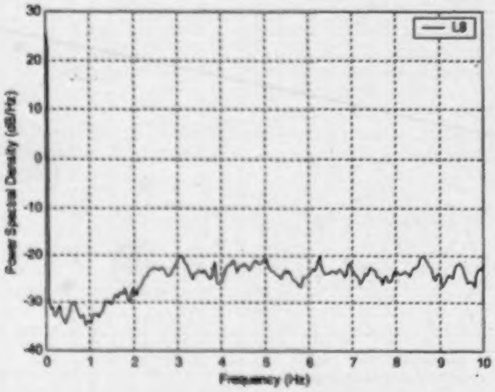

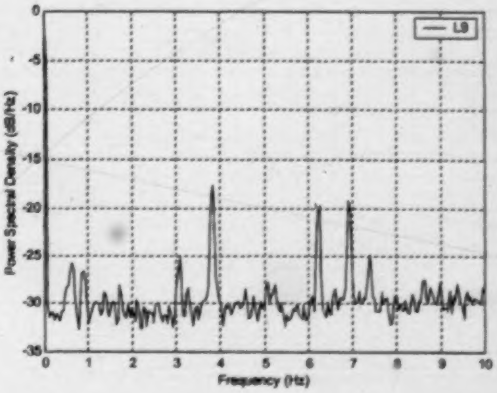

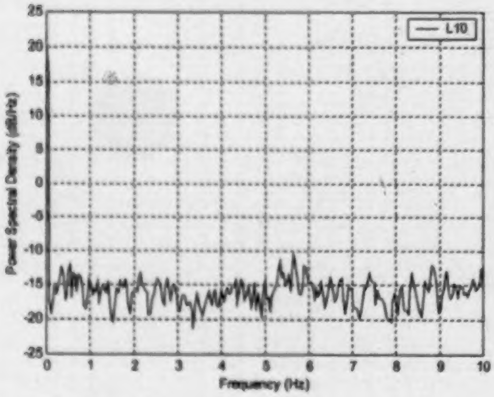

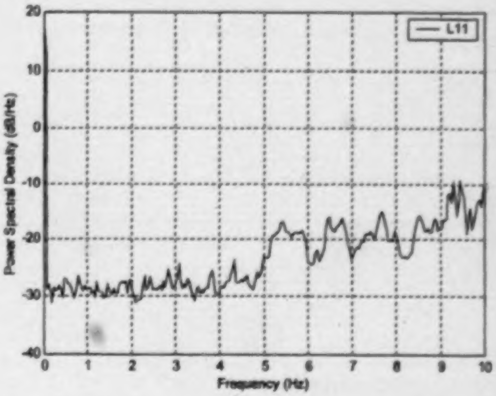

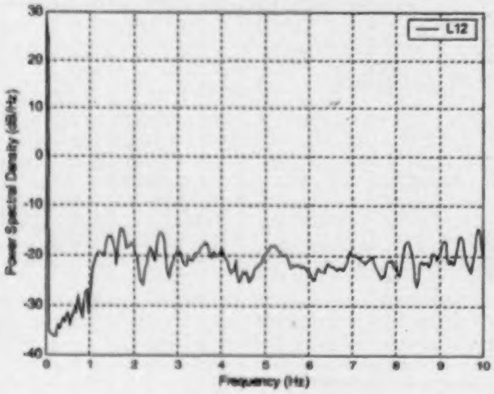

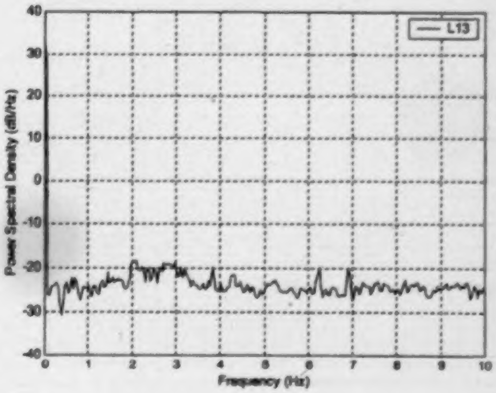

July 18, 1999
2:40 PM

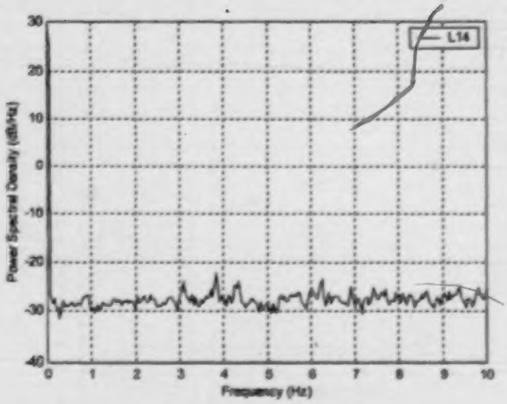

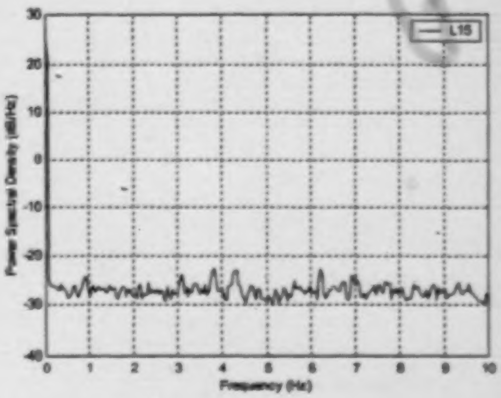

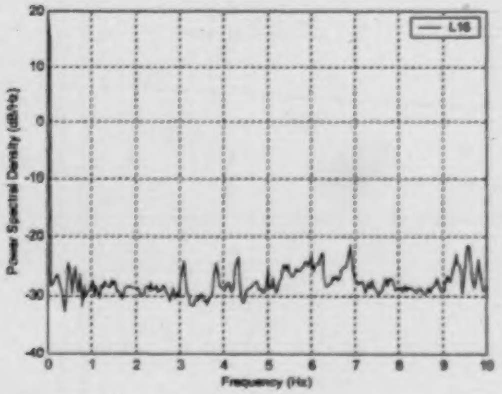

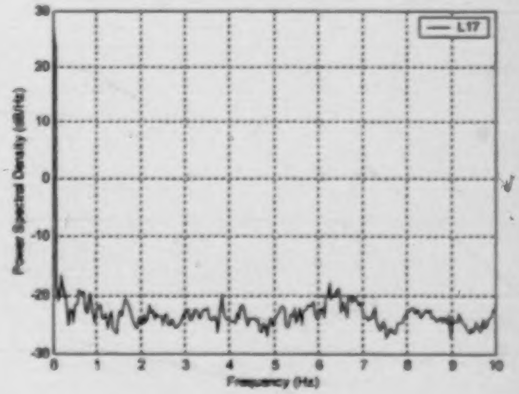

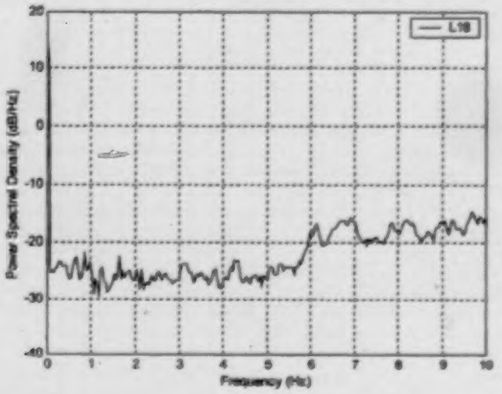

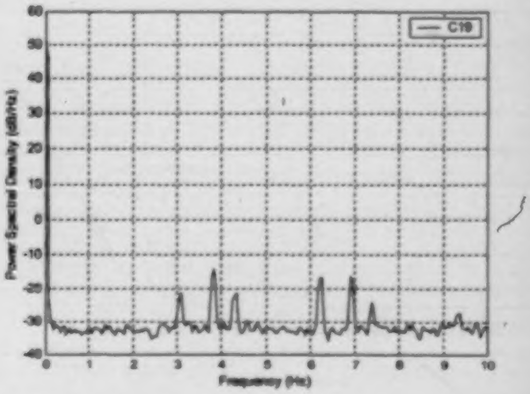

July 18, 1999
2:40 PM

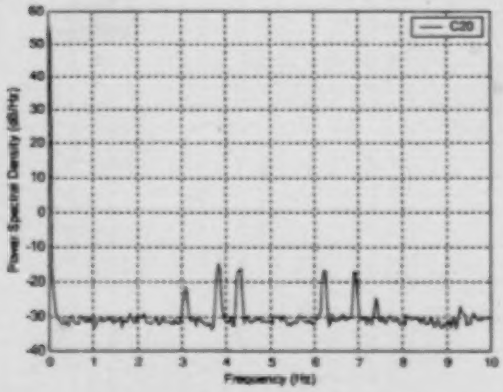

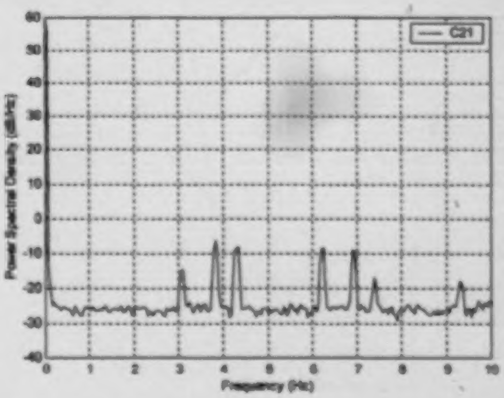

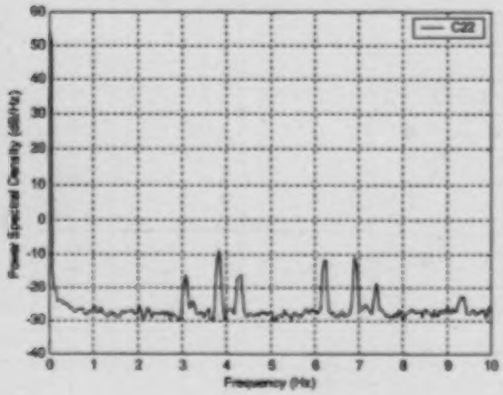

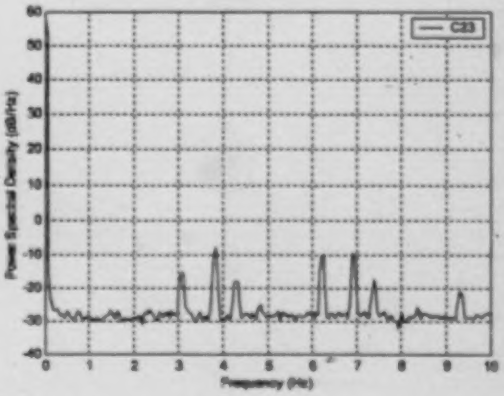

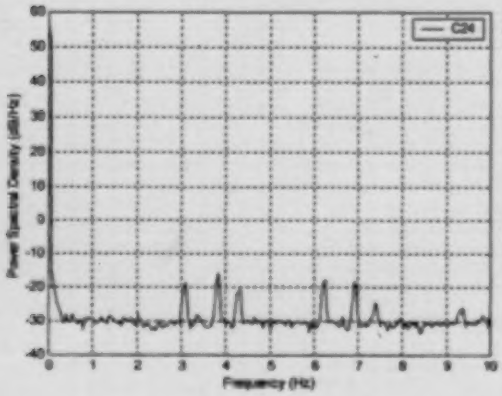

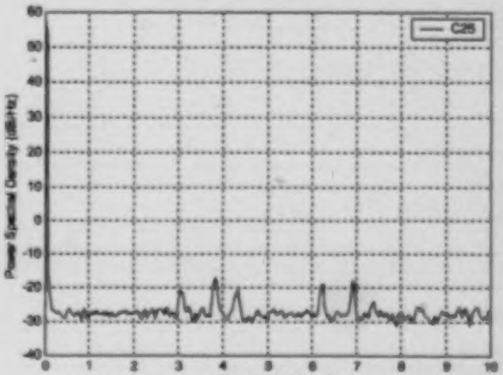

July 18, 1999
2:40 PM

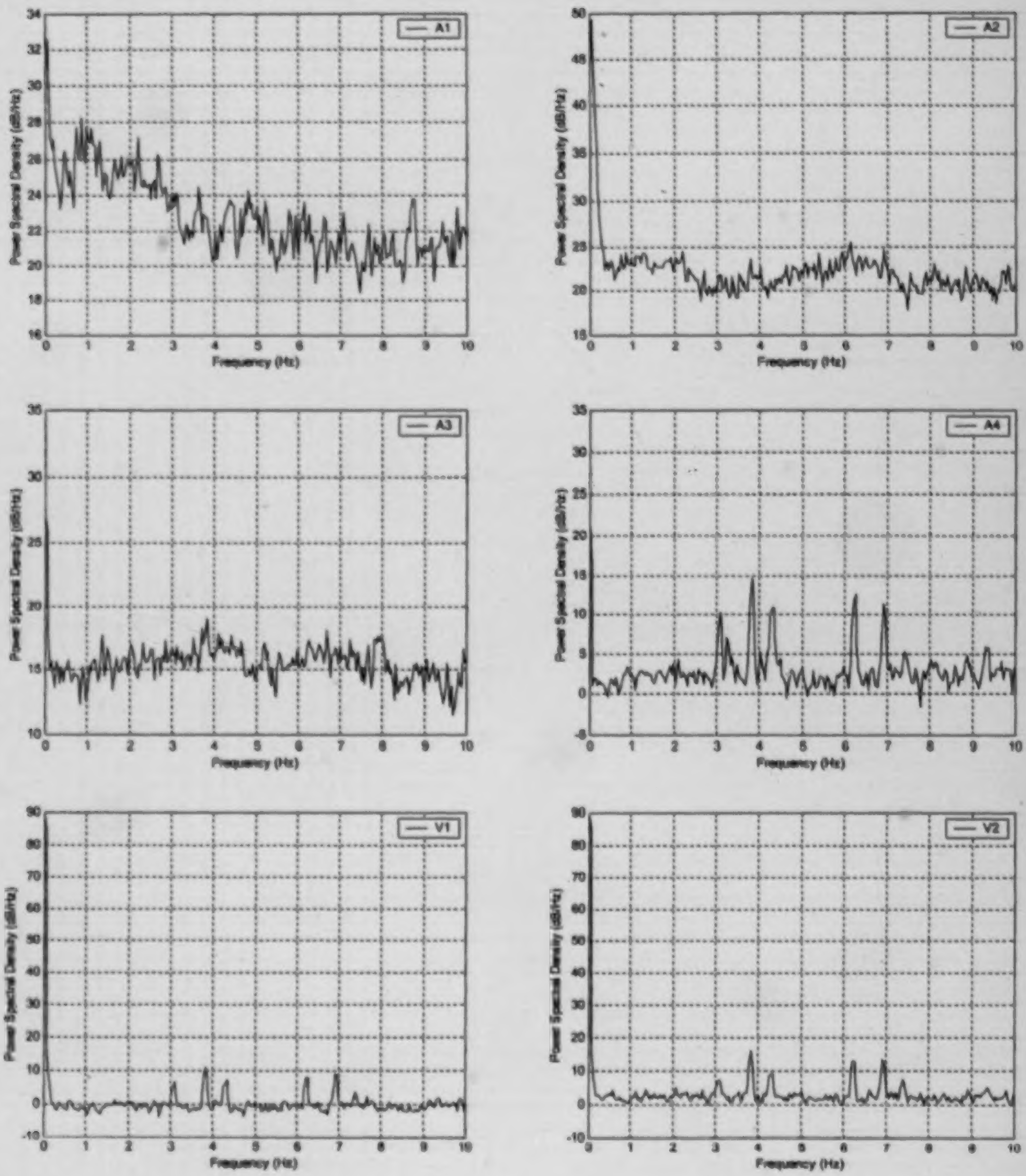

July 18, 1999
2:46 PM

July 18, 1999
2:46 PM

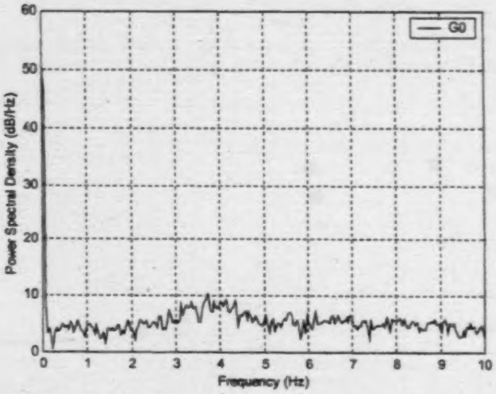

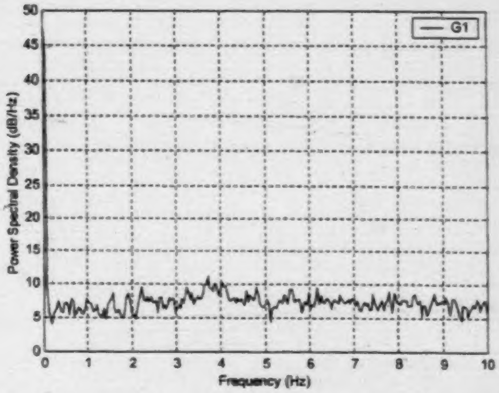

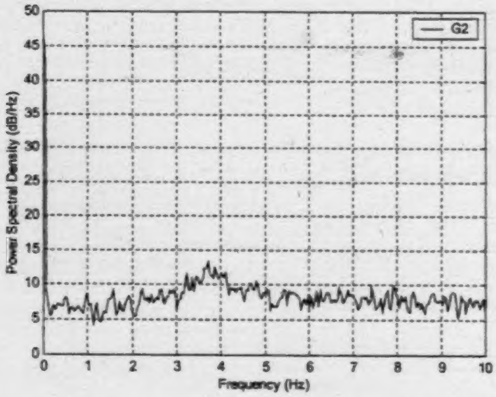

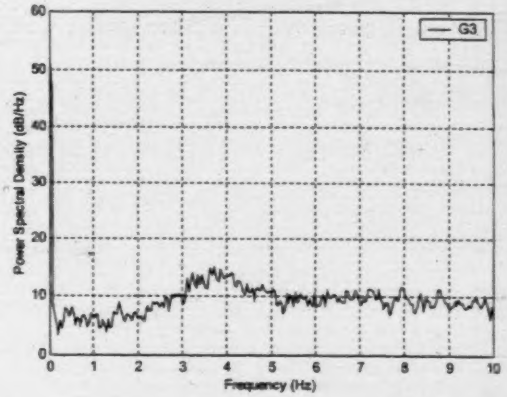

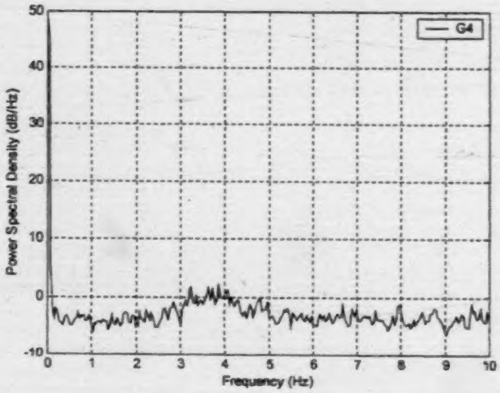

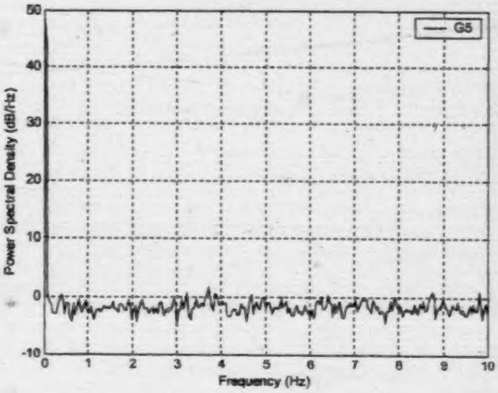

July 18, 1999
2:46 PM

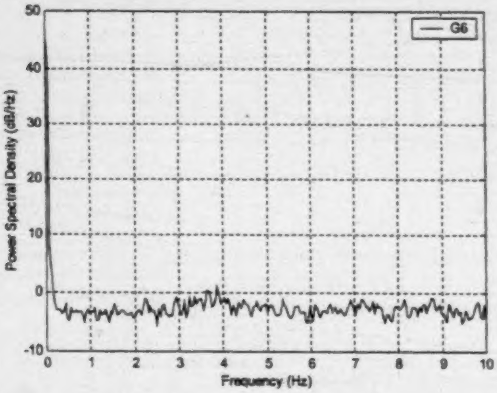

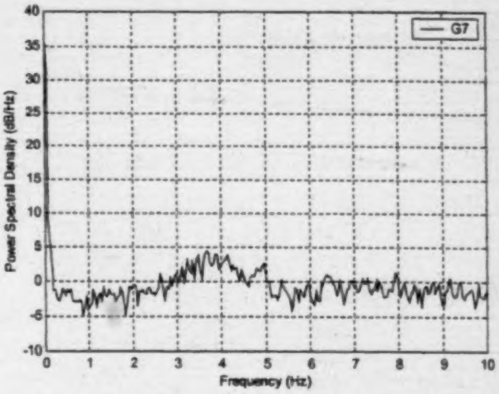

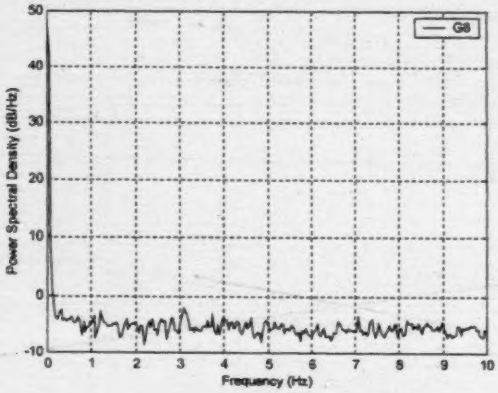

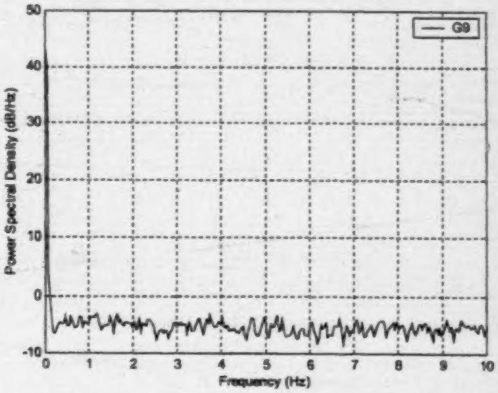

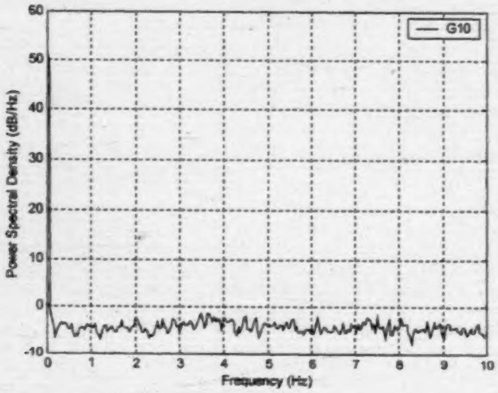

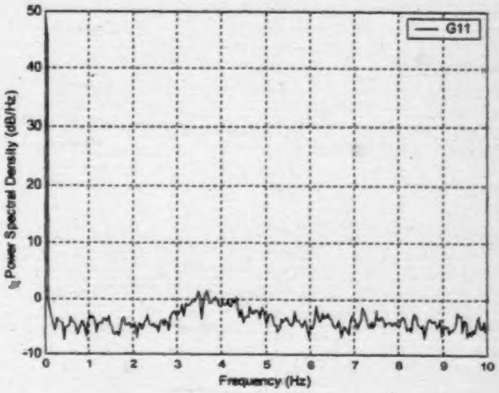

July 18, 1999
2:46 PM

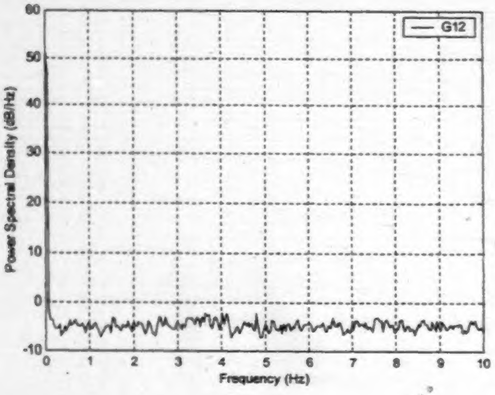

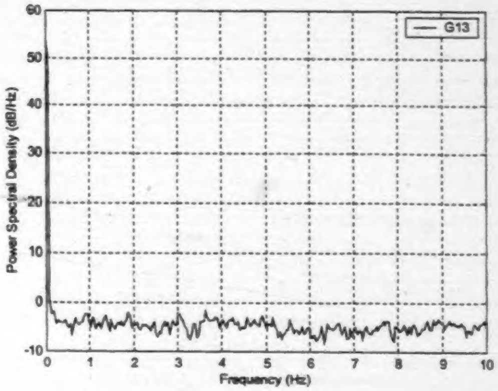

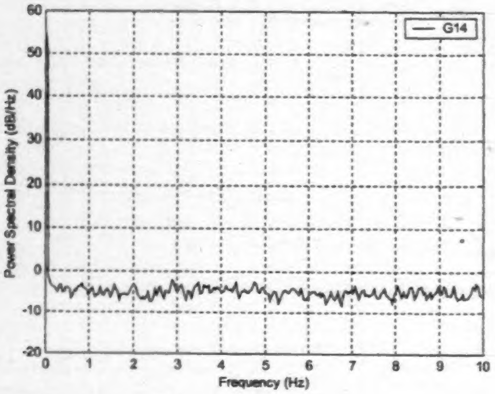

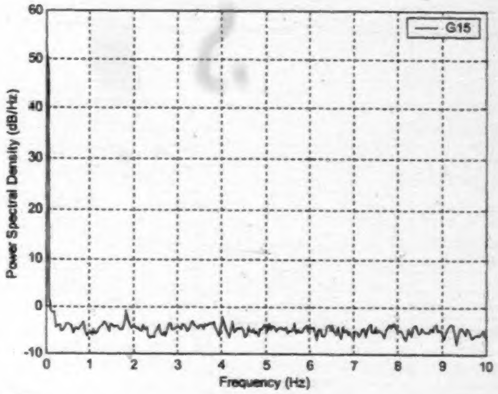

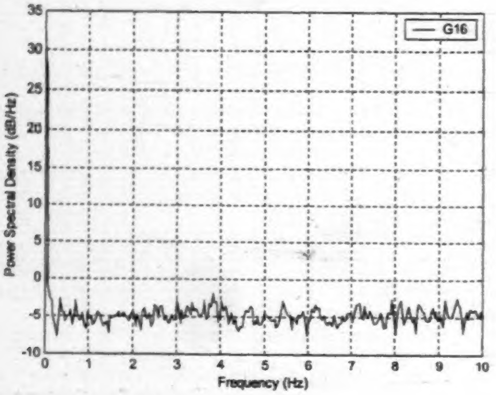

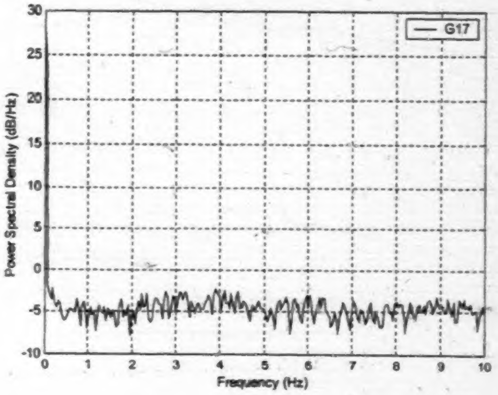

July 18, 1999
2:46 PM

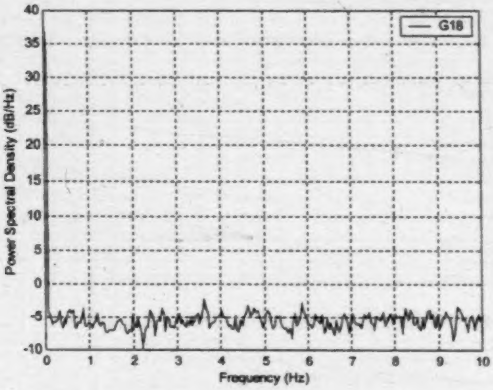

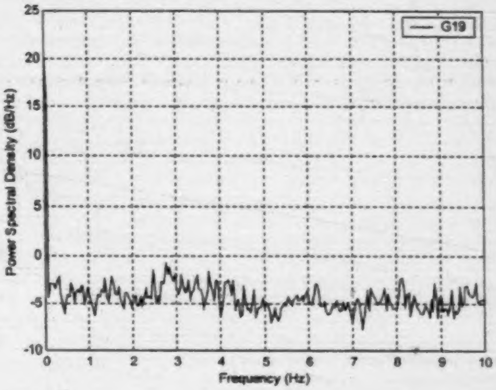

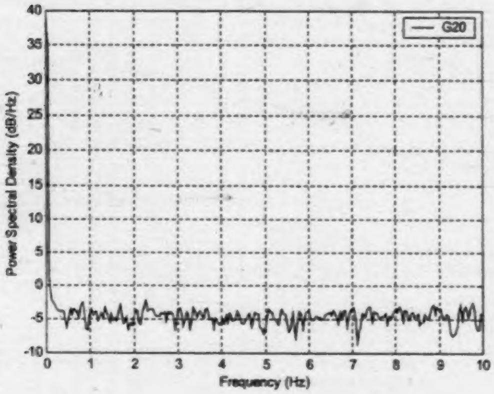

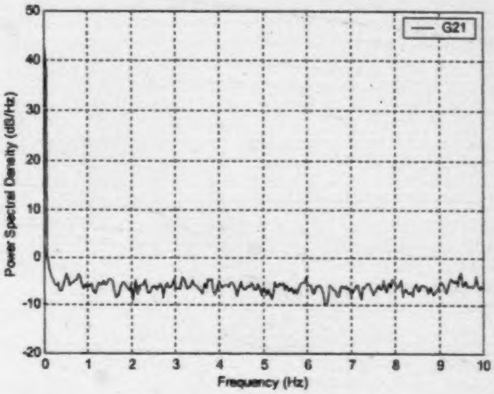

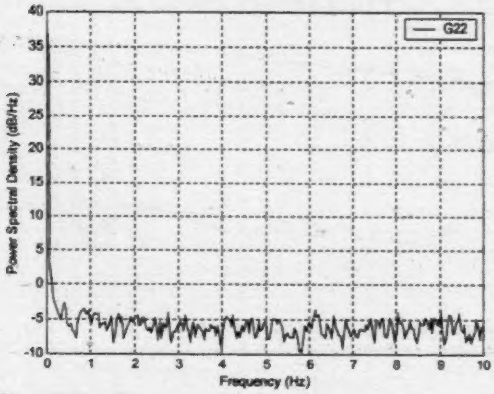

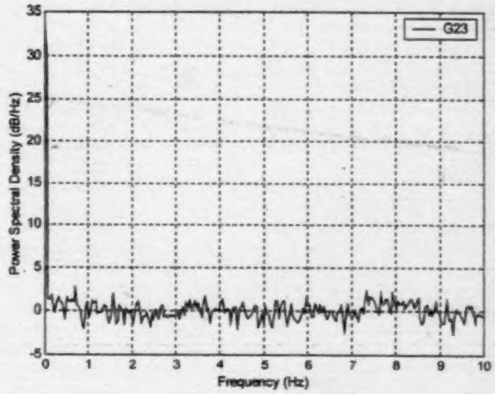

July 18, 1999
2:46 PM

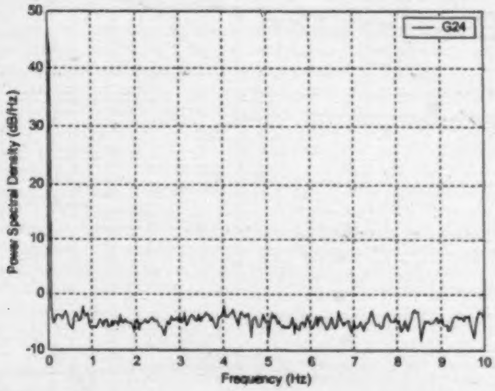

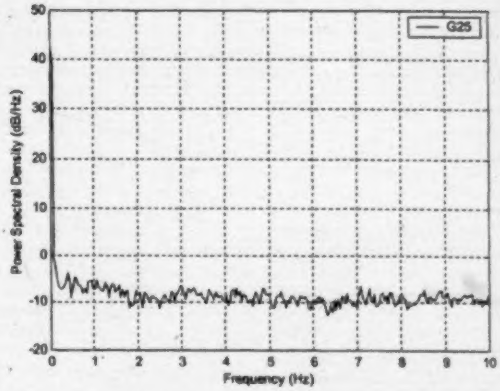

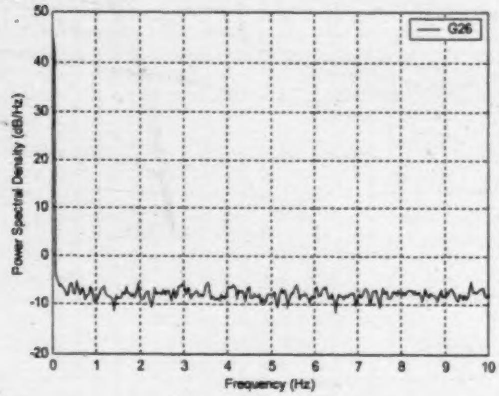

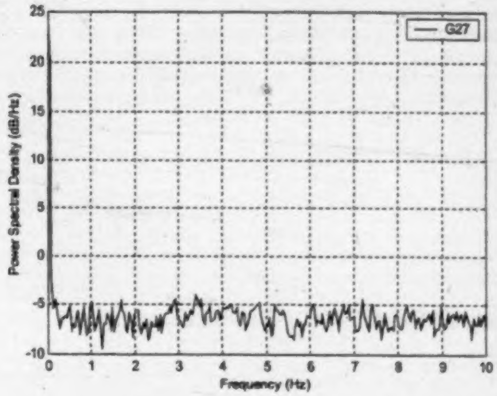

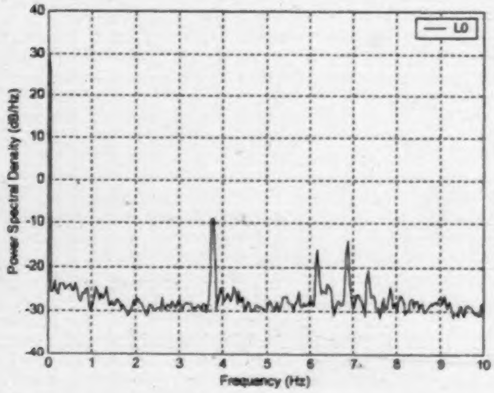

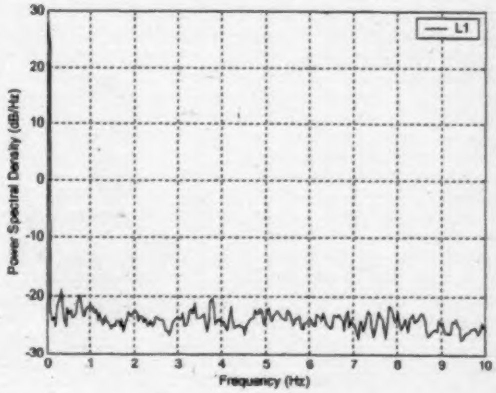

July 18, 1999
2:46 PM

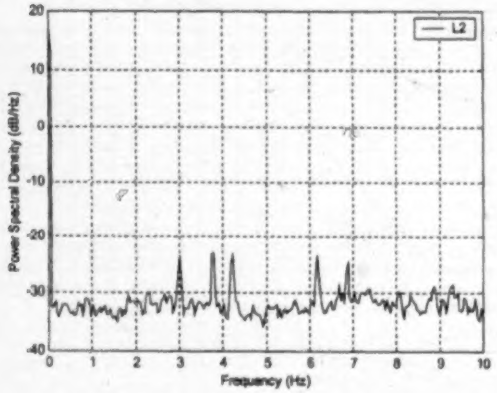

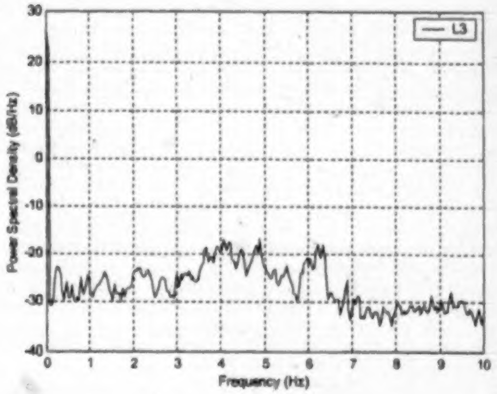

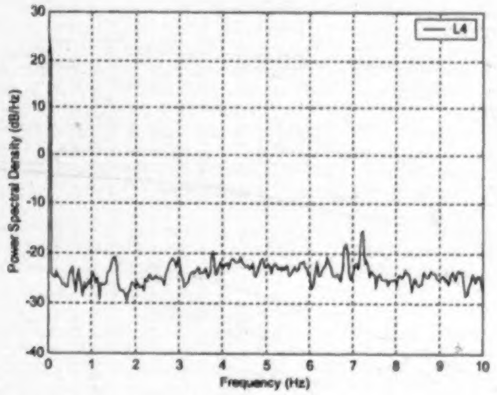

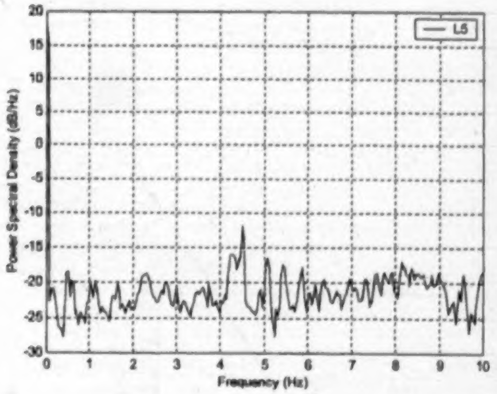

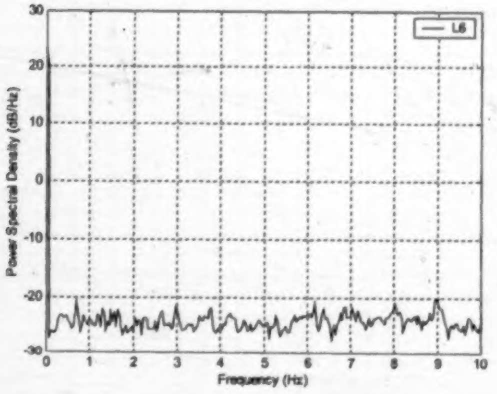

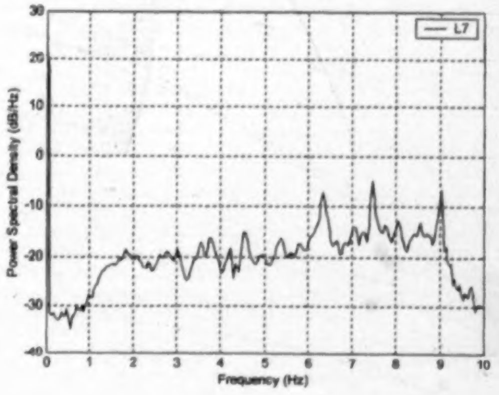

July 18, 1999
2:46 PM

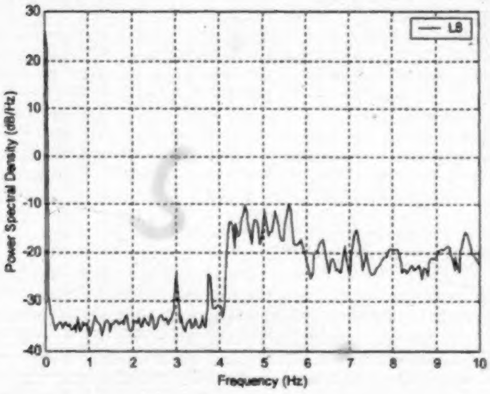

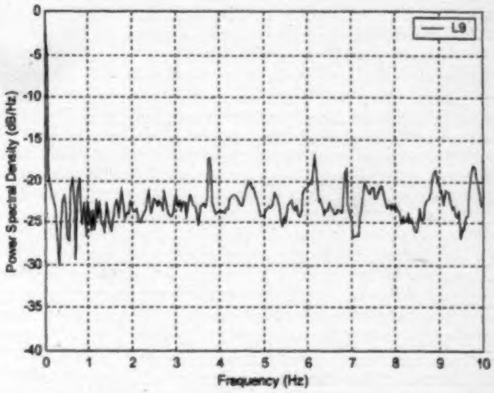

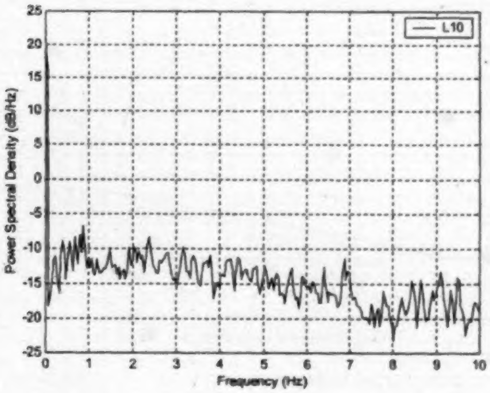

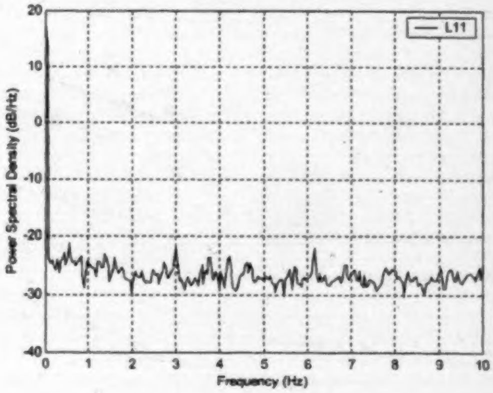

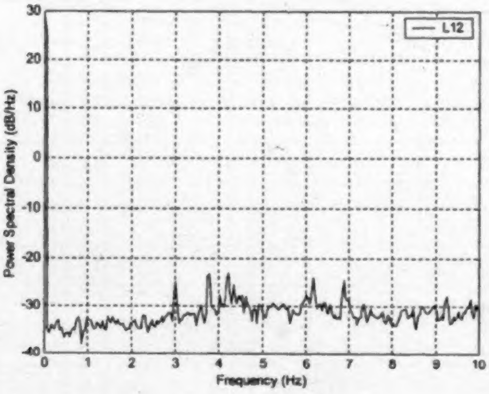

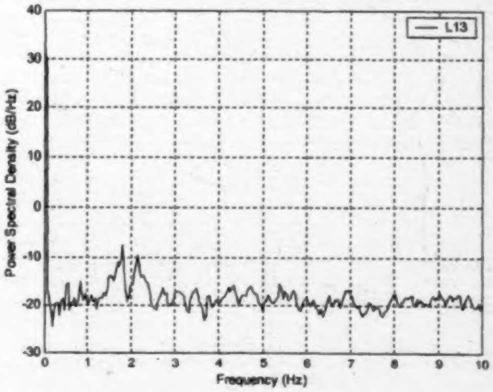

July 18, 1999
2:46 PM

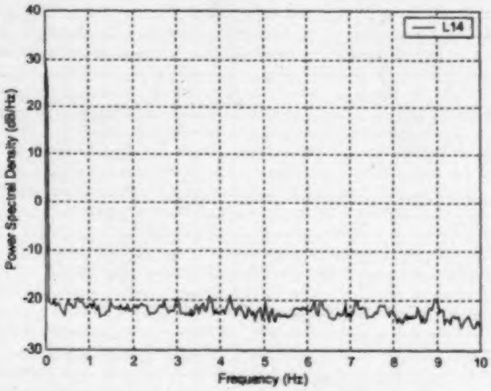

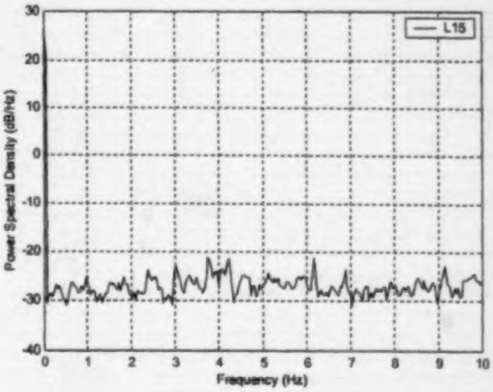

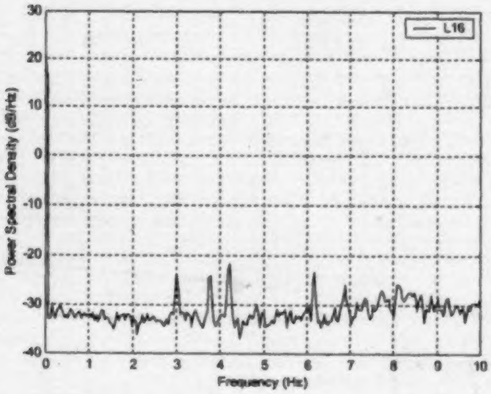

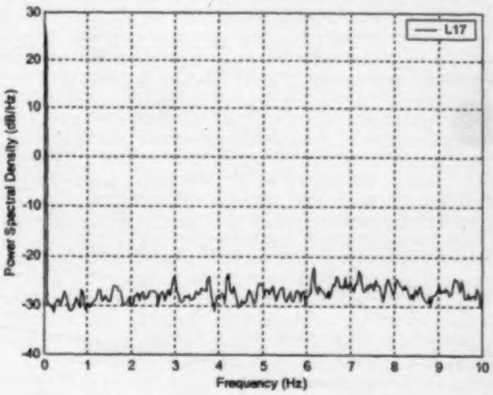

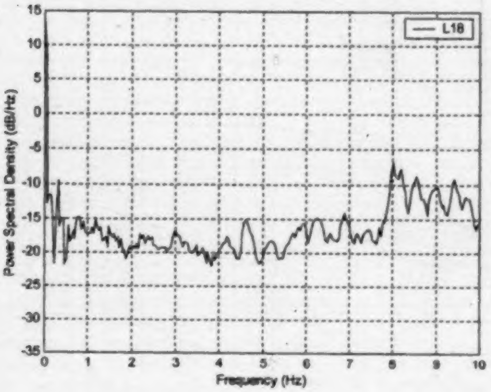

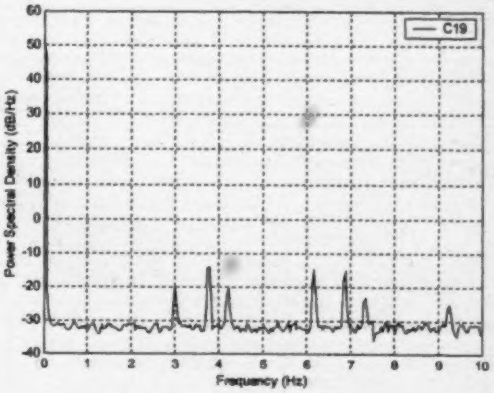

July 18, 1999
2:46 PM

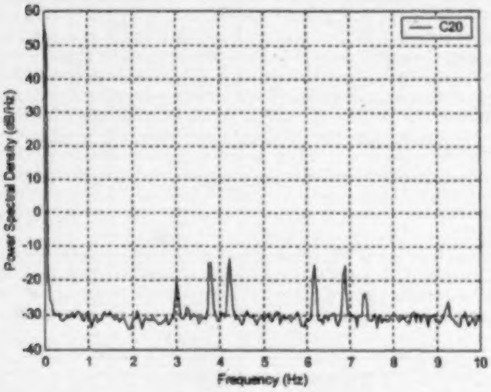

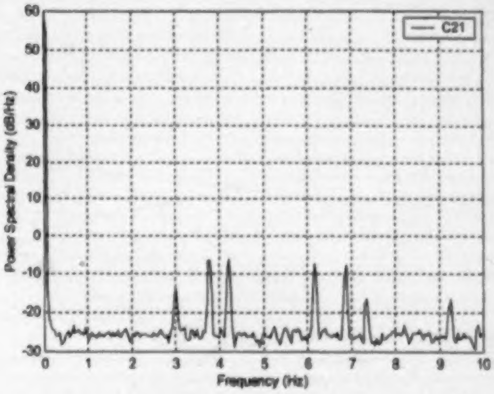

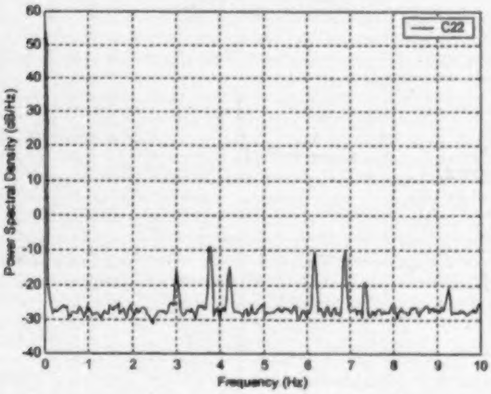

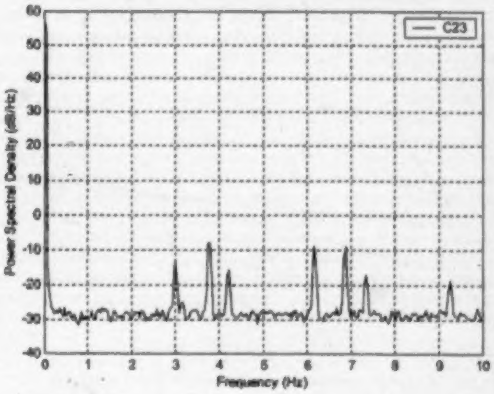

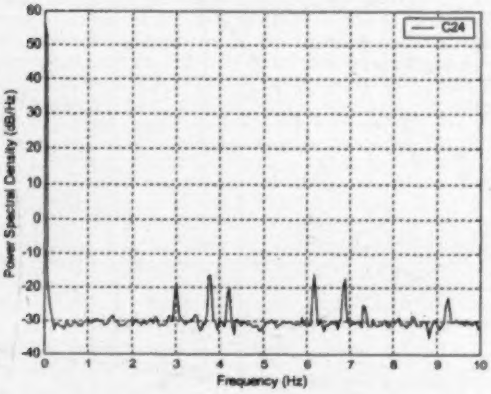

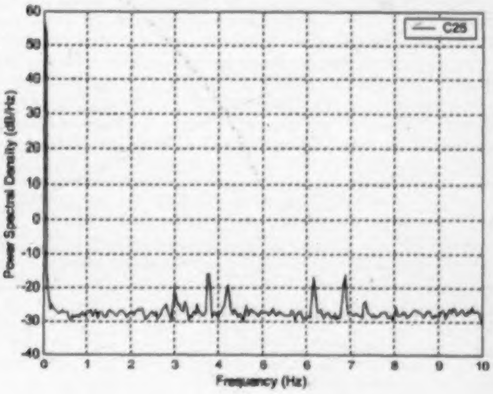

July 18, 1999
2:46 PM

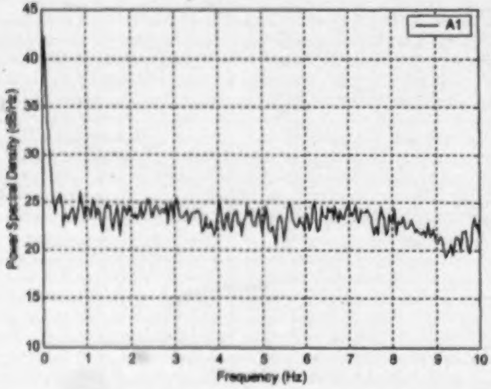

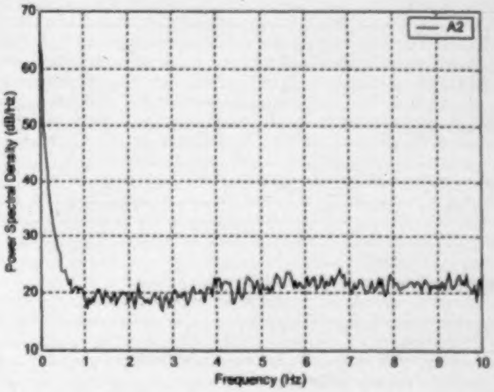

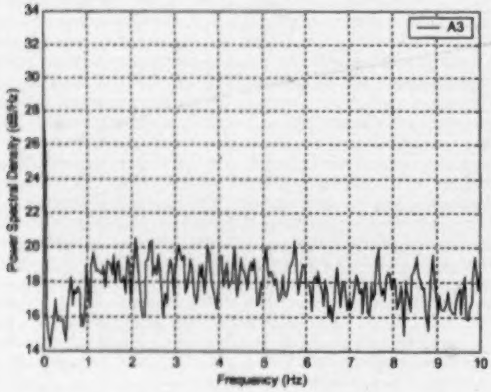

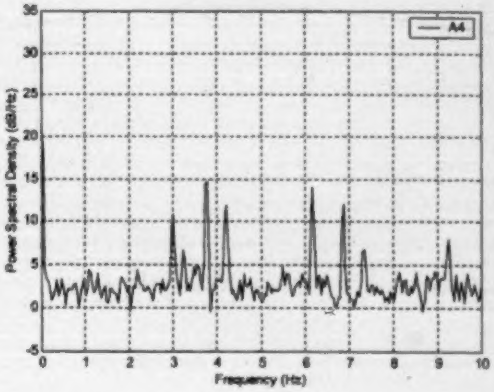

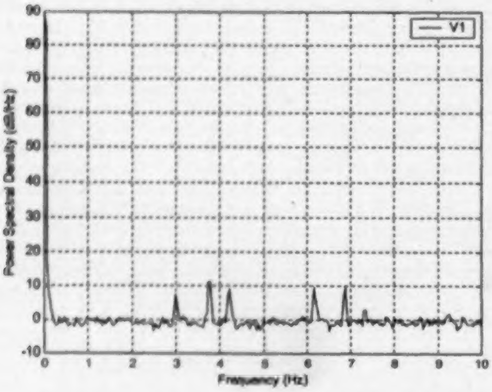

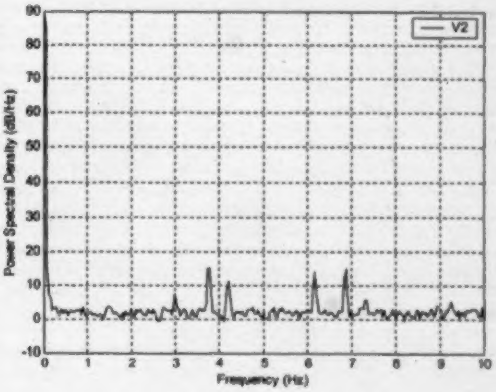

July 18, 1999
2:57 PM

July 18, 1999
2:57 PM

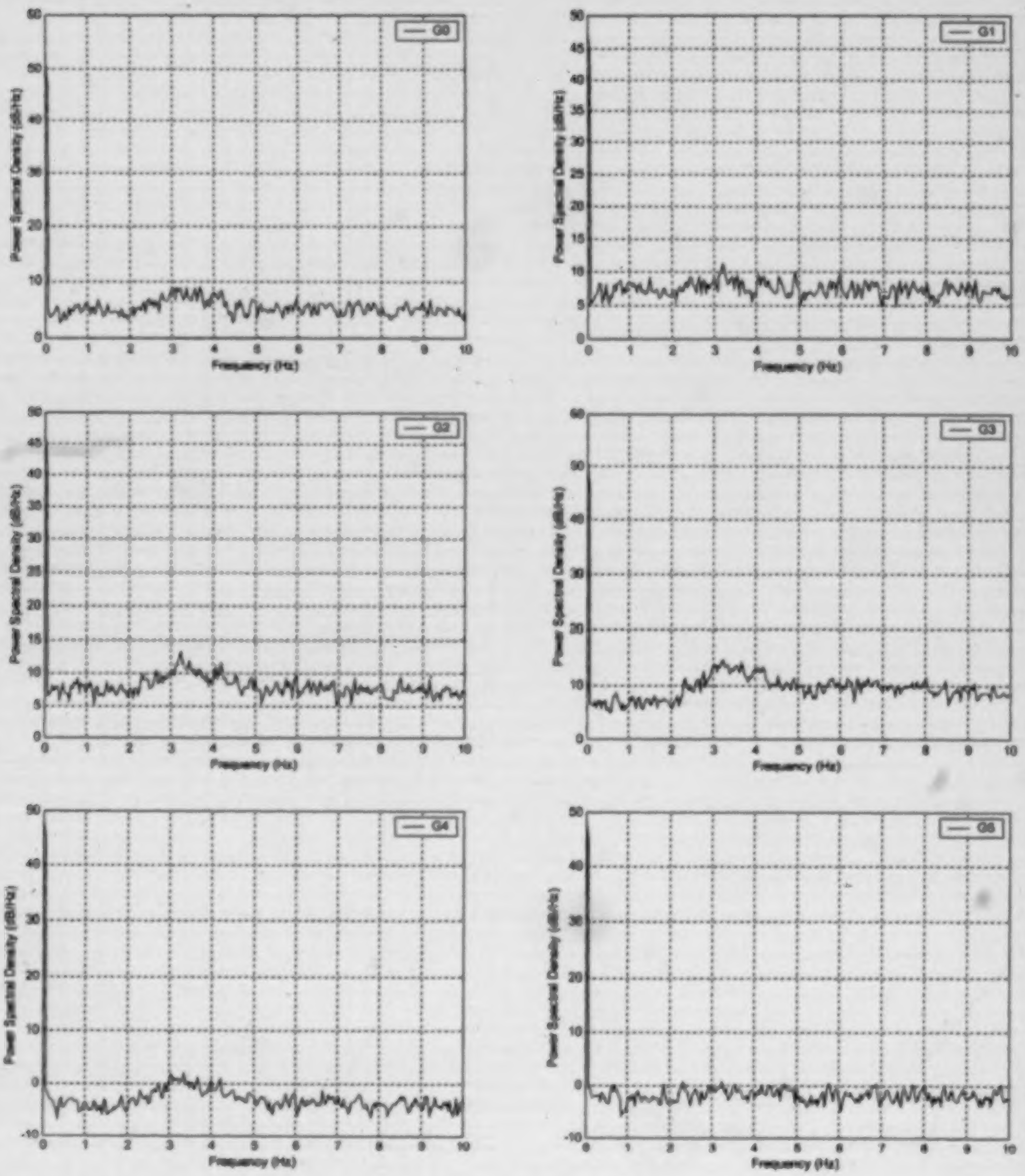

July 18, 1999
2:57 PM

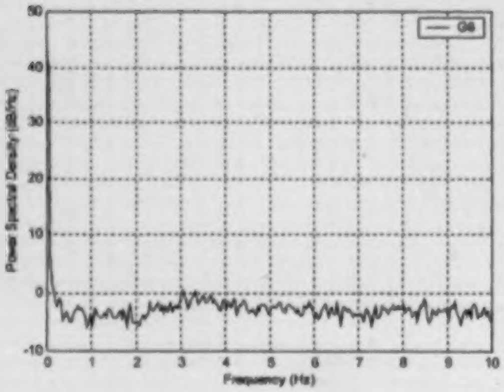

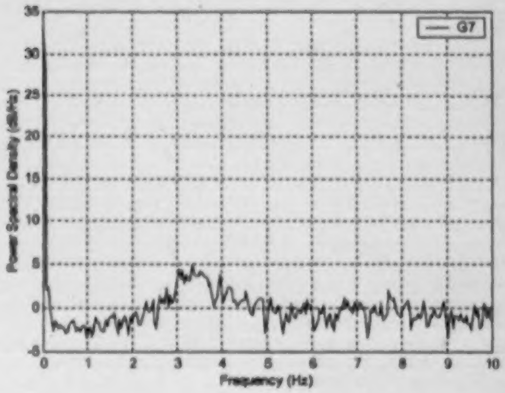

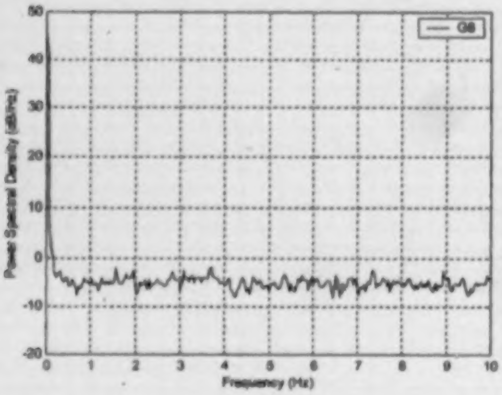

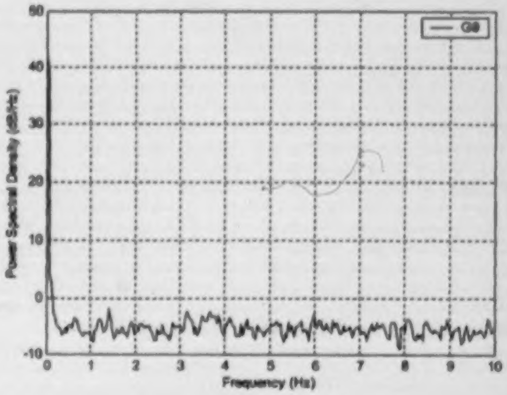

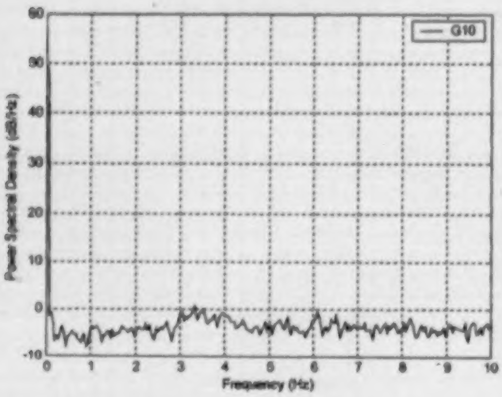

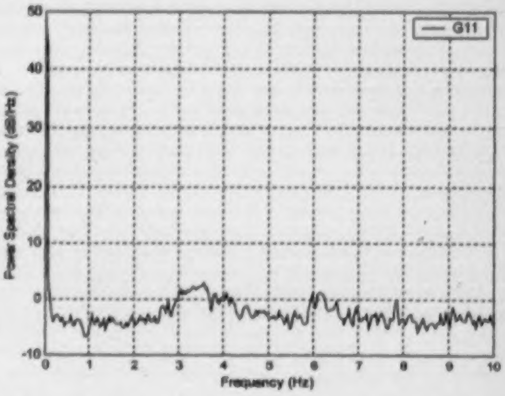

July 18, 1999
2:57 PM

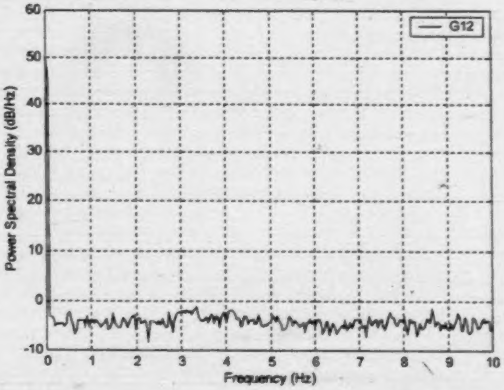

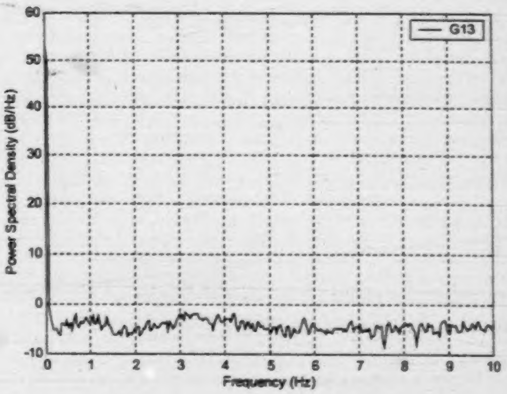

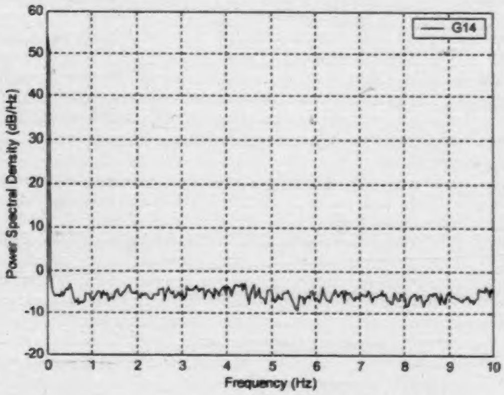

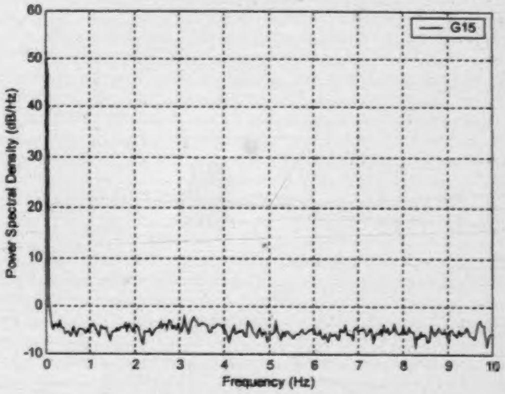

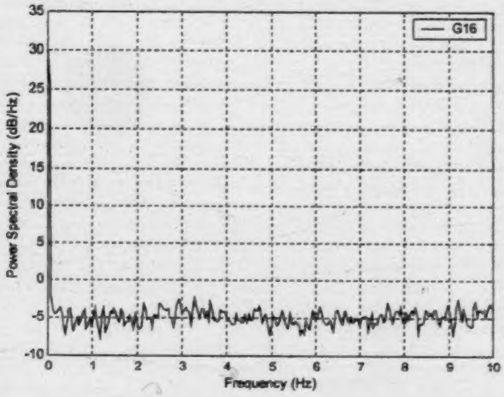

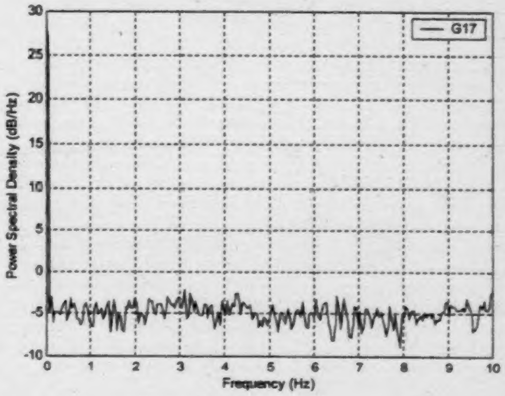

July 18, 1999
2:57 PM

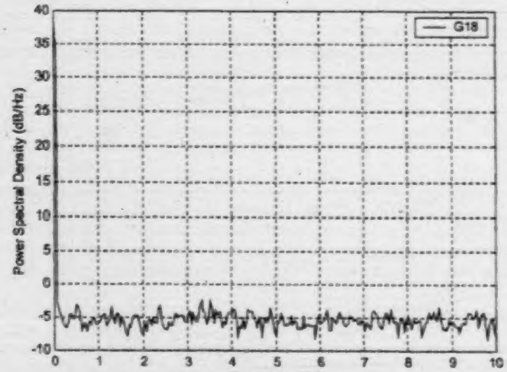

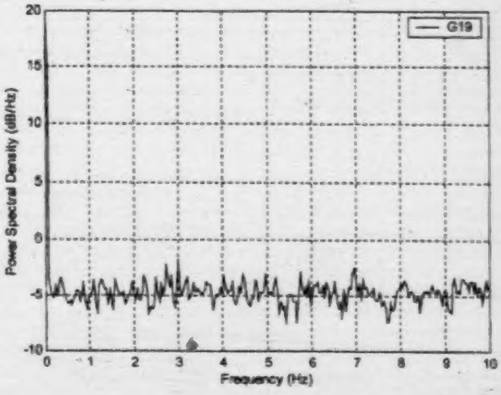

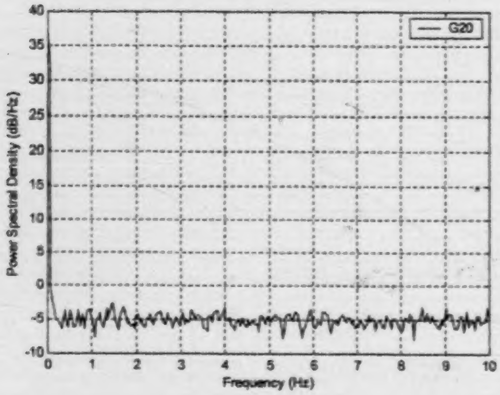

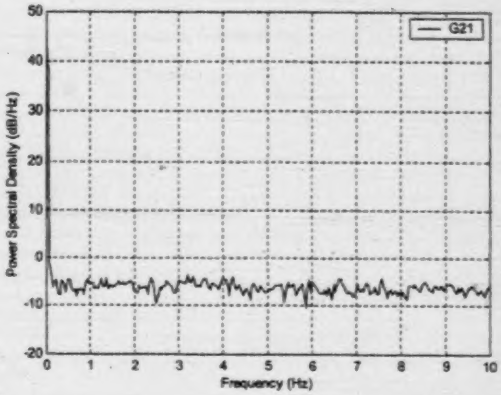

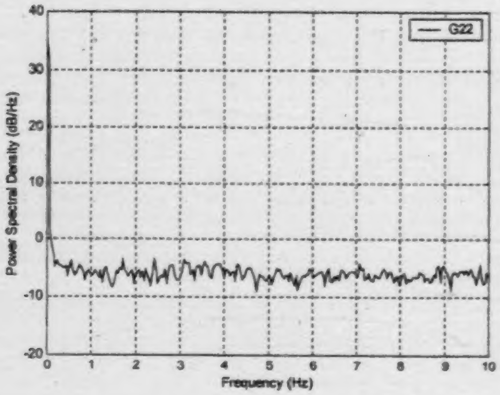

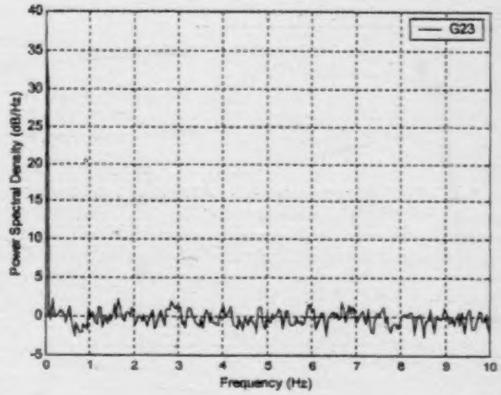

July 18, 1999
2:57 PM

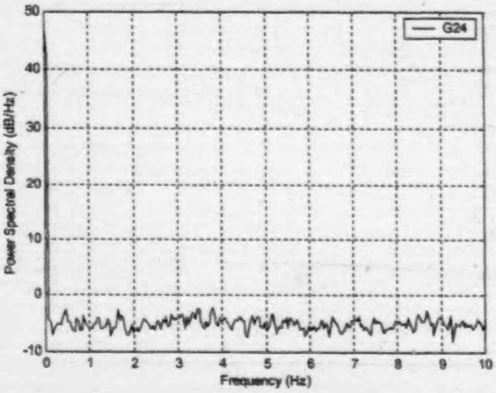

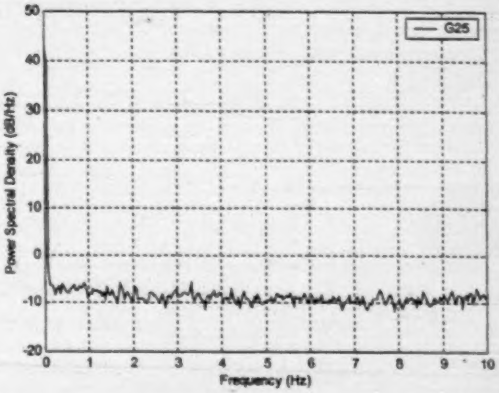

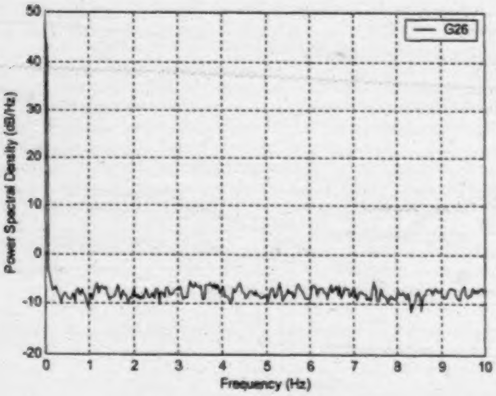

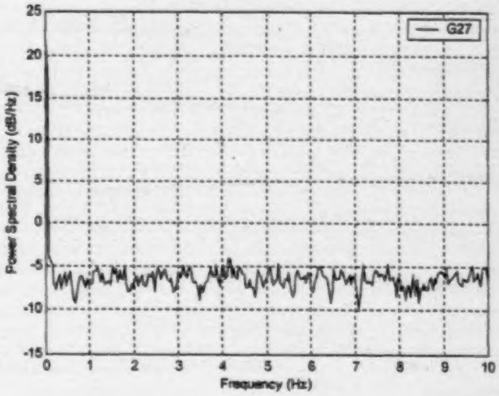

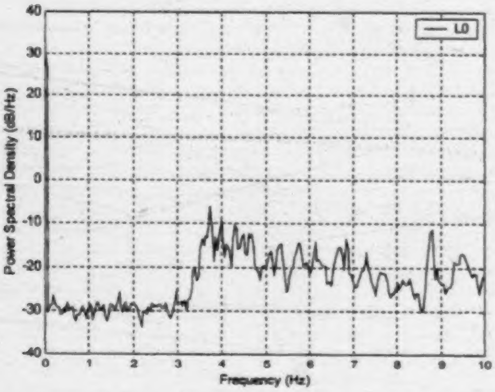

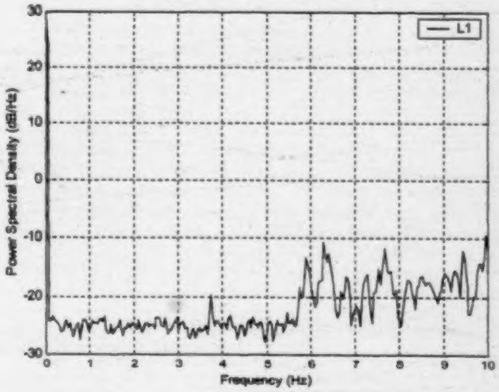

July 18, 1999
2:57 PM

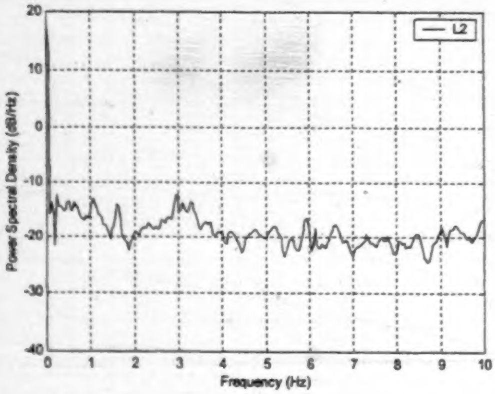

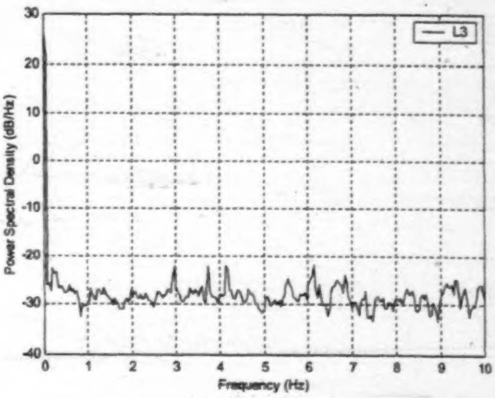

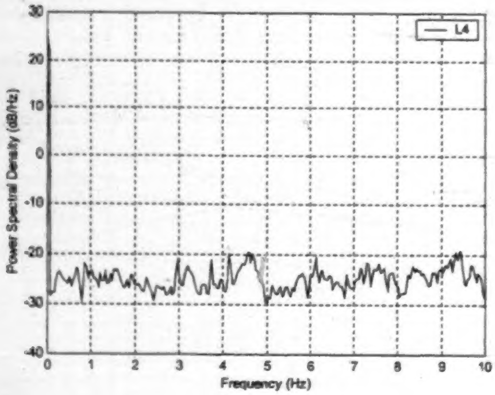

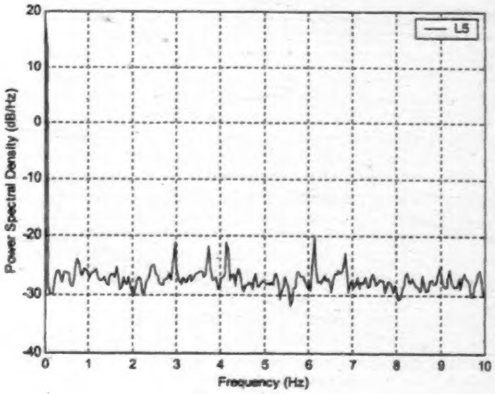

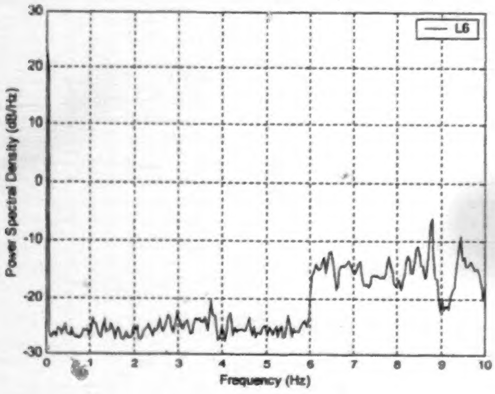

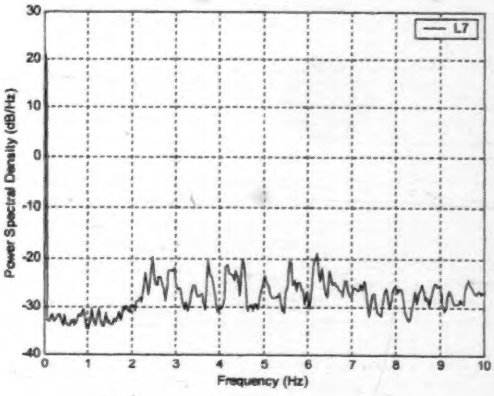

July 18, 1999
2:57 PM

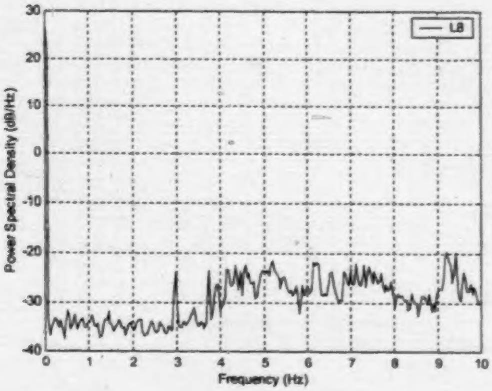

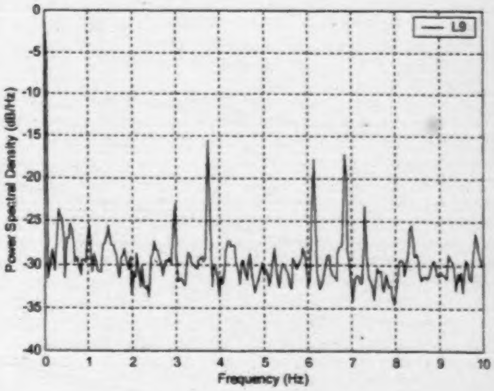

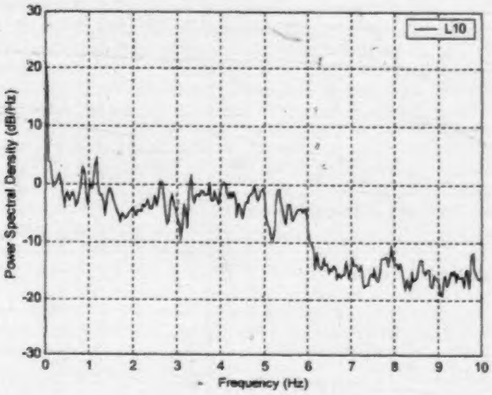

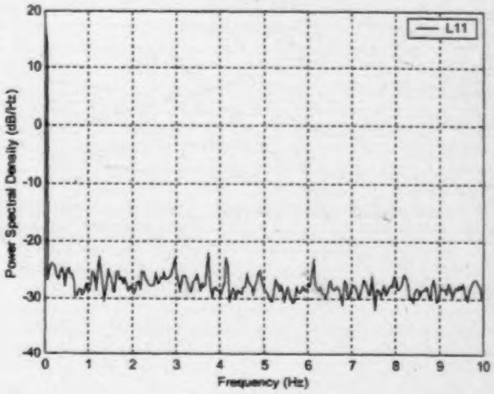

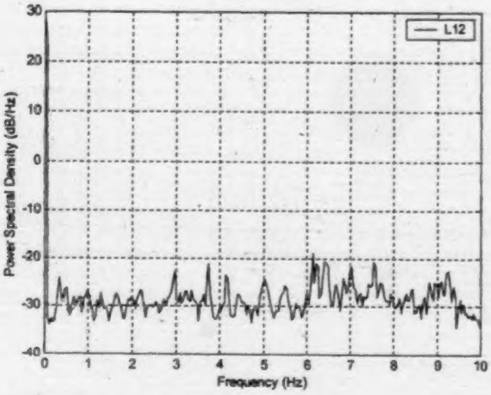

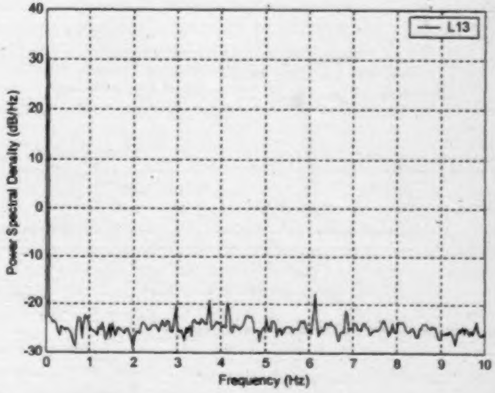

July 18, 1999
2:57 PM

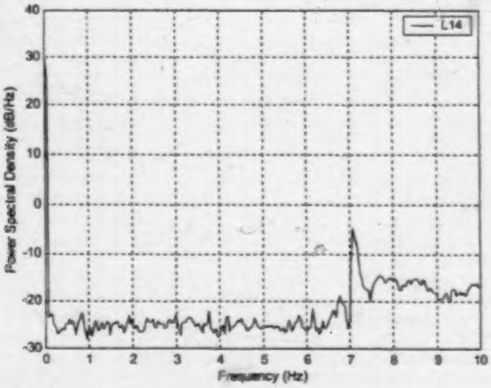

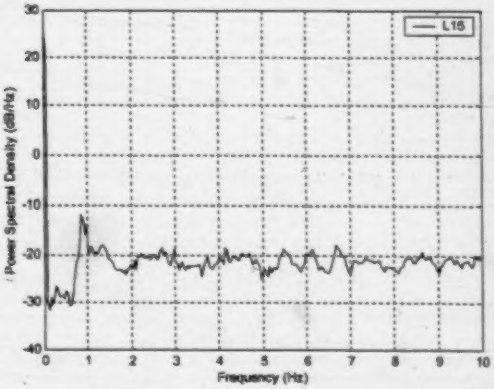

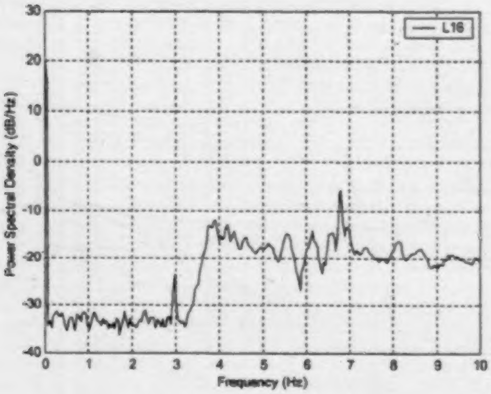

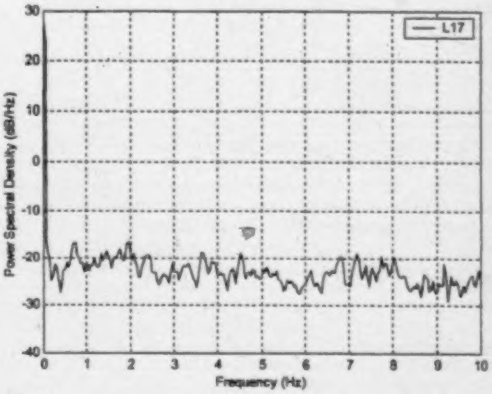

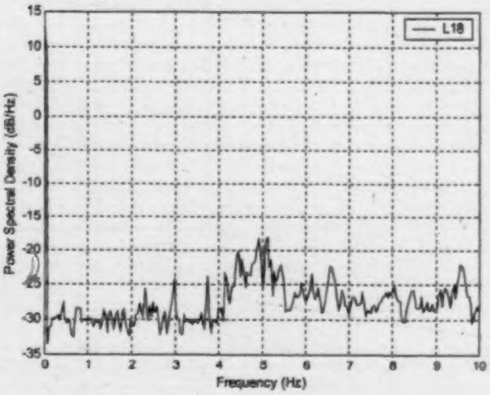

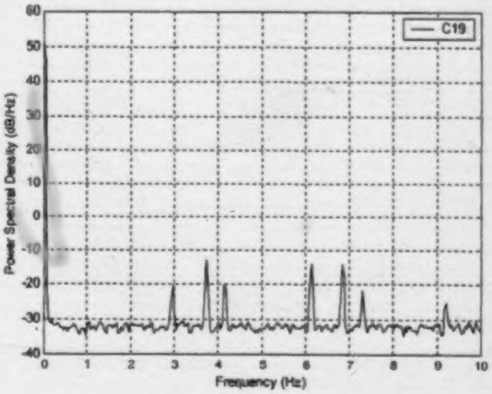

July 18, 1999
2:57 PM

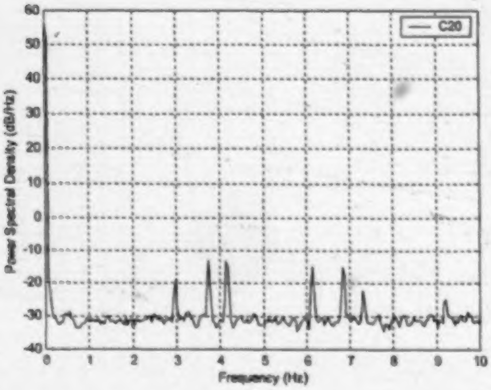

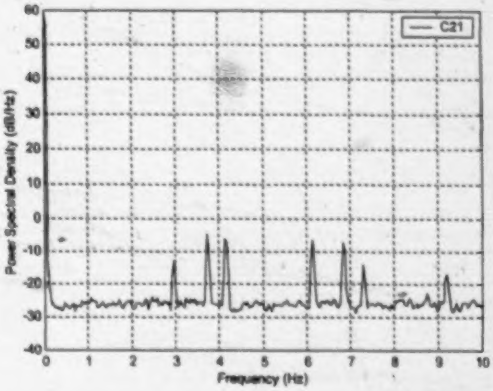

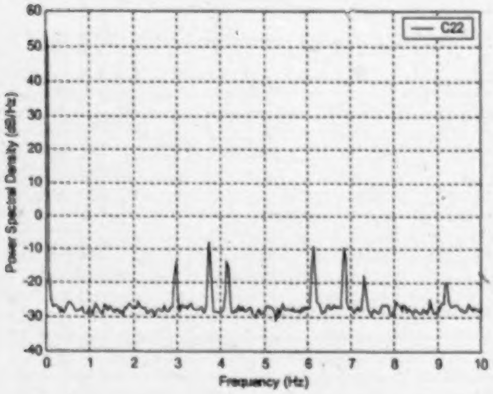

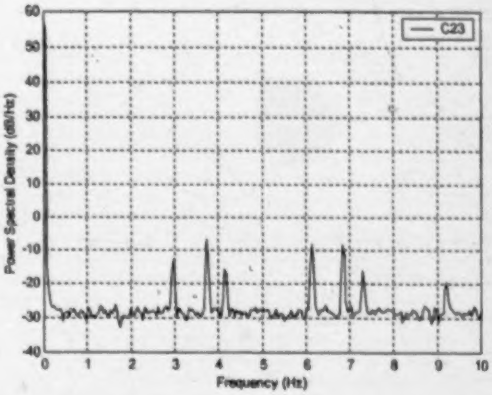

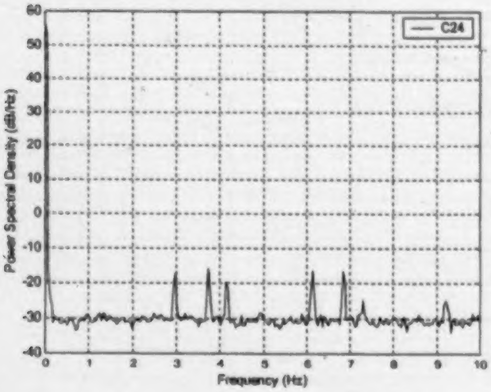

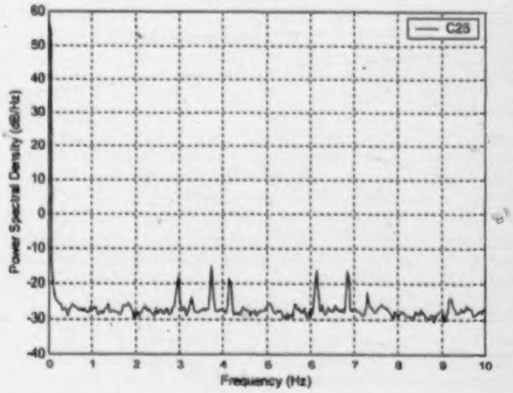

July 18, 1999
2:57 PM

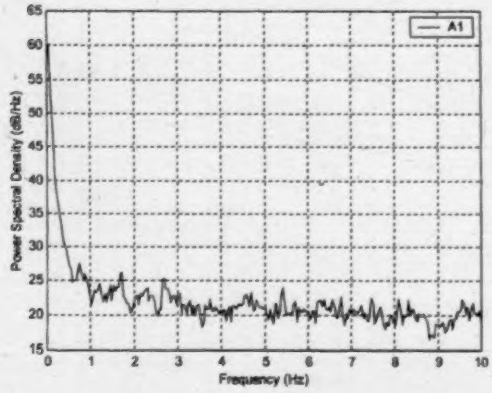

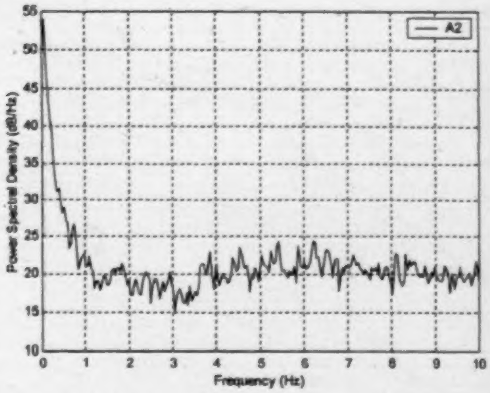

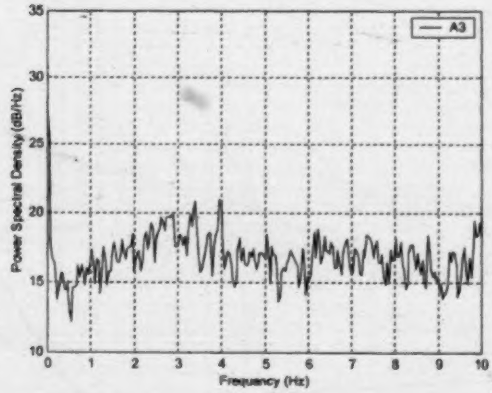

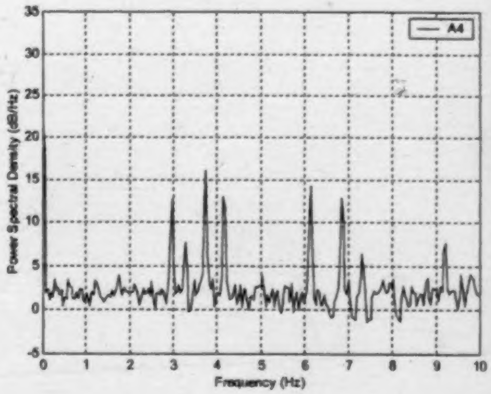

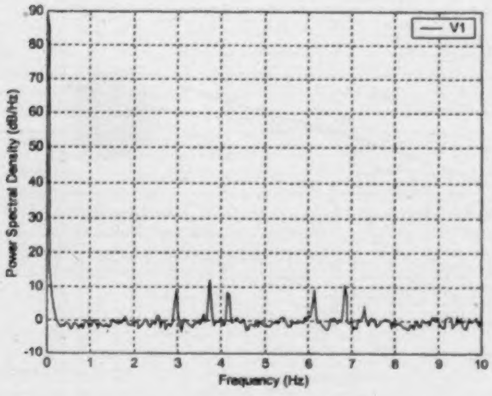

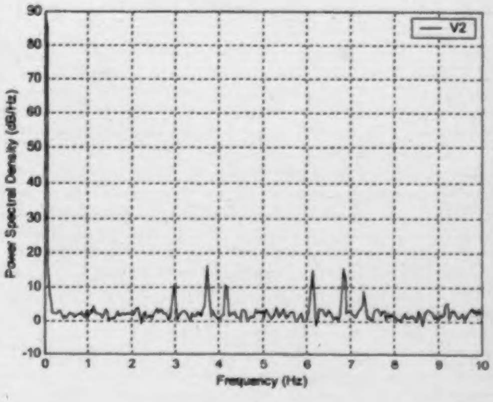

July 18, 1999
3:02 PM

July 18, 1999
3:02 PM

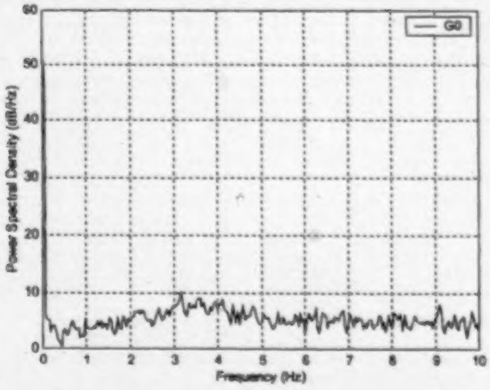

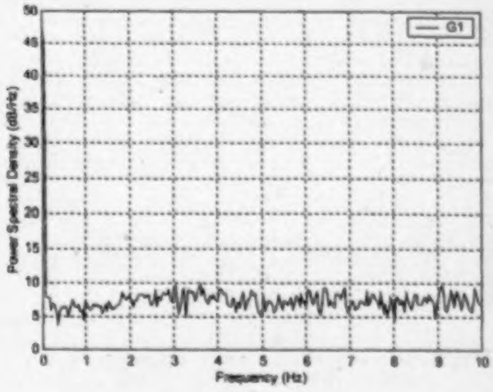

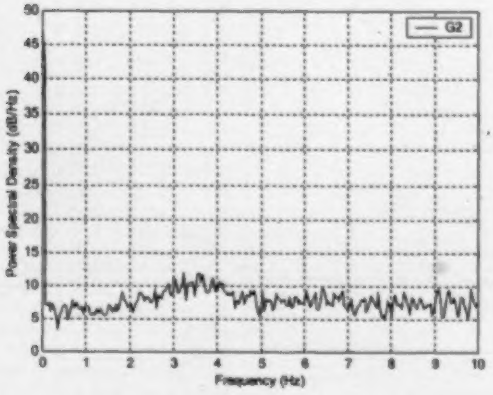

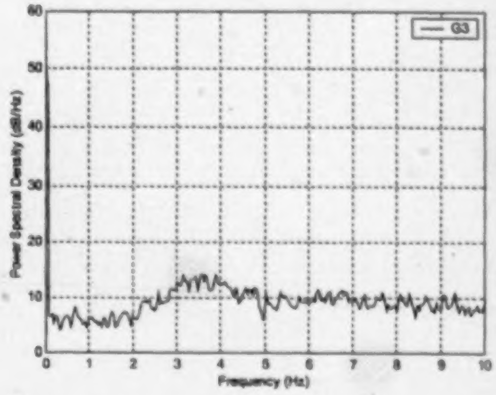

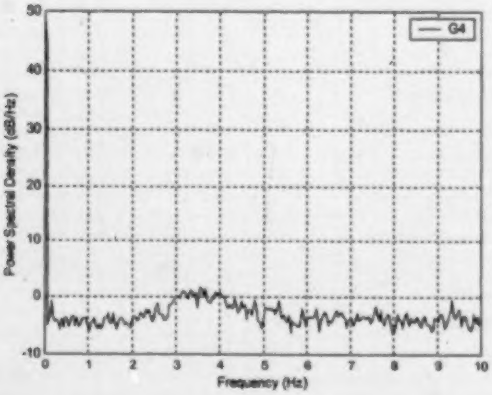

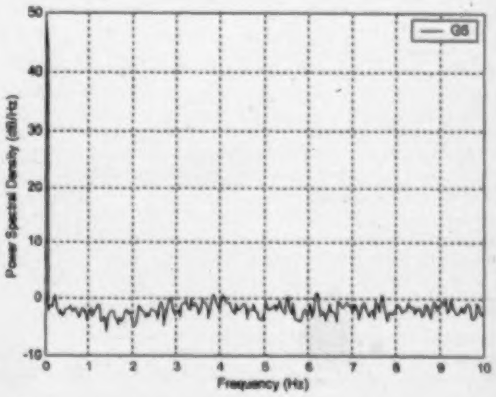

July 18, 1999
3:02 PM

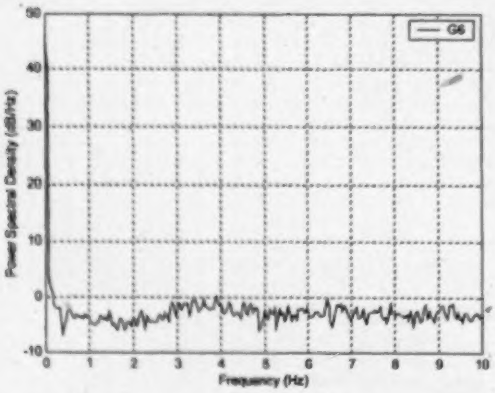

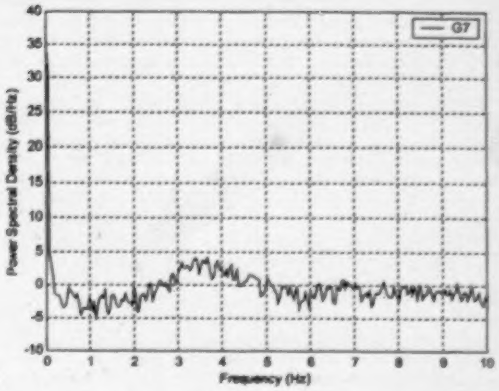

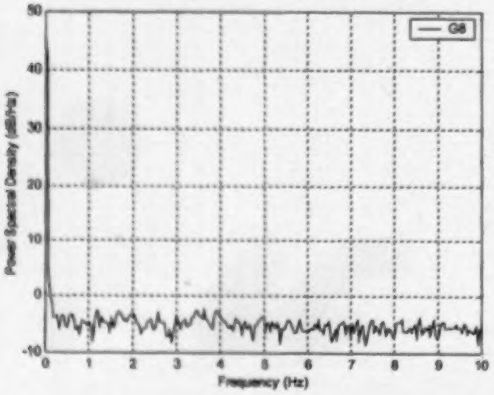

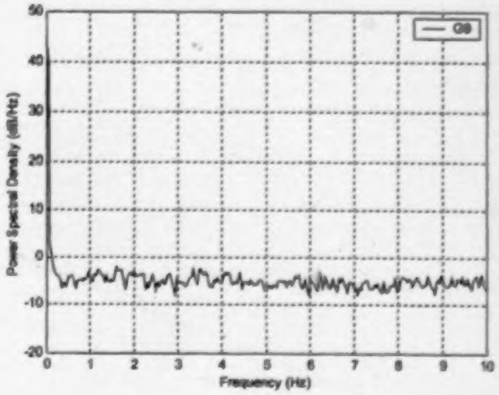

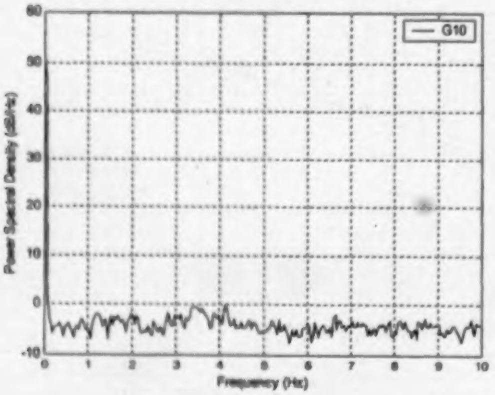

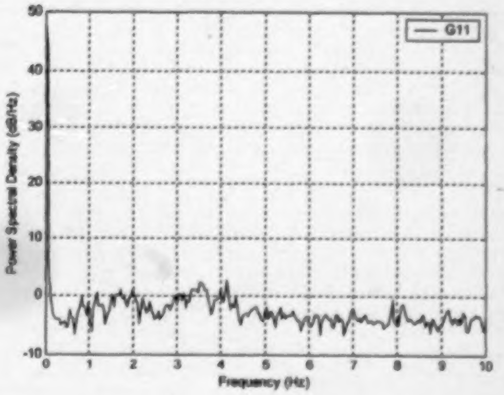

July 18, 1999
3:02 PM

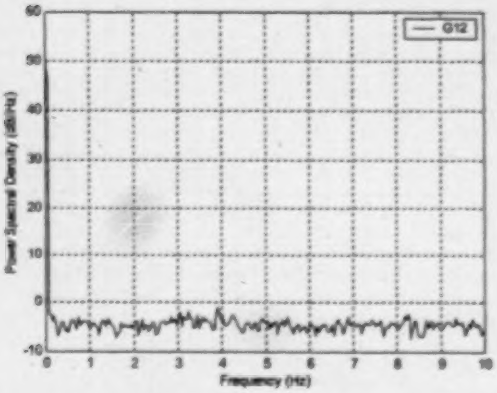

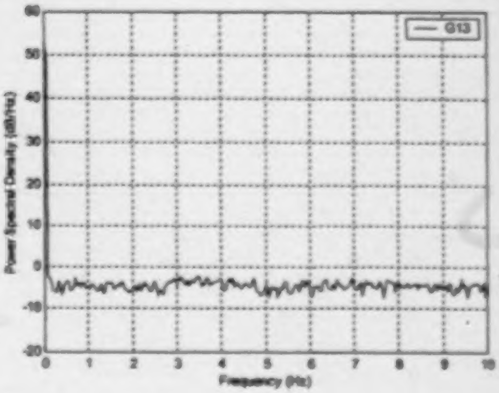

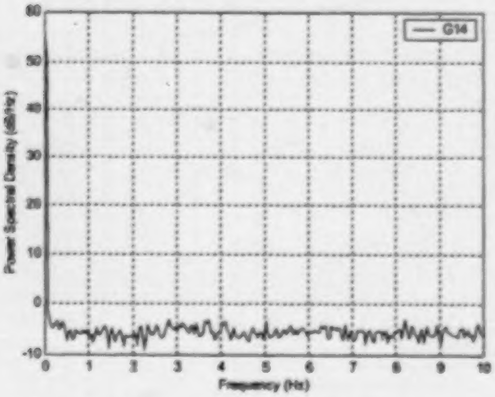

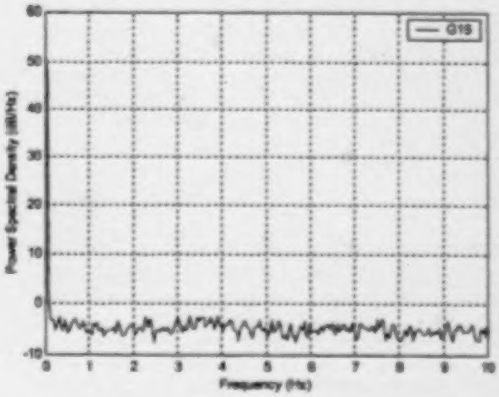

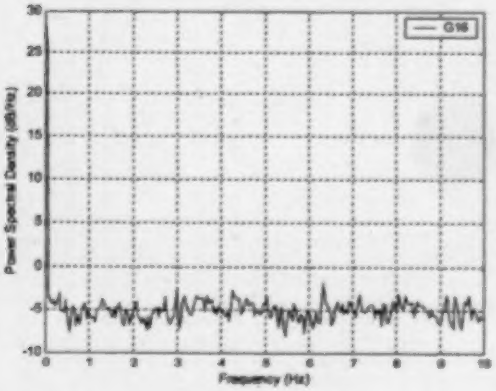

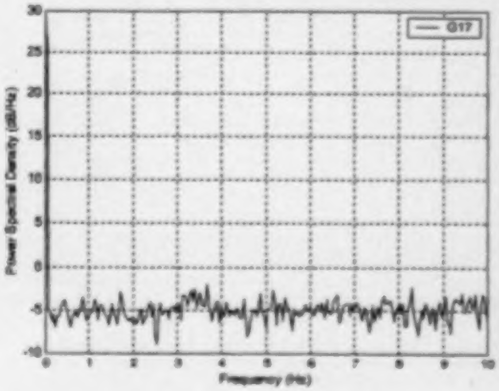

July 18, 1999
3:02 PM

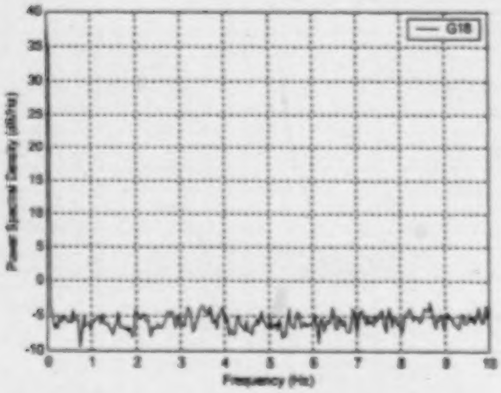

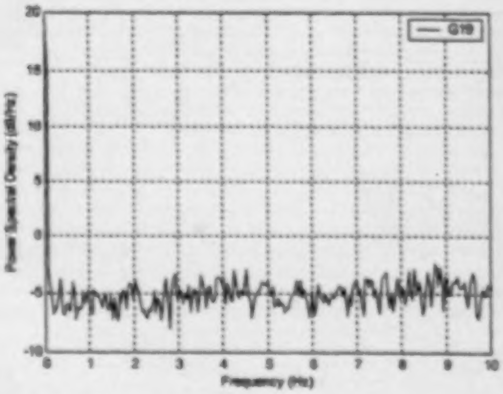

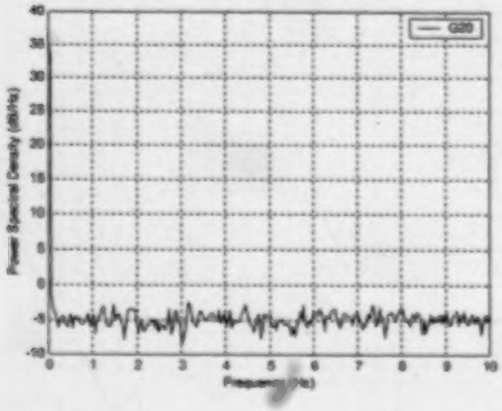

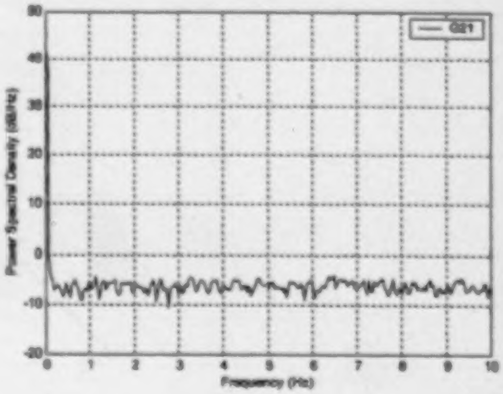

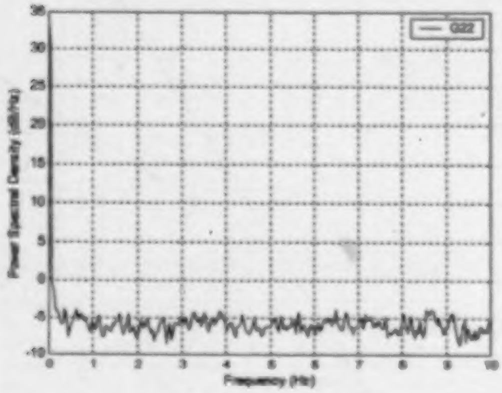

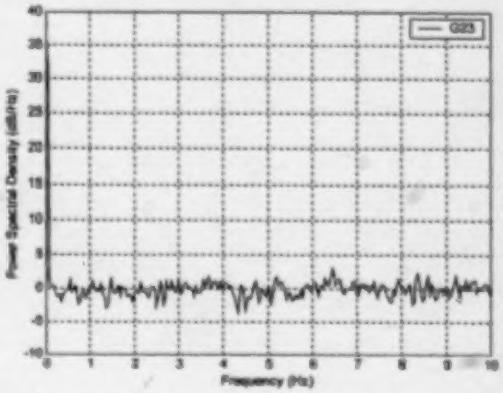

July 18, 1999
3:02 PM

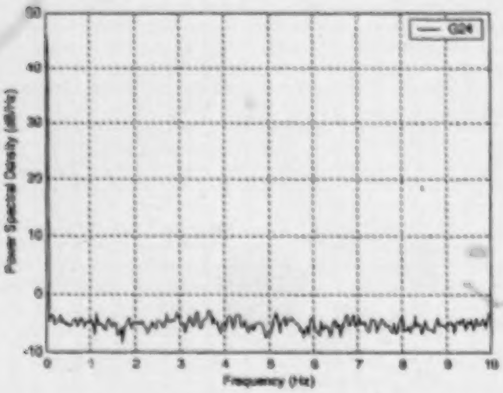

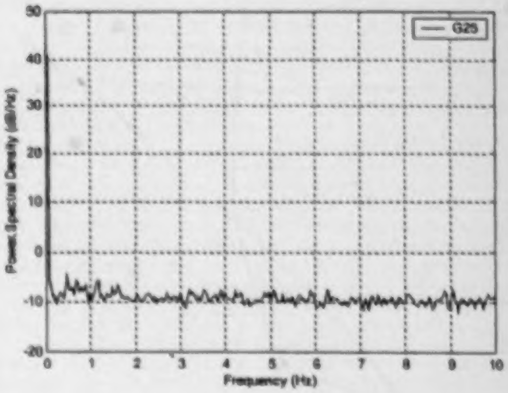

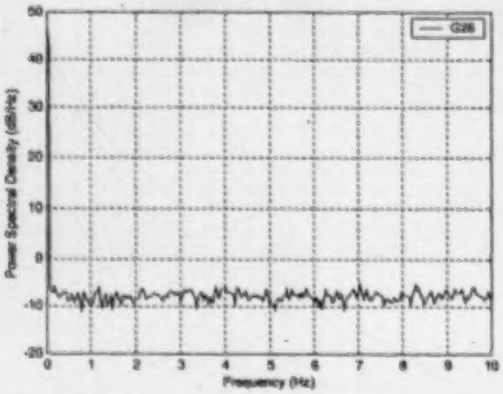

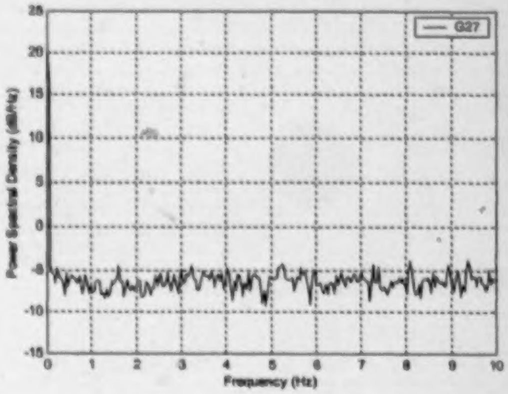

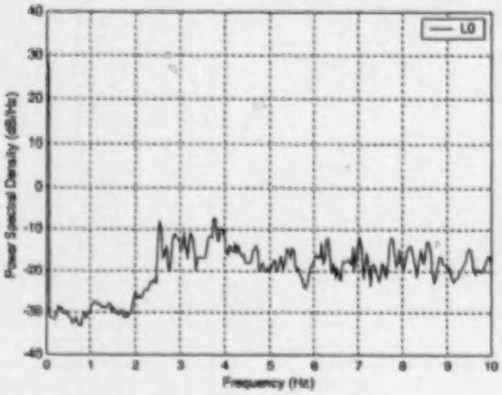

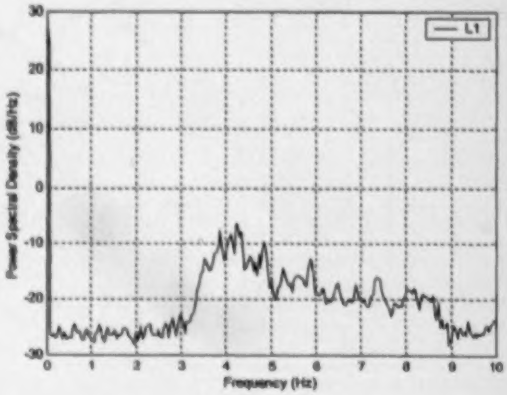

July 18, 1999
3:02 PM

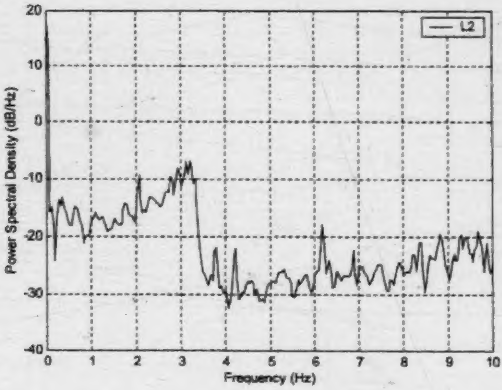

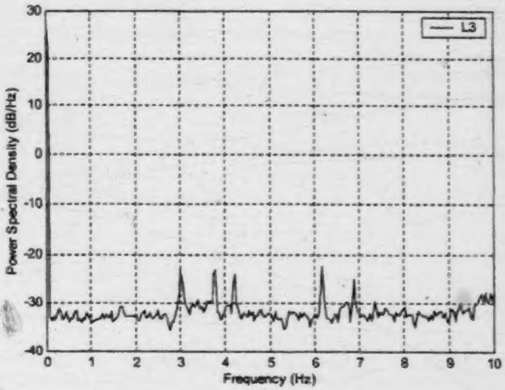

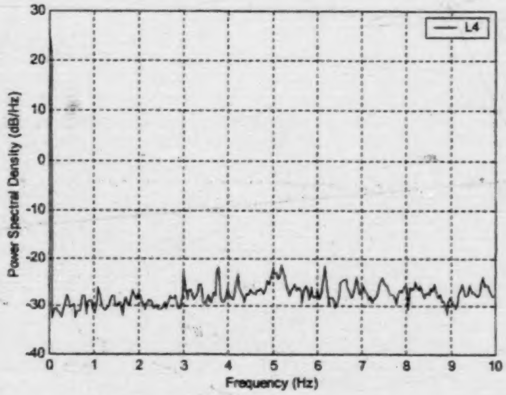

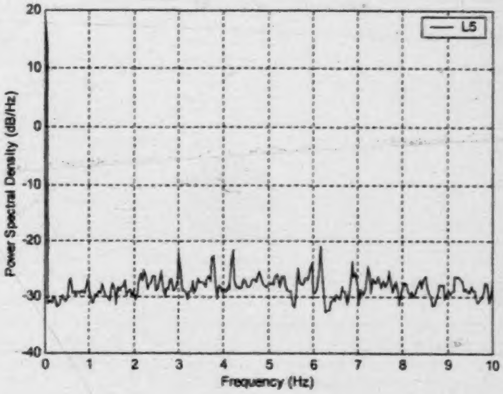

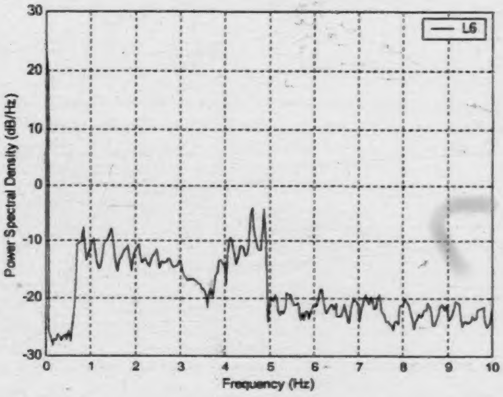

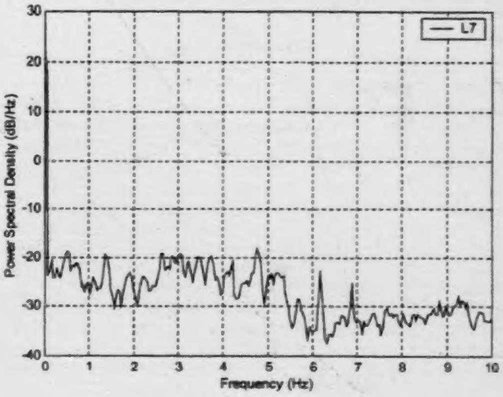

July 18, 1999
3:02 PM

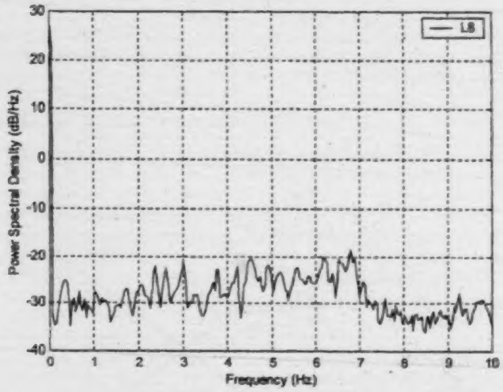

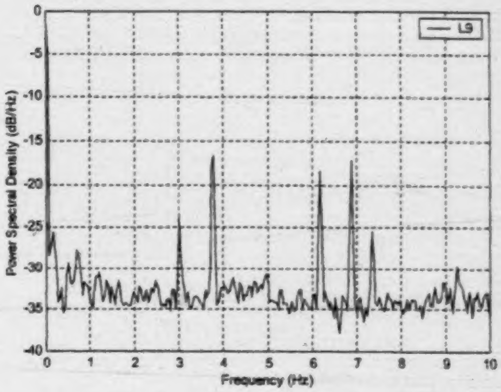

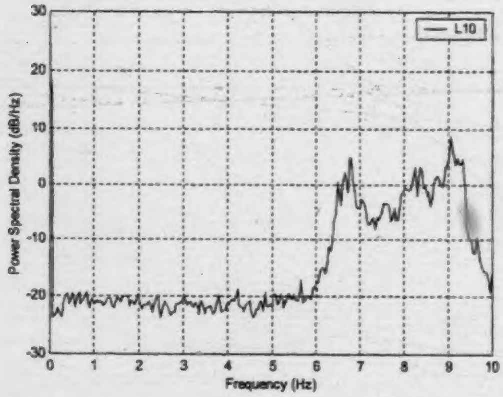

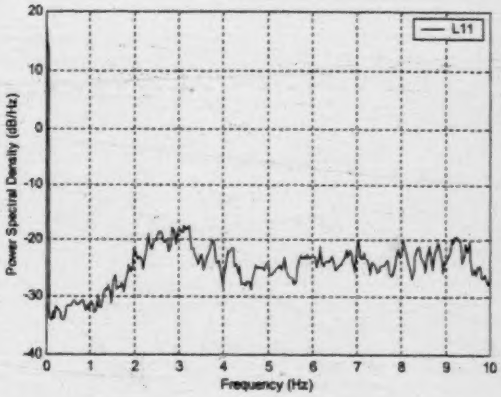

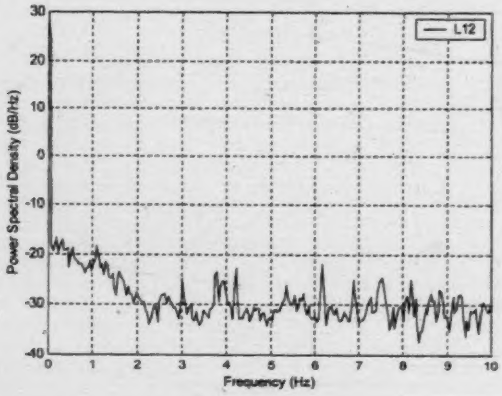

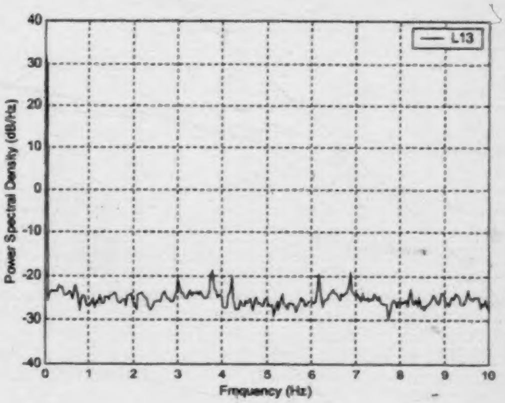

July 18, 1999
3:02 PM

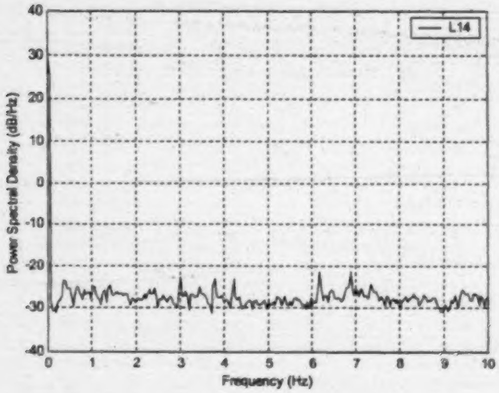

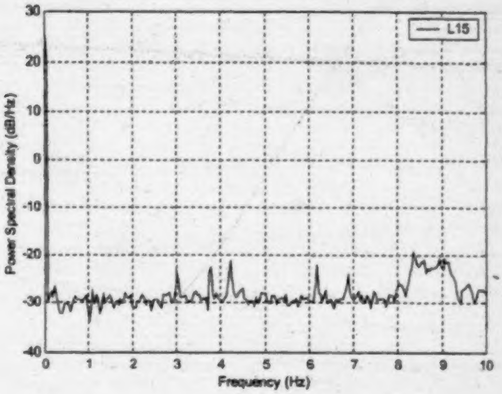

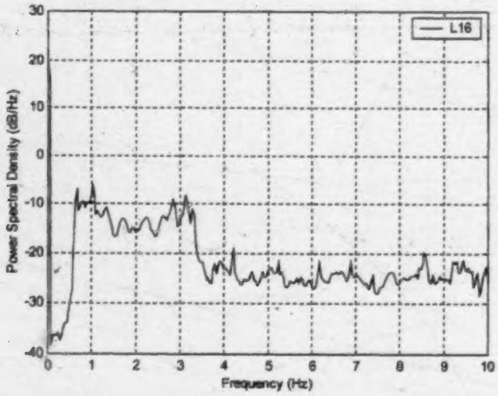

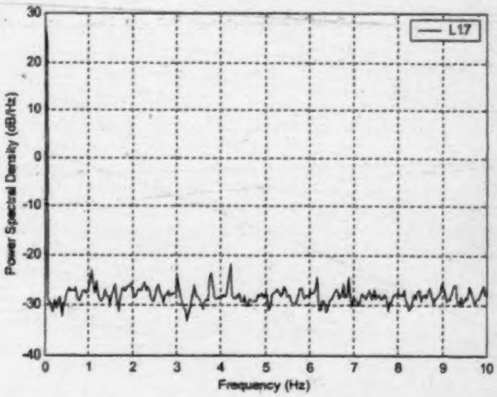

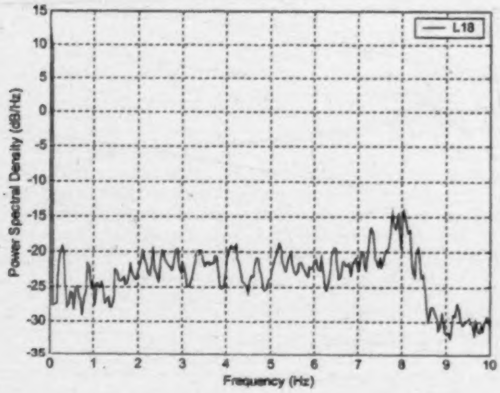

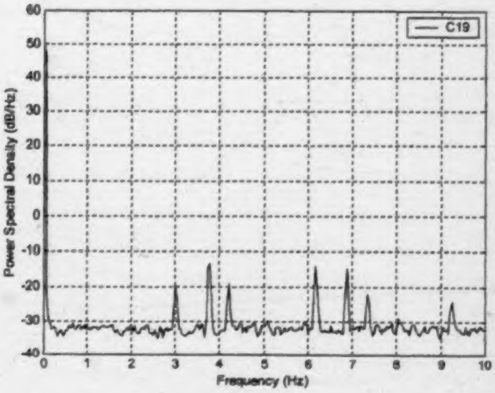

July 18, 1999
3:02 PM

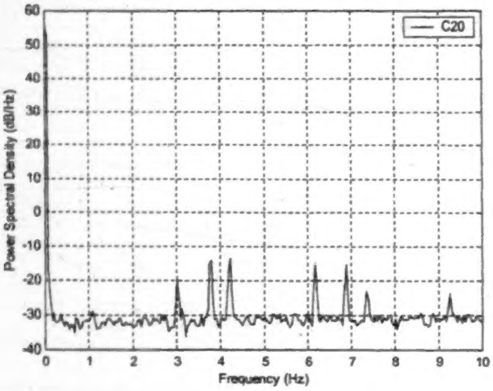

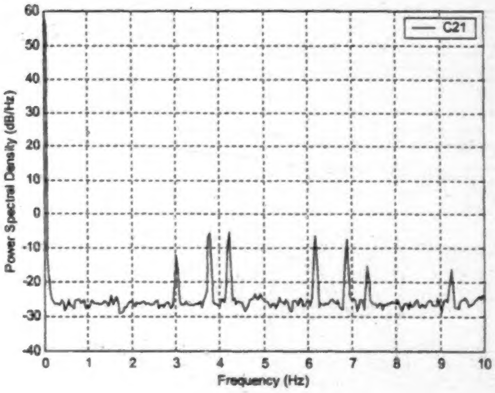

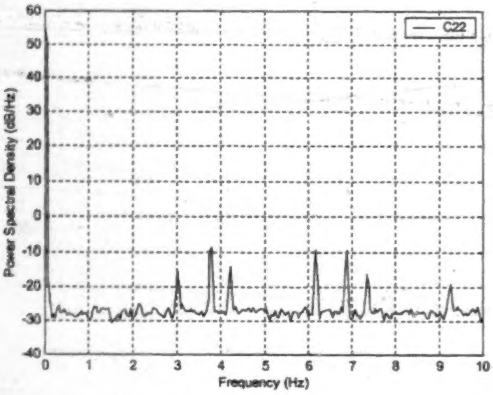

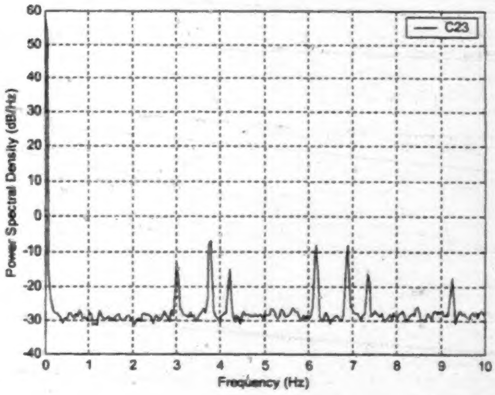

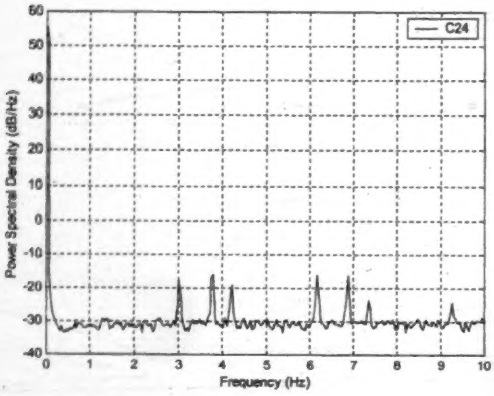

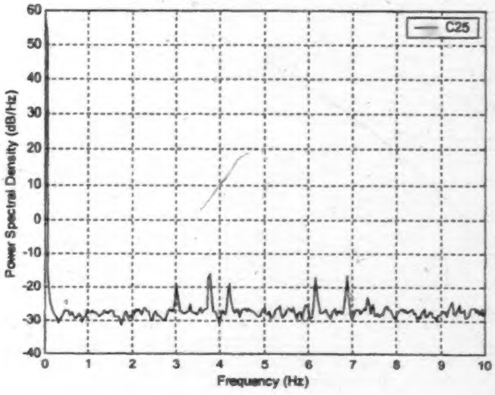

July 18, 1999
3:02 PM

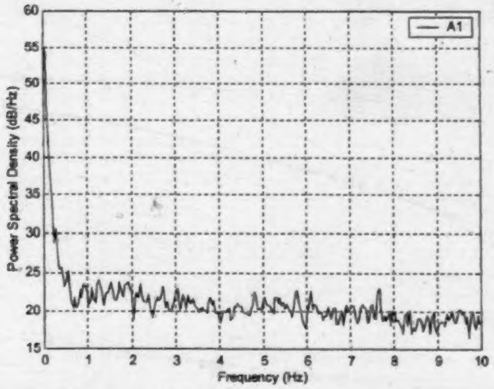

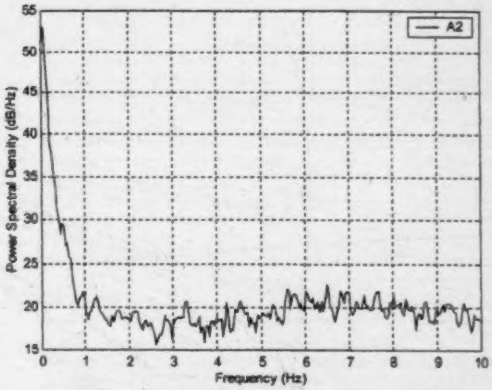

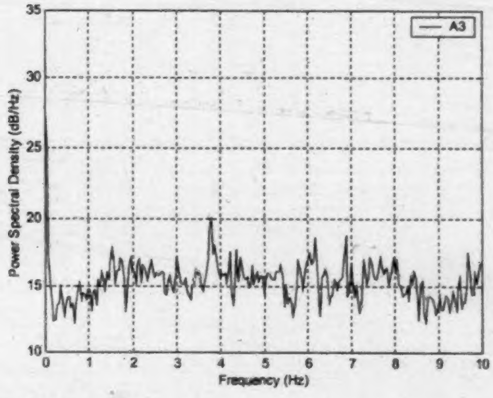

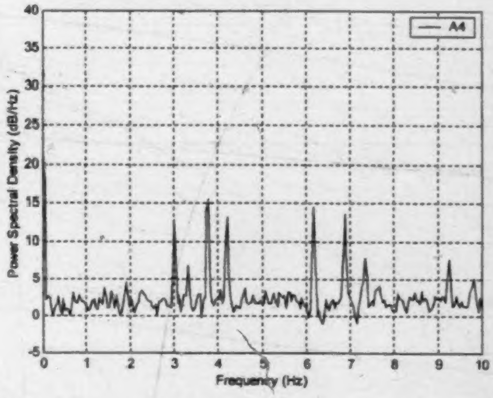

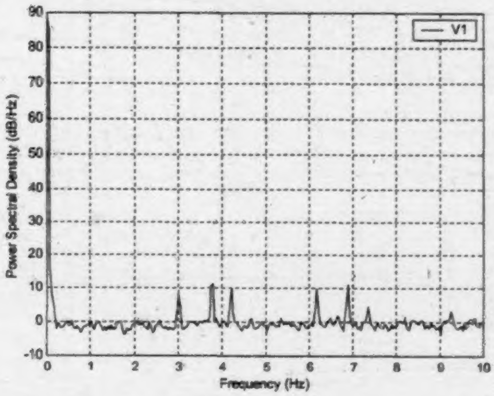

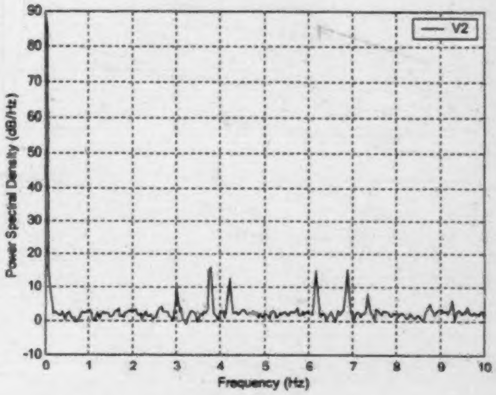

July 18, 1999
3:08 PM

July 18, 1999
3:08 PM

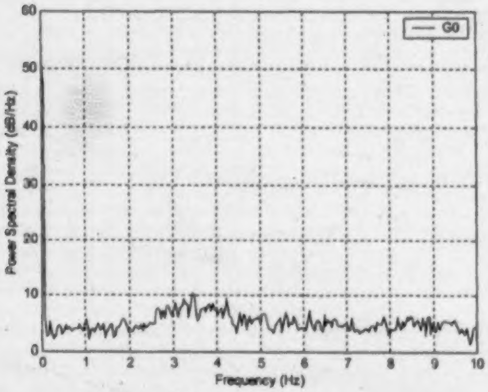

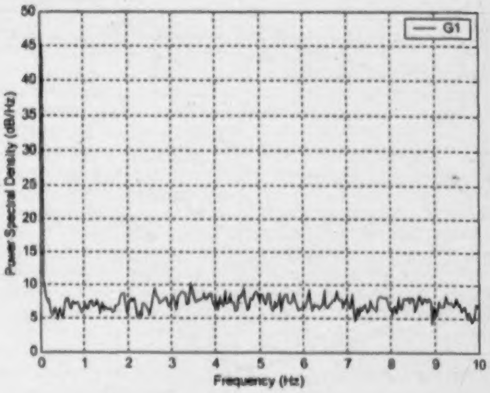

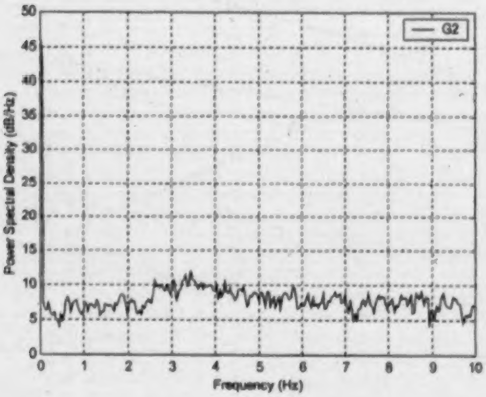

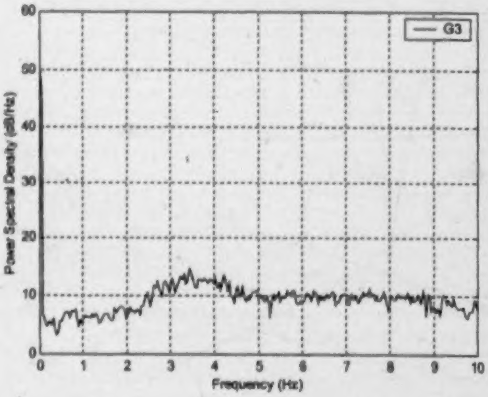

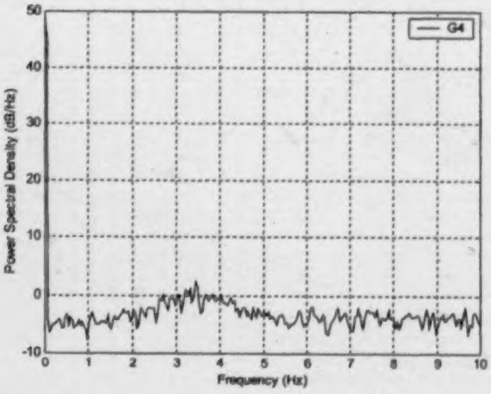

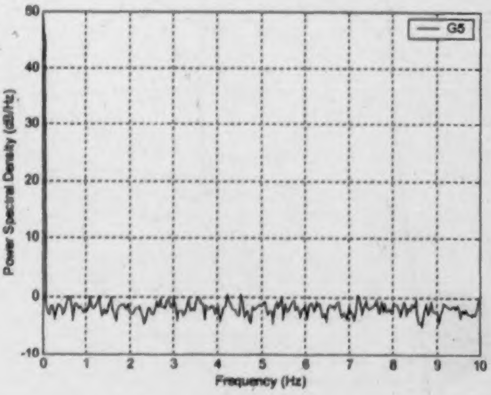

July 18, 1999
3:08 PM

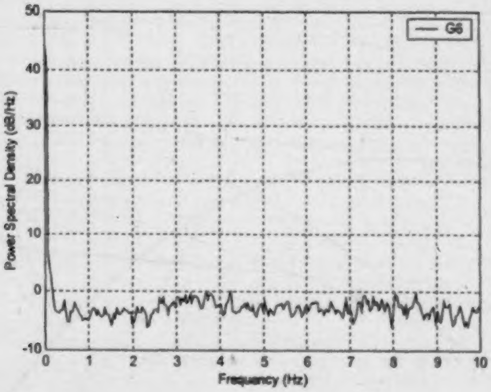

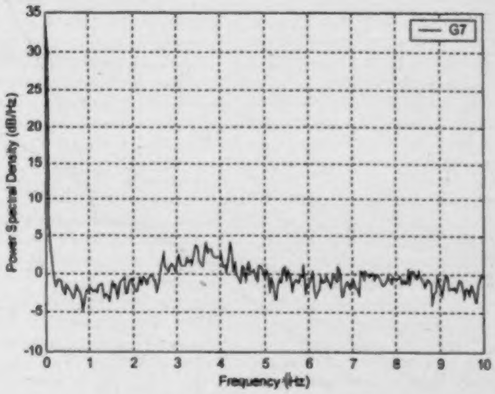

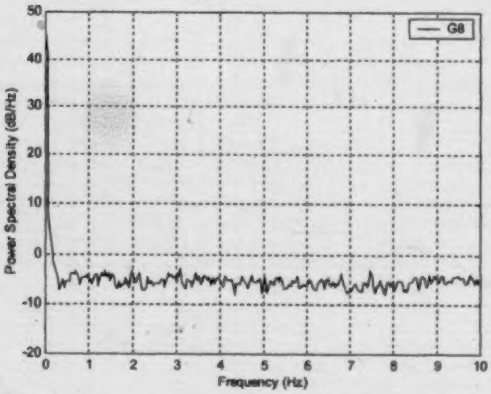

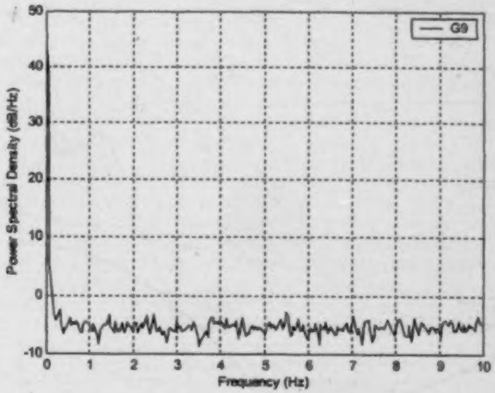

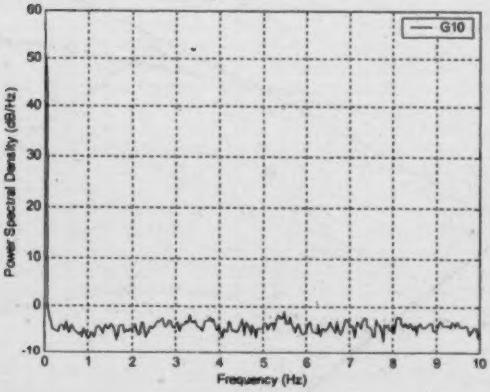

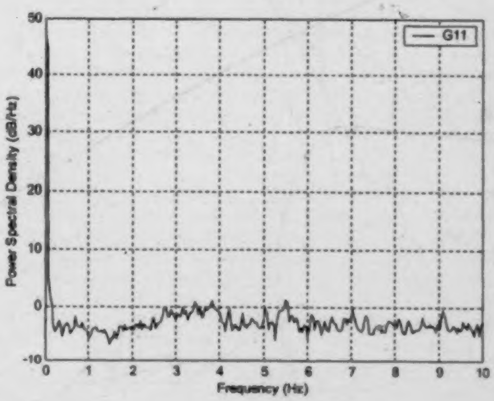

July 18, 1999
3:08 PM

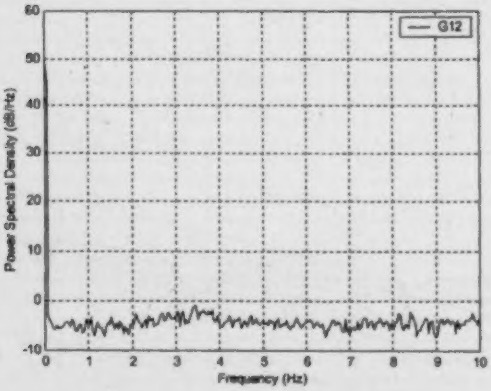

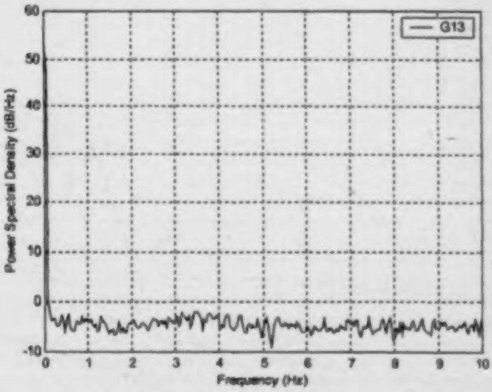

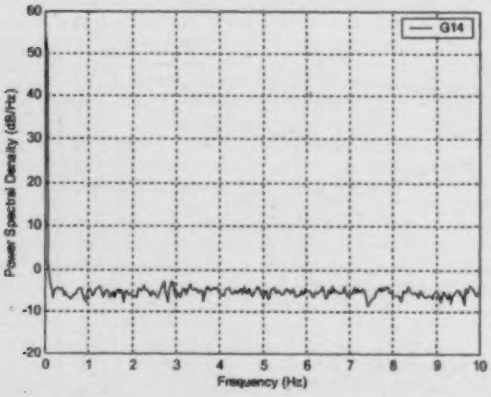

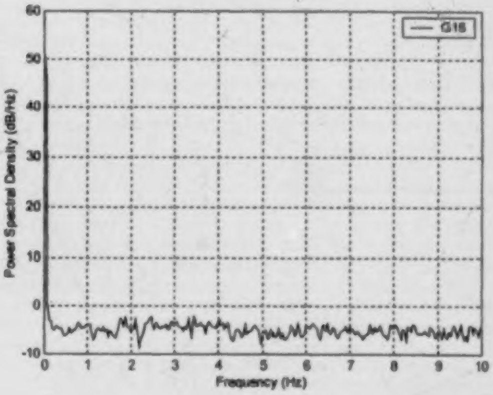

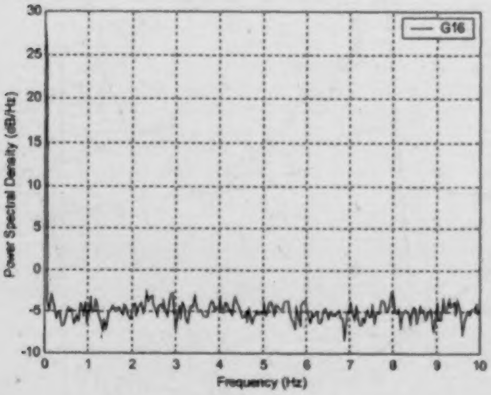

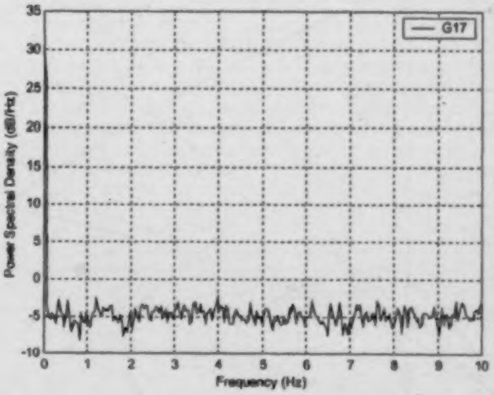

July 18, 1999
3:08 PM

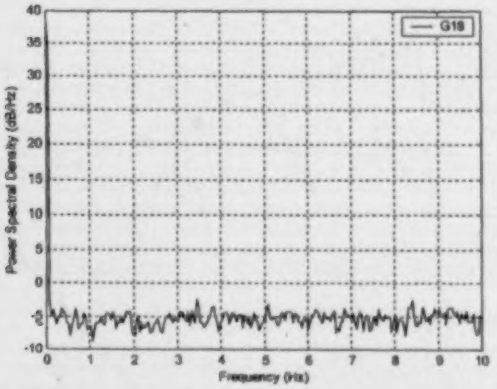

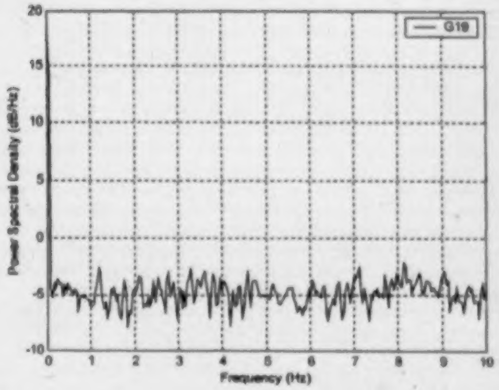

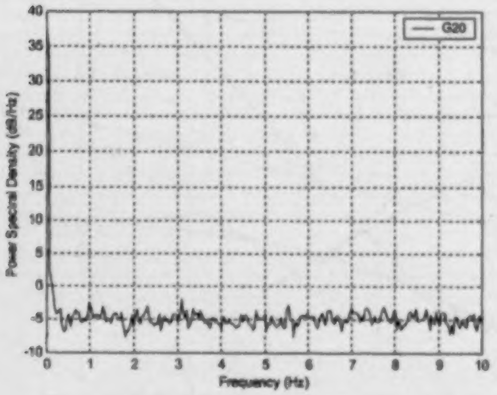

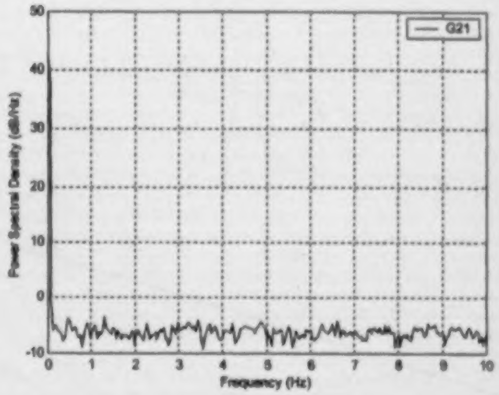

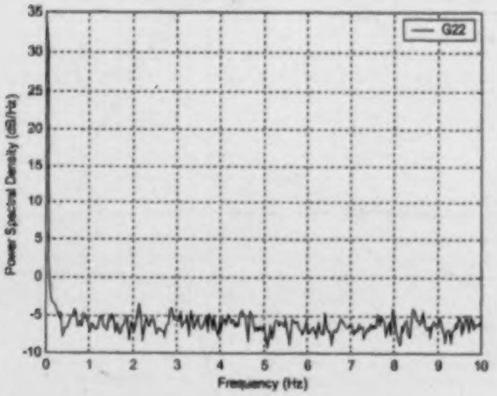

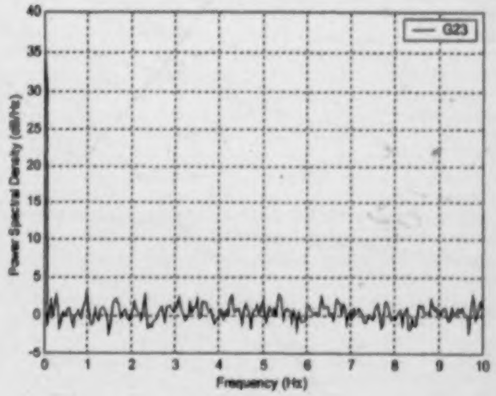

July 18, 1999
3:08 PM

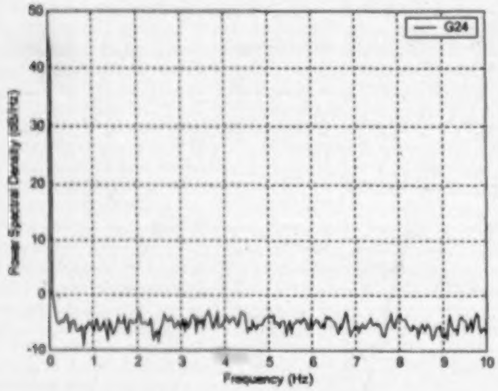

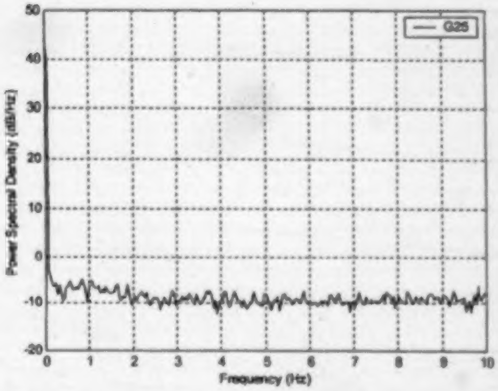

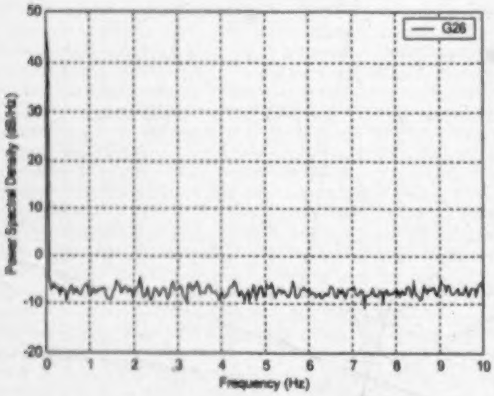

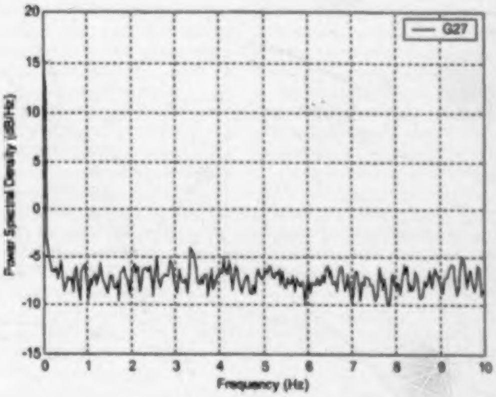

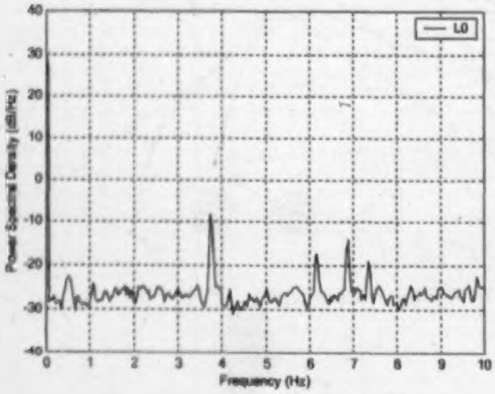

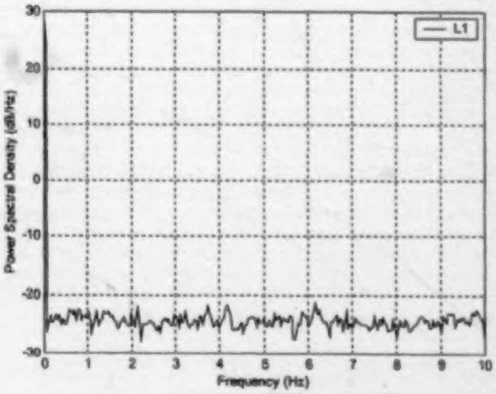

July 18, 1999
3:08 PM

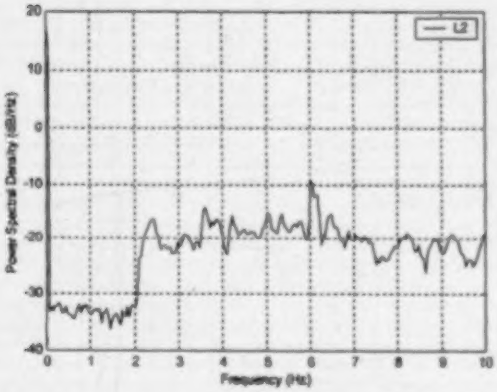

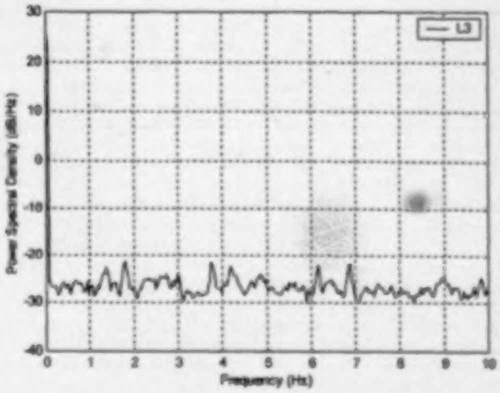

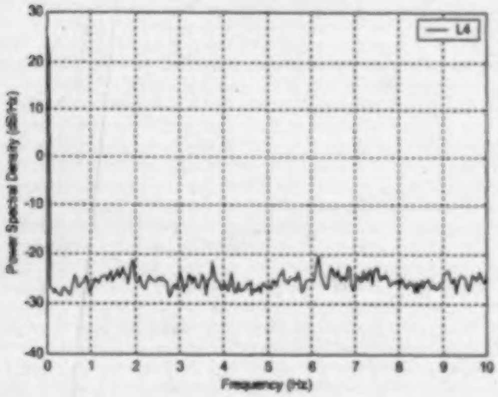

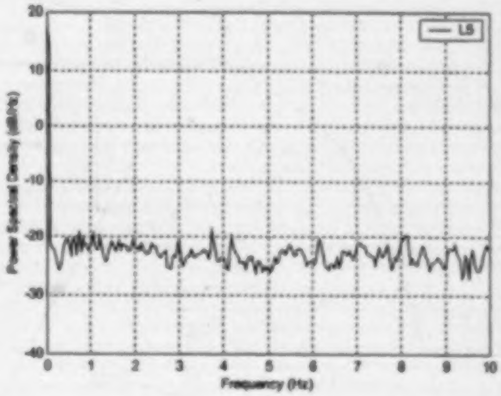

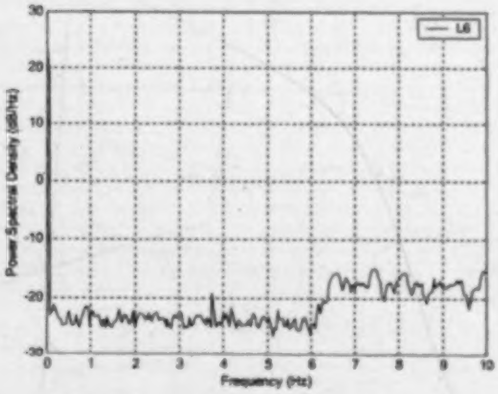

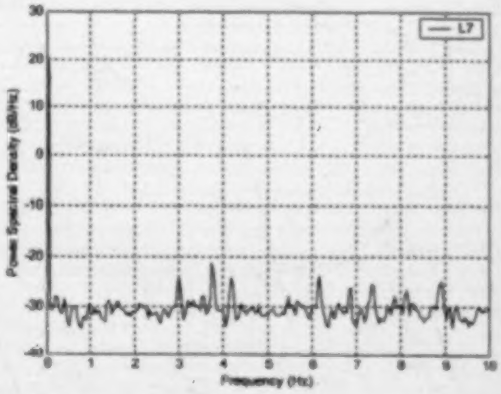

July 18, 1999
3:08 PM

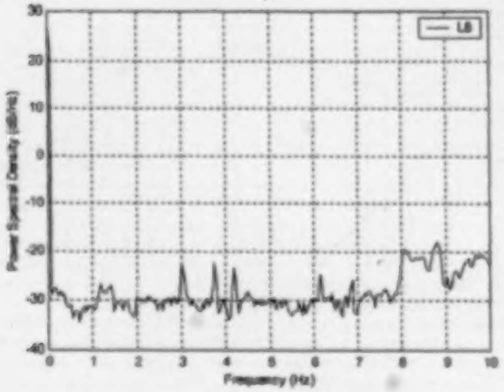

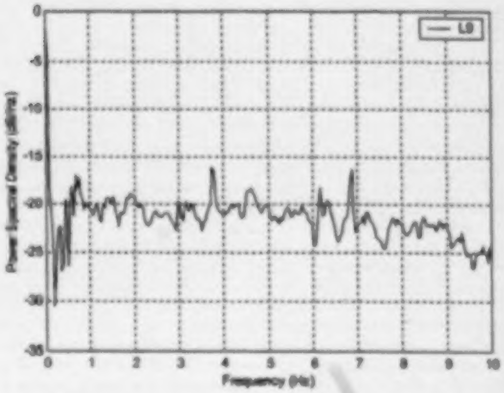

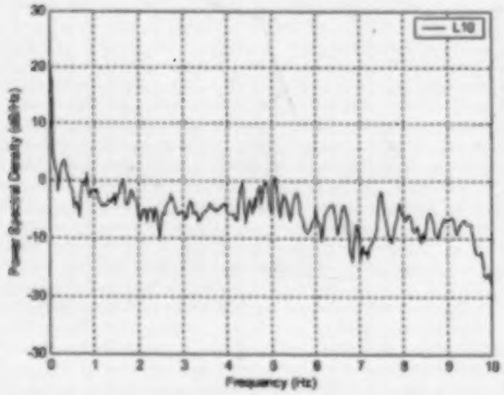

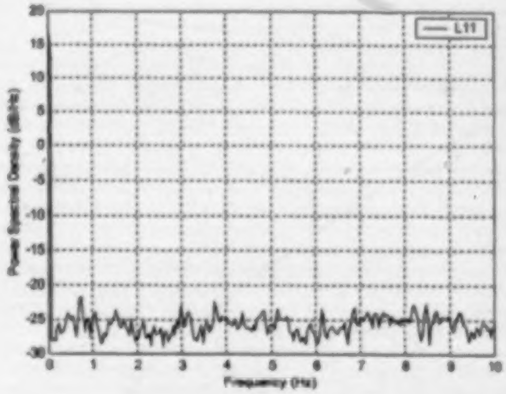

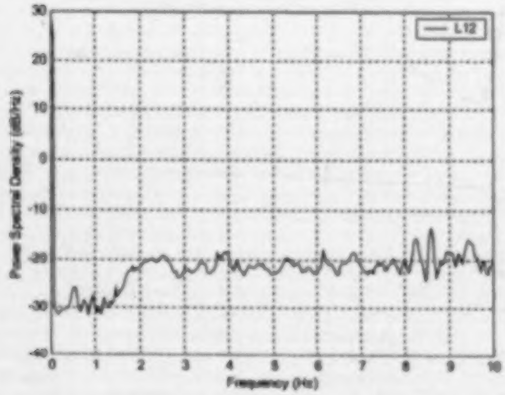

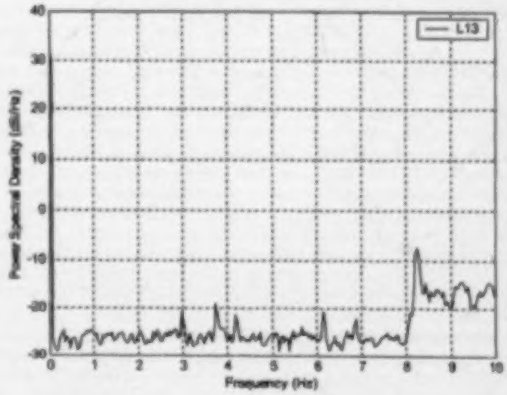

July 18, 1999
3:08 PM

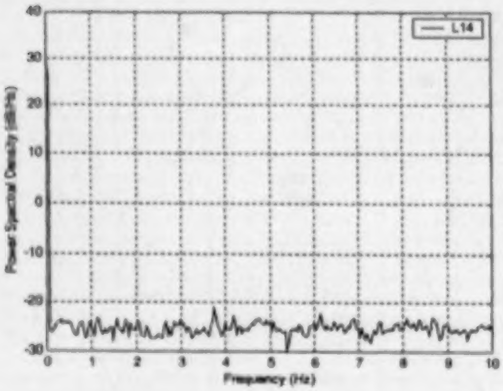

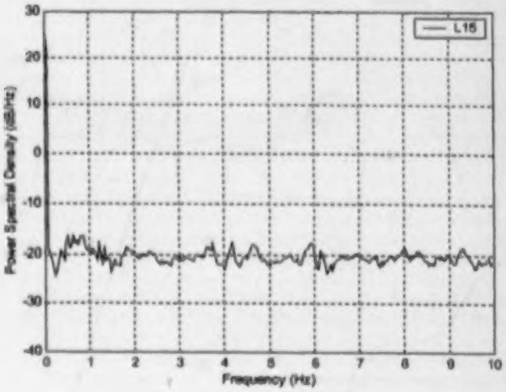

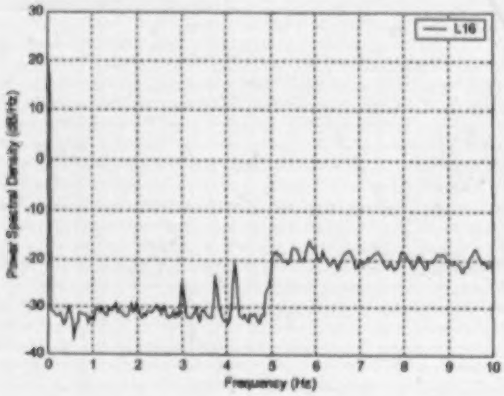

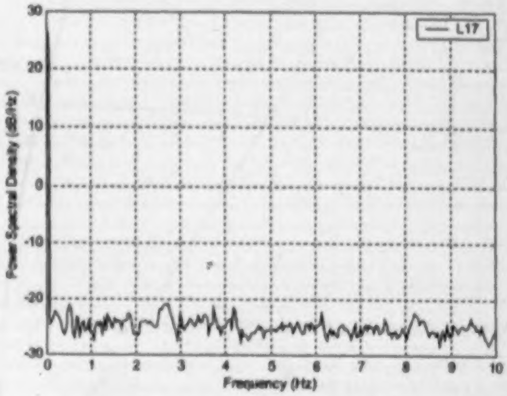

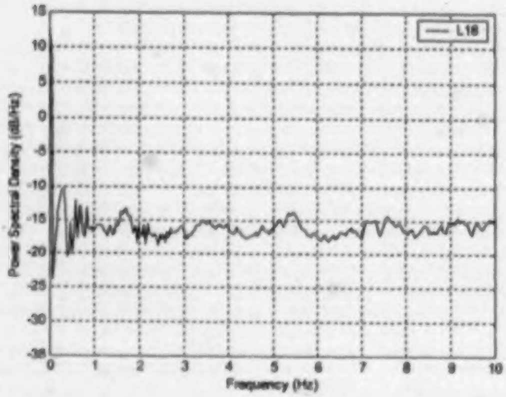

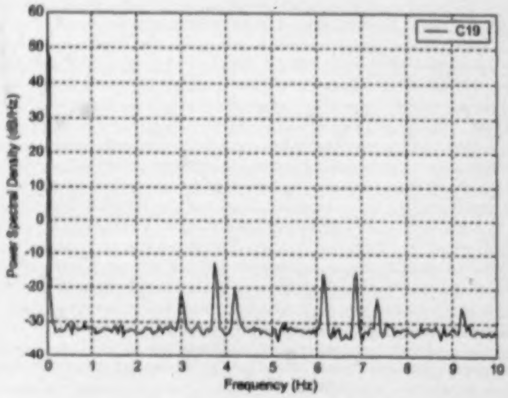

July 18, 1999
3:08 PM

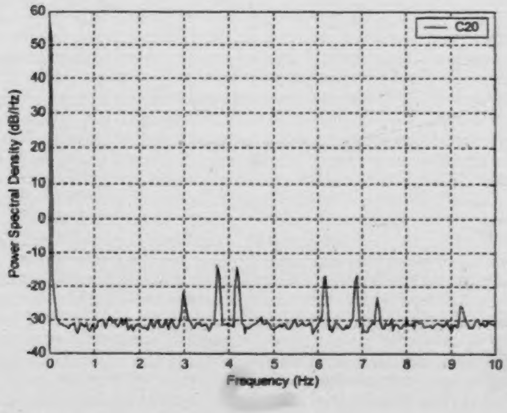

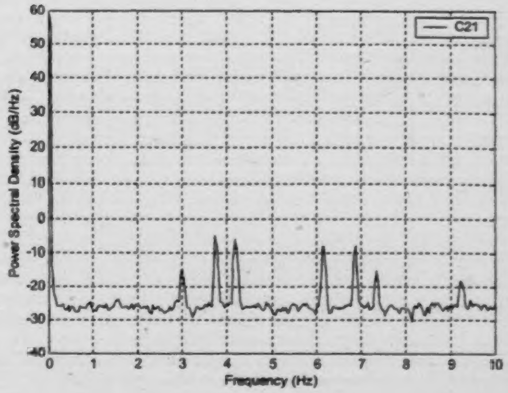

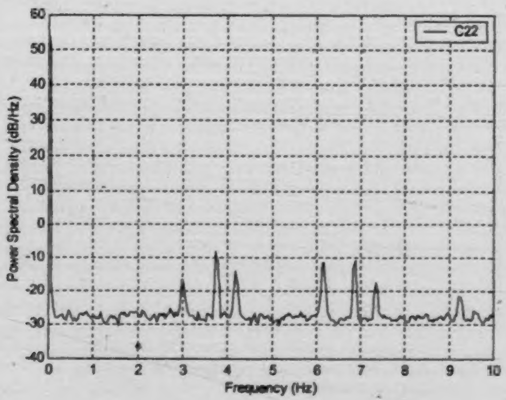

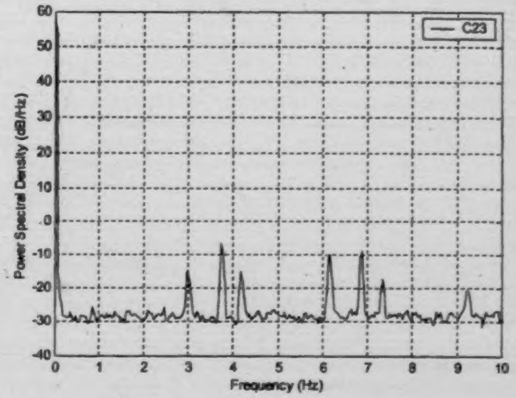

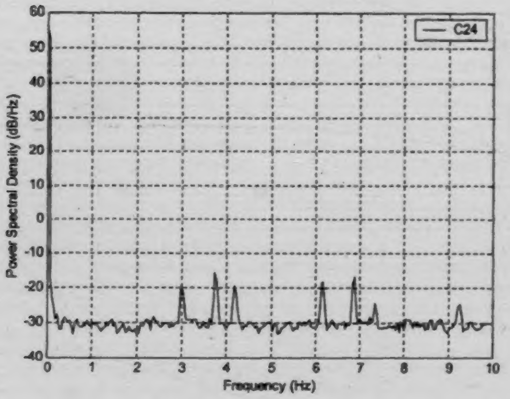

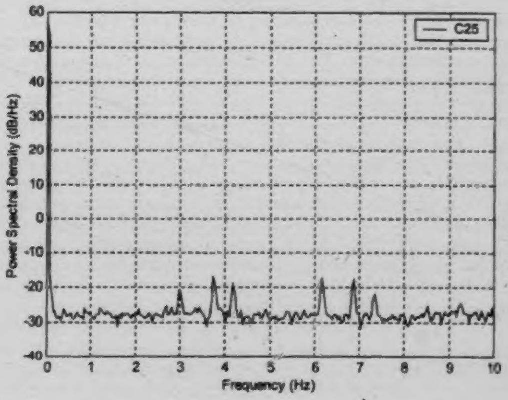

July 18, 1999
3:08 PM

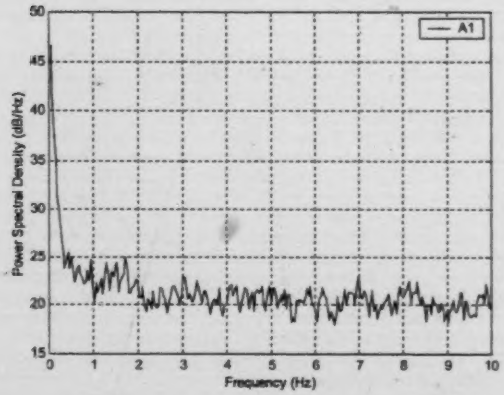

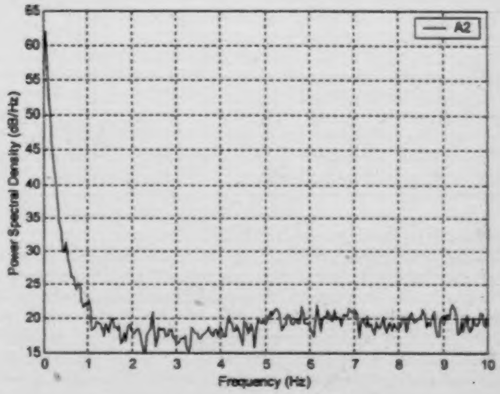

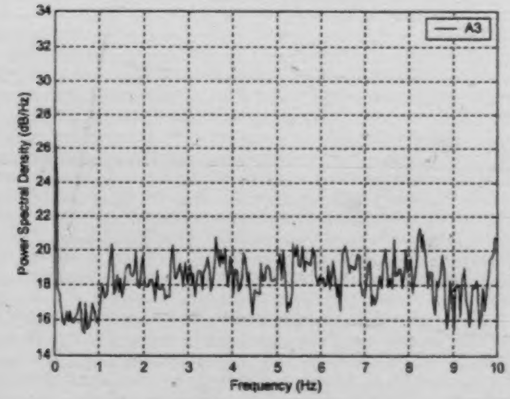

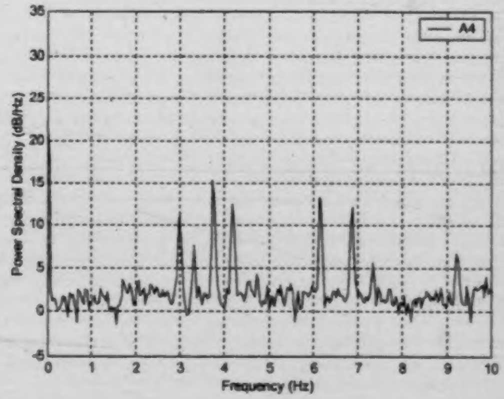

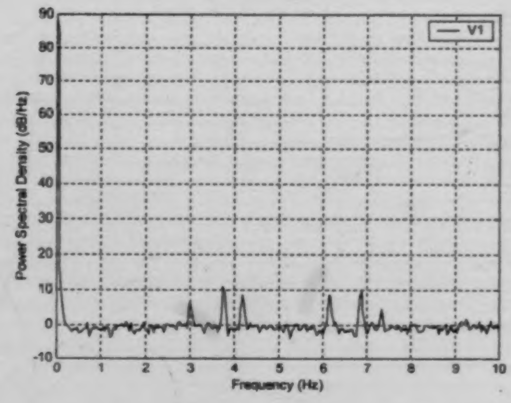

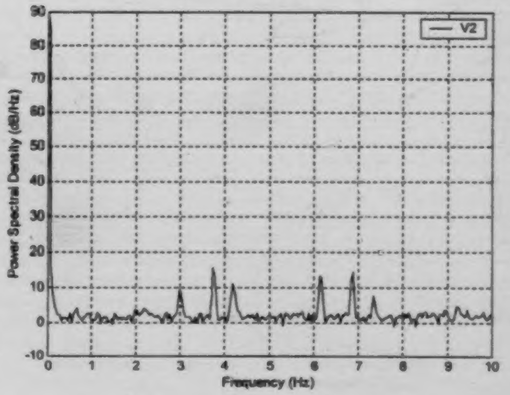

July 18, 1999
3:15 PM

July 18, 1999
3:15 PM

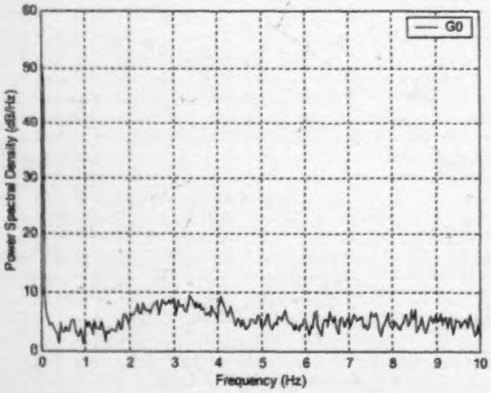

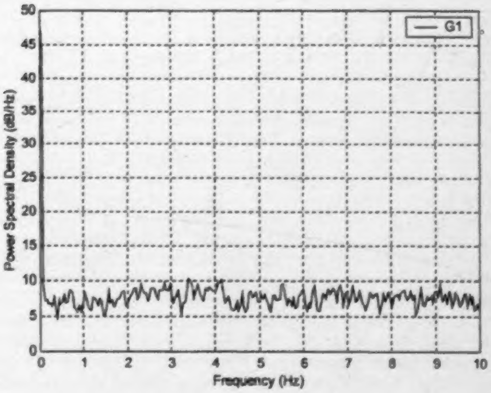

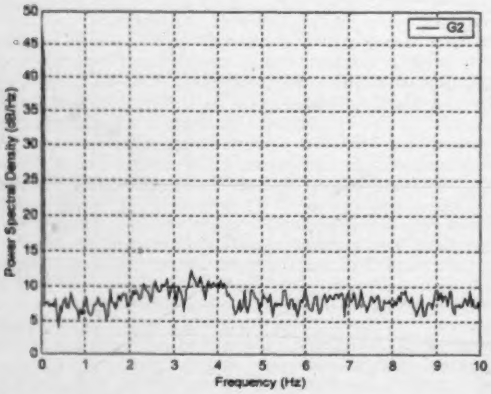

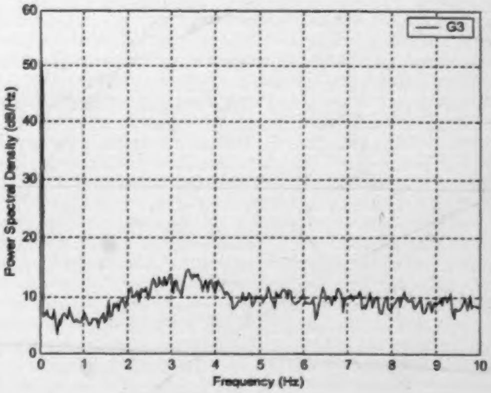

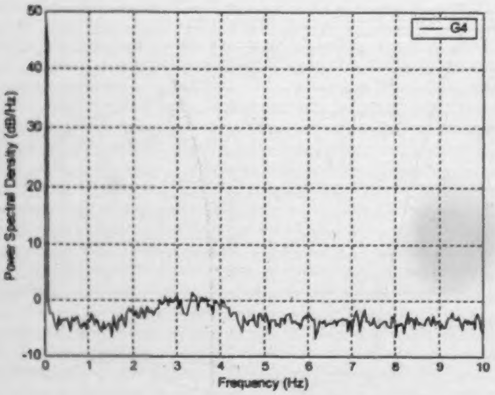

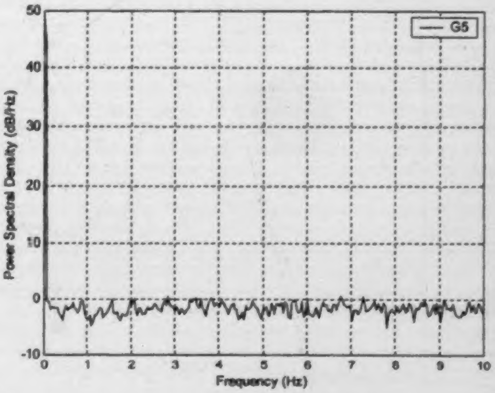

July 18, 1999
3:15 PM

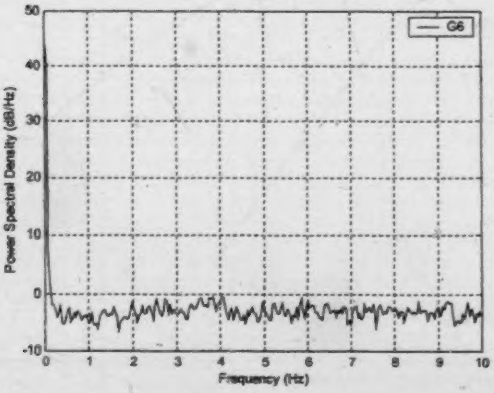

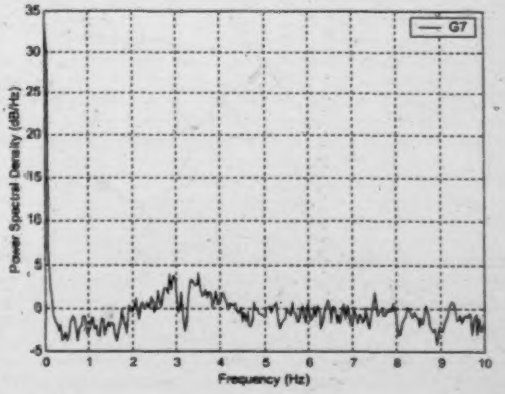

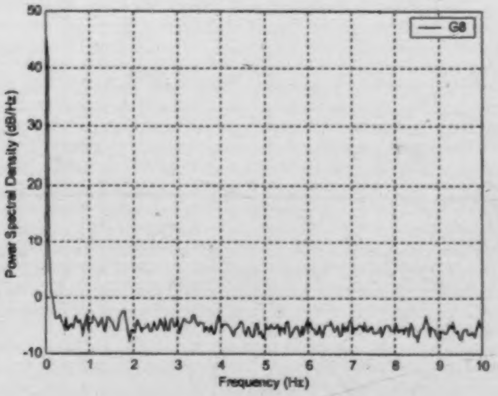

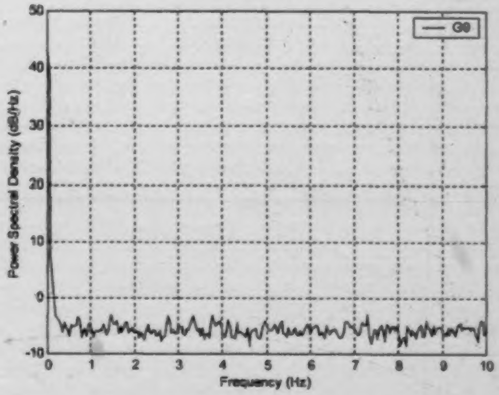

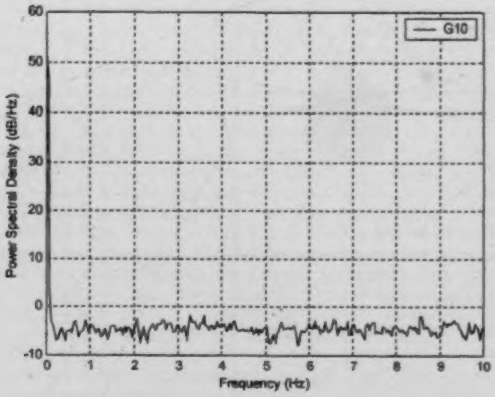

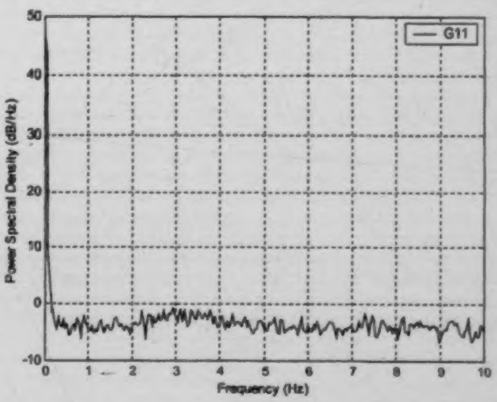

July 18, 1999
3:15 PM

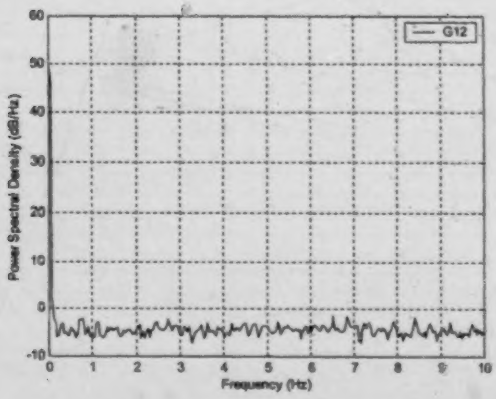

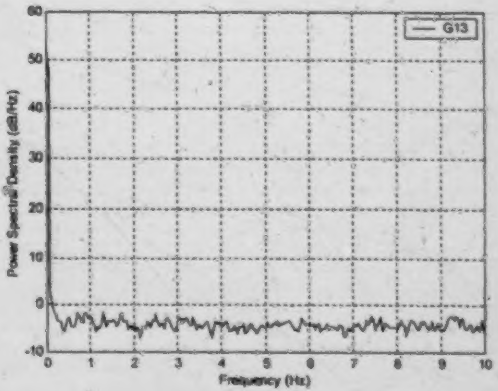

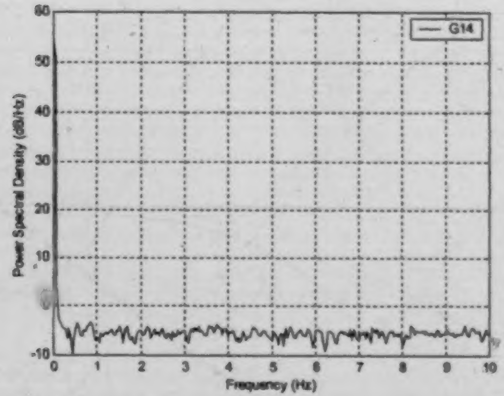

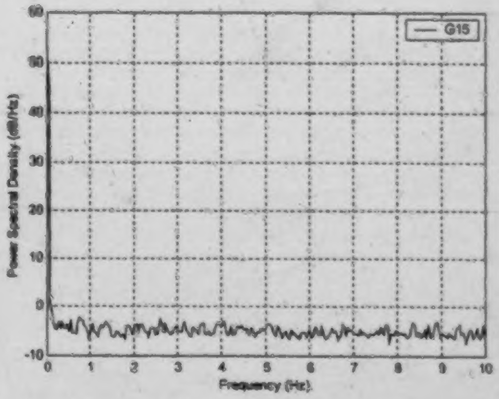

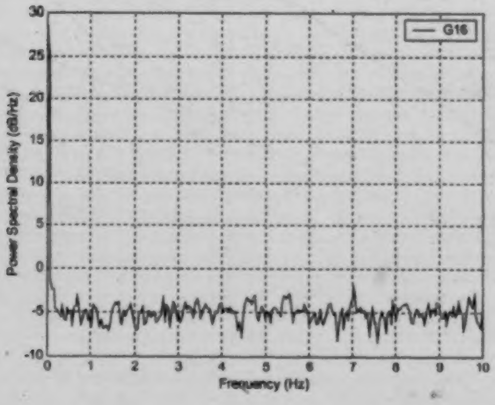

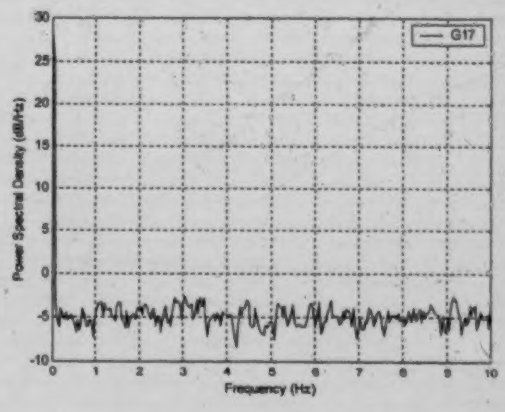

July 18, 1999
3:15 PM

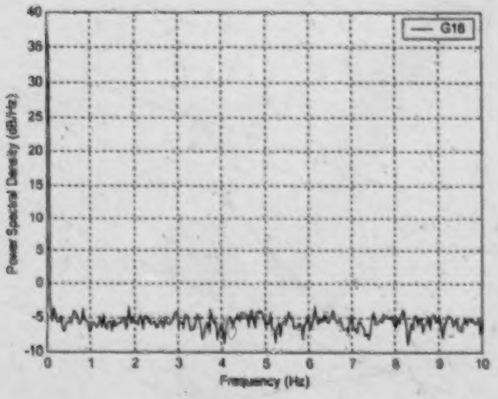

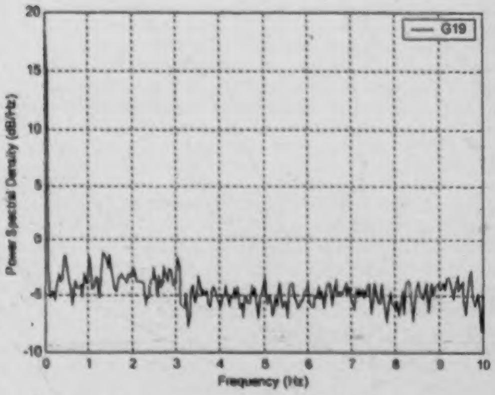

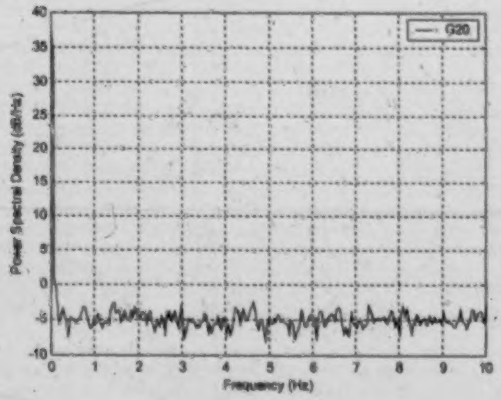

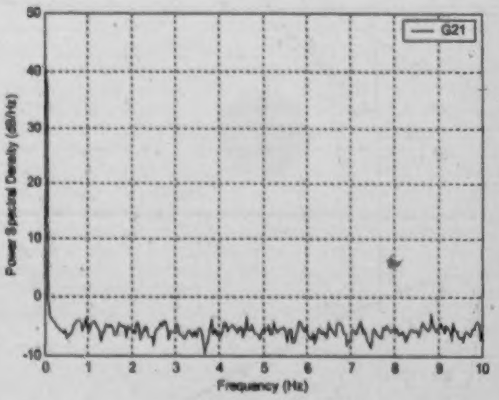

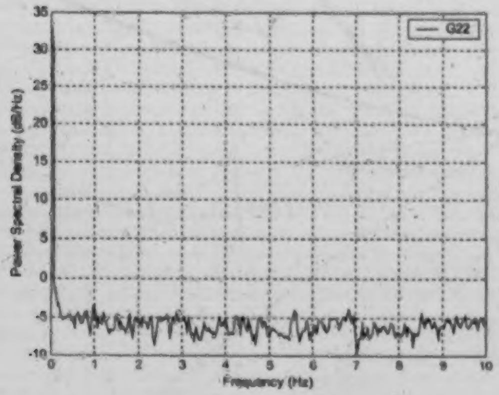

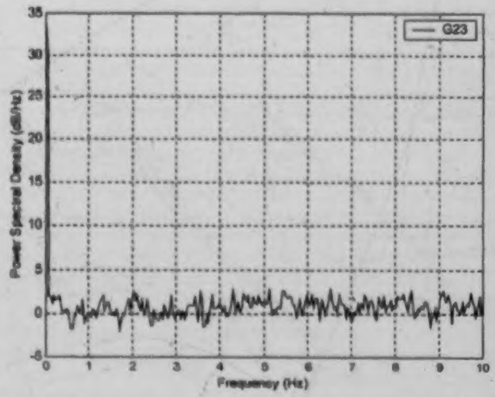

July 18, 1999
3:15 PM

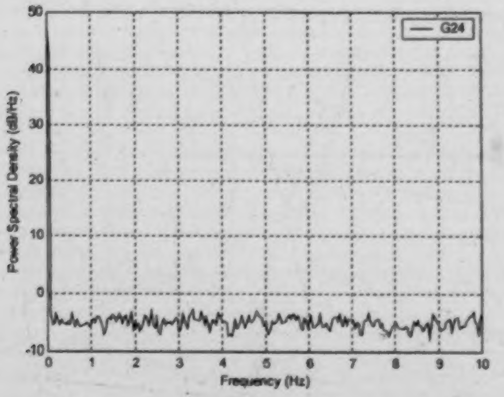

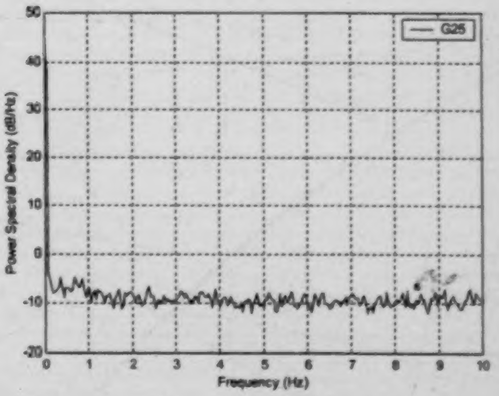

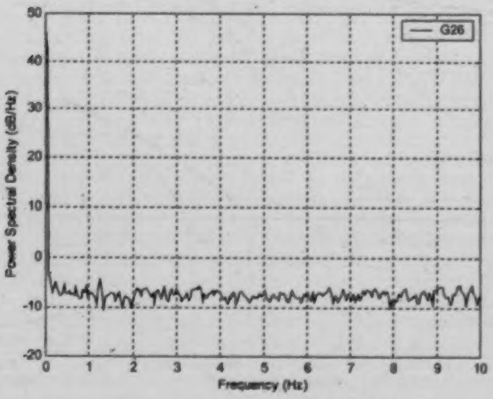

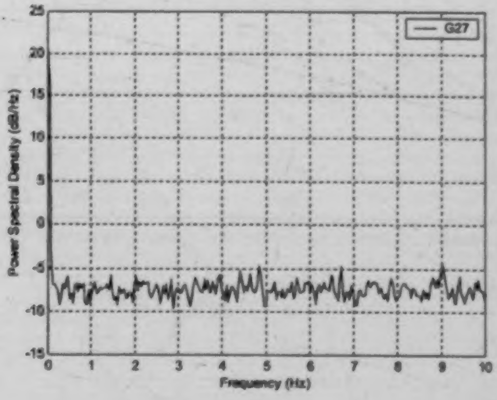

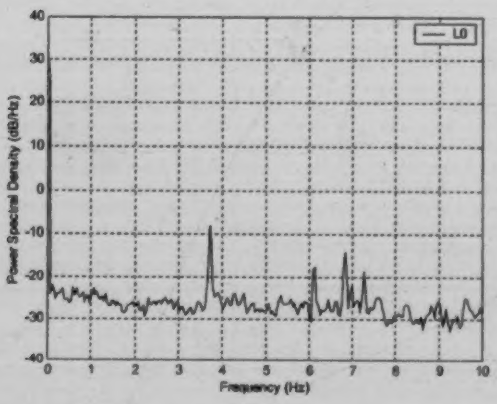

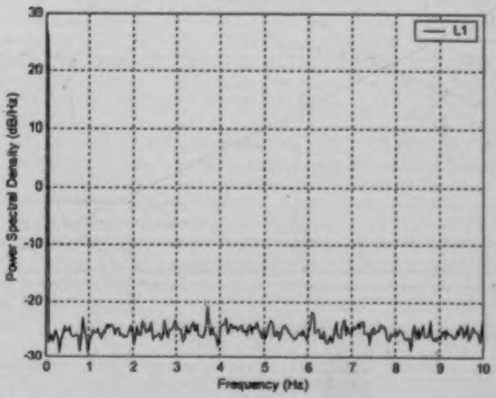

July 18, 1999
3:15 PM

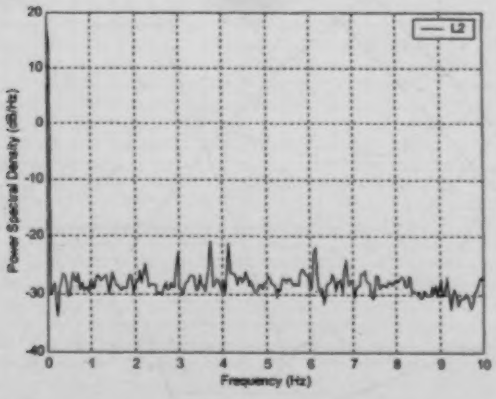

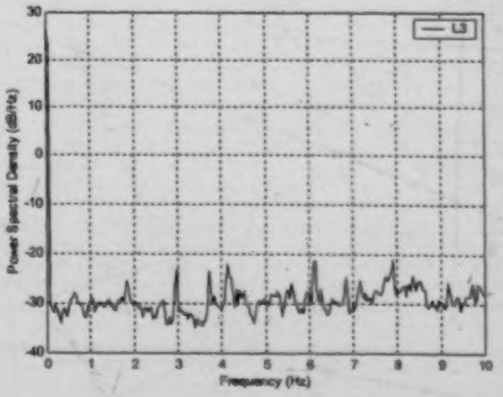

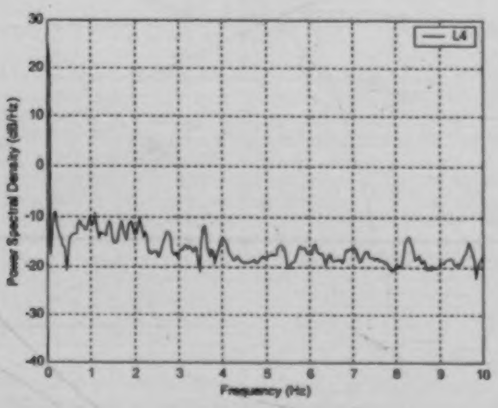

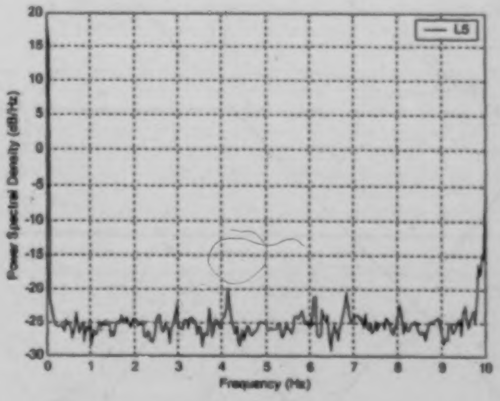

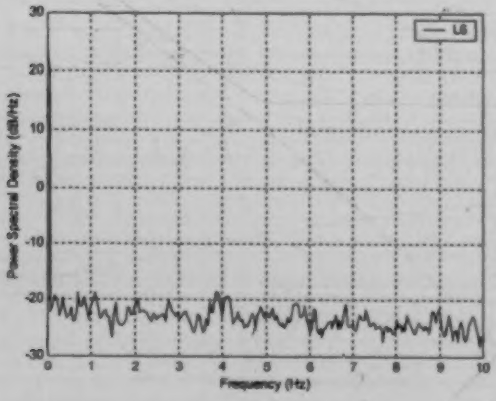

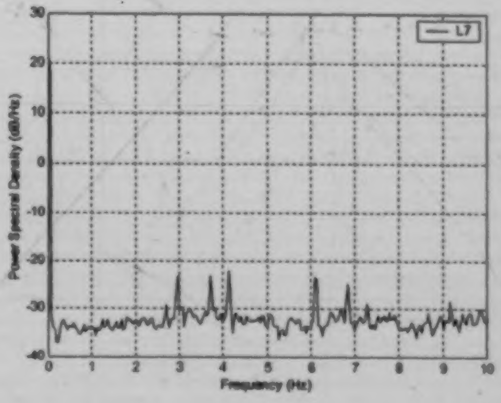

July 18, 1999
3:15 PM

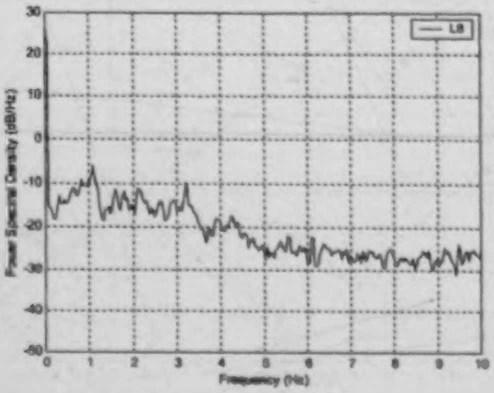

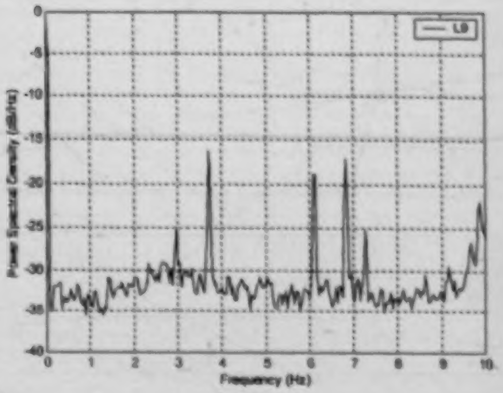

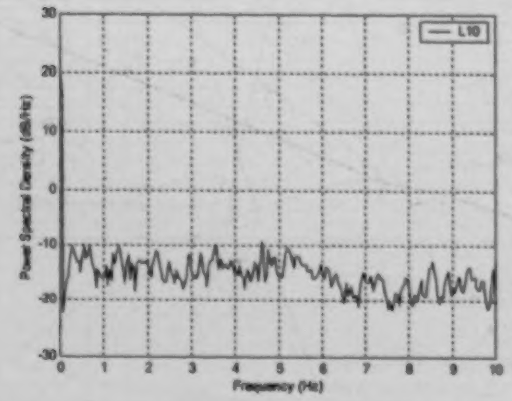

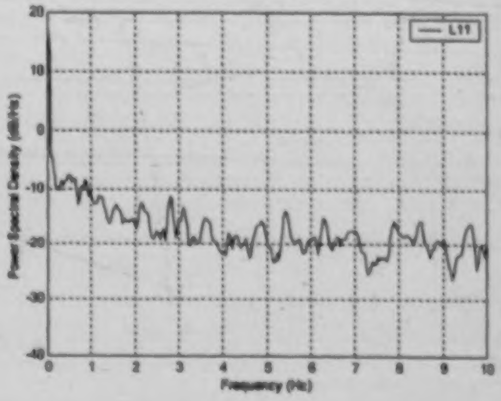

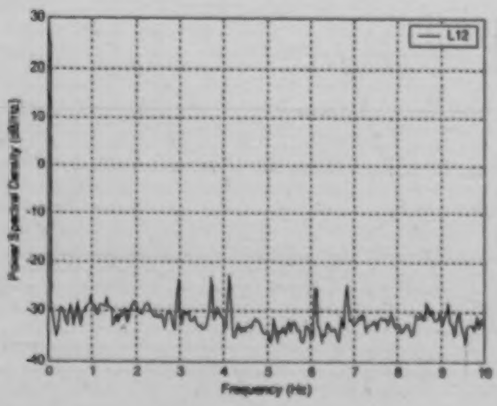

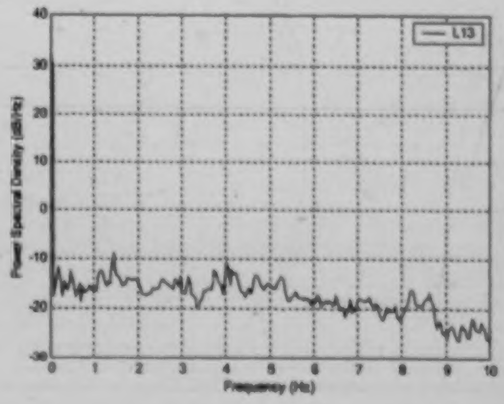

July 18, 1999
3:15 PM

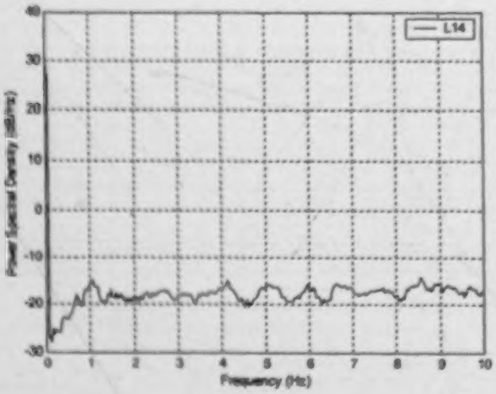

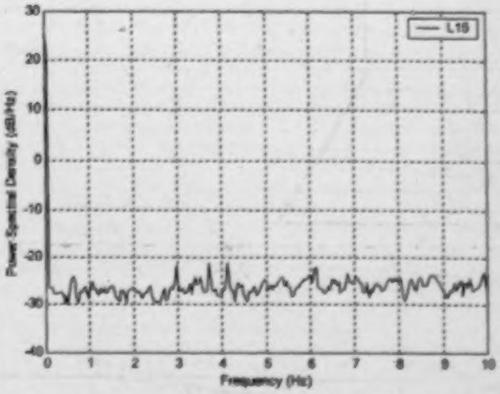

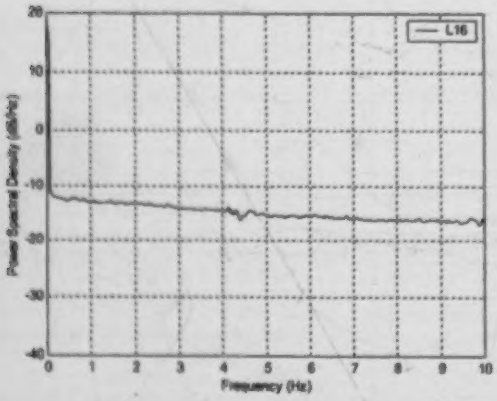

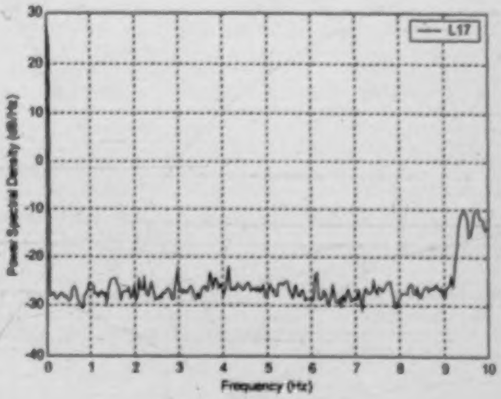

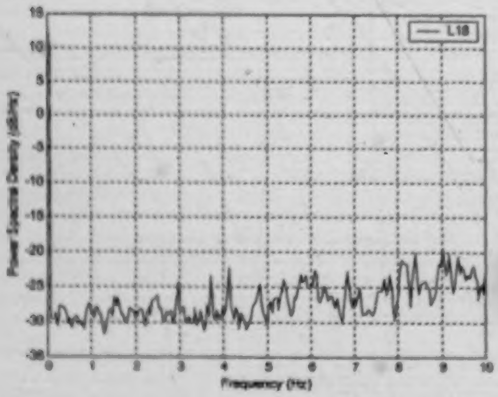

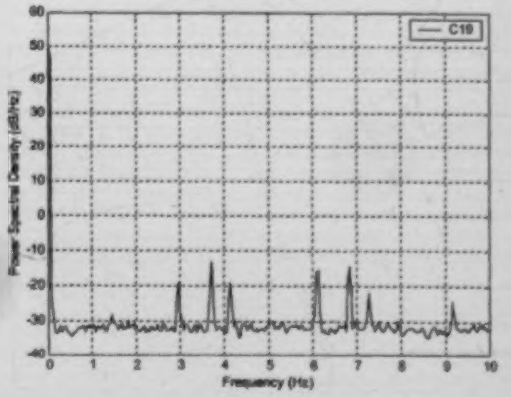

July 18, 1999
3:15 PM

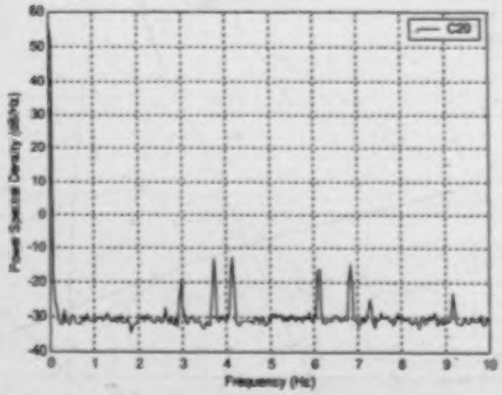

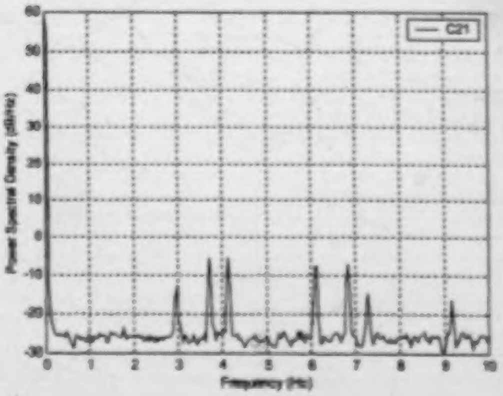

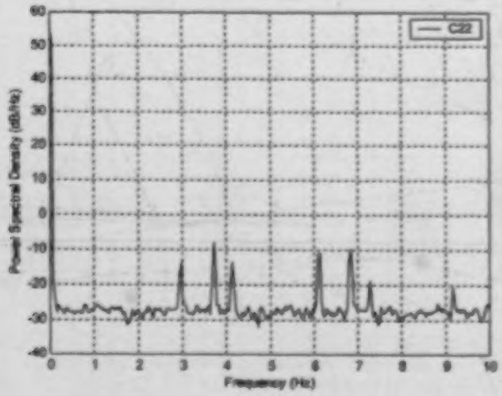

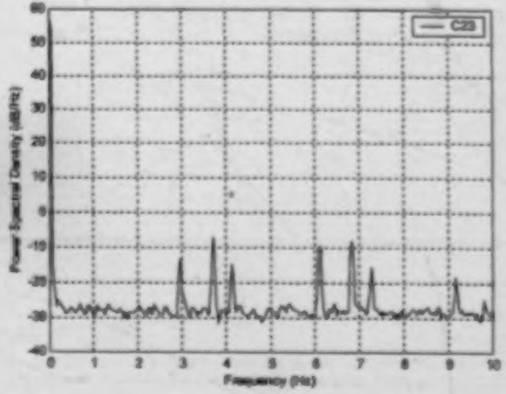

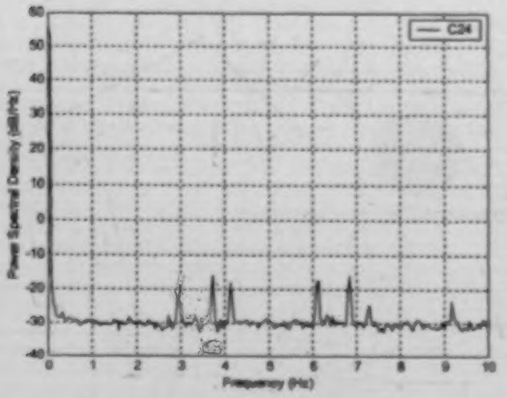

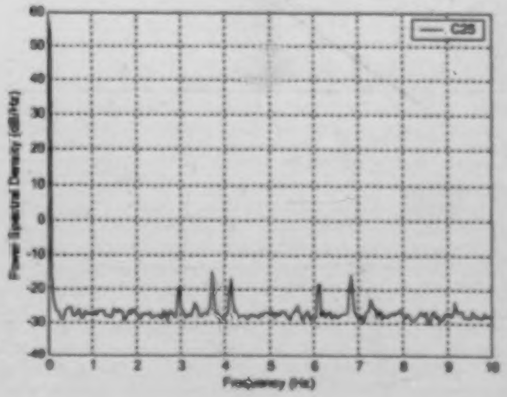

July 18, 1999
3:15 PM

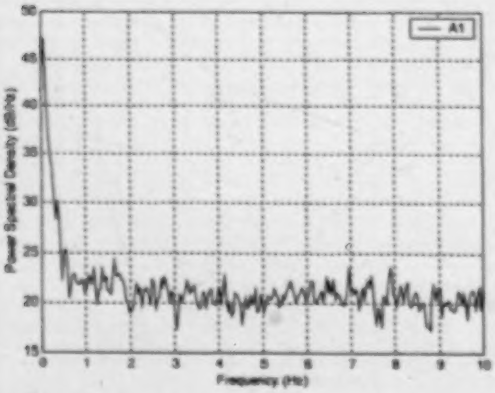

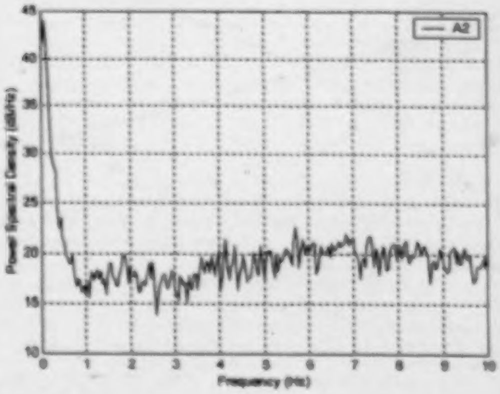

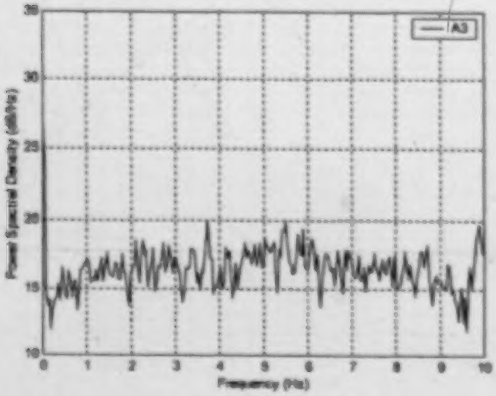

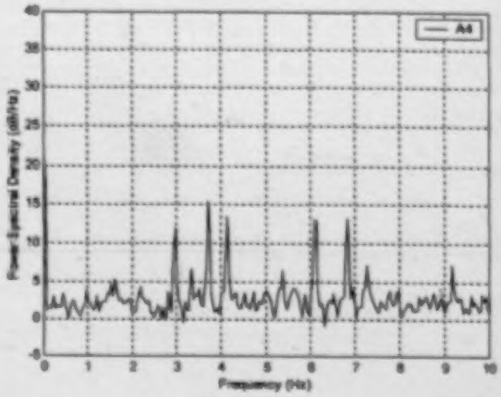

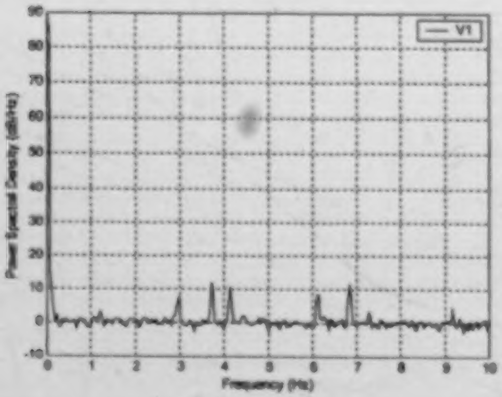

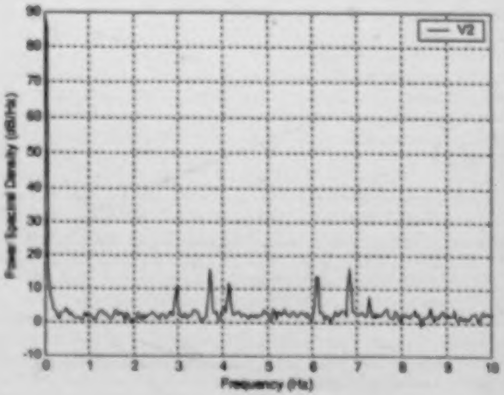

July 18, 1999
3:20 PM

July 18, 1999
3:20 PM

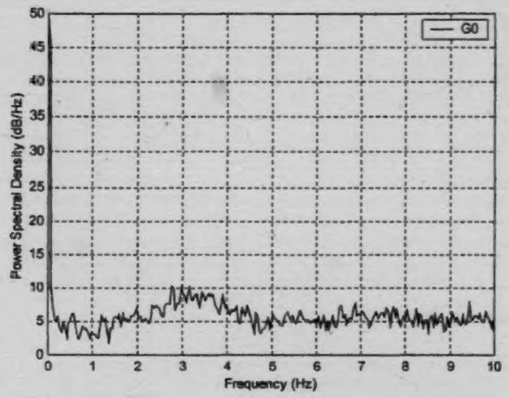

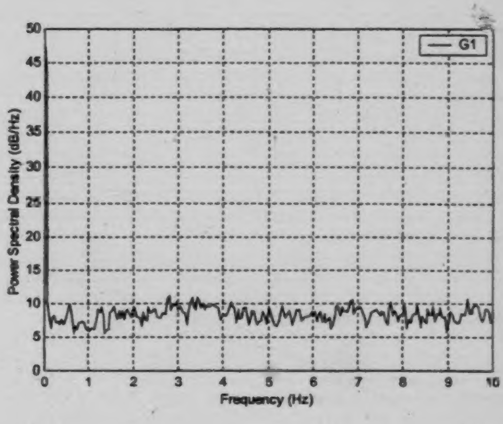

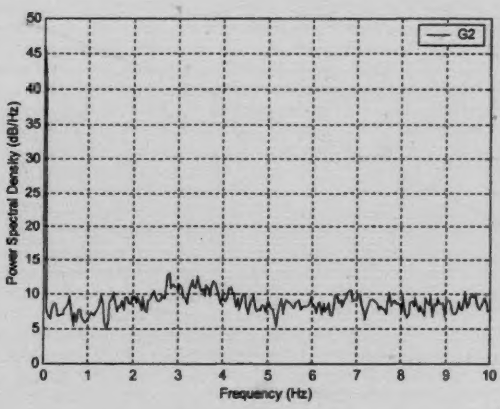

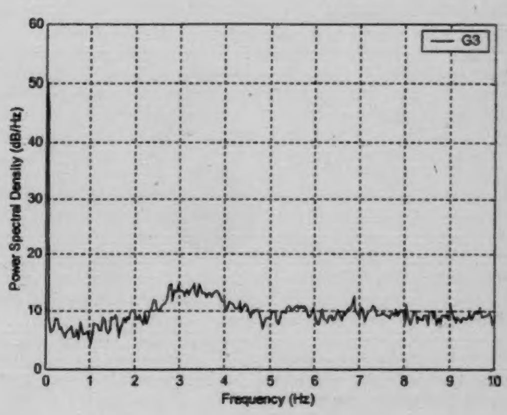

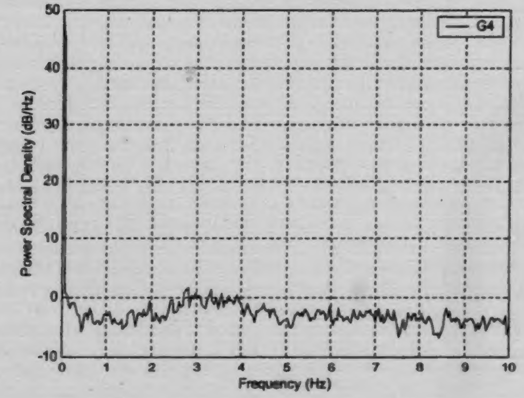

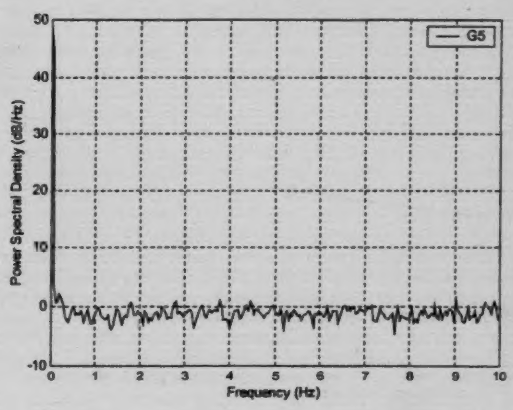

July 18, 1999
3:20 PM

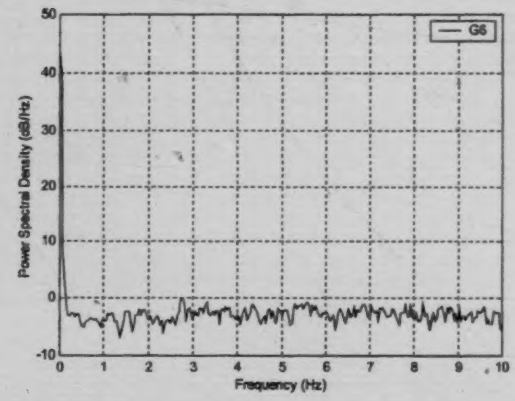

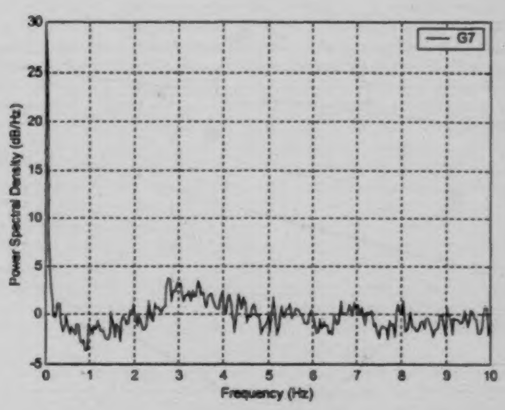

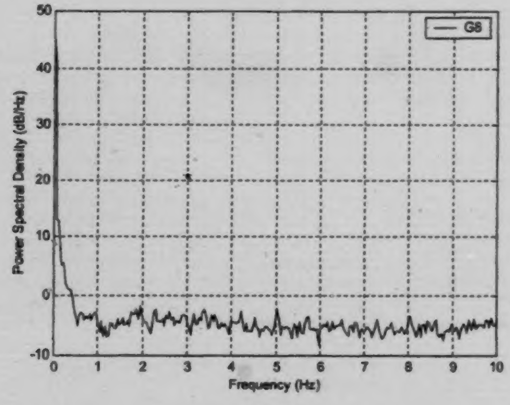

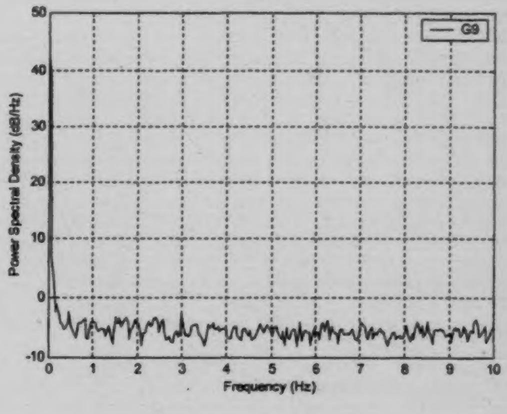

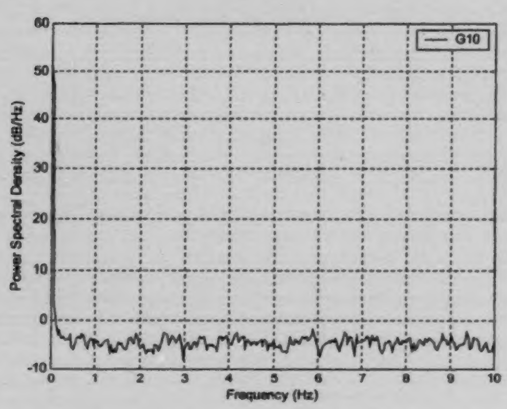

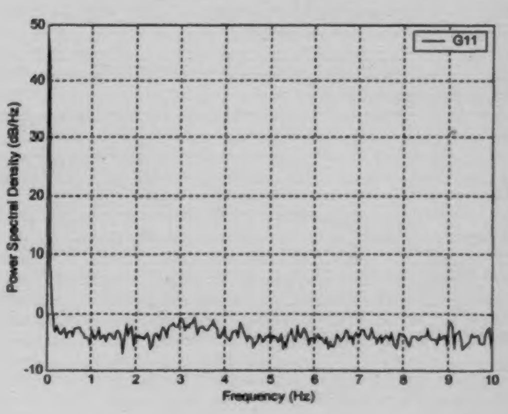

July 18, 1999
3:20 PM

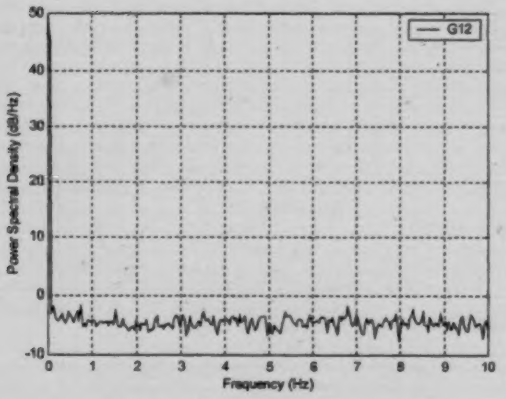

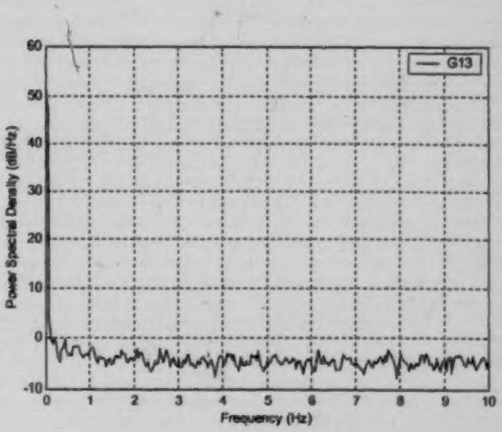

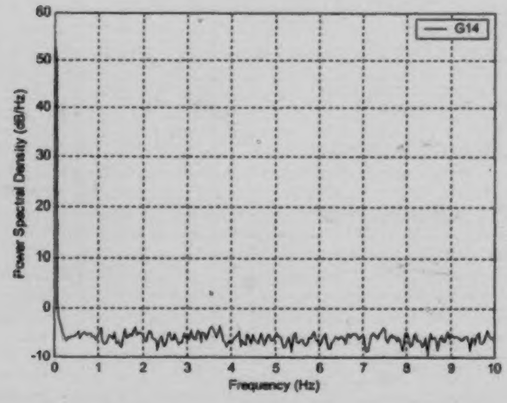

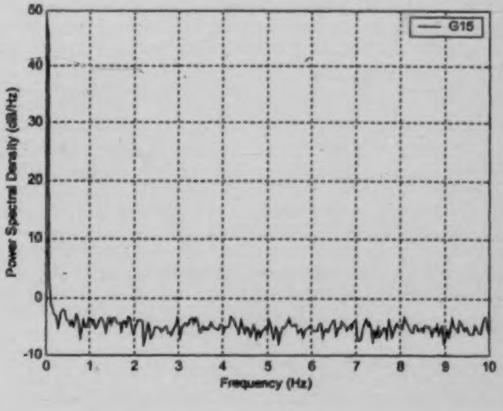

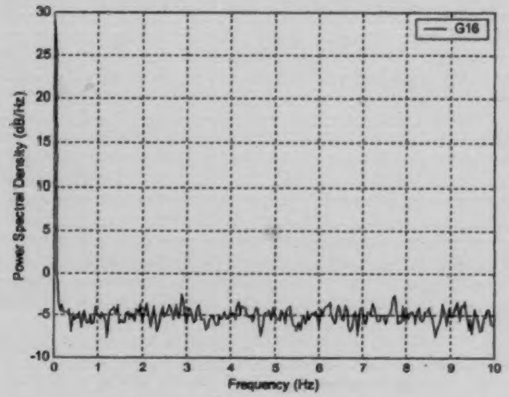

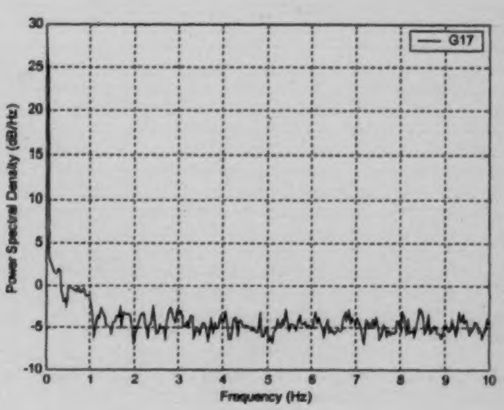

July 18, 1999
3:20 PM

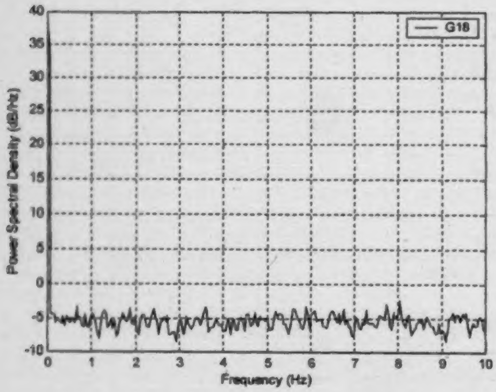

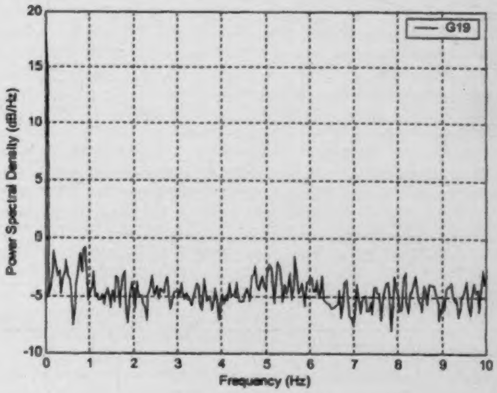

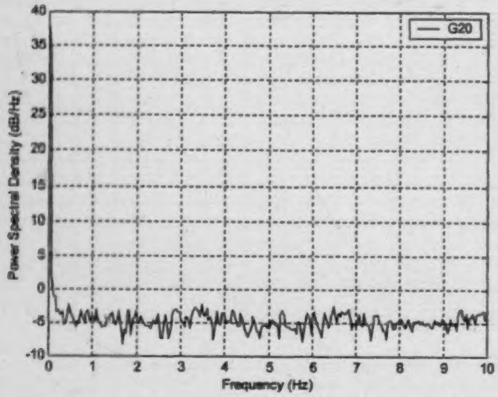

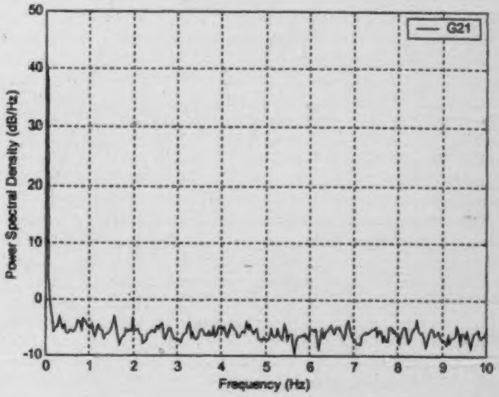

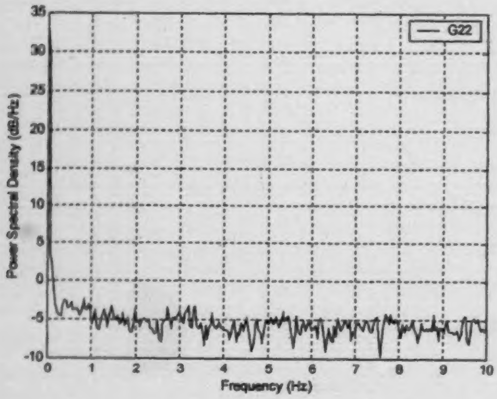

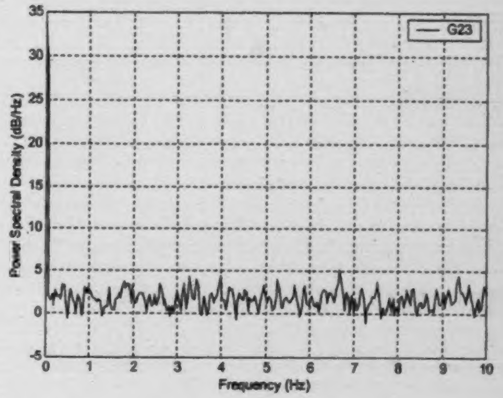

July 18, 1999
3:20 PM

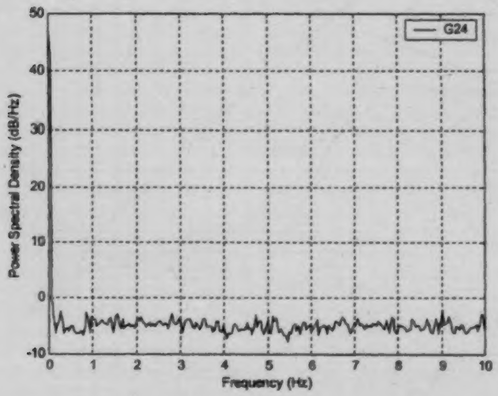

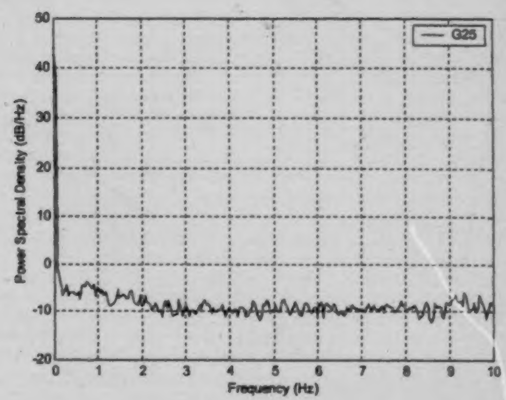

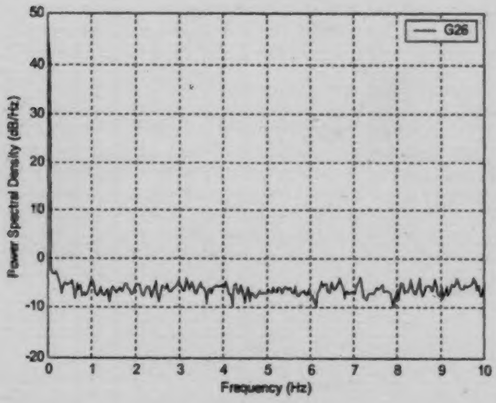

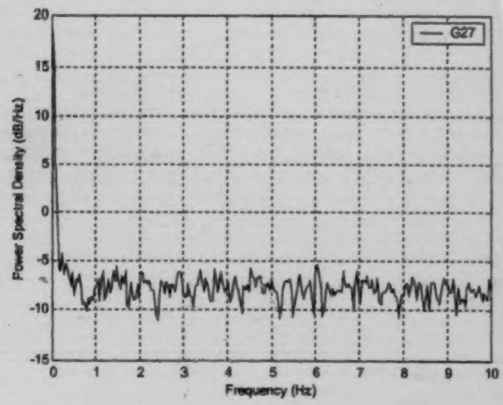

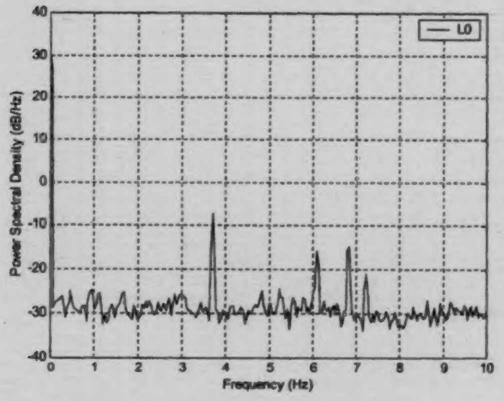

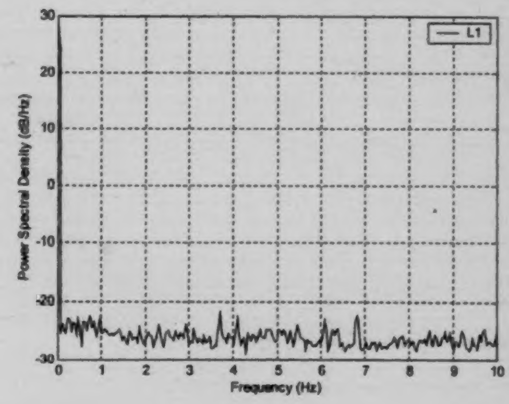

July 18, 1999
3:20 PM

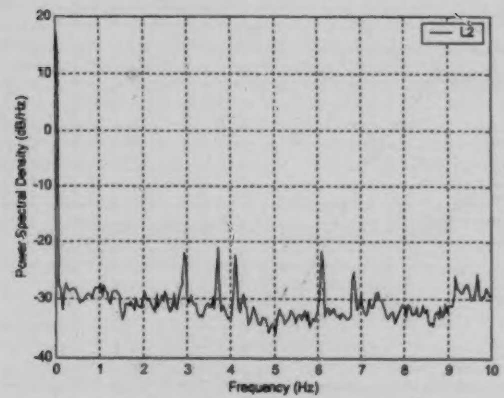

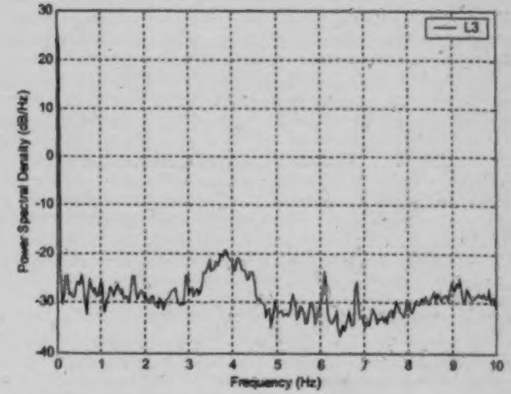

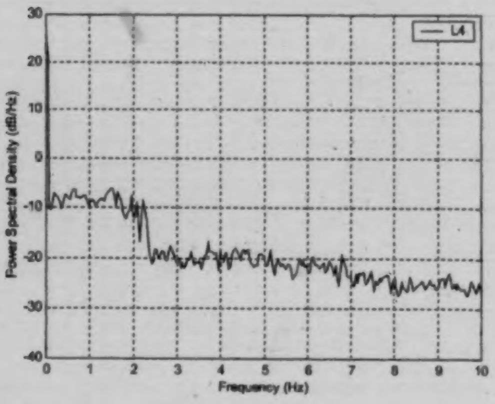

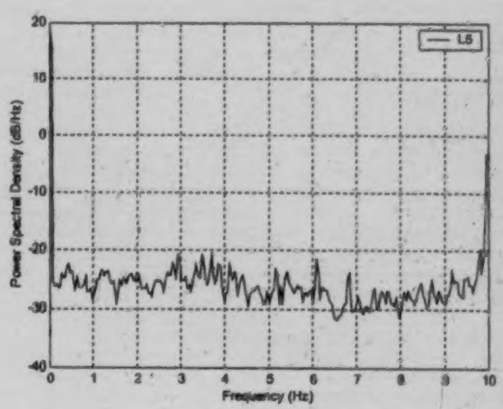

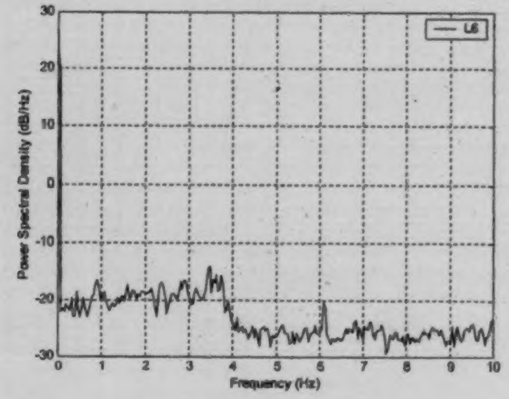

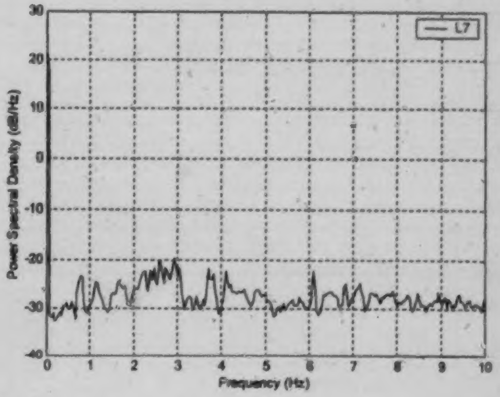

July 18, 1999
3:20 PM

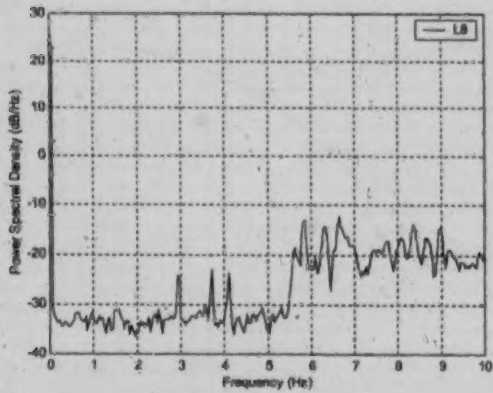

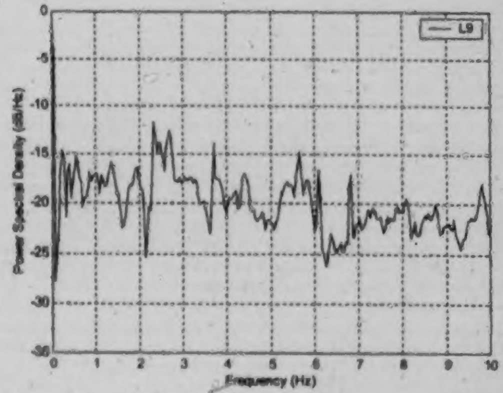

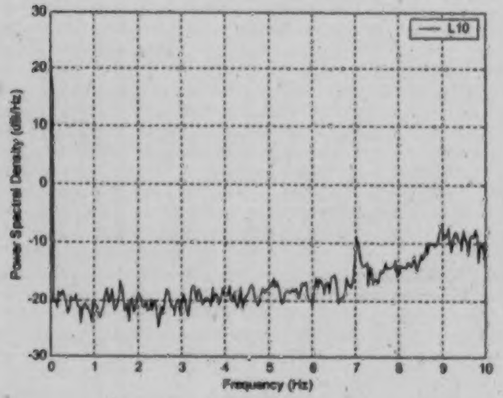

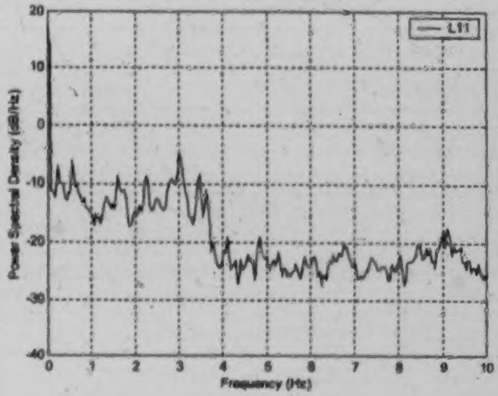

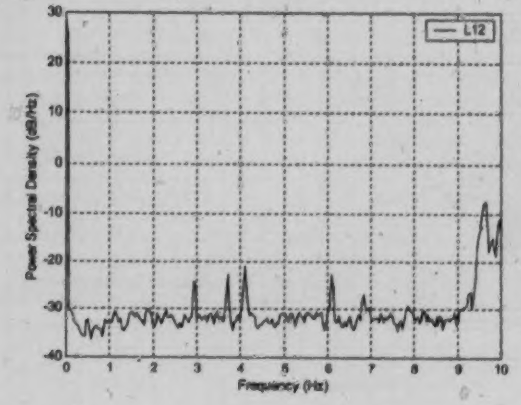

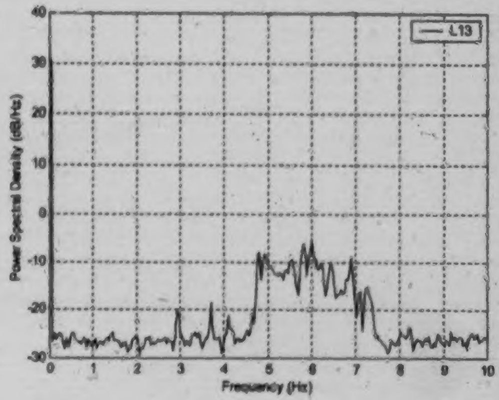

July 18, 1999
3:20 PM

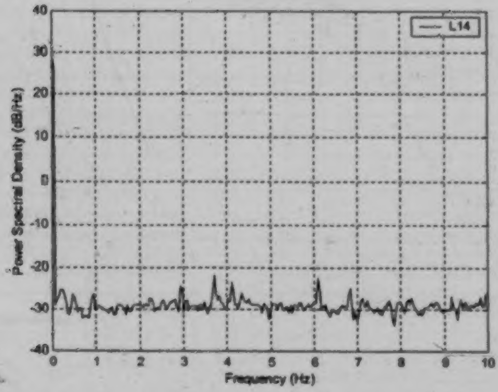

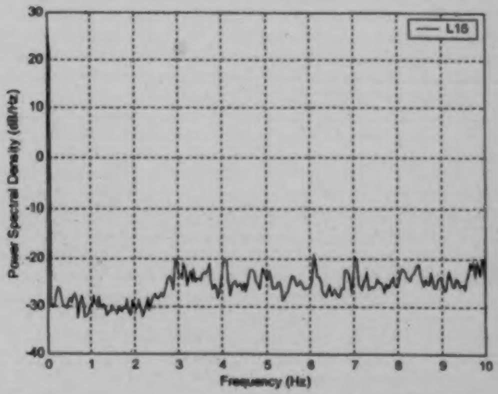

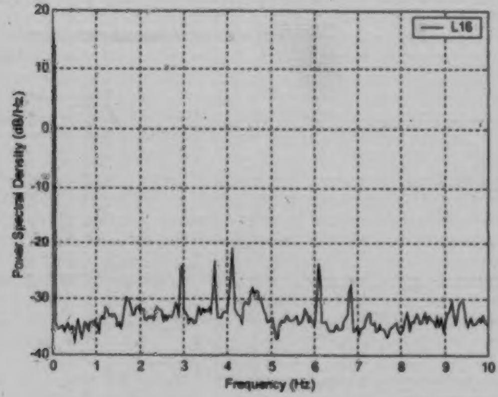

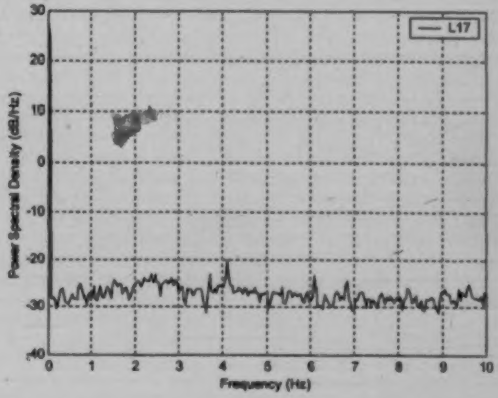

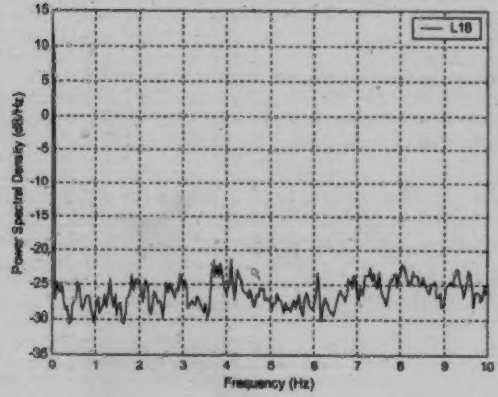

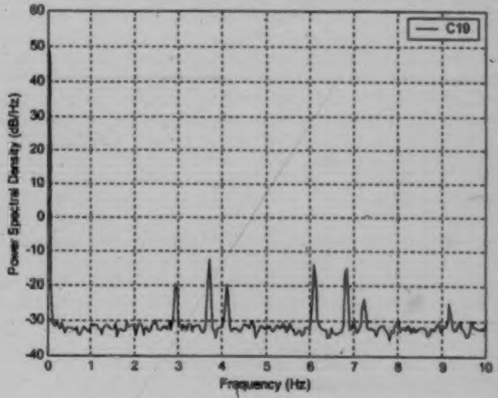

July 18, 1999
3:20 PM

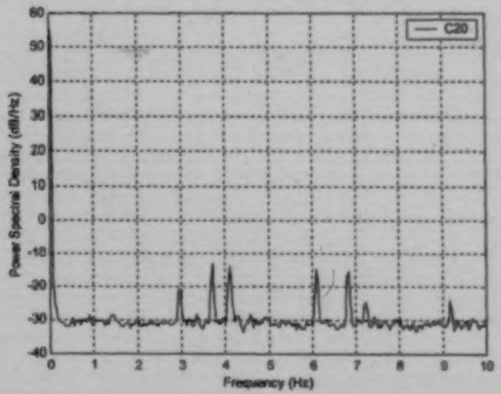

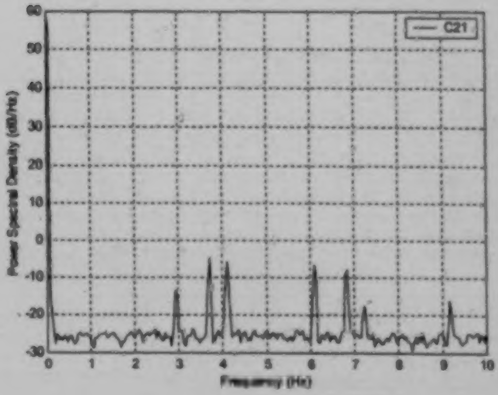

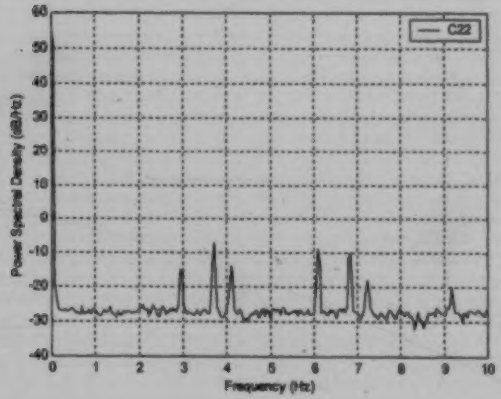

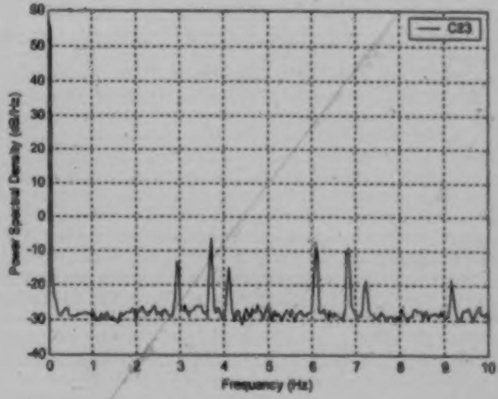

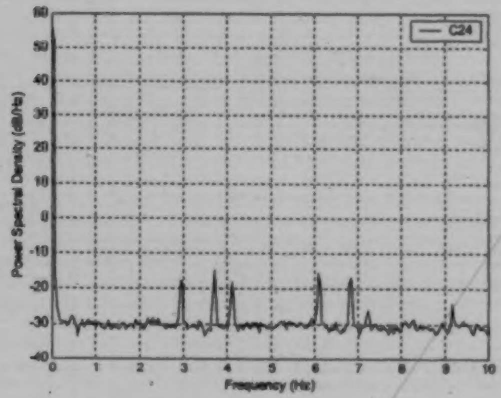

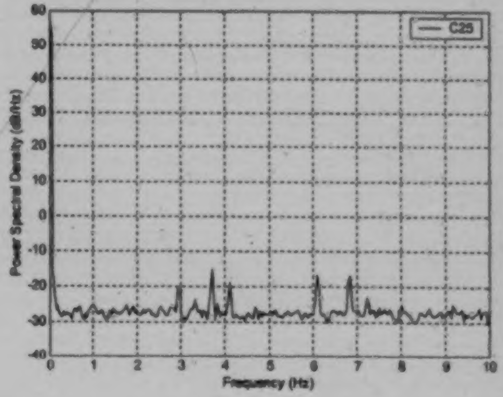

July 18, 1999
3:20 PM

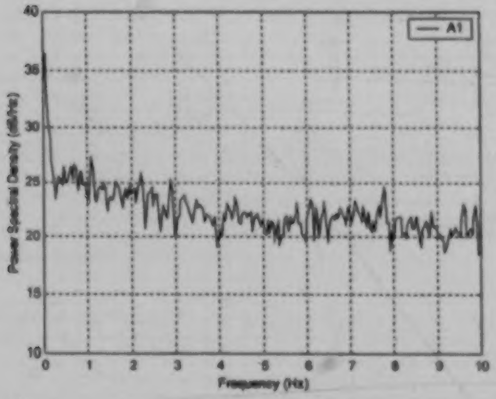

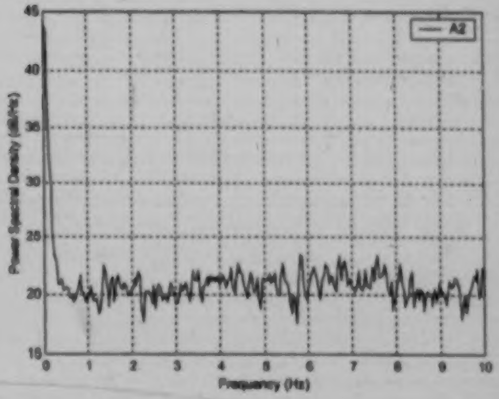

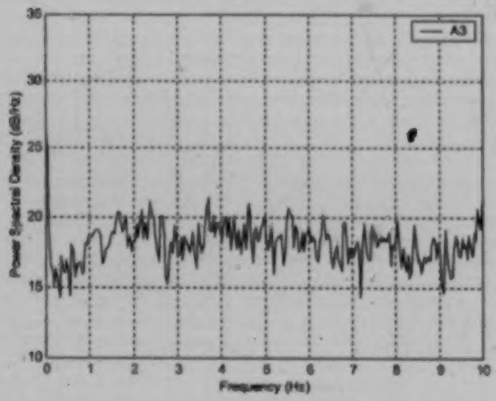

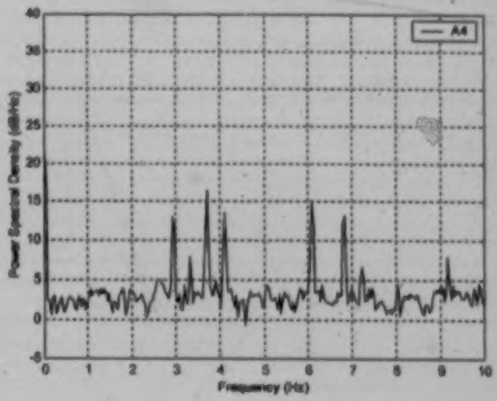

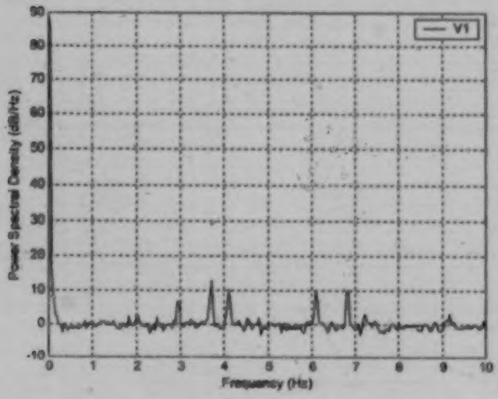

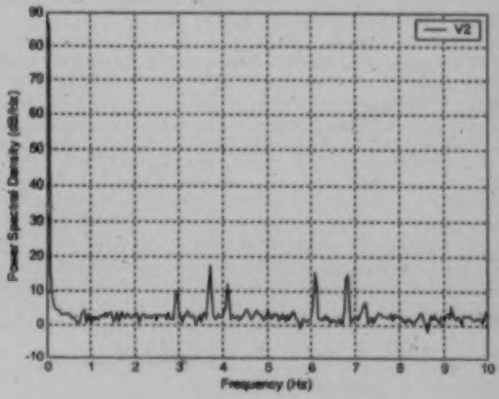

July 18, 1999
3:26 PM

July 18, 1999
3:26 PM

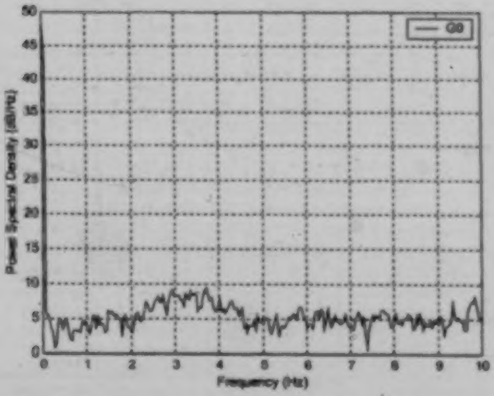

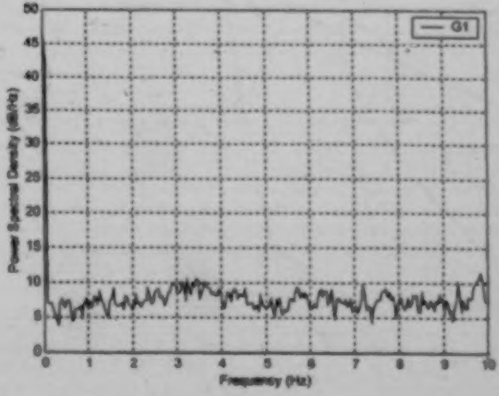

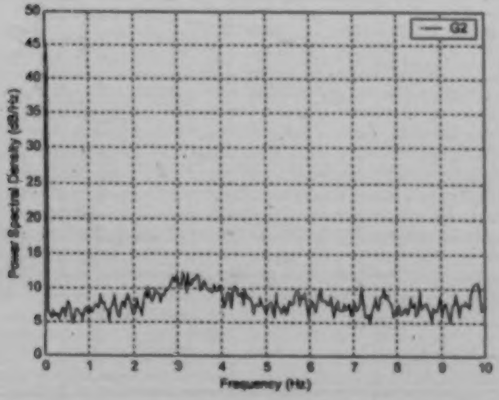

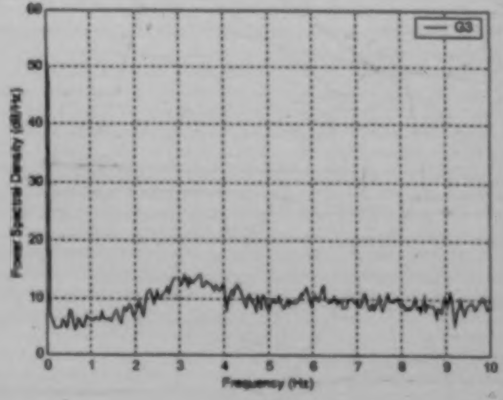

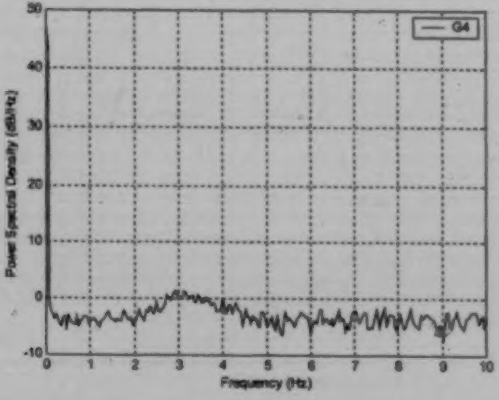

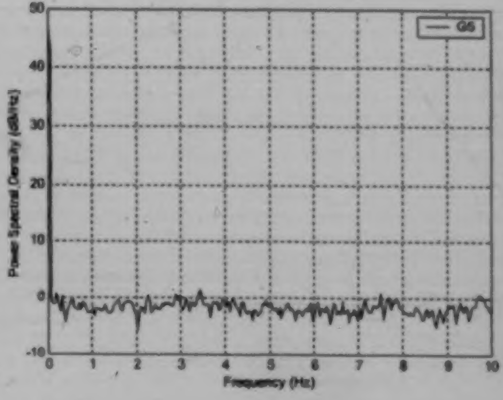

July 18, 1999
3:26 PM

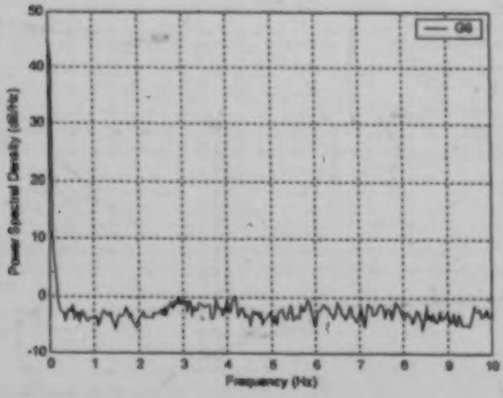

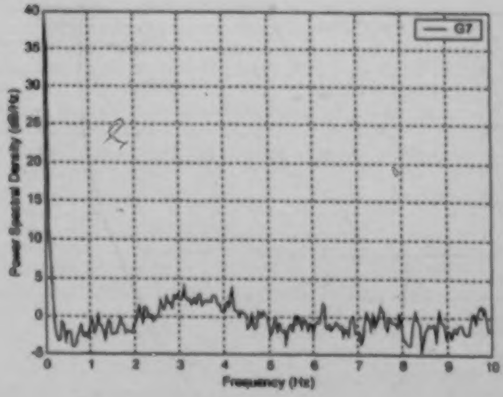

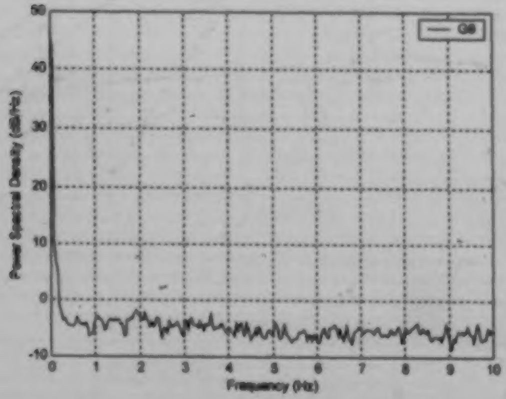

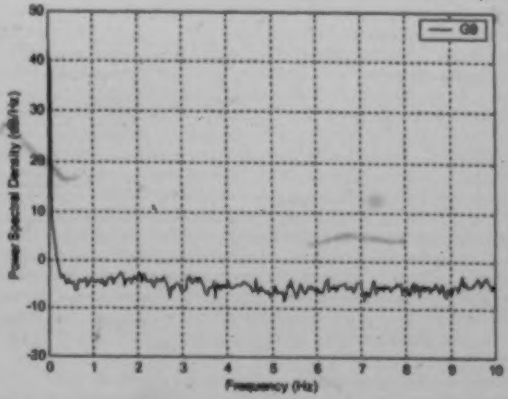

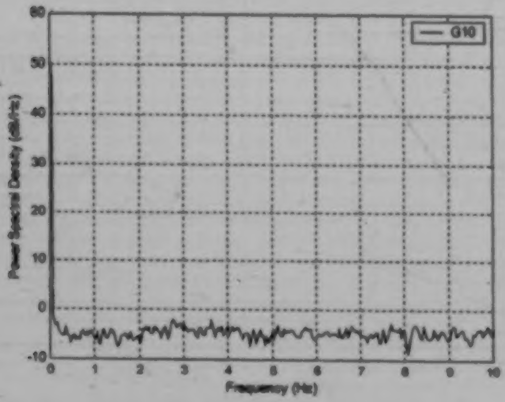

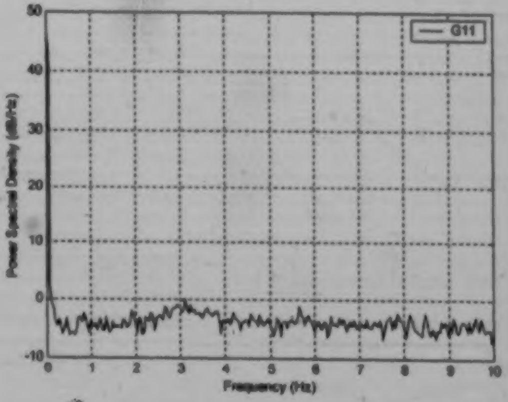

July 18, 1999
3:26 PM

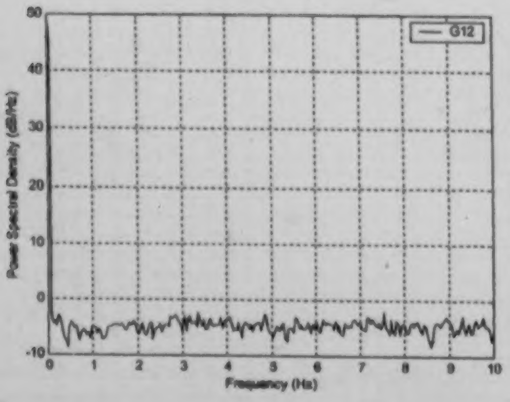

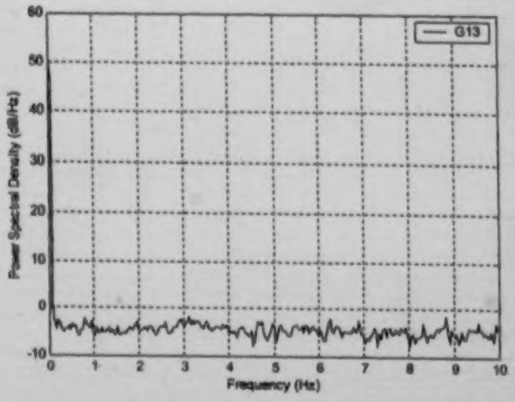

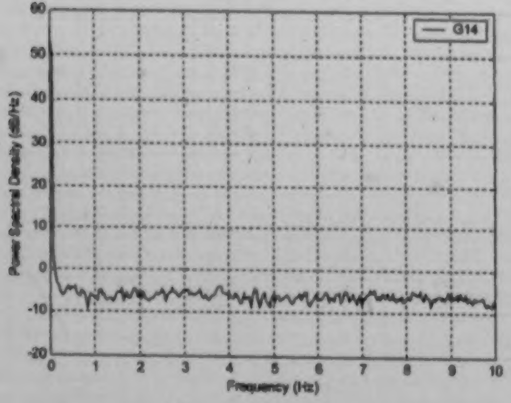

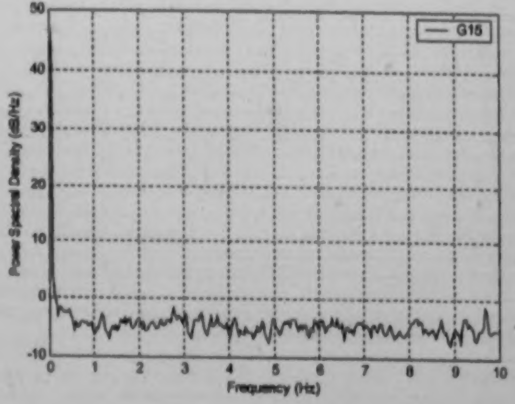

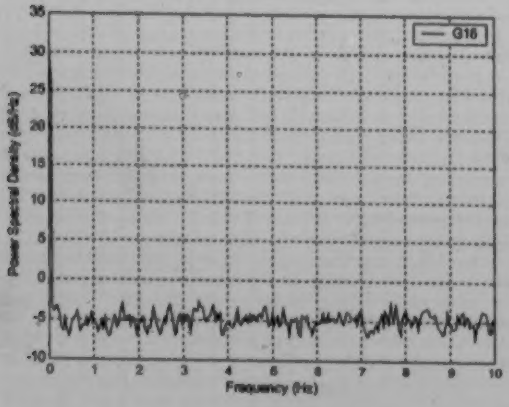

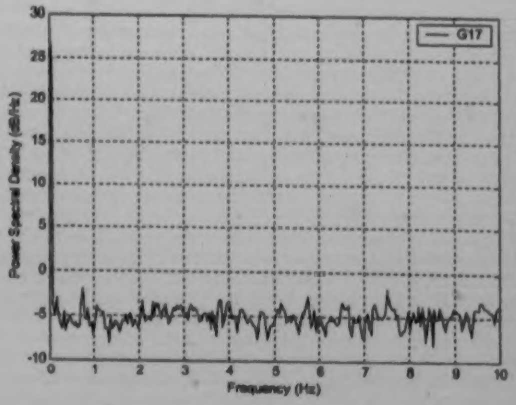

July 18, 1999
3:26 PM

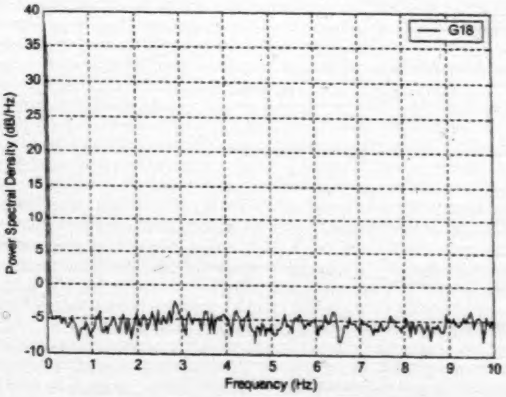

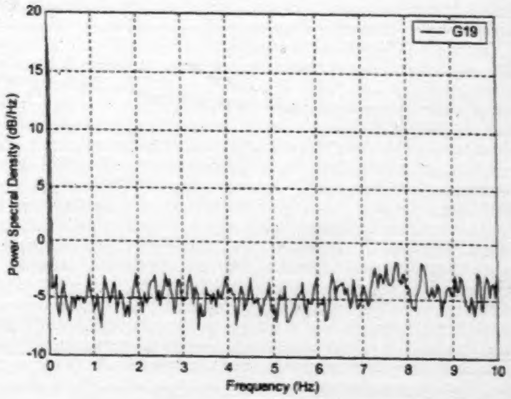

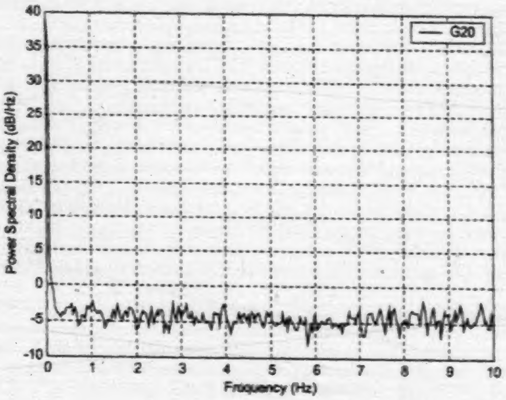

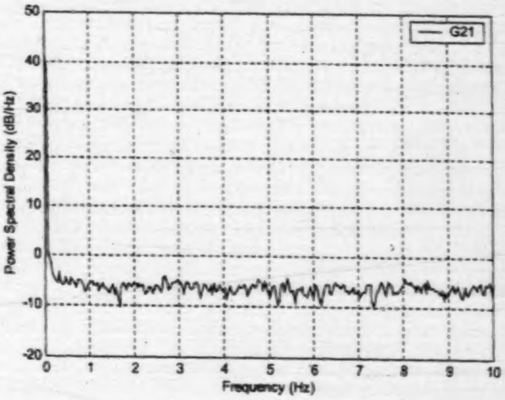

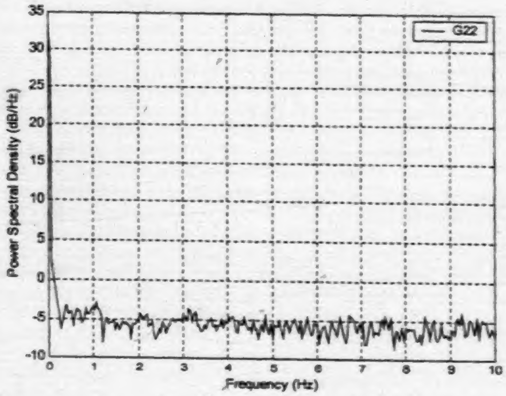

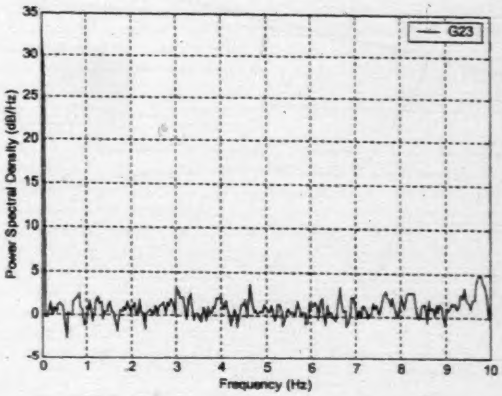

July 18, 1999
3:26 PM

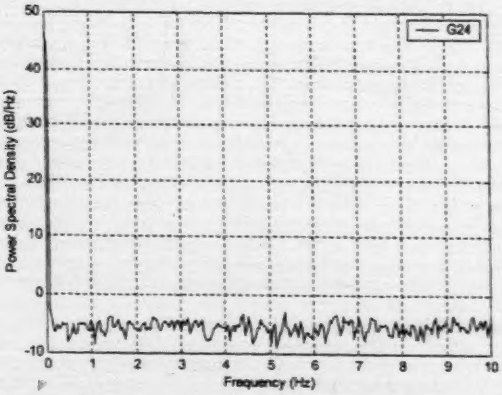

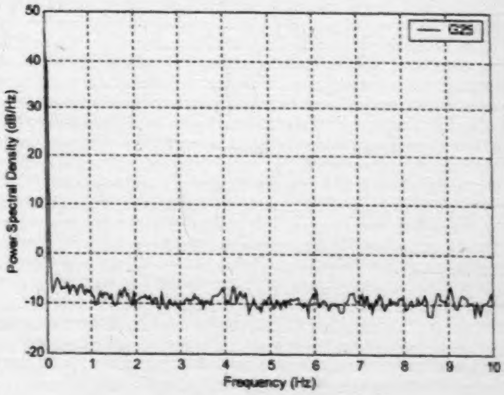

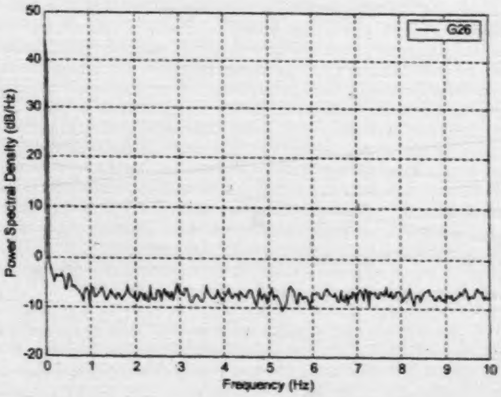

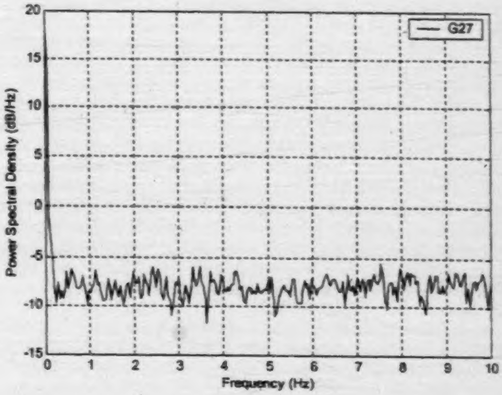

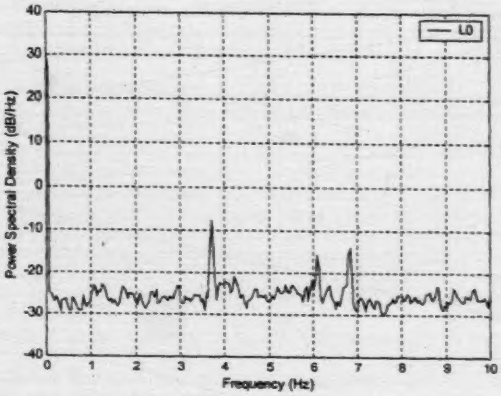

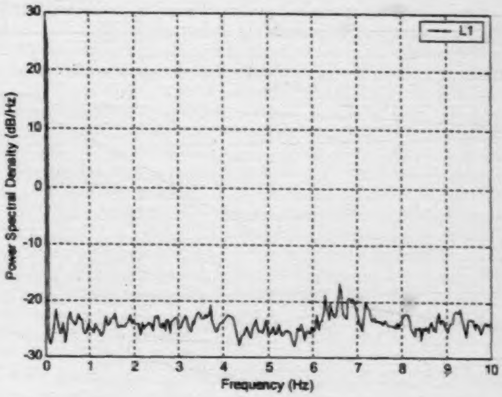

July 18, 1999
3:26 PM

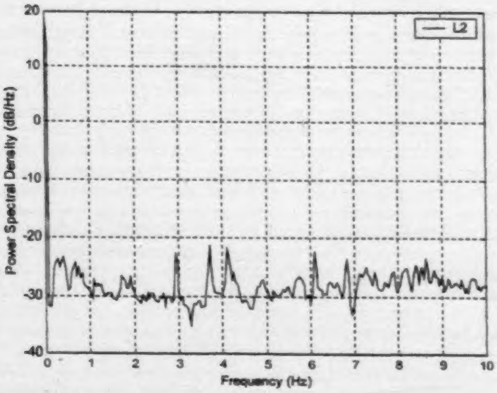

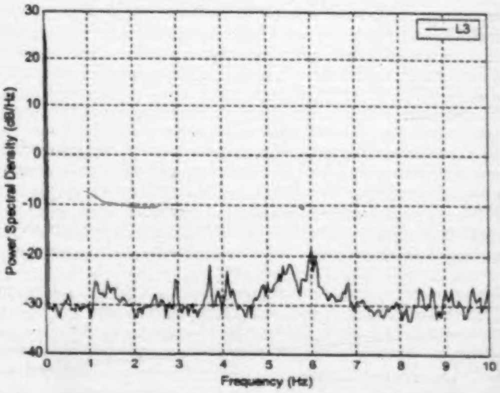

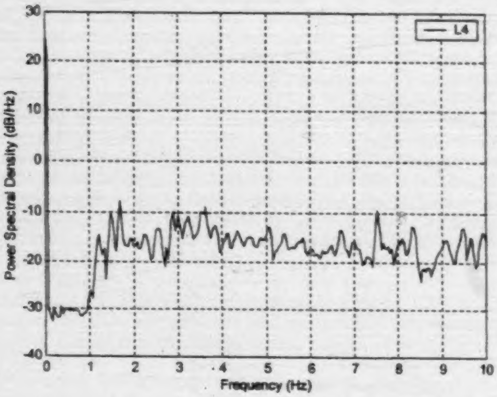

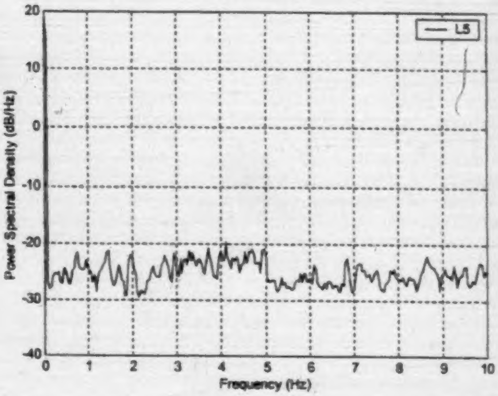

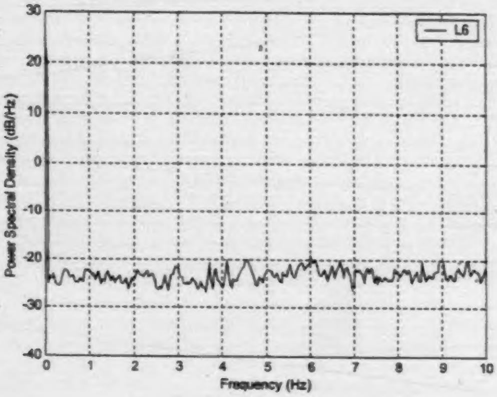

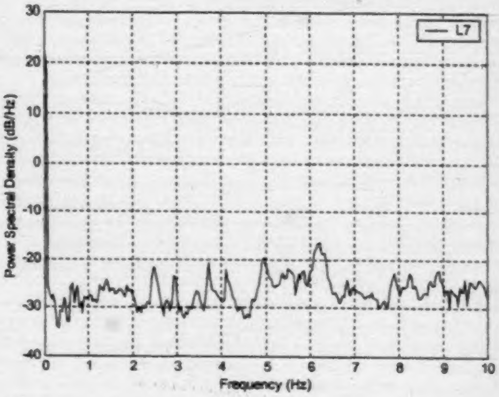

July 18, 1999
3:26 PM

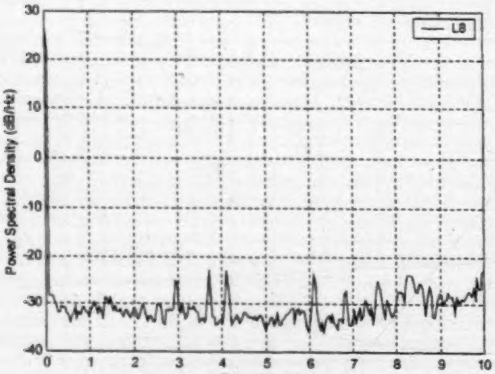

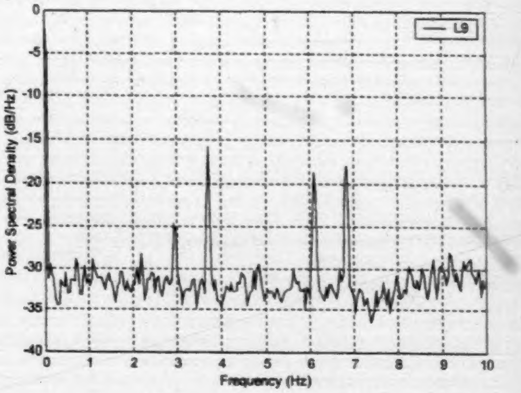

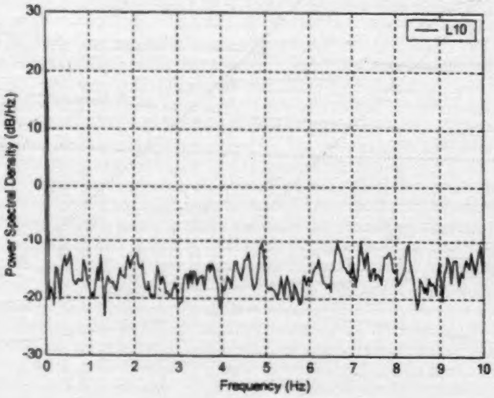

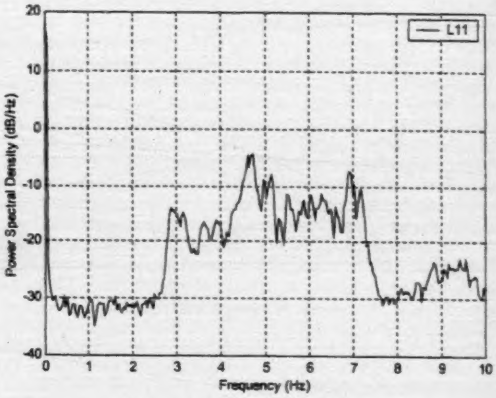

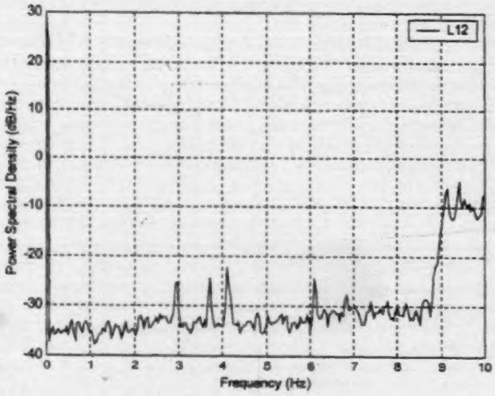

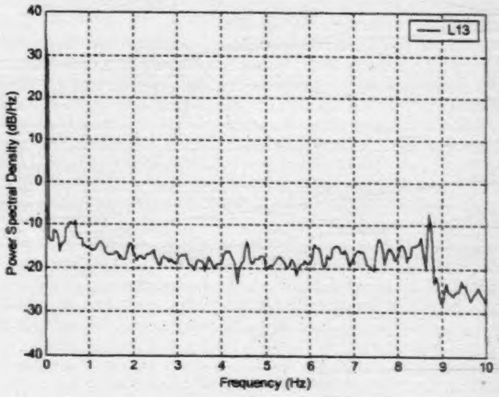

July 18, 1999
3:26 PM

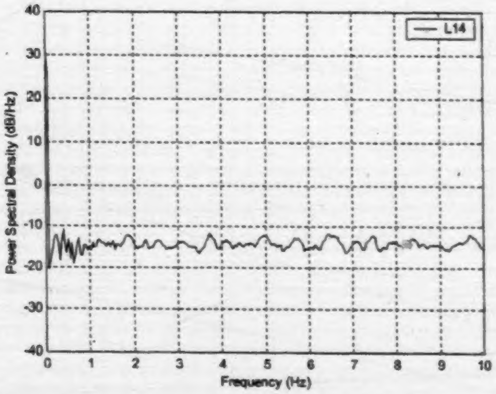

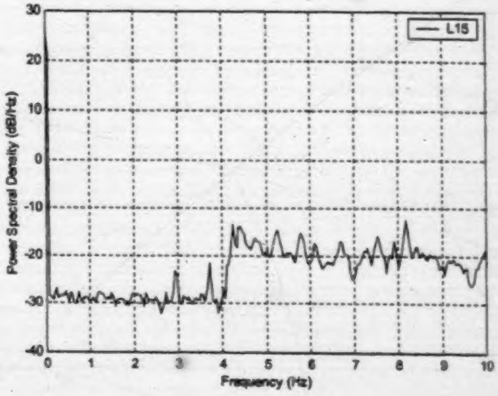

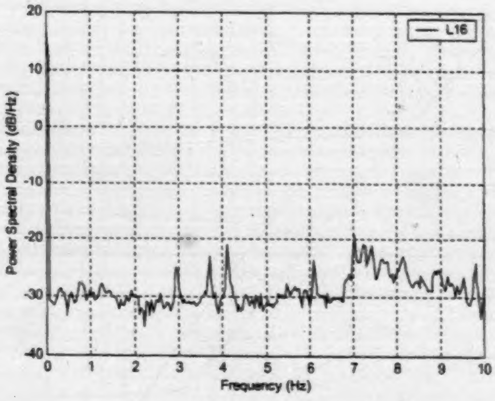

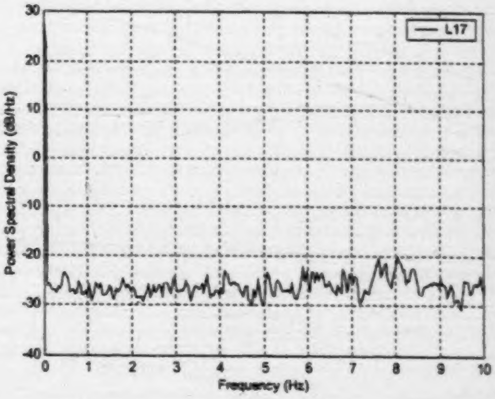

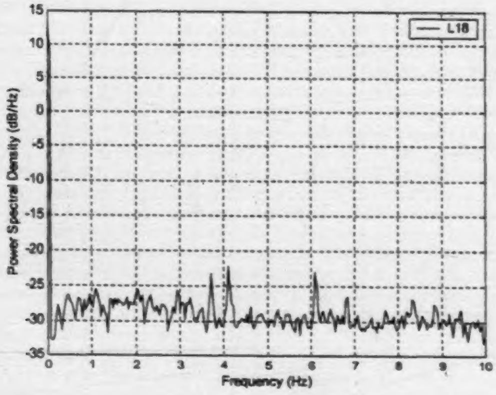

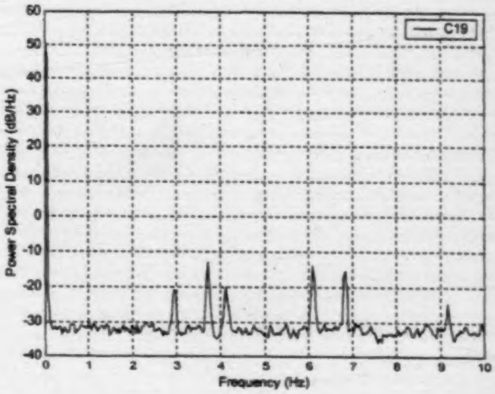

July 18, 1999
3:26 PM

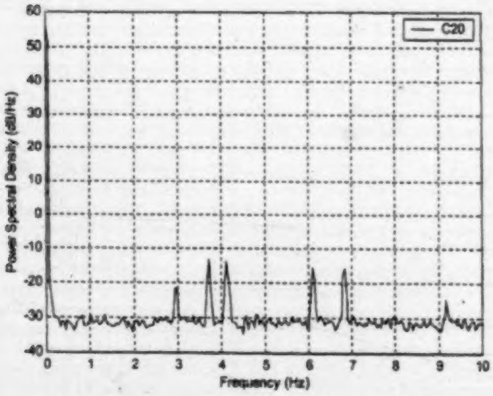

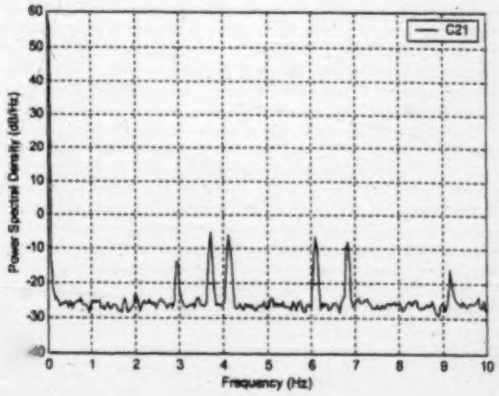

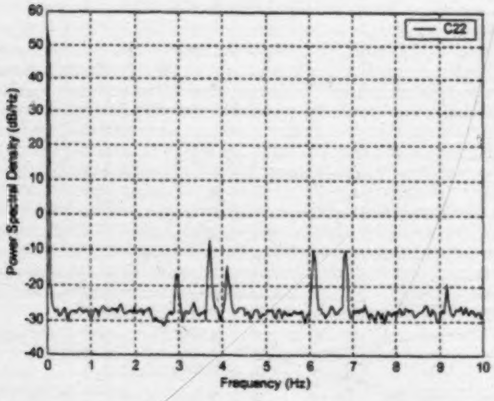

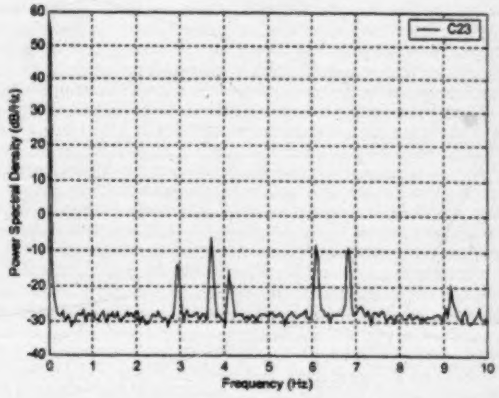

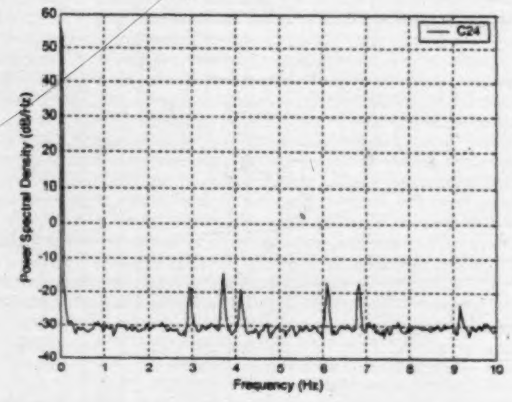

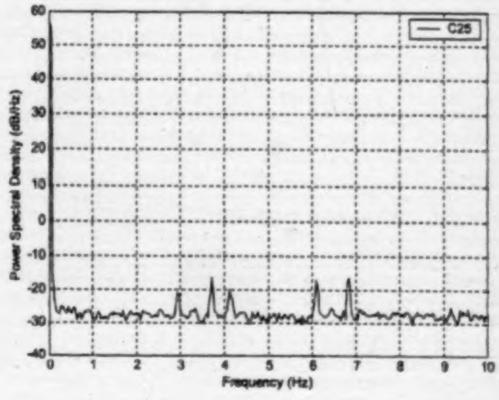

July 18, 1999
3:26 PM

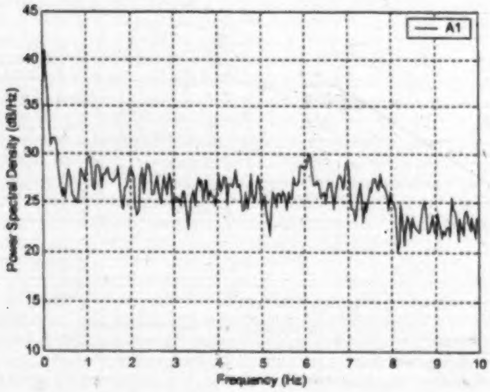

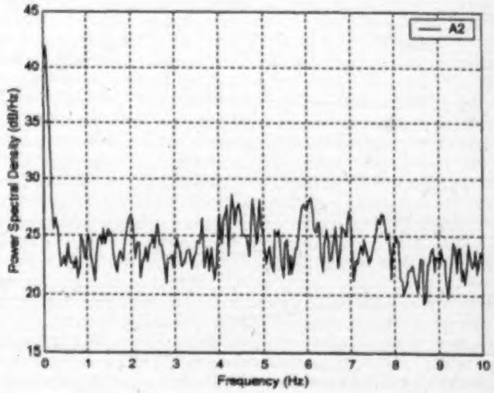

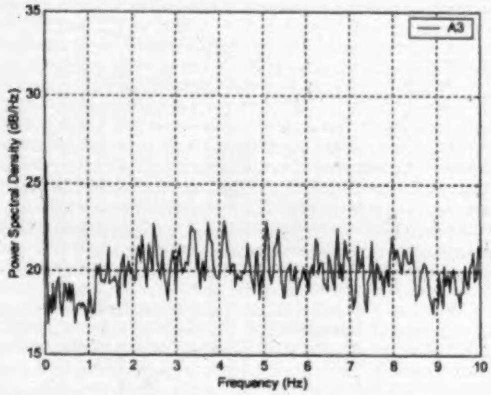

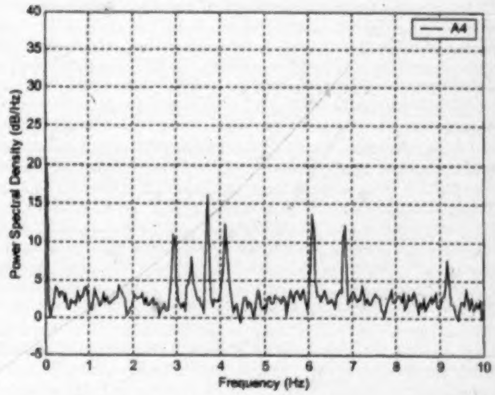

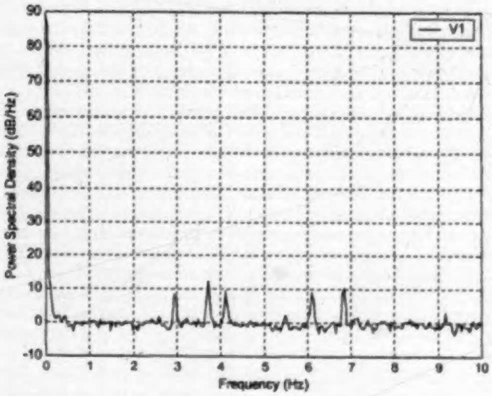

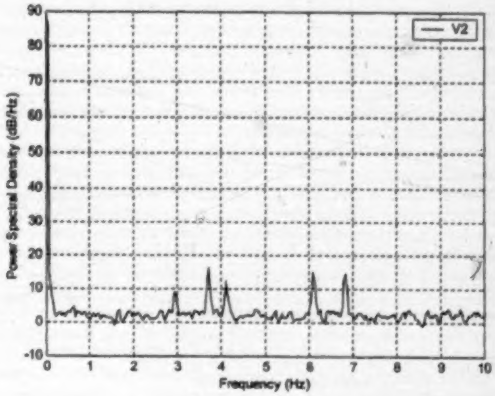

July 18, 1999
3:32 PM

July 18, 1999
3:32 PM

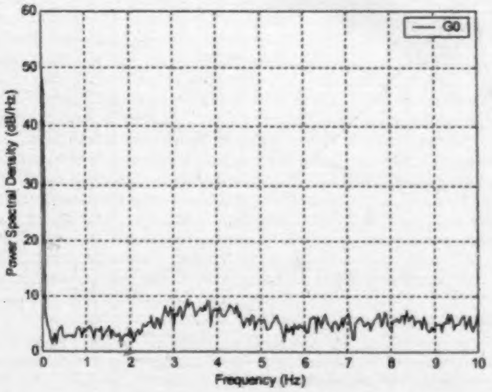

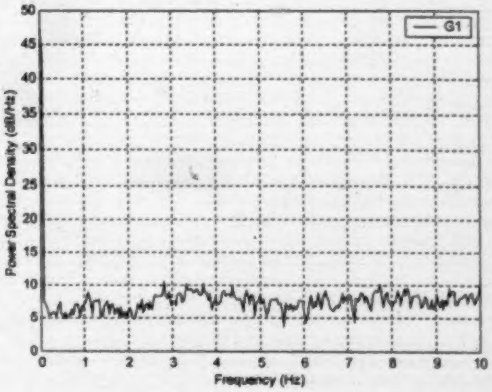

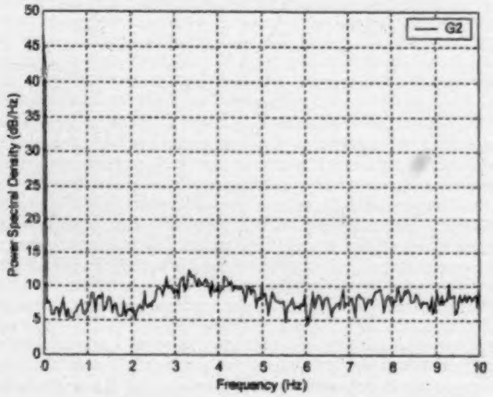

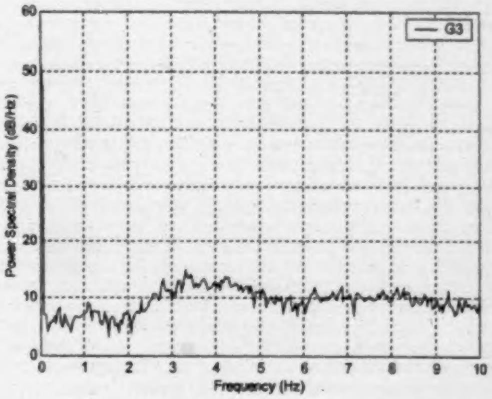

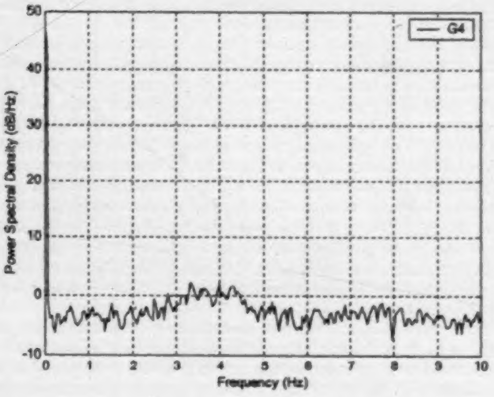

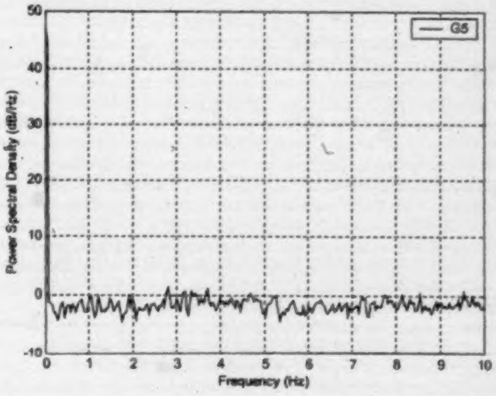

July 18, 1999
3:32 PM

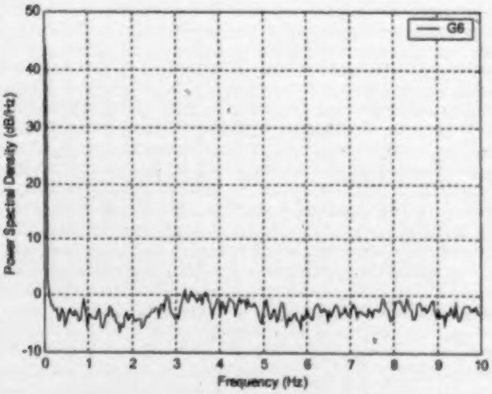

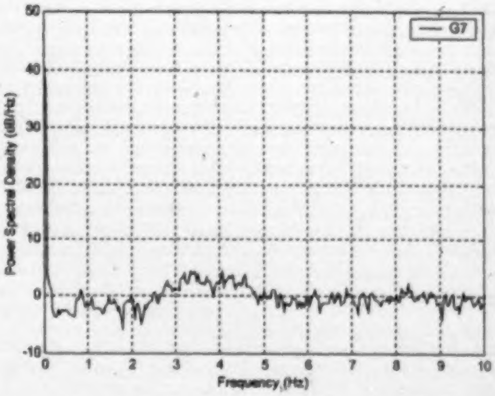

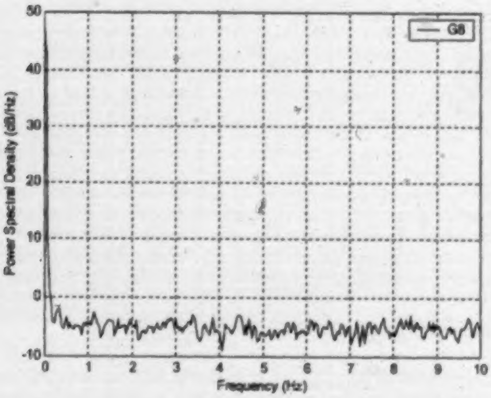

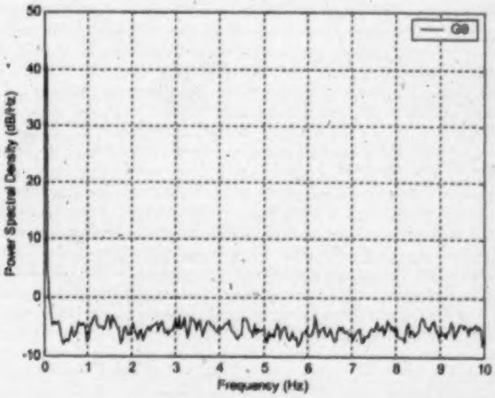

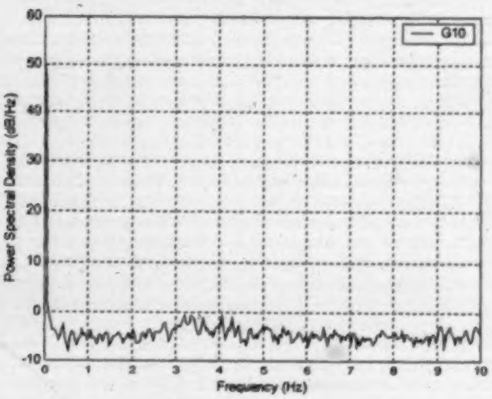

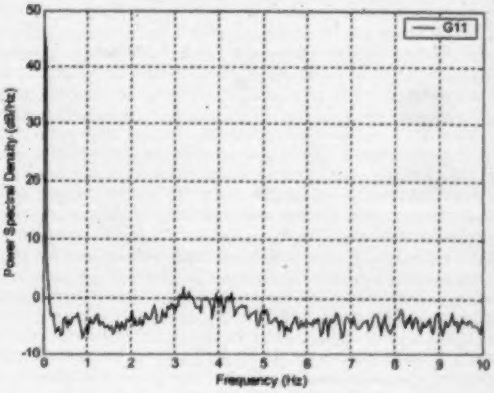

July 18, 1999
3:32 PM

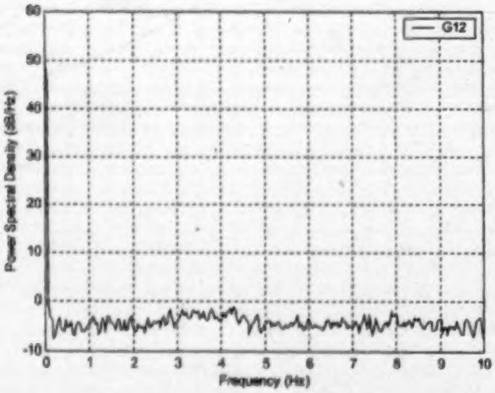

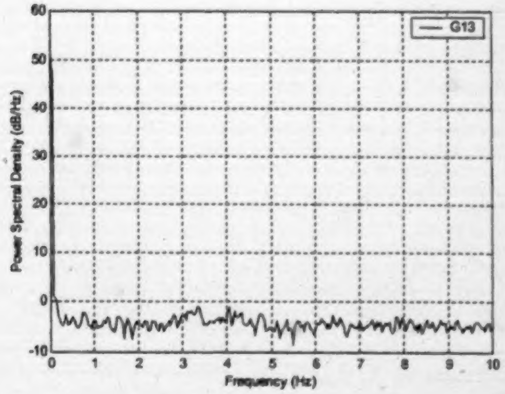

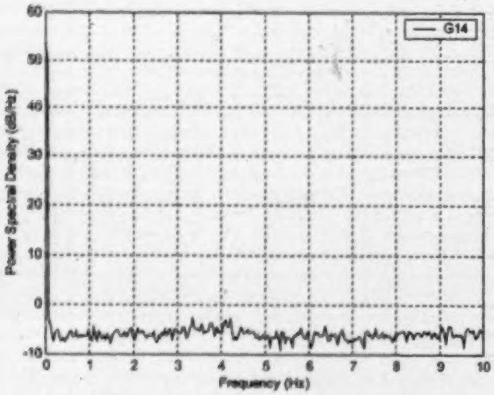

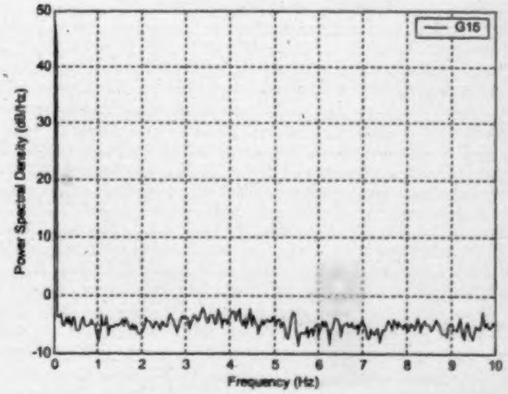

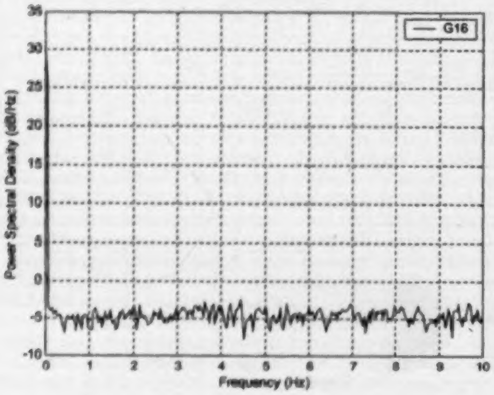

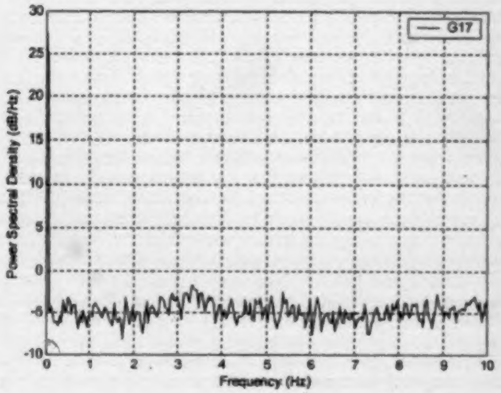

July 18, 1999
3:32 PM

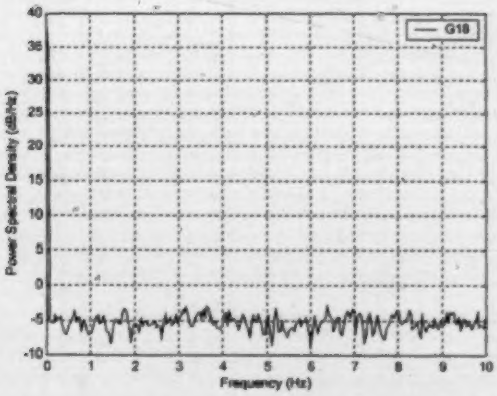

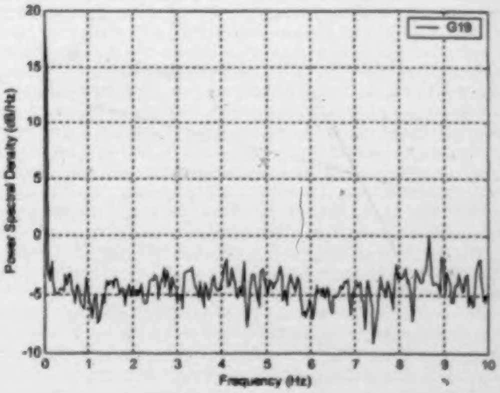

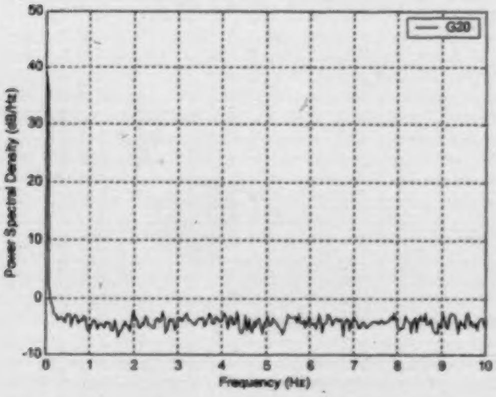

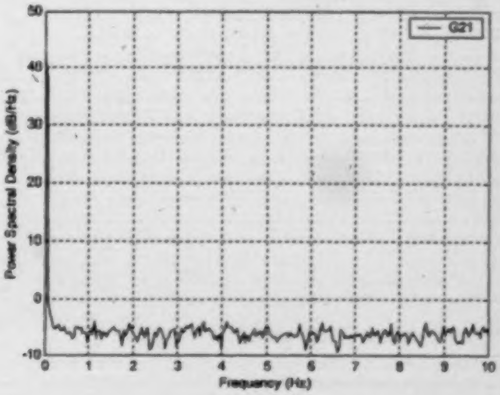

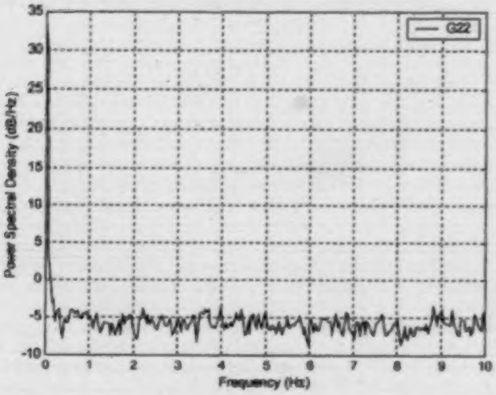

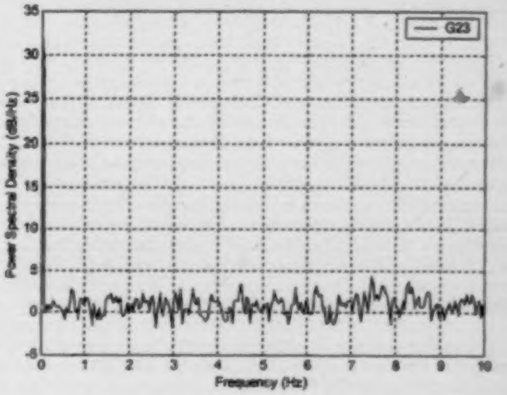

July 18, 1999
3:32 PM

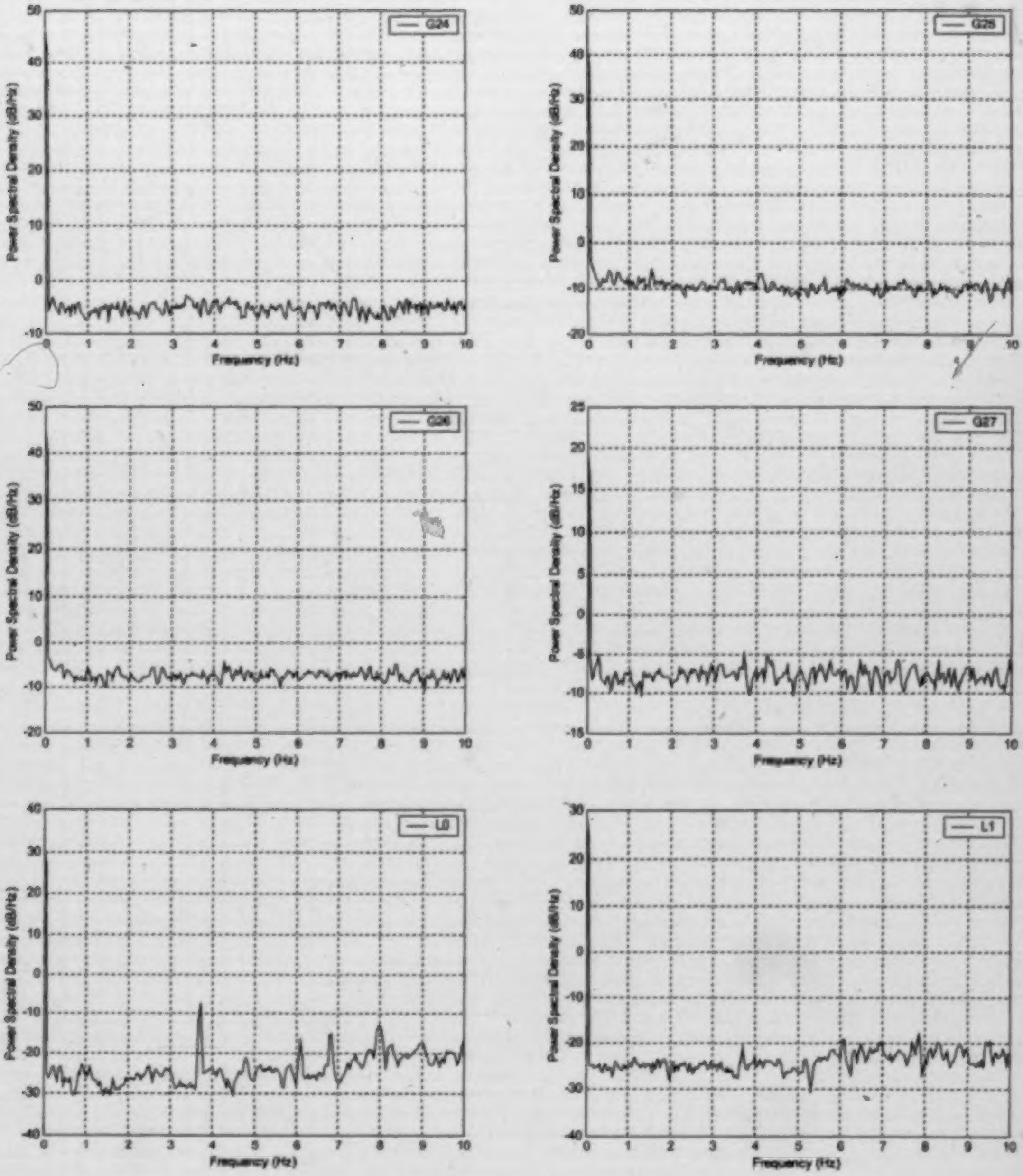

July 18, 1999
3:32 PM

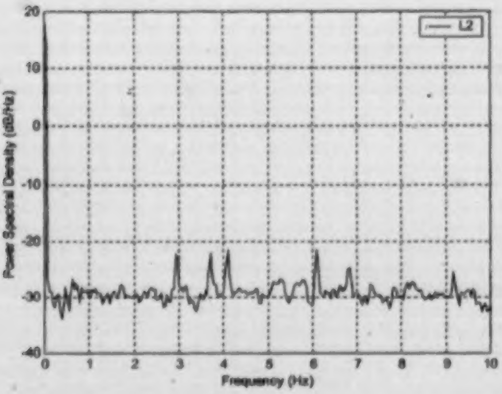

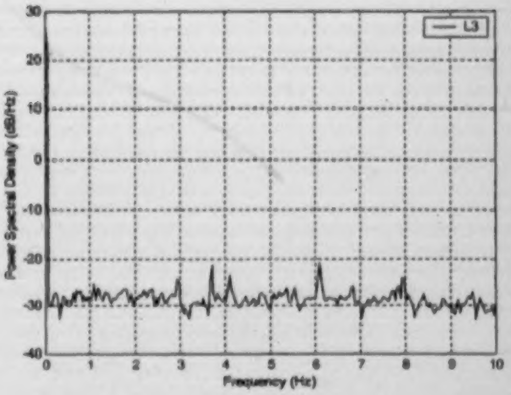

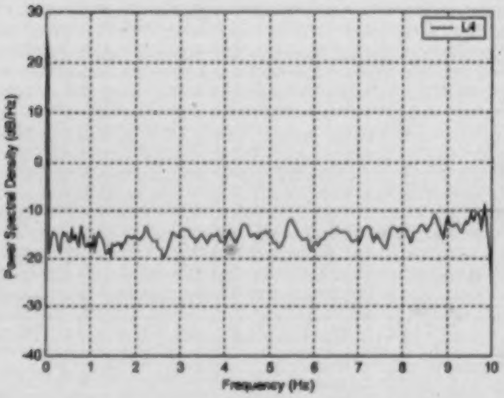

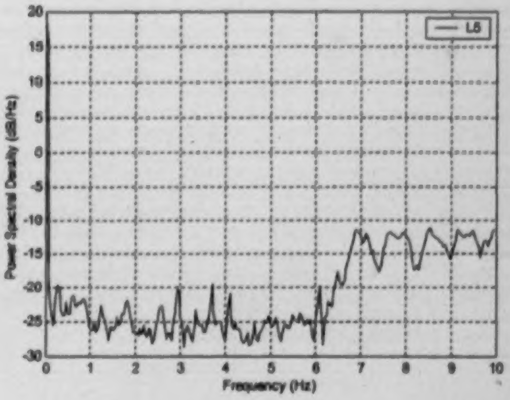

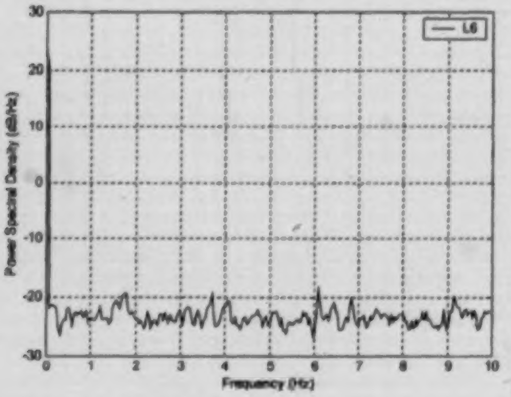

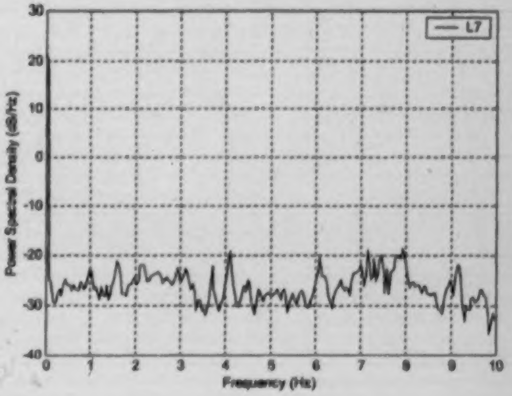

July 18, 1999
3:32 PM

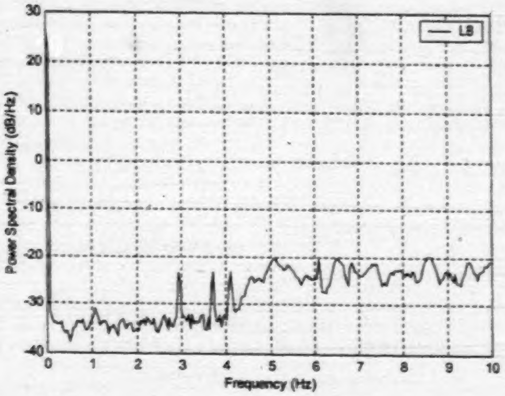

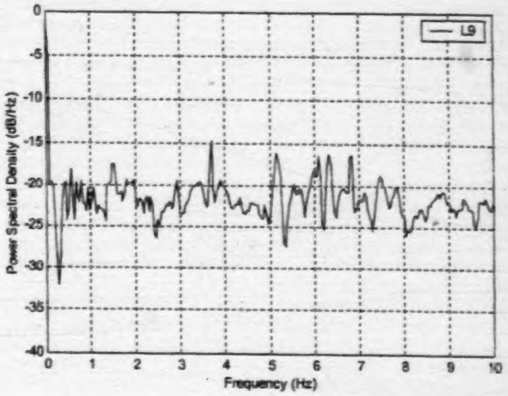

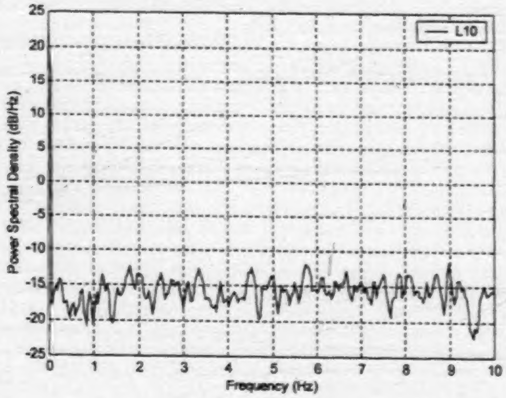

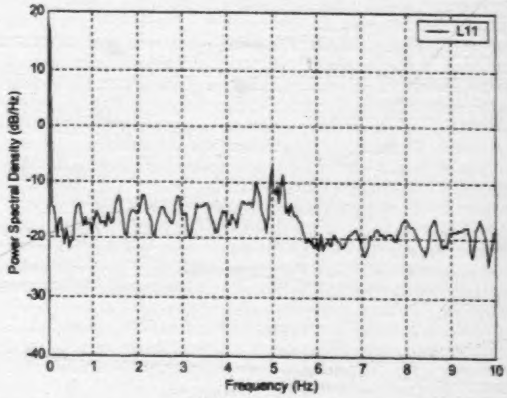

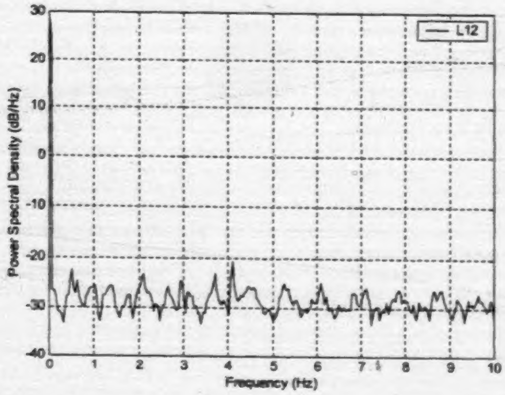

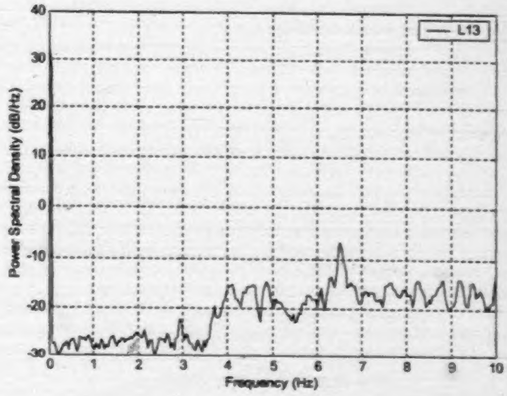

July 18, 1999
3:32 PM

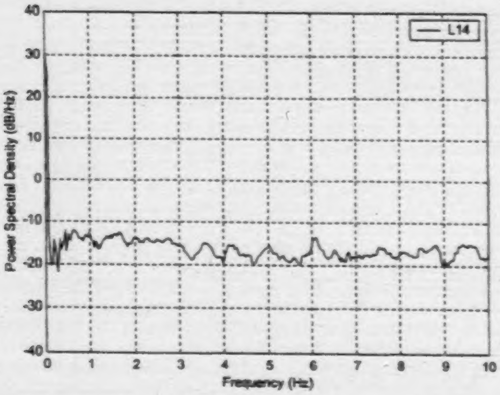

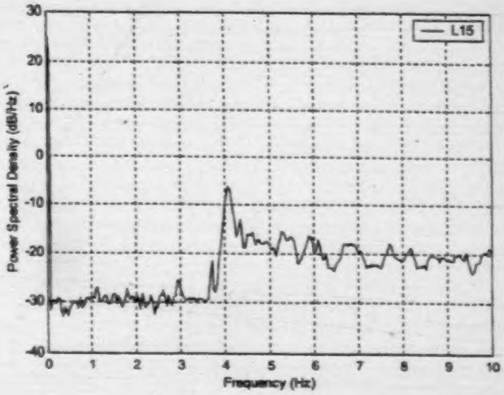

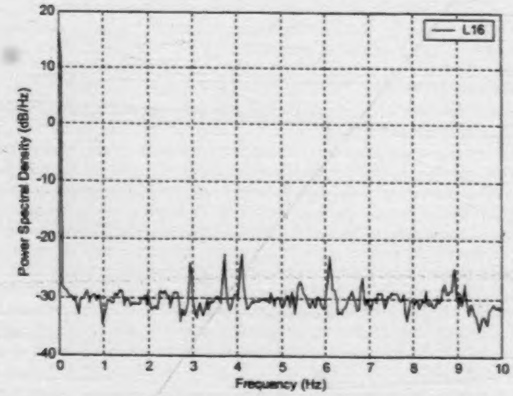

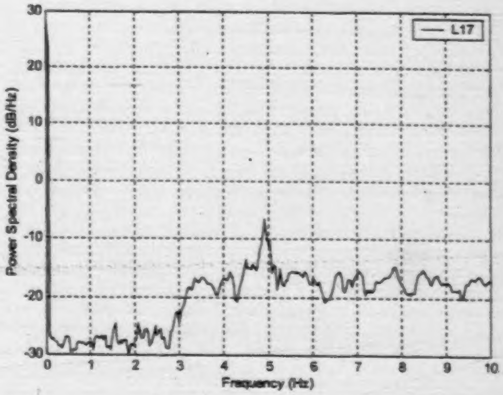

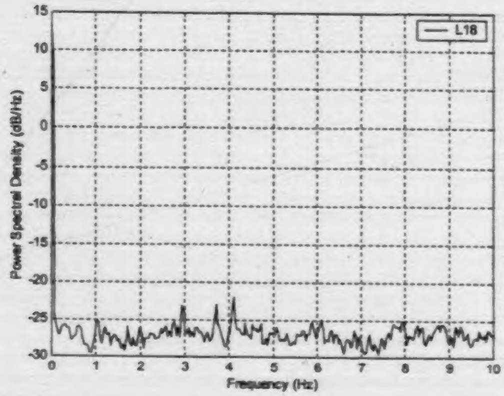

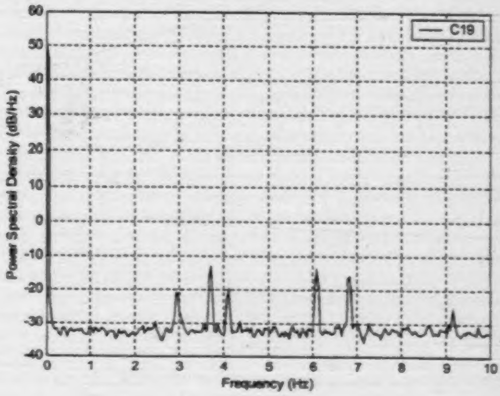

July 18, 1999
3:32 PM

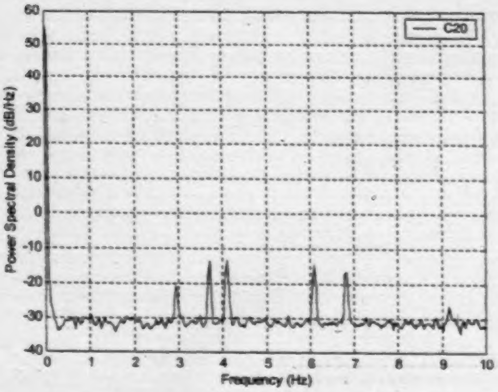

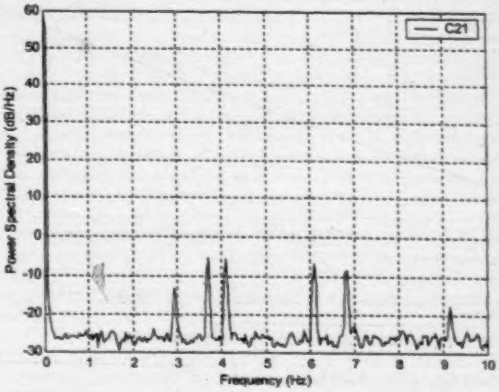

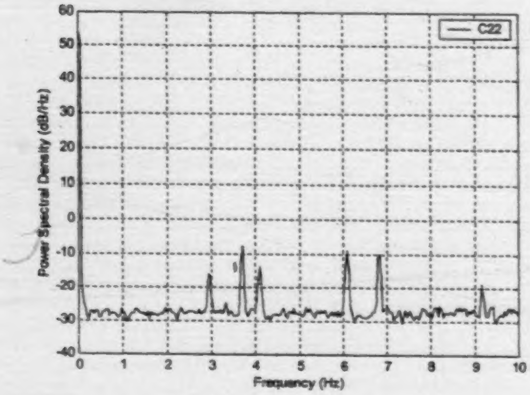

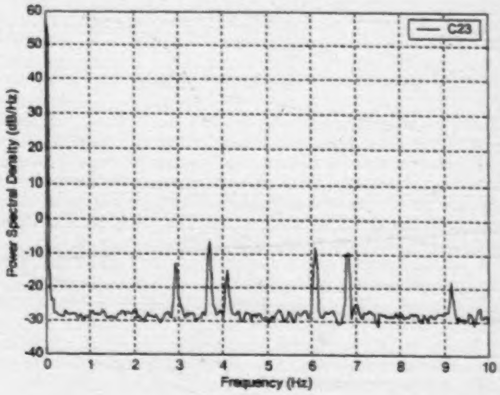

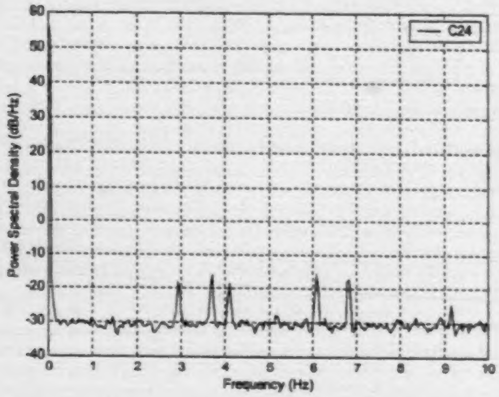

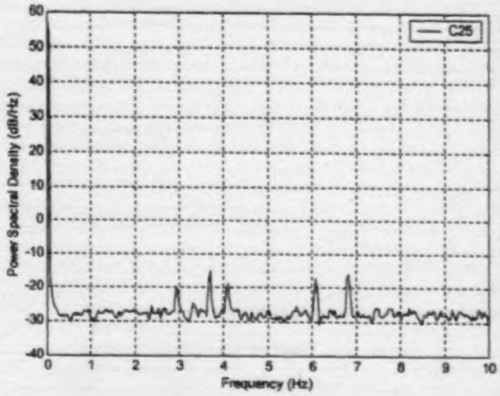

July 18, 1999
3:32 PM

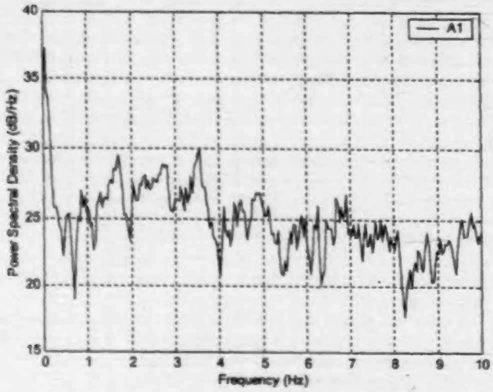

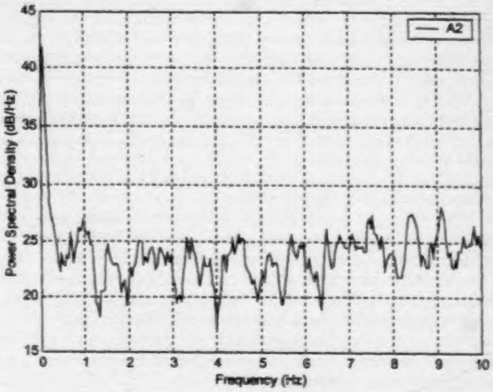

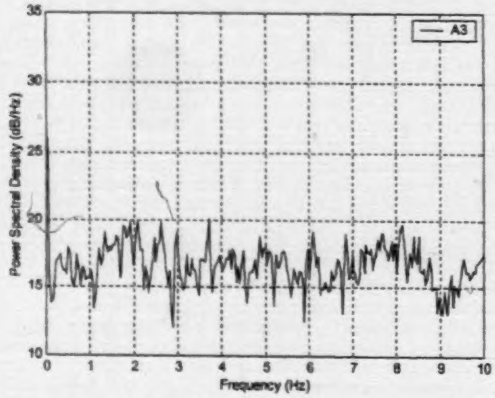

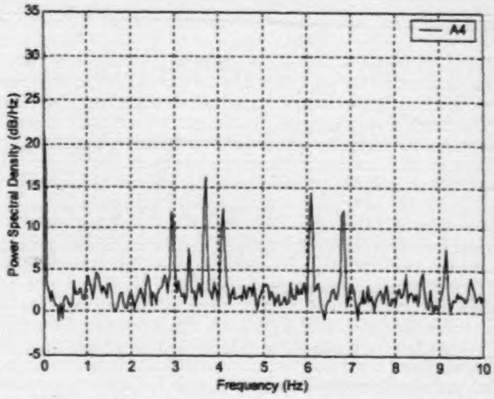

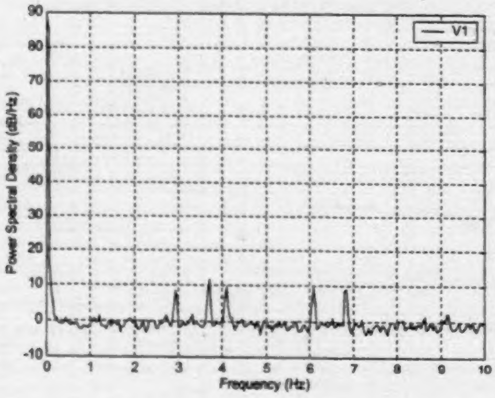

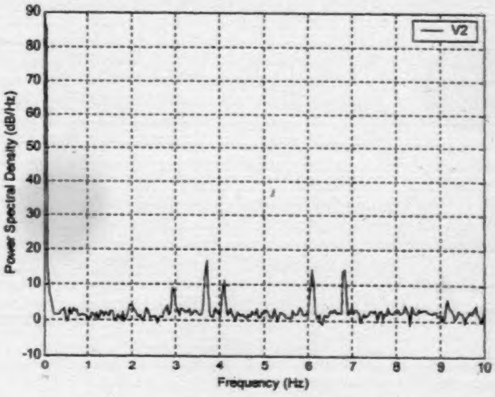

July 18, 1999
3:37 PM

July 18, 1999
3:37 PM

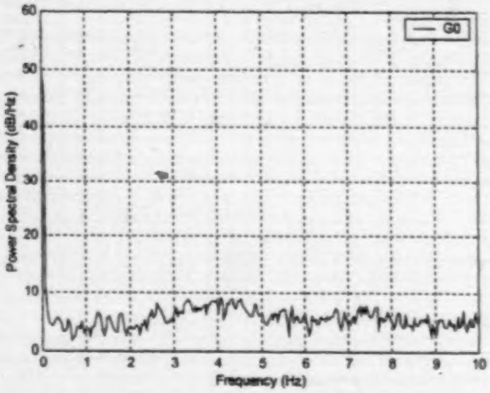

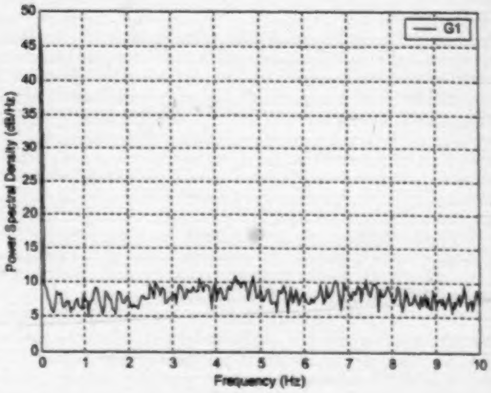

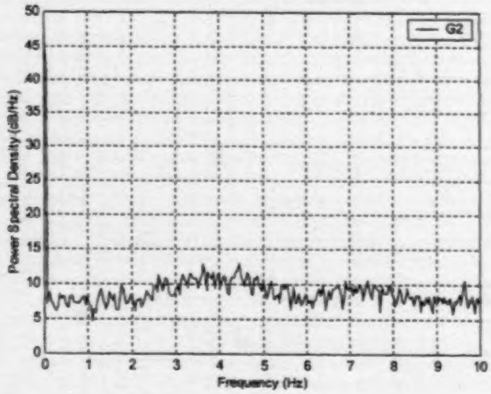

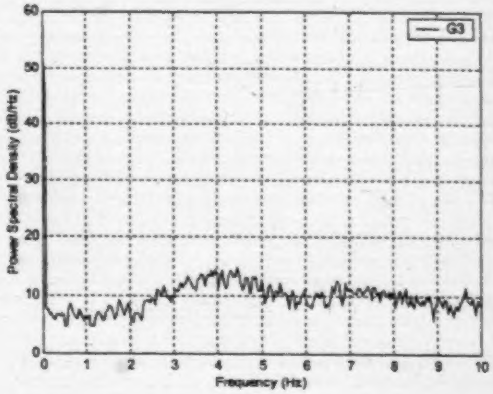

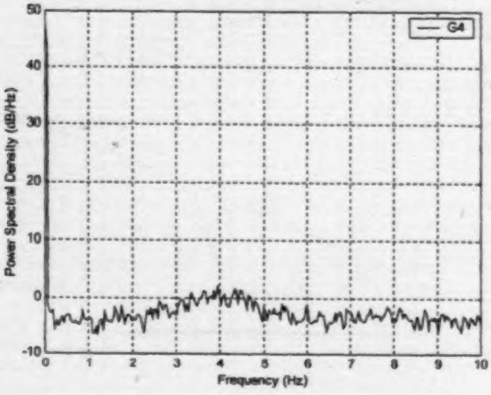

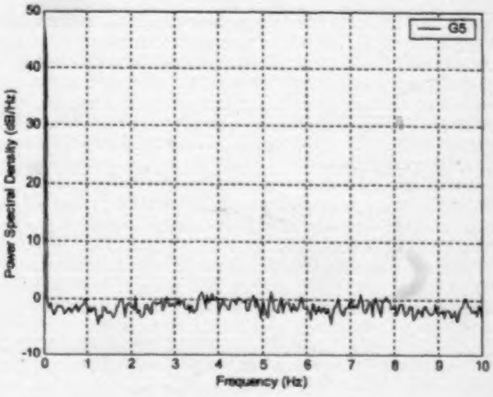

July 18, 1999
3:37 PM

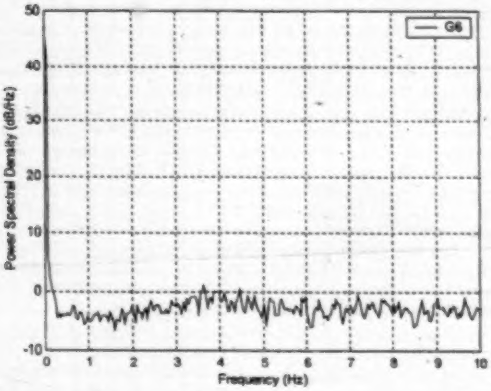

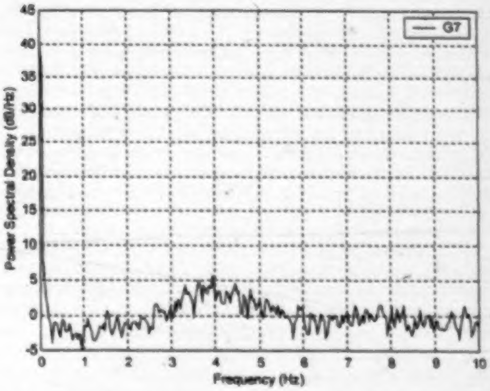

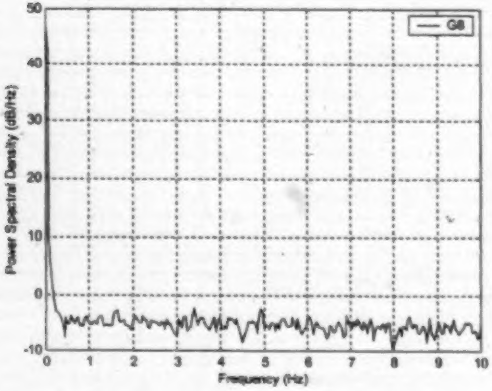

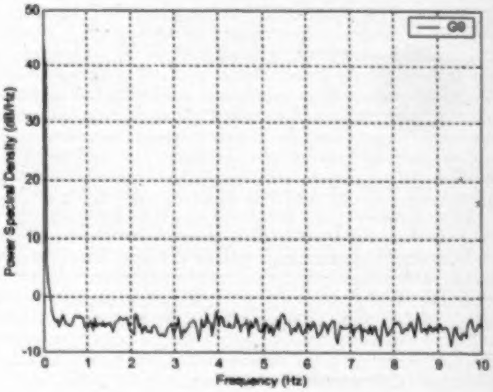

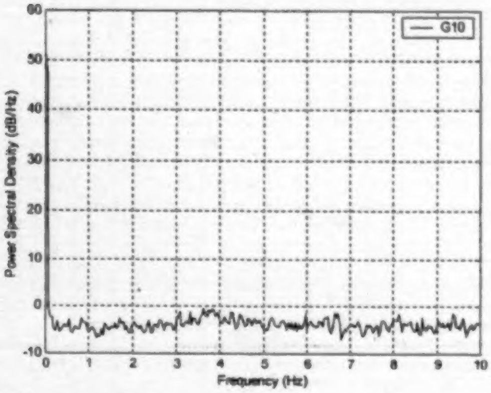

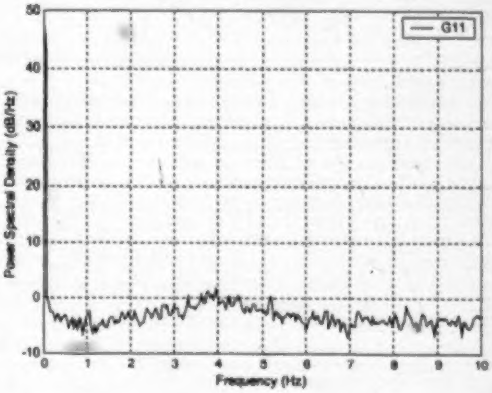

July 18, 1999
3:37 PM

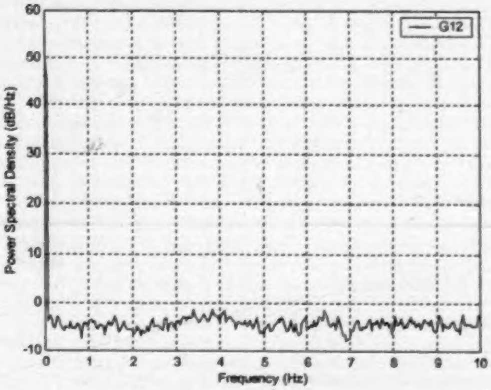

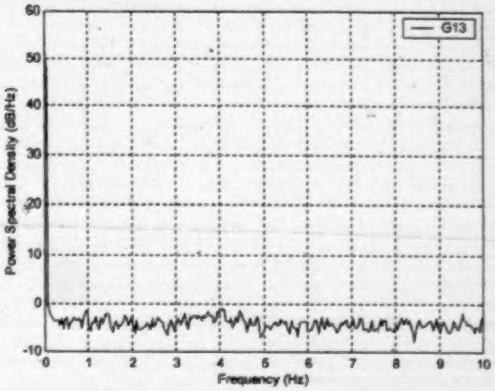

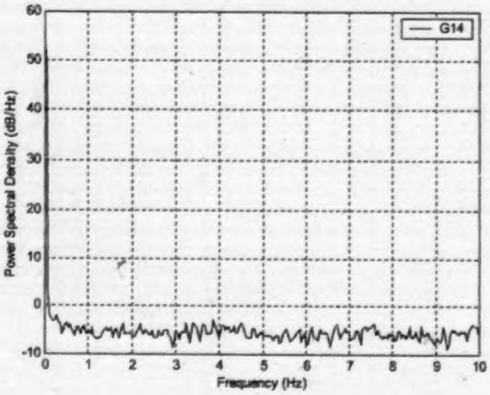

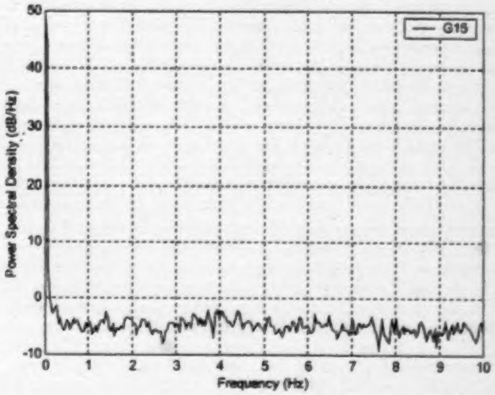

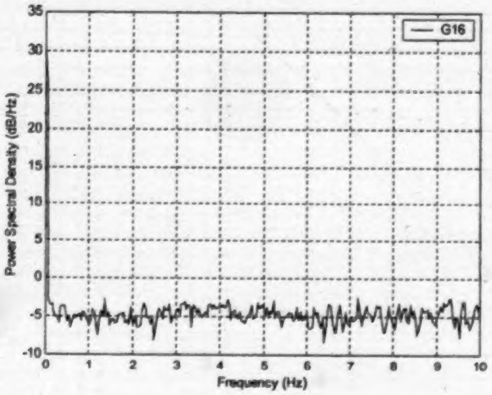

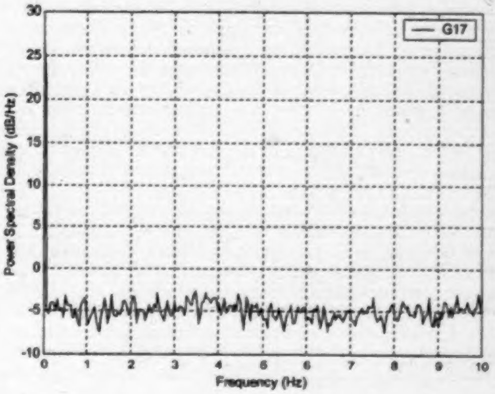

July 18, 1999
3:37 PM

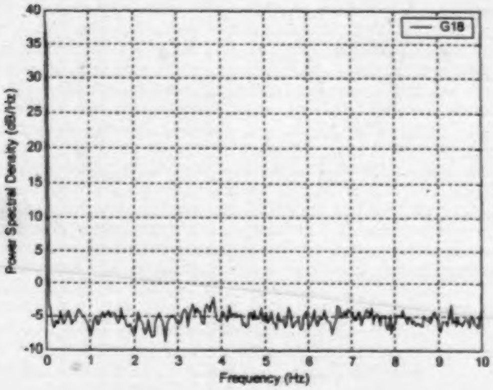

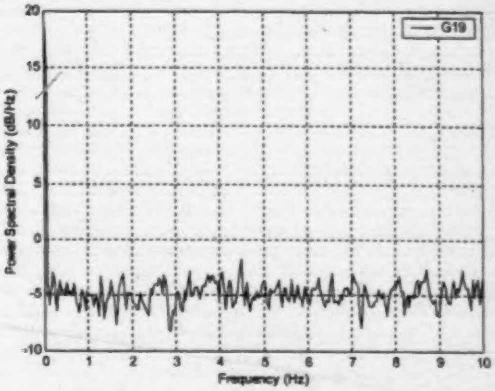

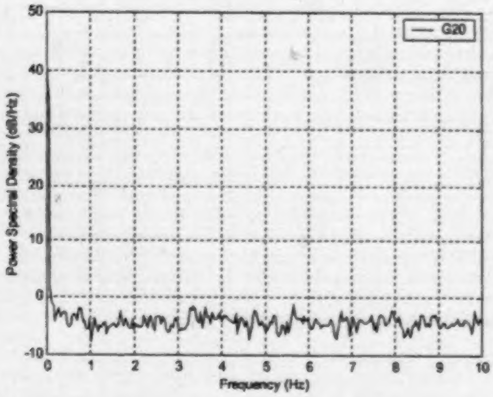

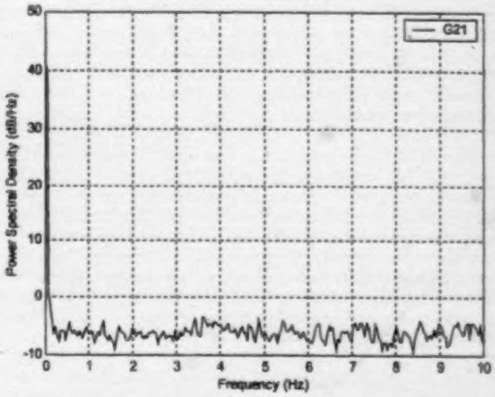

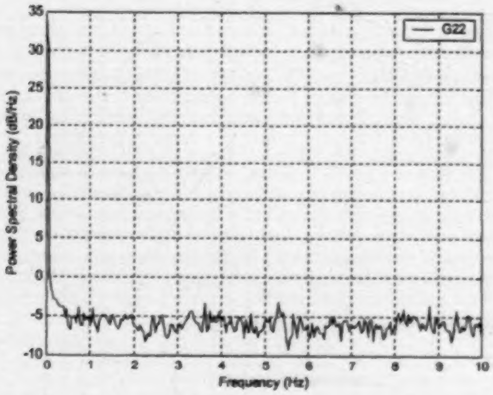

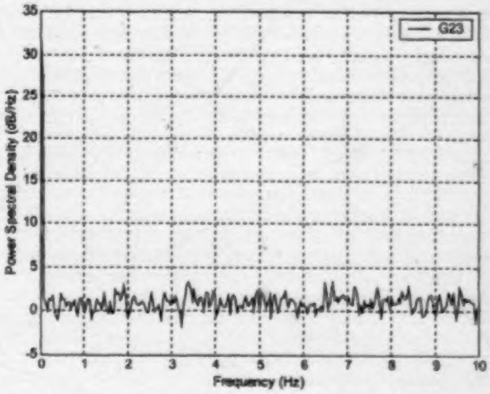

July 18, 1999
3:37 PM

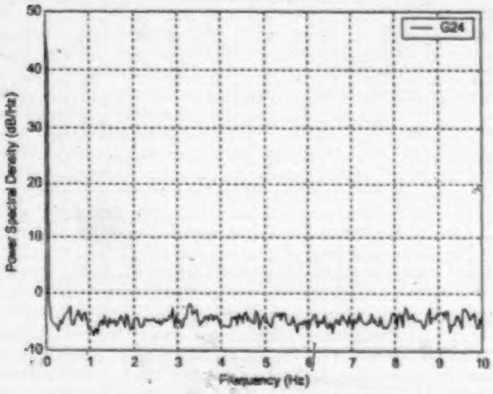

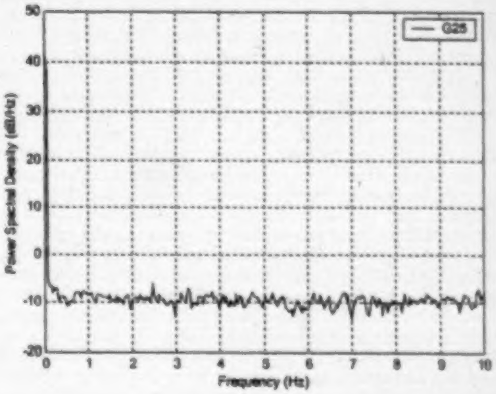

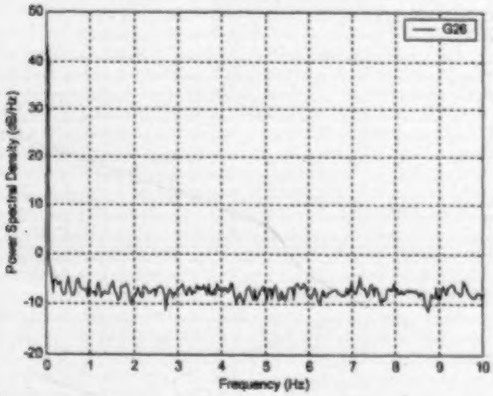

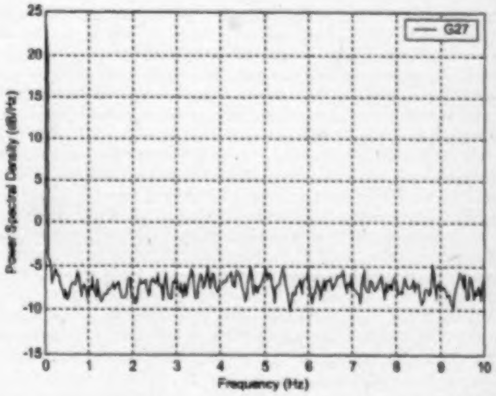

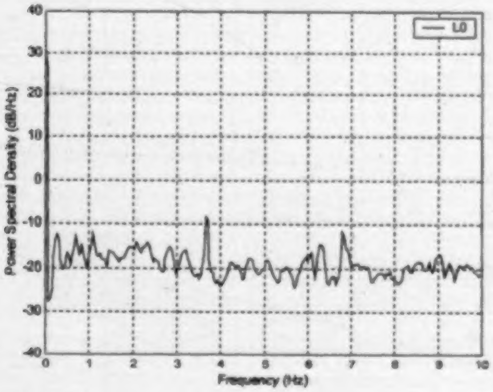

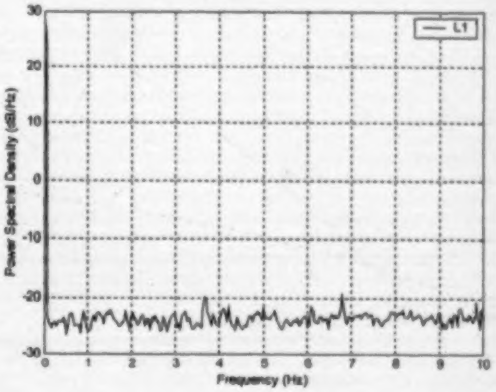

July 18, 1999
3:37 PM

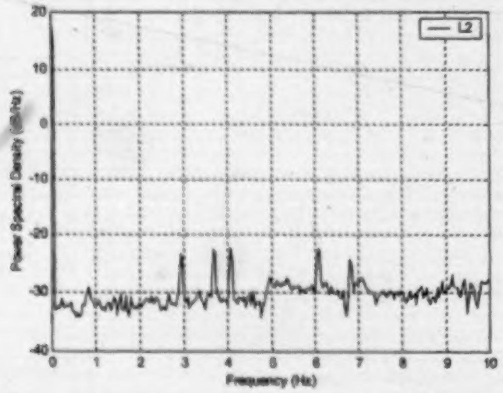

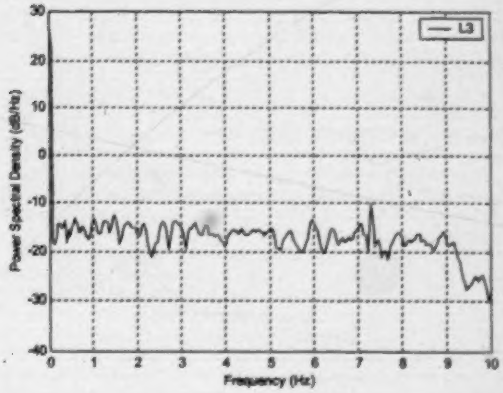

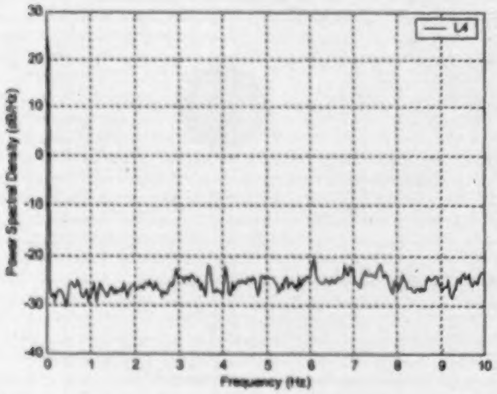

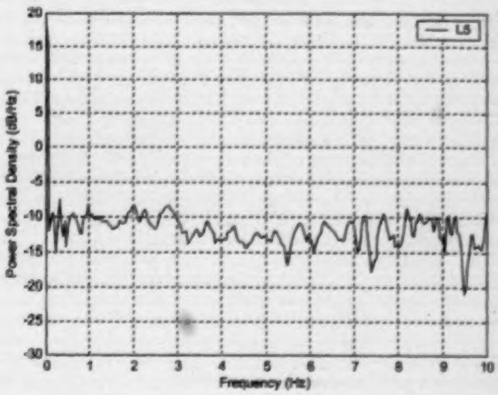

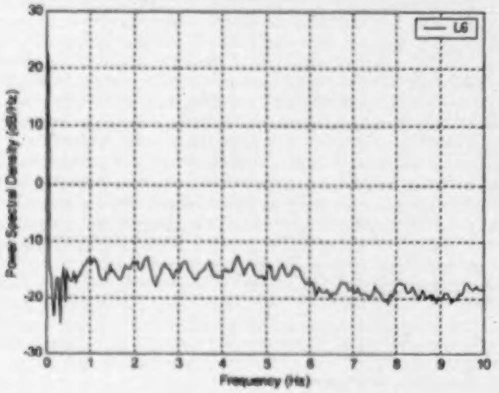

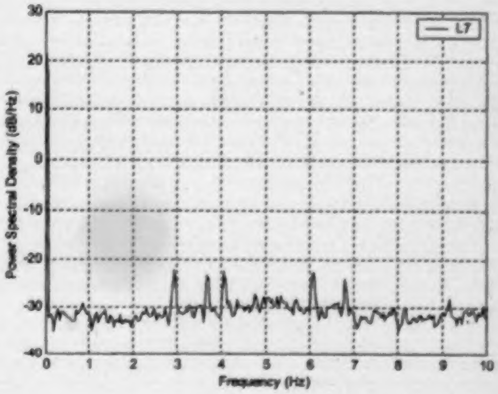

July 18, 1999
3:37 PM

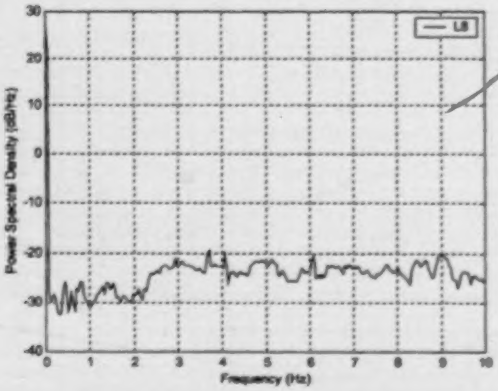

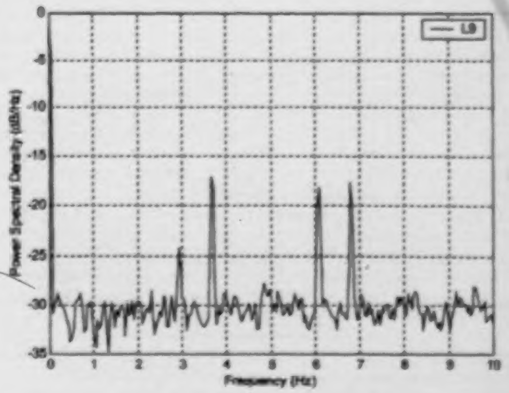

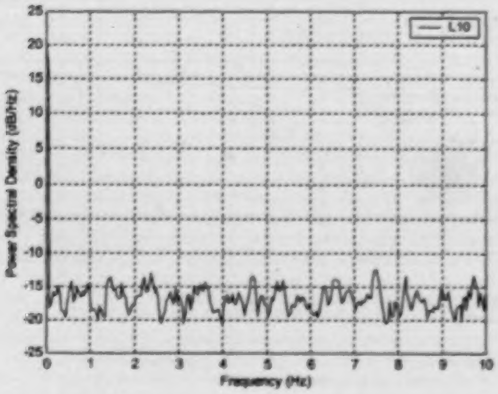

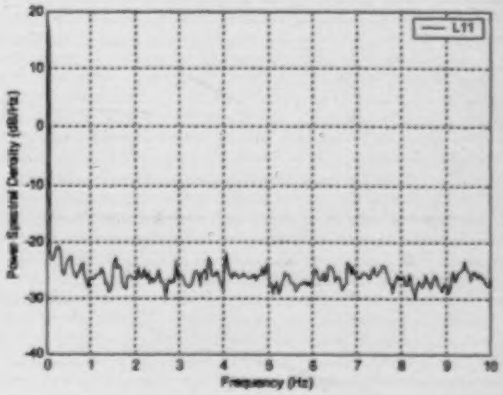

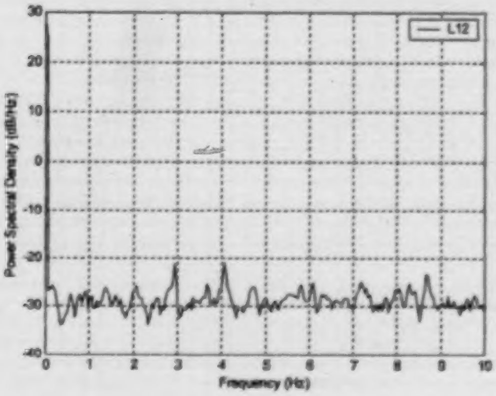

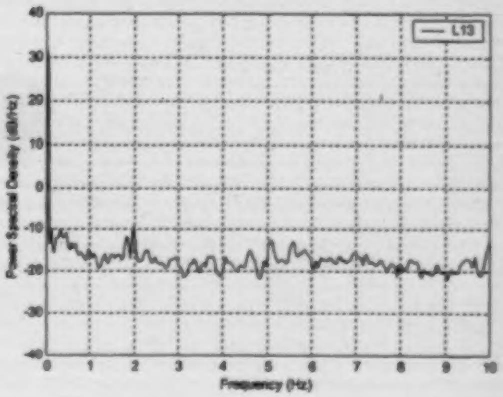

July 18, 1999
3:37 PM

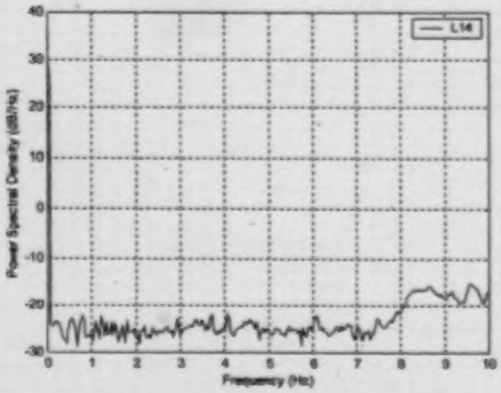

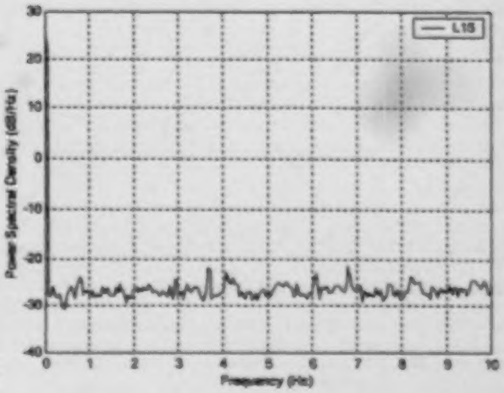

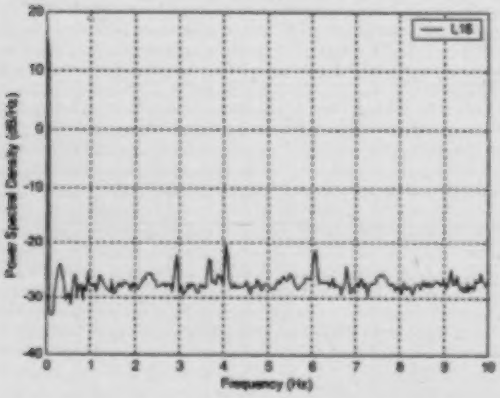

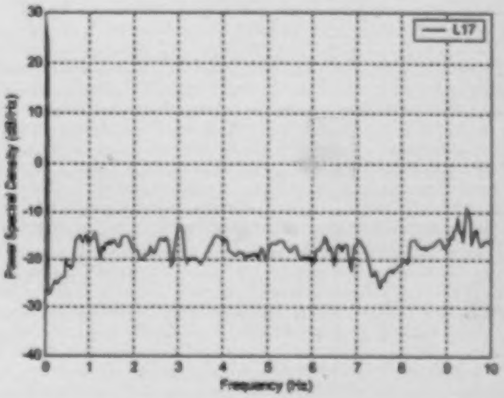

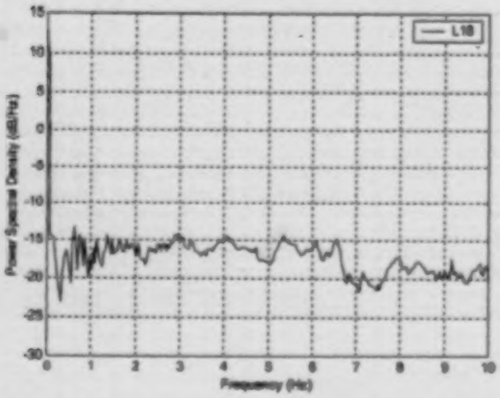

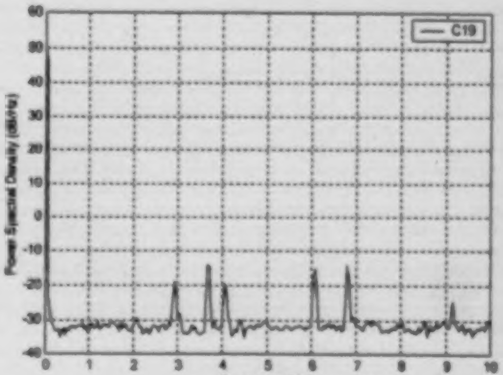

July 18, 1999
3:37 PM

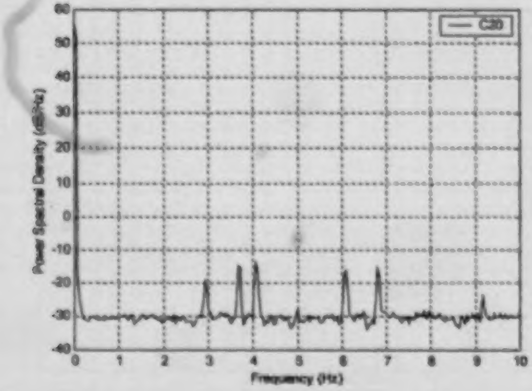

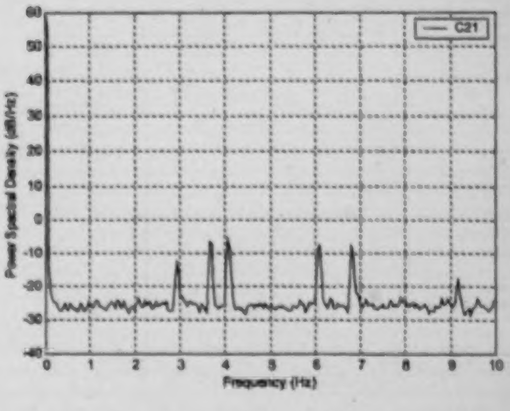

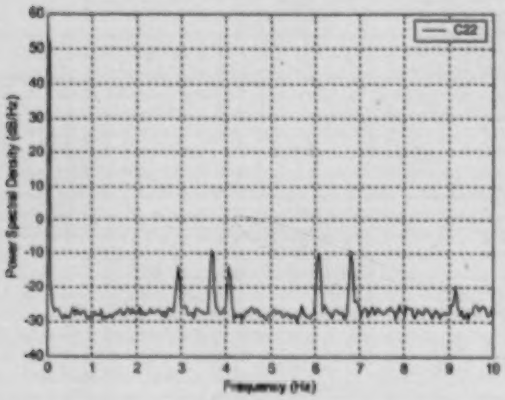

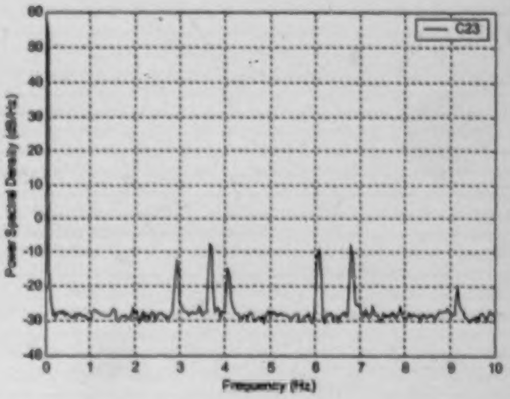

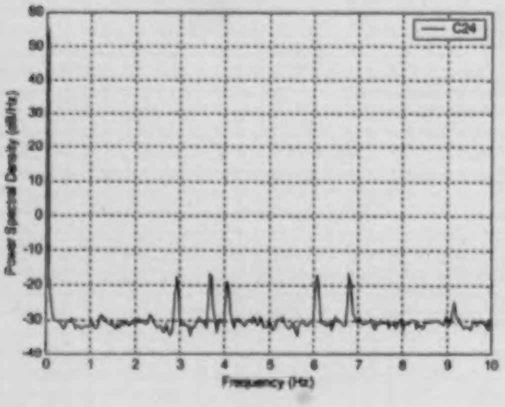

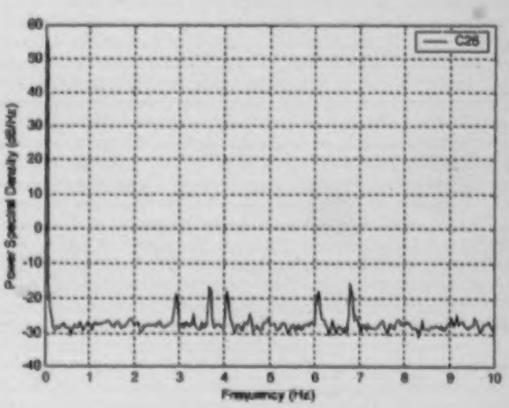

July 18, 1999
3:37 PM

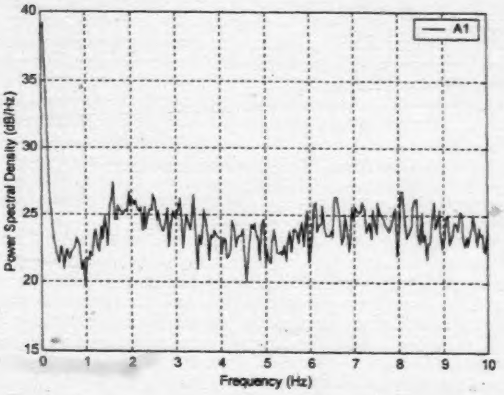

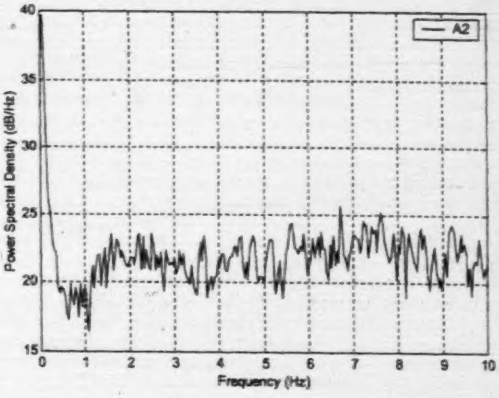

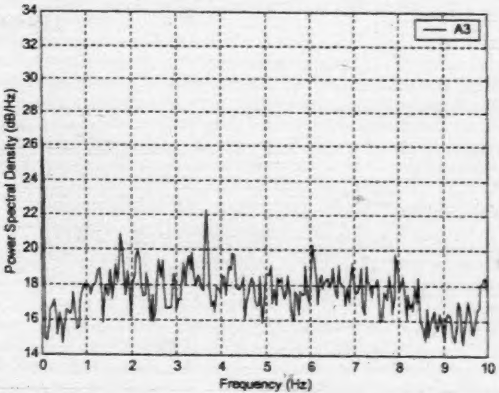

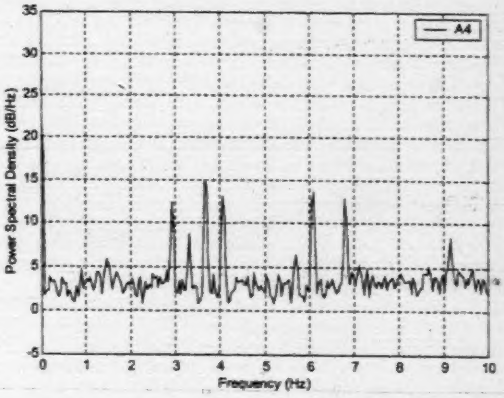

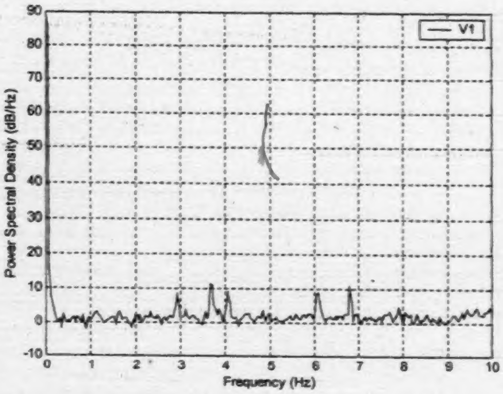

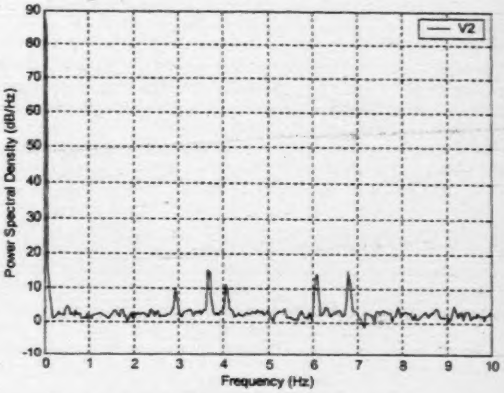

July 18, 1999
3:43 PM

July 18, 1999
3:43 PM

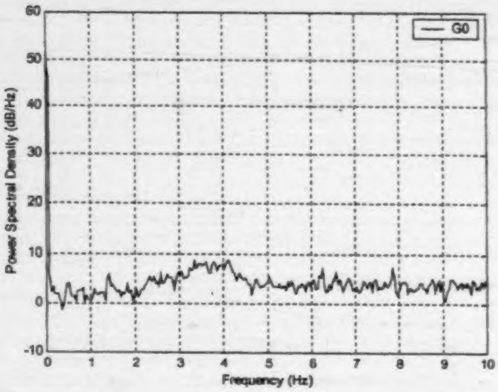

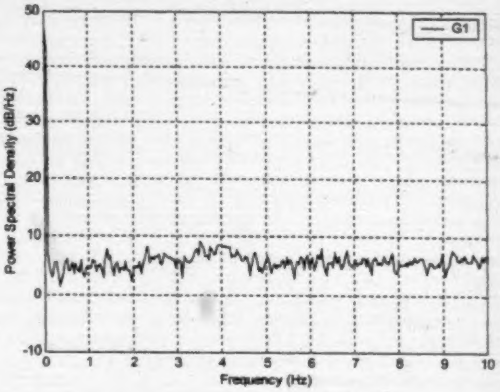

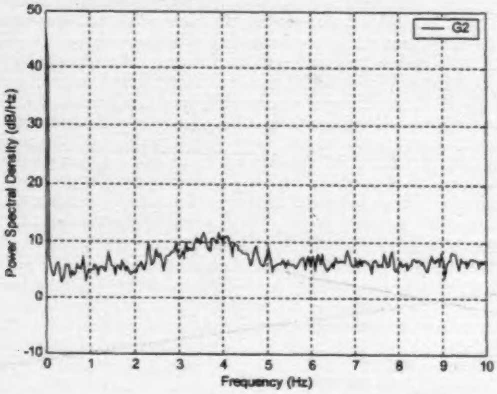

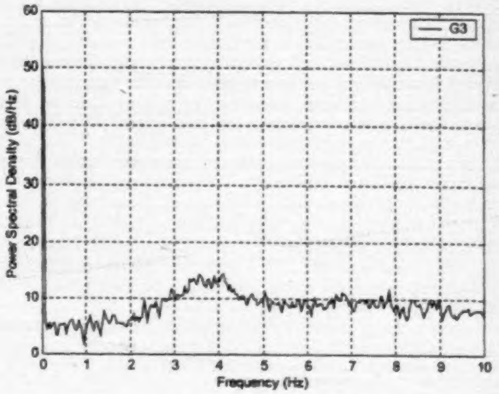

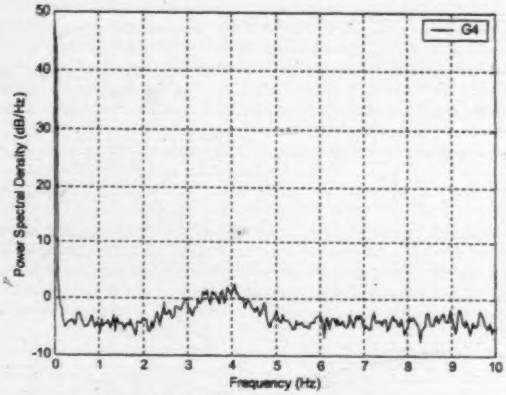

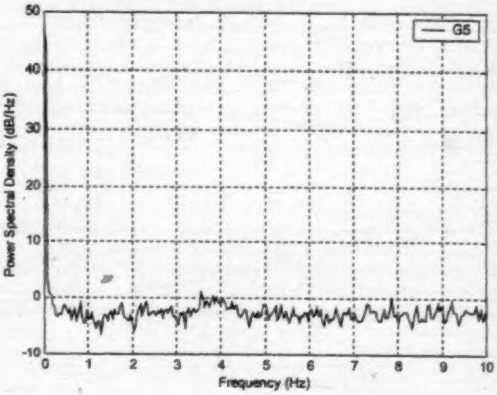

July 18, 1999
3:43 PM

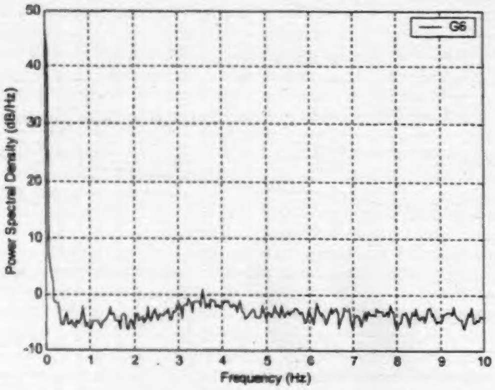

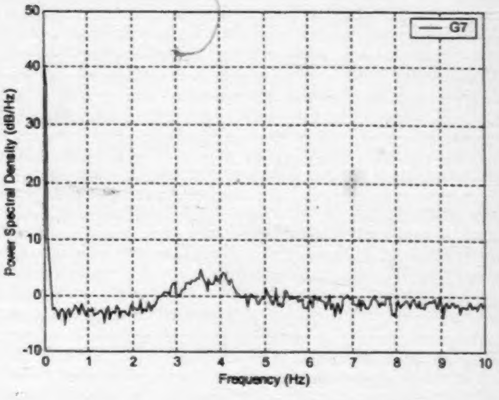

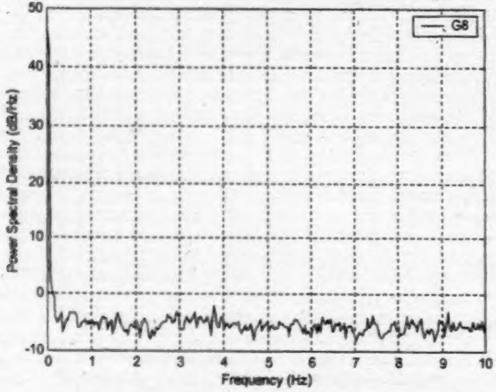

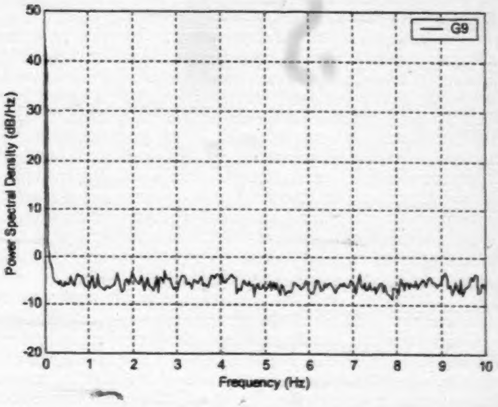

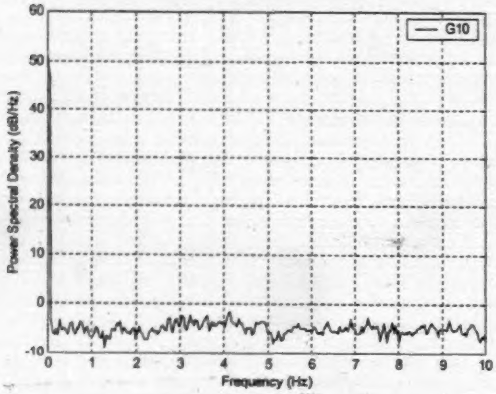

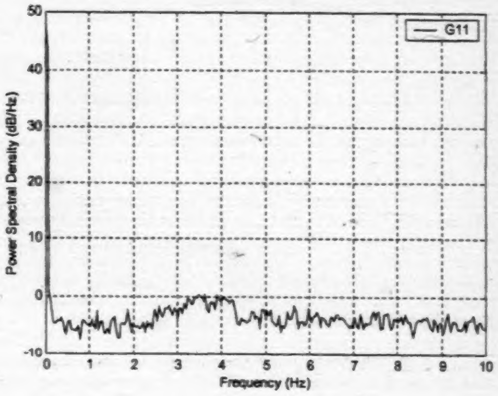

July 18, 1999
3:43 PM

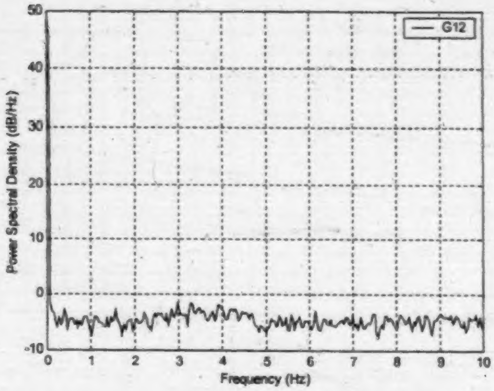

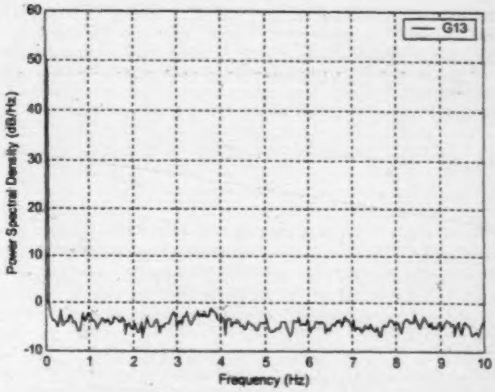

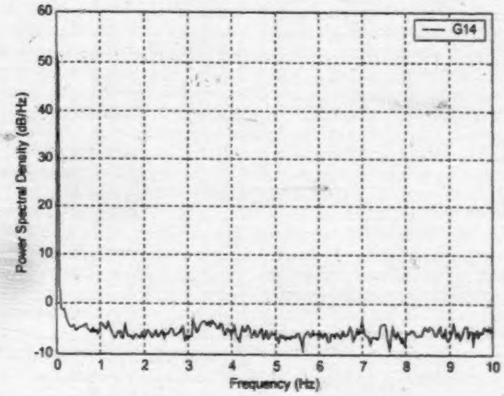

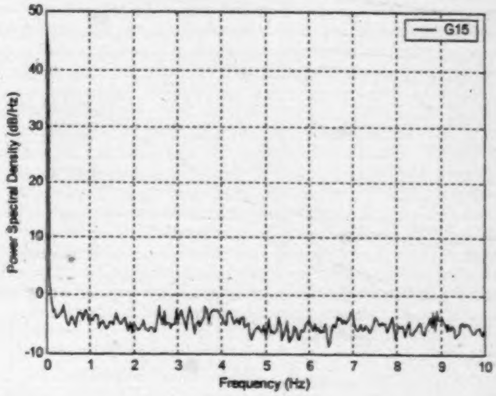

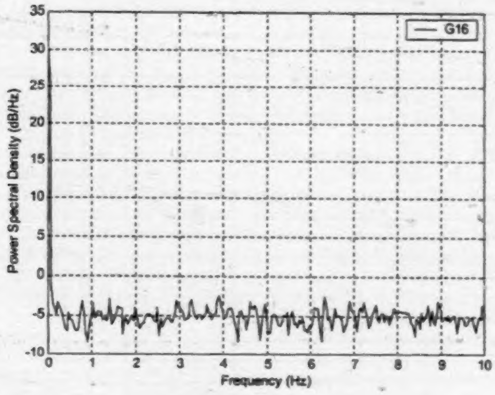

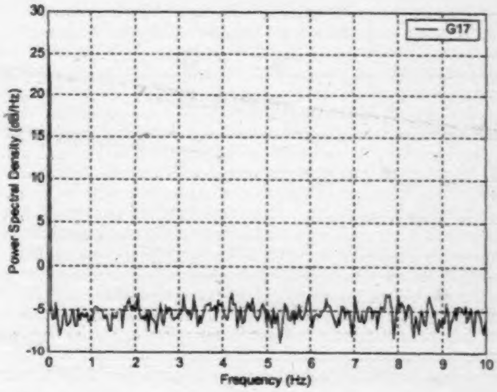

July 18, 1999
3:43 PM

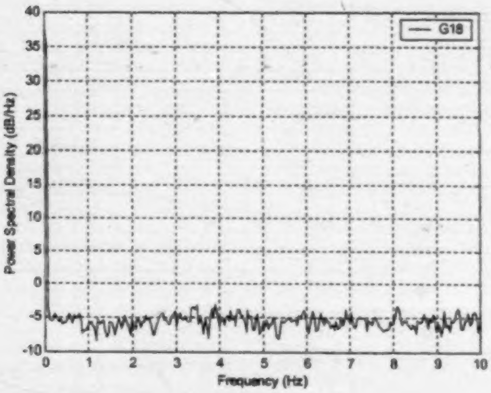

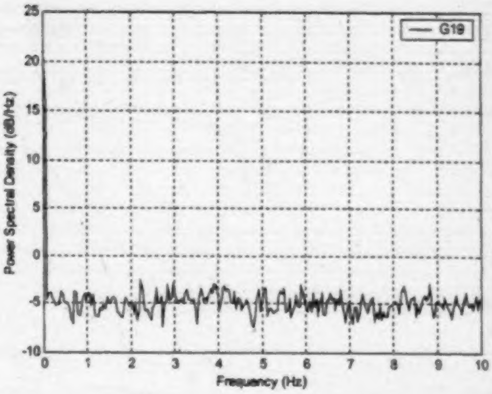

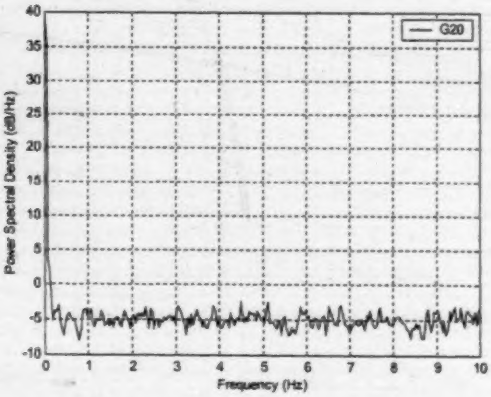

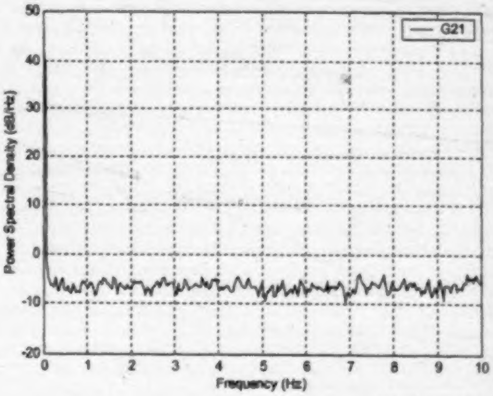

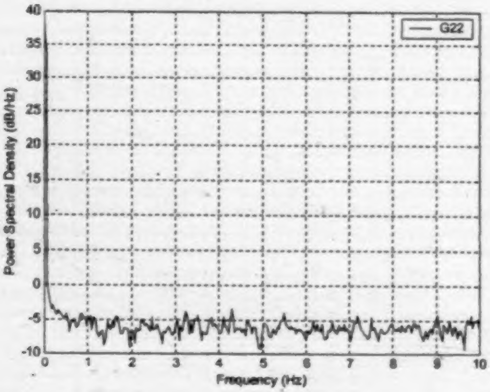

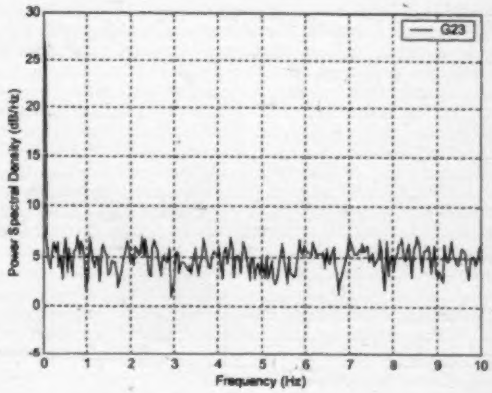

July 18, 1999
3:43 PM

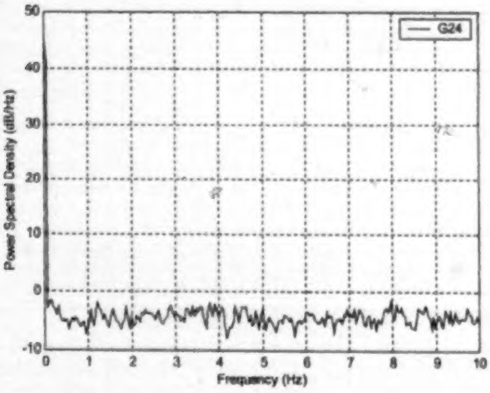

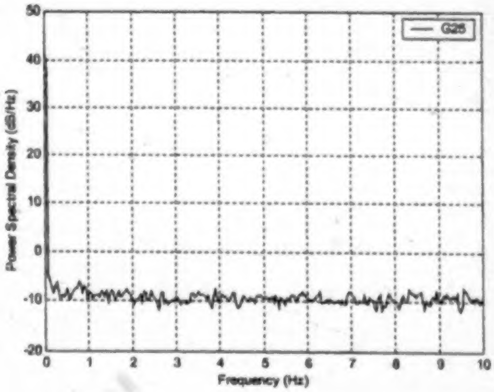

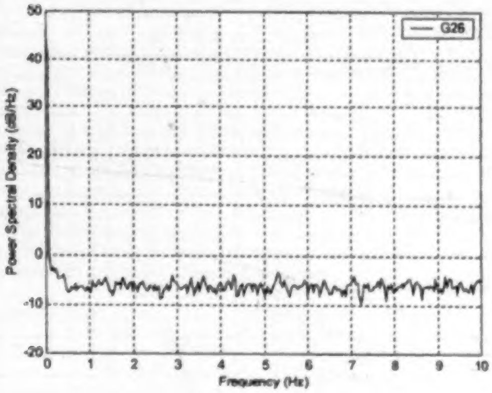

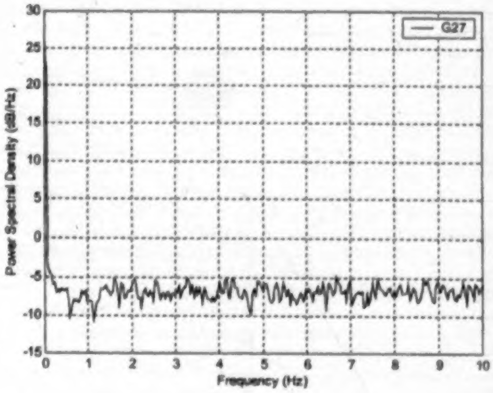

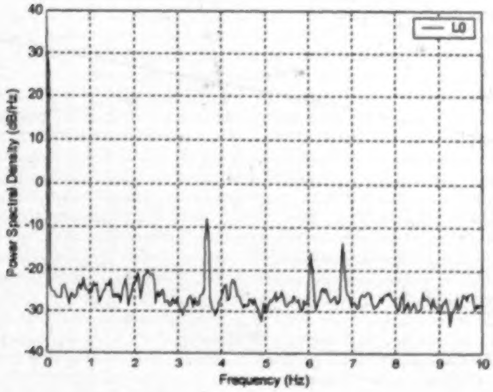

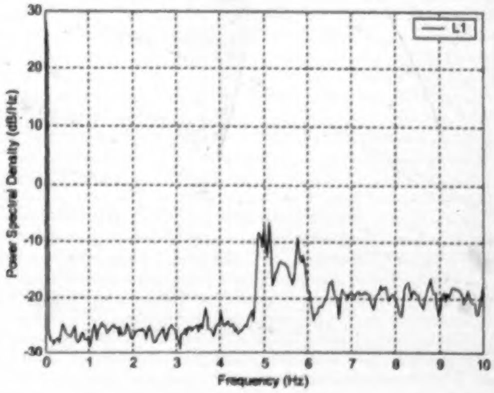

July 18, 1999
3:43 PM

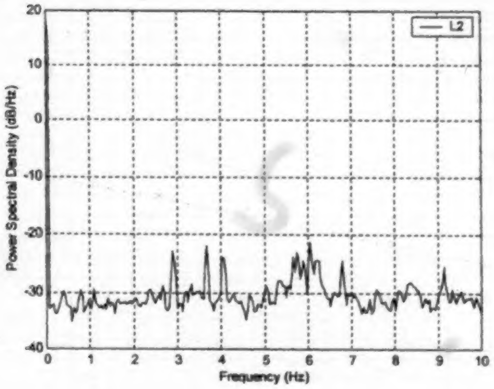

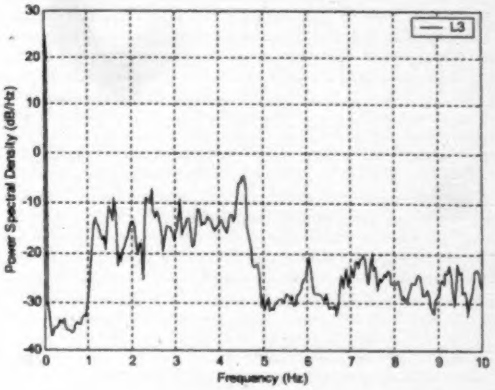

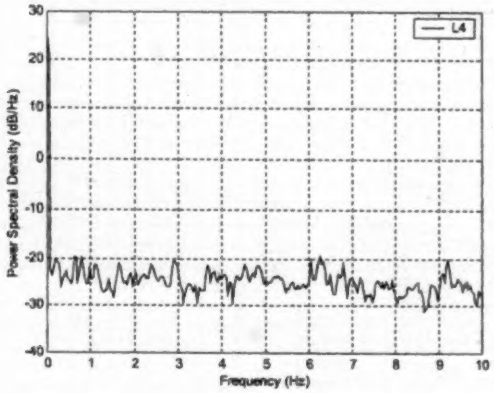

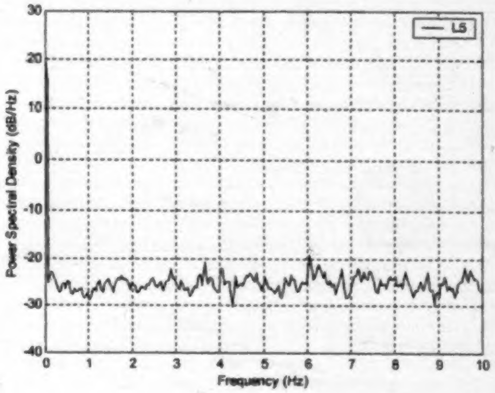

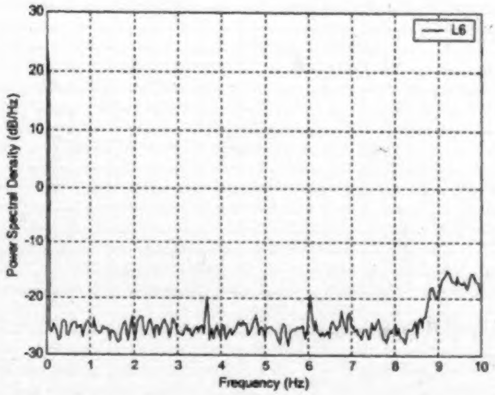

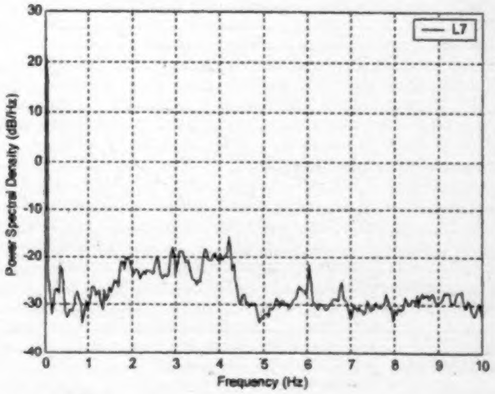

July 18, 1999
3:43 PM

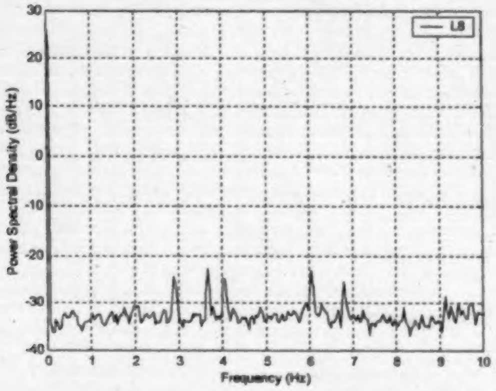

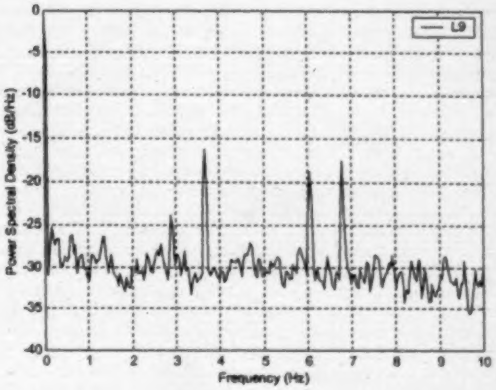

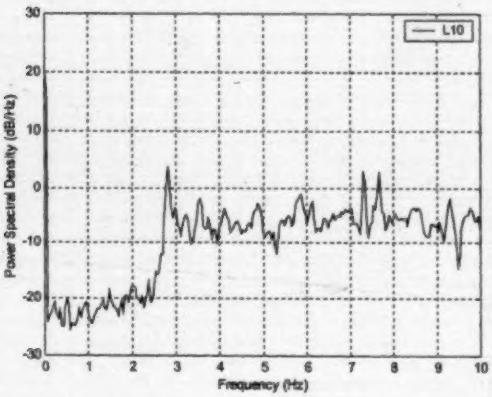

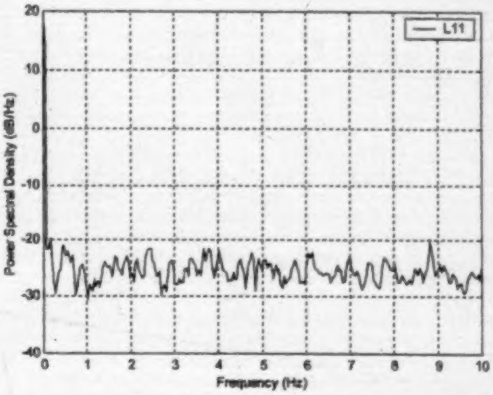

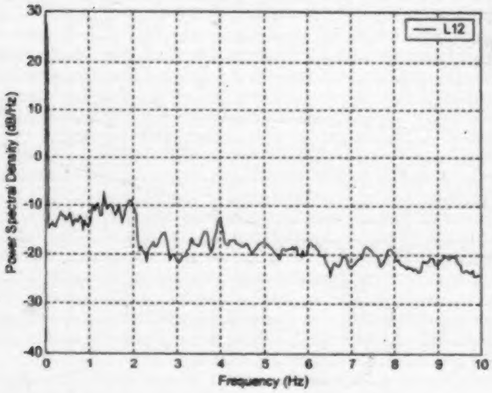

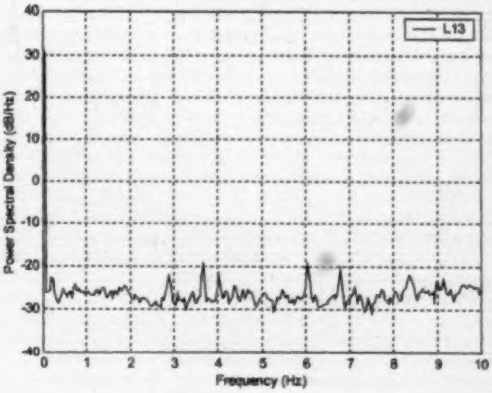

July 18, 1999
3:43 PM

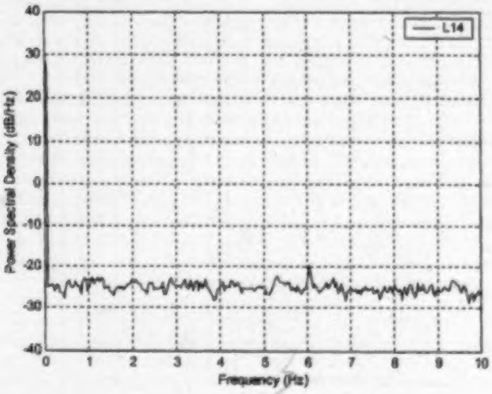

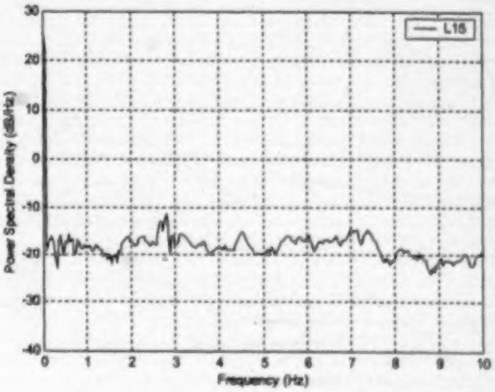

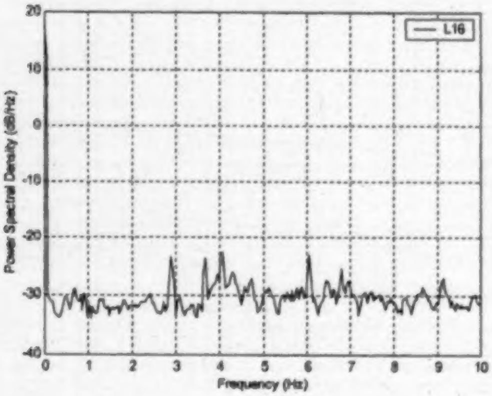

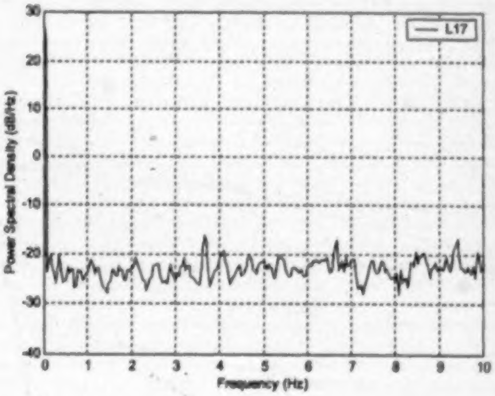

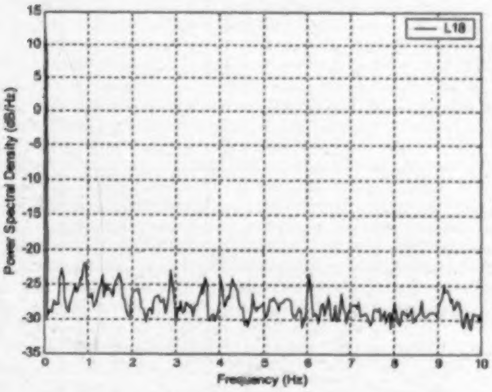

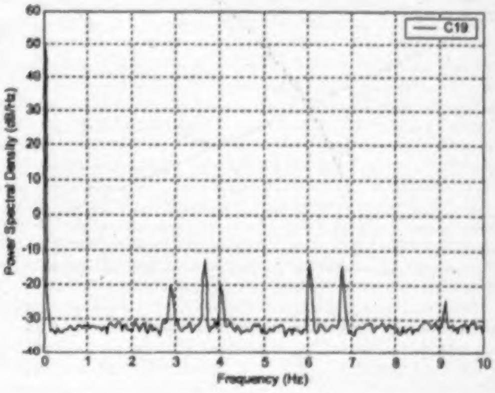

July 18, 1999
3:43 PM

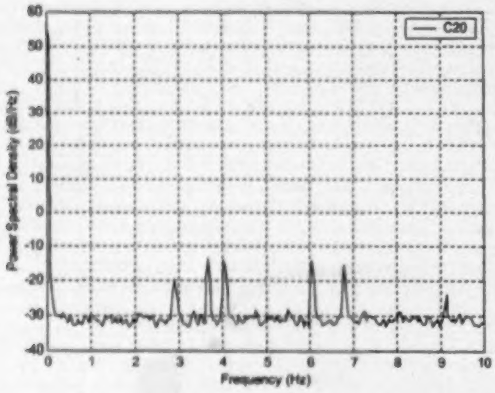

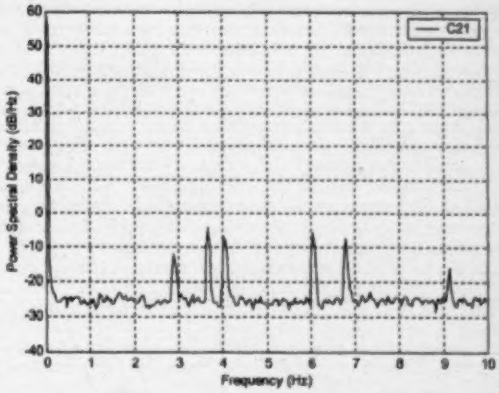

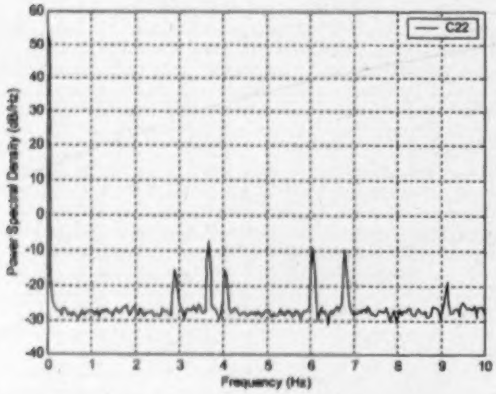

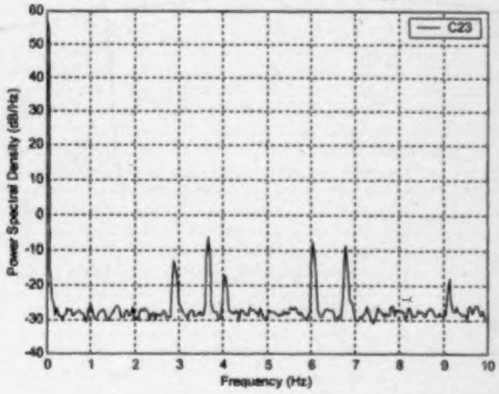

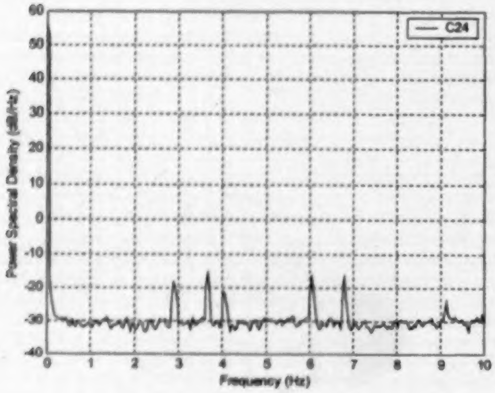

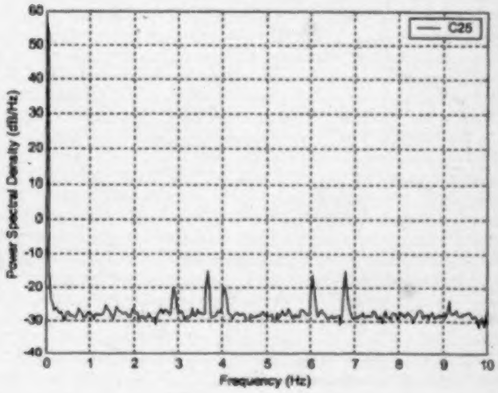

July 18, 1999
3:43 PM

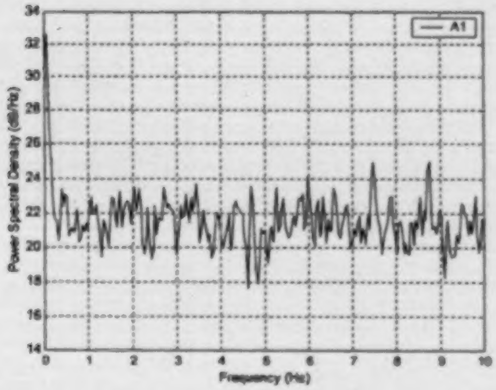

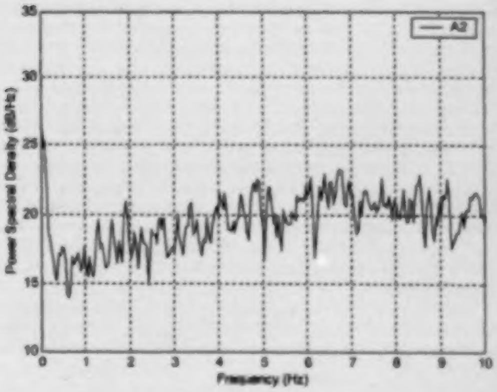

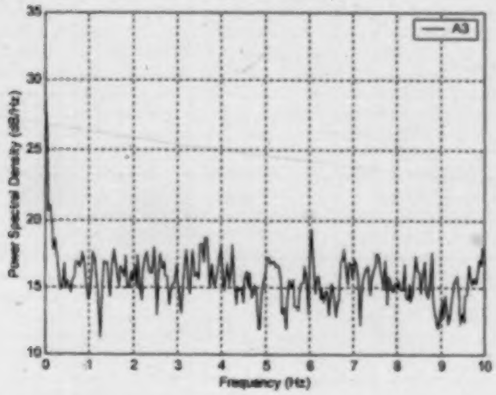

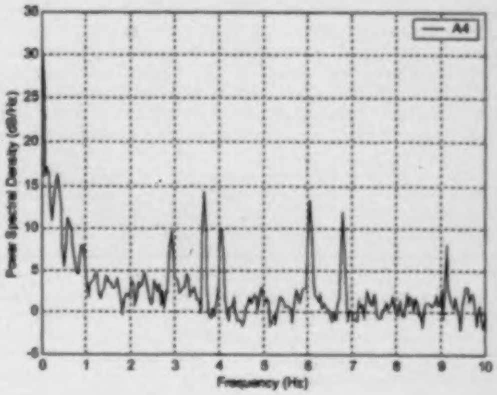

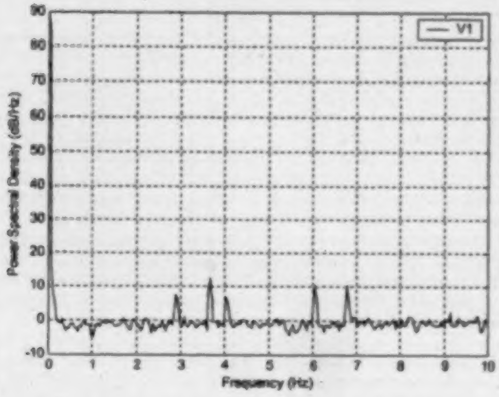

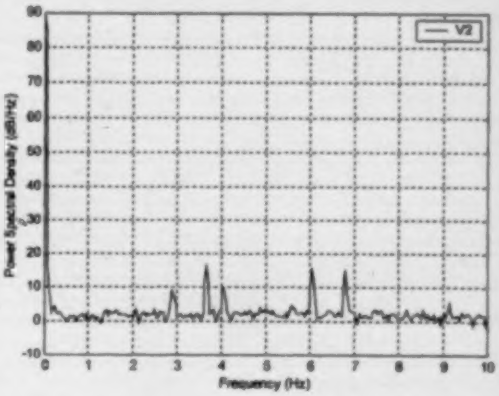

July 18, 1999
3:49 PM

July 18, 1999
3:49 PM

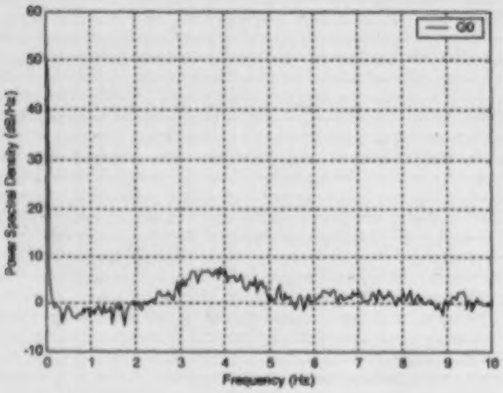

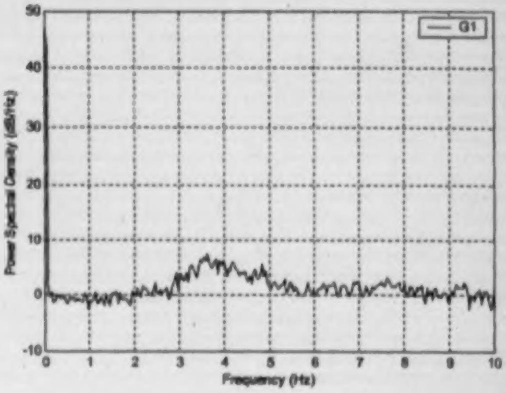

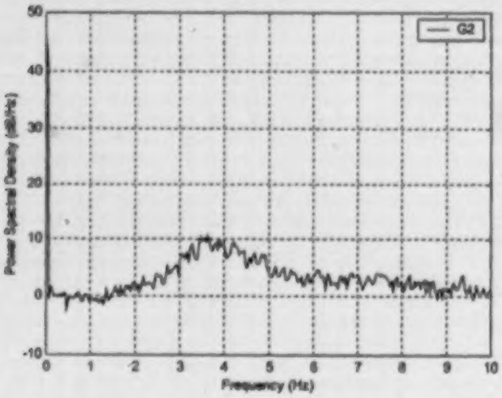

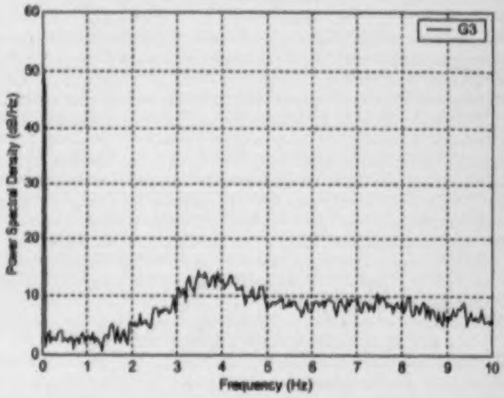

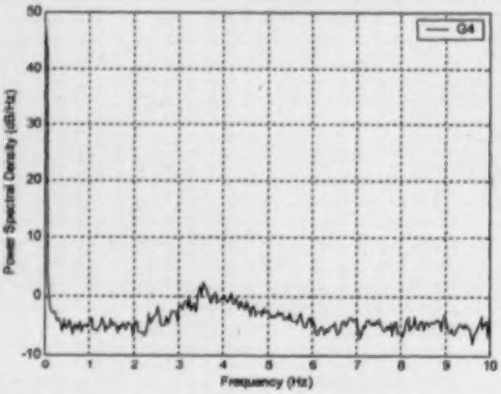

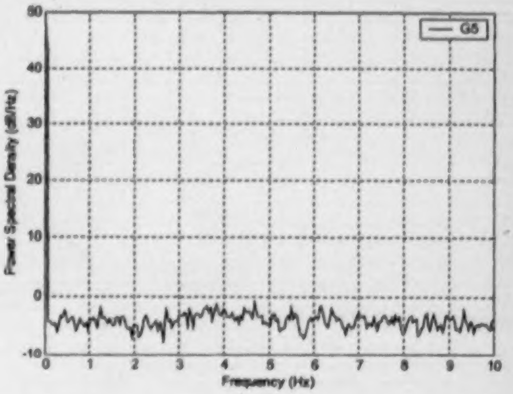

July 18, 1999
3:49 PM

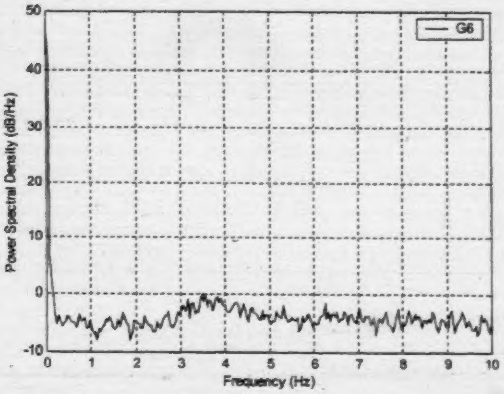

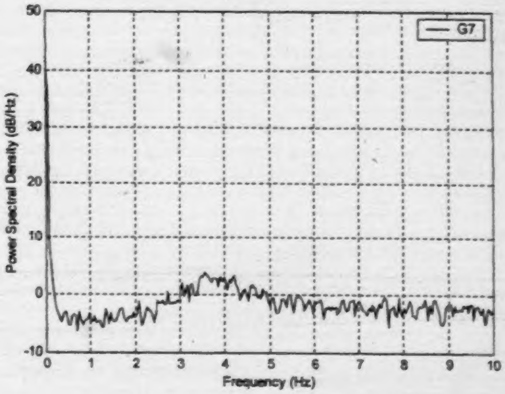

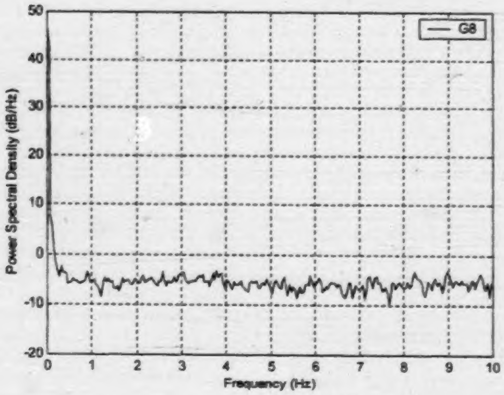

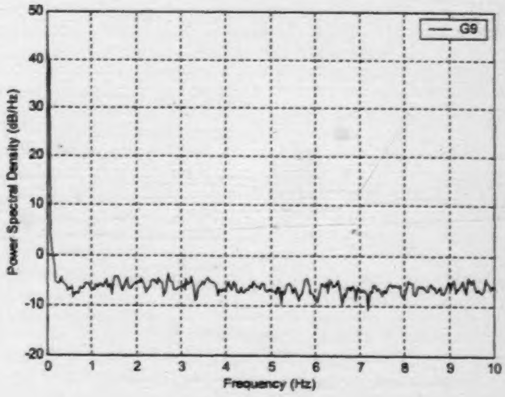

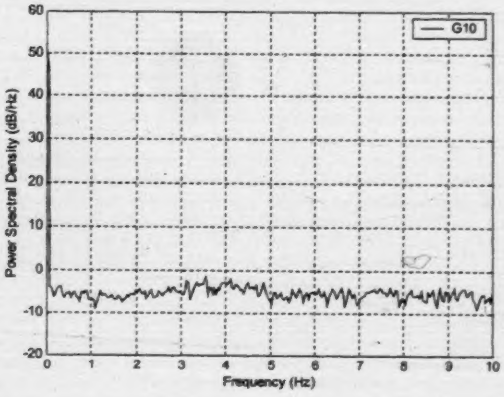

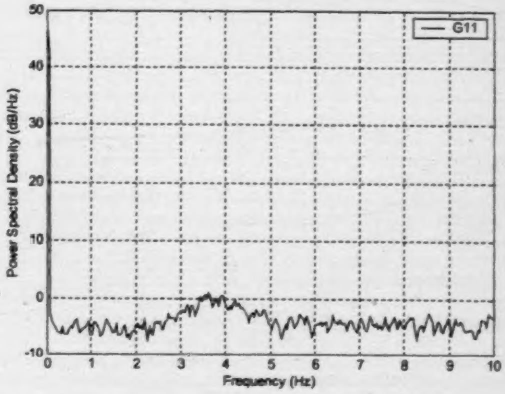

July 18, 1999
3:49 PM

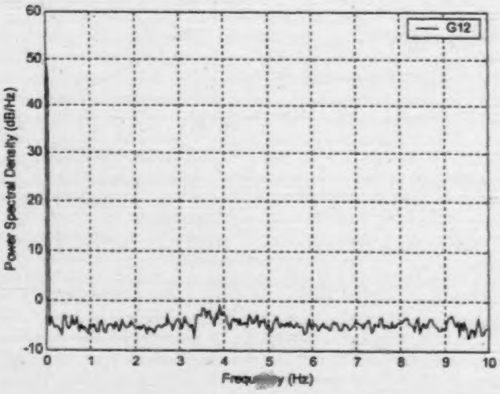

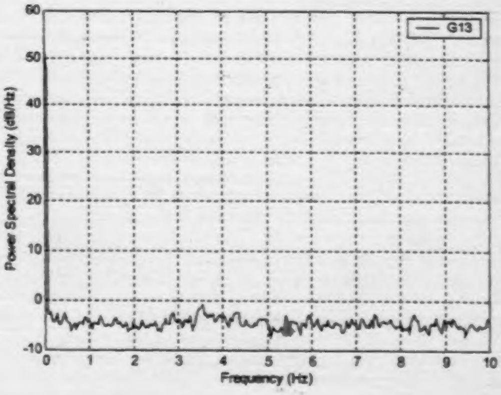

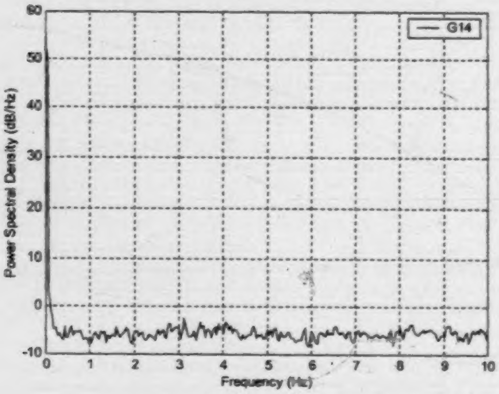

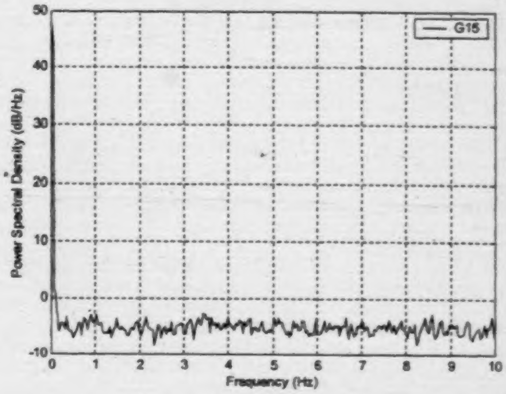

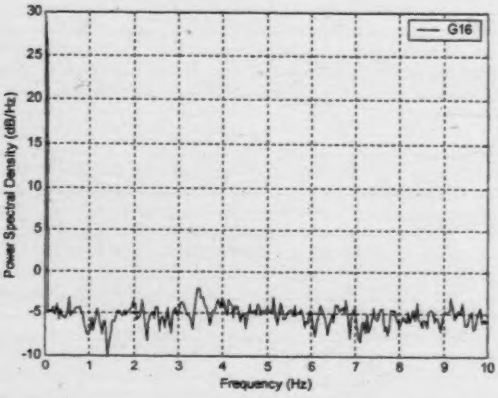

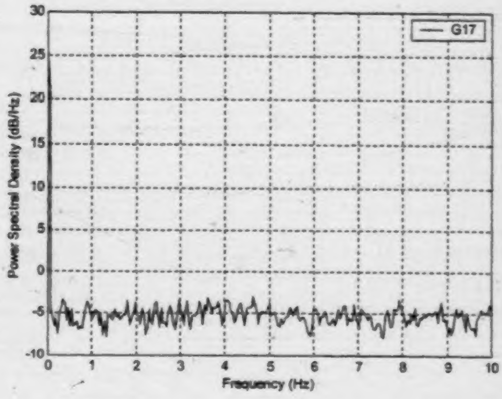

July 18, 1999
3:49 PM

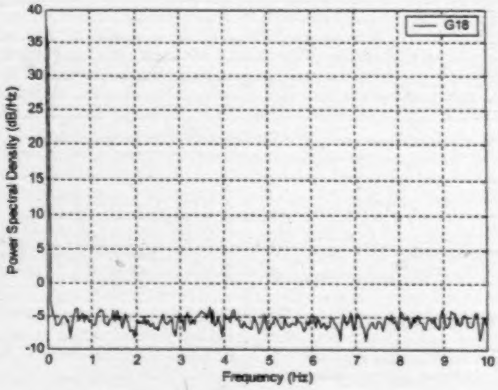

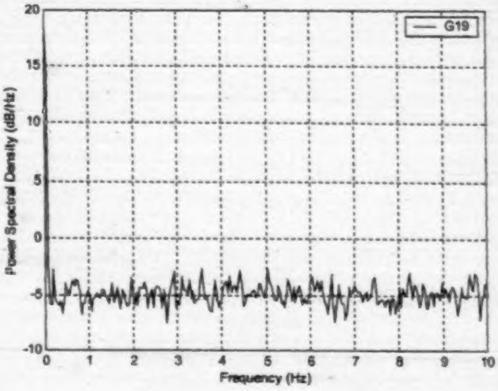

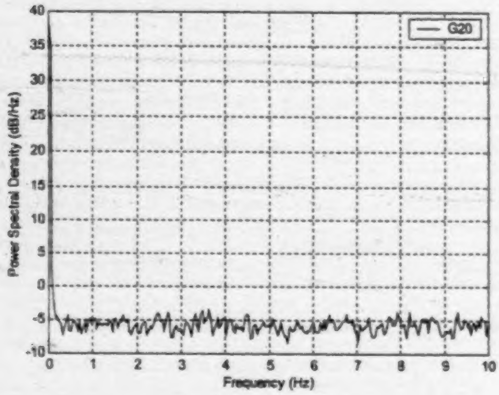

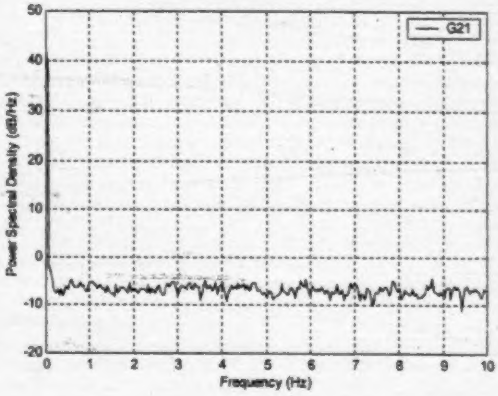

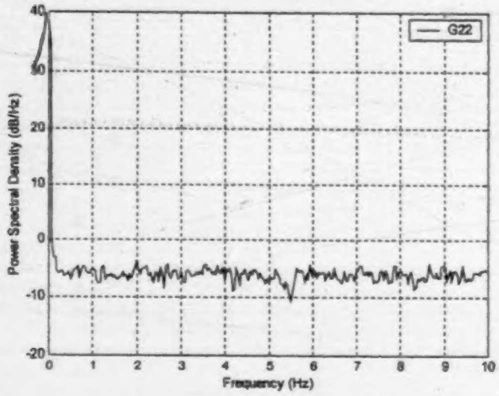

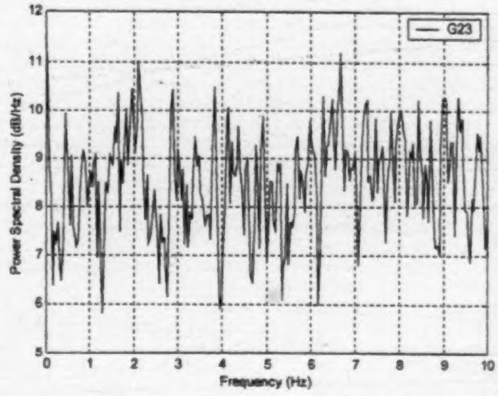

July 18, 1999
3:49 PM

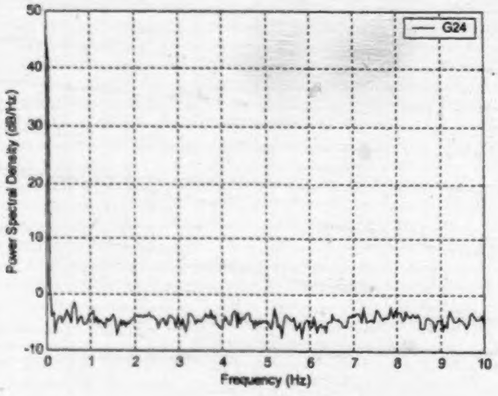

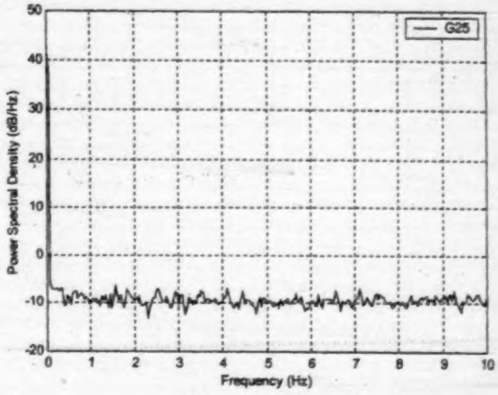

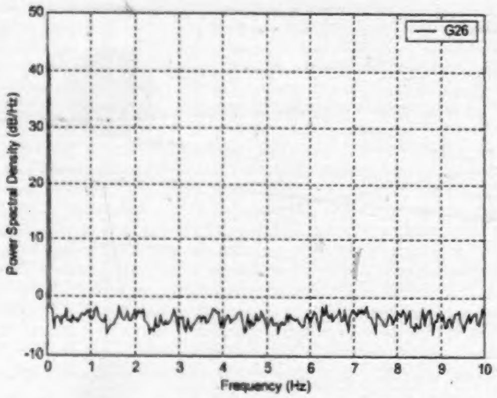

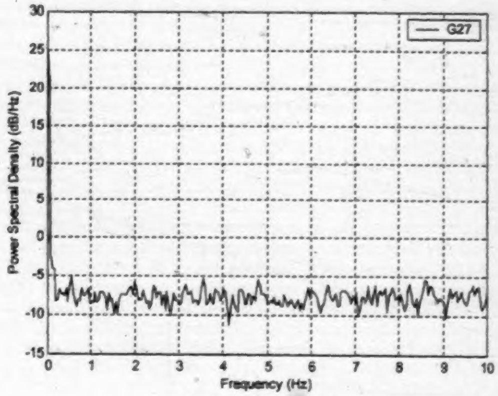

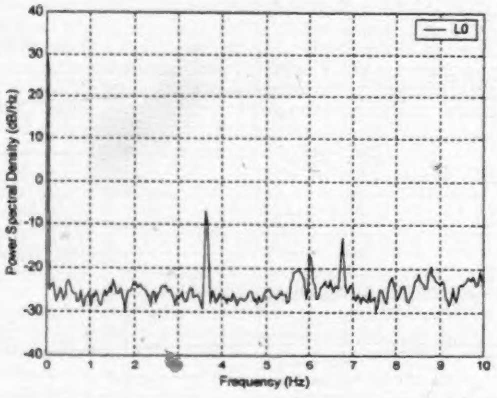

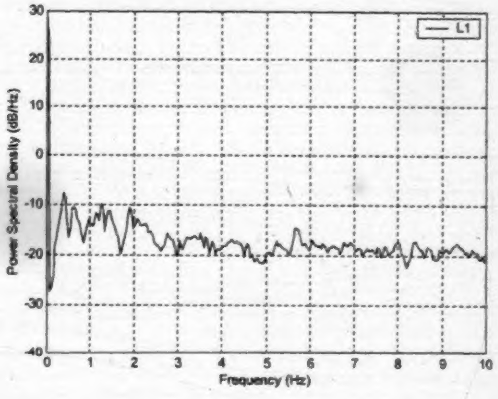

July 18, 1999
3:49 PM

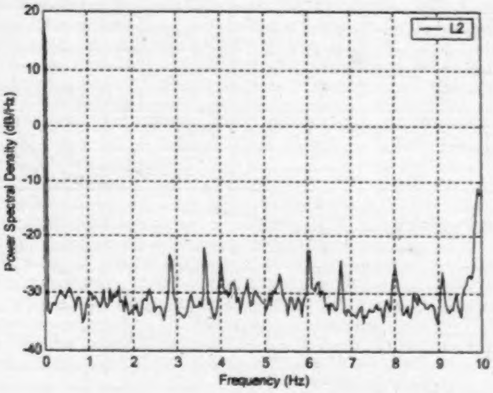

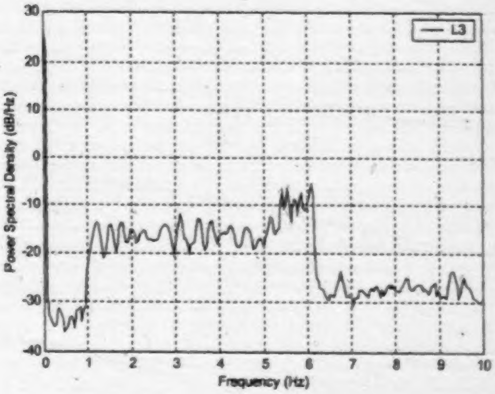

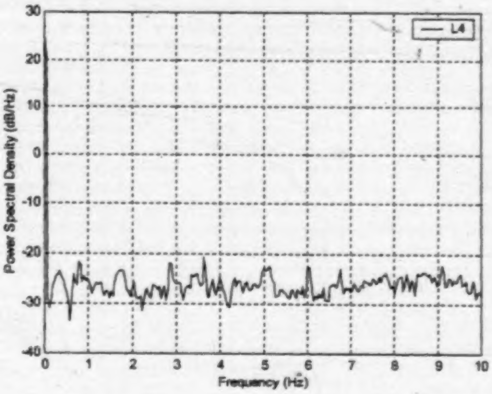

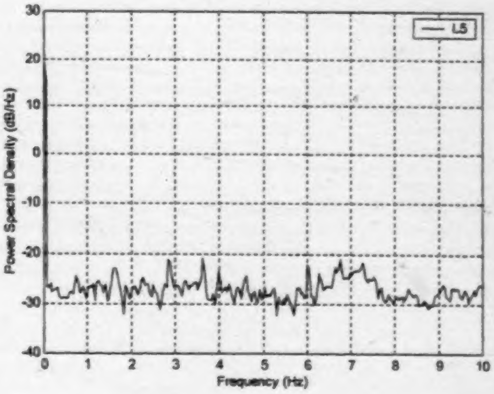

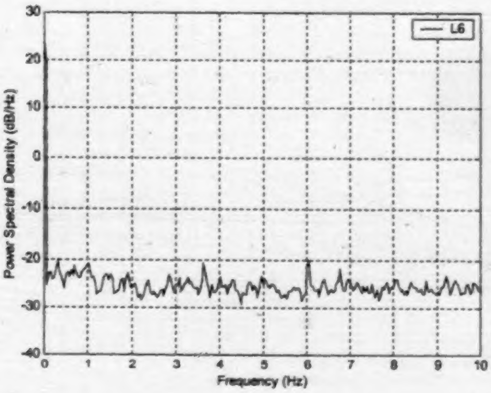

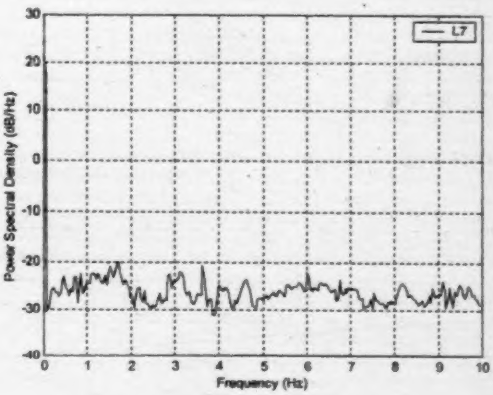

July 18, 1999
3:49 PM

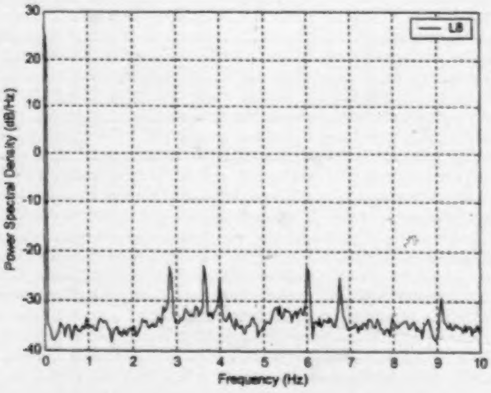

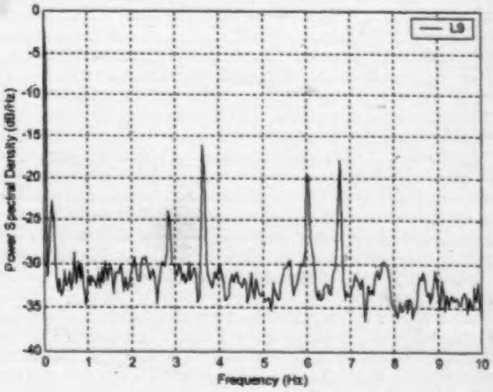

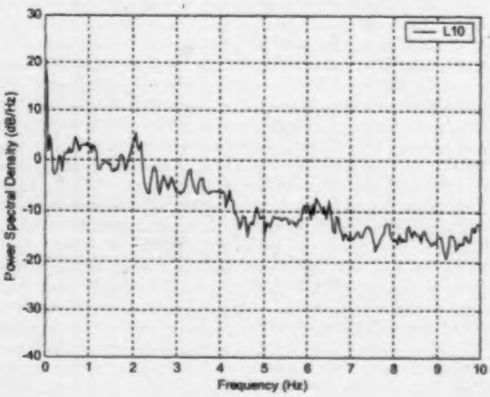

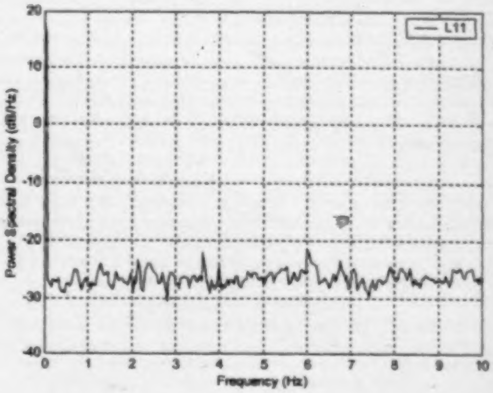

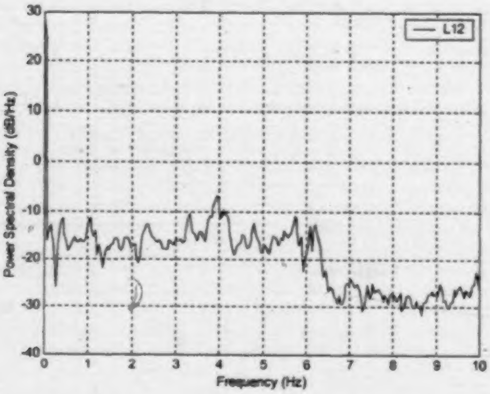

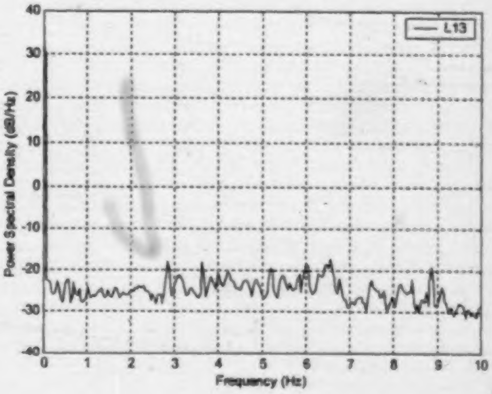

July 18, 1999
3:49 PM

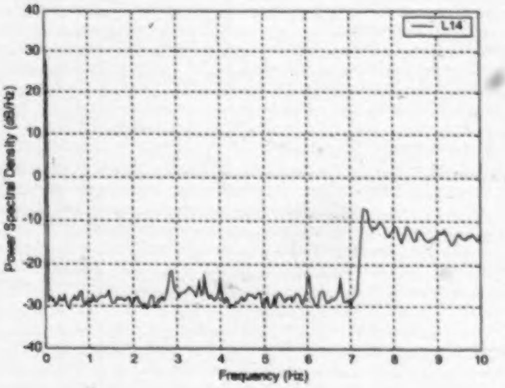

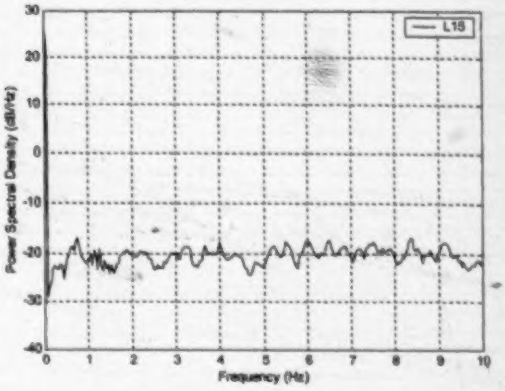

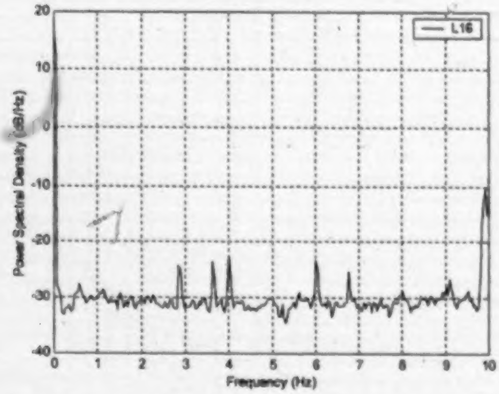

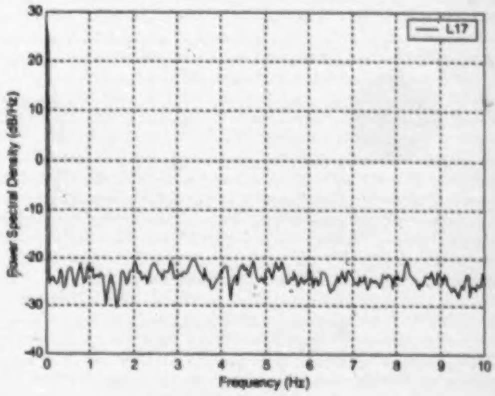

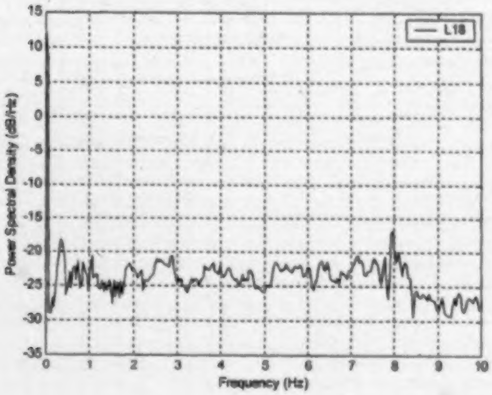

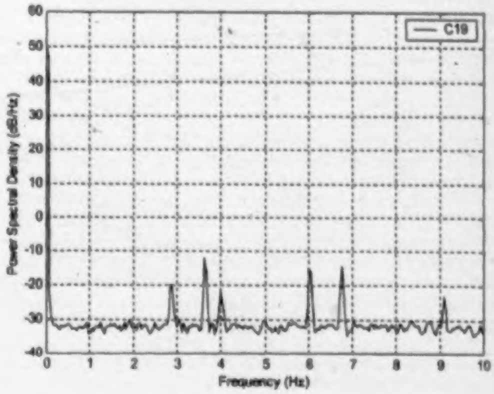

July 18, 1999
3:49 PM

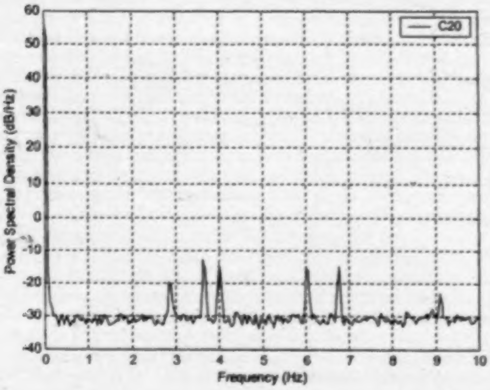

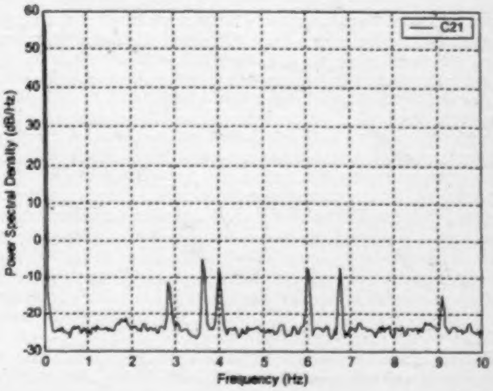

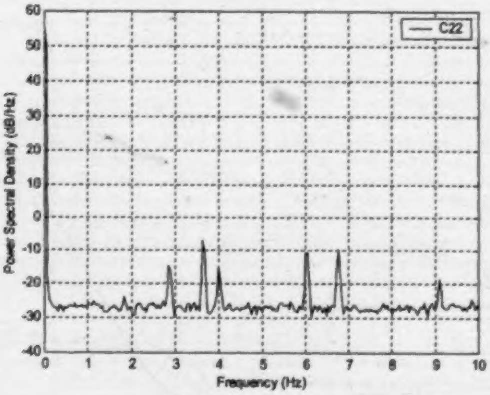

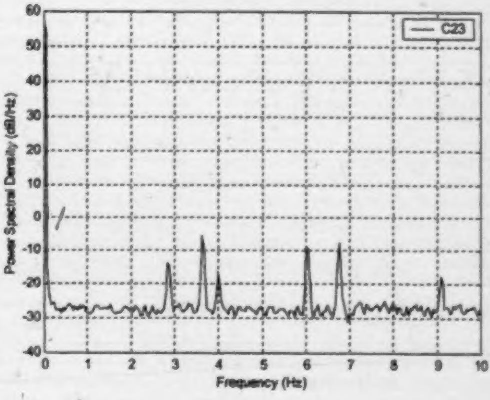

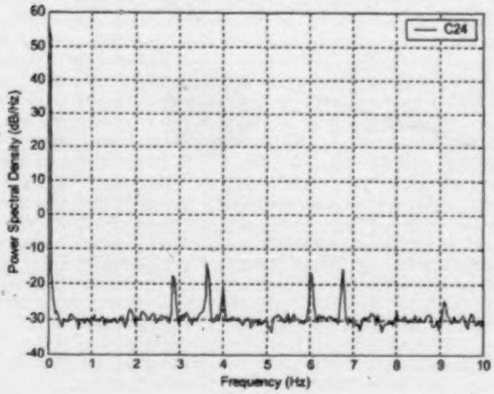

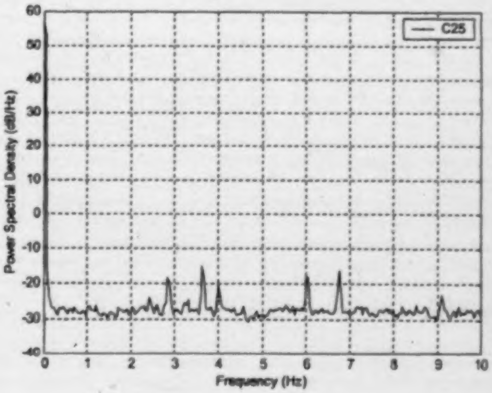

July 18, 1999
3:49 PM

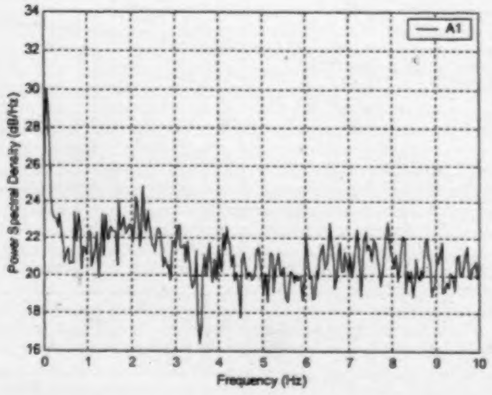

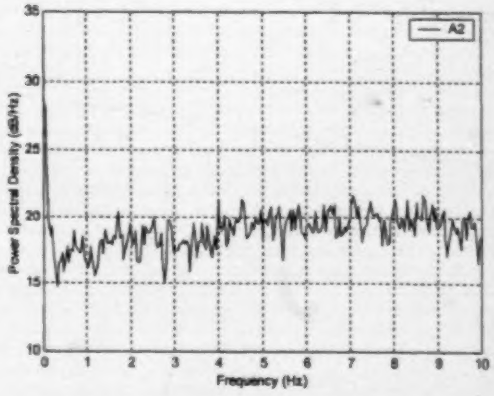

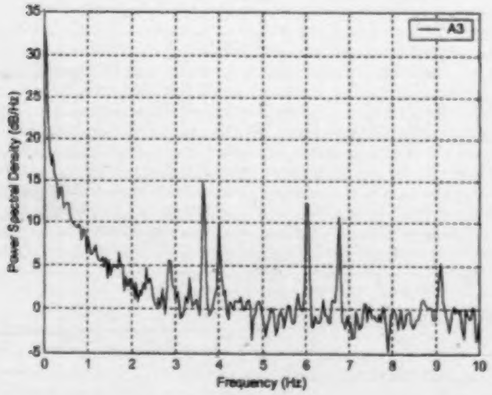

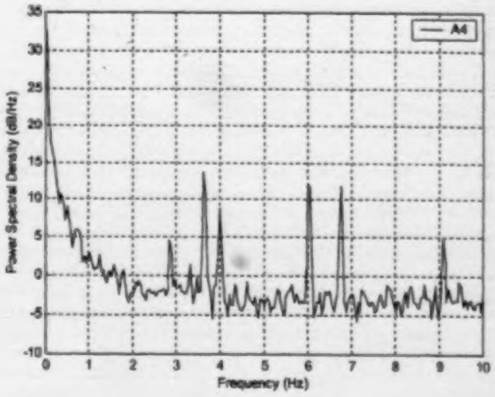

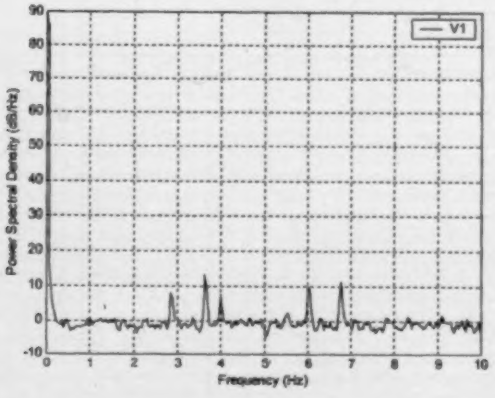

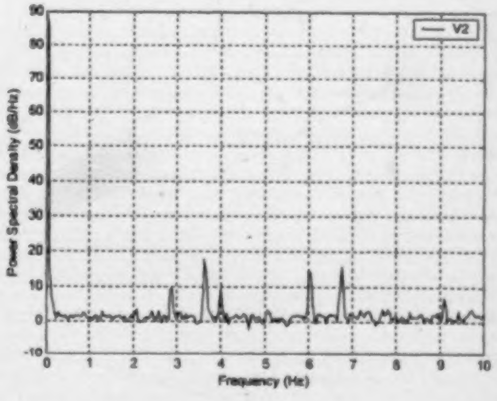

July 18, 1999
3:54 PM

July 18, 1999
3:54 PM

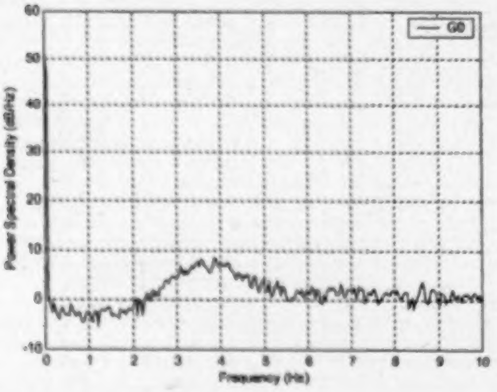

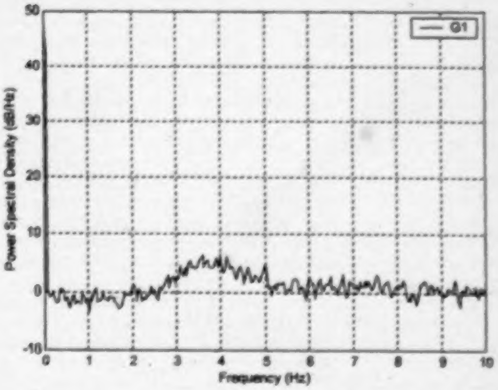

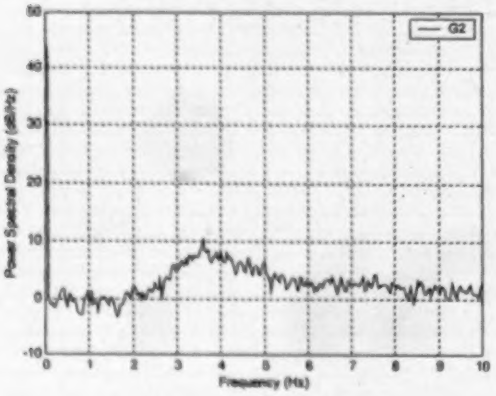

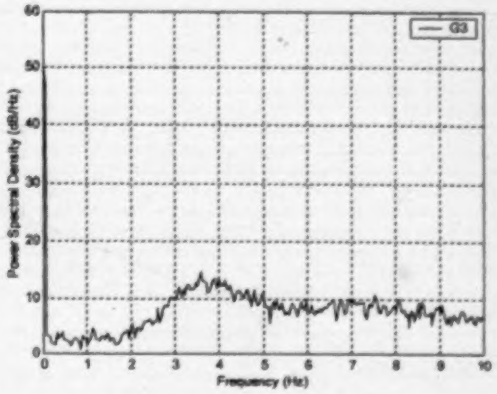

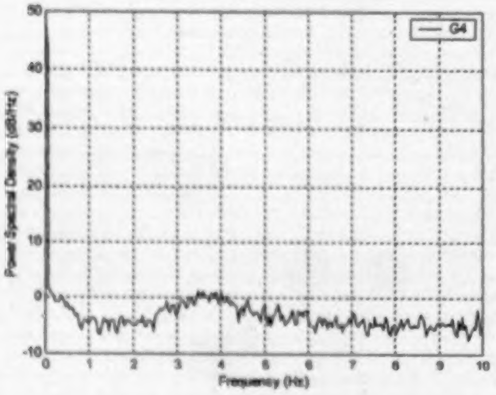

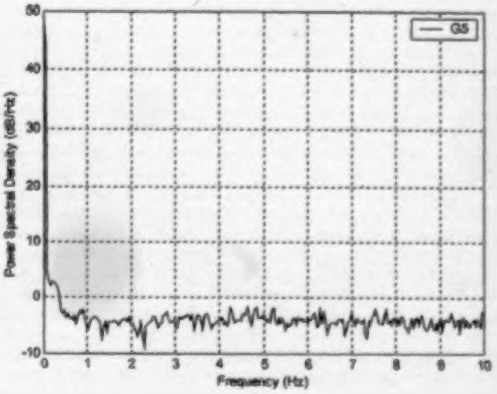

July 18, 1999
3:54 PM

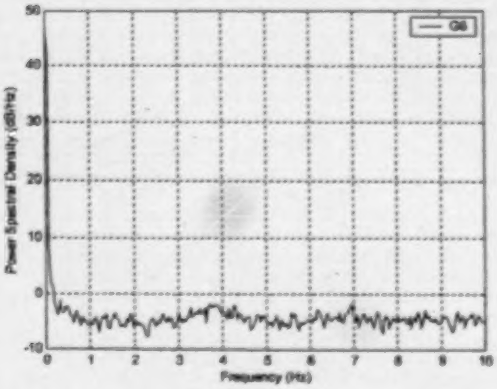

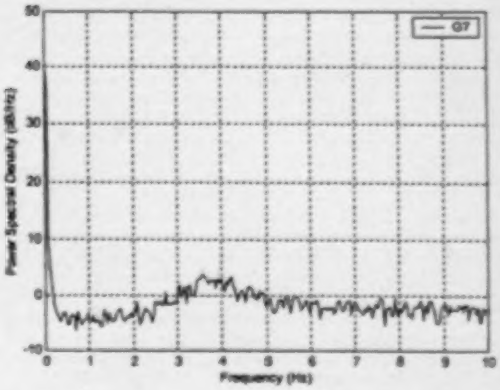

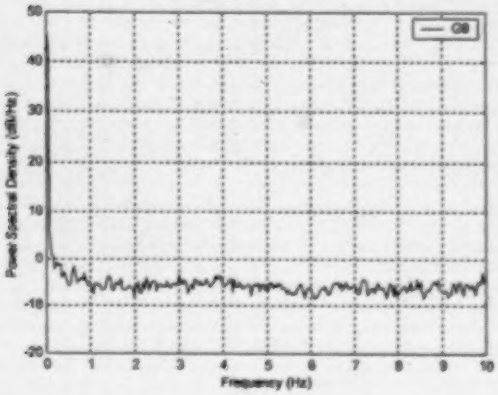

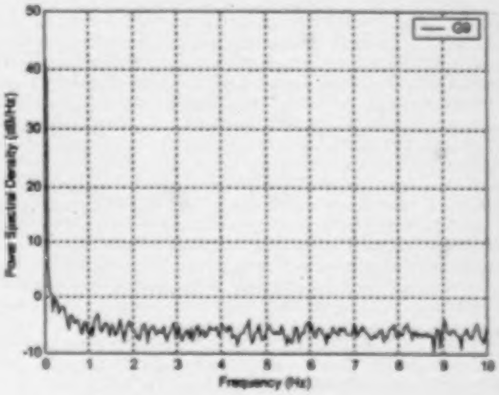

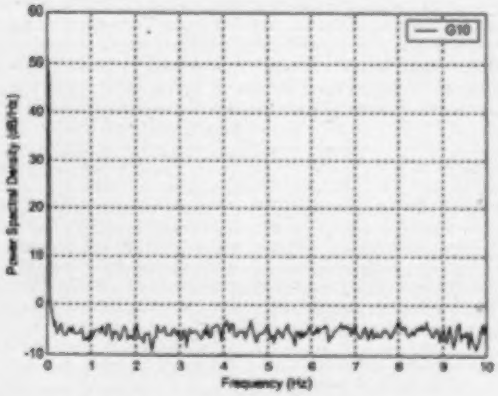

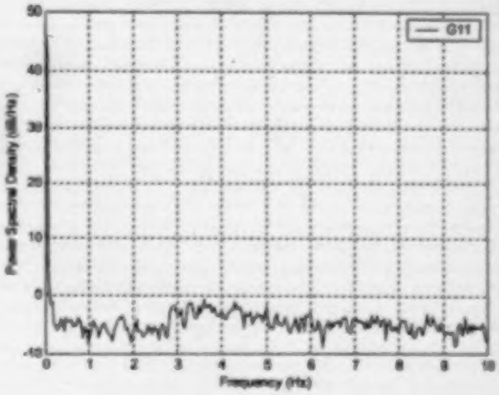

July 18, 1999
3:54 PM

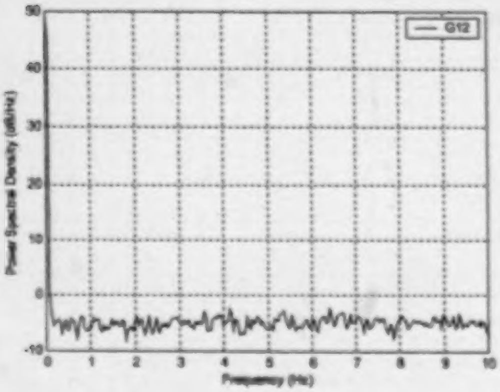

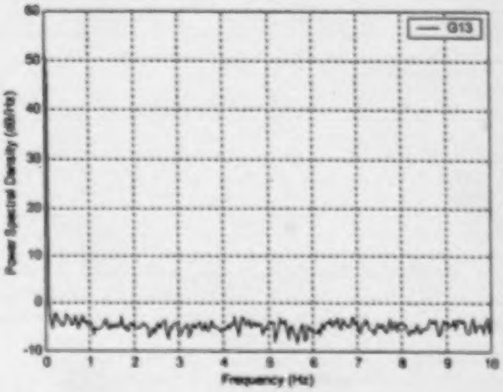

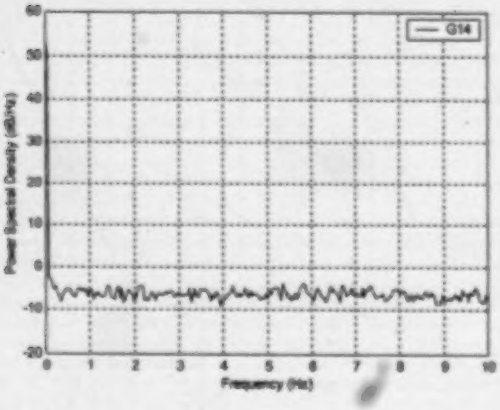

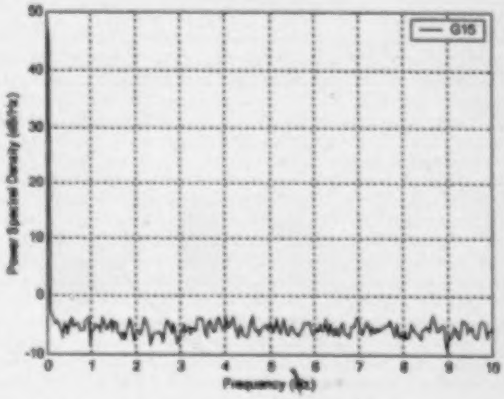

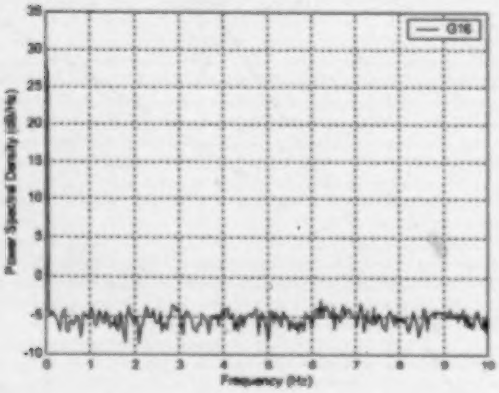

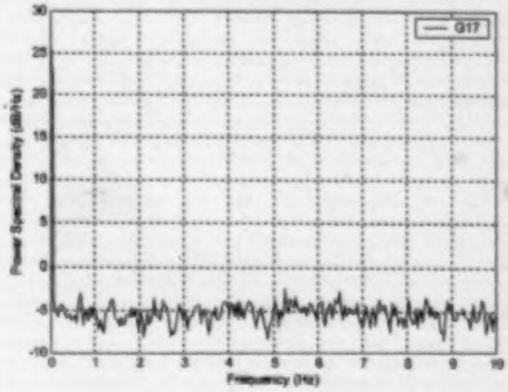

July 18, 1999
3:54 PM

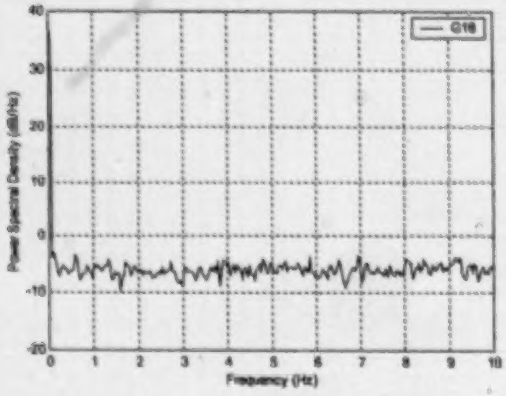

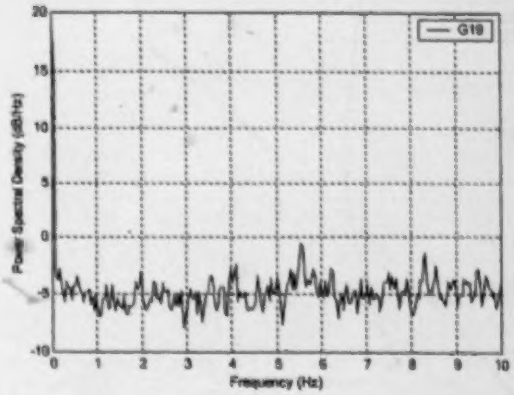

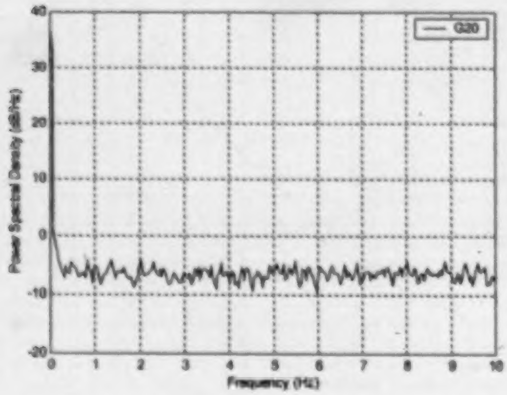

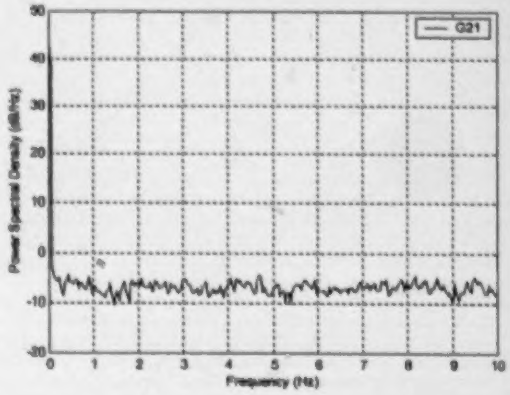

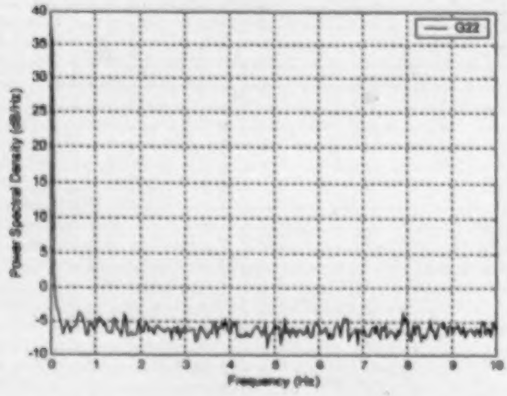

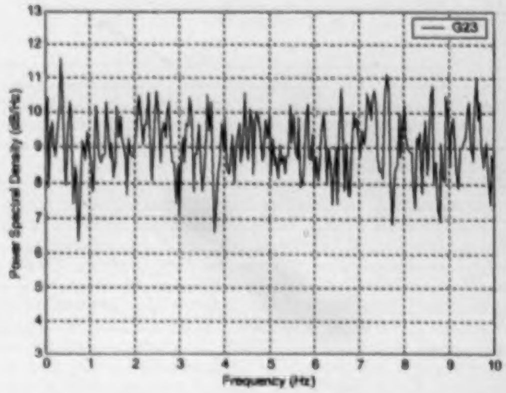

July 18, 1999
3:54 PM

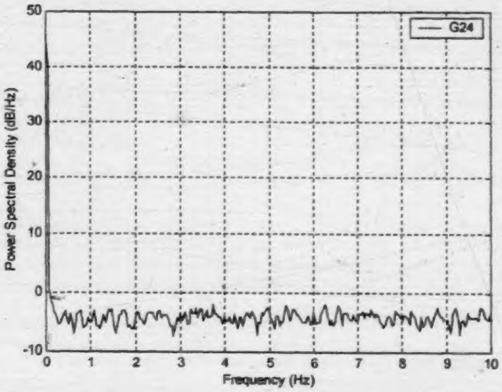

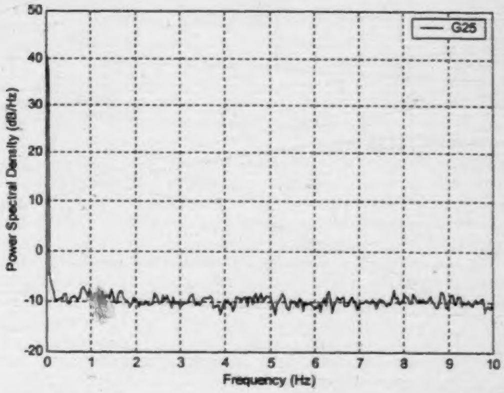

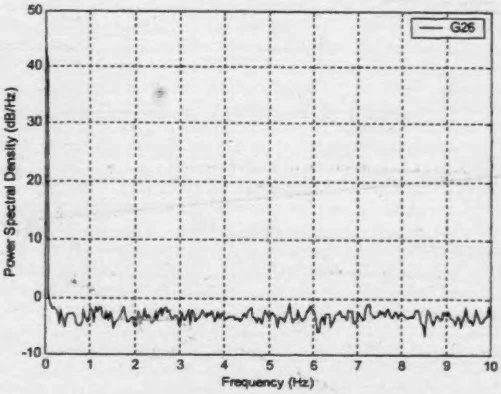

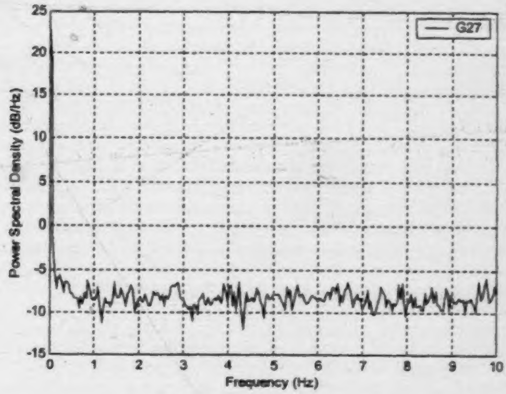

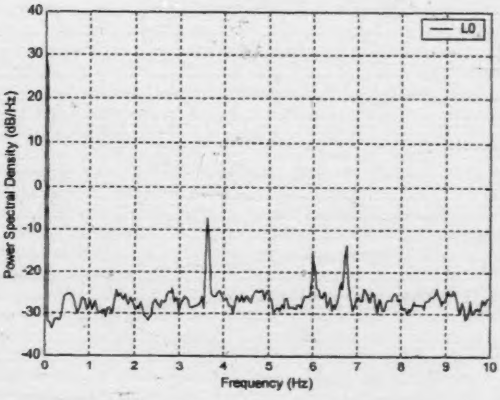

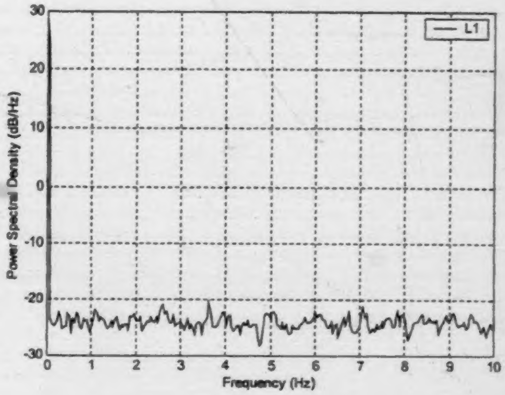

July 18, 1999
3:54 PM

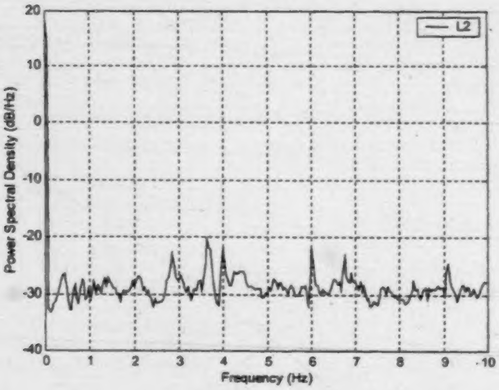

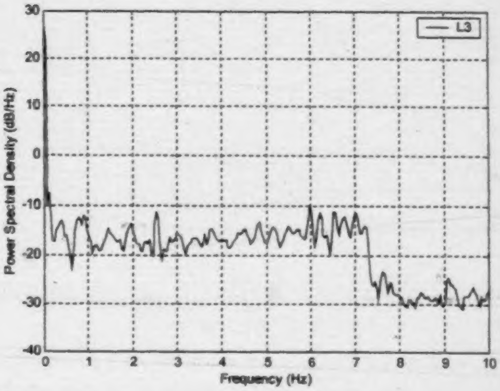

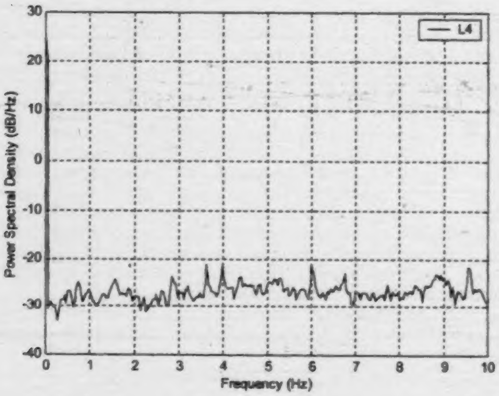

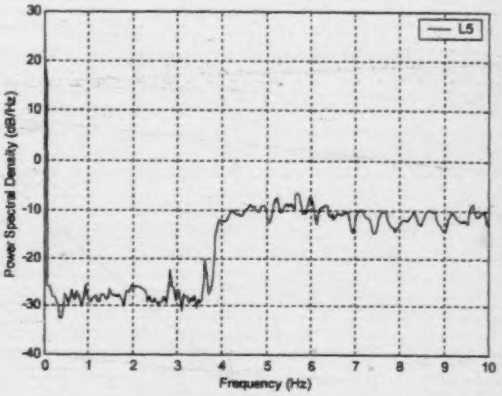

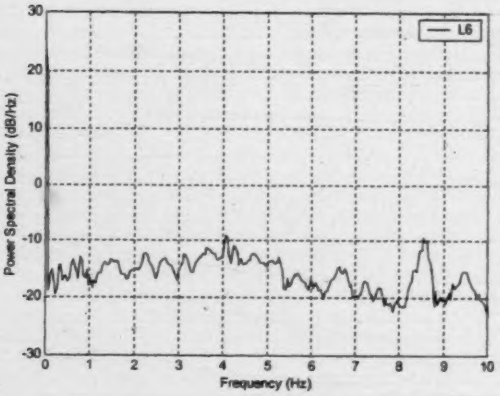

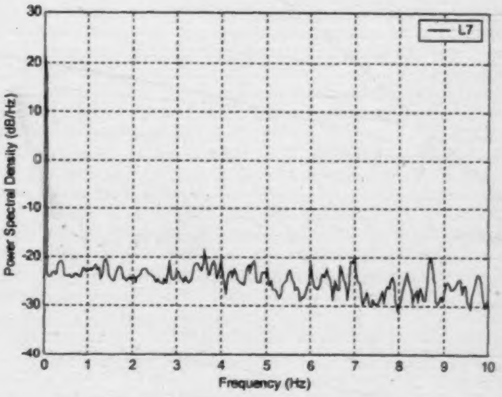

July 18, 1999
3:54 PM

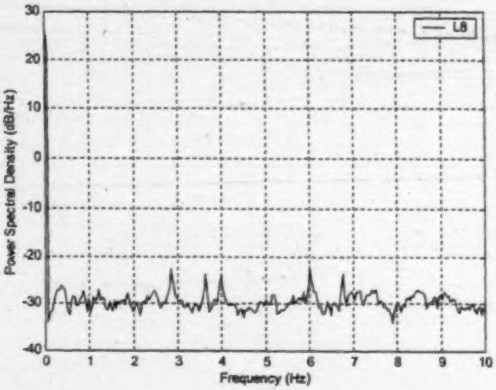

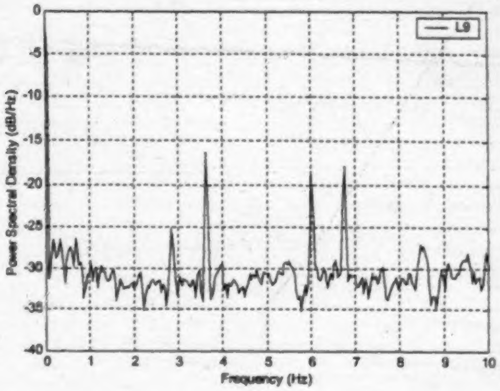

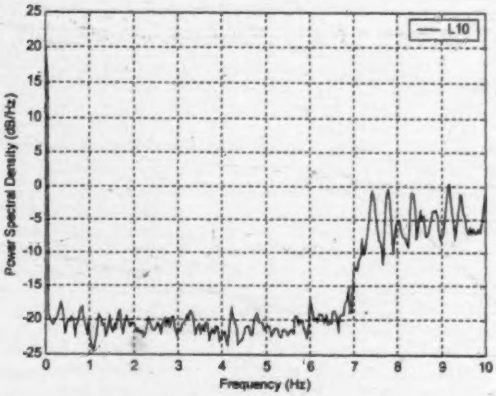

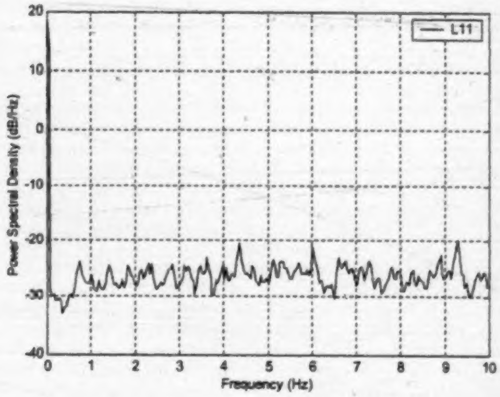

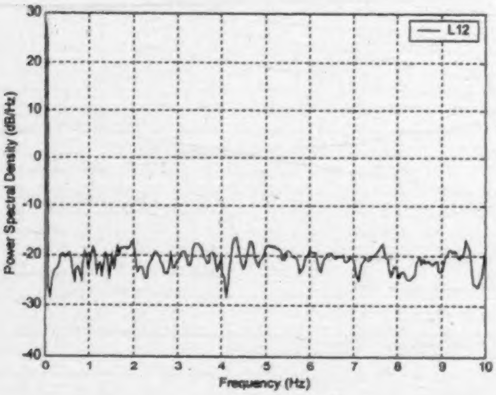

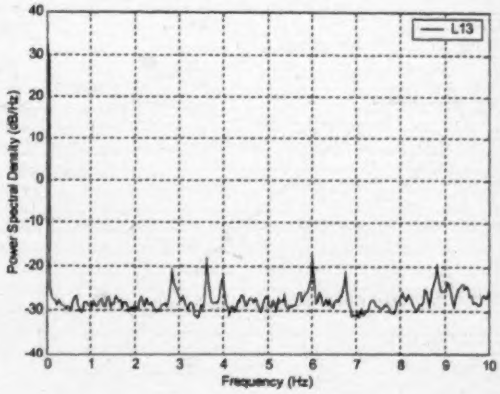

July 18, 1999
3:54 PM

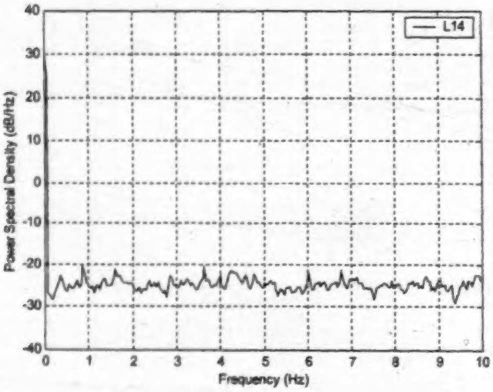

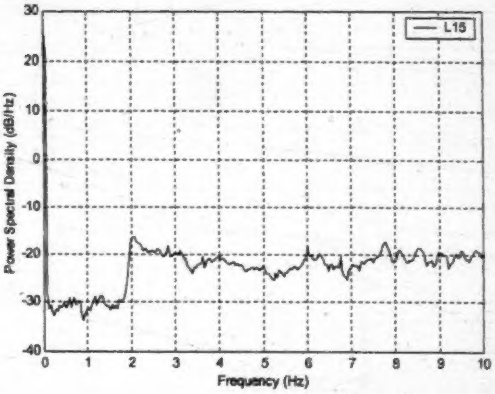

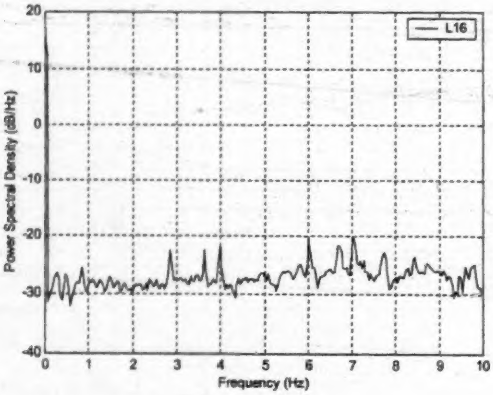

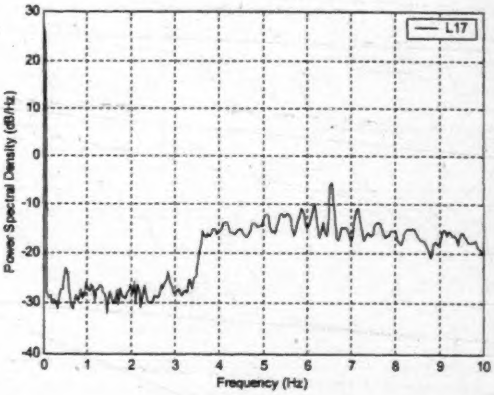

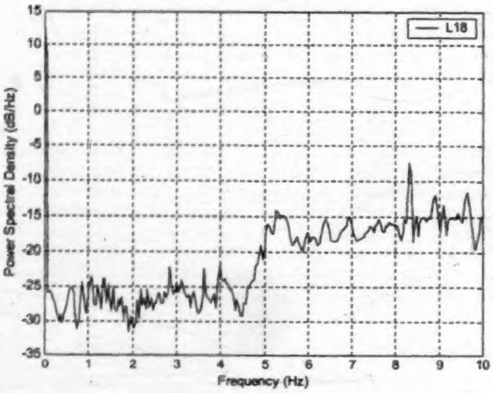

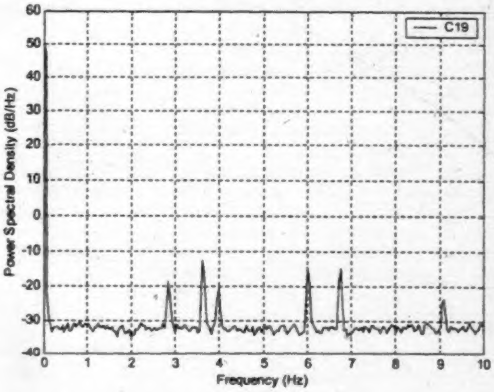

July 18, 1999
3:54 PM

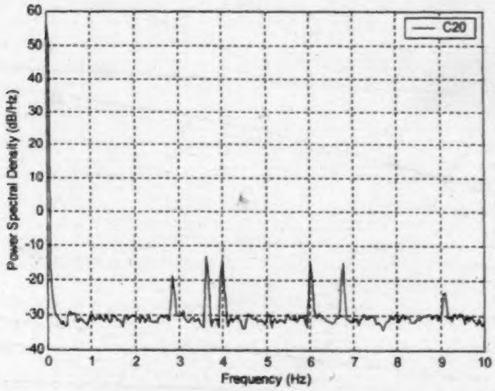

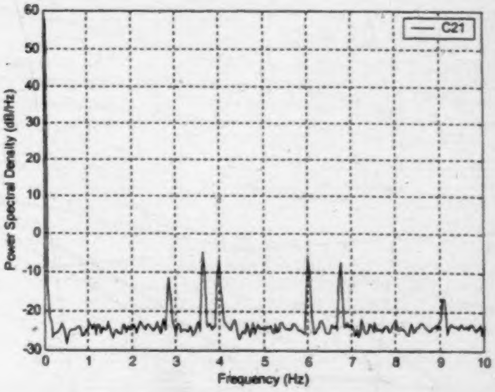

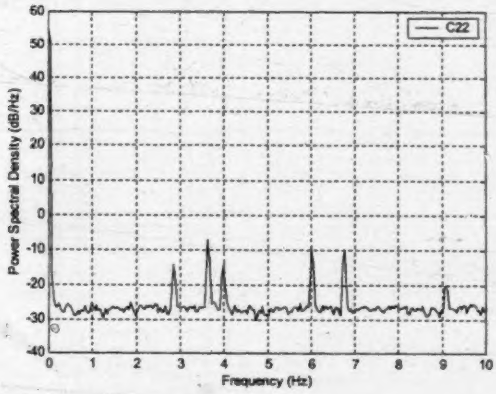

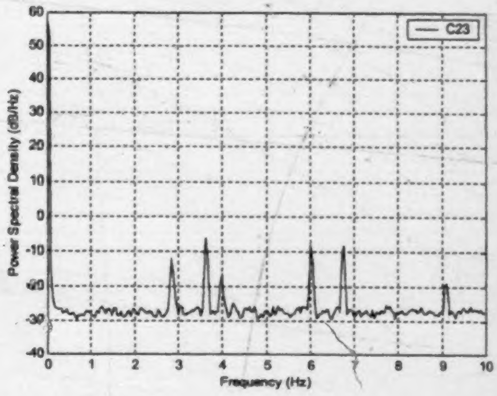

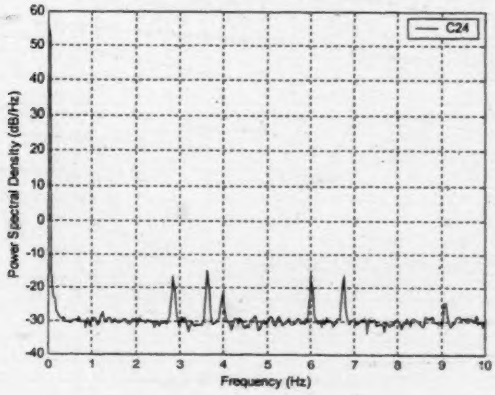

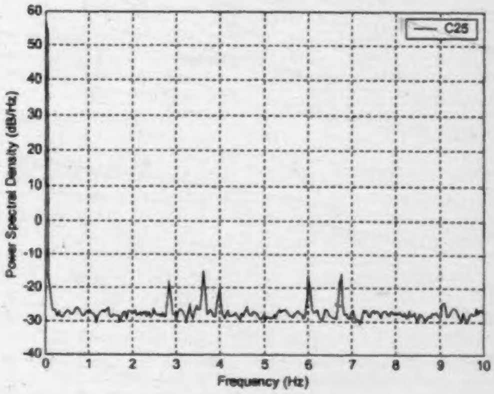

July 18, 1999
3:54 PM

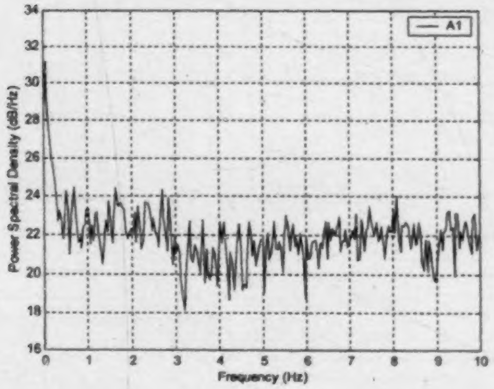

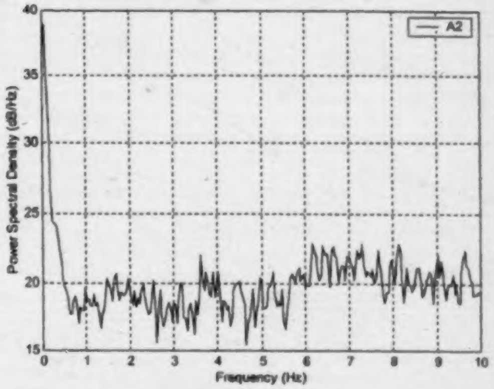

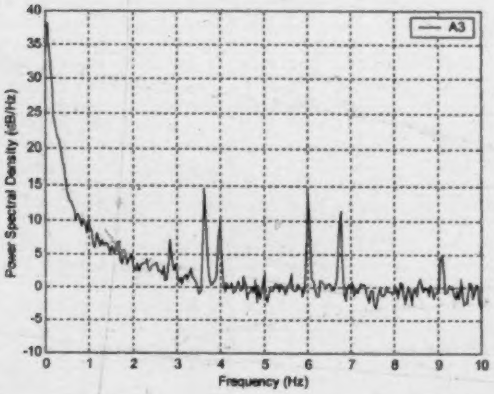

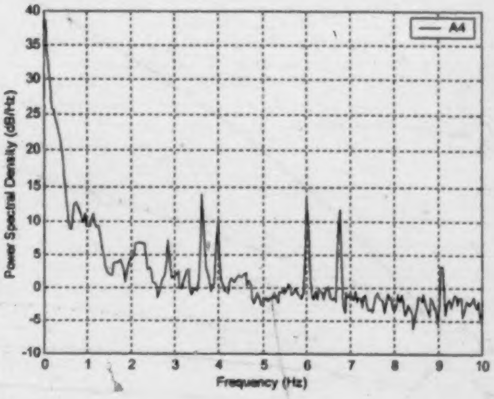

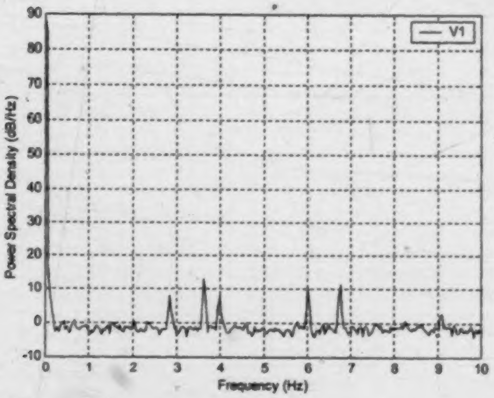

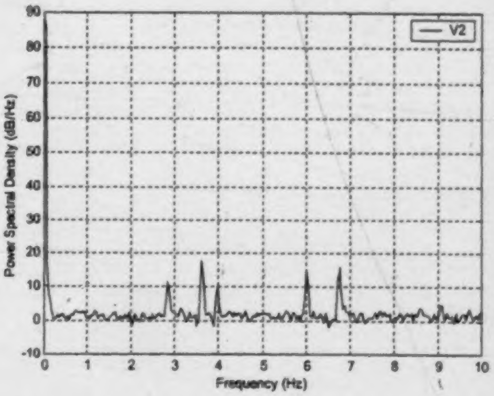

July 18, 1999
4:00 PM

July 18, 1999
4:00 PM

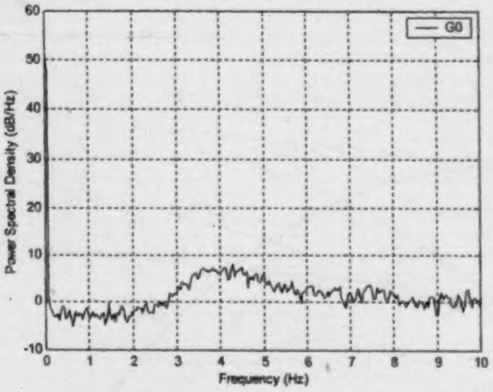

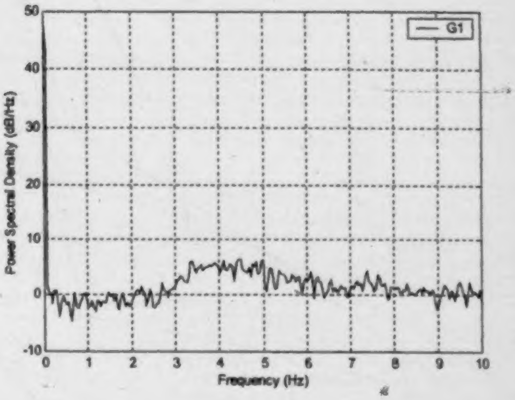

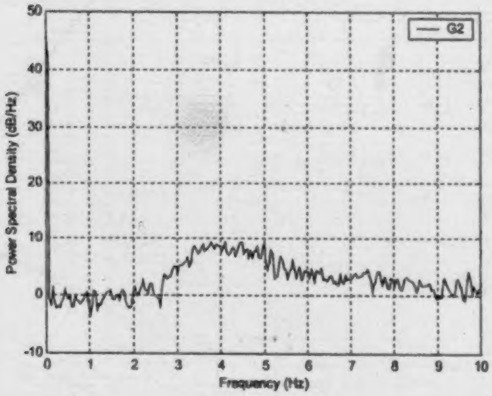

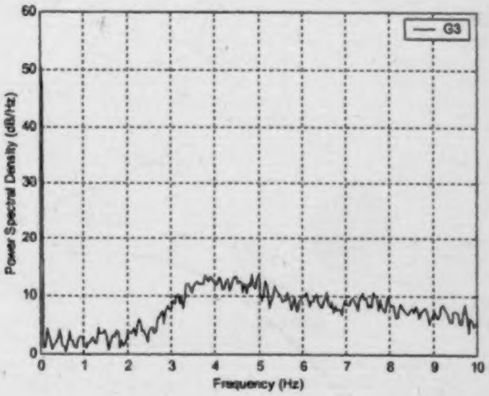

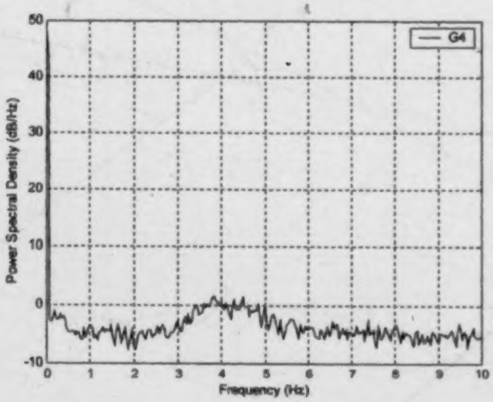

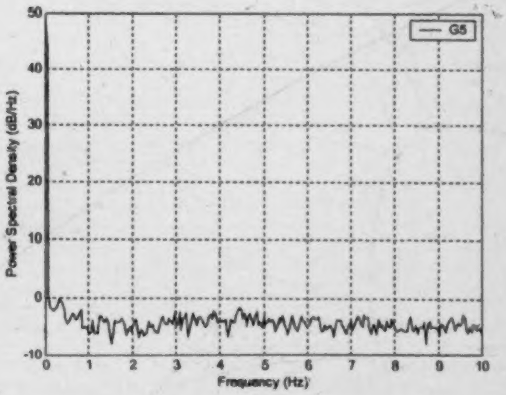

July 18, 1999
4:00 PM

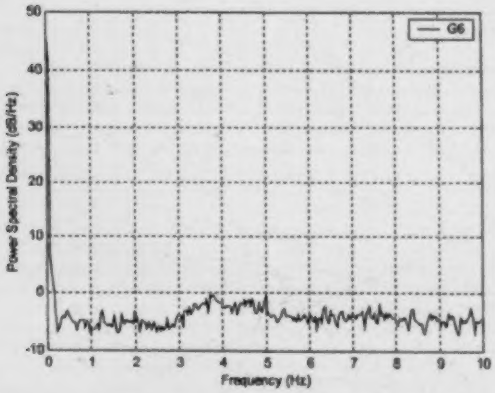

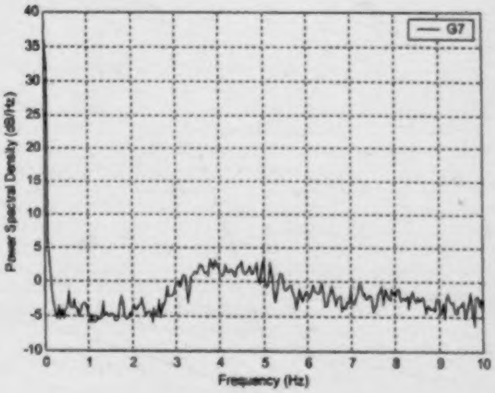

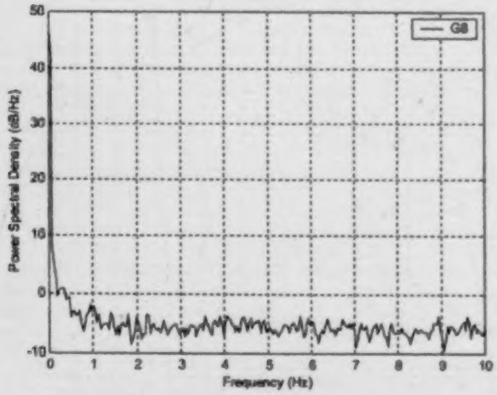

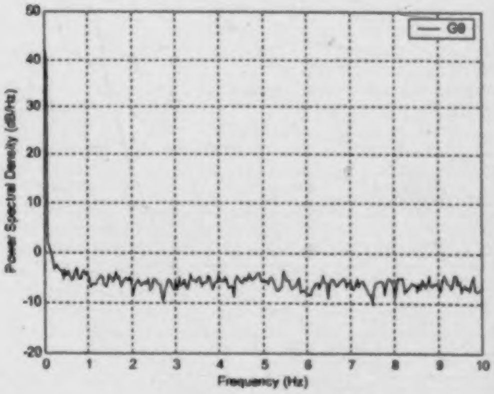

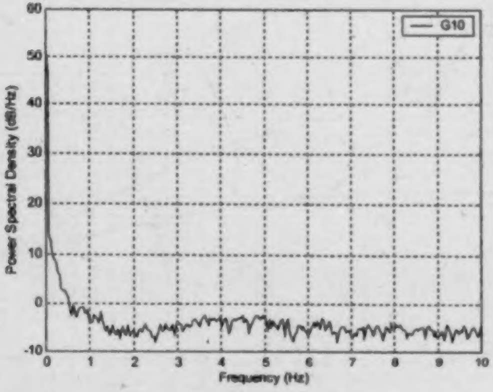

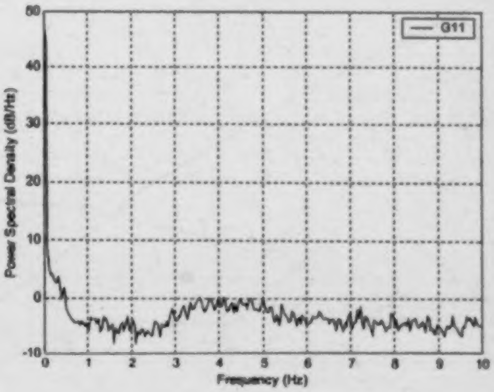

July 18, 1999
4:00 PM

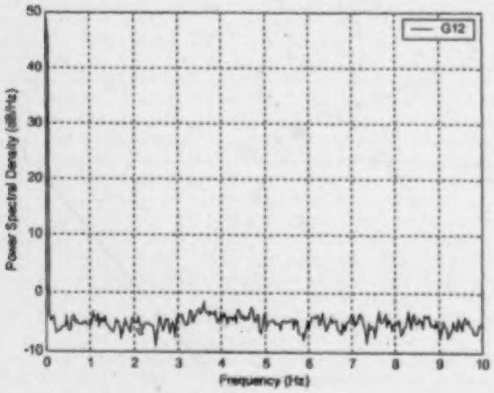

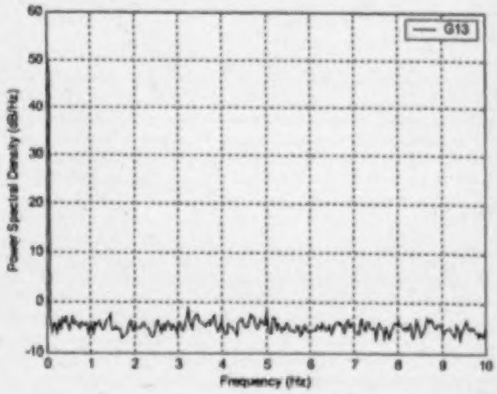

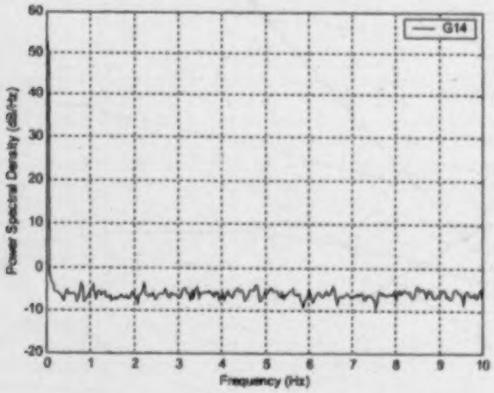

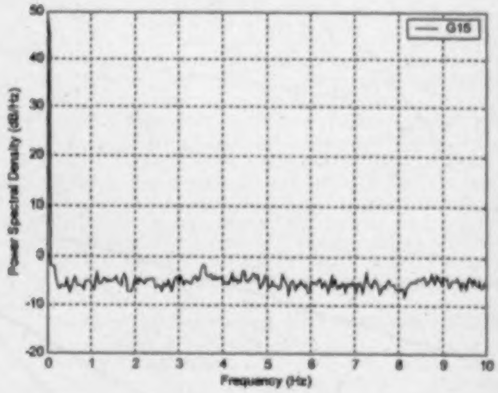

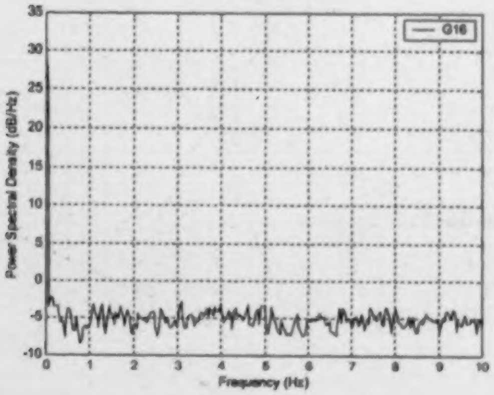

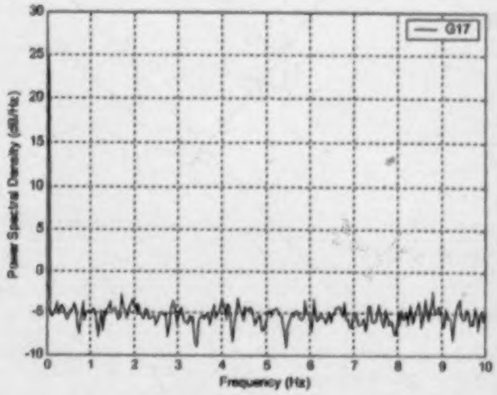

July 18, 1999
4:00 PM

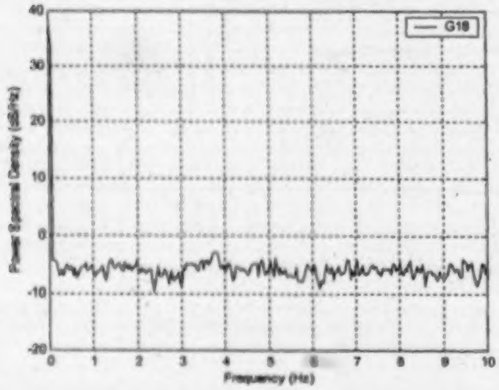

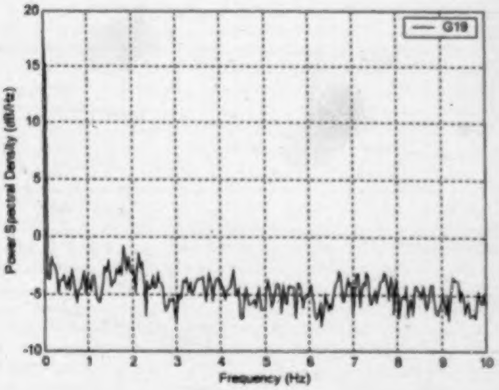

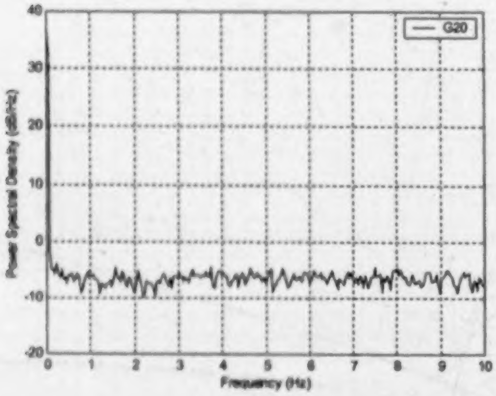

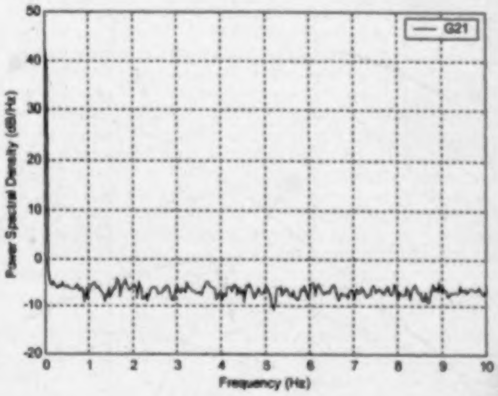

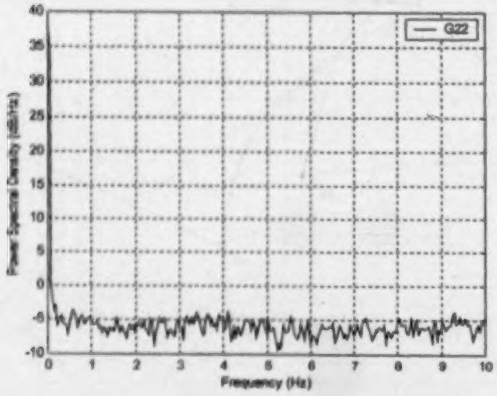

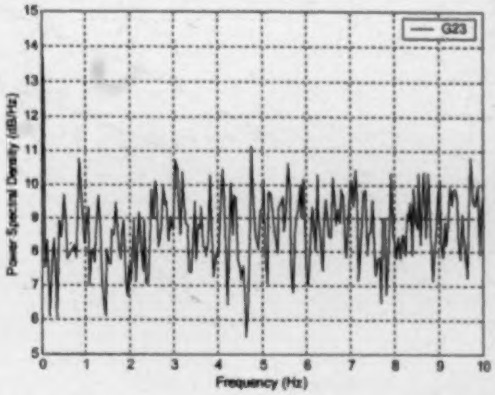

July 18, 1999
4:00 PM

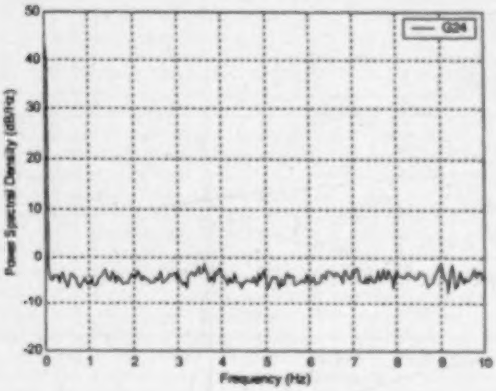

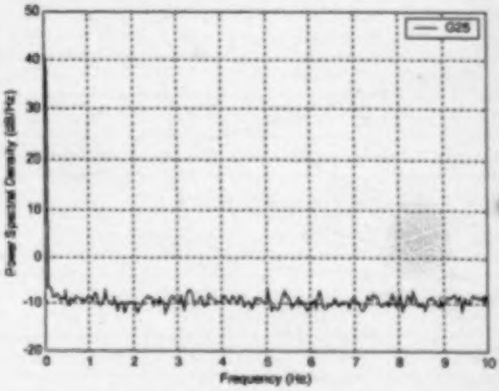

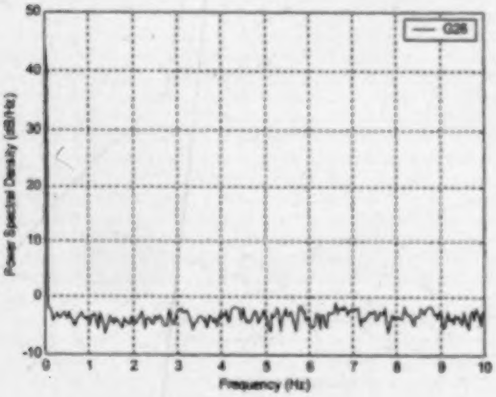

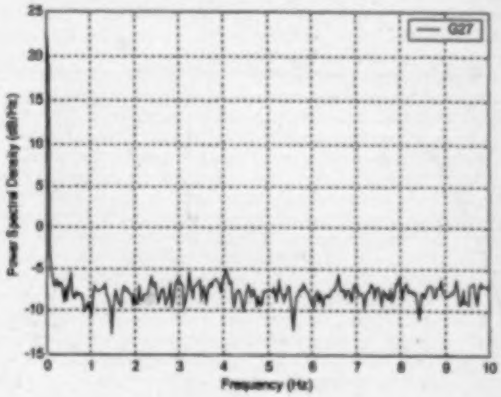

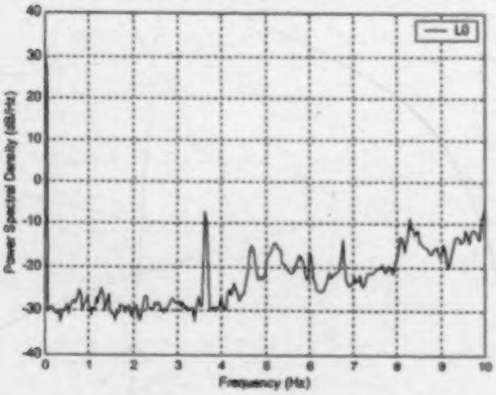

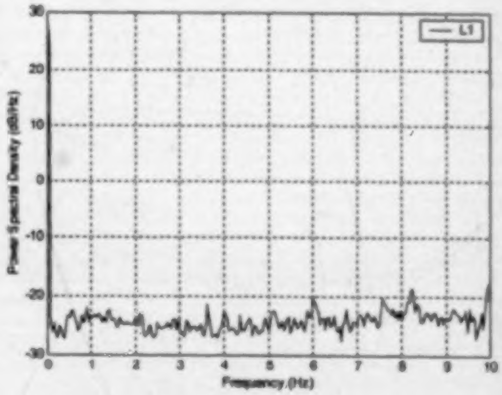

July 18, 1999
4:00 PM

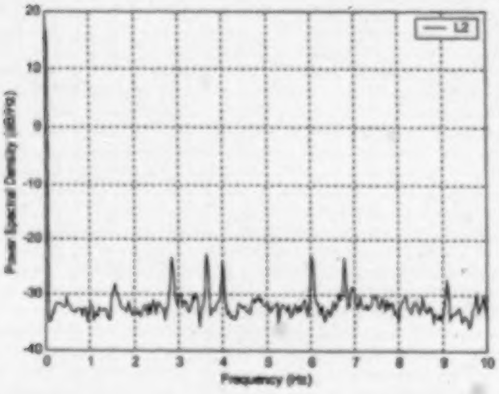

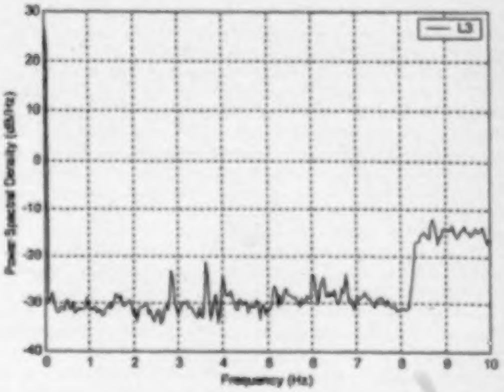

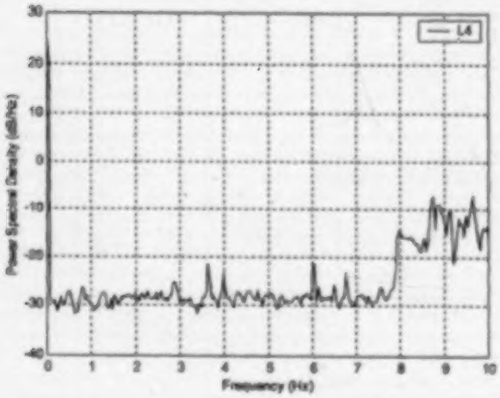

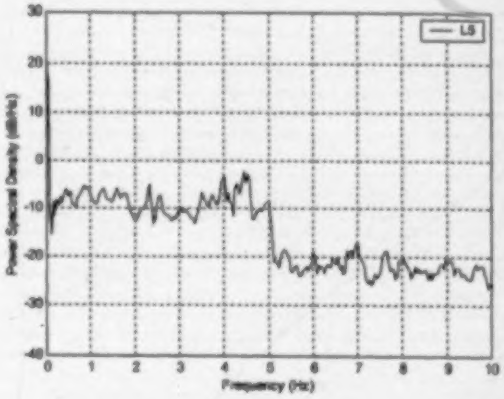

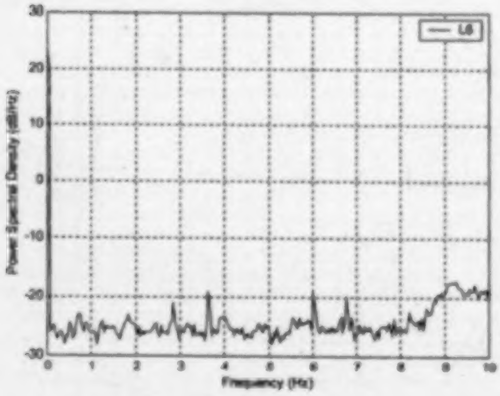

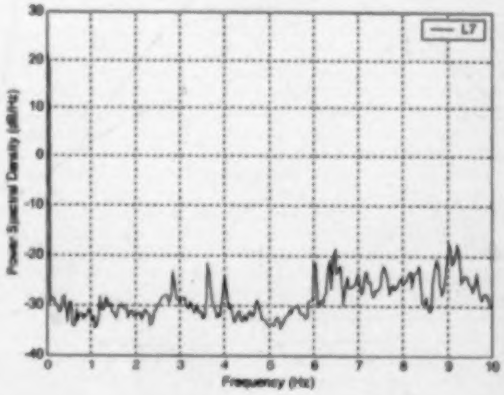

July 18, 1999
4:00 PM

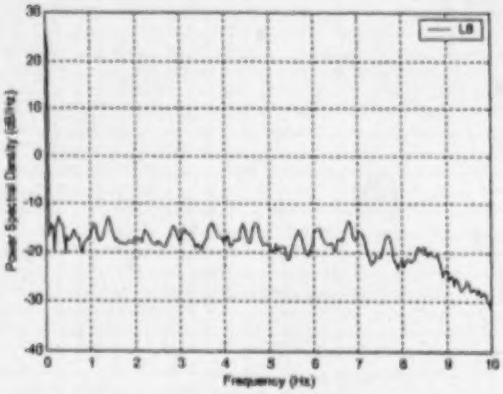

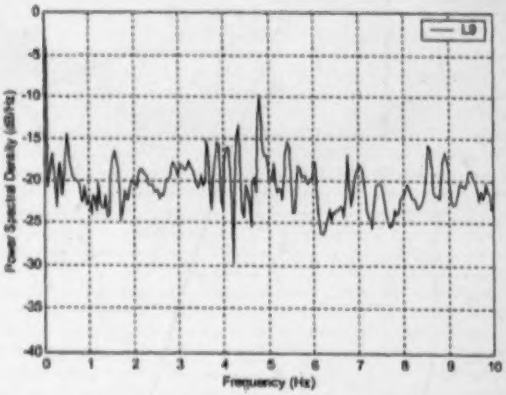

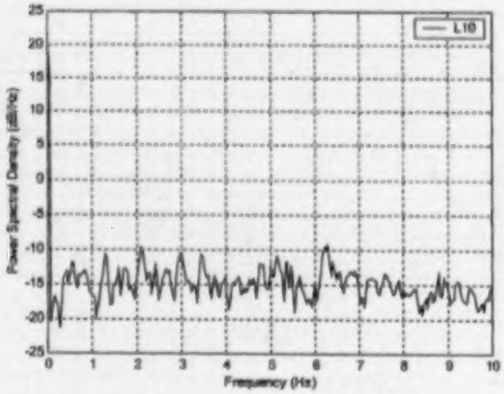

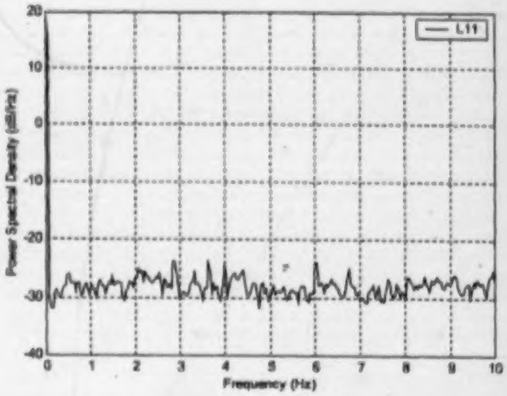

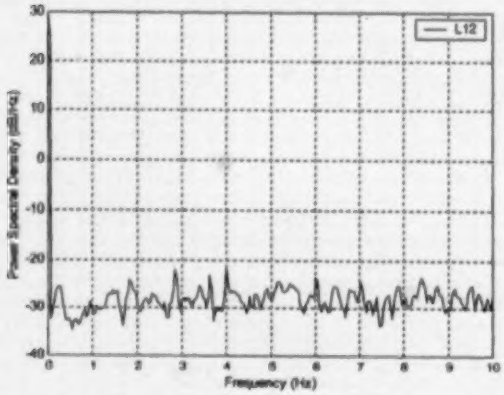

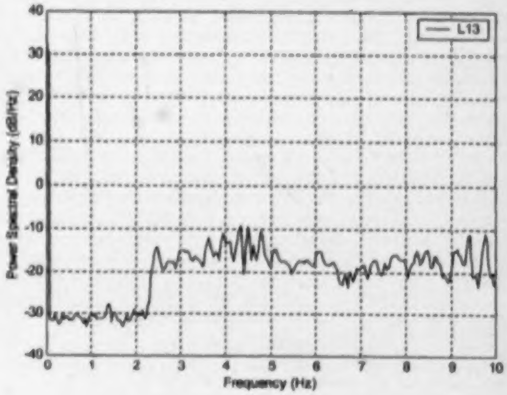

July 18, 1999
4:00 PM

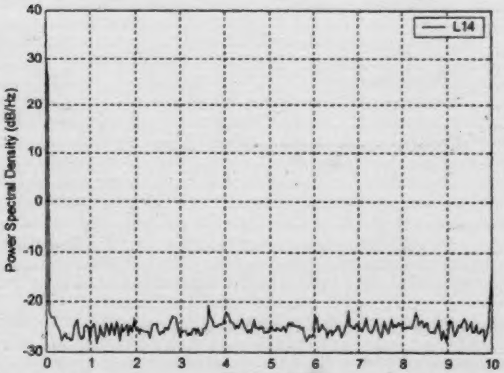

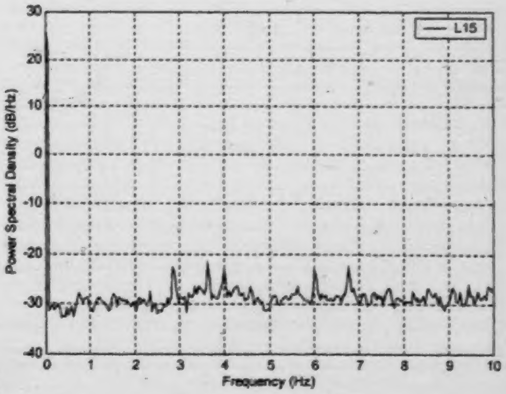

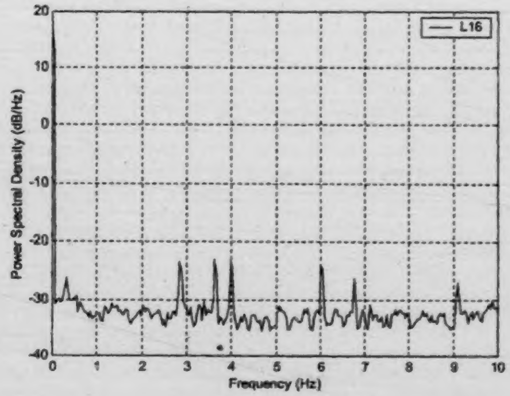

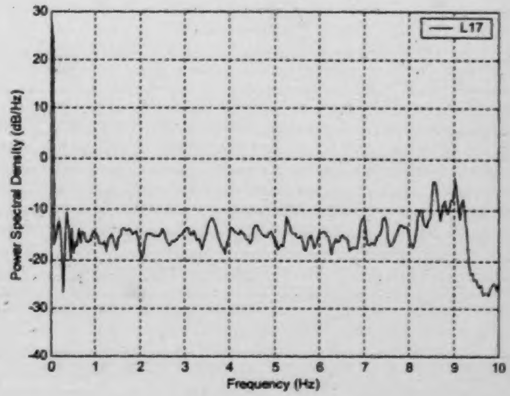

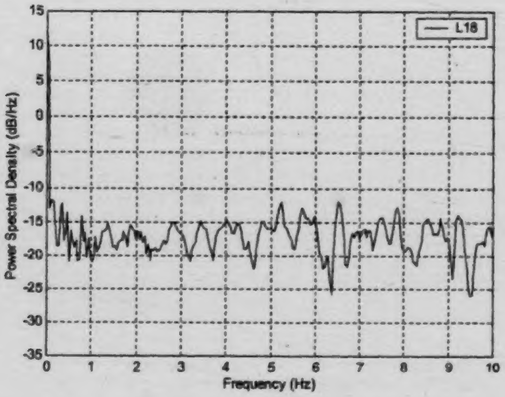

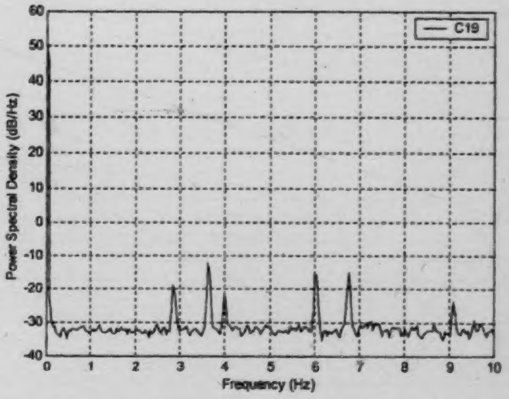

July 18, 1999
4:00 PM

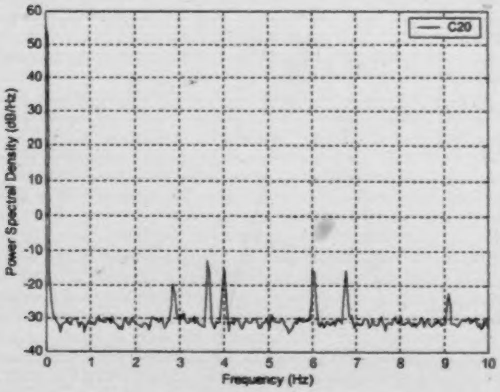

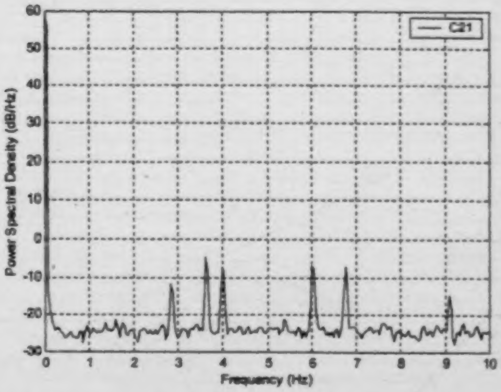

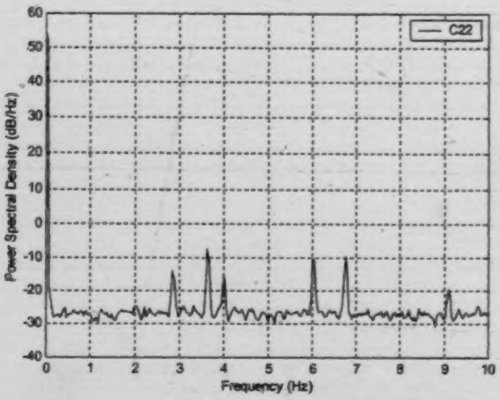

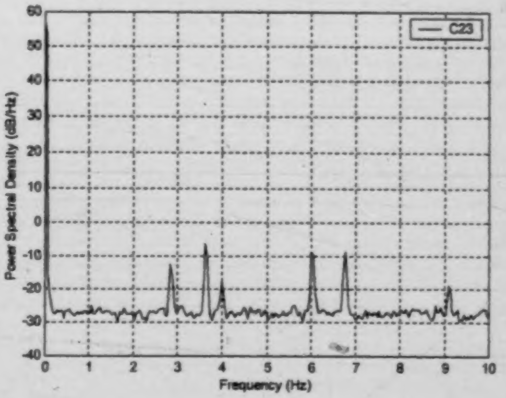

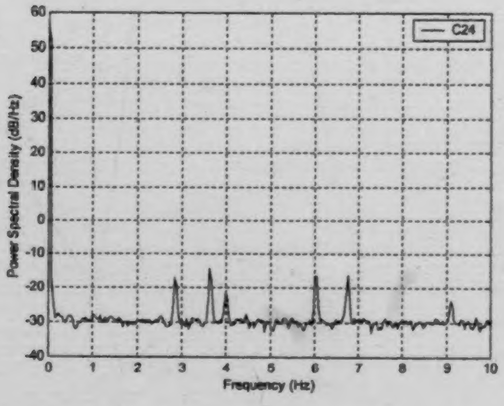

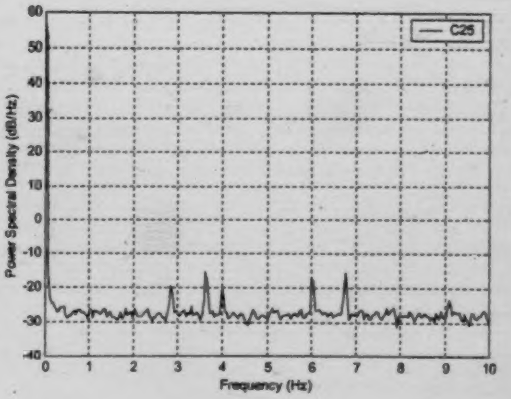

July 18, 1999
4:00 PM

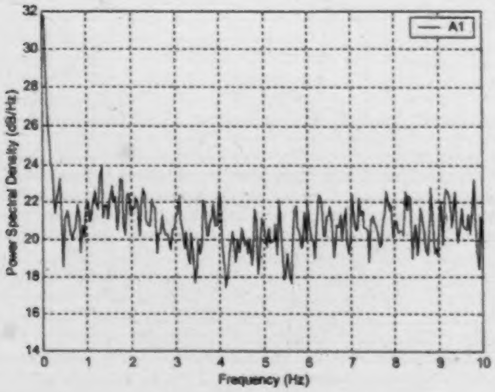

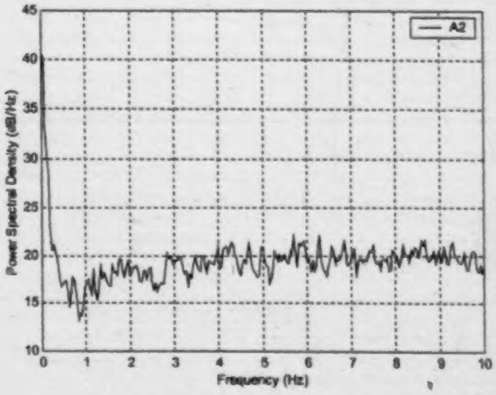

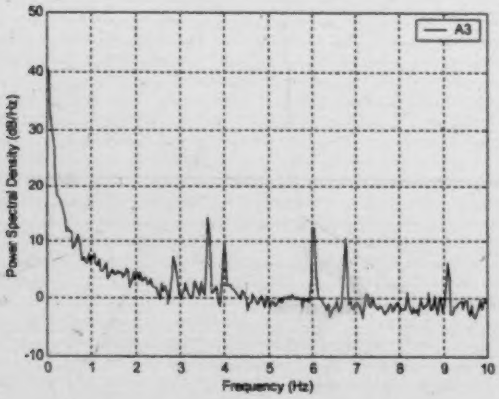

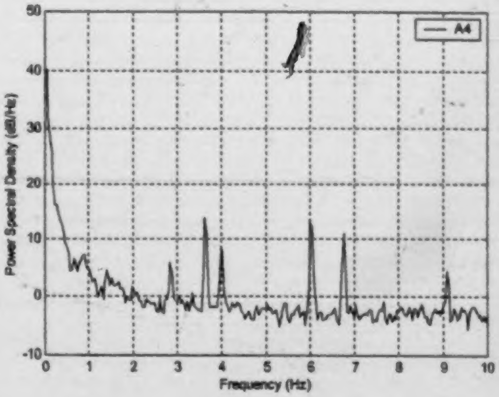

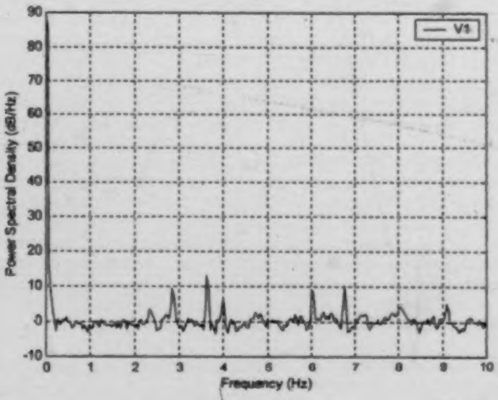

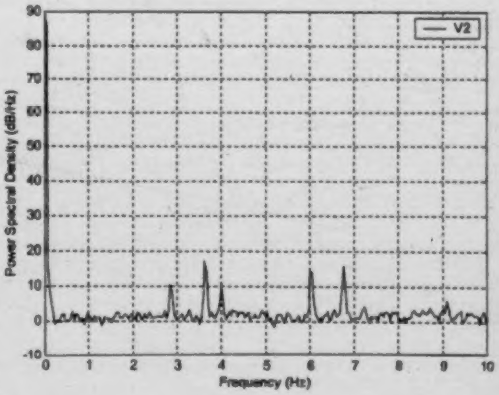

July 18, 1999
4:05 PM

July 18, 1999
4:05 PM

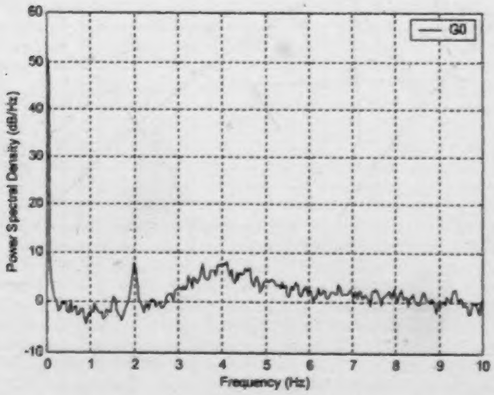

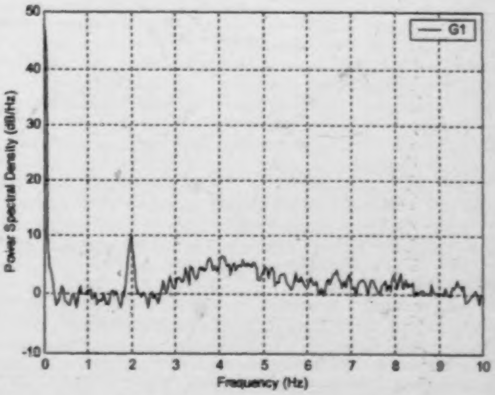

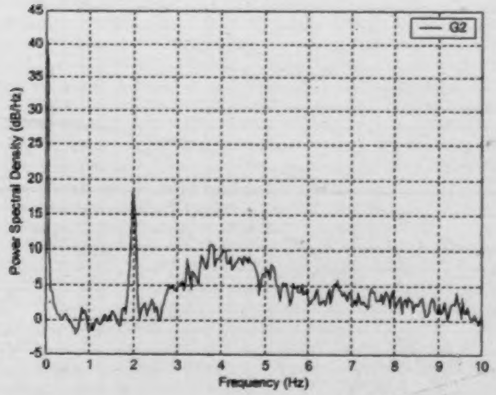

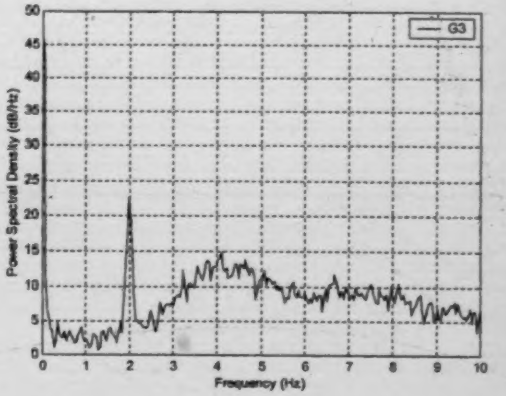

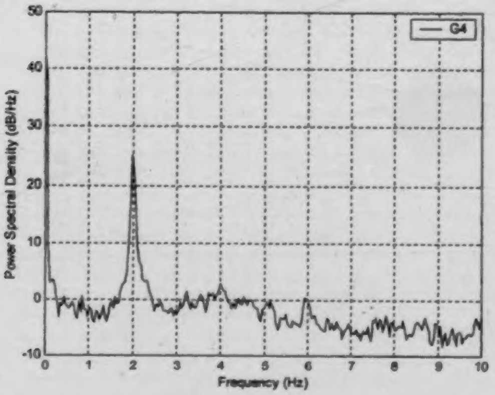

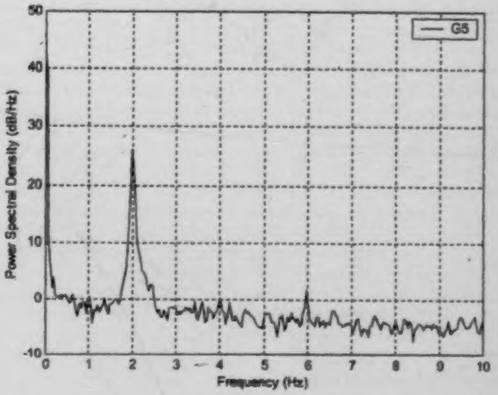

July 18, 1999
4:05 PM

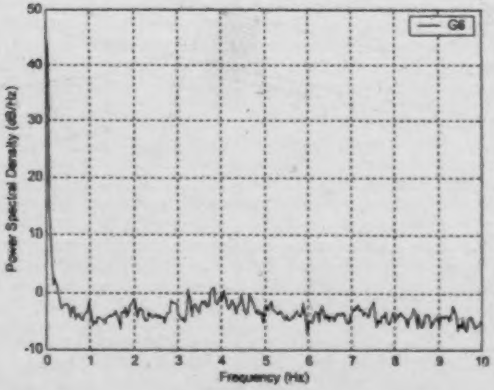

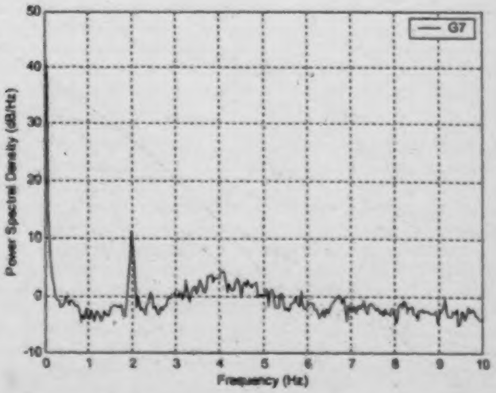

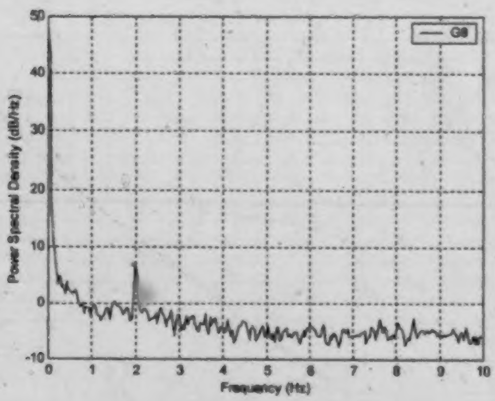

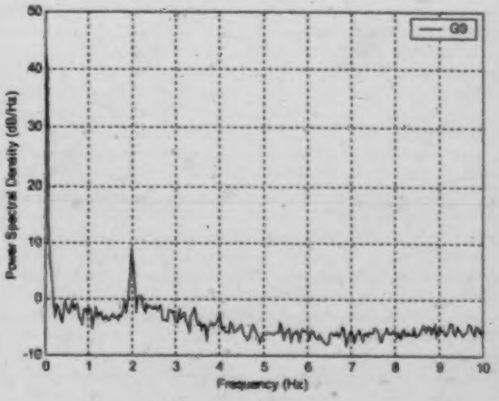

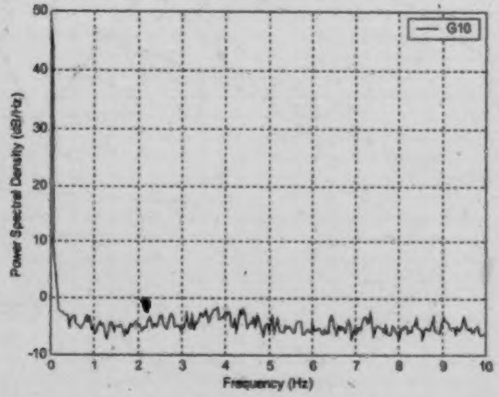

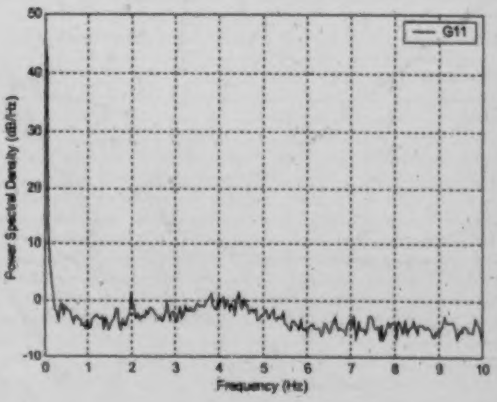

July 18, 1999
4:05 PM

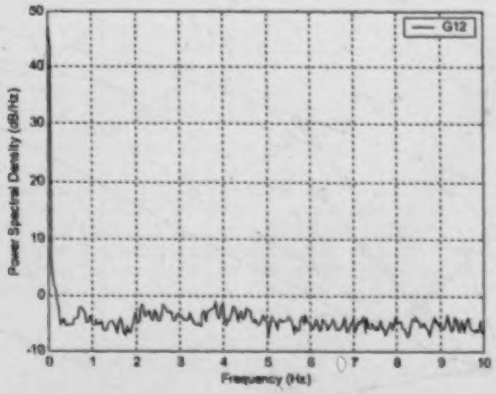

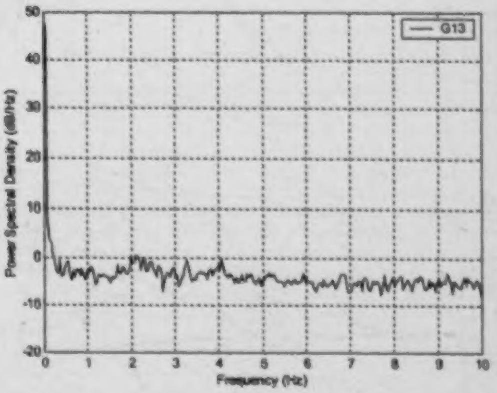

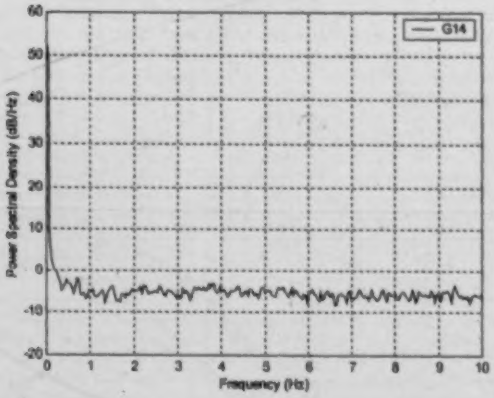

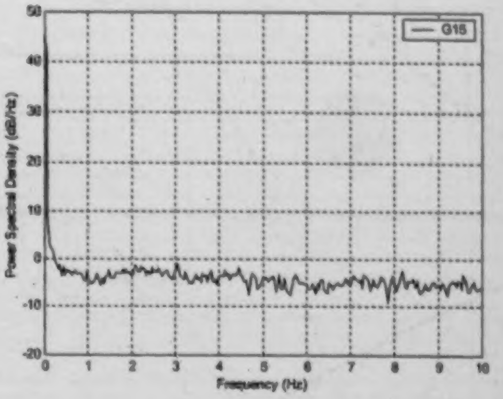

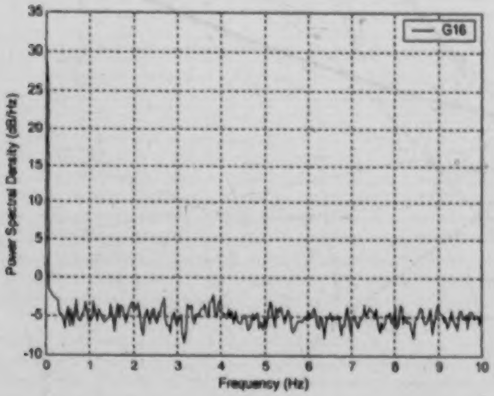

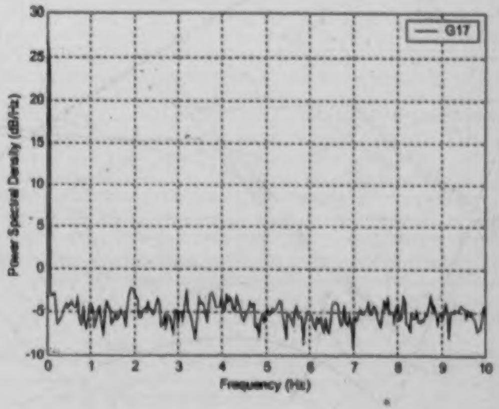

July 18, 1999
4:05 PM

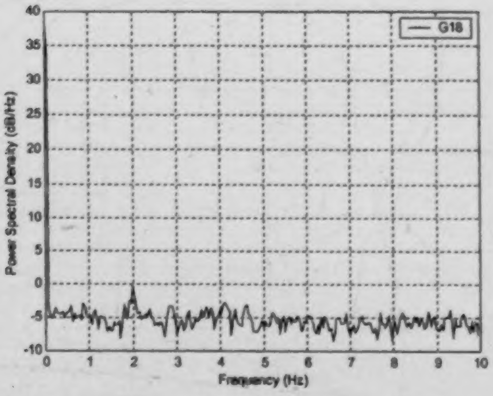

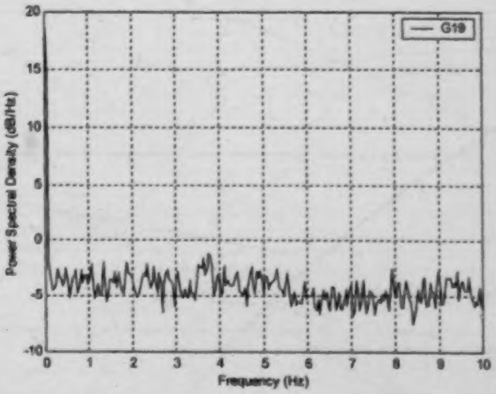

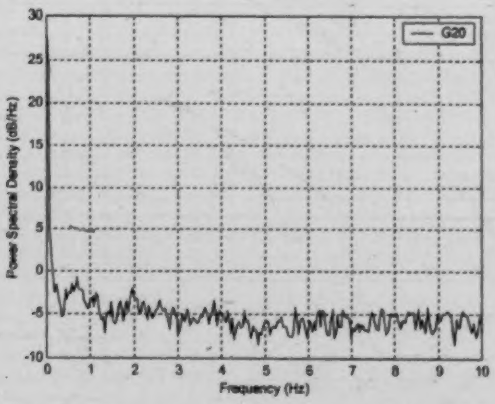

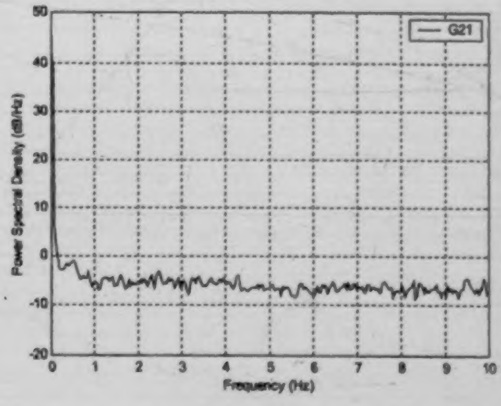

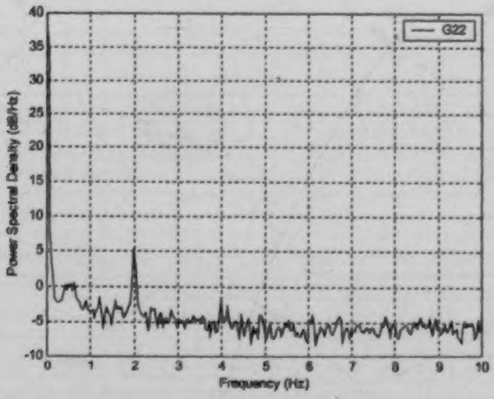

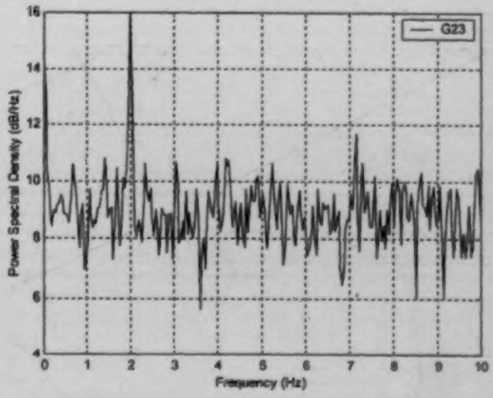

July 18, 1999
4:05 PM

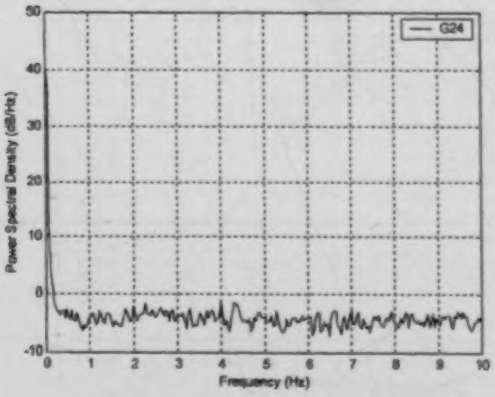

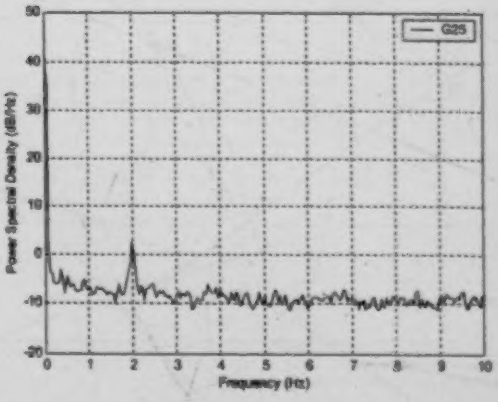

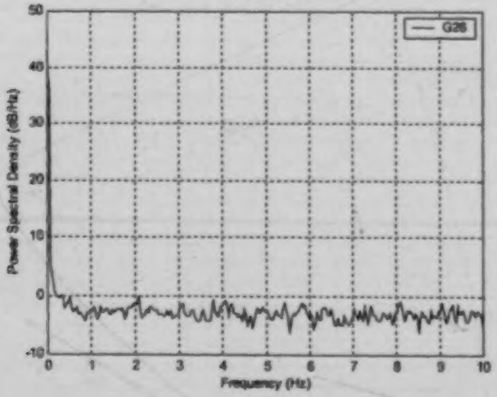

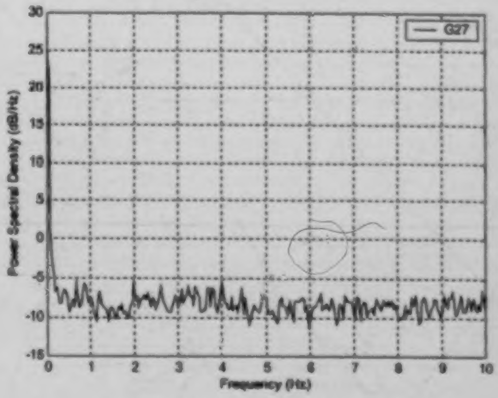

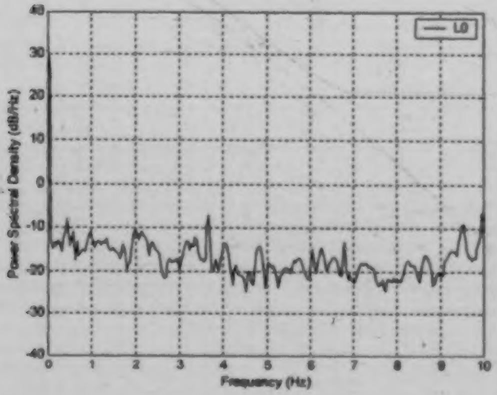

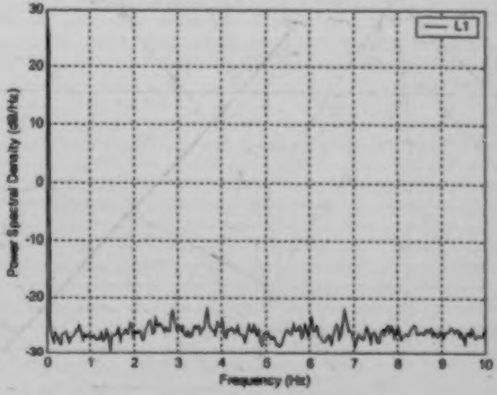

July 18, 1999
4:05 PM

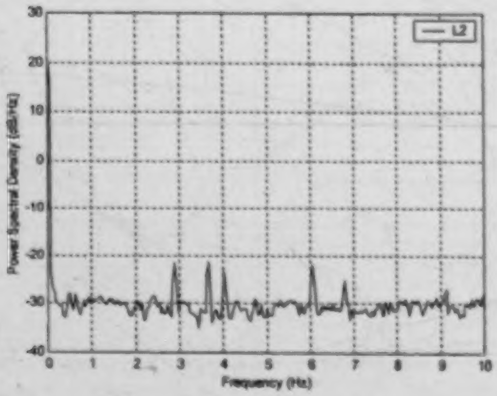

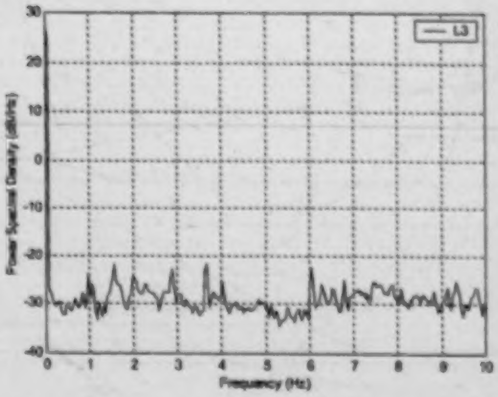

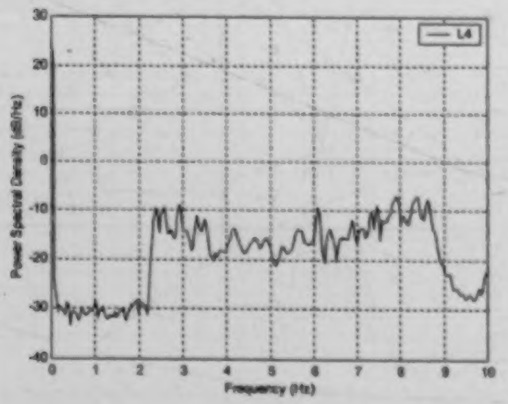

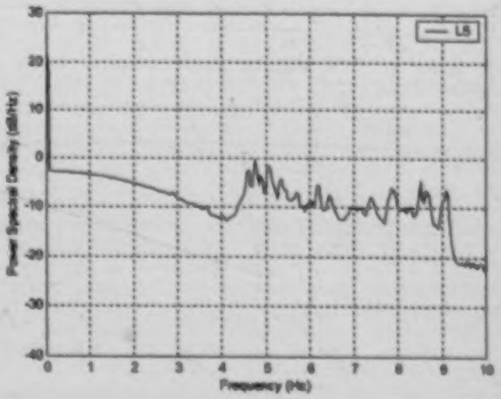

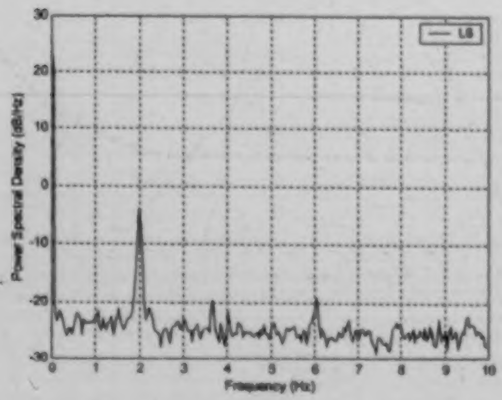

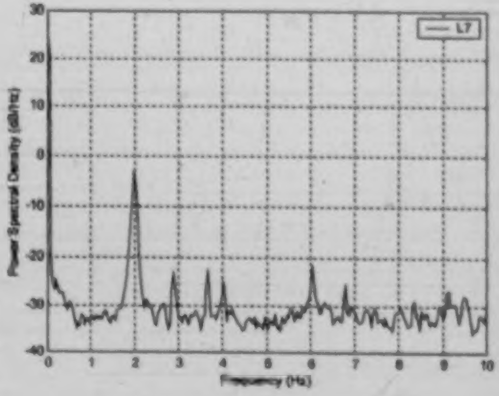

July 18, 1999
4:05 PM

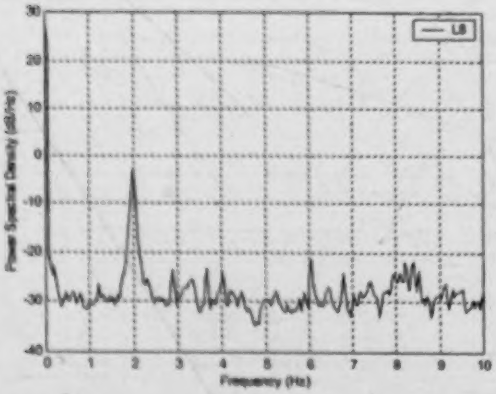

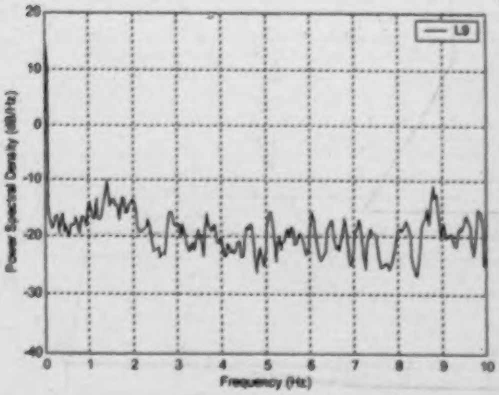

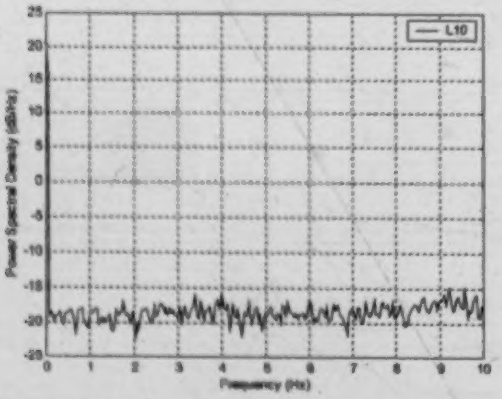

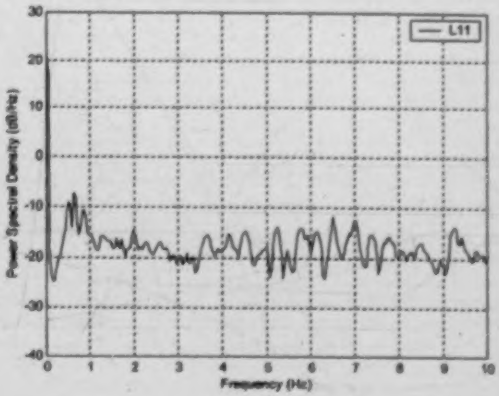

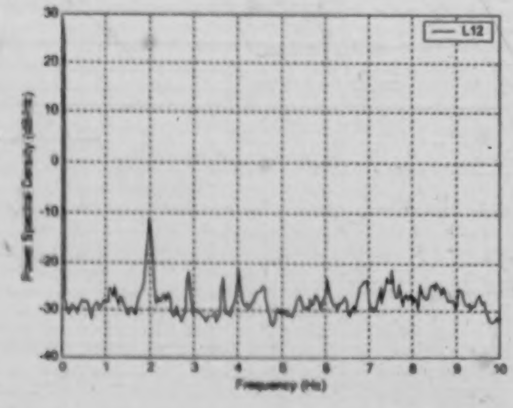

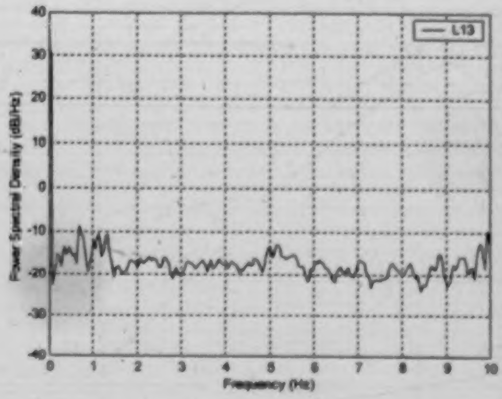

July 18, 1999
4:05 PM

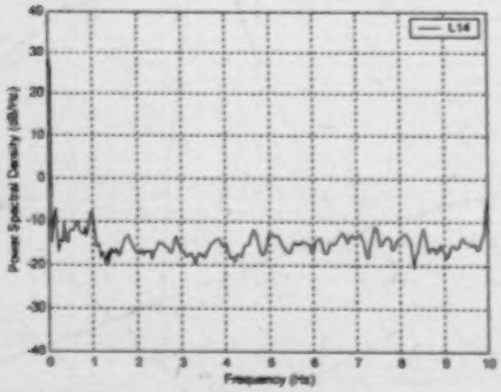

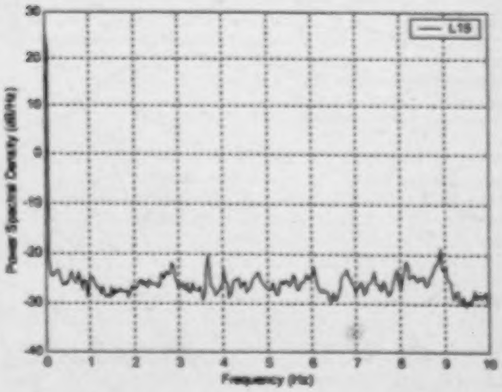

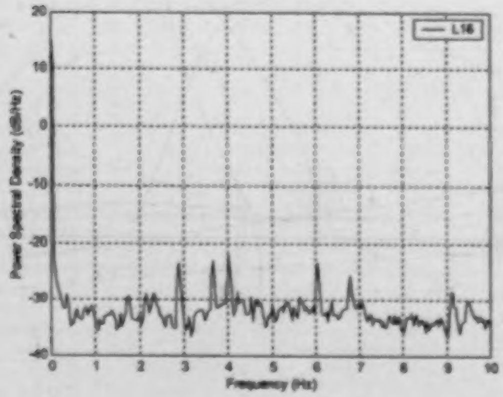

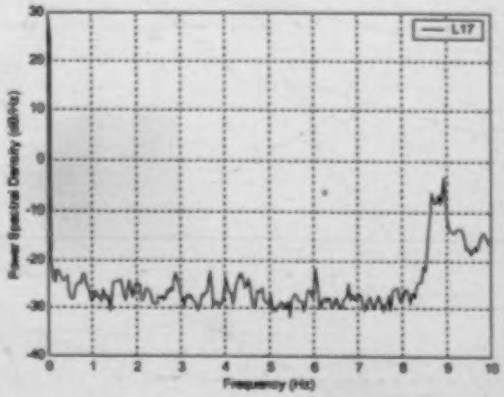

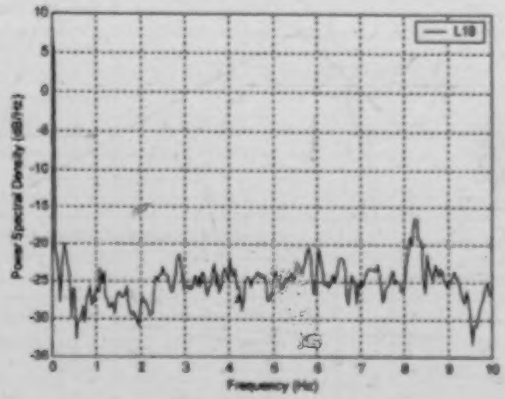

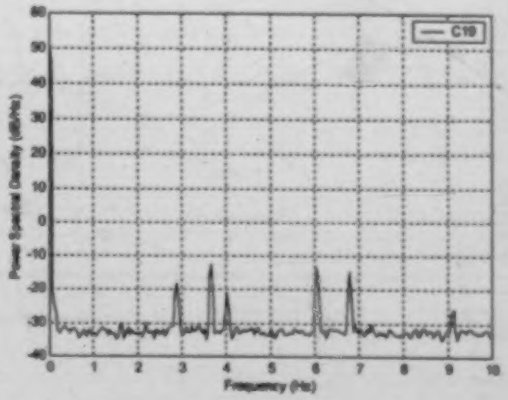

July 18, 1999
4:05 PM

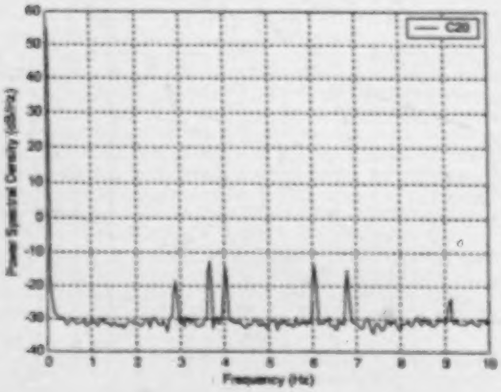

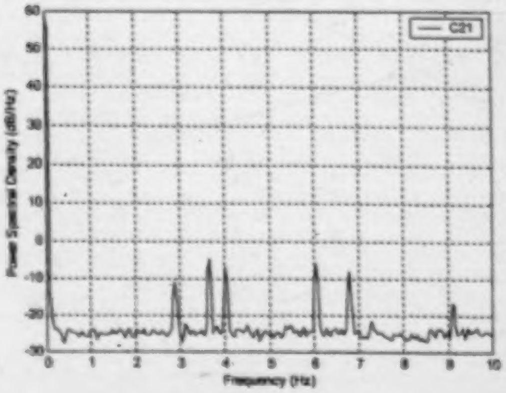

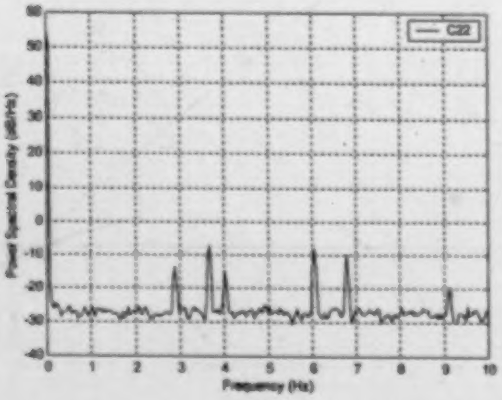

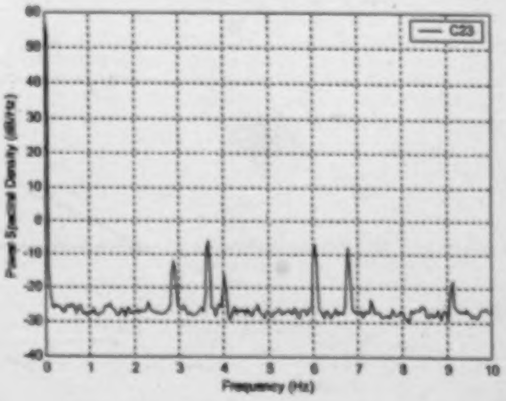

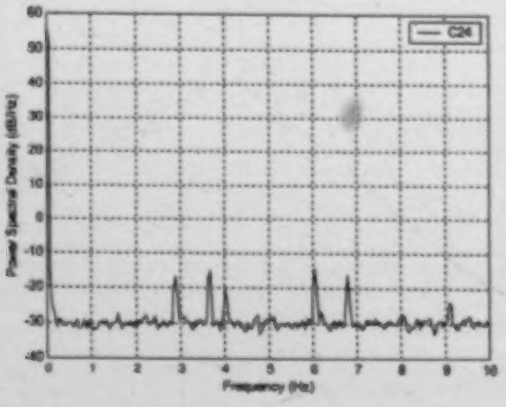

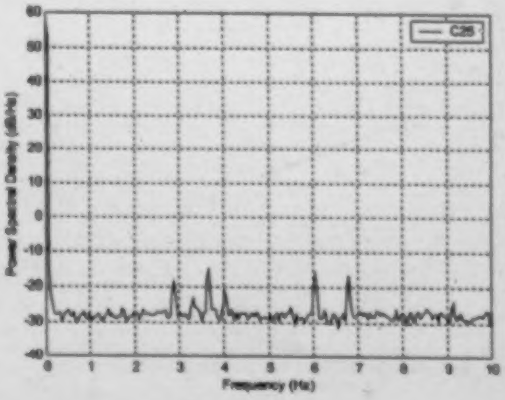

July 18, 1999
4:05 PM

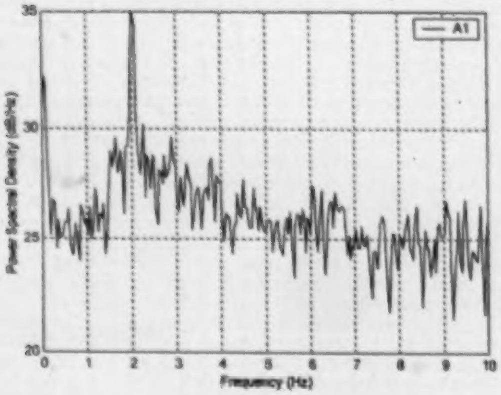

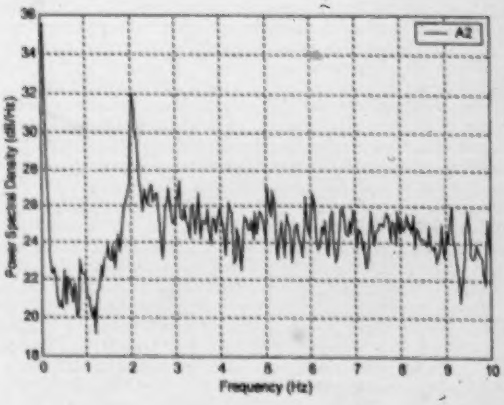

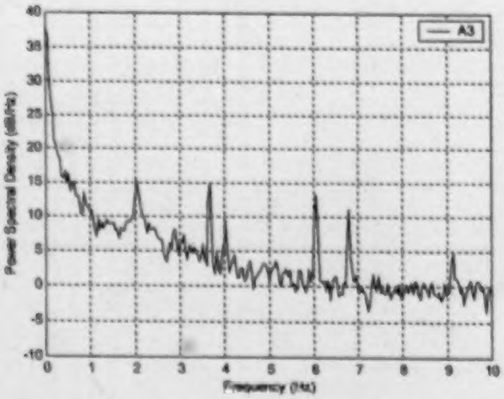

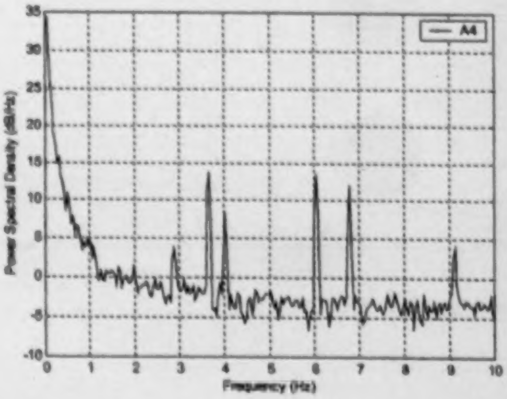

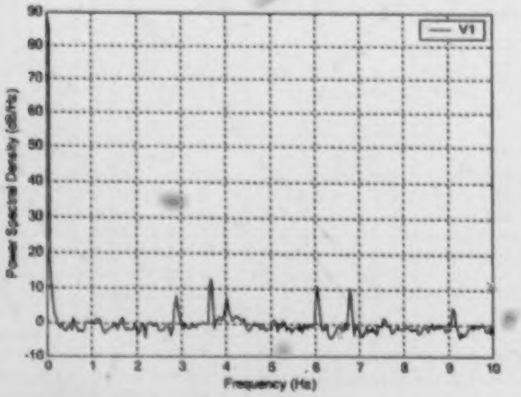

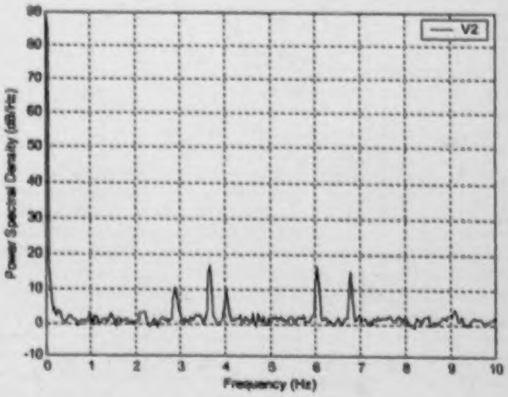

July 18, 1999
4:11 PM

July 18, 1999
4:11 PM

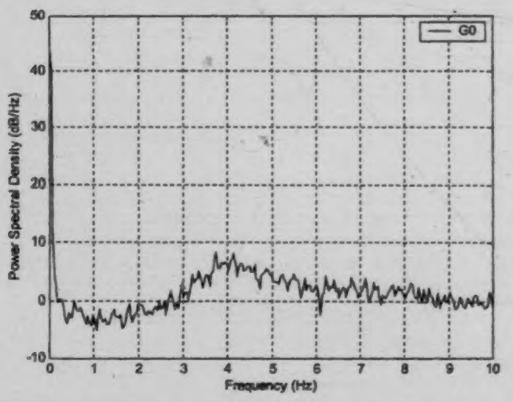

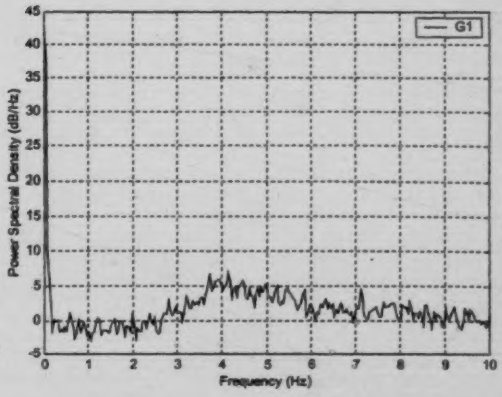

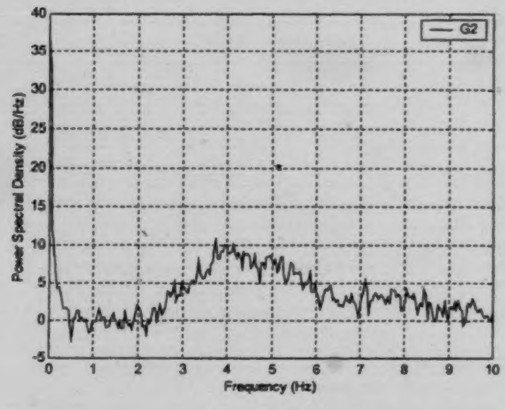

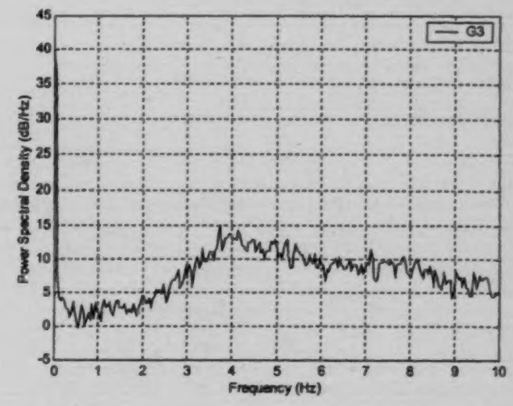

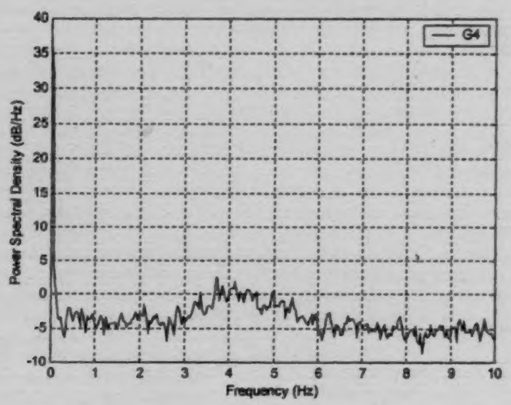

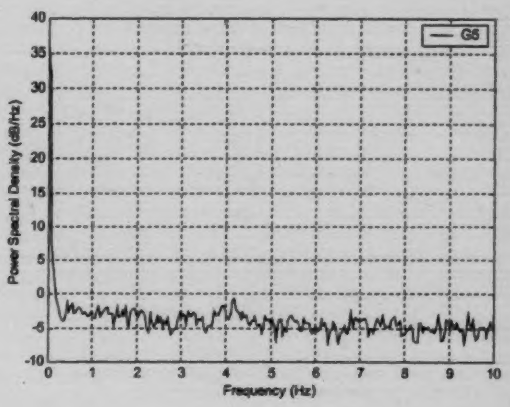

July 18, 1999
4:11 PM

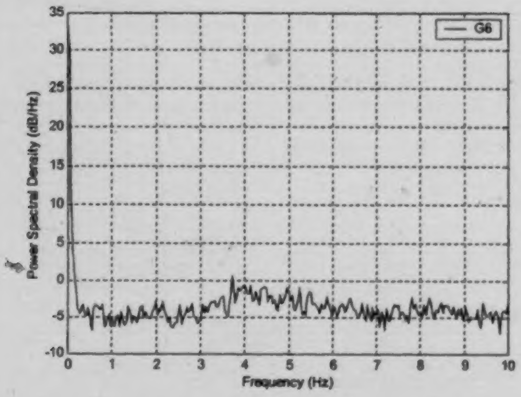

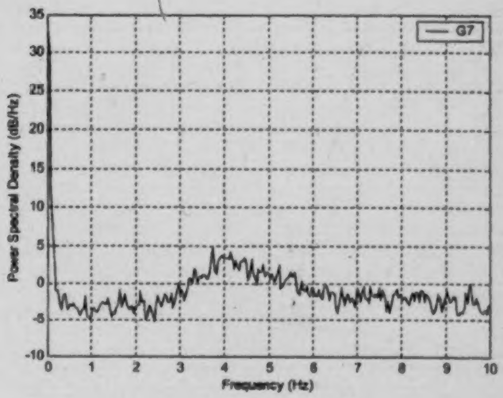

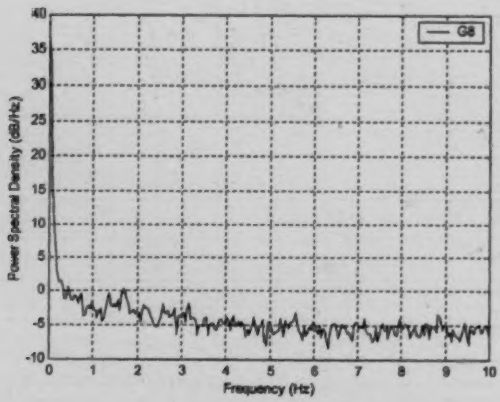

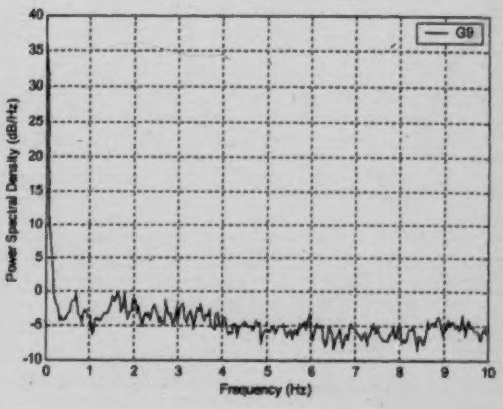

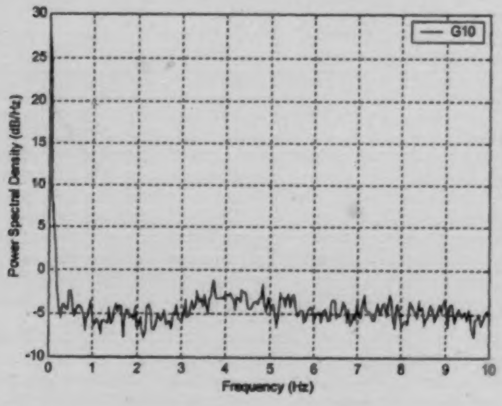

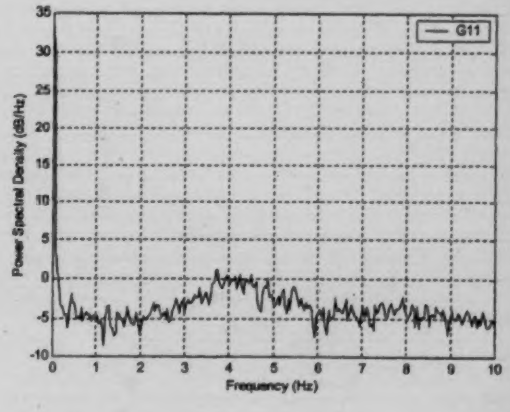

July 18, 1999
4:11 PM

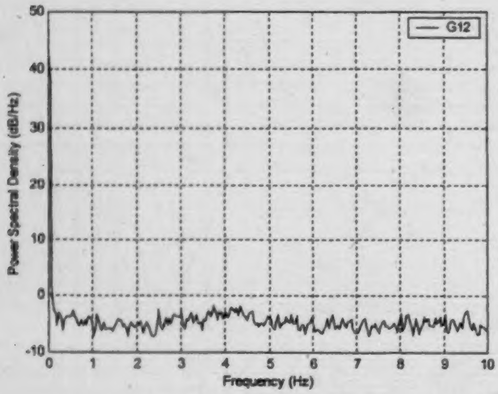

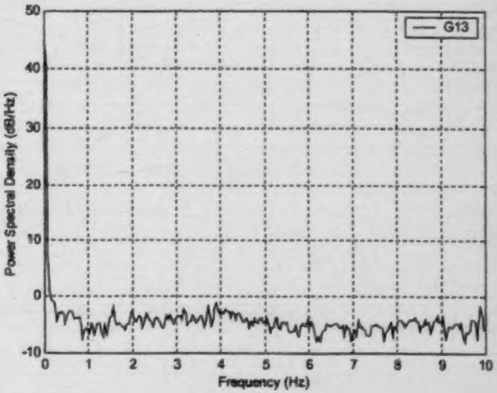

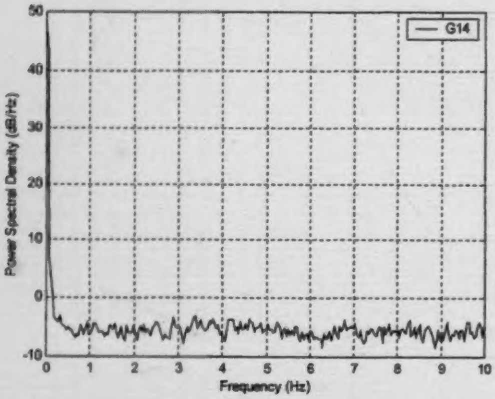

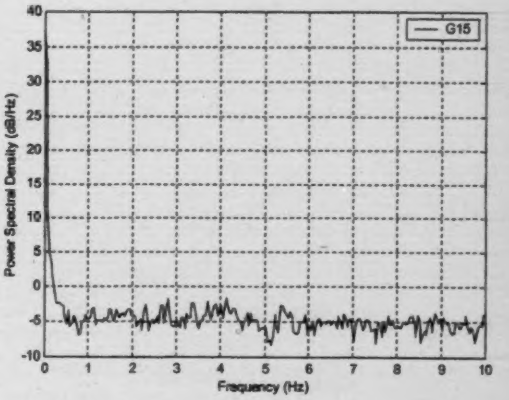

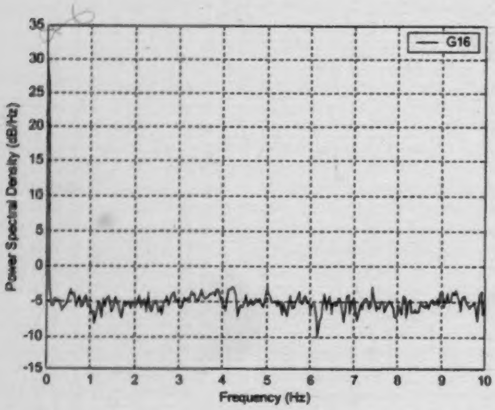

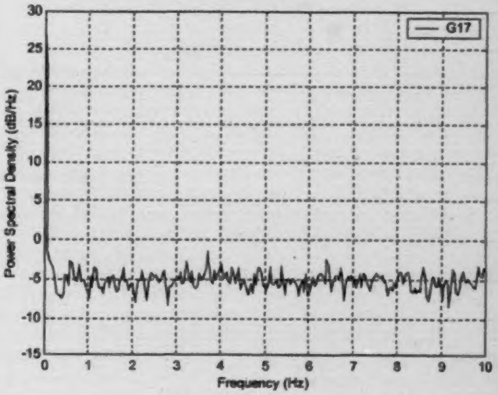

July 18, 1999
4:11 PM

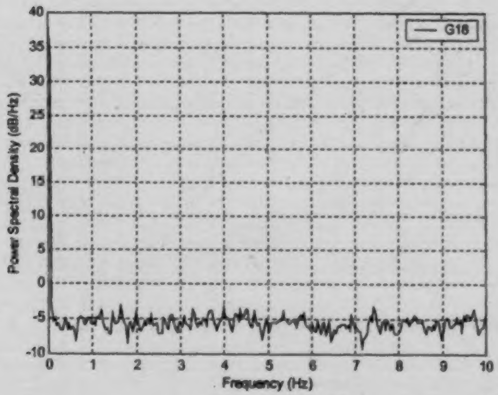

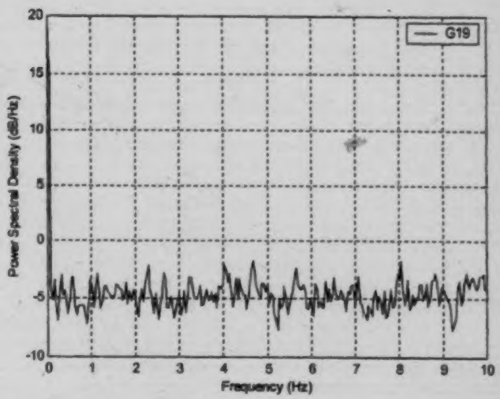

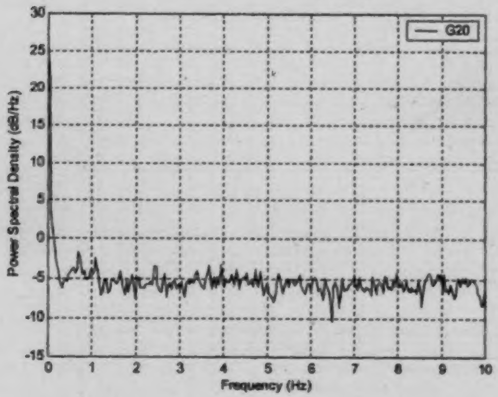

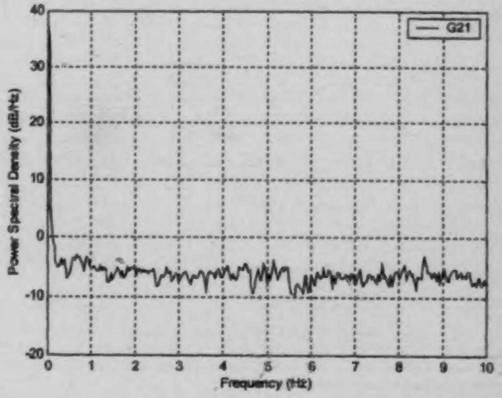

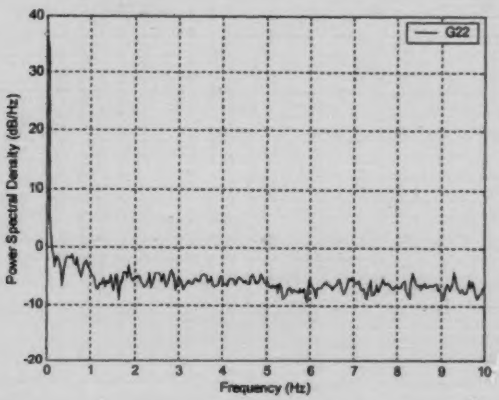

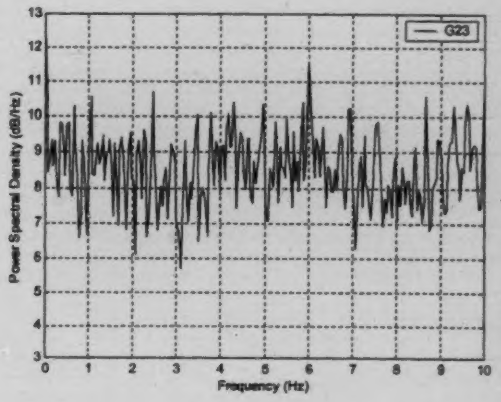

July 18, 1999
4:11 PM

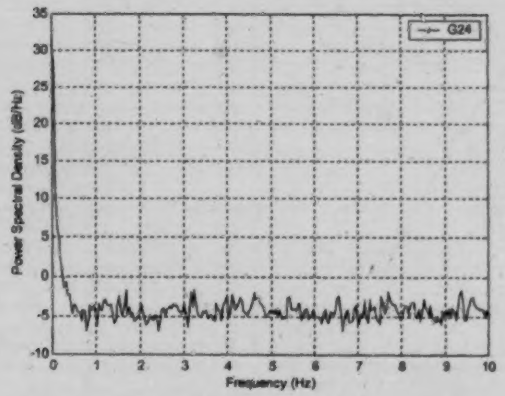

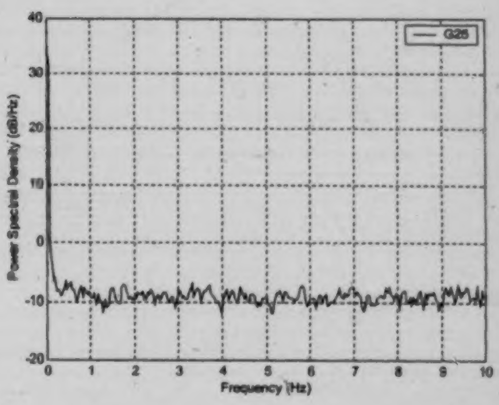

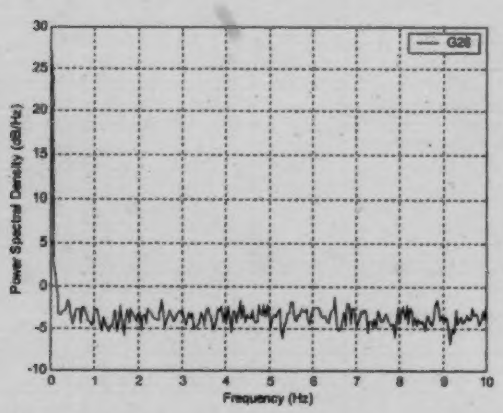

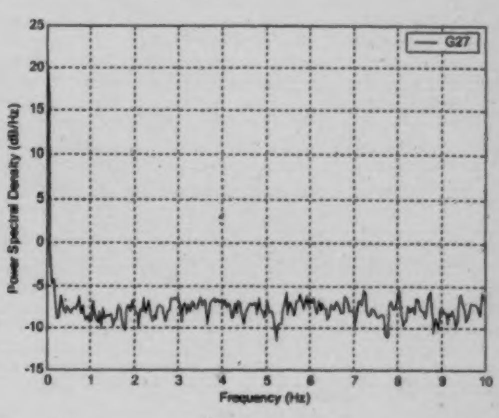

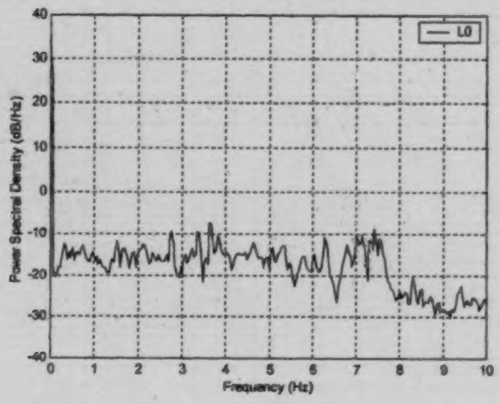

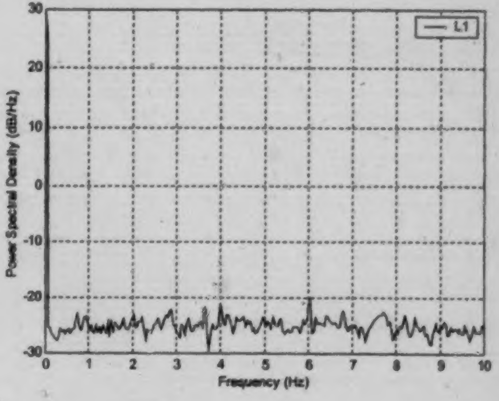

July 18, 1999
4:11 PM

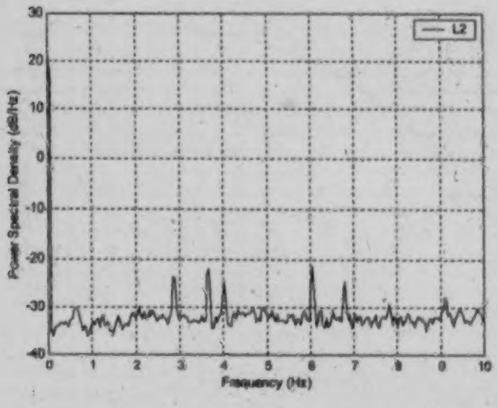

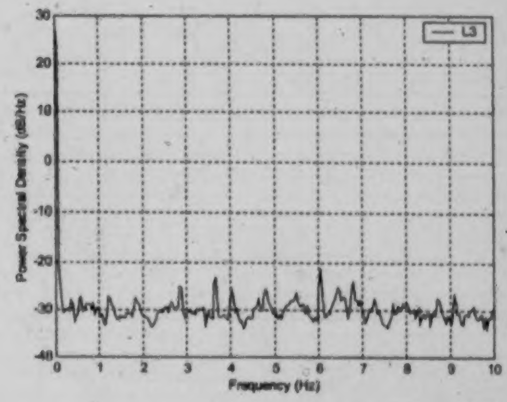

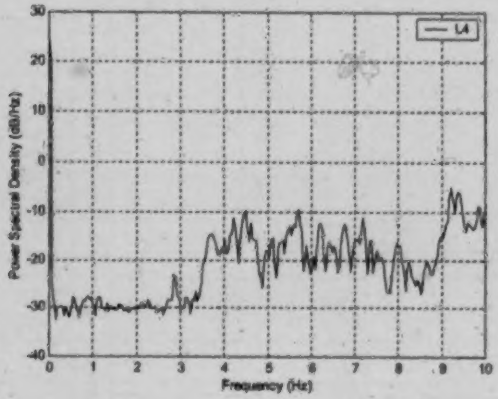

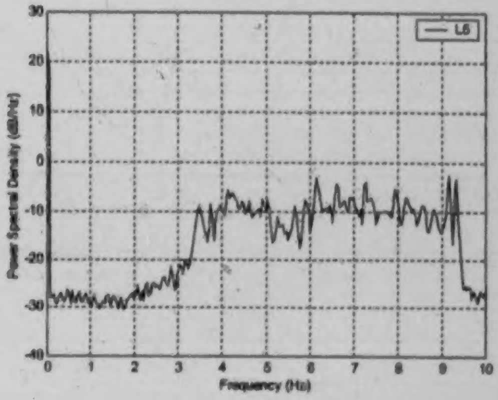

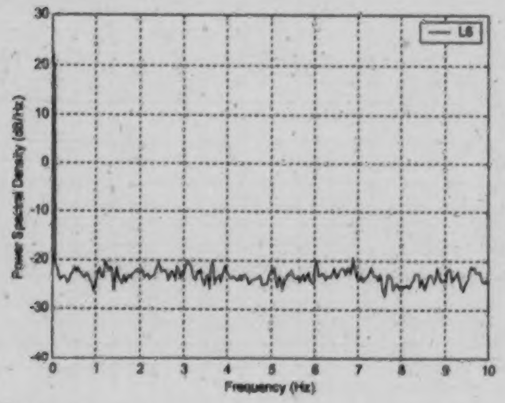

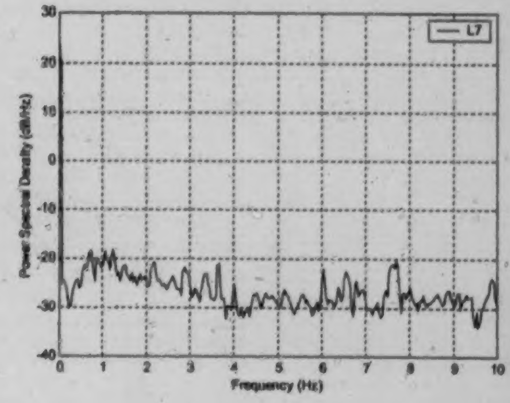

July 18, 1999
4:11 PM

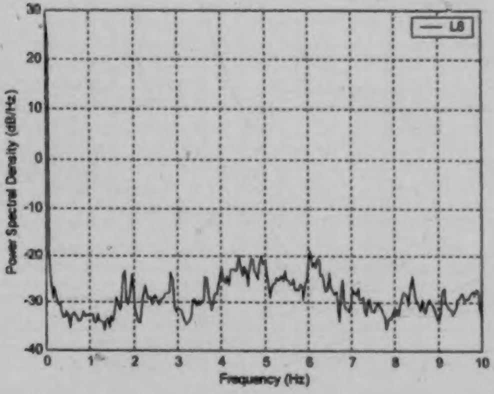

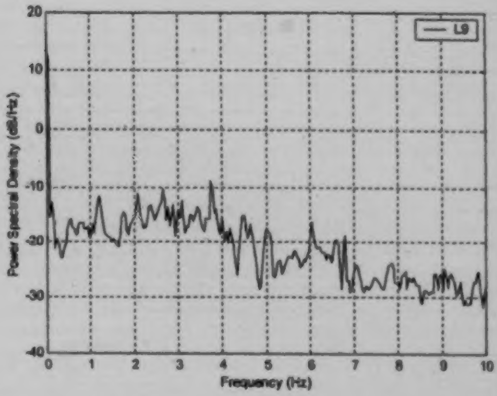

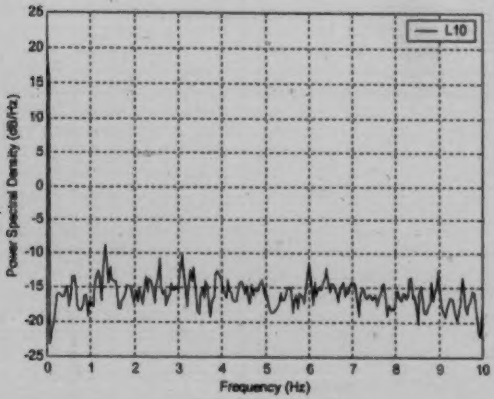

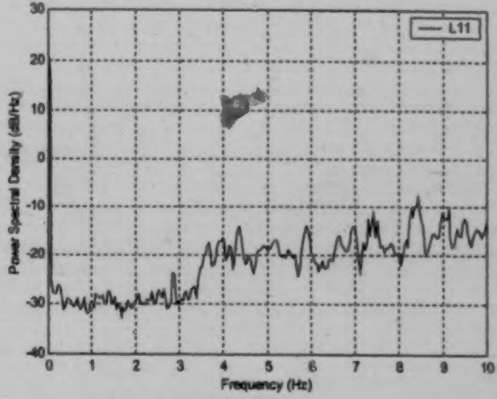

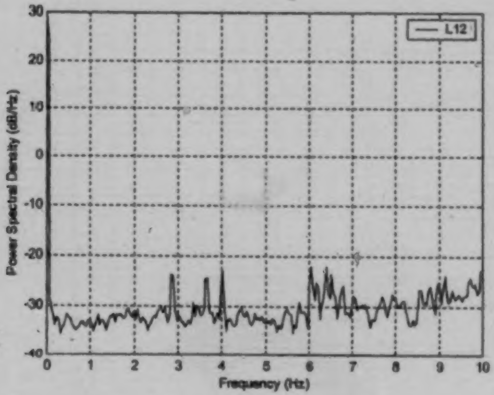

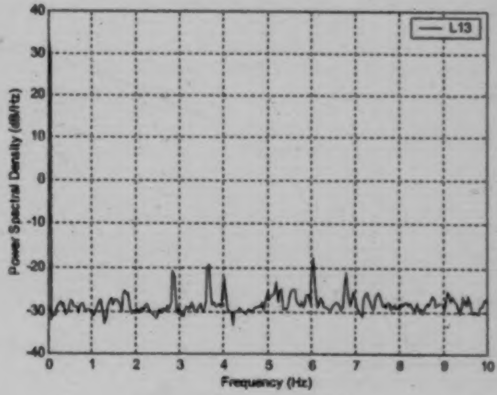

July 18, 1999
4:11 PM

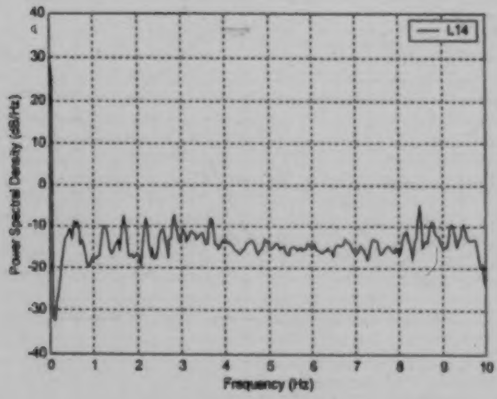

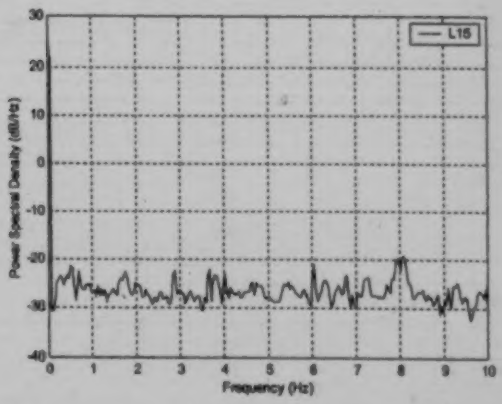

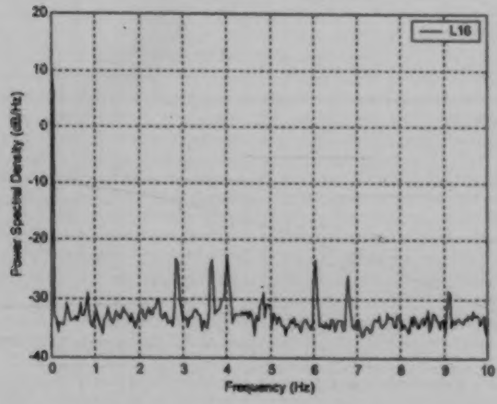

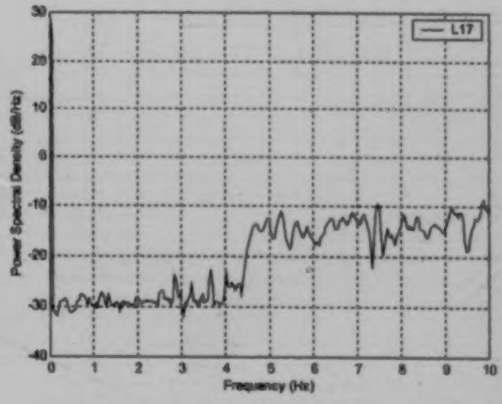

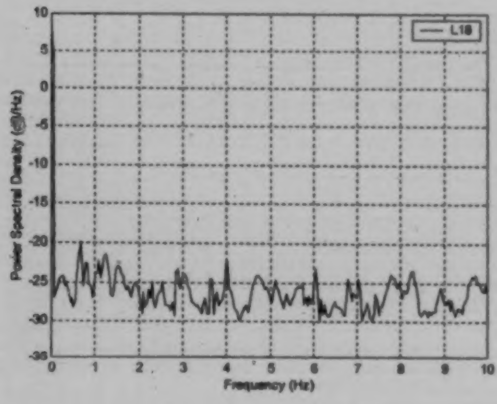

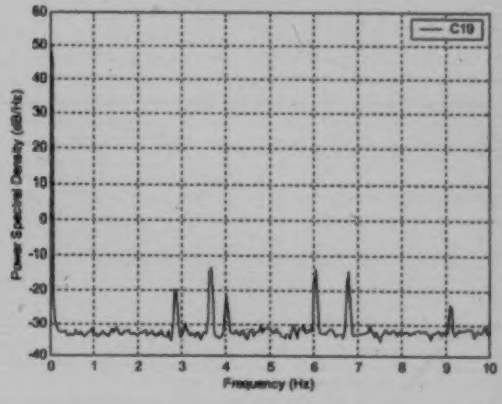

July 18, 1999
4:11 PM

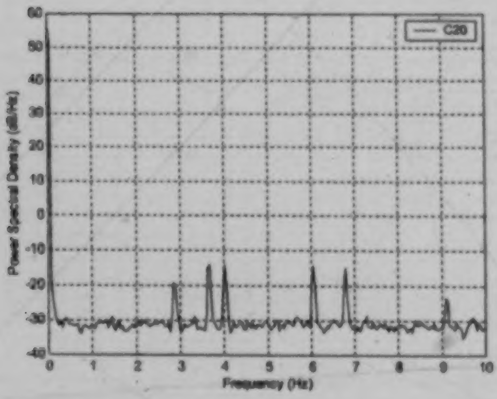

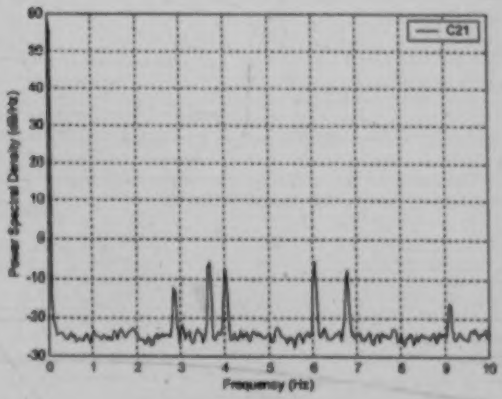

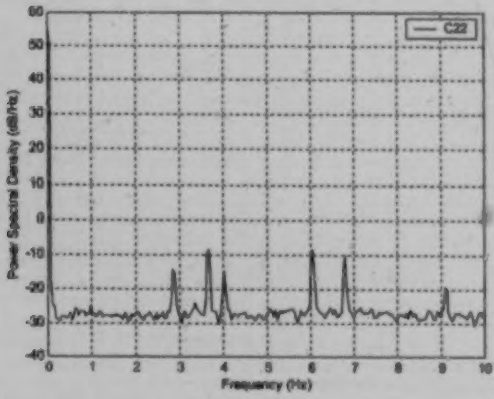

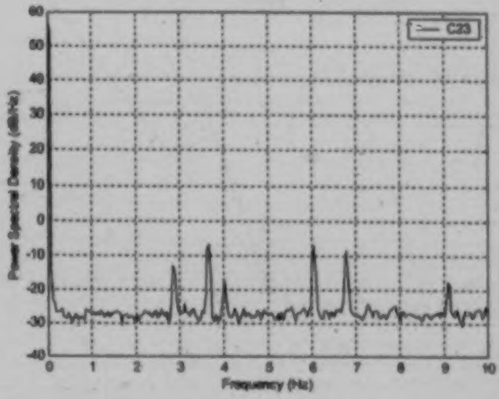

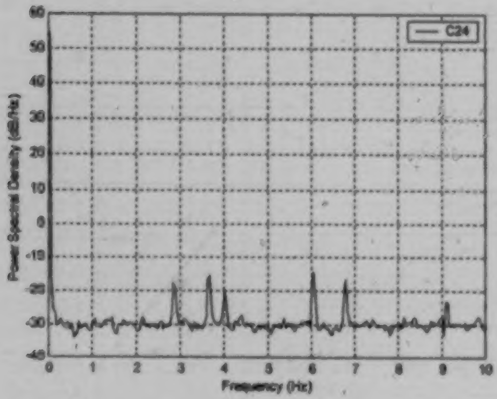

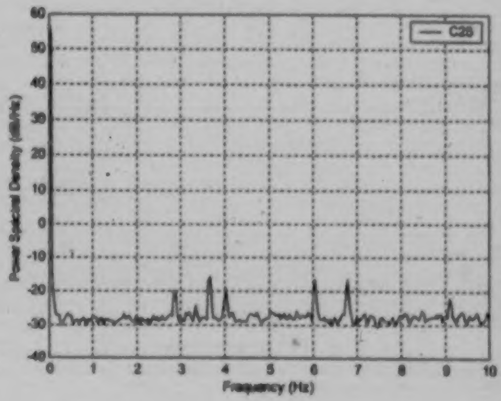

July 18, 1999
4:11 PM

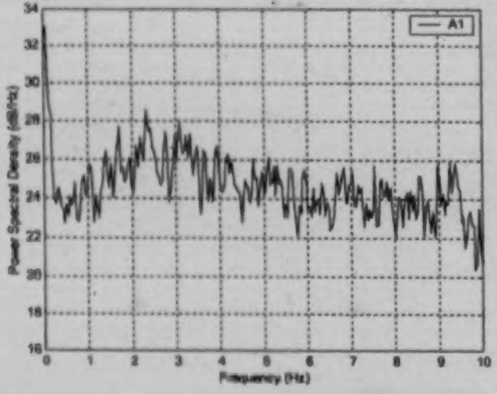

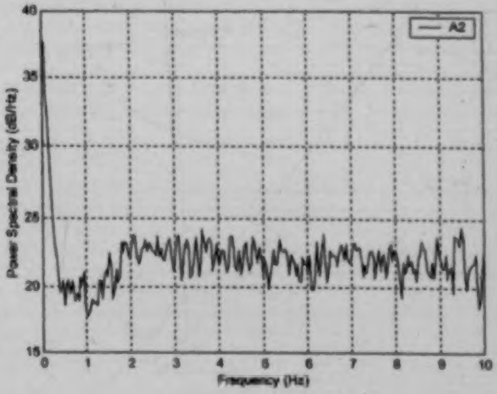

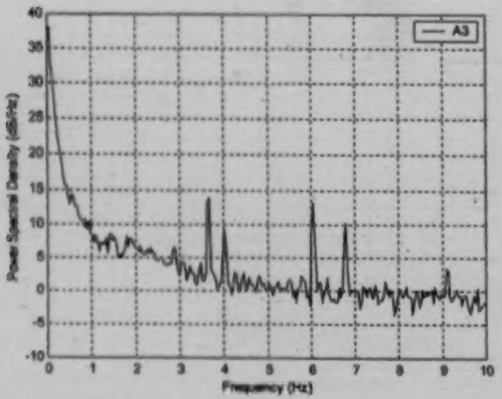

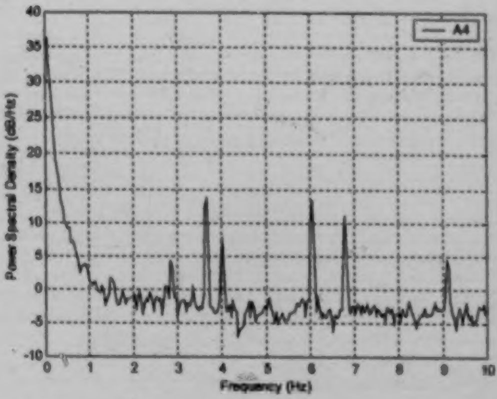

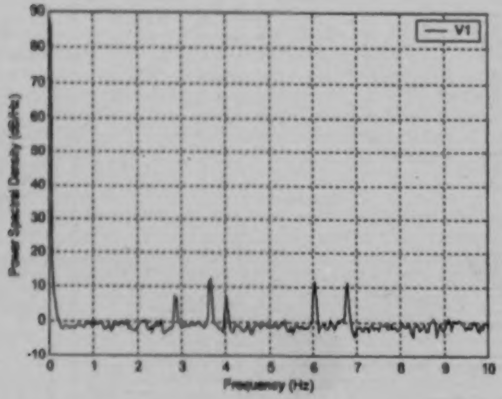

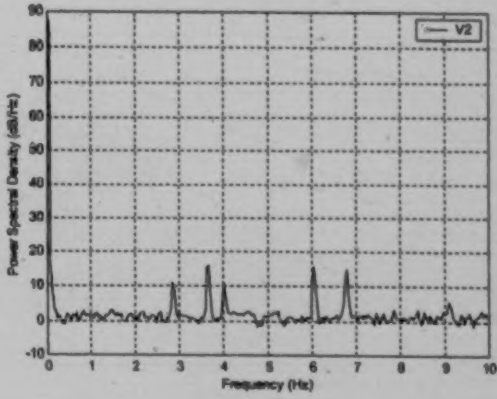

July 18, 1999
4:17 PM

July 18, 1999
4:17 PM

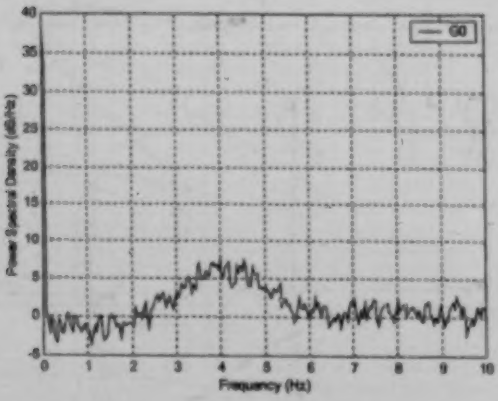

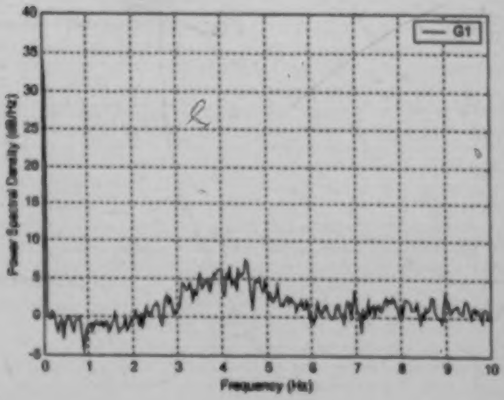

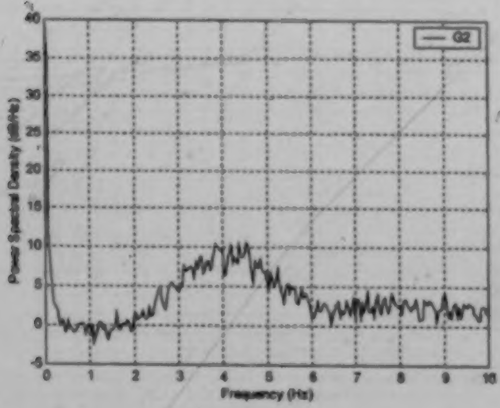

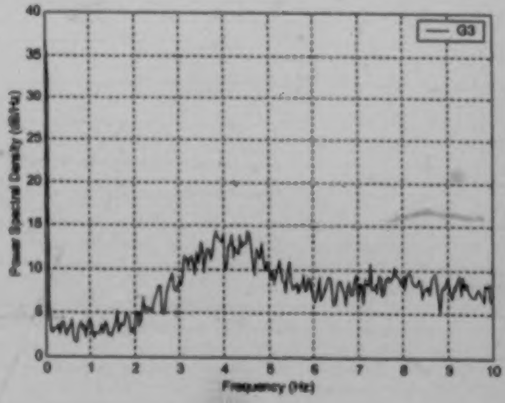

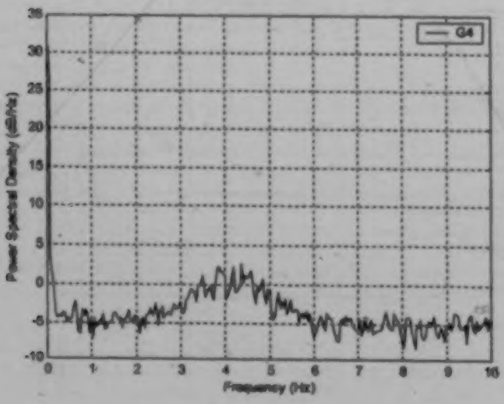

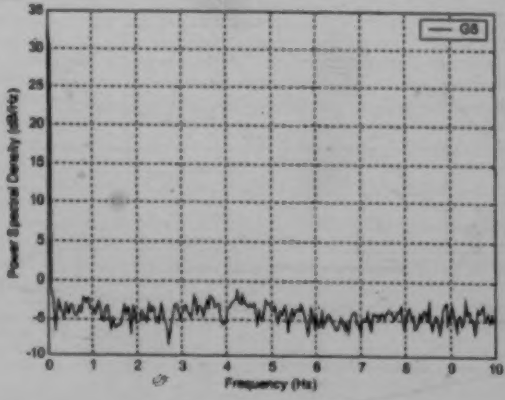

July 18, 1999
4:17 PM

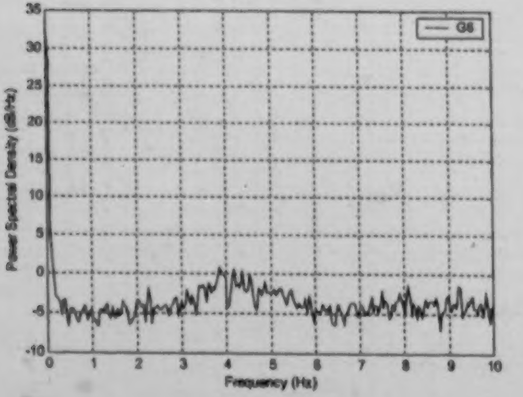

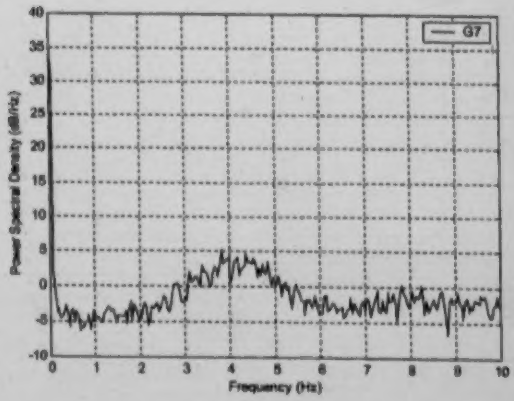

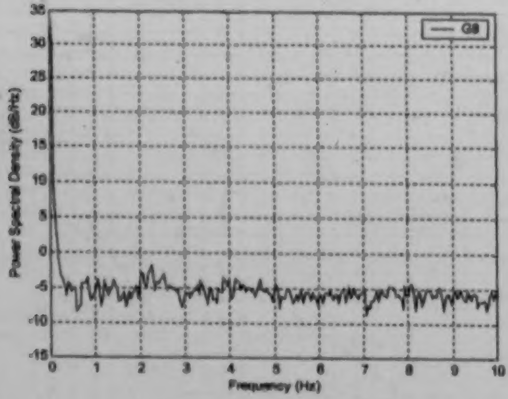

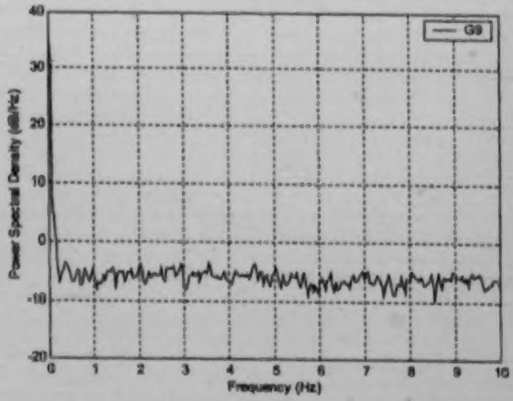

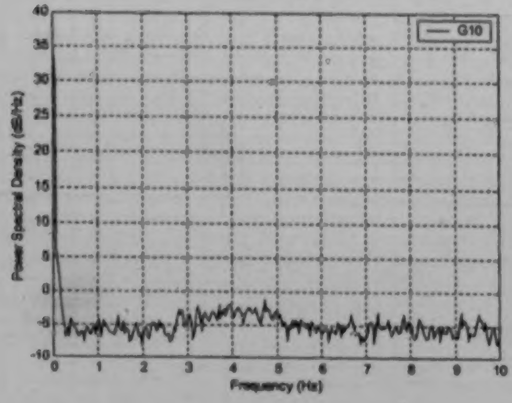

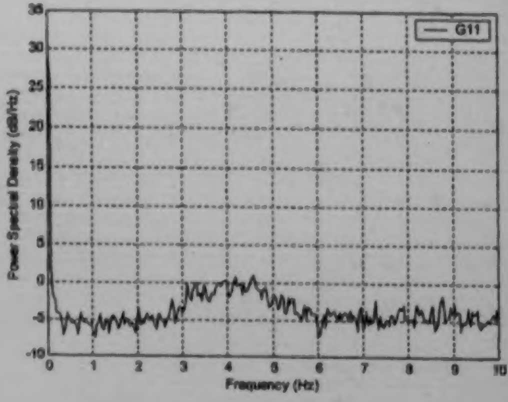

July 18, 1999
4:17 PM

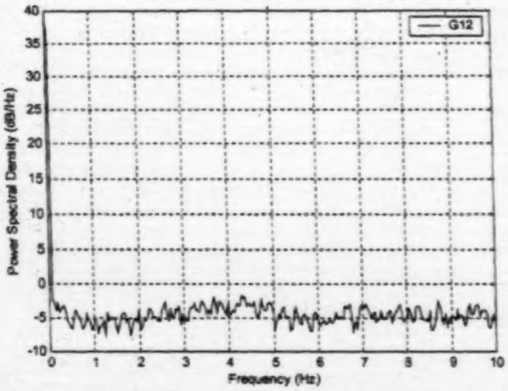

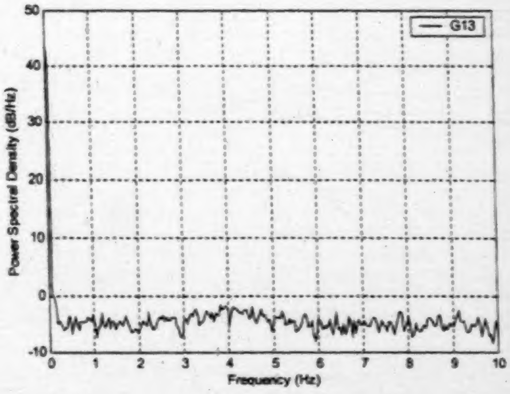

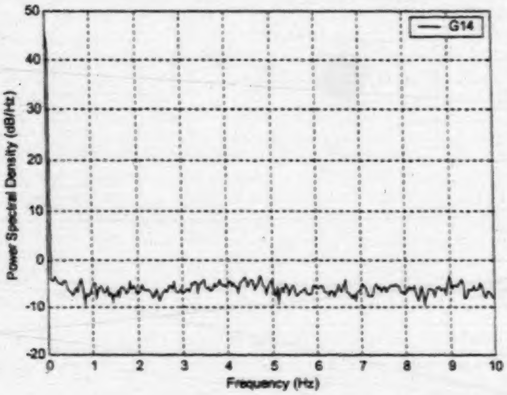

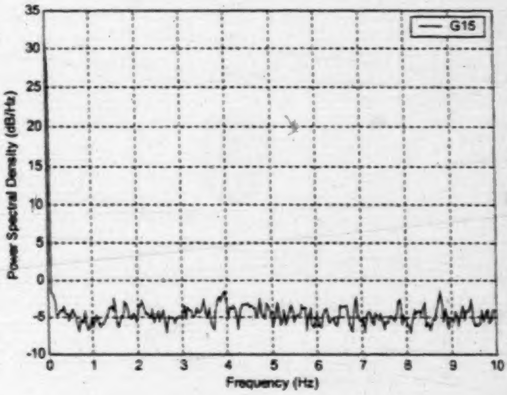

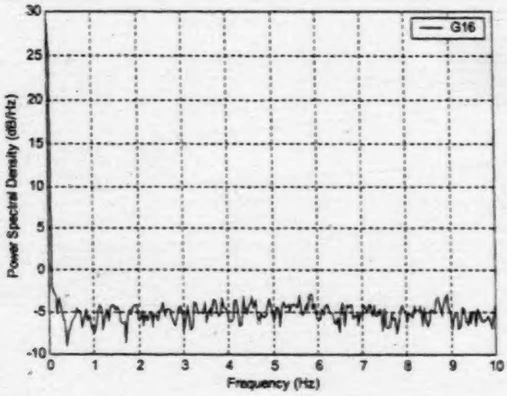

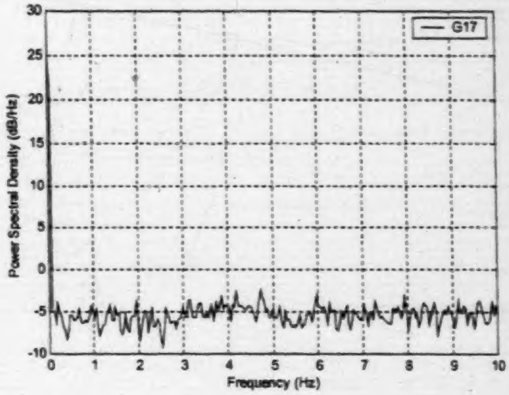

July 18, 1999
4:17 PM

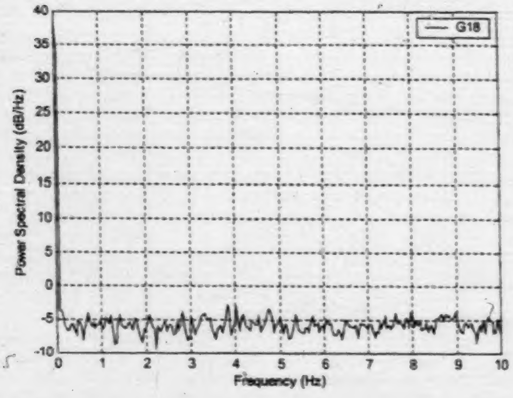

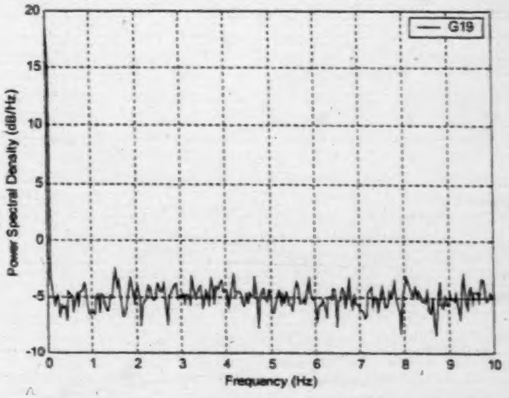

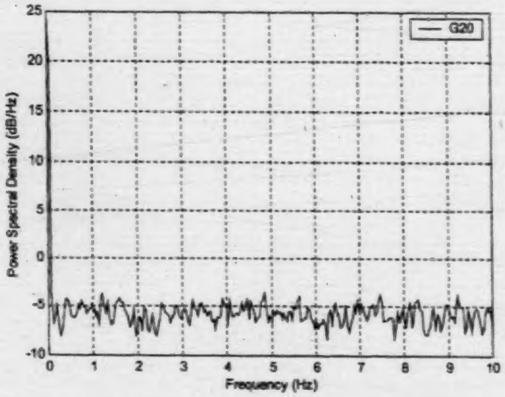

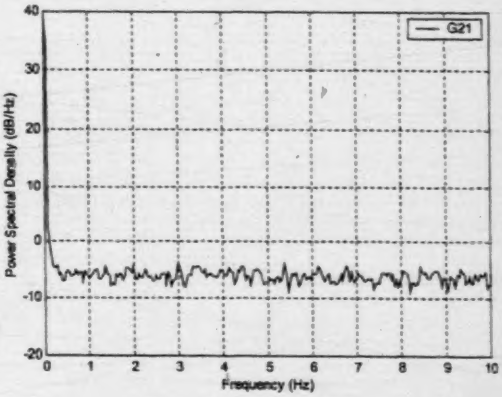

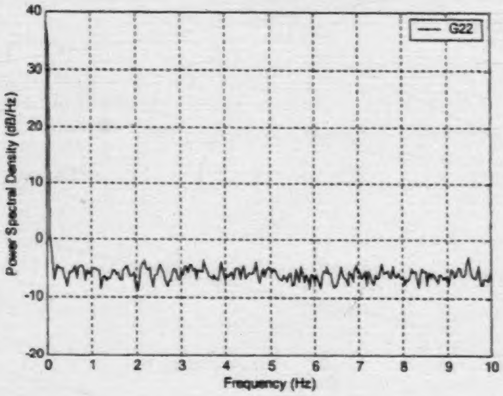

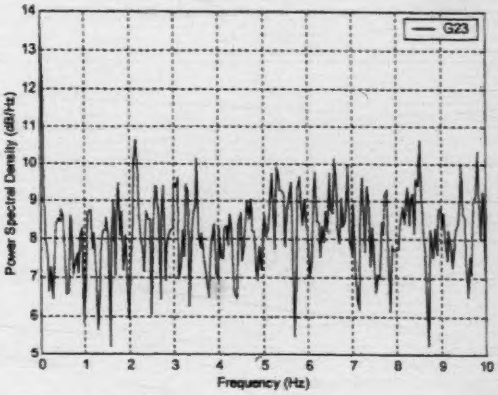

July 18, 1999
4:17 PM

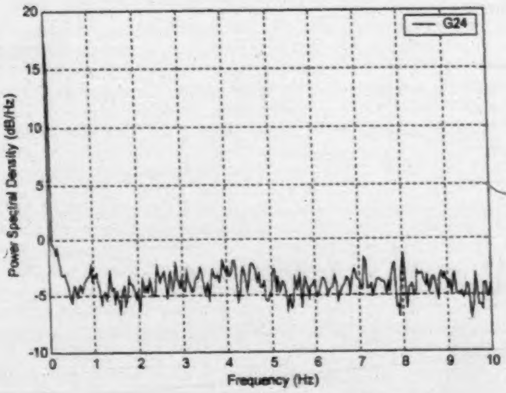

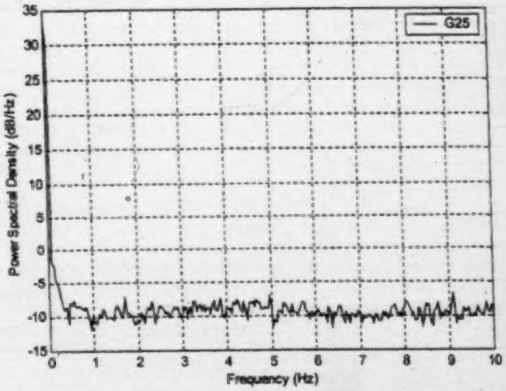

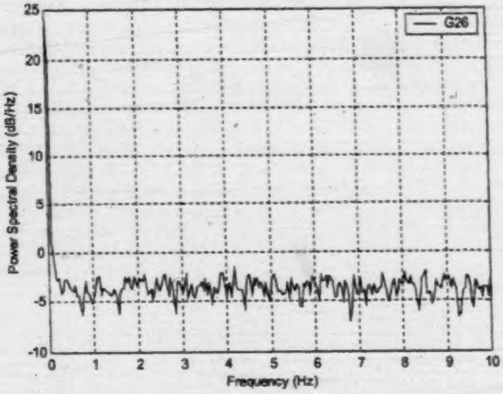

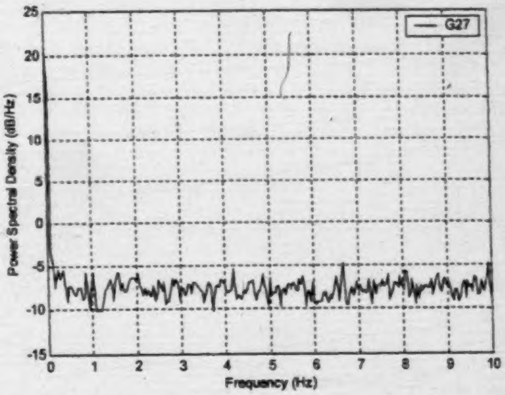

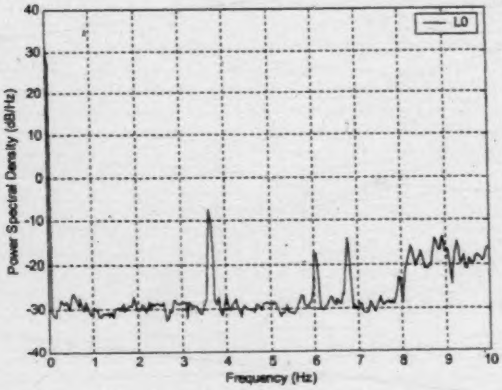

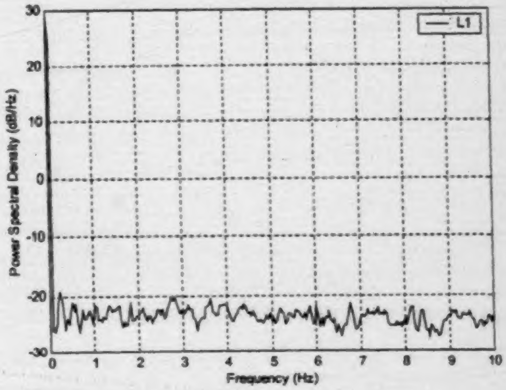

July 18, 1999
4:17 PM

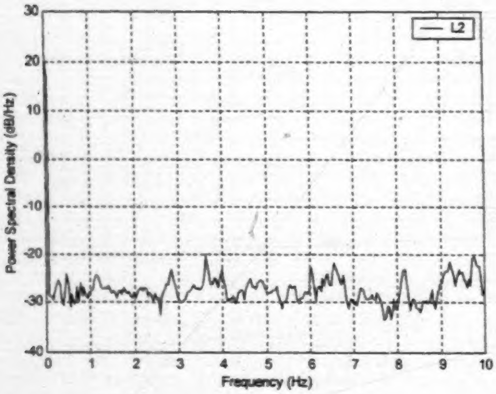

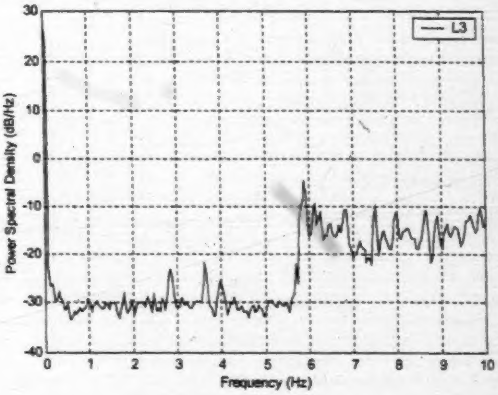

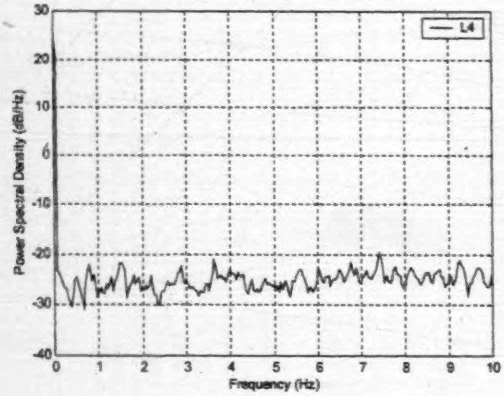

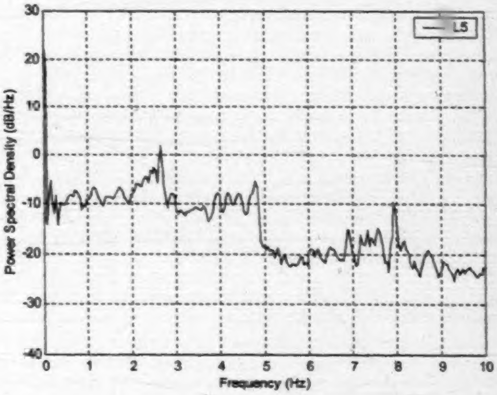

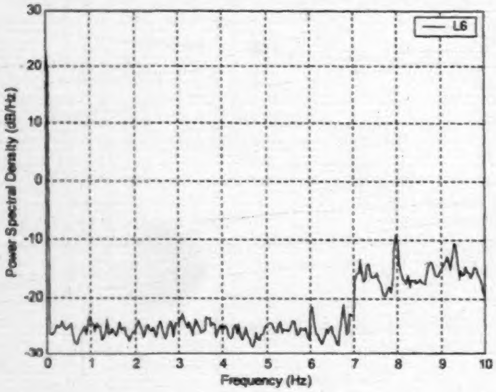

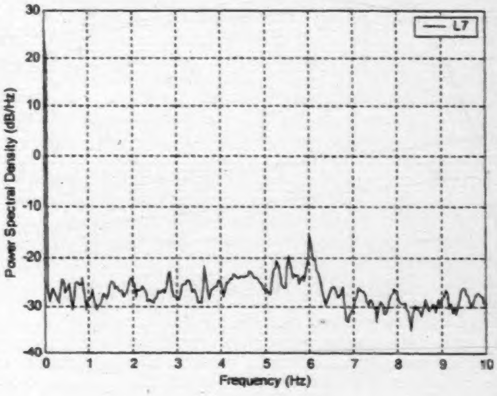

July 18, 1999
4:17 PM

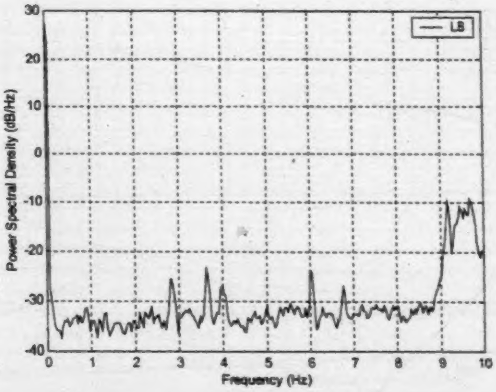

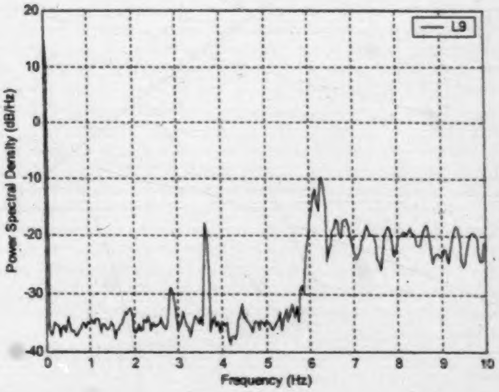

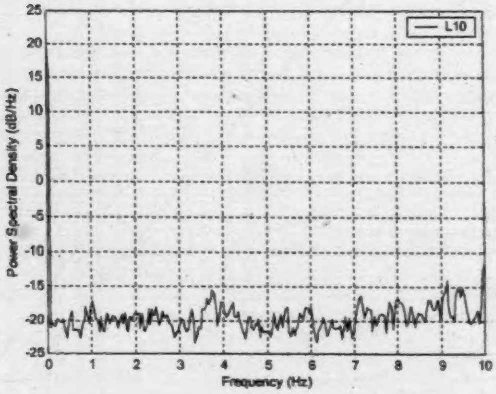

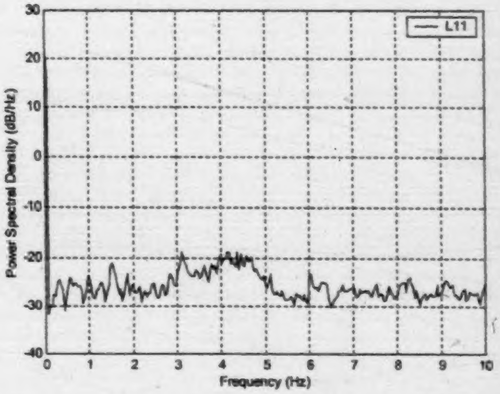

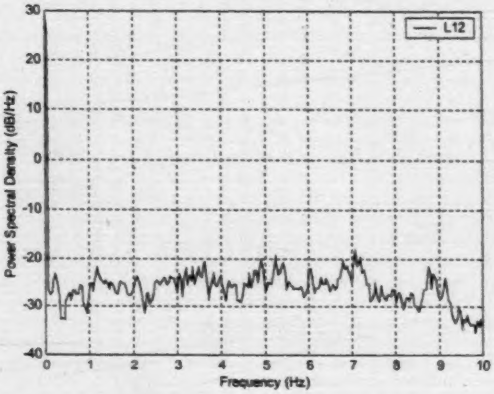

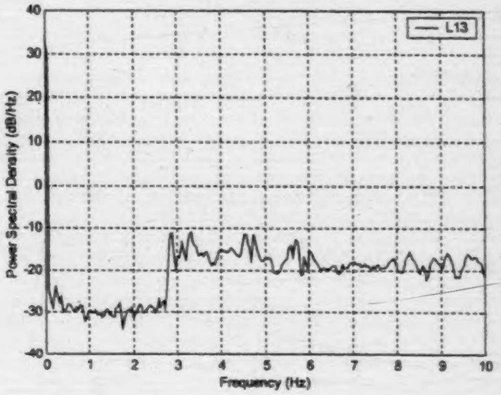

July 18, 1999
4:17 PM

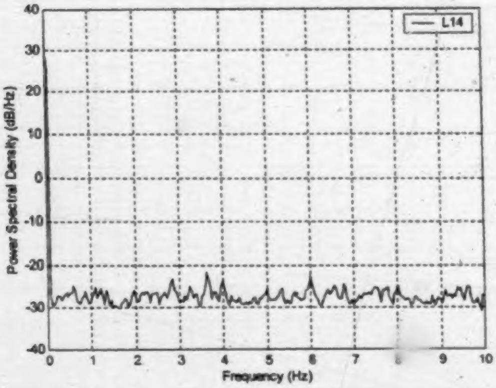

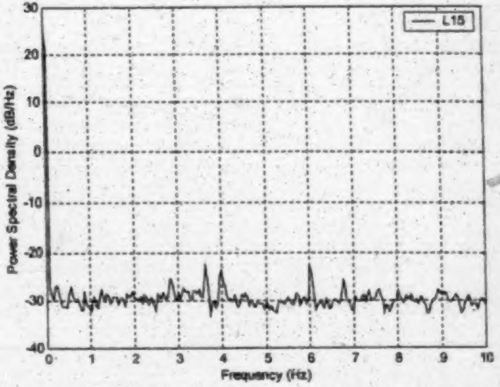

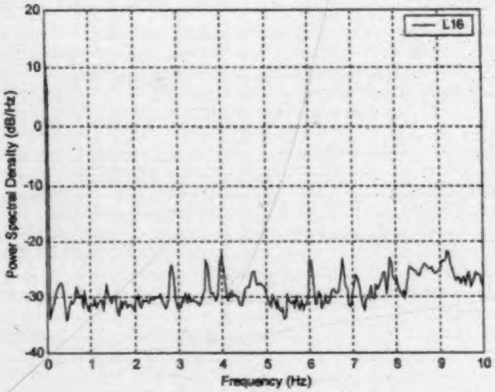

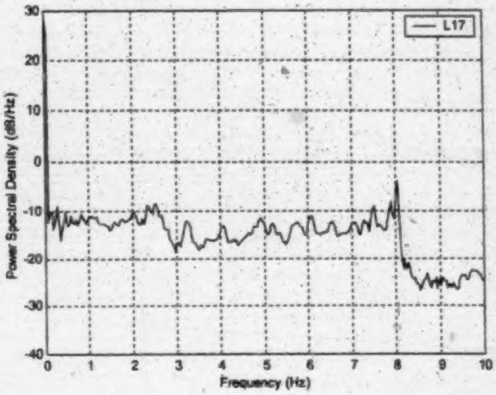

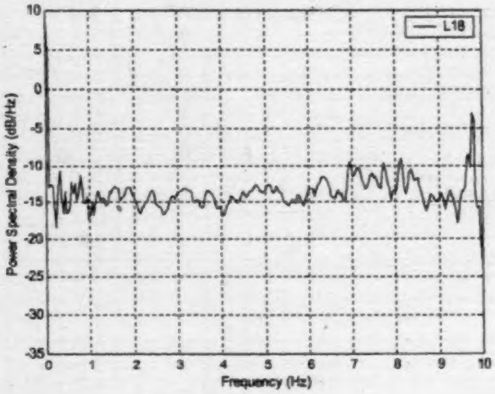

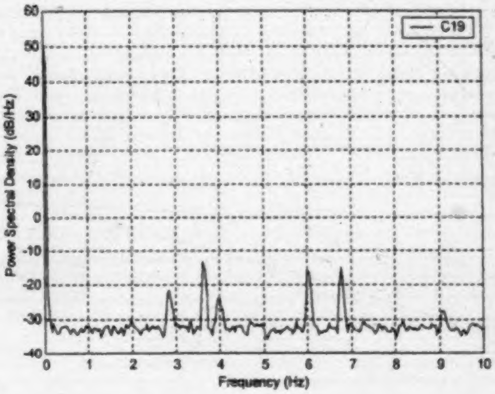

July 18, 1999
4:17 PM

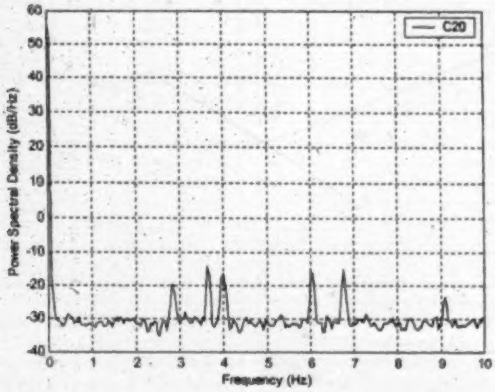

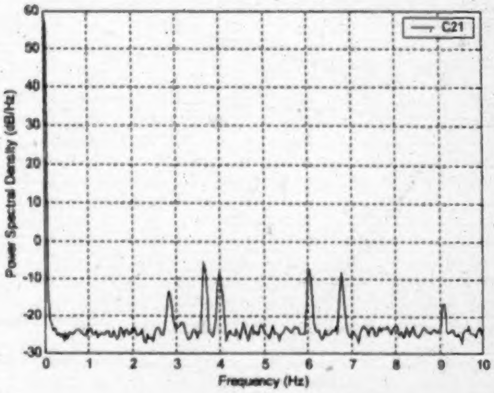

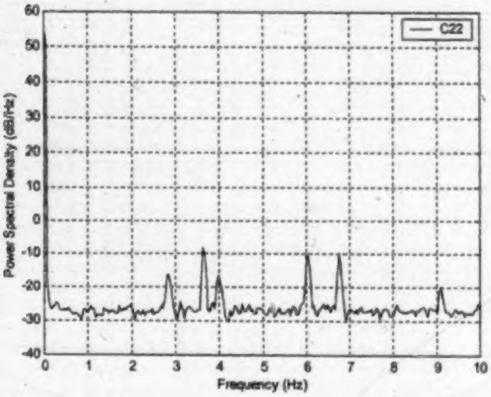

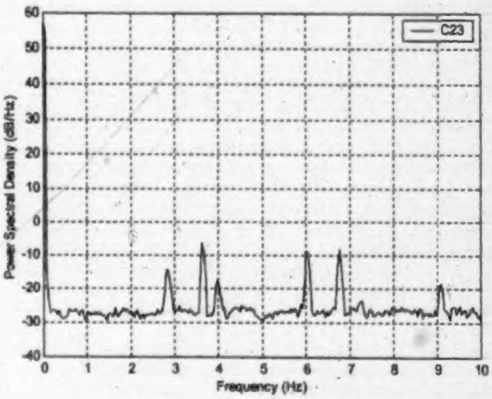

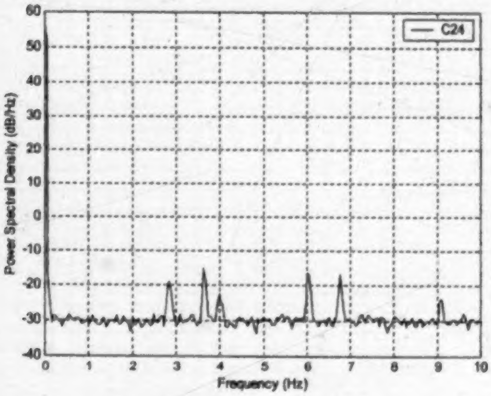

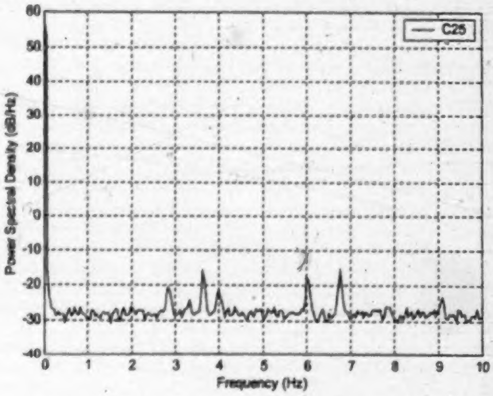

July 18, 1999
4:17 PM

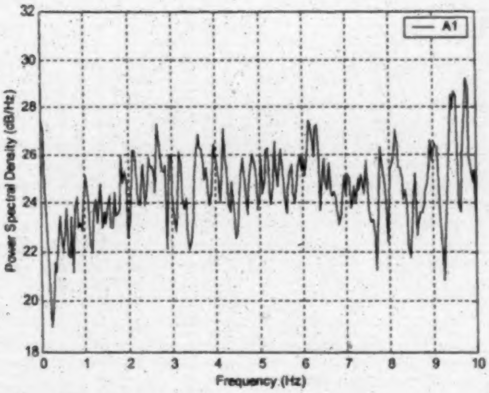

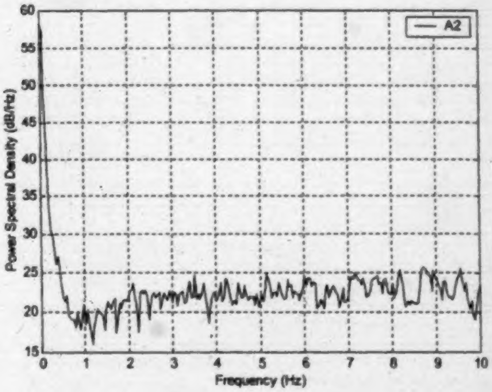

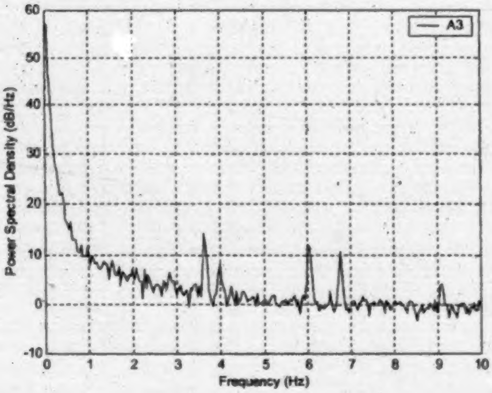

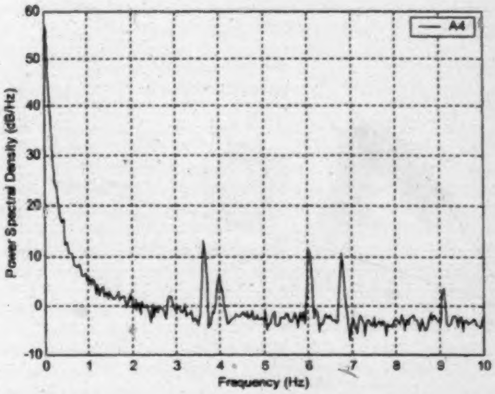

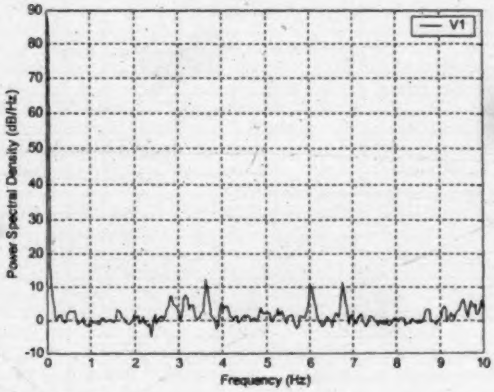

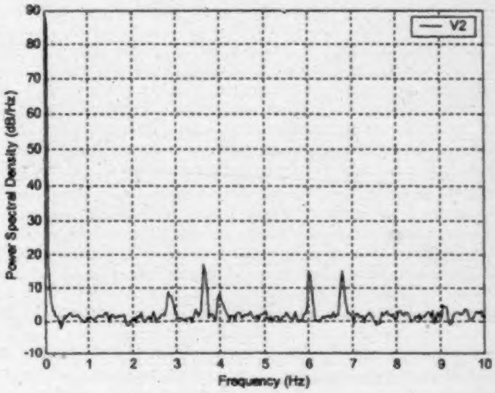

July 18, 1999
4:22 PM

July 18, 1999
4:22 PM

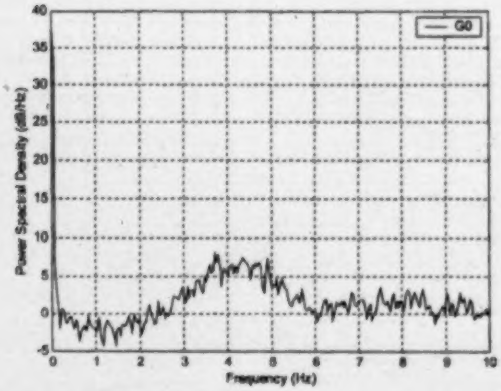

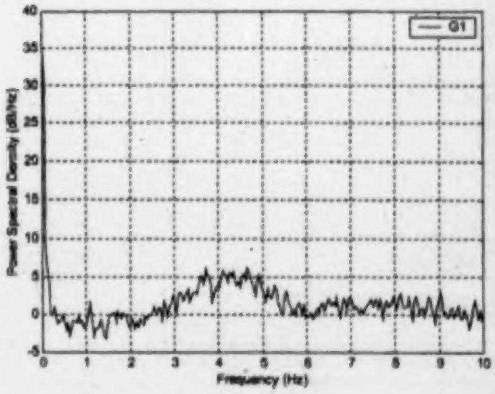

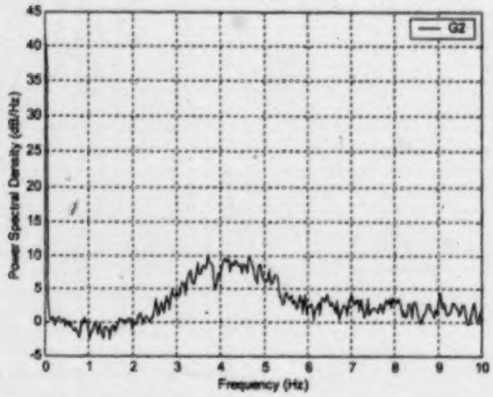

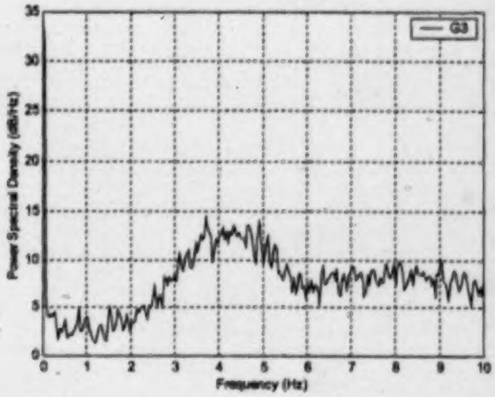

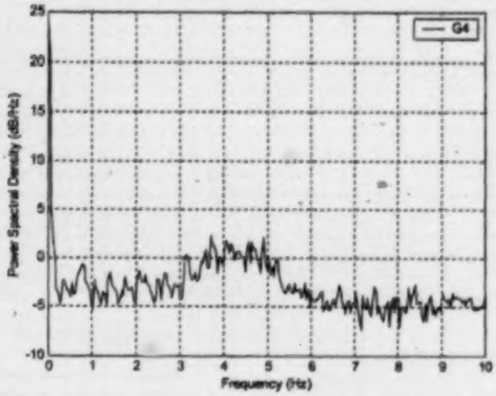

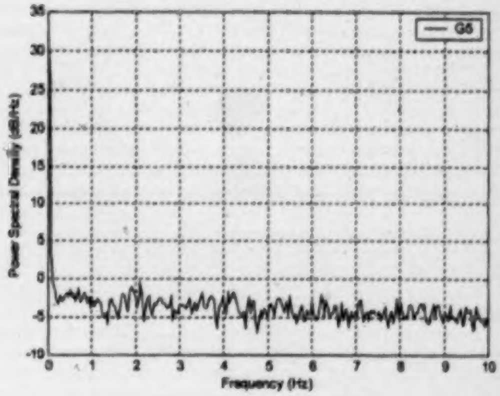

July 18, 1999
4:22 PM

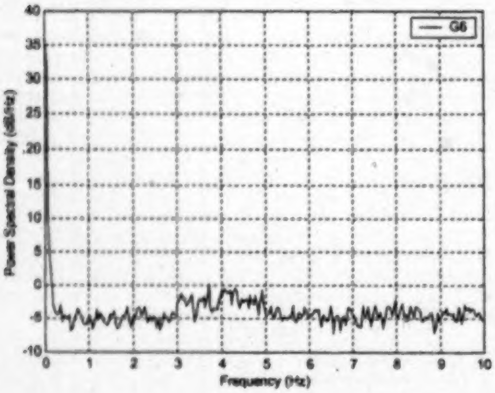

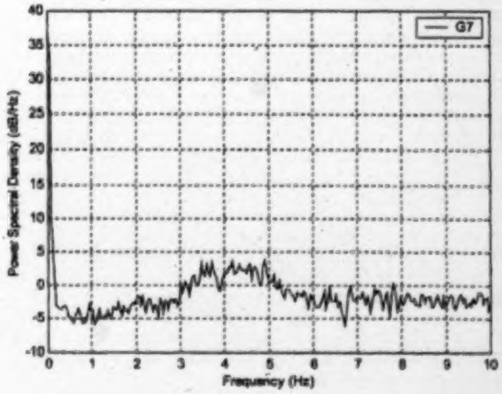

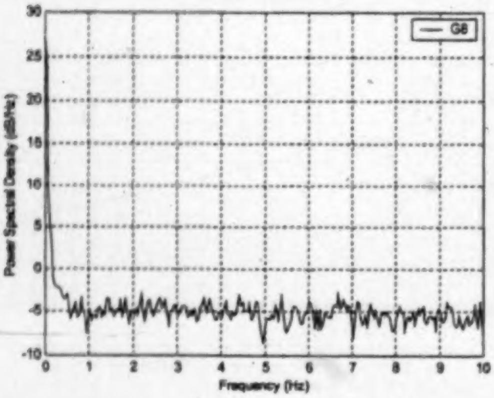

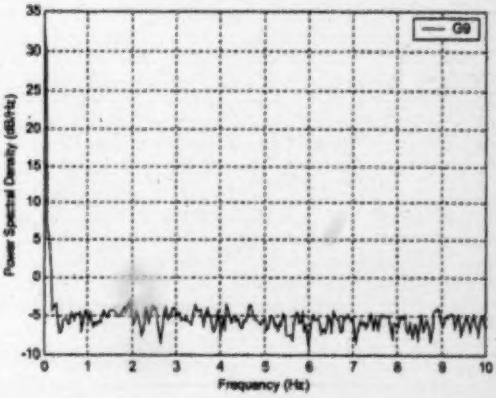

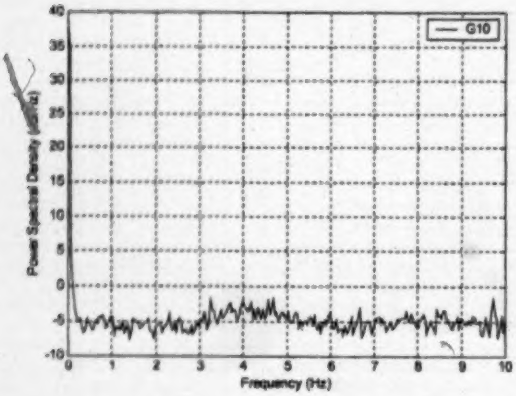

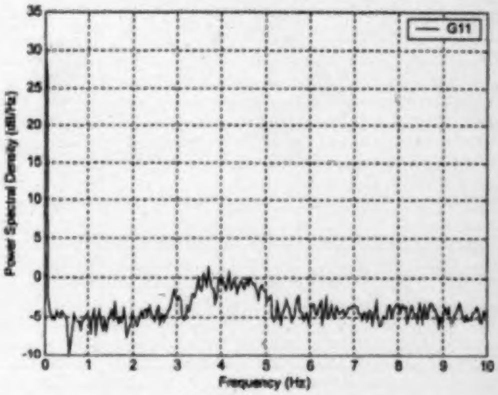

July 18, 1999
4:22 PM

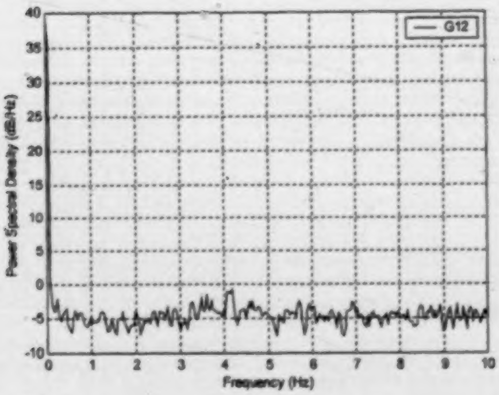

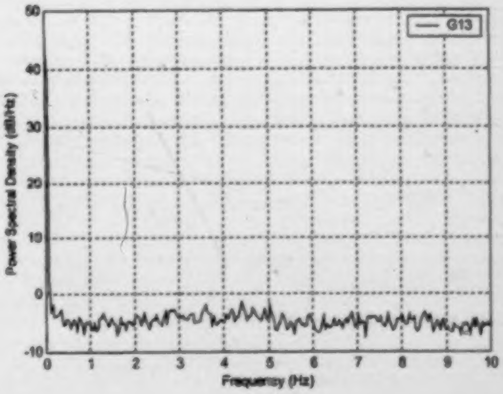

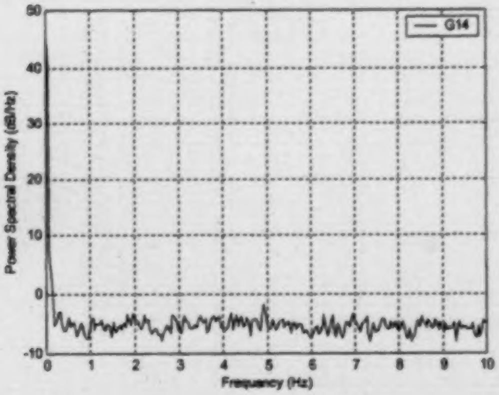

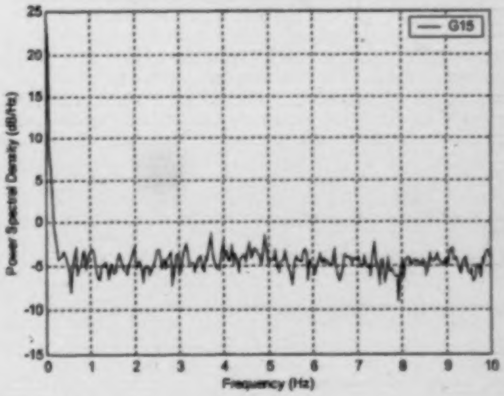

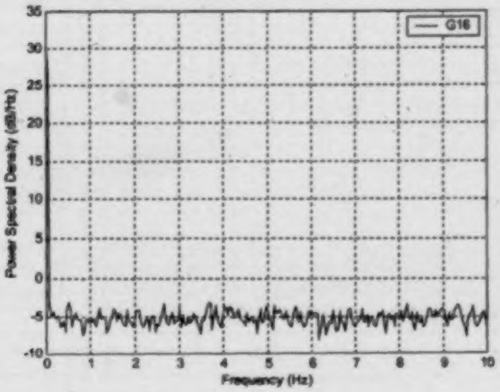

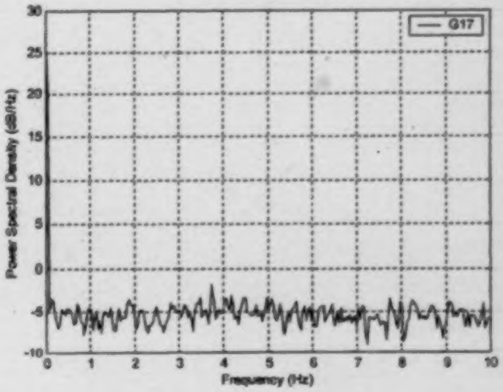

July 18, 1999
4:22 PM

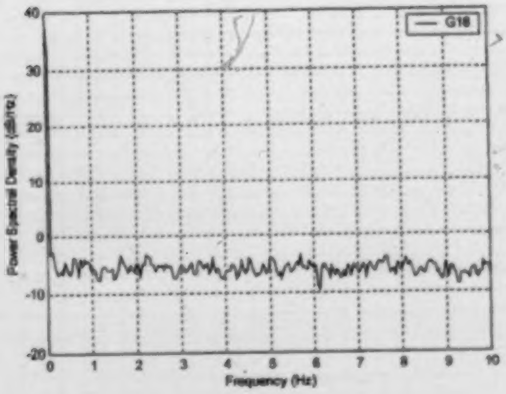

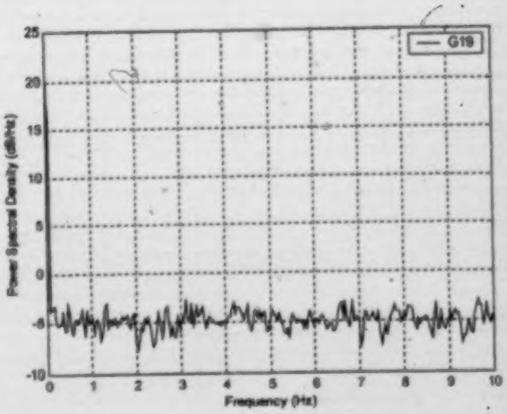

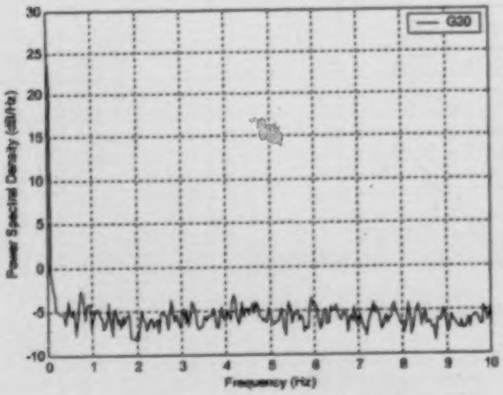

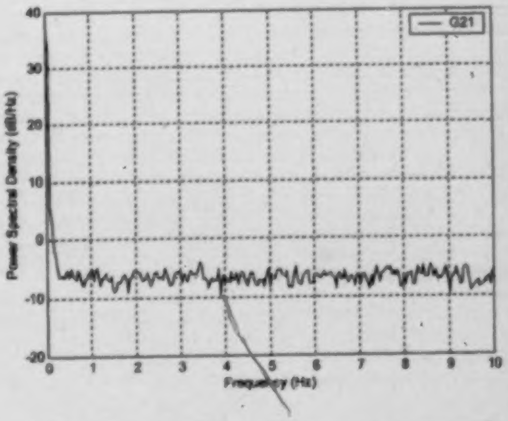

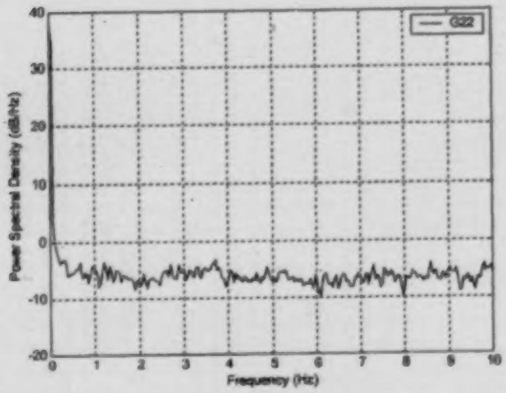

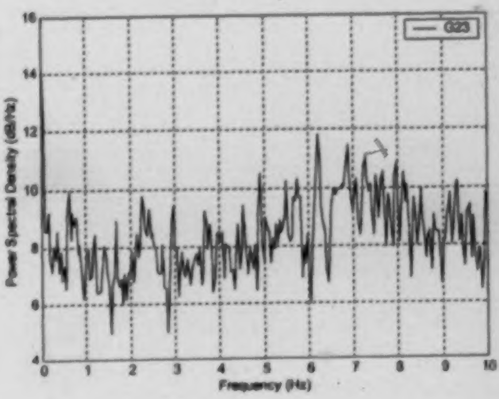

July 18, 1999
4:22 PM

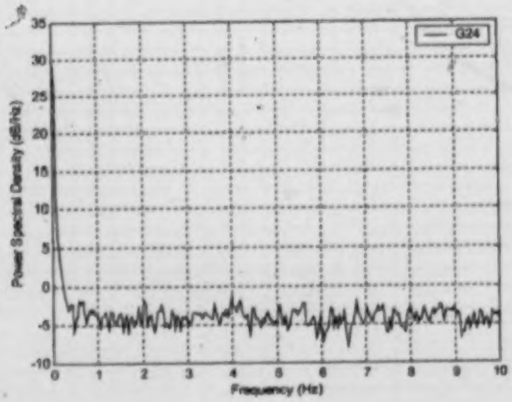

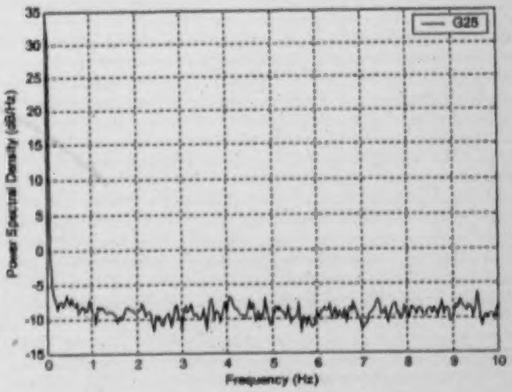

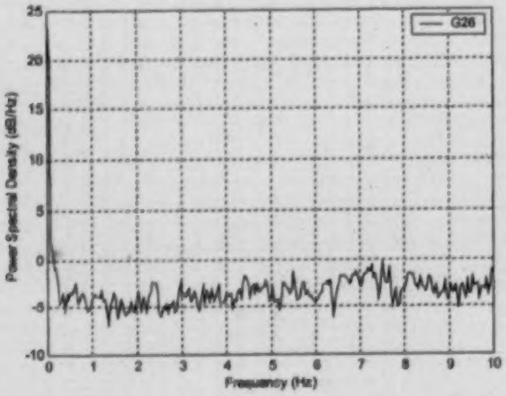

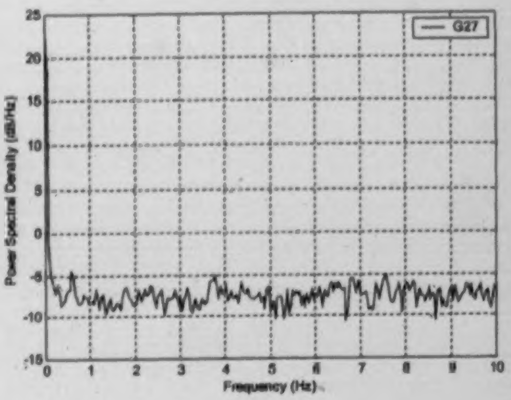

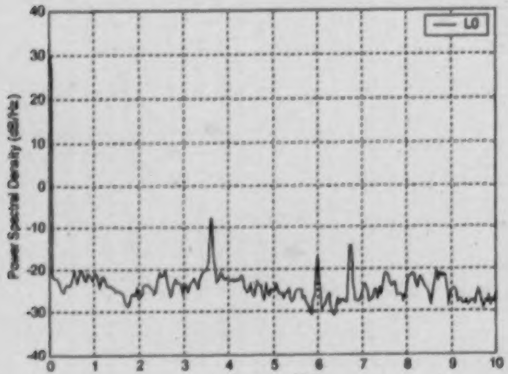

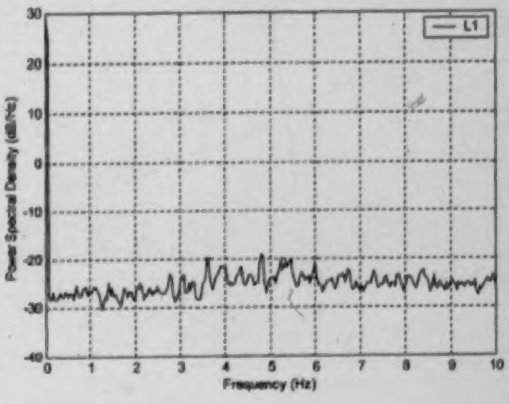

July 18, 1999
4:22 PM

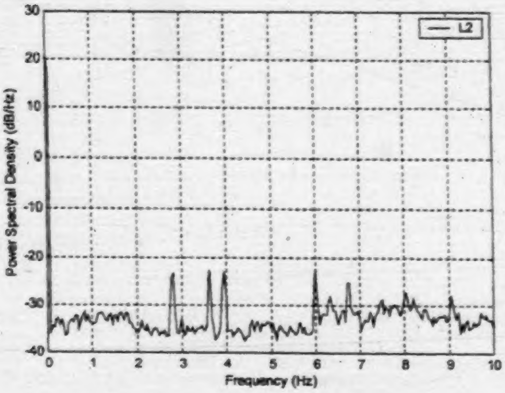

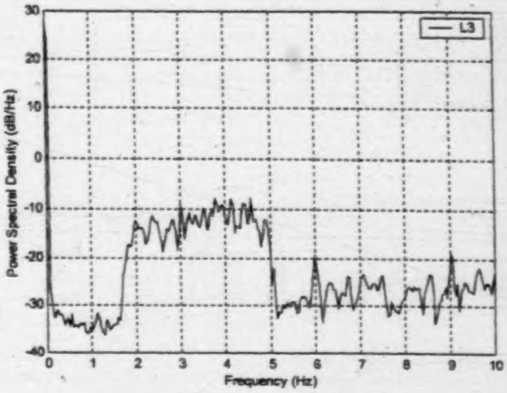

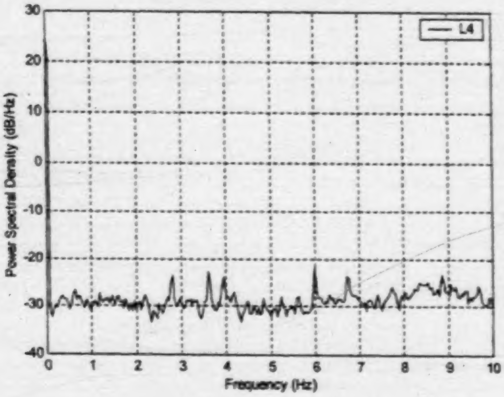

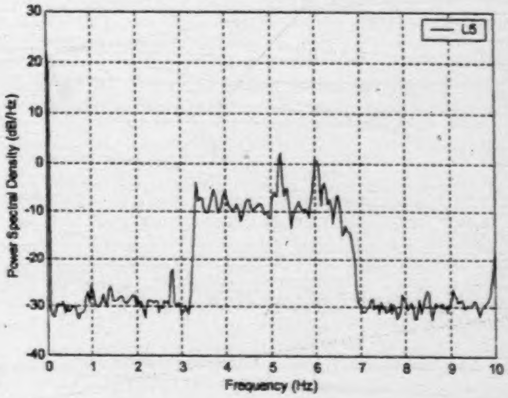

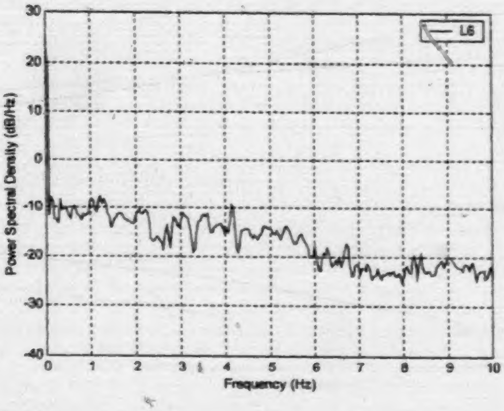

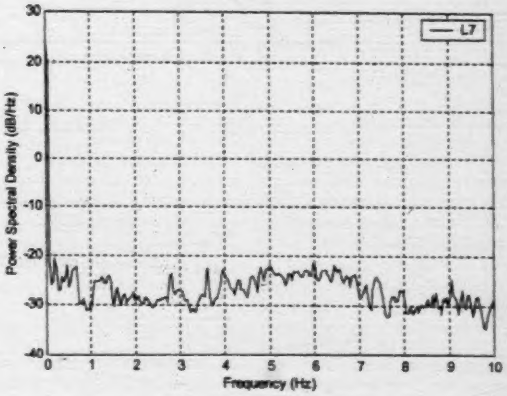

July 18, 1999
4:22 PM

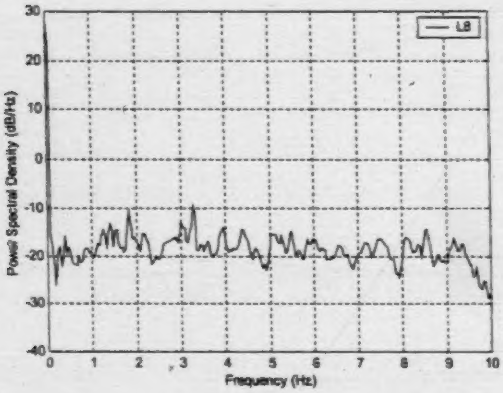

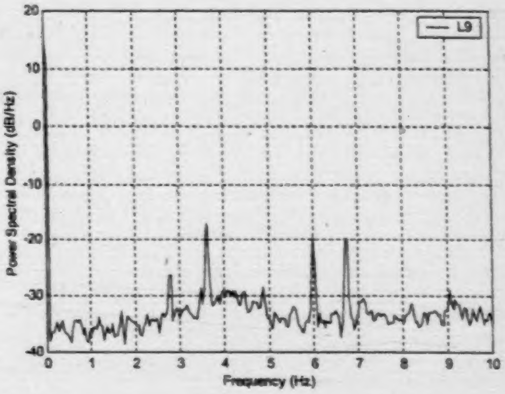

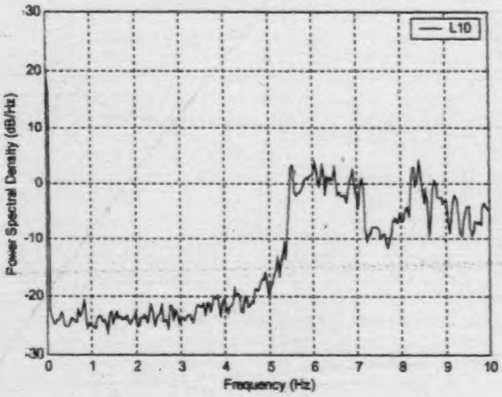

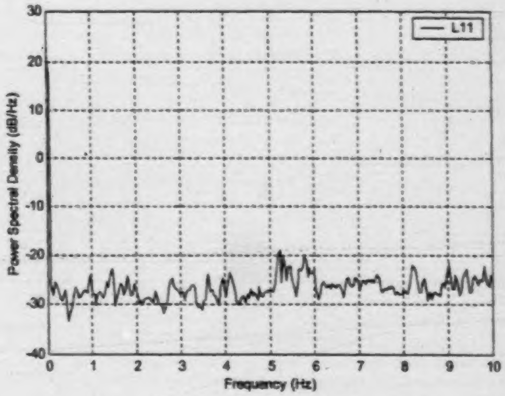

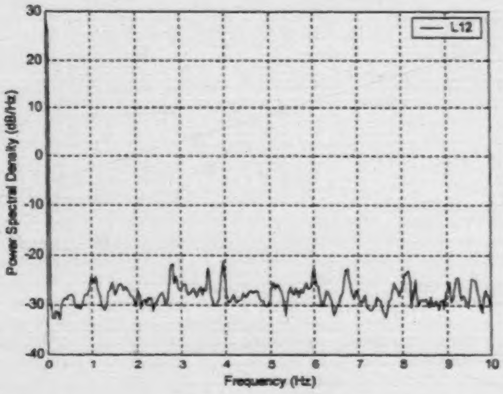

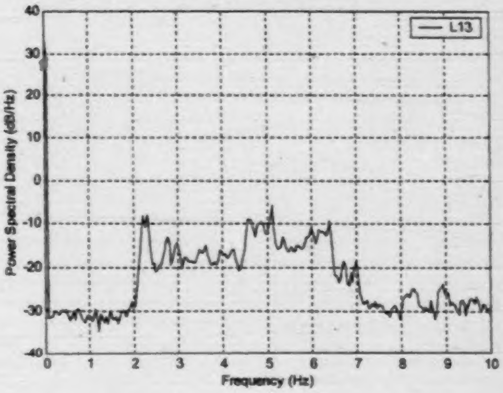

July 18, 1999
4:22 PM

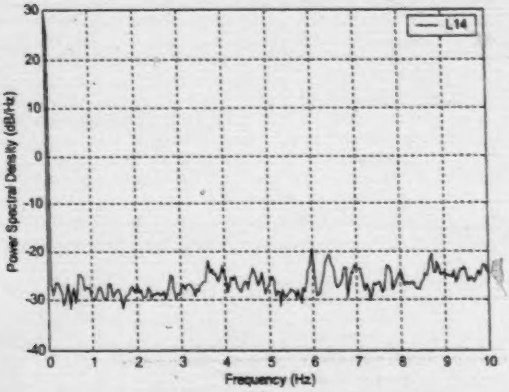

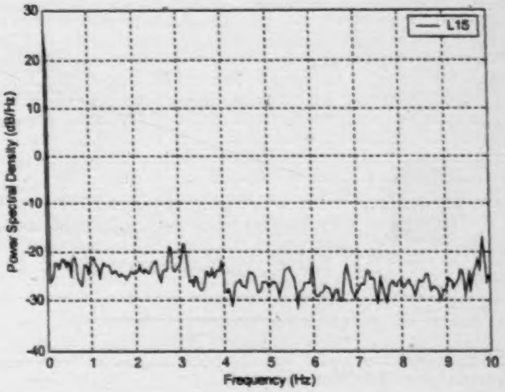

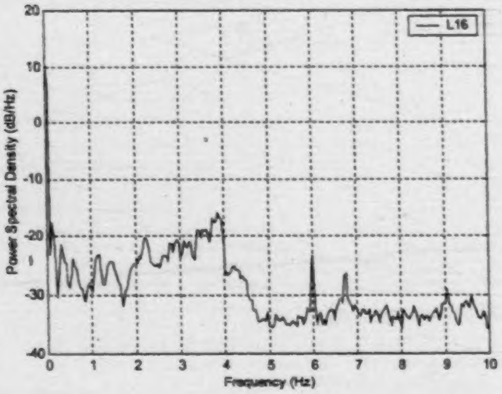

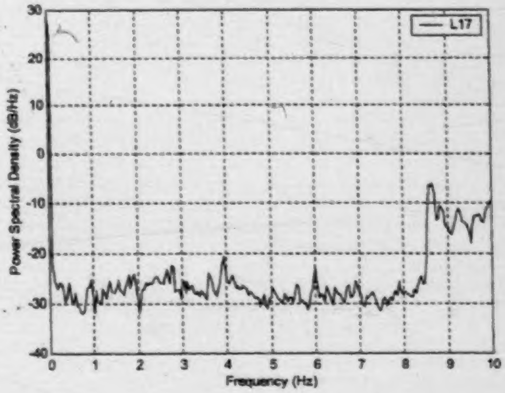

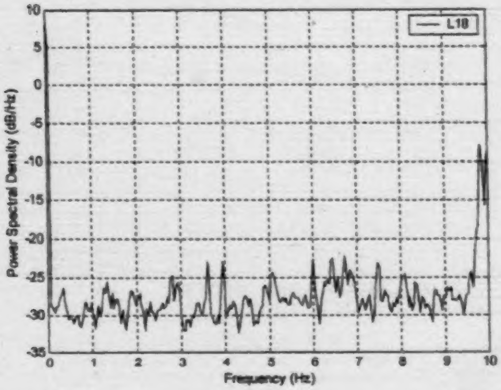

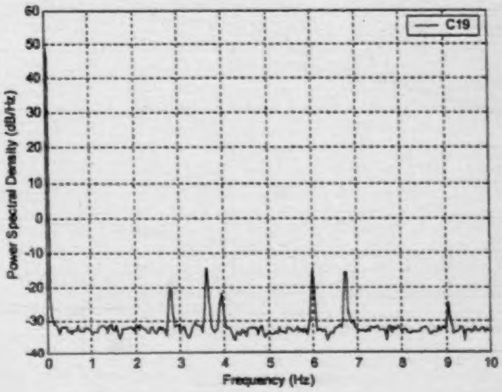

July 18, 1999
4:22 PM

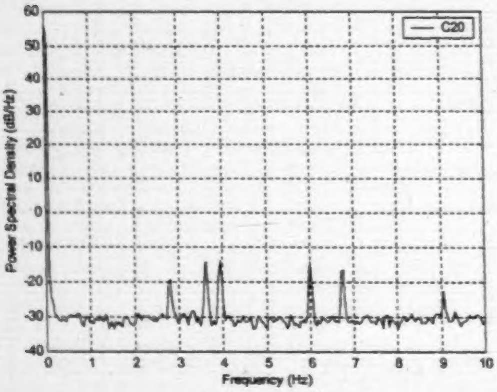

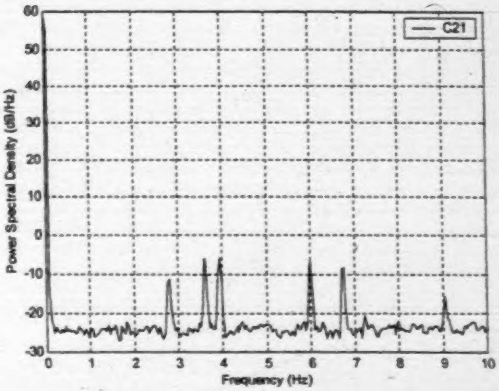

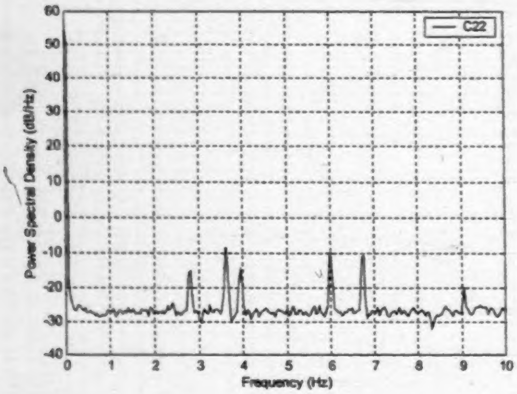

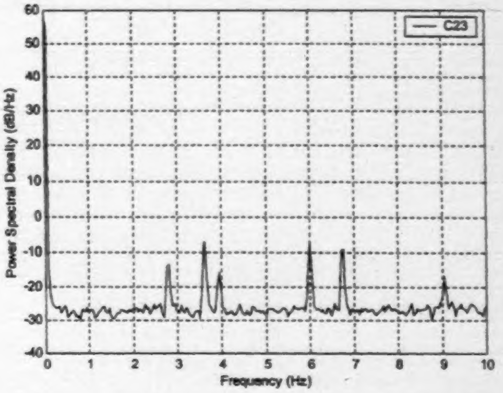

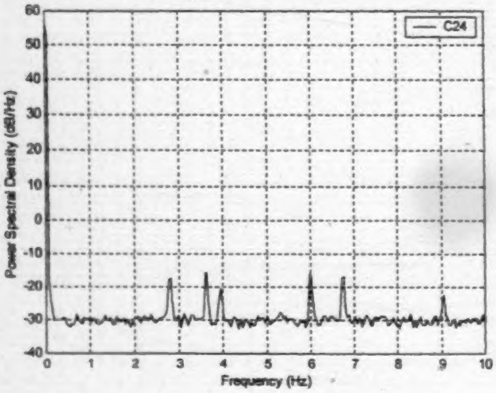

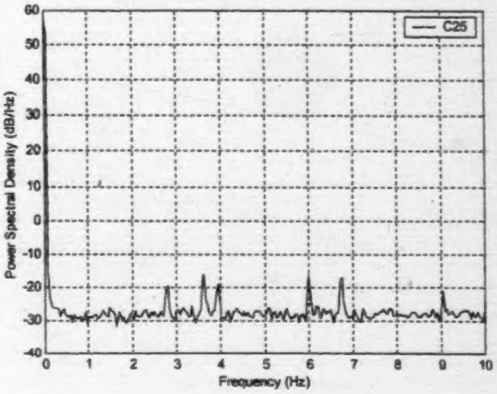

July 18, 1999
4:22 PM

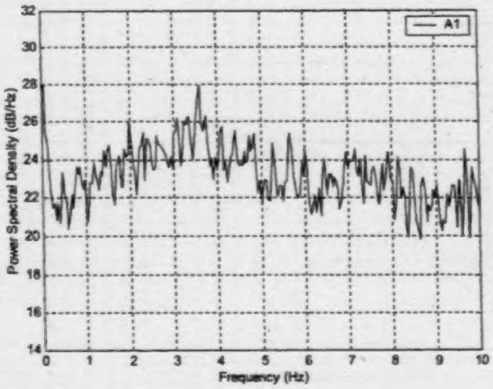

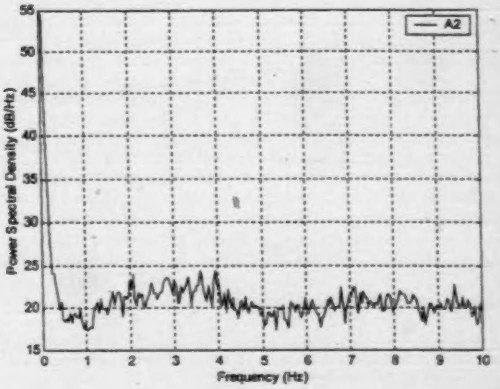

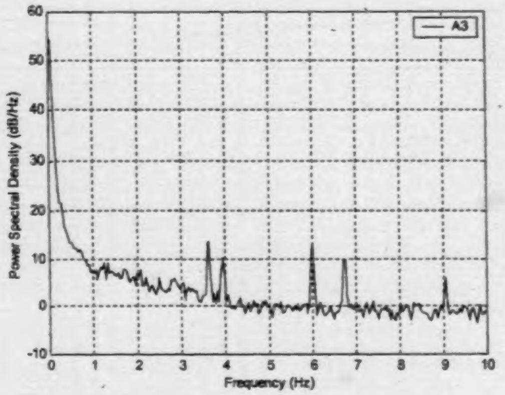

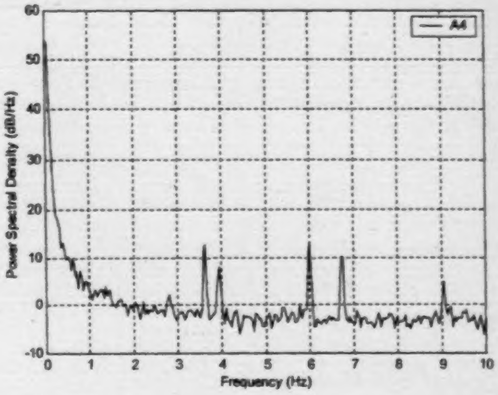

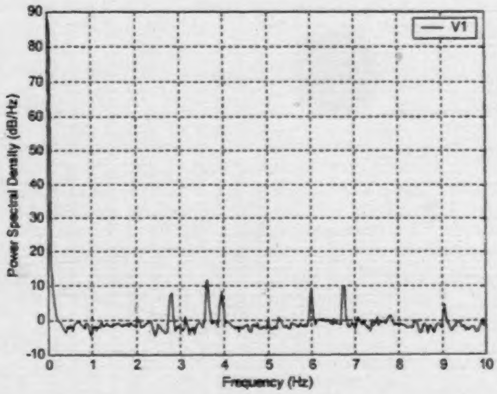

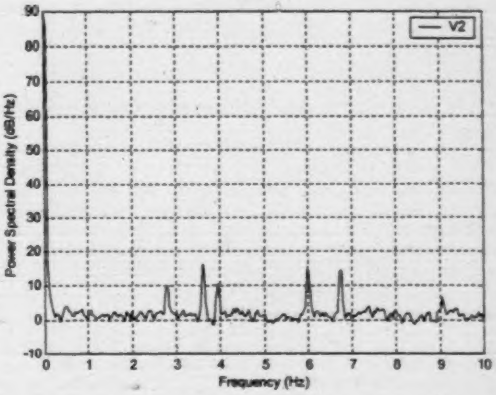

July 18, 1999
4:28 PM

July 18, 1999
4:28 PM

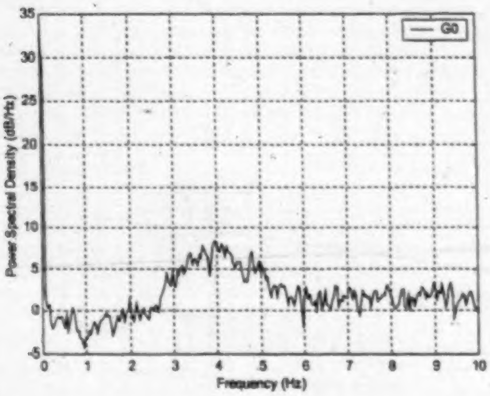

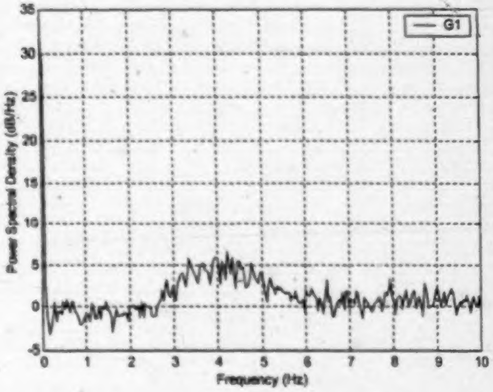

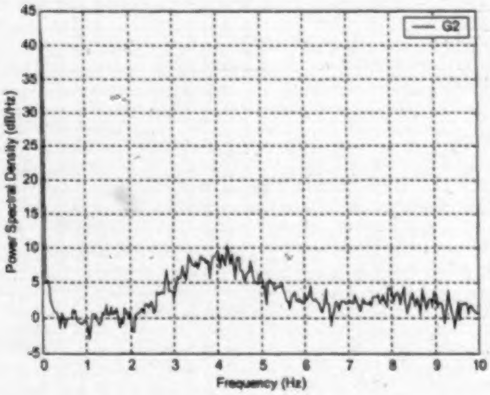

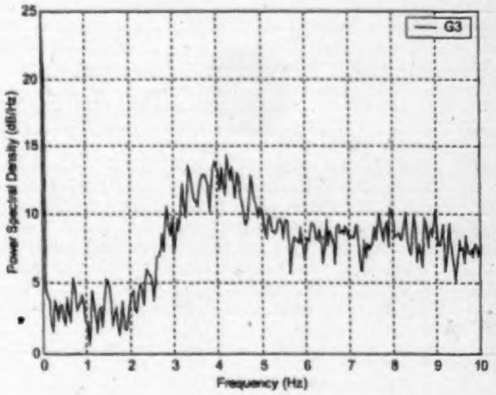

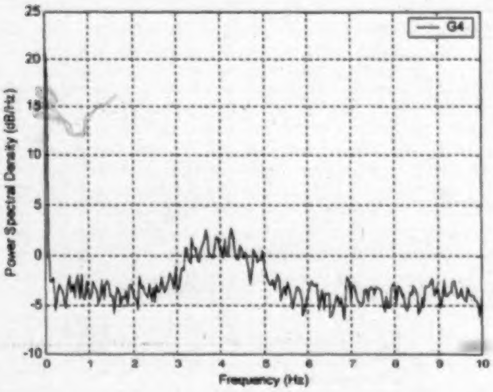

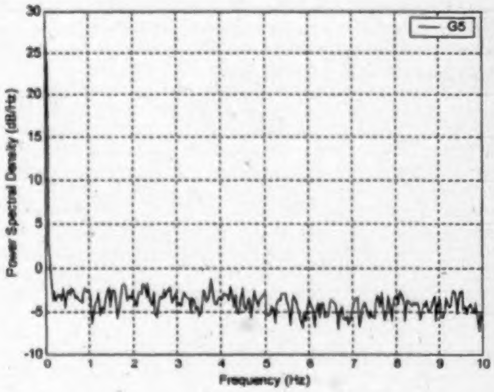

July 18, 1999
4:28 PM

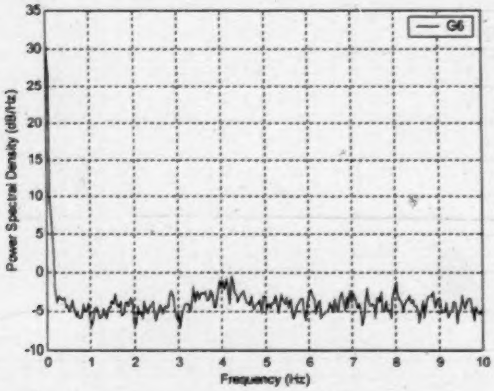

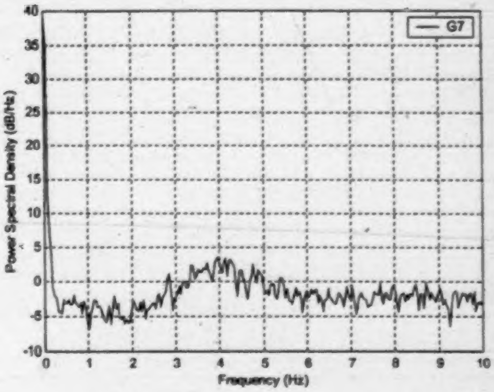

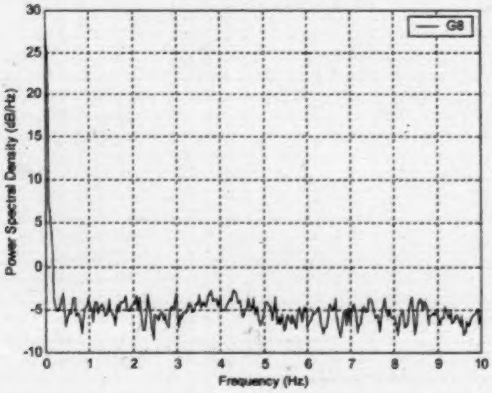

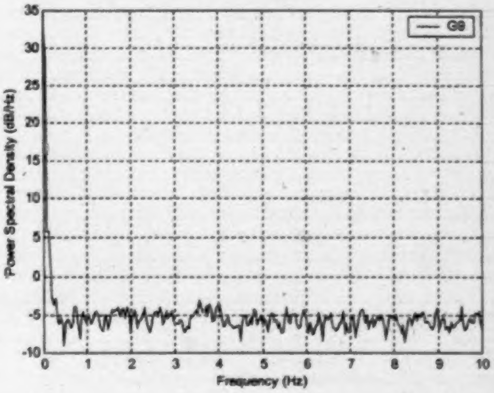

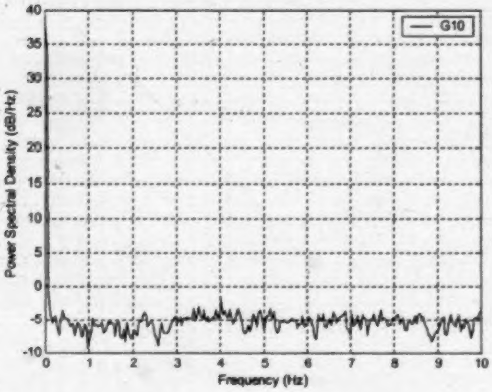

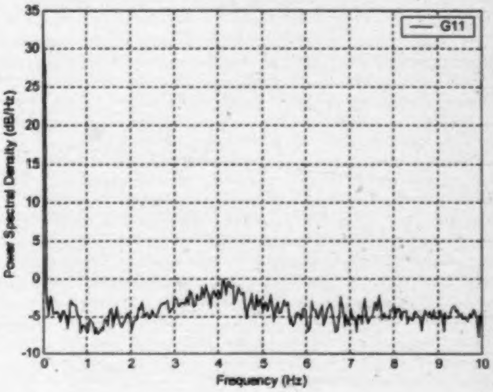

July 18, 1999
4:28 PM

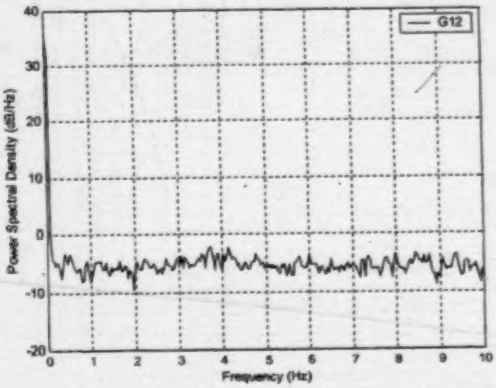

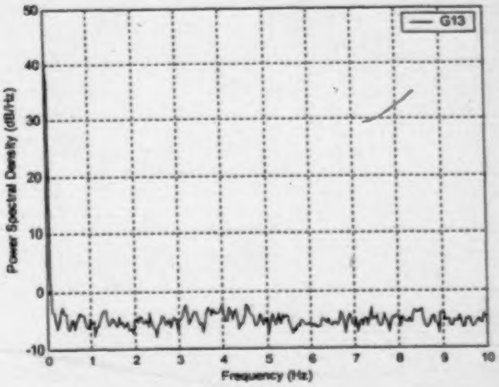

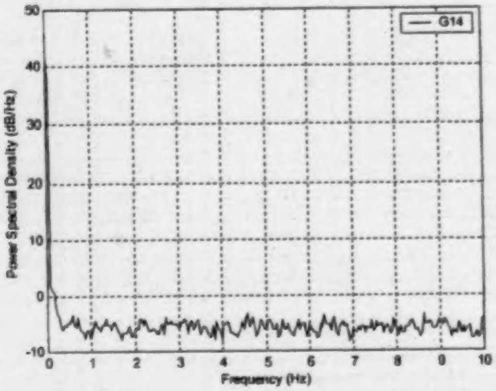

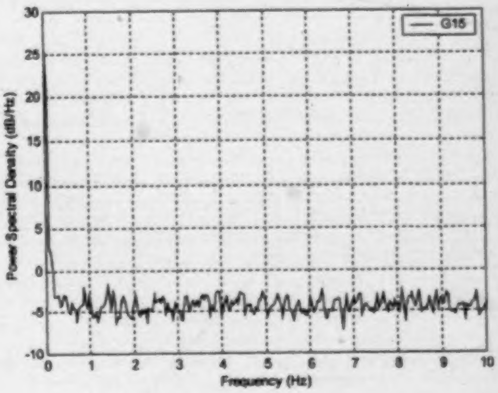

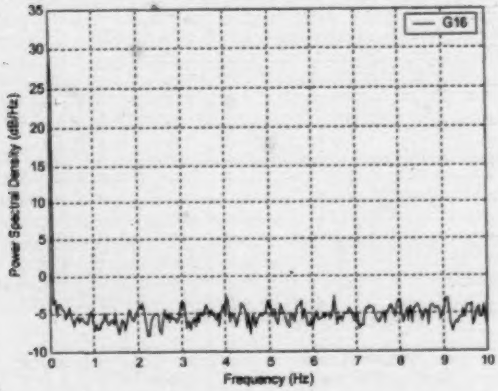

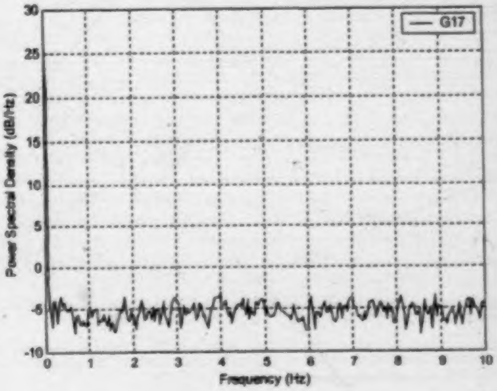

July 18, 1999
4:28 PM

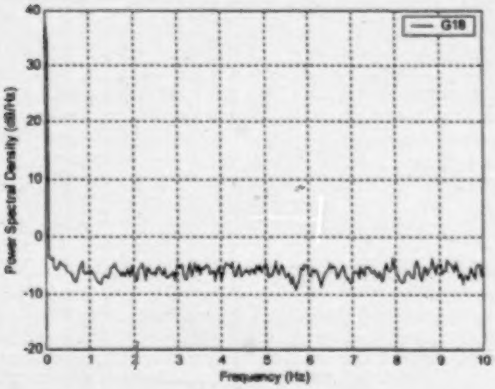

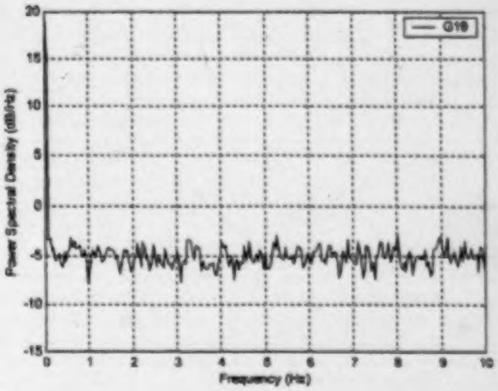

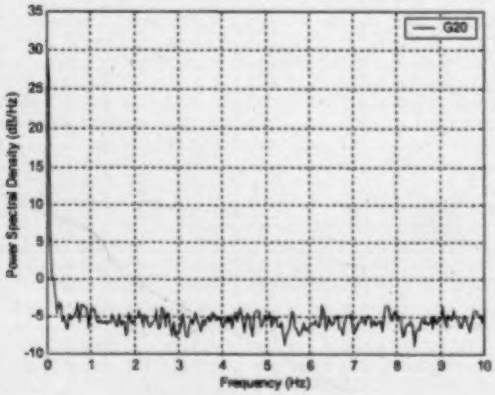

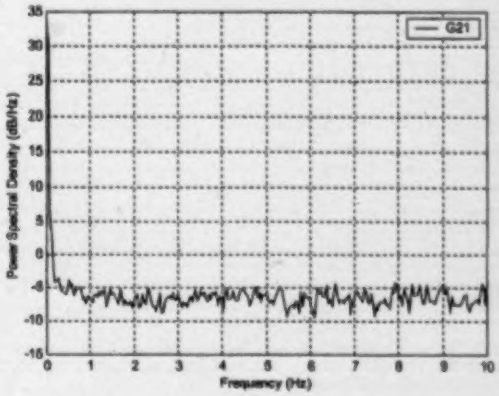

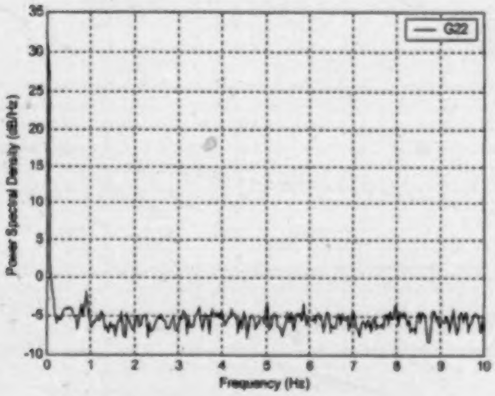

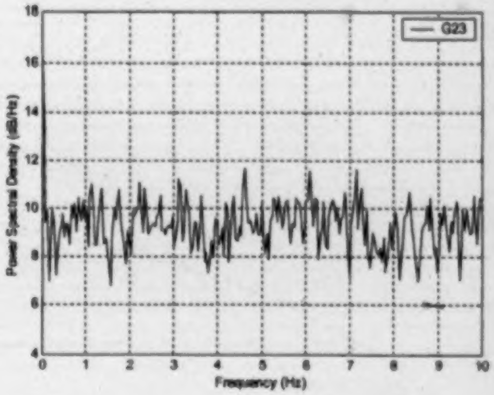

July 18, 1999
4:28 PM

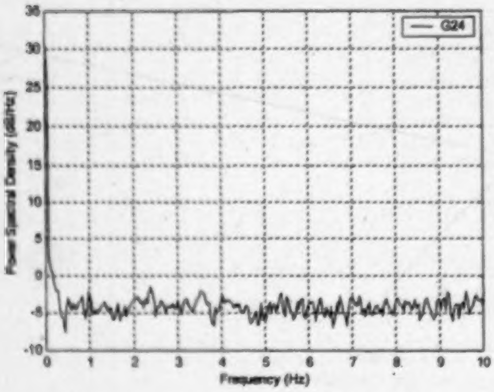

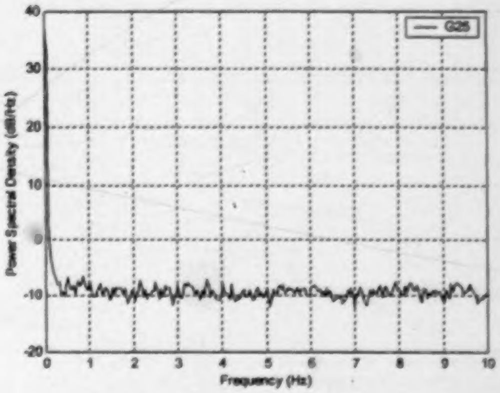

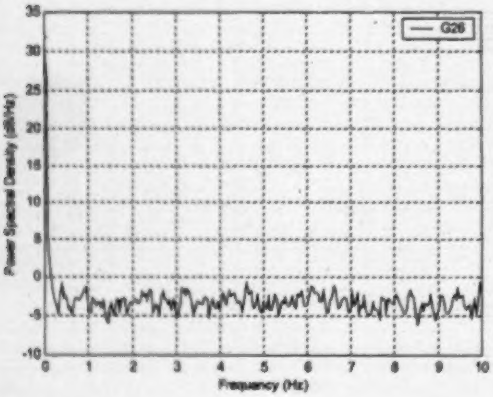

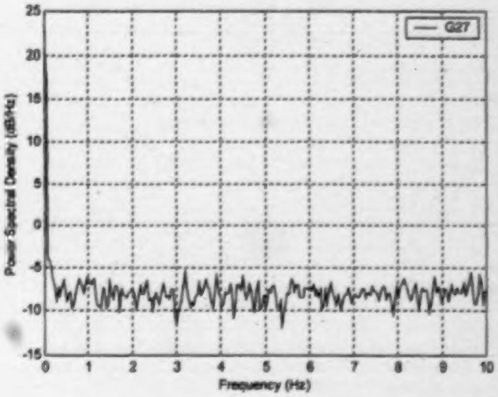

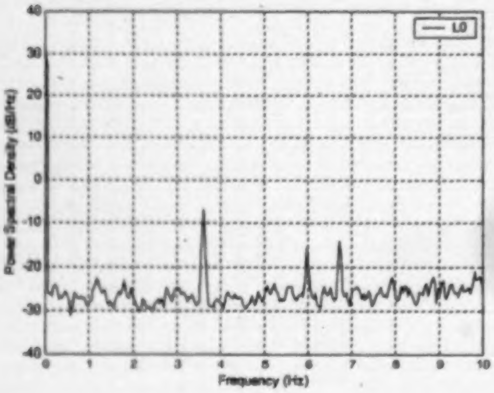

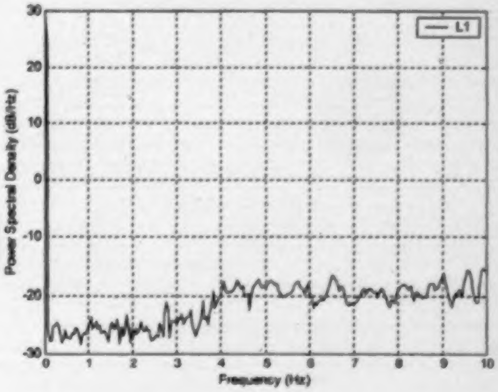

July 18, 1999
4:28 PM

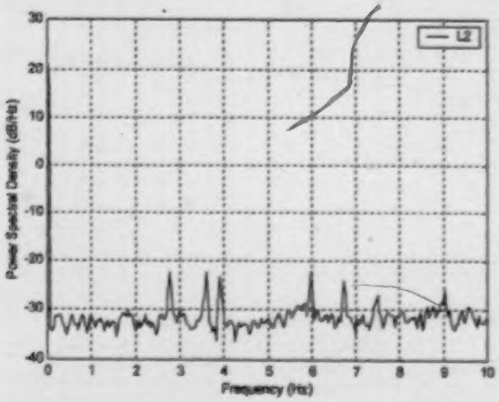

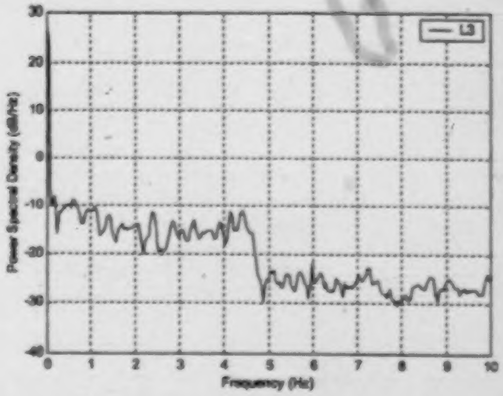

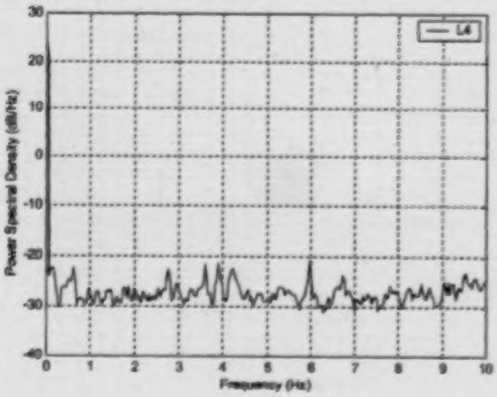

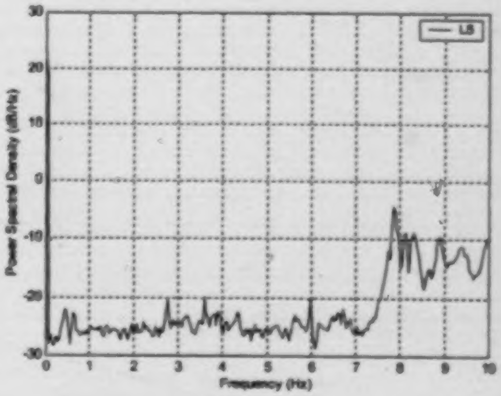

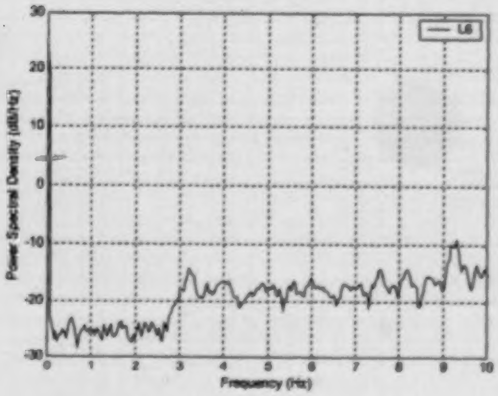

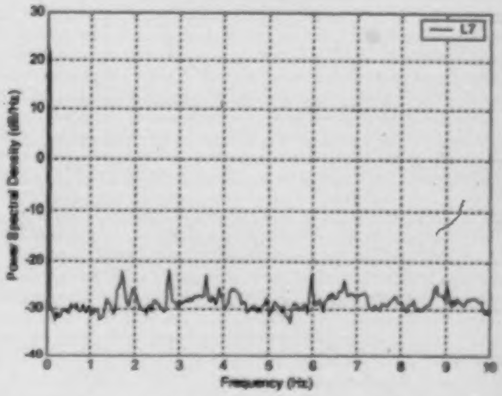

July 18, 1999
4:28 PM

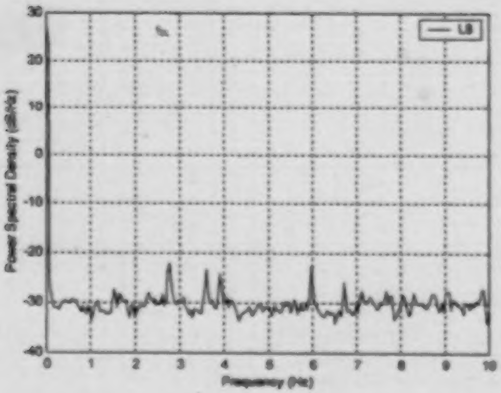

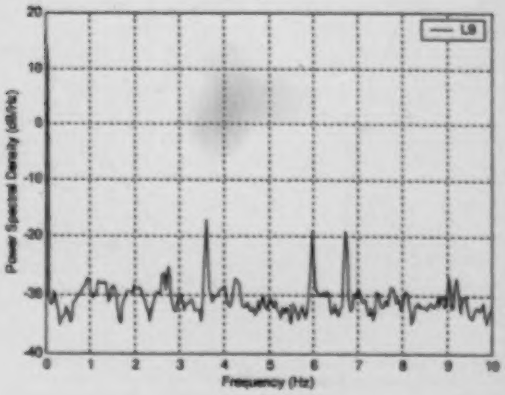

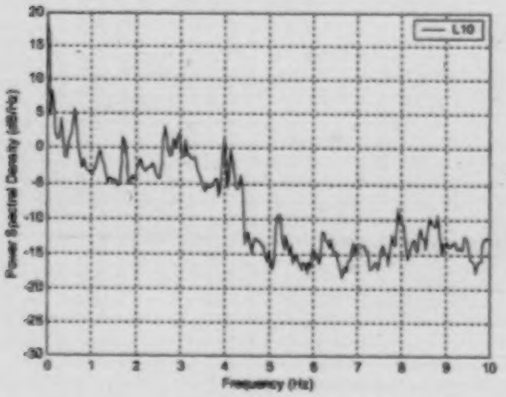

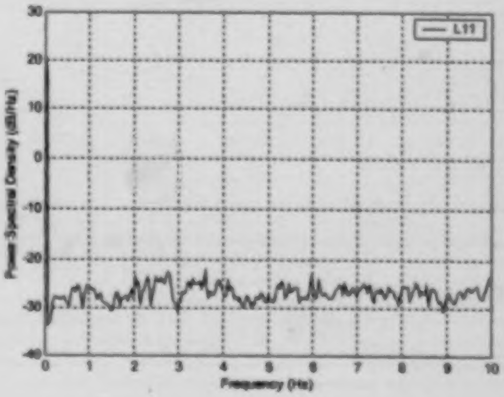

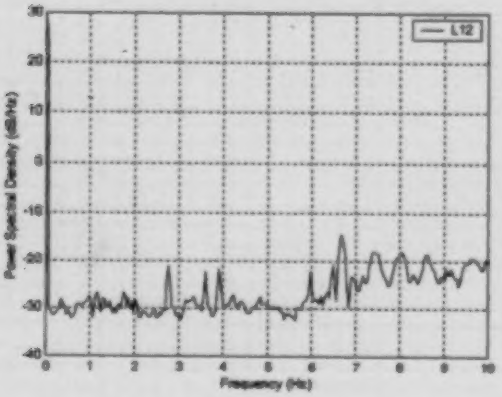

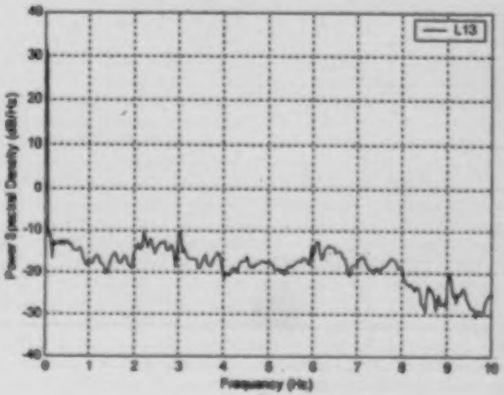

July 18, 1999
4:28 PM

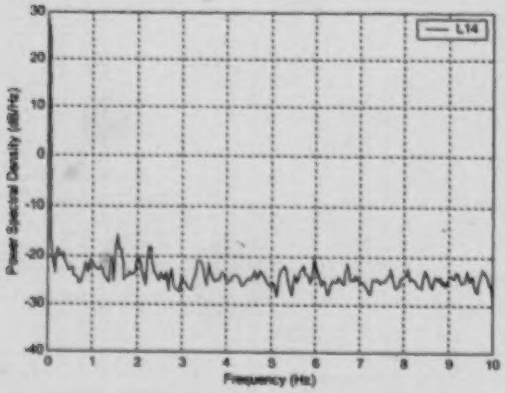

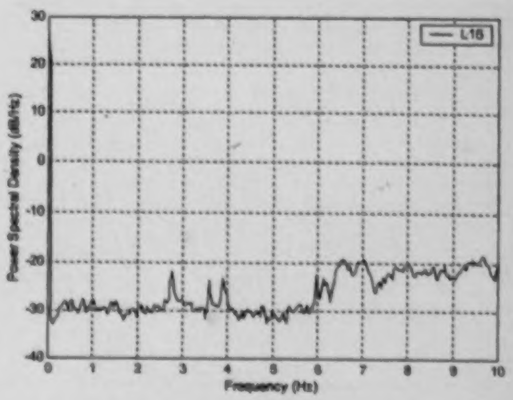

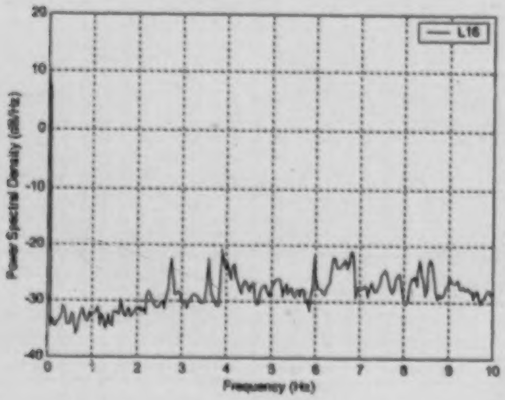

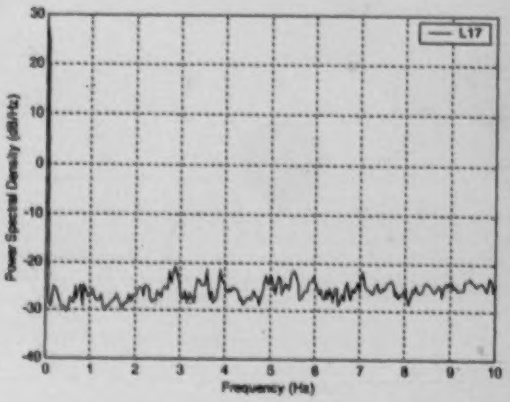

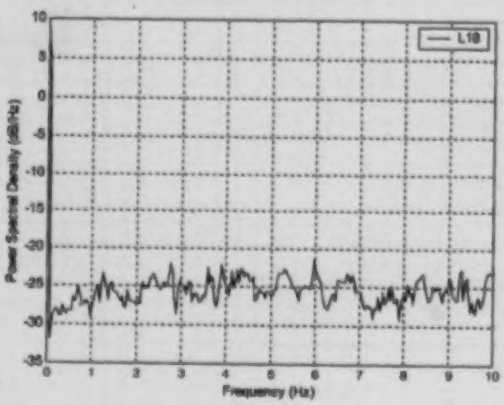

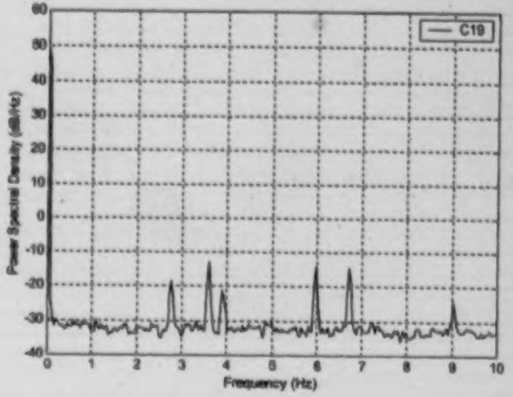

July 18, 1999
4:28 PM

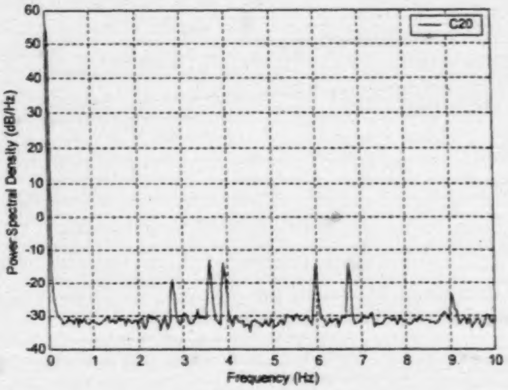

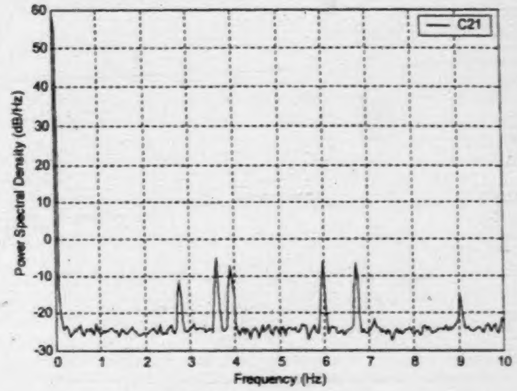

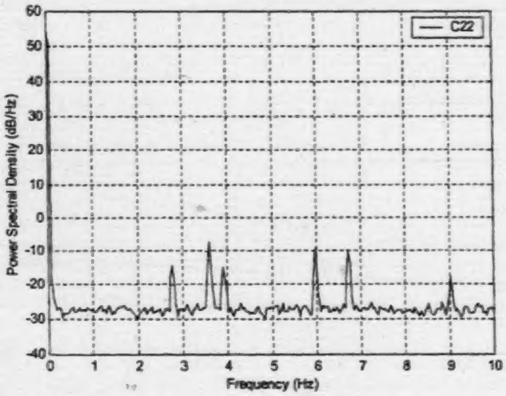

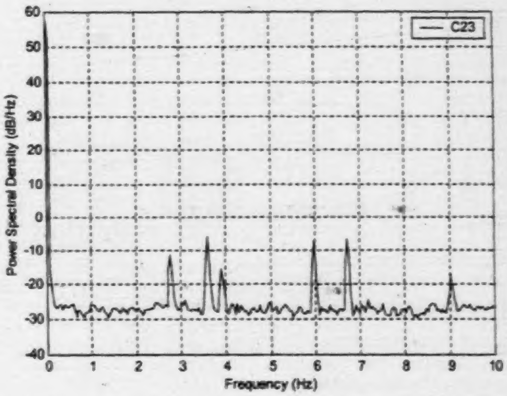

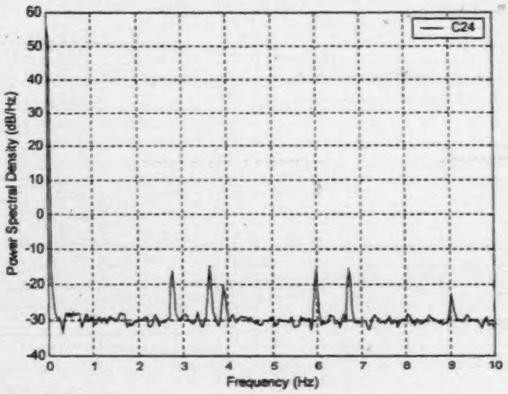

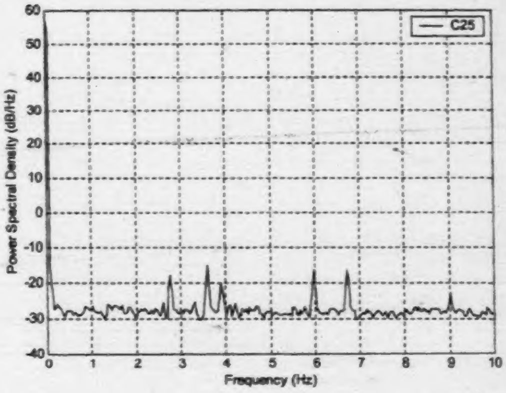

July 18, 1999
4:28 PM

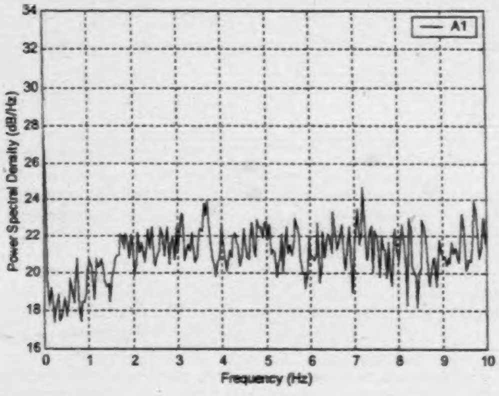

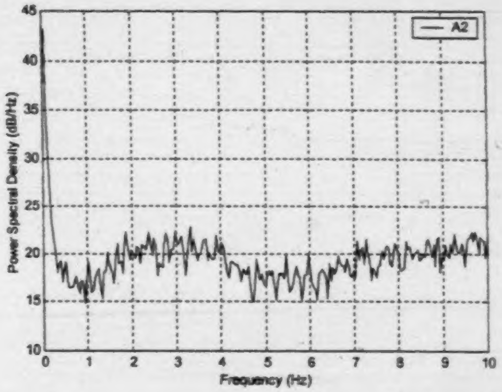

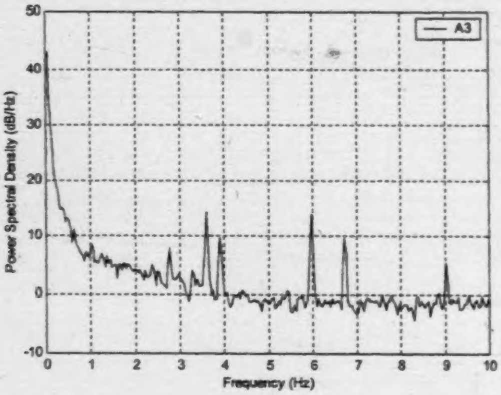

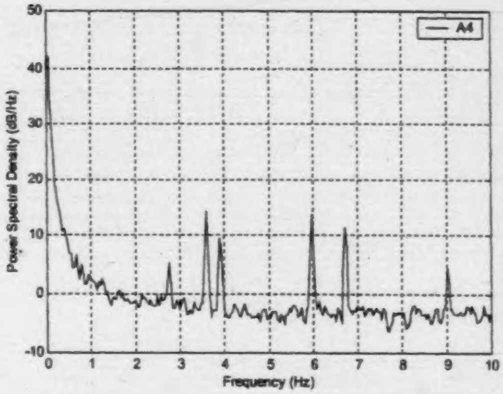

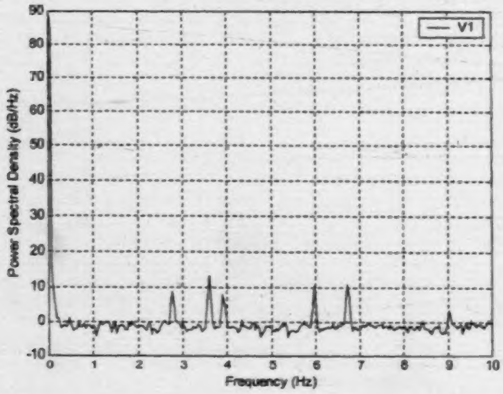

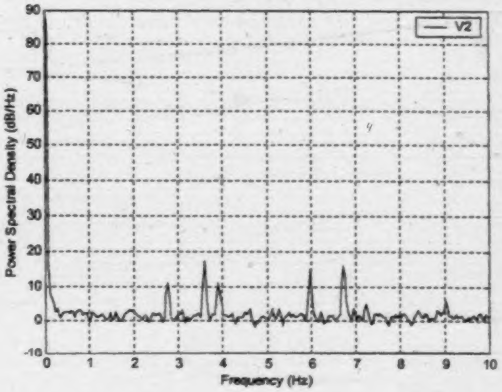

July 18, 1999
4:33 PM

July 18, 1999
4:33 PM

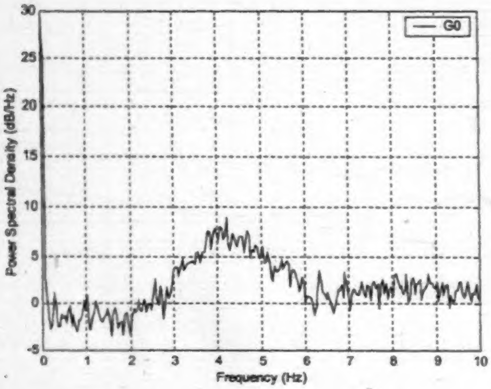

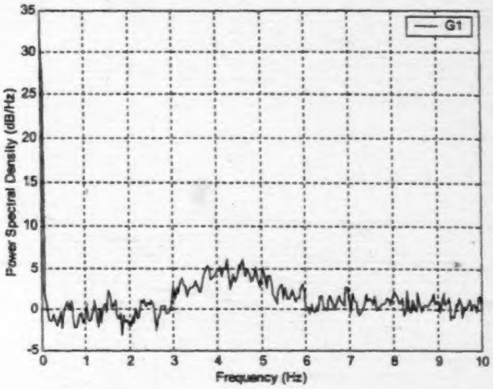

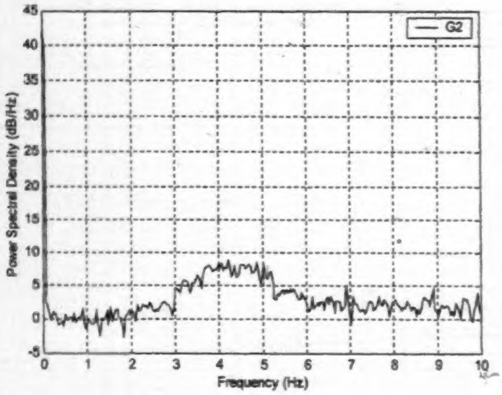

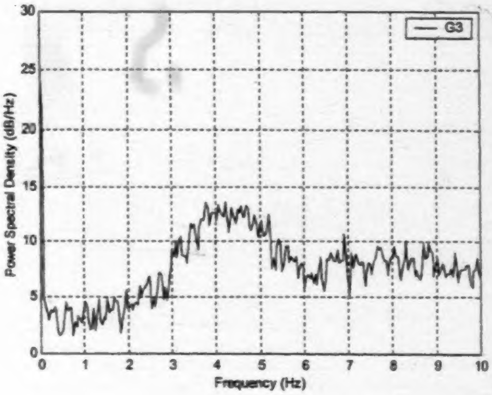

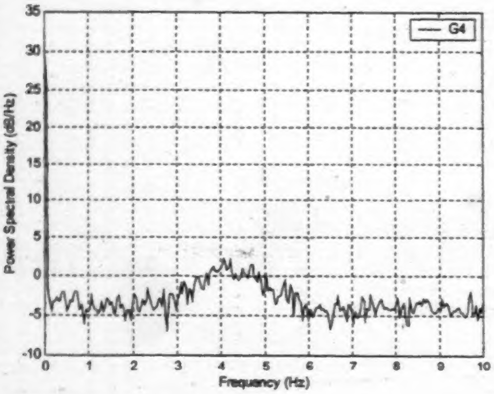

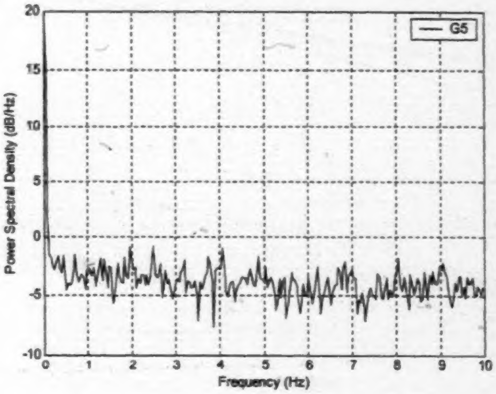

July 18, 1999
4:33 PM

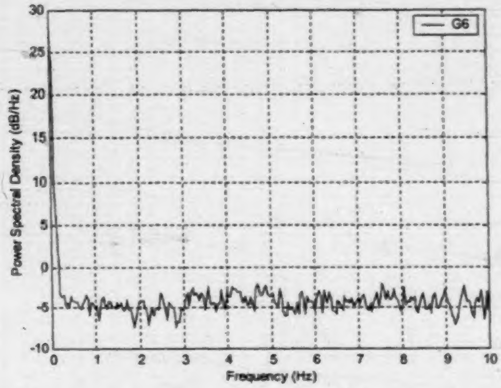

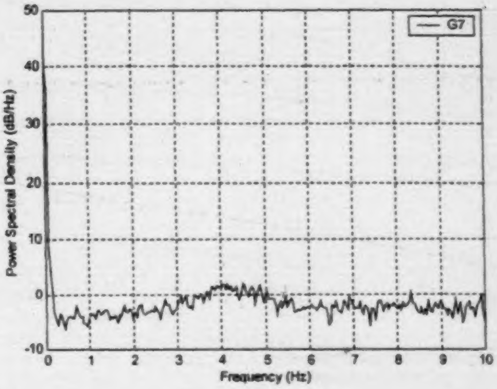

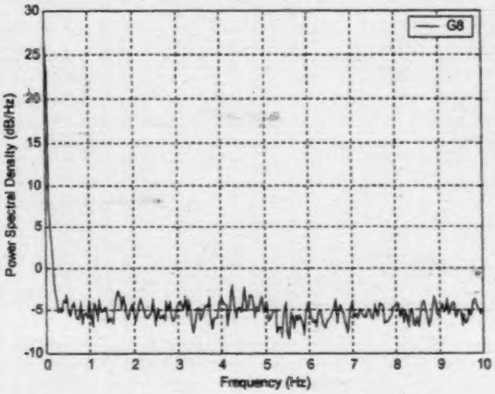

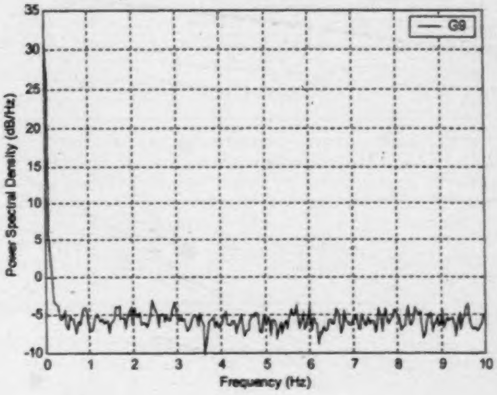

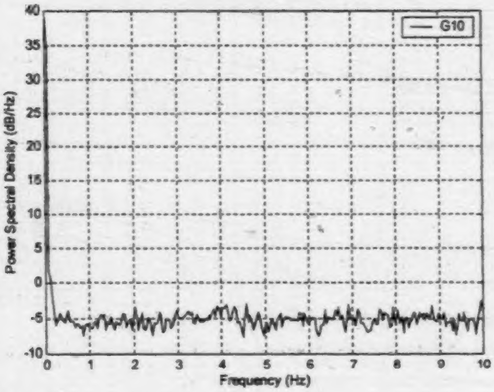

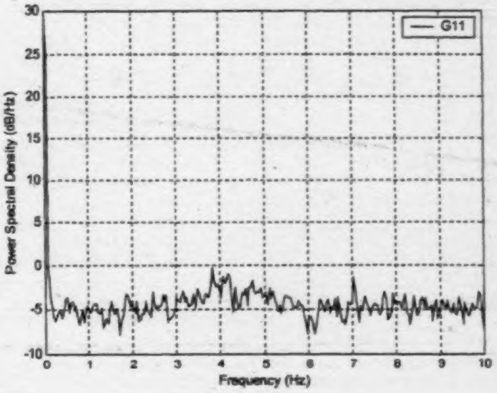

July 18, 1999
4:33 PM

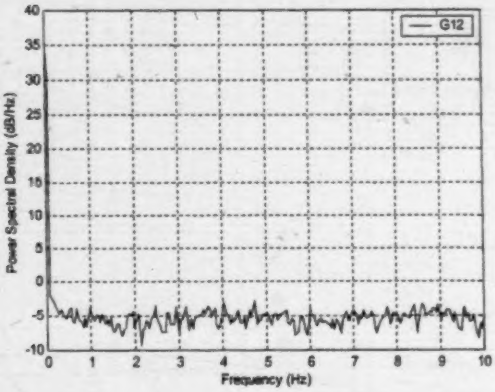

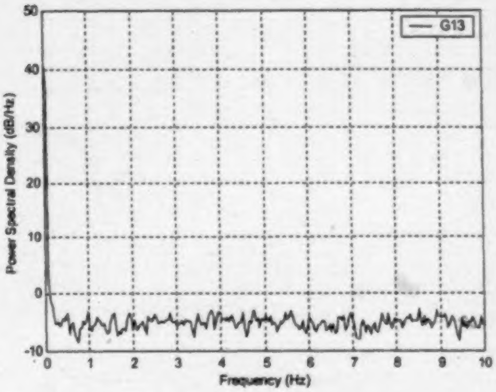

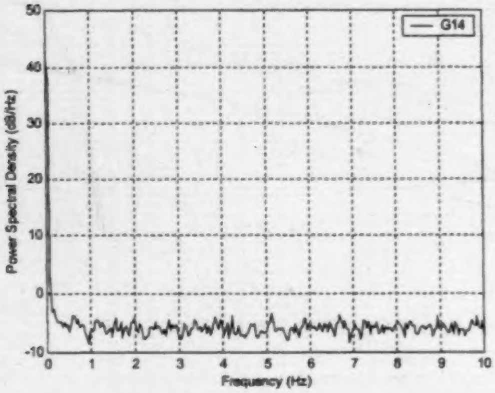

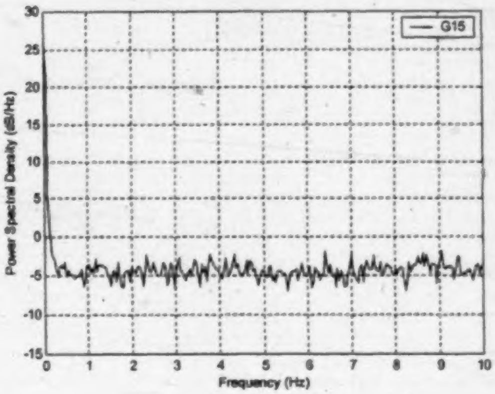

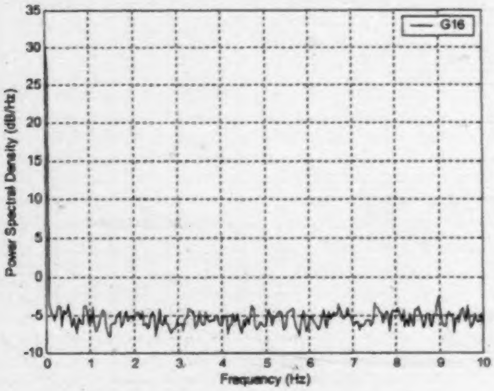

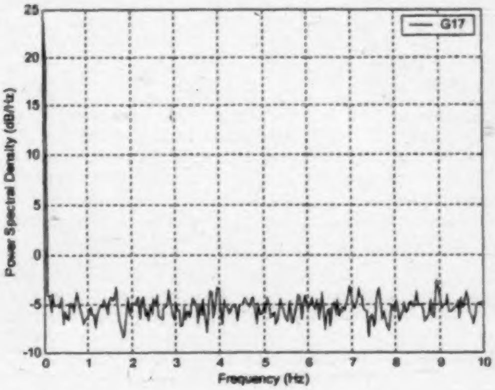

July 18, 1999
4:33 PM

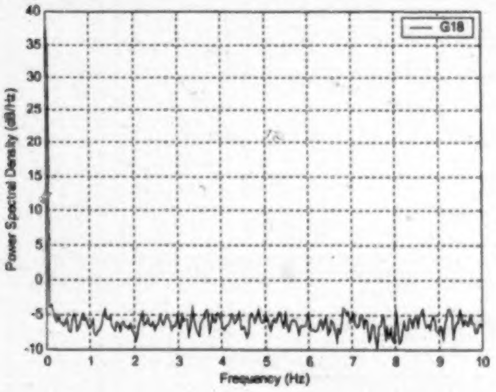

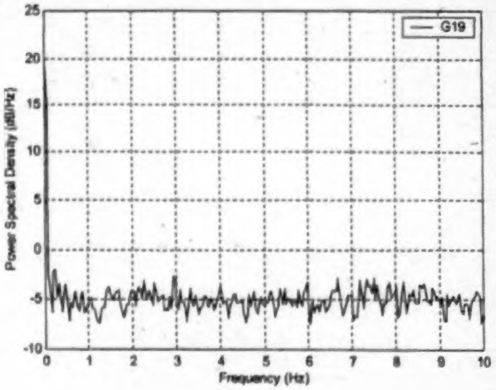

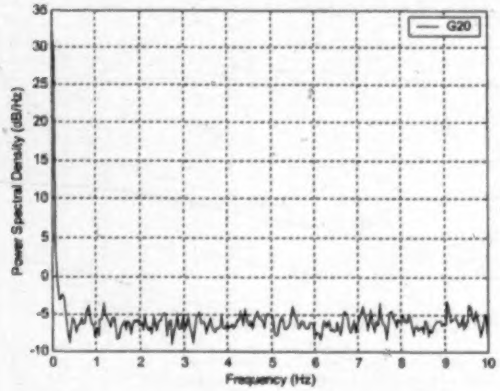

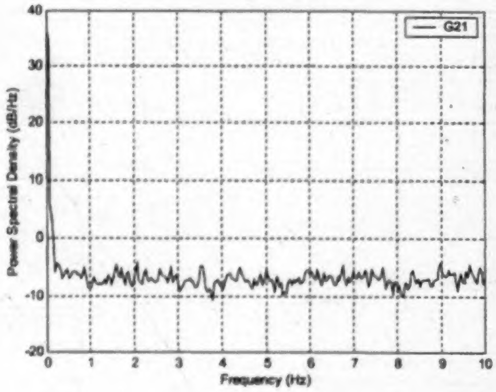

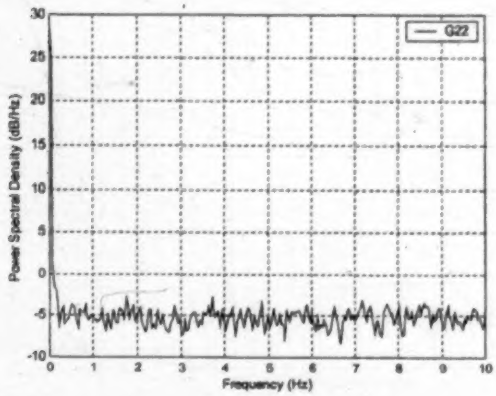

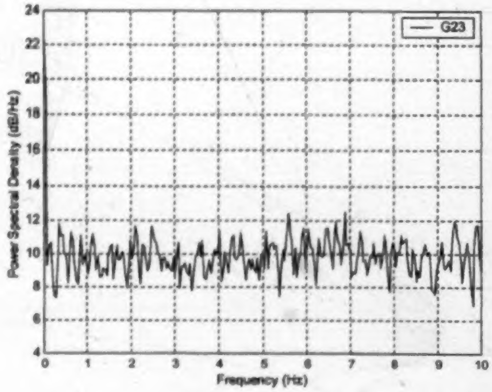

July 18, 1999
4:33 PM

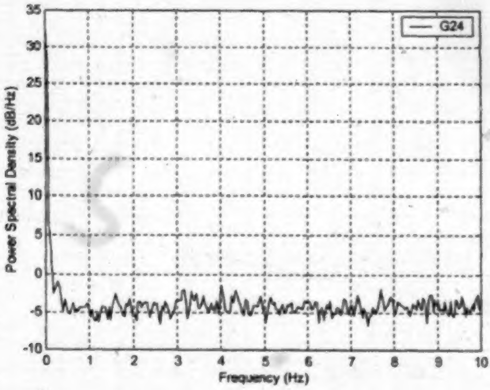

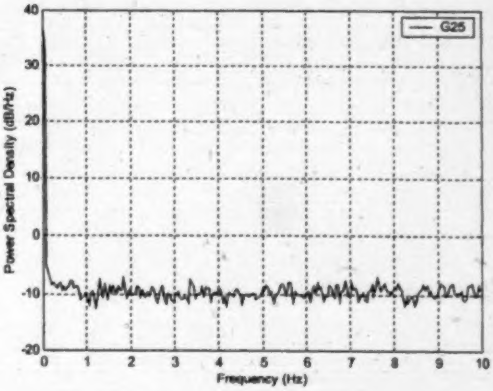

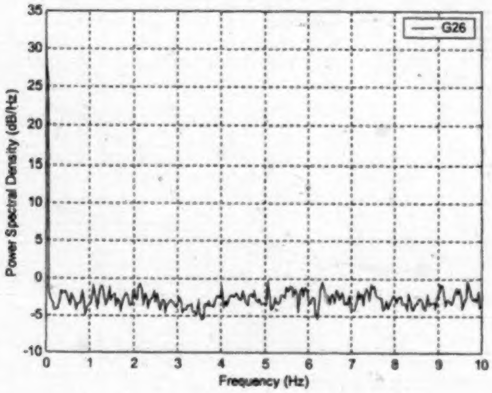

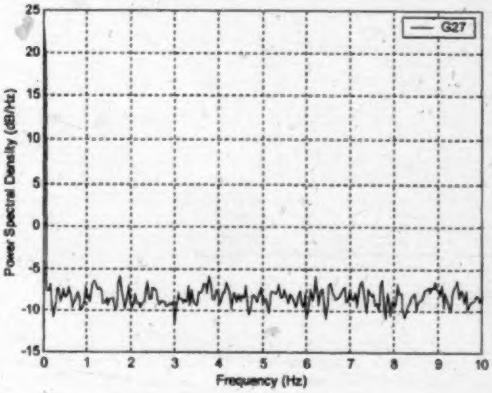

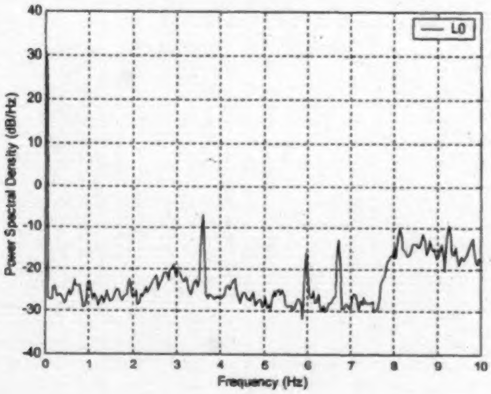

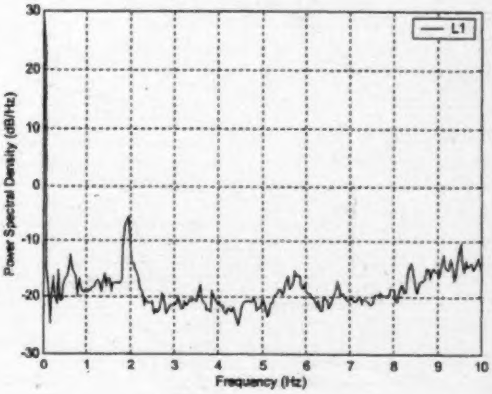

July 18, 1999
4:33 PM

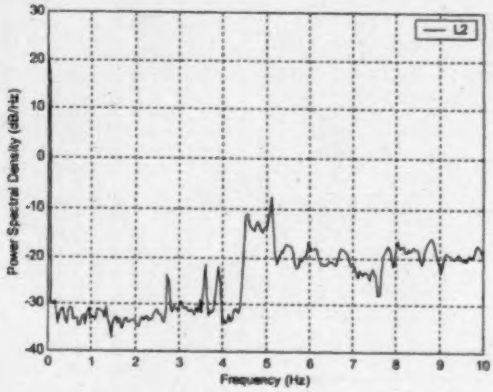

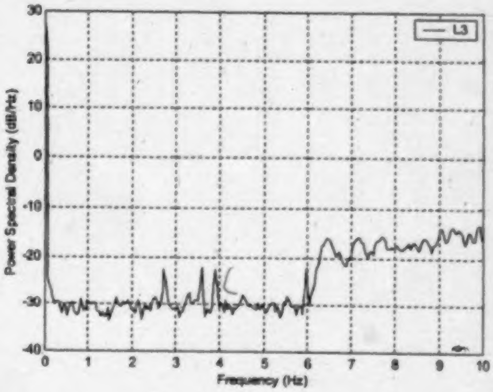

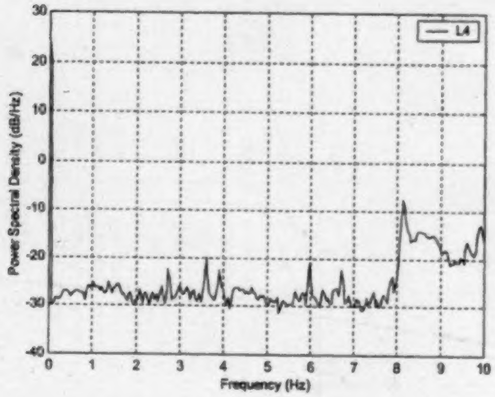

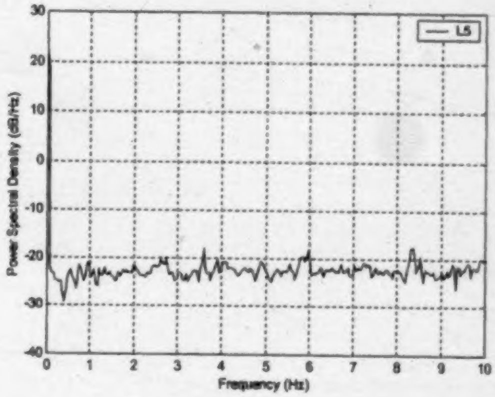

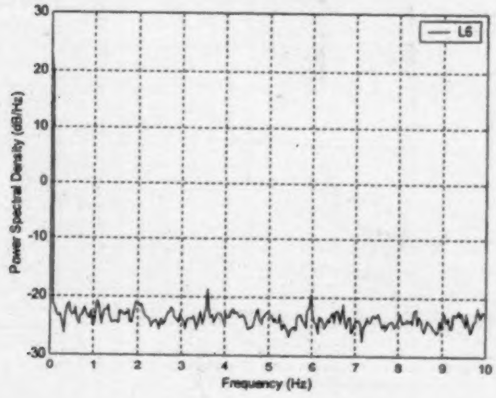

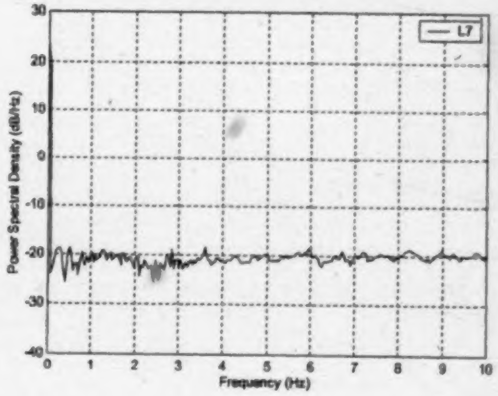

July 18, 1999
4:33 PM

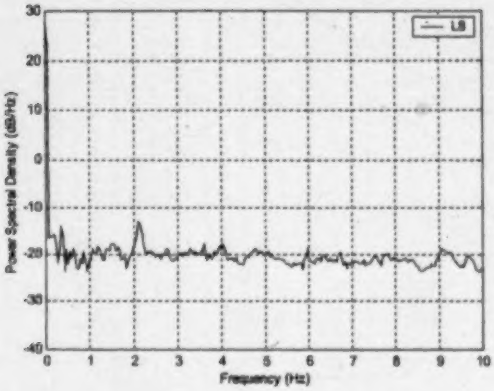

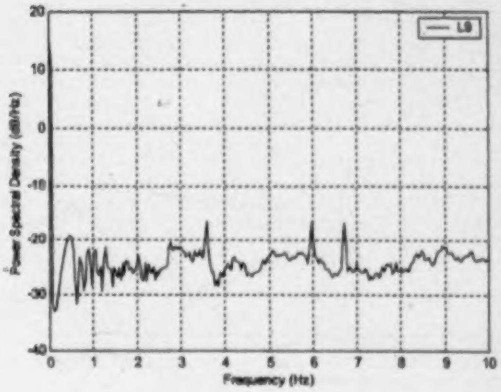

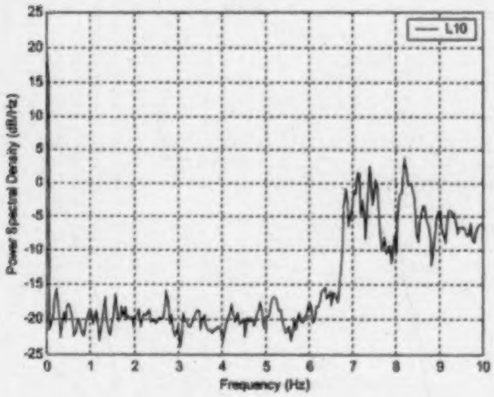

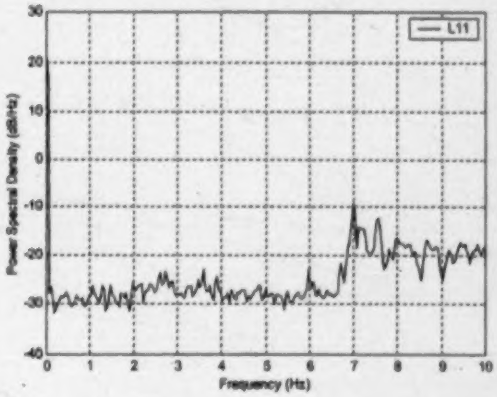

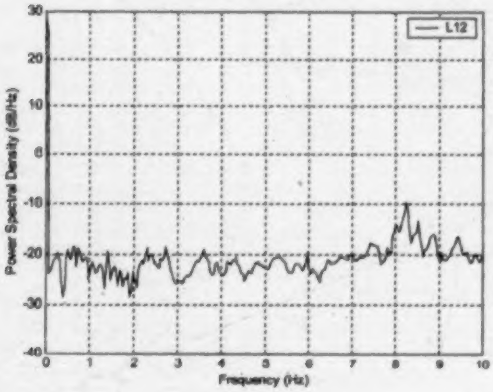

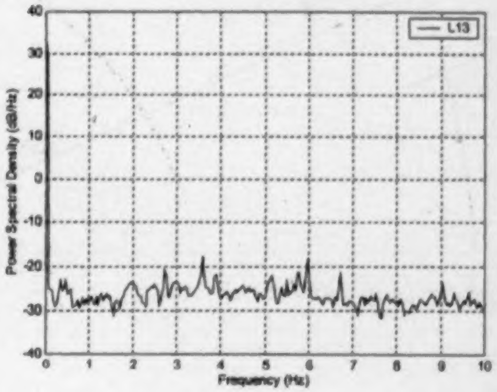

July 18, 1999
4:33 PM

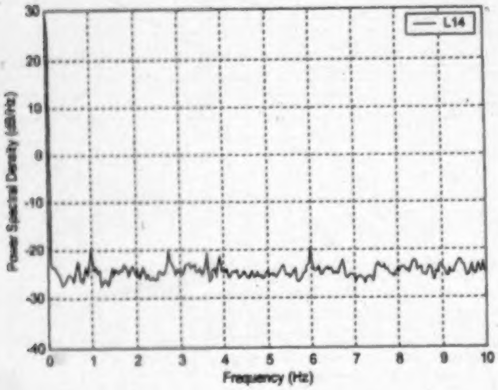

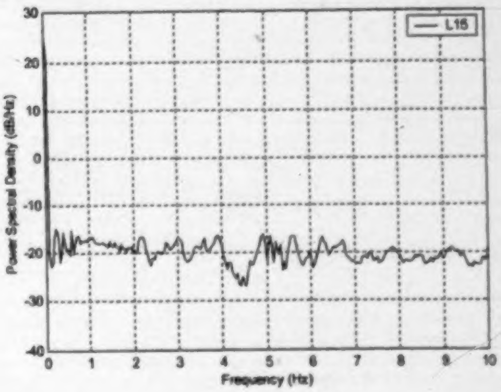

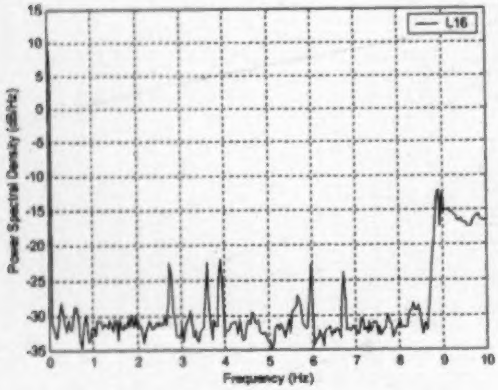

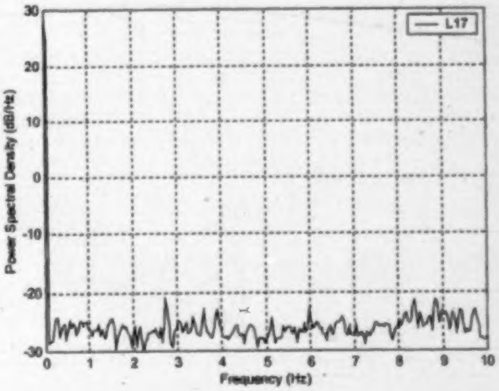

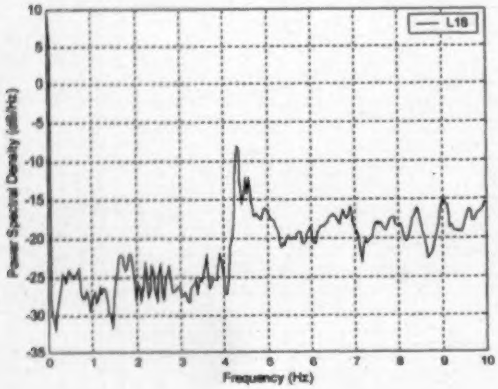

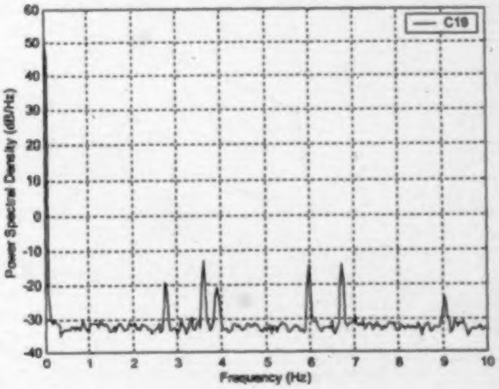

July 18, 1999
4:33 PM

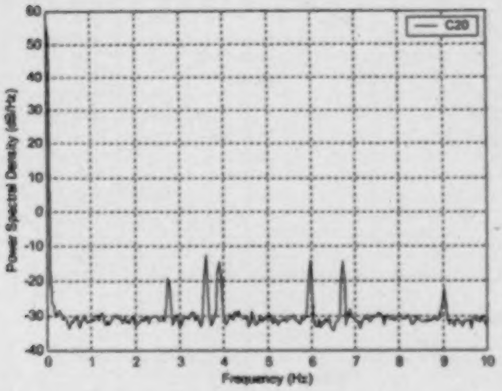

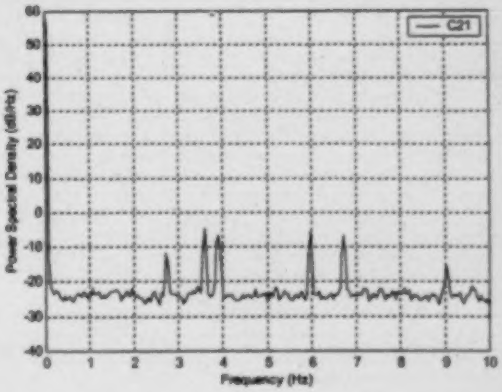

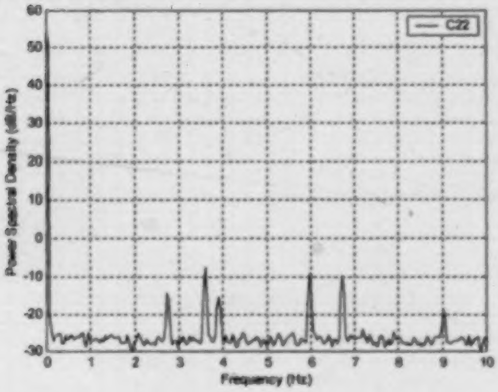

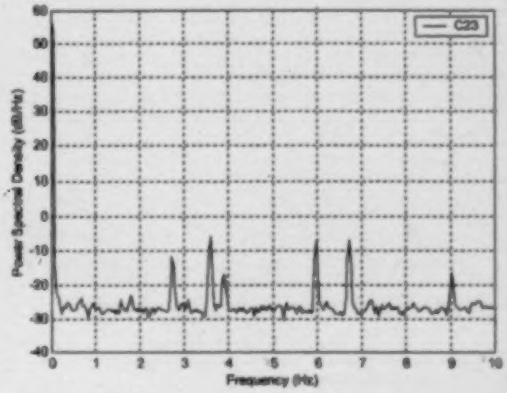

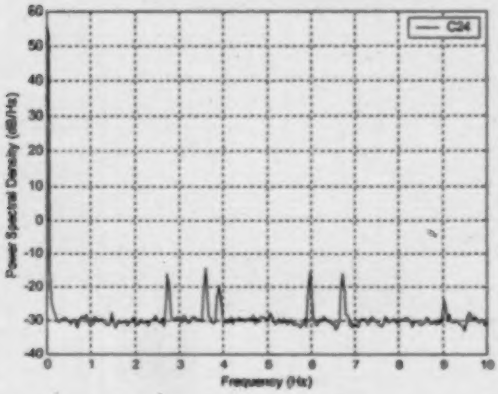

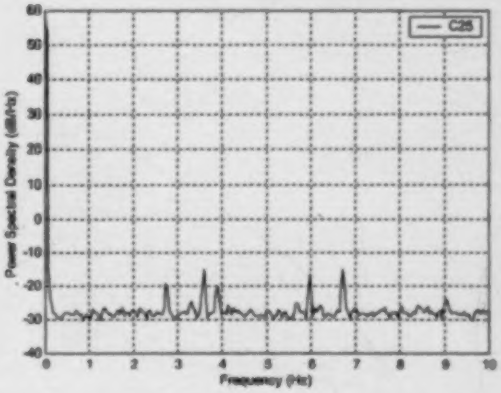

July 18, 1999
4:33 PM

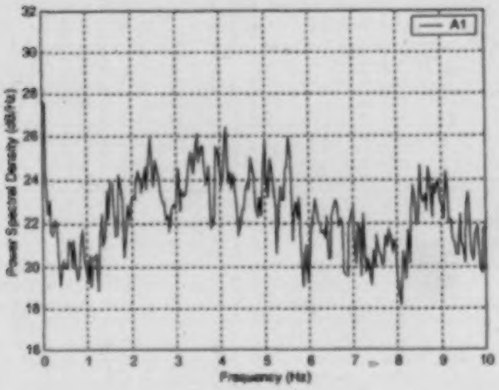

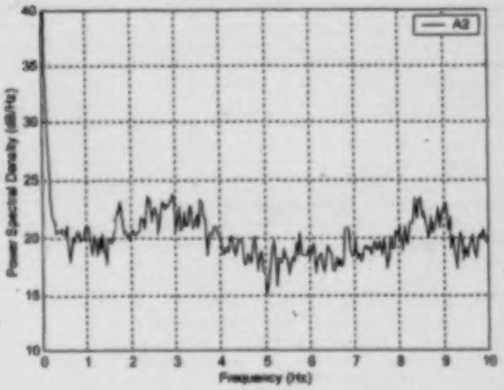

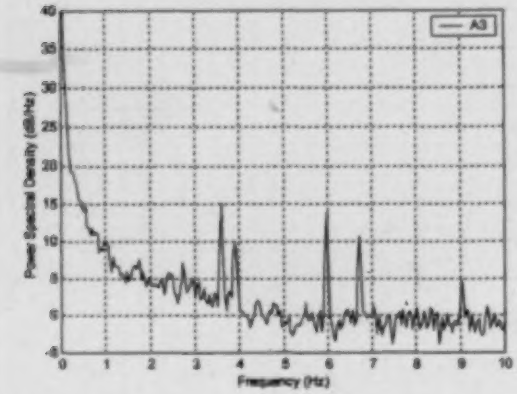

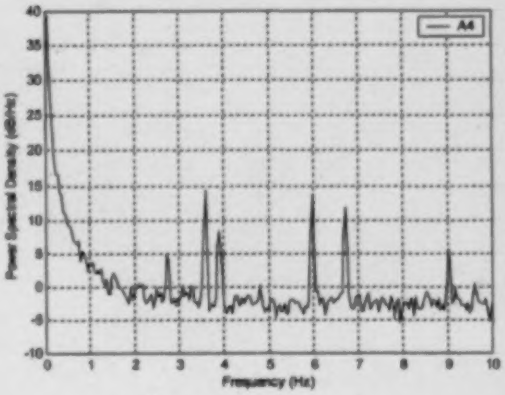

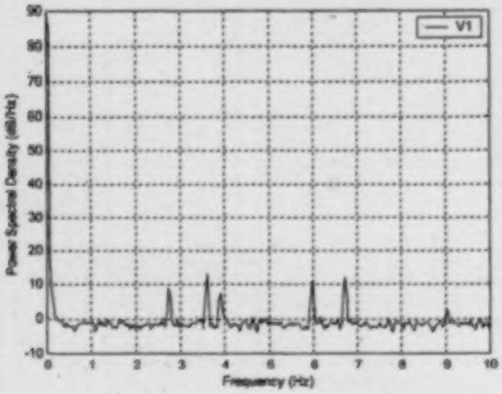

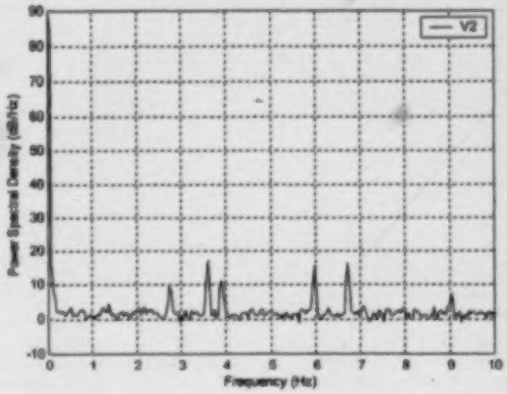

July 18, 1999
5:39 PM

July 18, 1999
5:39 PM

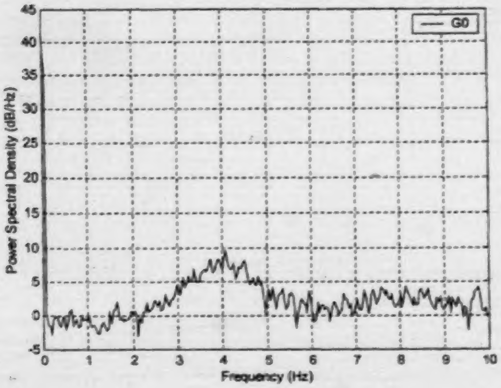

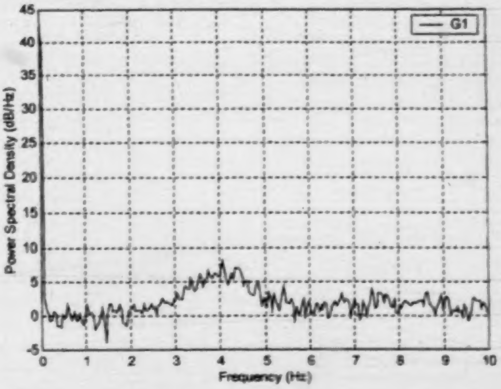

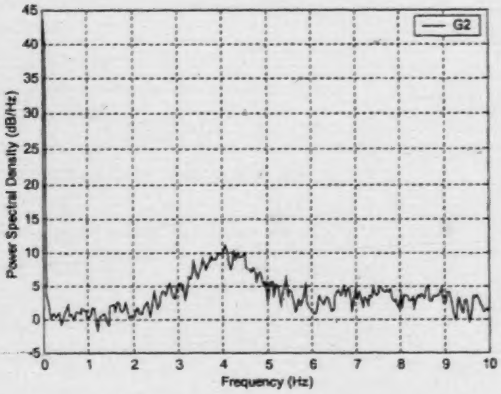

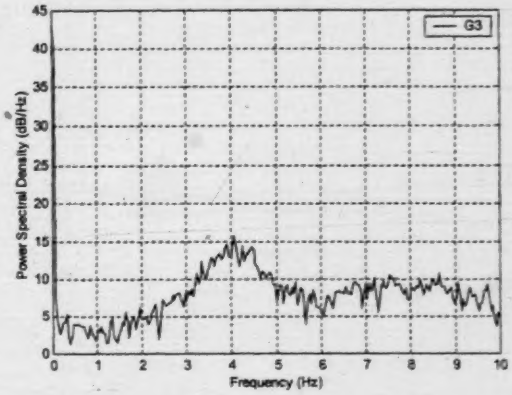

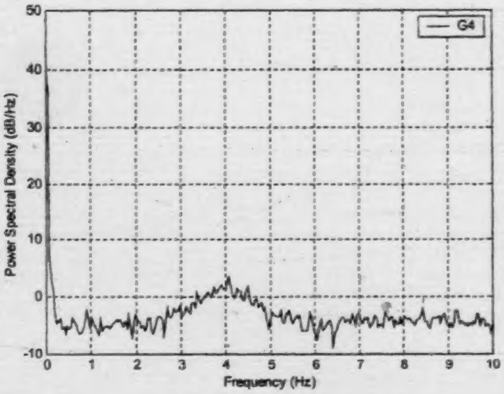

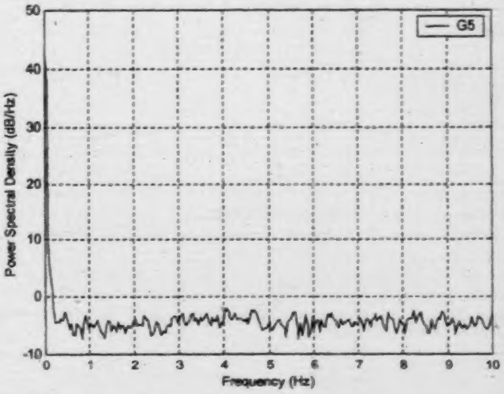

July 18, 1999
5:39 PM

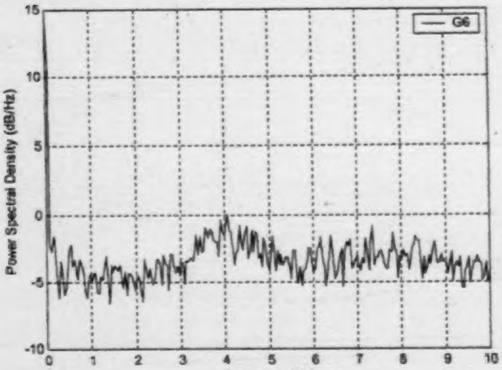

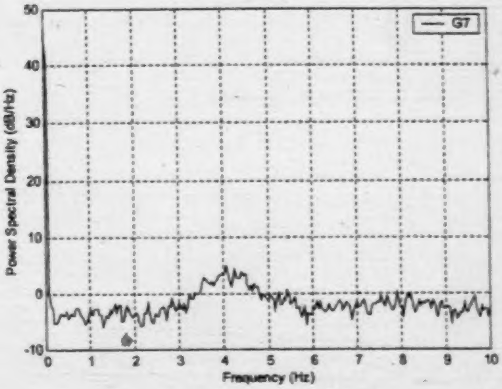

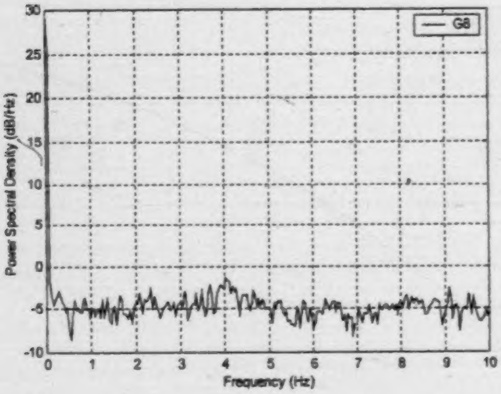

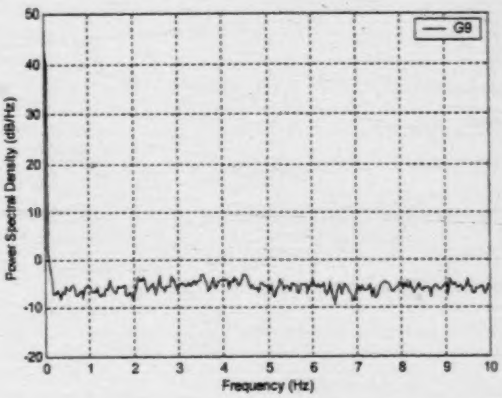

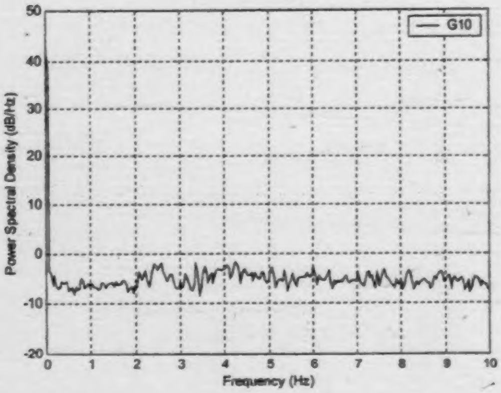

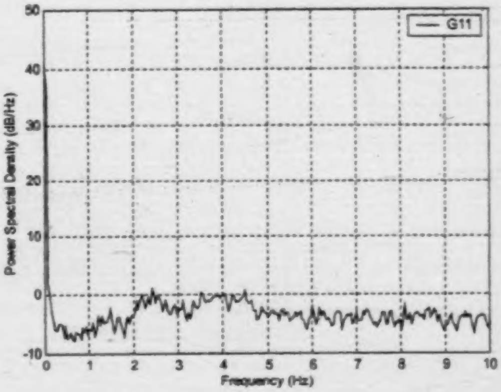

July 18, 1999
5:39 PM

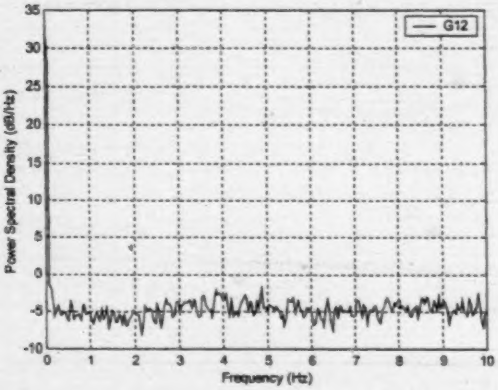

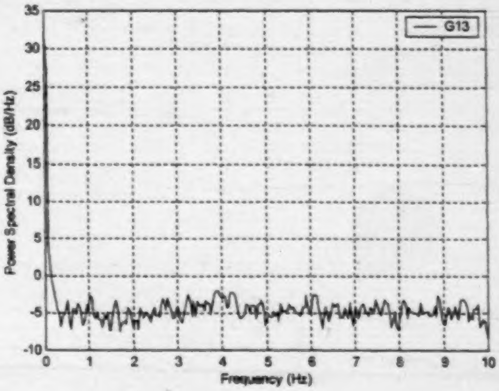

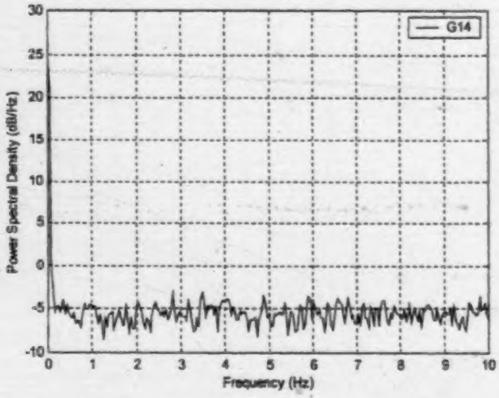

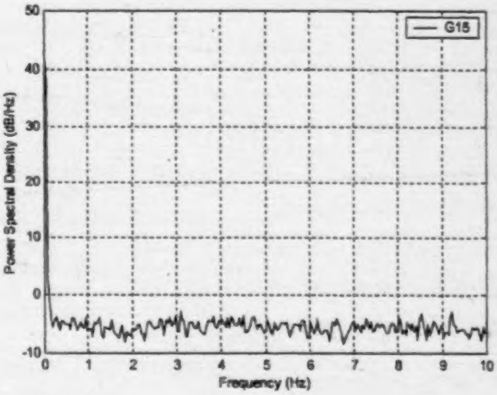

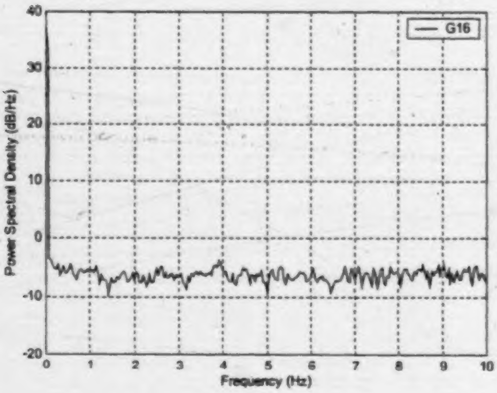

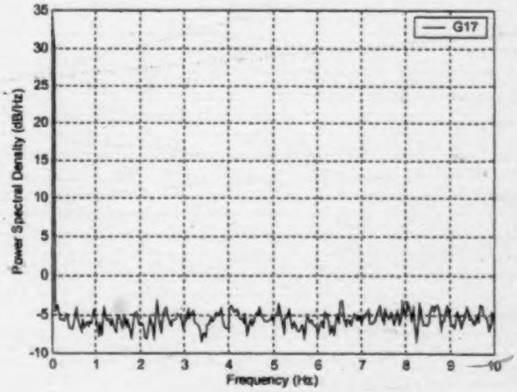

July 18, 1999
5:39 PM

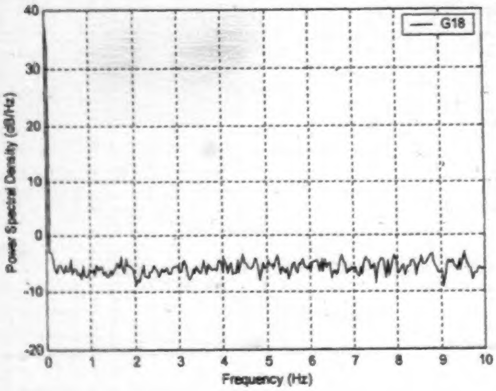

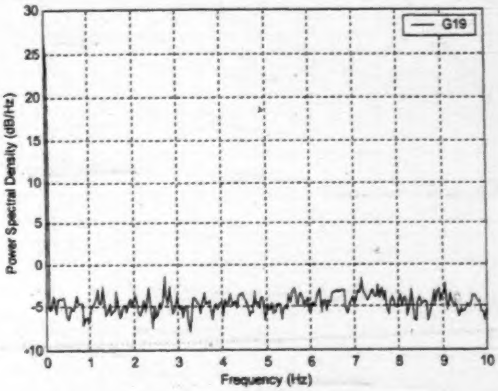

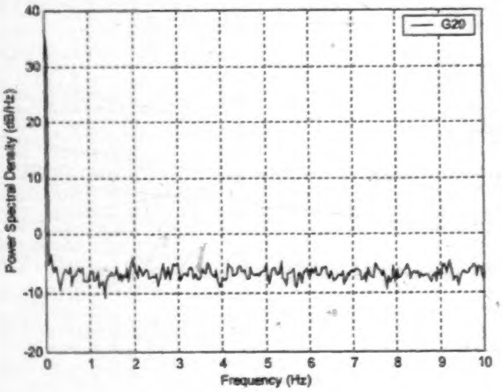

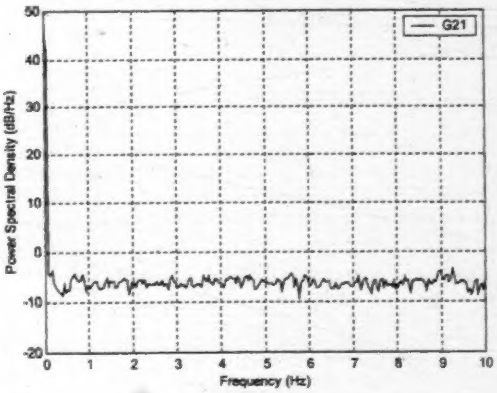

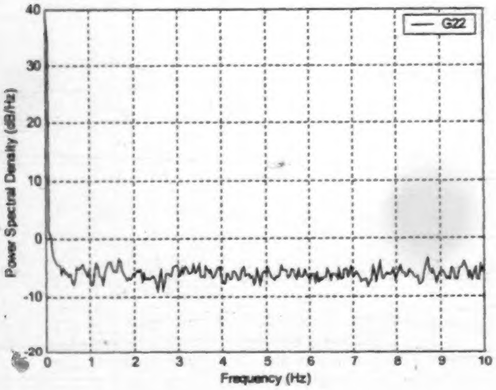

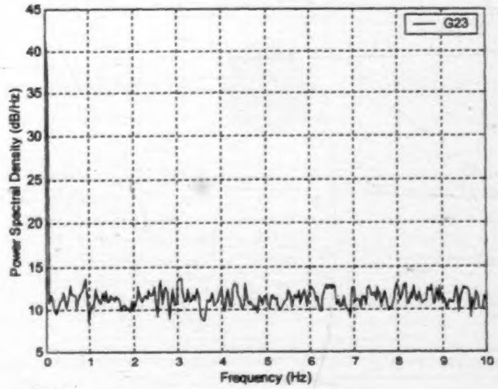

July 18, 1999
5:39 PM

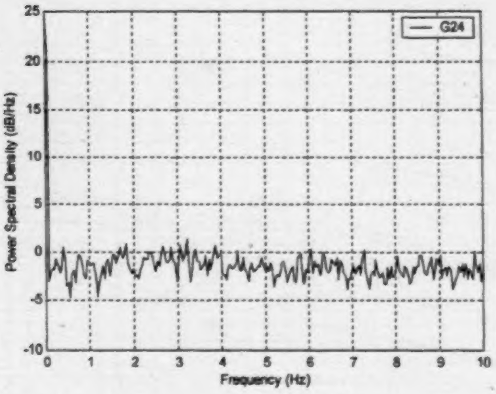

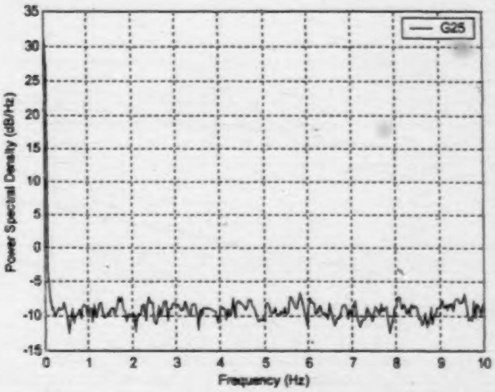

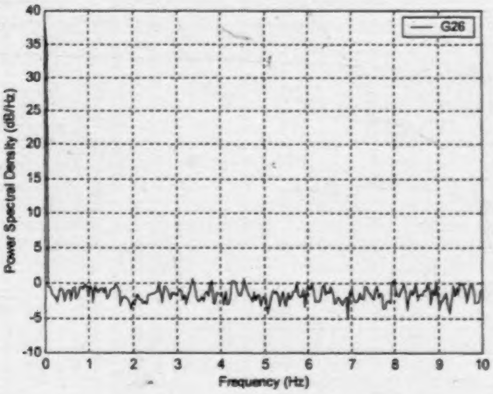

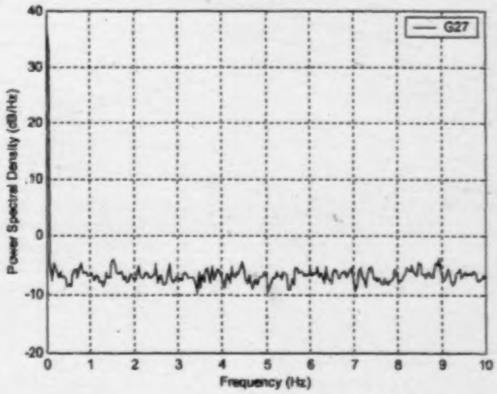

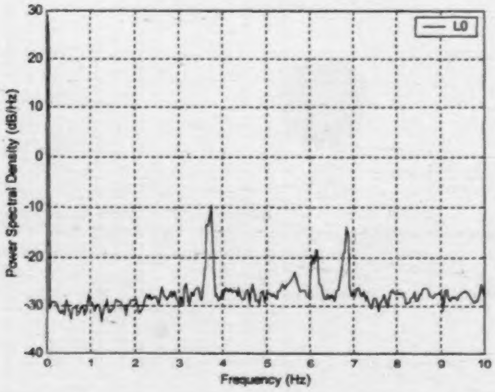

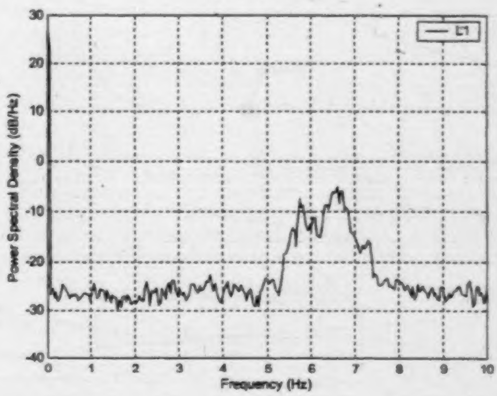

July 18, 1999
5:39 PM

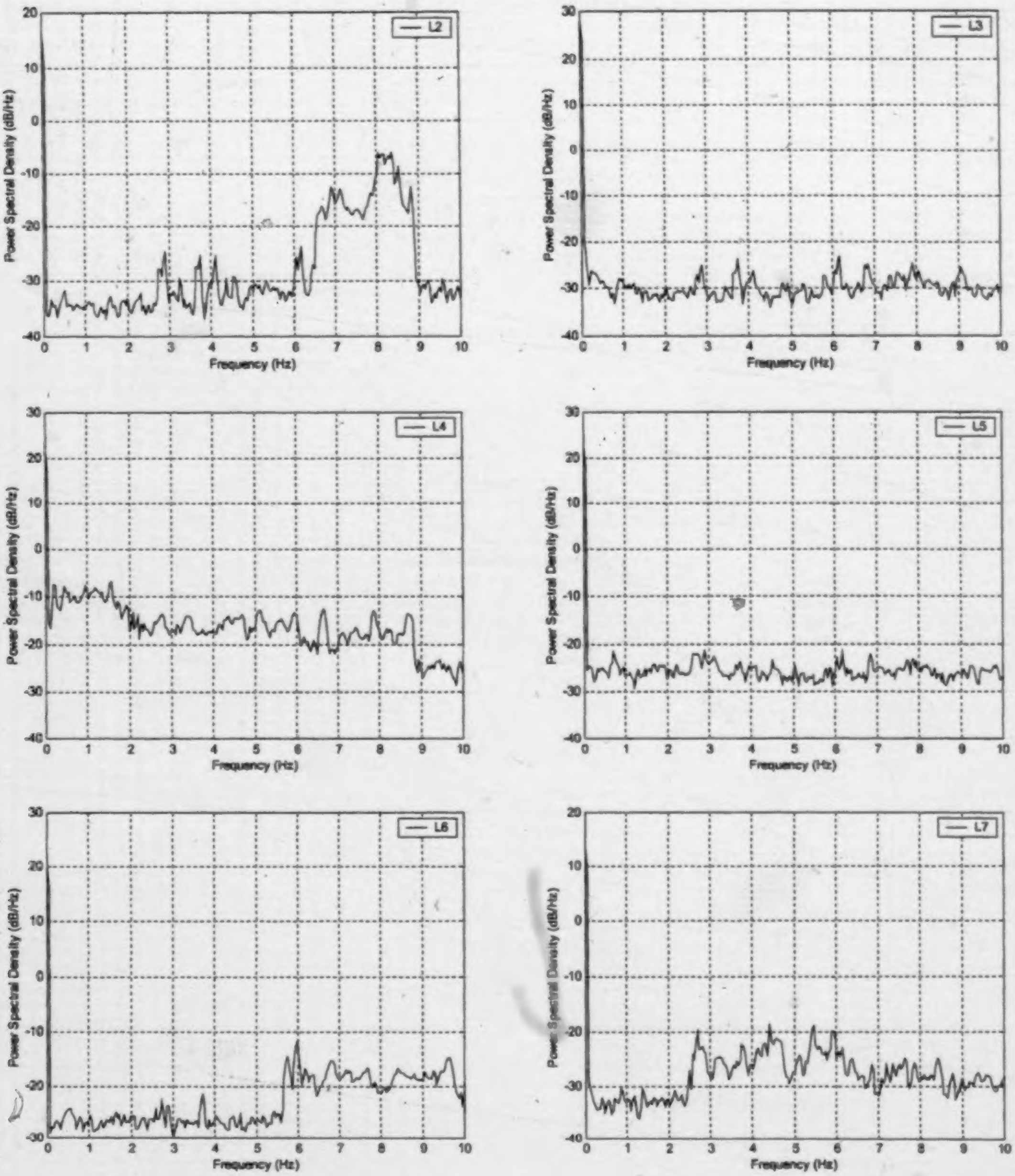

July 18, 1999
5:39 PM

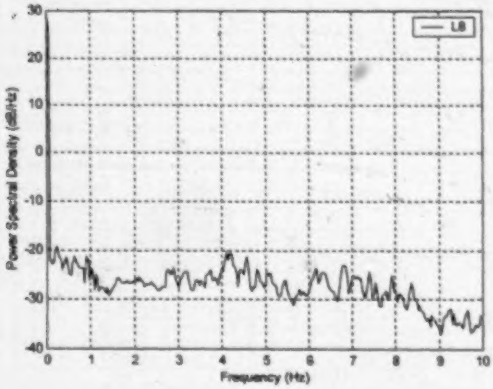

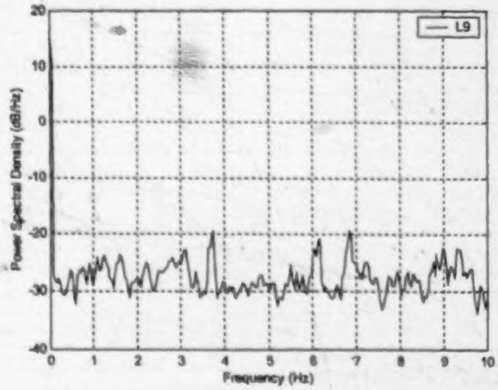

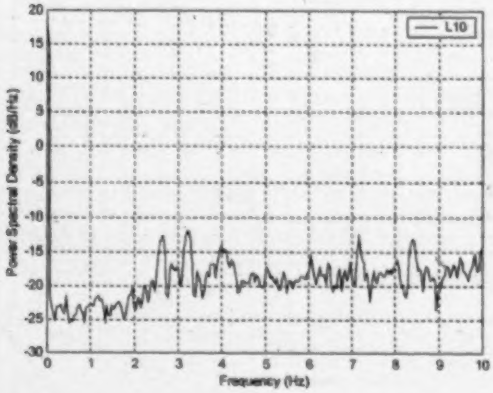

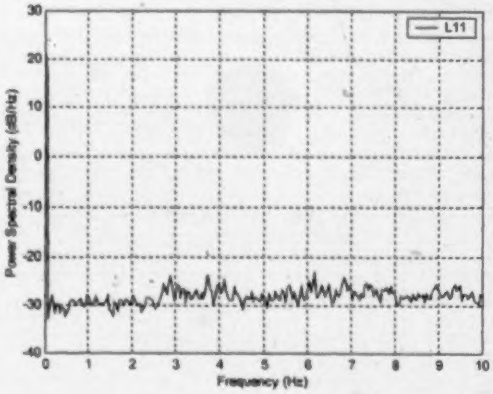

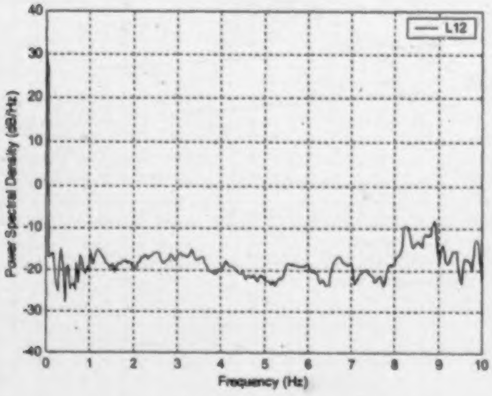

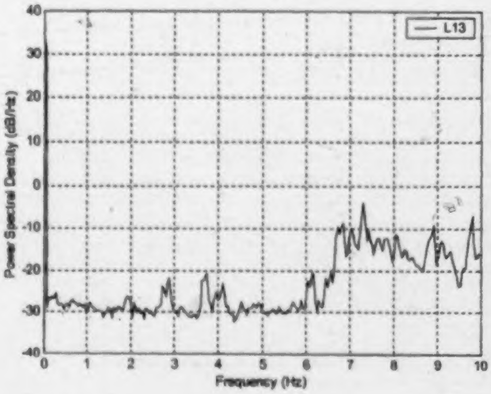

July 18, 1999
5:39 PM

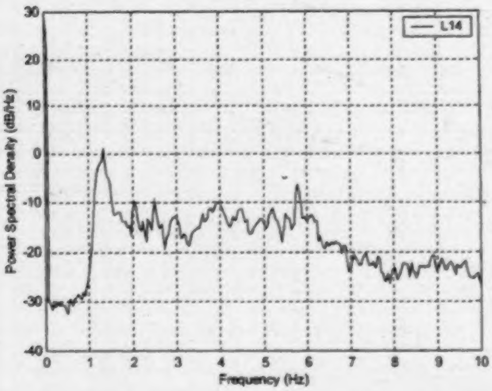

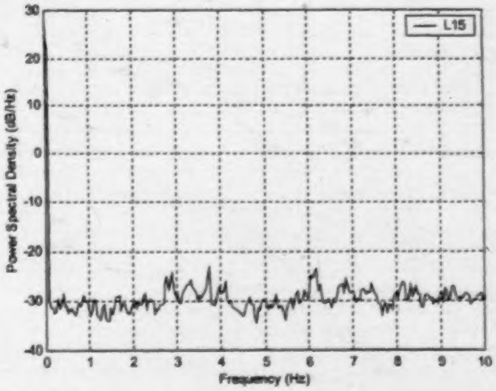

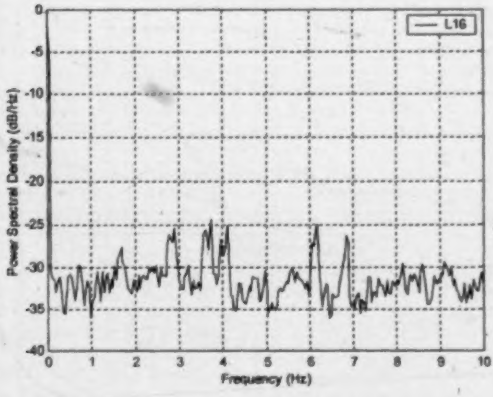

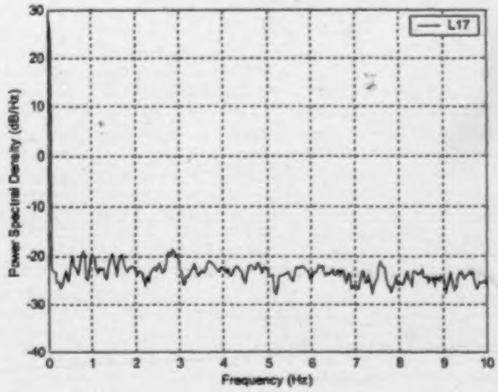

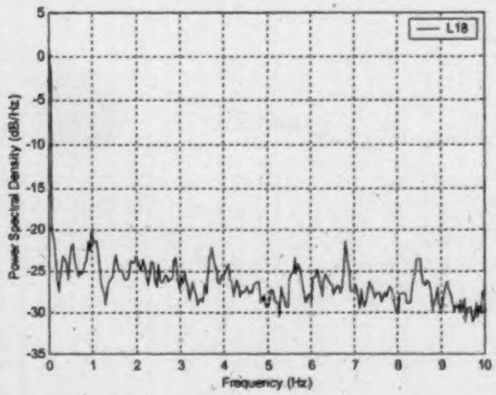

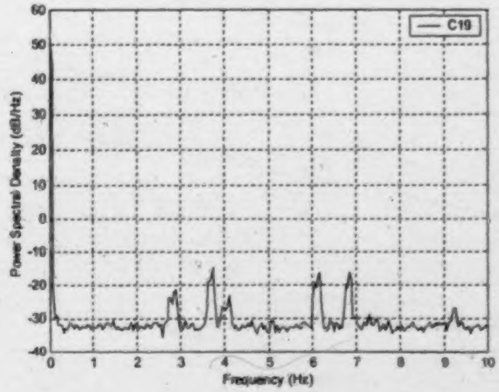

July 18, 1999
5:39 PM

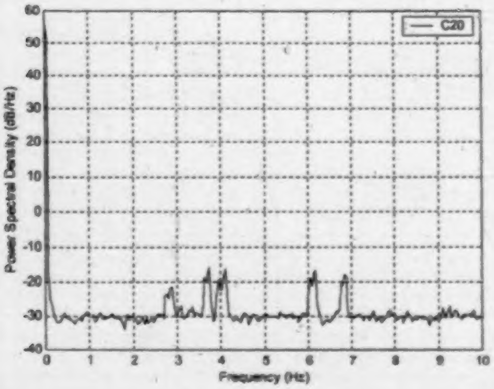

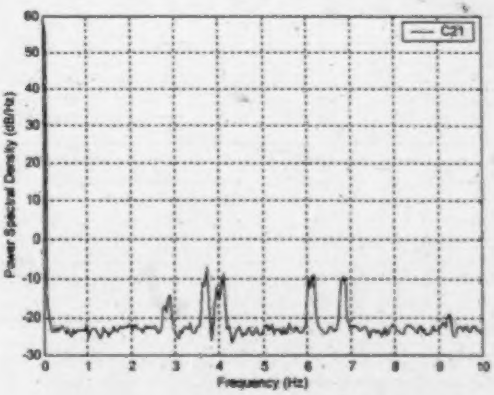

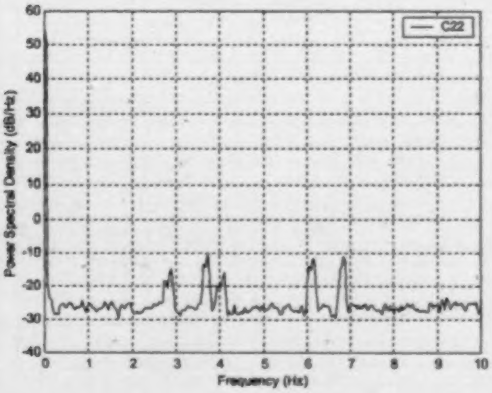

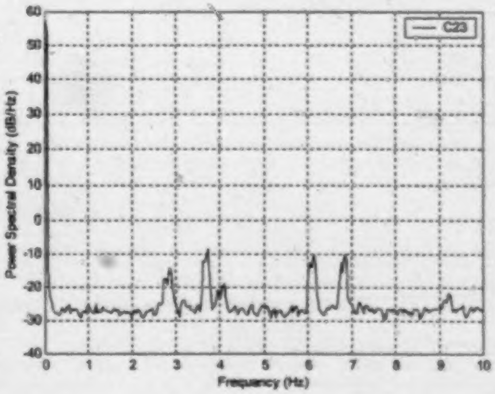

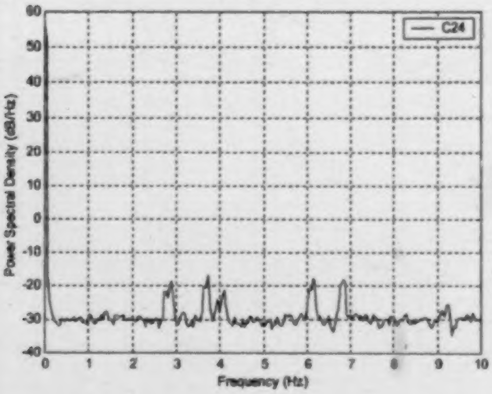

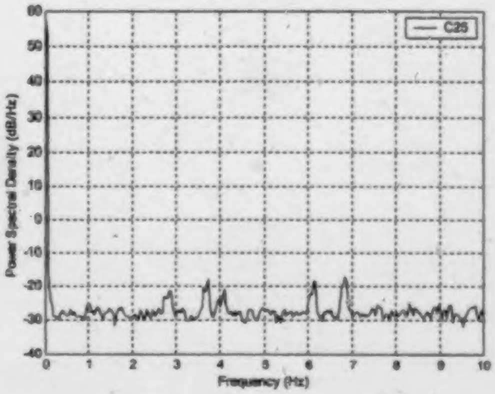

July 18, 1999
5:39 PM